

Swansea University E-Theses

Evaluation of mineral magnetic properties and thermal activation characteristics of soil material in reconstructing post-fire sediment redistribution and fire history, Sydney Basin, Australia.

Farwig, Victoria Jane

How to cite:

Farwig, Victoria Jane (2006) *Evaluation of mineral magnetic properties and thermal activation characteristics of soil material in reconstructing post-fire sediment redistribution and fire history, Sydney Basin, Australia..* thesis, Swansea University.

<http://cronfa.swan.ac.uk/Record/cronfa43195>

Use policy:

This item is brought to you by Swansea University. Any person downloading material is agreeing to abide by the terms of the repository licence: copies of full text items may be used or reproduced in any format or medium, without prior permission for personal research or study, educational or non-commercial purposes only. The copyright for any work remains with the original author unless otherwise specified. The full-text must not be sold in any format or medium without the formal permission of the copyright holder. Permission for multiple reproductions should be obtained from the original author.

Authors are personally responsible for adhering to copyright and publisher restrictions when uploading content to the repository.

Please link to the metadata record in the Swansea University repository, Cronfa (link given in the citation reference above.)

<http://www.swansea.ac.uk/library/researchsupport/ris-support/>

Evaluation of mineral magnetic properties
and Thermal Activation Characteristics of
soil material in reconstructing post-fire
sediment redistribution and fire history,
Sydney Basin, Australia

Victoria Jane Farwig

Submitted to the University of Wales Swansea in part fulfilment of
the requirements for the degree of Doctor of Philosophy.
Department of Geography, University of Wales Swansea,
September 2006.



ProQuest Number: 10821587

All rights reserved

INFORMATION TO ALL USERS

The quality of this reproduction is dependent upon the quality of the copy submitted.

In the unlikely event that the author did not send a complete manuscript and there are missing pages, these will be noted. Also, if material had to be removed, a note will indicate the deletion.



ProQuest 10821587

Published by ProQuest LLC (2018). Copyright of the Dissertation is held by the Author.

All rights reserved.

This work is protected against unauthorized copying under Title 17, United States Code
Microform Edition © ProQuest LLC.

ProQuest LLC.
789 East Eisenhower Parkway
P.O. Box 1346
Ann Arbor, MI 48106 – 1346

*"Success is a journey, not a destination.
The doing is often more important than the outcome."
Arthur Ashe*

DECLARATION

This work has not previously been accepted in substance for any degree and is not being concurrently submitted in candidature for any degree

Signed(candidate)

Date18th February 2007.....

STATEMENT 1

This thesis is the result of my own investigations, except where otherwise stated. All other sources are acknowledged by explicit references.

Signed(candidate)

Date18th February 2007.....

STATEMENT 2

I hereby give consent for my thesis, if accepted, to be made available for photocopying and for inter-library loan, and for the title and abstract to be made available to outside organisations.

Signed(candidate)

Date18th February 2007.....

ABSTRACT

This thesis explores the applicability of mineral magnetic properties and Thermal Activation Characteristics (TAC), in reconstructing: (i) heating due to wildfire; (ii) the temperature reached during fire; and (iii) fire history from reservoir-floor sediments in Lake Burragorang, Sydney Basin, Australia and soil in its catchment. Heating of soil modifies its magnetic minerals by creating a secondary ferrimagnetic form and TAC plot curves can indicate emission of luminescence from quartz following stimulation by progressive heating. Mineral magnetic properties were examined in laboratory-heated soil samples from long-unburnt foot-slope, mid-slope and ridge-top locations in the catchment. TAC were assessed for the foot-slope sample and a control sample of crushed rock previously unexposed to any major heating. These findings were applied to dated reservoir sediments in seven cores to ascertain the reliability of the two techniques in reconstructing both the soil temperatures reached in fire-related sediment and fire history.

Both techniques were found to be restricted to the maximum temperature experienced in any fire to which the soil or sediment had been subjected and not the most recent one. The results suggested that ridge-top and mid-slope samples represented unheated sub-surface soil exposed by post-fire erosion, since modification to mineral magnetic properties for these samples occurred at temperatures as low as $\sim 50^{\circ}\text{C}$. In contrast, samples from the foot-slope site appeared to retain a heating signal from previous fires and only became enhanced at temperatures $>450^{\circ}\text{C}$, suggesting that this slope unit acted largely as a sink for eroded sediment from upslope. The TAC results proved more useful than those for the mineral magnetic properties in reconstructing fire effects. The shape of the TAC curve and the peak value were able to be used to suggest the timing and degree of heating over a large temperature range ($0\text{--}800^{\circ}\text{C}$).

In the sediment cores, magnetic parameters showed elevated values in conjunction with different signatures related to the composition of the material. TAC showed that quartz grains in fire-related sediment had experienced temperatures of $400\text{--}500^{\circ}\text{C}$. Dating evidence suggested that virtually all the retrieved fire-related material originated from the 1964-1965 fire events. This is supported by the similarity in the indicated soil temperatures. Broadly similar chronologies were obtained for the seven cores.

Despite some limitations, both techniques show considerable promise in sediment-source tracing of wildfire-affected eroded sediment and in reconstructing fire history from lake and reservoir sediments. It is, however, recommended that these methods are also evaluated in other environments to assess their wider applicability.

ACKNOWLEDGEMENTS

There are a large number of people to whom I owe a great deal. I would especially like to thank the following for their contributions to this study.

First of all, I wish to give a special thank you to my supervisors Rick Shakesby and Stefan Doerr for their unfailing enthusiasm and encouragement throughout. A big thank you also goes to Geoff Humphreys for teaching me about Australian soils and Will Blake for mineral magnetics advice. Both have provided invaluable supervisory support. I would also like to extend my thanks to Ed Rhodes for his interest and enthusiasm for my research on Thermal Activation Characteristics. I am particularly indebted to Zoë Hardiman for her superb fieldwork assistance and friendship during my second fieldwork visit.

In the Geography Department at the University of Wales Swansea, I would like to thank everyone for friendship and support, for which Helena, Hannah, Chris, Amber, Penny, Phil, Addy, and Aimee deserve particular mention. I also owe thanks to Phil, Alan, Nicola and Anna for technical help. Additionally, thanks to Emma, Sarah, and Mel for being great friends and for their hospitality during visits to Swansea while writing up.

I would also like to thank Tony Morris for the use of the Agico KLY3s anisotropy system in the geodynamics and palaeomagnetism laboratory at the University of Plymouth.

I am indebted to many people for making my visits to Australia successful and full of happy memories. In Sydney, I would like to thank the staff from Macquarie University in Sydney for their extensive and very willing support for my fieldwork. They very kindly allowed me access to field equipment and provided office space. Sydney Catchment Authority staff from the Warragamba office managed by Glen Capararo kindly allowed access to the Lake Burragorang catchment and provided a barge from which to carry out the coring. Chris Chafer provided ancillary data used in this study and advice on site selection. Staff at Wirrimbirra Flora and Fauna Sanctuary provided accommodation, access to their office, laboratory space and support, I would especially like to thank Joy Hafey and Robert Sloss, who showed great interest in my research whilst at the Sanctuary. Mark, Kerrie and the Lamaro family provided accommodation during time spent in Sydney. In Canberra, I would like to thank Peter Wallbrink and Danny Hunt of the Commonwealth Scientific Industrial Research Organisation (CSIRO) for provision of coring equipment and for providing laboratory space, and Gary Hancock for advice on dating of sediment core samples. Norman Hill and Cynthja Bolton provided technical support during TAC laboratory work. The staff and postgraduates at Australian National University in Canberra made me more than welcome during my stay at University House.

Lastly and most importantly, thanks to my wonderful family for their unfailing support, patience, encouragement and love and to my friends for their excellent company during the roller coaster ride of this PhD!

Funding from NERC studentship NER/S/A/2002/10414 is gratefully acknowledged.

TABLE OF CONTENTS

| | |
|---|-----------|
| Declaration | i |
| Abstract | ii |
| Acknowledgements | iii |
| Table of Contents | iv |
| List of Figures | v |
| 1 INTRODUCTION | 1 |
| 2 LITERATURE REVIEW | 4 |
| 2.1 INTRODUCTION | 4 |
| 2.2 FOREST FIRES | 5 |
| 2.2.1 FIRE RISK MANAGEMENT | 7 |
| 2.2.2 FIRE INTENSITY, SEVERITY AND FREQUENCY | 8 |
| 2.2.3 FIRE MOVEMENT AND BEHAVIOUR | 14 |
| 2.2.3.1 <i>The effect of weather on fire movement and behaviour</i> | 15 |
| 2.2.3.2 <i>The effect of topography on fire movement and behaviour</i> | 16 |
| 2.2.3.3 <i>The effect of fuel load on fire movement and behaviour</i> | 17 |
| 2.3 FOREST FIRE IMPACTS ON SOIL, LITTER AND VEGETATION | 20 |
| 2.3.1 FOREST FIRE EFFECTS ON VEGETATION | 20 |
| 2.3.1.1 <i>Fire severity and vegetation removal</i> | 20 |
| 2.3.1.2 <i>Vegetation regeneration after fire</i> | 21 |
| 2.3.2 FOREST FIRE EFFECTS ON SOILS AND LITTER | 24 |
| 2.3.3 FIRE EFFECTS ON SOIL PHYSICAL PROPERTIES | 25 |
| 2.3.4 Fire effects on soil mineral magnetic properties | 26 |
| 2.3.4.1 <i>Magnetic properties of soil</i> | 26 |
| 2.3.4.2 <i>The behaviour of fires</i> | 32 |
| 2.3.4.3 <i>The type of soil being heated</i> | 34 |
| 2.3.4.4 <i>Summary of the effects of heating on mineral magnetic properties</i> | 37 |
| 2.3.5 FIRE EFFECTS ON THERMAL ACTIVATION CHARACTERISTICS | 38 |
| 2.3.6 FIRE EFFECTS ON SOIL CHEMICAL PROPERTIES | 42 |
| 2.3.6.1 <i>Chemical properties</i> | 42 |
| 2.3.6.2 <i>Water repellency</i> | 43 |
| 2.3.6.2.1 <i>Moisture effect on fire</i> | 43 |
| 2.3.6.2.2 <i>Initial soil state prior to burning</i> | 45 |
| 2.3.6.2.3 <i>The severity of the fire</i> | 45 |
| 2.3.6.2.4 <i>The duration of the burn</i> | 45 |
| 2.3.6.2.5 <i>Longevity of fire-induced changes to soil hydrophobicity</i> | 46 |
| 2.4 FIRE EFFECTS ON HYDROLOGY | 47 |
| 2.4.1 FIRE EFFECTS ON INFILTRATION | 47 |
| 2.4.2 FIRE EFFECTS ON INFILTRATION | 49 |

| | | |
|-----------|--|----|
| 2.4.2.1 | <i>The relevance of macro-pores to infiltration processes</i> | 49 |
| 2.4.3 | OVERLAND FLOW AND RUNOFF | 50 |
| 2.5 | FIRE EFFECTS ON SOIL EROSION | 52 |
| 2.5.1 | RAINSPLASH DETACHMENT | 53 |
| 2.5.2 | OVERLAND FLOW, RILL AND GULLY DEVELOPMENT | 55 |
| 2.5.3 | OTHER FIRE-INDUCED EROSIONAL EFFECTS | 57 |
| 2.5.3.1 | <i>Wind erosion</i> | 57 |
| 2.5.3.2 | <i>Mass wasting</i> | 57 |
| 2.5.3.3 | <i>Dry Ravel</i> | 57 |
| 2.5.3.4 | <i>Debris flows</i> | 58 |
| 2.5.4 | FIRE EFFECTS ON EROSION AT THE SLOPE-SCALE | 59 |
| 2.5.4.1 | <i>Pedestals and exposed roots</i> | 59 |
| 2.5.4.2 | <i>Litter dams</i> | 59 |
| 2.5.4.3 | <i>Bioturbation</i> | 60 |
| 2.6 | TRANSPORTATION AND DEPOSITION OF ERODED SEDIMENTS | 62 |
| 2.6.1 | ENTRAINMENT AS A RESULT OF INCREASED FLOW VELOCITY | 62 |
| 2.6.2 | RESPONSE OF HYDROLOGIC MECHANISMS IN A POST-FIRE ENVIRONMENT | 63 |
| 2.6.3 | TRANSPORTATION THROUGH THE RIVER SYSTEM | 67 |
| 2.6.4 | DELTA DEPOSITION | 67 |
| 2.6.4.1 | <i>Agradation above the reservoir</i> | 70 |
| 2.6.5 | SEDIMENT MOVEMENT WITHIN LAKE AND RESERVOIR ENVIRONMENTS | 70 |
| 2.6.5.1 | <i>Climate effects on erosion, sedimentation deposition</i> | 71 |
| 2.6.5.2 | <i>Processes within lakes and reservoirs affecting sedimentation and</i> | 72 |
| 2.6.5.3.1 | Wind | 72 |
| 2.6.5.3.2 | River inflow | 72 |
| 2.6.5.3.3 | Solar heating | 72 |
| 2.6.5.3.4 | Sediment distribution | 73 |
| 2.6.6 | MODELLING SEDIMENT DISTRIBUTION IN RESERVOIRS | 74 |
| 2.7 | RESERVOIR MANAGEMENT | 74 |
| 2.7.1 | EFFECT OF DRAW-DOWN ON RESERVOIR SEDIMENTATION | 74 |
| 2.7.1.1 | <i>Management solutions to sedimentation</i> | 75 |
| 2.7.2 | RECORD OF FIRE IN SEDIMENTS | 75 |
| 2.8 | FIRE FREQUENCY AND ITS EFFECTS OF EROSION AND SEDIMENTATION | 77 |
| 2.8.1 | TEMPORAL PATTERNS OF FIRE AND EFFECTS ON SOIL EROSION CYCLES | 77 |
| 2.8.2 | TEMPORAL PATTERNS OF FIRE ON VEGETATION | 77 |
| 2.8.3 | TEMPORAL PATTERNS OF FIRE AND SOIL EROSION CYCLES | 78 |
| 2.8.4 | SCALE PROBLEMS (DIFFERENCE BETWEEN SMALL AND LARGE SCALE RESEARCH) | 80 |
| 2.9 | SUMMARY AND RESEARCH GAPS | 83 |
| 3 | STUDY AREA | 86 |
| 3.1 | INTRODUCTION | 86 |
| 3.2 | GEOLOGY | 91 |
| 3.3 | RELIEF AND SLOPE FORM | 93 |
| 3.4 | SOILS | 97 |

| | | |
|-------------|---|------------|
| 3.5 | VEGETATION AND LAND USE | 98 |
| 3.6 | CLIMATE | 102 |
| 3.6.1 | TEMPERATURE AND HUMIDITY | 102 |
| 3.6.2 | RAINFALL | 103 |
| 3.7 | FIRE HISTORY | 106 |
| 3.8 | HYDROLOGY | 121 |
| 3.8.1 | RESERVOIR LEVEL | 123 |
| 3.8.2 | RIVER FLOW | 123 |
| 3.9 | LAKE BATHYMETRY AND CURRENTS | 127 |
| 3.10 | PREVIOUS WORK ON SOIL EROSION, WATER REPELLENCY, SEDIMENT MOVEMENT AND DEPOSITION IN THE STUDY AREA OF LAKE BURRAGORANG | 130 |
| 3.10.1 | SOIL EROSION AND MOVEMENTS WITHIN THE CATCHMENT OF LAKE BURRAGORANG | 130 |
| 3.10.2 | EFFECTS OF FIRE ON SOIL PROPERTIES WITHIN THE STUDY REGION | 133 |
| 3.10.3 | SEDIMENTOLOGICAL STUDIES WITHIN CATCHMENTS OF LAKE BURRAGORANG | 139 |
| 3.11 | SUMMARY OF RESEARCH GAPS ARISING FROM RESEARCH WITHIN THE CATCHMENT OF LAKE BURRAGORANG | 144 |
| 4 | RESEARCH DESIGN AND RATIONALE | 145 |
| 4.1 | INTRODUCTION | 145 |
| 4.2 | RESEARCH DESIGN AND RATIONALE | 146 |
| 5 | EFFECTS OF HEATING ON SOIL MINERAL MAGNETIC PROPERTIES | 150 |
| 5.1 | INTRODUCTION | 150 |
| 5.2 | METHODOLOGY | 153 |
| 5.2.1 | SAMPLE DETAILS | 153 |
| 5.2.2 | FURNACE HEATING PROCEDURE | 154 |
| 5.2.3 | MAGNETIC MEASUREMENTS PROCEDURE | 155 |
| 5.2.3.1 | <i>Preparation of samples for magnetic measurements</i> | 156 |
| 5.2.3.2 | <i>Measurement and calculation of low frequency susceptibility (X_{lf}) and frequency dependent susceptibilities (χ_{fd} and $\chi_{fd\%}$)</i> | 156 |
| 5.2.3.3 | <i>Remanence measurements</i> | 159 |
| 5.2.3.4 | <i>Anhyseretic remnant magnetisation: measurement and calculation</i> | 159 |
| 5.2.3.5 | <i>Isothermal remnant magnetisation: measurement and calculation</i> | 161 |
| 5.2.4 | CHANGES IN χ_{LF} DURING HEATING AND COOLING | 162 |
| 5.3 | FURNACE HEATING EFFECTS ON MAGNETIC PROPERTIES OF LONG UNBURNT SOIL | 164 |
| 5.3.1 | FURNACE-HEATED SAMPLES: ACTUAL TEMPERATURES | 164 |
| 5.3.2 | RESPONSES OF MAGNETIC PARAMETERS TO FURNACE HEAT TREATMENTS | 165 |
| 5.3.3 | RESPONSES OF MAGNETIC PARAMETERS TO FURNACE HEAT TREATMENTS BIVARIATE PLOTS | 173 |
| 5.4 | HEATING AND COOLING EFFECT ON χ OF LONG UNBURNT SOIL | 178 |
| 5.4.1 | χ CHANGES: FOOT-SLOPE SAMPLE | 178 |
| 5.4.2 | χ CHANGES: MID-SLOPE SAMPLE | 183 |

| | | |
|------------|---|-----|
| 5.4.3 | χ CHANGES: RIDGE-TOP SAMPLE | 185 |
| 5.5 | DISCUSSION | 188 |
| 5.5.1 | ENHANCED χ > 400 °C | 188 |
| 5.5.1.1 | <i>Mineralogy and soil type</i> | 188 |
| 5.5.1.2 | <i>Previous heating history</i> | 190 |
| 5.5.1.3 | <i>Rate of heating</i> | 191 |
| 5.5.1.4 | <i>Heating duration</i> | 192 |
| 5.5.2 | DIFFERENT TEMPERATURE THRESHOLDS FOR MAGNETIC ENHANCEMENT | 192 |
| 5.5.3 | EFFECT OF REDUCING ATMOSPHERE ON MAGNETIC ENHANCEMENT | 193 |
| 5.6 | CHAPTER SUMMARY | 194 |
| 6 | EFFECTS OF HEATING ON THERMAL ACTIVATION CHARACTERISTICS (TAC) OF QUARTZ GRAINS IN SOIL AND SEDIMENT | 196 |
| 6.1 | INTRODUCTION | 197 |
| 6.2 | METHODOLOGY | 199 |
| 6.2.1 | SAMPLE DETAILS | 199 |
| 6.2.2 | FURNACE HEATING PROCEDURE | 200 |
| 6.2.3 | SAMPLE PREPARATION FOR $tl\chi$ MEASUREMENTS | 200 |
| 6.2.4 | THERMOLUMINESCENCE SENSITIVITY MEASUREMENTS: PROCEDURE | 201 |
| 6.2.5 | CALCULATION OF $tl\chi$ AND PRODUCTION OF TAC | 202 |
| 6.3 | FURNACE HEATING ON TAC OF LONG UNBURNT SOIL | 203 |
| 6.3.1 | TAC OF FURNACE HEATED LONG UNBURNT FOOT-SLOPE SAMPLE | 203 |
| 6.3.1.1 | <i>TAC of recently furnace heated sample</i> | 203 |
| 6.3.1.2 | <i>TAC of samples with simulated early Holocene heating</i> | 204 |
| 6.3.2 | SINGLE GRAIN ANALYSIS OF 'UNHEATED' SAMPLE | 207 |
| 6.4 | UNHEATED AND FURNACE-HEATED TAC OF SANDSTONE BEDROCK SAMPLE | 212 |
| 6.4.1 | $tl\chi$ OF THE 110 °C PEAK | 212 |
| 6.4.2 | TAC OF FURNACE-HEATED BEDROCK | 213 |
| 6.4.2.1 | <i>TAC of a recently heated unexposed bedrock sample</i> | 213 |
| 6.4.2.2 | <i>TAC of a sample of unexposed bedrock simulated to have been heated ca. 10,000 years ago</i> | 214 |
| 6.4.3 | SINGLE GRAIN ANALYSIS OF UNEXPOSED BEDROCK | 217 |
| 6.4.4 | SINGLE GRAIN ANALYSIS OF UNEXPOSED BEDROCK SAMPLE FURNACE HEATED TO 600°C | 222 |
| 6.4.5 | FEATURES OF TAC OF THE FURNACE HEATED BEDROCK (BR) SAMPLE | 224 |
| 6.5 | DISCUSSION | 229 |
| 6.5.1 | INCREASE IN 110 °C $tl\chi$ PEAK WITH FURNACE HEATING TO TEMPERATURES ≤ 400 °C | 229 |
| 6.5.2 | USE OF TAC CURVE TO DISTINGUISH BETWEEN SOIL HEATED TO (I) <400 °C; (II) 400-500 °C AND (III) 600-800 °C | 230 |
| 6.5.3 | USE OF TAC IN DETERMINING TEMPERATURES REACHED IN SOIL | 231 |
| 6.5.4 | TAC CAN BE USED TO SUGGEST THE TIMING OF PREVIOUS HEATING | 233 |
| 6.6 | CHAPTER SUMMARY | 235 |

| | | |
|-----------|--|------------|
| 7 | EVIDENCE FOR WILDFIRE TIMING AND POST-FIRE EROSION: SEDIMENT CORES FROM LAKE BURRAGORANG | 237 |
| 7.1 | INTRODUCTION | 237 |
| 7.2 | METHODOLOGY | 241 |
| 7.2.1 | CORE COLLECTION | 241 |
| 7.2.2 | LABORATORY PROCEDURES | 243 |
| 7.2.2.1 | <i>Core description</i> | 243 |
| 7.2.2.2 | <i>Dating methods applied to the core sediments</i> | 244 |
| 7.2.2.3 | <i>Particle size analysis</i> | 246 |
| 7.2.2.4 | <i>Total Organic Carbon (TOC) analysis</i> | 247 |
| 7.2.2.5 | <i>Mineral magnetic analysis</i> | 247 |
| 7.2.2.6 | <i>Thermal Activation Characteristics (TAC)</i> | 247 |
| 7.2.2.7 | <i>Bulk density and porosity</i> | 247 |
| 7.3 | RESULTS | 248 |
| 7.3.1 | Core 6 | 250 |
| 7.3.1.1 | <i>Visual description</i> | 250 |
| 7.3.1.2 | <i>TOC measurements</i> | 251 |
| 7.3.1.3 | <i>Particle size data</i> | 251 |
| 7.3.1.4 | <i>Bulk density and porosity</i> | 251 |
| 7.3.1.5 | <i>Dating</i> | 254 |
| 7.3.1.5.1 | ¹⁴ C | 254 |
| 7.3.1.5.2 | ²¹⁰ Pb | 256 |
| 7.3.1.5.3 | ¹³⁷ Cs | 256 |
| 7.3.1.5.4 | Pu | 257 |
| 7.3.1.6 | <i>Mineral Magnetism</i> | 258 |
| 7.3.1.7 | <i>TAC</i> | 262 |
| 7.3.2 | CORES 5, 4 AND 7 | 271 |
| 7.3.2.1 | <i>Core 5</i> | 271 |
| 7.3.2.2 | <i>Cores 4 and 7</i> | 271 |
| 7.3.2.3 | <i>Mineral magnetic properties of Cores 5, 4 and 7</i> | 274 |
| 7.4 | DISCUSSION OF FINDINGS | 278 |
| 7.4.1 | USE OF ENHANCED MINERAL MAGNETIC PARAMETERS TO DETECT FIRE | 278 |
| 7.4.2 | USE OF TAC TO DETERMINE SOIL TEMPERATURES DURING FIRE | 280 |
| 7.4.3 | RELIABILITY OF FIRE HISTORY RECORDS CONTAINED WITHIN SEDIMENT CORES FROM AUSTRALIAN RESERVOIR ENVIRONMENTS | 281 |
| 7.4.3.1 | <i>Post-fire rainfall</i> | 283 |
| 7.4.3.2 | <i>Location of fire</i> | 284 |
| 7.5 | CHAPTER SUMMARY OF KEY FINDINGS | 286 |
| 8 | SYNTHESIS AND CONCLUSIONS | 287 |
| 8.1 | INTRODUCTION | 287 |
| 8.2 | KEY FINDINGS | 288 |
| 8.3 | RECONSTRUCTING SOIL AND SEDIMENT TEMPERATURES | 291 |
| 8.3.1 | PROBLEMS WITH USING MINERAL MAGNETIC MEASUREMENTS TO RECONSTRUCT SOIL AND SEDIMENT TEMPERATURES | 292 |

| | | |
|------------|---|------------|
| 8.3.2 | PROSPECTS FOR USING MINERAL MAGNETIC MEASUREMENTS TO RECONSTRUCT SOIL AND SEDIMENT TEMPERATURES | 292 |
| 8.3.3 | FUTURE DIRECTIONS FOR USING MINERAL MAGNETIC MEASUREMENTS TO RECONSTRUCT SOIL AND SEDIMENT TEMPERATURES | 293 |
| 8.3.4 | PROBLEMS WITH USING TAC TO RECONSTRUCT SOIL AND SEDIMENT TEMPERATURES | 294 |
| 8.3.5 | PROSPECTS FOR USING TAC TO RECONSTRUCT SOIL AND SEDIMENT TEMPERATURES | 294 |
| 8.3.6 | FUTURE DIRECTIONS FOR USING TAC TO RECONSTRUCT SOIL AND SEDIMENT TEMPERATURES | 294 |
| 8.4 | DETECTING FIRE EVENTS IN RESERVOIR CORES | 295 |
| 8.4.1 | PROBLEMS WITH DETECTING FIRE EVENTS IN RESERVOIR CORES | 295 |
| 8.4.2 | PROSPECTS FOR DETECTING FIRE EVENTS IN RESERVOIR CORES | 295 |
| 8.4.3 | FUTURE DIRECTIONS FOR DETECTING FIRE EVENTS IN SEDIMENTARY ENVIRONMENTS | 296 |
| 8.5 | RECONSTRUCTING FIRE HISTORY USING AUSTRALIAN RESERVOIR SEDIMENTS | 296 |
| 8.5.1 | PROBLEMS WITH RECONSTRUCTING FIRE HISTORY USING AUSTRALIAN RESERVOIR SEDIMENTS | 296 |
| 8.5.2 | POTENTIAL FOR RECONSTRUCTING FIRE HISTORY USING AUSTRALIAN RESERVOIR SEDIMENTS | 297 |
| 8.5.3 | FUTURE DIRECTIONS FOR RECONSTRUCTING FIRE HISTORY USING AUSTRALIAN RESERVOIR SEDIMENTS | 298 |
| 8.6 | CONCLUSIONS | 299 |

LIST OF FIGURES

2 LITERATURE REVIEW

| | | |
|------|---|----|
| 2.1 | Coincidence of fires seasons and major El Niño episodes in Australia. | 6 |
| 2.2 | Depths at which increased soil temperatures are experienced within the soil profile adapted from data by Chandler <i>et al</i> (1983). | 11 |
| 2.3 | The development of conical flumes and the influence on air entrainment. | 19 |
| 2.4 | The determinants of wildland fire behaviour and their relation to fire modelling. | 19 |
| 2.5 | Schematic representation of the distribution of magnetisation vector in crystals showing the resultant spontaneous magnetisation . | 27 |
| 2.6 | The range of magnetic susceptibility values for environmental materials and minerals (data from diverse published and unpublished sources). | 28 |
| 2.7 | The extent and nature of magnetic enhancement in burnt topsoil (Blake <i>et al.</i> 2006b) | 28 |
| 2.8 | Simplified schematic diagram of the physical processes responsible for luminescence dating. | 38 |
| 2.9 | Simplified model of electron traps and centres adapted from Zimmerman (1971) and Bailey (2001) | 40 |
| 2.10 | (A) Soil water-repellency in unburned brush is found in the litter, fermenting litter and mineral soil layers immediately beneath the shrub plants. (B) When fire burns, hydrophobic substances are vaporized, moving downward along temperature gradients. (C) After the fire has passed, a water repellent layer is present below and parallel to the soil surface on the burned area (De Bano 1981). | 44 |
| 2.11 | Schematic diagram of the displacement of particles by rainsplash | 54 |

| | | |
|-------------------------|---|-----|
| 2.12 | Rill formation during rainstorms following fire involves: (A) saturation of the wettable soil surface; (B) a failure at the boundary between wettable and water repellent layers; (C) loss of the wettable surface layer, with the flow of water over the water repellent layer (D) erosion of the water repellent layer; (E) erosion through the water repellent layer and infiltration into the underlying wettable soil; and (F) development of a well-defined rill (adapted from Wells, 1987; De Bano, 2000). | 56 |
| 2.13 | Formation of litter dams after fire | 60 |
| 2.14 | Erosion and deposition thresholds in relation to flow velocity | 63 |
| 2.15 | Location and thickness of wildfire-related sediment in the upper end of the Strontia Springs Reservoir, Colorado. (A) The pre-fire 1993 surface is shown for comparison with the post-fire September 1996 and June 1997 surfaces. (B) The location of the delta for five surveys in 1997, 1998 and 1999 (Moodv and Martin 2001). | 69 |
| 2.16 | Lake responses to various forms of physical forcing functions | 71 |
| 2.17 | Distribution of sediment from a river inflow into a thermally stratified lake | 73 |
| 2.18 | Cross Section of sediment deposits, Lake Barcroft, Virginia | 74 |
| 2.19 | A hypothetical model of the variation of sediment yield for several fire rotations for a steep-land chaparral system (A) and a <i>Pseudotsuga menziesii</i> western Cascade Mountain system (B) * denotes occurrence of fire. Note different scales (Swanson 1978). | 79 |
| 2.20 | Sediment losses between slope and catchment scales | 81 |
| 2.21 | Conceptual framework showing process relationships between different scales for two different catchments in Spain | 82 |
| 3 STUDY AREA | | |
| 3.1 | Location of Lake Burragorang in New South Wales (NSW), southeast Australia. | 87 |
| 3.2 | Main areas of Lake Burragorang. | 88 |
| 3.3 | (a) stratigraphic columns for the southern and western sections of the Sydney basin, NSW; (b) geology of the catchment of lakes. | 92 |
| 3.4 | Topographical variations within the lower Nattai catchment. | 93 |
| 3.5 | The lower reaches of the Nattai river. | 94 |
| 3.6 | General slope formation showing micro- and meso-scale features relevant to post-fire erosion. | 95 |
| 3.7 | Daily rainfall (solid line) and annual rainfall (dashed line) for 8 rainfall stations located in southern Lake Burragorang (See Figure 3.2 for station locations). | 104 |
| 3.8 | Average monthly rainfall for 1981-1999 and 2000-2003 for the rainfall stations the Causeway, Hilltop and Starlights located in the Nattai catchment. | 105 |
| 3.9 | Percentage of lake Burragorang and Nattai catchments burnt between the 1979/1980 and 2001/2002 fire seasons. | 107 |
| 3.10a | Areas burnt between the 1962/63 and 1967/68 fire seasons. | 110 |
| 3.10b | Areas burnt during the 1968-1969 fire season. | 112 |
| 3.10c | Burnt areas between the 1969/70 and 1974/75 fire seasons. | 114 |
| 3.10d | Areas burnt between the 1979/80 and 1985/86 fire seasons. | 116 |
| 3.10e | Areas burnt between the 1986/87 and 1996/1997 fire seasons. | 118 |
| 3.10f | Areas burnt during the 2001/2002 fire season. | 120 |
| 3.11 | Hydrological catchment of the Nattai River (adapted from Colliton [, 2001 #525]) | 122 |
| 3.12 | (a) Daily reservoir water level since 1960, (b) daily flow data for the Nattai River (catastrophic flood events are labelled in red and high magnitude events are labelled in black), and (c) daily flow data for the Wollondilly River. | 124 |

| | | |
|----------|---|------------|
| 3.13 | Nattai river flow during 2002 fieldwork: (a) before; (b) 3-days after; and (c) 5 days after a storm. | 125 |
| 3.14 | Bathymetry of the Nattai arm of Lake Burragorang. | 128 |
| 3.15 | Occurrence of erosion in the region of Lake Burragorang identified by CALM survey in 1965. | 132 |
| 3.16 | Distinctive magnetic signatures attributed to different slope units from the Blue Gum Creek study site following the 2001/2002 fires. | 134 |
| 4 | RESEARCH DESIGN AND RATIONALE | 145 |
| 4.1 | Research Design. | 145 |
| 5 | EFFECTS OF HEATING ON SOIL MINERAL MAGNETIC PROPERTIES | |
| 5.1 | Summary of research questions addressed and techniques applied to investigate the effects of heating on mineral magnetic properties of soils from the Lake Burragorang catchment. | 151 |
| 5.2 | Vegetation at long unburnt foot-slope site near Sheehys Creek. | 153 |
| 5.3 | The Bartington MS2B dual-frequency susceptibility sensor and Bartington MS2 magnetic susceptibility meter. | 157 |
| 5.4 | The demagnetiser and ARM attachment. | 160 |
| 5.5 | Nature of applied magnetic field using the Molspin a.f. Demagnetiser and ARM equipment during induction of χ_{ARM} into a sample. | 160 |
| 5.6 | (a) Thermocouple inserted in glass vessel with sample; (b) Sample (in glass vessel) inserted in rotary arm. | 162 |
| 5.7 | Maximum sample temperature during furnace heating, accounting for thermal lag caused by heating the silica trays. | 164 |
| 5.8 | The influence of furnace heating on: (a) χ_{if} ; (b) χ_{fd} ; and (c) χ_{ARM} . (Values displayed are normalised to the measurements made at 22 °C). | 167 |
| 5.9 | The influence of furnace heating on: (a) $\text{soft}_{IRM}\%$; and (b) $\chi_{fd}\%$. (Values displayed are normalised to the measurements made at 22 °C). | 169 |
| 5.10 | The influence of furnace heating on: (a) χ_{ARM} / SIRM ; and (b) χ_{fd} / χ_{ARM} . (Values displayed are normalised to the measurements made at 22 °C). | 170 |
| 5.11 | The influence of furnace heating on SIRM. | 171 |
| 5.12 | Bivariate plot of: (a) χ_{ARM} / SIRM ; (b) $\text{IRM}_{300} / \text{SIRM} / \text{IRM}_{20} / \text{SIRM}$. | 174 |
| 5.13 | Bivariate plot of: (a) $\chi_{fd} / \chi_{ARM} / \text{SIRM}$; (b) $\chi_{if} / \text{IRM}_{100}$. | 175 |
| 5.14 | Bivariate plot of $\chi_{ARM} / \chi_{if} / \chi_{ARM} / \chi_{fd}$. | 176 |
| 5.15 | X changes while heating and cooling of a foot-slope sample to: (a) 100 °C; (b) 200 °C; (c) 300 °C; and (d) 400 °C; (e) 500 °C; (f) 600 °C; and (g) 700 °C; (h) final enhancement of χ following heating and cooling. | 180 |
| 5.16 | X changes to the long unburnt mid-slope sample while heating and cooling to: (a) 100 °C; (b) 200 °C; (c) 300 °C; (d) 400 °C; (e) 500 °C; (f) 600 °C; and (g) 700 °C; and (h) final enhancement of χ following heating and cooling. | 184 |
| 5.17 | X changes to the long unburnt ridge top sample while heating and cooling to: (a) 100 °C; (b) 200 °C; (c) 300 °C; (d) 400 °C; (e) 500 °C; (f) 600 °C; and (g) 700 °C; and (h) final enhancement of χ following heating and cooling. (Note different scales for graphs (e) and (g)). | 186 |

6 EFFECTS OF HEATING ON THERMAL ACTIVATION CHARACTERISTICS (TAC) OF QUARTZ GRAINS IN SOIL AND SEDIMENT

| | | |
|------|---|-----|
| 6.1 | Summary of research questions addressed and techniques applied to investigate the effects of heating on TAC of a long unburnt foot-slope soil sample (Stage 3) and a sample of unexposed unheated bedrock (Stage 4) from the Lake Burragorang catchment. | 198 |
| 6.2 | Previously unexposed bedrock (BR) sample of Hawkesbury Sandstone – the white unweathered section was used for this investigation owing to concerns about uranium gathering in the iron-stained sandstone. | 200 |
| 6.3 | TAC showing: (a) late activation; and (b) early activation. | 202 |
| 6.4 | TAC for the long unburnt foot-slope soil furnace heated to temperatures between 50-800 °C (Horizontal axis shows the temperature reached by the sample prior to TAC measurement; vertical axis shows normalized TL χ). | 205 |
| 6.5 | TAC following application of a 10 Gy β dose to simulate heating occurring <i>ca.</i> 10,000 years ago for the long unburnt foot-slope soil furnace heated to temperatures between 50-800 °C. (Horizontal axis shows the temperature reached by the sample prior to TAC measurement; vertical axis shows normalized TL χ). | 206 |
| 6.6 | Single grains: (a) 1-20; (b) 21-40; and (c) 41-60 from the sample heated to 50 °C, used as a proxy for an unheated sample. | 208 |
| 6.7 | Histogram of the temperatures allocated to the 60 single grains from the ‘unheated sample’ that were suggested by comparison with the TAC plots produced for the various furnace heat treatments in Figure 6.6 and 6.7. | 211 |
| 6.8 | Effect of furnace heating the unexposed bedrock sample on the 110 °C TL χ peak. (Values are normalized to the 1 st measurement of each sample. | 213 |
| 6.9 | TAC for the unexposed bedrock sample furnace heated to temperatures of 50-800 °C. Horizontal axis shows the temperature reached by the sample prior to TAC measurement; vertical axis shows normalized TL χ . Grey dotted lines mark features of the TAC used for analysis in Table 6.2. | 215 |
| 6.10 | TAC following application of a 10 Gy β dose to simulate heating occurring <i>ca.</i> 10,000 years ago for the unexposed bedrock sample, furnace heated to temperatures between 50-800 °C. Horizontal axis shows the temperature reached by the sample prior to TAC measurement; vertical axis shows normalized TL χ . | 216 |
| 6.11 | Single grains: (a) 1-20; (b) 21-40; and (c) 41-60 from the unexposed unheated bedrock sample. | 219 |
| 6.12 | TAC for 20 single grains from the bedrock sample furnace-heated to 600 °C Horizontal axis shows the temperature reached prior to TL χ measurement; Vertical axis shows the normalized TL χ . | 223 |
| 6.13 | Features of the TAC including: (a) χ_0 ; (b) χ_{2N} ; (c) χ_{3N} ; and (d) χ_{FN} produced for the bedrock samples furnace heated to temperatures of 0-800 °C. | 226 |
| 6.14 | Bivariate plots TAC features: (a) χ_{2N}/χ_0 ; (b) χ_{FN}/χ_{3N} ; and (c) χ_{3N}/χ_{2N} (Dotted lines represent a suggestion of the development of hysteretic behaviour. | 227 |

7 EVIDENCE FOR WILDFIRE TIMING AND POST-FIRE EROSION: SEDIMENT CORES FROM LAKE BURRAGORANG

| | | |
|-----|--|-----|
| 7.1 | Summary of research questions addressed and techniques applied to investigate fire history within the 7 closely spaced sediment cores obtained from two locations in the Nattai arm of Lake Burragorang reservoir. | 238 |
| 7.2 | Depth transects of the Nattai channel showing targeted coring locations for core 4, 5, 6 and 7. | 241 |

| | | |
|----------|--|-----|
| 7.3 | The coring device. | 242 |
| 7.4 | Location map of the Nattai cores. Inset: (a) spatial relationship between cores 1 to 3; and inset: (b) spatial relationship between cores 4 to 7. | 243 |
| 7.5 | Radioactive decay series of ^{238}U leading to the formation of ^{210}Pb (Appleby 2001). | 245 |
| 7.6 | Comparison of the visual description of Cores 4-7. | 249 |
| 7.7 | Profiles of Core 6 showing: (a) a schematic representation of lithostratigraphical units; (b) photo of core 6 prior to dissection; (c) a schematic representation of fire horizons; (d) TOC; (e) particle size composition; (f) $^{210}\text{Pb} / ^{137}\text{Cs}$; and (g) bulk density and porosity. | 253 |
| 7.8 | Calibration of the ^{14}C values obtained for samples from Core 6 from depths of 8.5, 19.5 and 29 cm. | 254 |
| 7.9 | ^{14}C date obtained from the charcoal sample from a depth of 43.8 cm in Core 6. | 256 |
| 7.10 | Mineral magnetic properties for Core 6. | 261 |
| 7.11 | TAC for multi-grain samples from Core 6 to elucidate previous heating history. | 263 |
| 7.12 | Temperatures experienced by samples taken from core 6 at depths of 0-5, 19-29, 35-57 and 43-45 cm (a) χ_{3N} (b) χ_{FN} (c) χ_{FN}/χ_{3N} . | 264 |
| 7.13 | 20 TAC for single grains from the core sampled between (a) 0-5 cm (b) 19-29 and (c) 43-45 cm. | 267 |
| 7.14 | Histograms of the temperatures allocated to the 20 single grains from the core samples at: (a) 0-5 cm; (b) 19-29; and (c) 43-45 cm that were suggested by comparison with the TAC produced for the various furnace heat treatments in Figures 6.11 and 6.12. | 270 |
| 7.15 | Profiles of Core 5 showing: (a) a schematic representation of lithostratigraphical units; (b) photo of core 5 prior to dissection; (c) a schematic representation of fire horizons; (d) TOC; and (e) particle size composition. | 272 |
| 7.16 | Profiles of Core 4 showing: (a) a schematic representation of lithostratigraphical units; (b) photo of core 4 prior to dissection; (c) a schematic representation of fire horizons; (d) TOC; (e) particle size composition; (f) $^{210}\text{Pb} / ^{137}\text{Cs}$; and (g) bulk density and porosity. | 273 |
| 7.17 | Profiles of Core 7 showing: (a) a schematic representation of lithostratigraphical units; (b) photo of core 7 prior to dissection; (c) a schematic representation of fire horizons; (d) TOC; (e) particle size composition; (f) $^{210}\text{Pb} / ^{137}\text{Cs}$; and (g) bulk density and porosity. | 274 |
| 7.18 | Mineral magnetic properties for Core 5. | 275 |
| 7.19 | Mineral magnetic properties for Core 4. | 276 |
| 7.20 | Mineral magnetic properties for Core 7. | 277 |
| 8 | SYNTHESIS AND CONCLUSIONS | |
| 8.1 | Schematic diagram summarising the findings for each research aim identified in Chapter 4 and the overall implications. | 290 |

LIST OF TABLES

2 LITERATURE REVIEW

| | | |
|-----|---|----|
| 2.1 | Fire severity and intensity rating for eucalypt-dominated sclerophyll vegetation communities in southeastern Australia. | 10 |
| 2.2 | Classification of fire severity in relation to fire frequency. | 12 |

| | | |
|----------|---|-----|
| 2.3 | Thermochemical reactions involving magnetic minerals. | 13 |
| 2.4 | Effect of fire on soil chemical properties | 29 |
| 2.5 | Effect of temperature on the enhancement of water repellent properties | 43 |
| 2.6 | Responses to post-fire environments | 45 |
| 3 | THE STUDY AREA | |
| 3.1 | Selected data about the catchment of Lake Burragorang. | 89 |
| 3.2 | Average concentrations of total free iron that is citrate-dithionite extractable; mobile / amorphous iron as oxalate extractable iron in soils of different depths, situated on Hawkesbury sandstone within the Avon Catchment. | 97 |
| 3.3 | Dominant vegetation in the Blue Gum Creek catchment and its respective position in the landscape. | 99 |
| 3.4 | Percentage distribution of land use in Lake Burragorang catchment in 1992. | 101 |
| 3.5 | High magnitude (normal font) and catastrophic (bold font) flood events in the Nattai Reservoir and reservoir water level (adapted from (Tomkins et al. in press)). | 125 |
| 3.6 | Summary of post-fire sediment redistribution in Blue Gum Creek catchment. | 135 |
| 3.7 | Mean loss/gain and absolute change results for erosion bridge sites: A) on Blue Gum Creek slopes, May 2002-February 2004; and B) on newly burnt terrain in Cataract River basin, January 2003-February 2004. | 138 |
| 3.8 | Summary of quantities and rates of different forms of bioturbation for different slope positions in sub-catchments H and L. | 139 |
| 3.9 | Summary of investigations on sedimentation in Lake Burragorang. | 142 |
| 4 | RESEARCH DESIGN AND RATIONALE | |
| 5 | EFFECTS OF HEATING ON SOIL MINERAL MAGNETIC PROPERTIES | |
| 5.1 | Details of soil samples used for measuring χ_{if} changes during progressive heating and cooling. | 154 |
| 5.3 | Peak enhancement and associated temperatures for χ_{if} for heating durations of 5, 10, 20 and 40 minutes. | 167 |
| 5.4 | Peak enhancement and associated temperatures for χ_{fd} for heating durations of 5, 10, 20 and 40 minutes. | 167 |
| 5.5 | Peak enhancement and associated temperatures for χ_{ARM} for heating durations of 5, 10, 20 and 40 minutes. | 167 |
| 5.6 | Enhancement and associated temperatures for χ_{ARM} / SIRM for heating durations of 5, 10, 20 and 40 minutes. | 170 |
| 5.7 | Enhancement and associated temperatures for χ_{fd} / χ_{ARM} for heating durations of 5, 10, 20 and 40 minutes. | 170 |
| 5.8 | Temperature thresholds of various magnetic parameters investigated for furnace heating of the long unburnt FS sample. | 194 |
| 6 | EFFECTS OF HEATING THERMAL ACTIVATION CHARACTERISTICS (TAC) OF QUATZ GRAINS WITHIN SOIL | |
| 6.1 | Sample details and codes used for investigating the response of TAC to different furnace heat treatments for a: (i) long-unburnt foot-slope soil sample; and (ii) an unexposed, previously unheated (since deposition) sample of bedrock. | 199 |
| 6.2 | Features identified by the TAC of the furnace heated bedrock sample. | 224 |
| 6.3 | Summary of the successful use of the glow curves to detect previous heat treatments. | 229 |

7 EVIDENCE FOR WILDFIRE TIMING AND POST-FIRE EROSION: SEDIMENT CORES FROM LAKE BURRAGORANG

| | | |
|-----|---|-----|
| 7.1 | Explanation of labels used for units in Core 6. | 250 |
| 7.2 | ^{14}C dates obtained for 4 samples from Core 6. | 255 |
| 7.3 | Plutonium measurements for Core 6. | 258 |

1 INTRODUCTION

Wildfires often cause accelerated soil erosion on hillslopes and widespread transfer of eroded sediment to the fluvial system. Where there is a reservoir downstream, this enhanced geomorphic activity may be recorded in the form of enhanced sediment accumulation on its floor (e.g. Rummary 1983; Clark 1986; Gedye *et al.* 2000; Blake *et al.* 2006b). The amount of downstream deposition is dependent on a number of factors including fire severity, catchment topography, the location and extent of the fire in the catchment and critically, the occurrence of post-fire rainfall sufficient to cause overland flow and runoff capable of removing material from hillslopes and transporting it through the catchment (Tomkins *et al.* in press). Immediate post-fire investigations aside, few techniques are available for detecting and reconstructing the timing and severity of past fire events from soils and eroded sediment, which provide a potential record of these events. As a result, it is often unclear as to the role wildfire has played in erosion and sediment deposition events in many fire-prone catchments.

The work for this thesis has been carried out as part of a larger collaborative research group which investigated soil erosion, water repellency, sediment movement and deposition following extensive naturally sparked fires in 2001/2002 in the eucalypt forests of the water supply catchment of Lake Burragorang in the Sydney Basin, Australia (Shakesby *et al.* 1993; Shakesby *et al.* 2003; Blake *et al.* 2004; Doerr *et al.* 2004; Shakesby *et al.* 2004; Tomkins *et al.* 2004; Blake *et al.* 2005; English *et al.* 2005; Blake *et al.* 2006a; Blake *et al.* 2006b; Blake *et al.* 2006c; Shakesby *et al.* 2006; Tomkins *et al.* In preparation; Tomkins *et al.* in press). Details of this work can be found in Section 3.10. This thesis investigates the usefulness of two relatively recently developed techniques concerning the mineral magnetic properties and Thermal Activation Characteristics (TAC) of soils and eroded sediment for: (i) detecting the passage of wildfire; (ii) determining the ground temperatures reached during the passage of fire; and (iii) reconstructing wildfire history. The eucalypt forests in this sandstone terrain have been subjected to wildfire over large areas on a number of well-documented occasions in the last few decades. Mineral magnetic measurements have been applied widely in Europe (Oldfield and Clark 1990; Dearing 1992; Dearing 2005), and developed particularly in

archaeological applications to detect the presence of campfire and kiln sites and to suggest the temperatures experienced (Linford and Canti 2001; Weston 2002). The application of mineral magnetic measurements in geomorphic studies in Australia has been demonstrated by Caitcheon (1993) and Blake *et al.* (2006a). As regards TAC, this soil property is obtained by measuring thermoluminescence sensitivity (TL χ) changes following heating to progressively higher temperatures. TAC have previously been used to ascertain thermal heat-treatments applied to archaeological artefacts (Godfrey-Smith *et al.* 2005; Lahaye *et al.* in press). In the present study, the application of this approach to detecting the temperatures and timing of heating in soils is explored for the first time.

Specifically, the thesis seeks to investigate the: (1) temperature thresholds apparent for thermally-enhanced soil parameters; (2) thermal memory of soil and sediment samples; (3) influence of catchment location and fire history in producing distinctive magnetic signatures; (4) applicability of mineral magnetic analysis and TAC in identifying burnt material within sediment cores; and (5) reliability of sediment cores obtained from dynamic reservoir environments as indicators of previous catchment fire events.

The thesis is divided into eight chapters. Following this introduction, Chapter 2 reviews previous work relating to the impact of fire frequency and behaviour on vegetation, soils, hydrology, soil erosion and sedimentation. Chapter 3 describes the location and environmental characteristics of the Lake Burragorang study region that are of particular relevance to fire history, soil erosion and sedimentation studies. It also summarises previous work on soil erosion and mineral magnetic investigations carried out in the study area. Chapter 4 details the research design used in this study. Chapters 5, 6, and 7 present the main results of this thesis. Chapter 5 investigates the temperature thresholds required to produce enhancement of the mineral magnetic parameters of three long-unburnt samples from a foot-slope, mid-slope and ridge-top location and assesses the effect of fire history retained by these samples. Chapter 6 investigates the temperature thresholds required to modify TAC of the long-unburnt foot-slope sample and a bedrock sample previously unexposed to heating. Chapter 7 investigates the potential application of mineral magnetism and TAC of sediment cores to distinguish between unburnt and burnt material as well as sediments subject

to different fire severities. Chapter 8 synthesises the main findings of this thesis, discusses their implications for detecting burnt material, and for reconstructing fire events and their severities, and suggests directions for future research.

2 LITERATURE REVIEW

2.1 INTRODUCTION

Forest fires occur on a global scale and can produce significant anthropogenic disturbance where they extend into residential areas (e.g. fires in Canberra in 2003; Portugal in 2006; and Los Angeles in 2007). Fire is important as it is complexly interlinked with climate and vegetation. Burning releases aerosols and greenhouse gases which impact upon the regional and global atmosphere (Görger *et al.* 2005). The climate influences the frequency of fire events by producing fuel and dry conditions to easily ignite vegetation. Fire affects the function, composition and structure of ecosystems by causing mortality or a change in ecosystem dynamics and biodiversity (Thonicke *et al.* 2001). The changes in vegetation cover that result from fire modify surface energy budgets through reduced surface albedo, available energy for partitioning into convective currents, increased substrate heat flux into the soil and modification to hydrological processes (Beringer *et al.* 2005).

The complex set of parameters that influence fire behaviour include ignition patterns, fuels, weather and topography (Figure 2.4) (Perry 1998). These make it difficult to create global generalisations regarding the behaviour and impact of fire, therefore, this literature review predominantly uses examples from South East Australia. It begins with the consideration of forest fire in terms of ignition, severity, movement and behaviour. The way that these factors are influenced by localised conditions such as weather, topography and fuel loading are then investigated. Forest fire impacts on hydrogeomorphological aspects of the environment are considered at length. These aspects include post-fire modifications to vegetation, soils and litter, and the consequences for hydrology and soil erosion. The focus then turns to the movement of sediment through river and reservoir environments. The literature that addresses the effect that fire has on erosion cycles and the influence of different temporal patterns of fire regimes is then discussed. There is also recognition of problems encountered when comparing material movement at hillslope and catchment spatial scales, before finally identifying the research gaps.

2.2 FOREST FIRES

This section firstly introduces the causes of forest fires. Section 2.2.1 reviews mitigation methods that are adopted to reduce the severity of fire events. Section 2.2.2 presents methods for evaluating fire intensity, severity and frequency. Section 2.2.3 identifies factors that influence fire movement and behaviour including the effects of weather, topography and fuel load, before an overview of components that are incorporated into fire models is given.

Wildfires may be initiated naturally by lightning striking trees or other vegetation during relatively dry or drought periods when the susceptibility of the vegetation to burning is high due to low moisture content. The risk is especially great at the end of a dry season, following a long period with little rain combined with an increased frequency of electrical storms as a result of the atmospheric transition to the wet season (Bowman 1988; Bowman and Wilson 1988; Gill *et al.* 1996). Regions where distinct dry seasons often lead to fire include the USA (Scott and Burgy 1956), Australia (Gould *et al.* 1997; Ward *et al.* 2001), the Mediterranean (Goldammer and Jenkins 1990; Shakesby *et al.* 1993), and South Africa (O' Hanlon 1995).

There is evidence from deep sea sediments to suggest that fire has occurred naturally since the Late Pleistocene (Verardo and Ruddiman 1996). Cave paintings have also documented the occurrence of natural forest fires over at least the last 100,000 years (Brian and Sillen 1988). Australia has a long and complex fire history which makes it difficult to decipher the impact of humans on fire regimes owing to the shifting settlement patterns of Aboriginies in the Late Quaternary period and disputed time frames for European colonization (Bowman 1998). There are contrasting theories regarding Aboriginal use of fire: either they used fire to manipulate the environment to suit their needs 'fire-stick farming' (Jones 1969) or that they did not appreciate the consequences of prescribed burning and had to adapt to the changes that they had induced (Flannery 1990; Bowman 1998). It is commonly assumed however that Aboriginies consistently used fire (Head 1989).

The impact of burning has modified the biodiversity of Australian ecosystems. Vegetation that is able to withstand frequent fire events has thrived. This explains the prominence of 'pyrogneic vegetation' that is dependent on fire to regenerate

(Gill and Bradstock 1995). This change in vegetation was demonstrated in a sediment core obtained from Lynch's Crater in Queensland, where a marked increase in burning was accompanied by a replacement of rainforest vegetation with fire-dependent sclerophyll vegetation (Turney *et al.* 2001). In this case the modification was attributed to human occupation. Conversely, a study in the Greater Blue Mountains by Black and Mooney (2006) found climate and human activity both affected fire regimes, however climate had the dominant control on fire activity. This suggests a potential increase in fire activity with projected rapid anthropogenic global climate change (Black and Mooney 2006) where a hotter, drier climate with an increased occurrence of low-pressure systems and associated stronger winds has been predicted in certain areas of the world, including Australia (Torn and Fried 1992). This is likely to create conditions similar to those experienced during El Niño episodes that increase vulnerability of forests to burning, as recognised in the correlation between El Niño events and major fire seasons in South Eastern Australia between 1940 and 1992 (Figure 2.1). This will require greater fire risk management in populated areas in the future (Section 2.2.1).

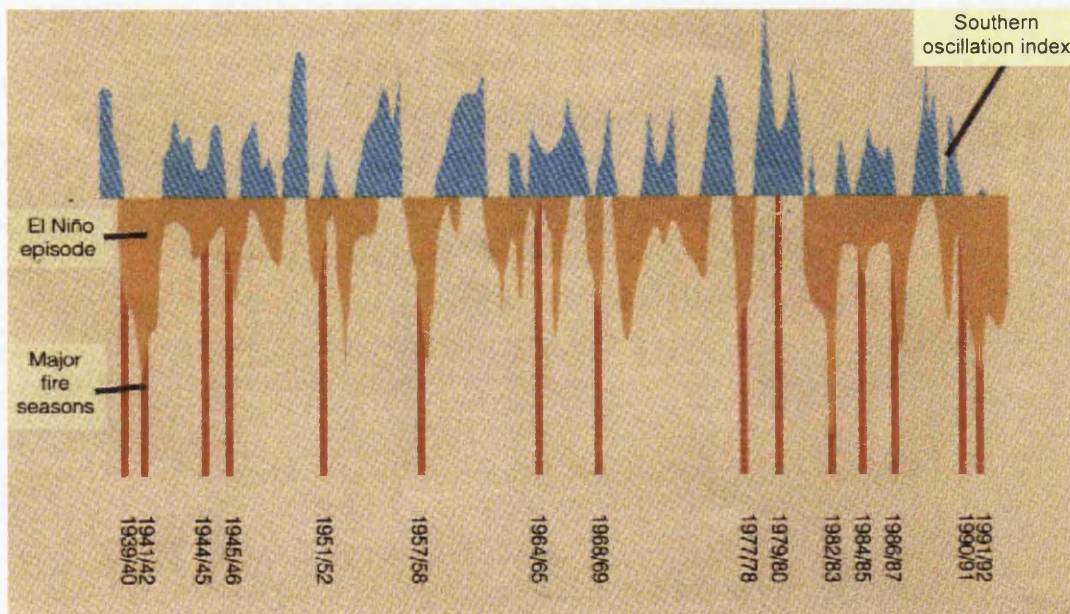


Figure 2.1: Coincidence of fires seasons and major El Niño episodes in South Eastern Australia between 1940-1992 (Source unknown)

2.2.1 FIRE RISK MANAGEMENT

Risk awareness of forest fires has led to the development of a number of mitigation measures (Wade, 1993). The most common precautionary method for managing and reducing the risk of fire hazards in forested areas is prescribed burning outside of the main 'fire season' period (Bradstock *et al.* 1998; Baeza *et al.* 2002). Alternative methods such as herbicide application and manual thinning of the vegetation reduce the height of vegetation, its cover and fuel loading. Herbicide application can be expensive and has other associated negative impacts on the environment such as contamination of water bodies. The treatment also takes a year to become effective as the shrubs die but remain standing, so in fact the fire risk increases for the first year after treatment due to the low moisture content of the dead material (Brose and Wade 2002).

Thinning is effective as it immediately reduces the fire risk by removing some of the vegetation from the site. However, this technique is labour intensive and the remaining vegetation provides seeds that regenerate within a short period after the land has been cleared. Consequently, the fuel reduction is short-lived. The most effective solution for reducing fire risk requires the relatively frequent application of controlled low intensity fires, which destroy some of the fuel load of vegetation and litter build-up, thus reducing the risk of high intensity fires. It is a successful and popular method because it is relatively inexpensive and non-labour intensive; however, concerns do exist about smoke management (Wade 1993) and the effects on the local ecology. Australian pyrogenic vegetation is dependent on fire to initiate regeneration, however low intensity fires associated with prescribed burn events do not provide enough heat to trigger the seed dispersal mechanisms which can reduce biodiversity (Section 2.3.1.2) (Whelan and York 1998; Ward *et al.* 2001). An extreme option to reduce the risk of fire is to isolate areas of woodland from the public during periods that are highly susceptible to burning. This minimises the chance of fires being initiated by accident, but can be unpopular with the public. However, it does not alleviate natural causes of fire as the Earth receives >60,000 lightning strikes per day (Watson and Holle 1996).

2.2.2 FIRE INTENSITY, SEVERITY AND FREQUENCY

Fire intensity, can be used to suggest the maximum temperature reached during a fire and may be assessed using the calculation of fire intensity (*I*). Fire intensity is a quantitative assessment of the temperature reached during a burn event and is often calculated using Bryam's (1959) fireline intensity formula (equation 2.1):

$$I = 0.0007 HWR$$

(equation 2.1)

Where **I** is the fire intensity (kw/m), **H** is the heat yield (cal/g), **W** is the fuel-loading (t/ha) and **R** is the rate of spread (m/min).

The values within this equation are influenced by factors such as atmospheric conditions, moisture content, fire frequency, topography and vegetation type, which are discussed later in this section. Bryam's equation is used widely for fire management purposes to predict the pattern of spread, because the flame length is proportional to the fire intensity (Luke and McArthur 1978). However, it has disadvantages: firstly, the value of fire intensity cannot be used to compare sites with dissimilar fuel types due to differences in structural composition (Cheney 1990); secondly, there are risks involved in collecting the data for this equation due to the requirement for working in close proximity to the fire edge.

There are more direct methods of assessing fire intensity. For example, Beaufait (1966) assessed fire intensity by measuring the amount of evaporation from buried water-filled drums to calculate the heat flux. The problems associated with this technique are likely to be related to the different conductive properties of the water in comparison to the soil. Other methods for identifying fire temperatures include the assessment of damage to heat-sensitive materials (that melt at known temperatures) inserted into the ground before the fire or by the use of thermocouples or thermistors (Cromer and Vines 1966) which could also be used to assess the depth of fire damage to soil. The above methods require preparation of the site before the burn event, which can be challenging to organise and set up in the event of a natural fire.

Temperatures reached in soil during bushfires have been recognised as being spatially variable (Raison *et al.* 1986; Bradstock and Auld 1995; Chafer *et al.* 2004) this is caused by a variety of factors (Section 2.2), including the duration of burn, which is influenced by fuel load, topography and weather (Luke and McArthur 1978; Pook and Gill 1993; Bradstock *et al.* 1998). The intensity reached during burning influences the extent of modifications to the soil's magnetic minerals. Various experiments have studied the effect of increasing temperature on magnetic properties, however few have looked at the changes to a full range of magnetic characteristics and none have studied the effects of heating above 60 °C on Australian soils. Despite the lack of information about the temperatures at which modification to soil properties occurs, burning of soil is commonly linked to the enhancement of magnetic minerals (Le Borgne 1955, 1960; Maher 1986). These changes have been used as a tool to identify burnt material within sediment cores e.g. (Rummery 1983; Gedye *et al.* 2000; Blake *et al.* in press). However, the level and duration of heating have not previously been studied. This work aims to ascertain the temperatures at which magnetic modifications occur to Australian soils through investigation of a range of parameters in order to confirm the use of this technique in hydrogeomorphological studies.

The temperatures reached within the soil during burning determine the extent of modification to soil properties at both the surface and within the soil profile. The level of heat created by fire is dependent on a number of variables (Section 2.2) (Luke and McArthur 1978; Pook and Gill 1993; Bradstock *et al.* 1998). These factors in turn control fire characteristics which influence the intensity of the fire, the rate of heating and the duration of the enhanced temperatures experienced by the soil at various depths. The high variability of soil temperatures induced by the above mentioned factors are indicated through the broad range of fire enhanced soil temperatures recognised within the literature (Table 2.1). These extend between 50-1000 °C at the surface, while the depths at which no enhanced temperature is detected has been identified below 22 cm. Figure 2.2 shows temperatures identified within the soil profile from different surface temperatures as found by Chandler *et al.* (1983).

Table 2.1: Soil temperatures reached in studies

| Fuel type | Temp (°C) | Depth | Av. /Max | Soil Type | Soil Location | Duration @ temperature | Reference | | |
|--------------------------------|-----------|-----------|----------|--|--|------------------------------------|--------------------------|--|------------------------------|
| Eucalyptus litter | 140 | 2 cm | Av | Dunes: Red siliceous sands Swales: heavier calcareous red earth | Low east-west oriented dunes, Mallee shrublands, central NSW | 50 mins @ 60–120°C | (Bradstock et al. 1992) | | |
| | 70 | 3.5 cm | | | | 30 mins @ >120°C (upper 2 cm only) | | | |
| | 50 | 5 cm | | | | | | | |
| | 40 | 7 cm | | | | | | | |
| | 35 | 9 cm | | | | | | | |
| Wood fuel mix | 456 | 1 cm | Max | Sandy Loam | Yarton, Oxfordshire, UK. | | (Canti and Linford 2000) | | |
| | 443 | | | | | | | | |
| | 433 | | | | | | | | |
| | 436 | | | | | | | | |
| | 570 | | | | | | | | |
| | 232 | 4 cm | | | | | | | |
| | 119 | | | | | | | | |
| | 276 | | | | | | | | |
| | 289 | | | | | | | | |
| | 318 | | | | | | | | |
| Light fire | 180 | Surface | Max | | | 7 minutes @ 100 °C | (Giovannini 1994) | | |
| | 50 | 2.5 cm | | | | | | | |
| | None | 5 cm | | | | | | | |
| Severe fire | 475 | Surface | Max | | | | | | > 60 minutes @ 100 °C |
| | 90 | 2.5 cm | | | | | | | |
| | 40 | 5 cm | | | | | | | |
| Slash burns | 900 – 320 | Surface | Max | Immature podzolic sandy loam & clay loam | NSW tablelands and coast | | | | (Humphreys and Lambert 1965) |
| | None | 2.5 cm | | | | | | | |
| | 400 | 20 cm | | | | | | | |
| | | Thick ash | | | | | | | |
| Mixed wood fuel | 433 | 1 cm | Max | Bare Gravel | Yarton, Oxfordshire, UK. | 1 day fire | (Linford and Canti 2001) | | |
| | 276 | 4 cm | | | | 4 day fire | | | |
| | 436 | 1 cm | | | | | | | |
| | 289 | 4 cm | | | | | | | |
| Eucalyptus logs | 666 | surface | Max | Sandy loam – ploughed 6 months prior to experiment | NSW tablelands and coast | 21 hours @ >100 °C @ 10 cm | (Roberts 1965) | | |
| | 112 | 22 cm | | | | | | | |
| Jarrah (eucalyptus Marginata) | 300 | Surface | Max | Pisolithic or massive laterite over a layer of Kaolinitic clay | Bauxite | 30 mins | (Smith et al. 2004) | | |
| | >100 | | Max | | | 3 hours | | | |
| | | | | | | | | | |
| | >100 | 1 cm | Max | | Ridge tops | 6 minutes | | | |
| | 49.9 | 2.5 cm | Max | | Ridge tops | | | | |
| | 80.4 | 1 cm | Max | | Furrows | 22 mins | | | |
| | 57.4 | 2.5 cm | Max | | Furrows | 24 mins @ > | | | |
| | <60 | >2.5cm | | | | | | | |
| Cedar (Juniperous virgin-iana) | 506.0 | 5 cm | Max | Clay | Stone hearths – Central Tennessee | | (Bennett 1999) | | |
| | 201 | 15 cm | Max | Clay | | | | | |
| | 72.1 | 25 cm | Max | Clay | | | | | |
| | 408 | 5 cm | Max | Sand | | | | | |
| | 244 | 15 cm | Max | Sand | | | | | |
| | 73.9 | 25 cm | Max | Sand | | | | | |

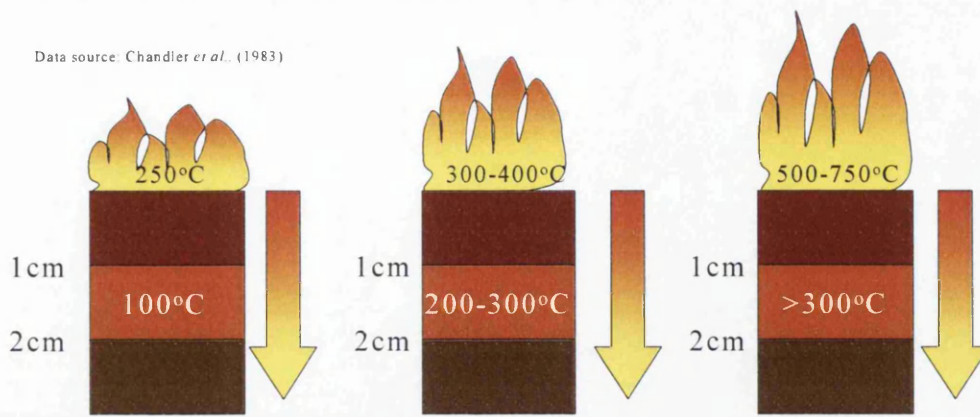


Figure 2.2: Depths at which increased soil temperatures are experienced within the soil profile adapted from data by Chandler *et al* (1983).

The large variation in soil temperatures identified in the literature (Table 2.1) can be attributed to a number of factors including different measuring techniques, microclimate and topographical variations, heating duration, fuel load and type and differences in soil texture and moisture content. The conductive properties of the soil determine the efficiency at which the heat is transferred. This is controlled by the bulk density, temperature and water content of the soil (Campbell *et al.* 1995). Temperatures of damp soil will not exceed 100°C until the majority of the moisture has been removed by evaporation (Doerr *et al.* 2004).

Different fire characteristics affect temperatures experienced within the soil. Low soil temperatures are associated with either prescribed fires, high moisture conditions or where fires burn within the canopy. This explains the poor link between NVDI generated fire severity ratings and soil temperature (Shakesby *et al.* 2003). High soil temperatures are more likely to be caused during ground-based fires that have dense vegetation providing a large amount of fuel load. Extreme soil temperatures occur under fallen logs due to the long slow burn enabling heat energy at the surface to penetrate to lower layers within the soil profile through conduction. The exception to this case is where a thick ash layer has developed, which has an insulating effect because of its poor conductive nature, thus reducing heat transferred to the soil.

Acknowledgement of temperatures experienced within the soil and the depth to which the heat penetrates is important for a number of reasons as it influences the level of modification to soil properties and the rate of post-fire recovery. Post fire

soil environments have been observed to have a reduced water content, increased compaction of the soil, reduced organic matter content and extractable Phosphorous (Snyman 2003) and increased daily temperatures experienced in the top 10 cm of the soil (O'Lear *et al.* 1996; Snyman 2003).

An alternative system for gauging the temperature reached during a burn event is to assess qualitative damage in a post-fire environment by using a number of established indicators in order to group fires into different severity categories of low, medium and high burns (Wells *et al.* 1979; USDA and NRCS August 2000). Table 2.2 shows an example of such a classification for a eucalypt-dominated forest in southeastern Australia as used by Cheney (1981) Jasper (1999), and Shakesby *et al.* (2003). In this classification, the description of the site recognises the damage to the ground and vegetation, identifying features that will be consumed at different fire severities. The maximum flame height relates to the visible amount of charring evident on the tree. However, this can easily be distorted if strong winds occur causing a decrease in flame angle. These visible characteristics are then incorporated into the appropriate severity rating classification group, which can be related to the likely energy of the fire. This technique is a very popular method due to its easy application and comparable results. However, a disadvantage of using such a methodology is that the specifications used will vary according to local site conditions and it is therefore not possible to devise a universal classification.

Table 2.2: Fire severity and intensity for eucalypt-dominated sclerophyll vegetation communities in southeastern Australia (modified from Cheney (1981) Jasper (1999), and Shakesby *et al.* (2003)).

| Severity and intensity rating | Fire intensity (kWm^{-1}) | Max. flame height (m) | Severity characteristics |
|-------------------------------|--------------------------------------|-----------------------|--|
| Low | <500 | 1.5 | Only ground fuel and shrubs <2m burnt |
| Moderate | 501-3000 | 5 | All ground fuel and shrub vegetation <4m consumed by fire |
| High | 3001-7000 | 10 | All ground and shrub vegetation consumed by fire and lower tree canopy <10m scorched |
| Very High | 7000-70000 | 10-30 | All green vegetation including tree canopy <30m, and woody vegetation <5mm diameter consumed by fire |
| Extreme | 70000+ | 20-40 | All green and woody vegetation <10mm diameter consumed by fire |

As mentioned earlier, the concept of prescribed burning increases the frequency of fires to reduce the severity of the burn. The fire frequency refers to the number of times that a fire event occurs within a given period. Areas with a low fire frequency enable complex ecosystems to develop, allowing mature vegetation to provide

habitats for a diverse range of species (Ward *et al.* 2001). The shelter provided by the canopy cover provides vital protection to the lower layers of vegetation from heat exhaustion, which in turn protects and stabilises the soil, consequently reducing erosion levels. Areas of high fire frequency have a shorter recovery period between fire events. This restricts the amount of vegetation build-up (fuel loading), which in relation to Bryam's fire intensity equation will produce a lower intensity fire, provided the other variables remain the same. Heinselman (1978b) took the concept of fire frequency into consideration when assessing the impact of fire on landscape evolution, and devised a classification of six kinds of fire regimes, recognised by the fire type, intensity, area and frequency (Table 2.3).

Table 2.3 Classification of fire severity in relation to fire frequency (Heinselman 1978b; Thomas 1993).

| Classification rating | Fire description |
|-----------------------|---|
| 0 | None (or very little) natural fire |
| 1 | Infrequent, light surface fires (>25years return period) |
| 2 | Frequent, light surface fires (1 to 25 year return period) |
| 3 | Infrequent, severe, surface fires (>25 years return period) |
| 4 | Short return interval, crown fires (25 to 100 year return period) |
| 5 | Long return interval, crown fires (100 to 300 year return period) |
| 6 | Very long return interval, crown fires (>300 year return period) |

For the assessment of longer-term fire occurrence there are several methods available, including: (i) burnt material and charcoal in lacustrine and marine sediments (Verardo and Ruddiman 1996; Gedye *et al.* 2000); (ii) charcoal deposits within land-based sediment stores (Tomkins *et al.* In preparation); and (iii) the position of fire scars in annual growth rings (Ward *et al.* 2001; Gavin *et al.* 2003). Fire-scarred tree rings are only reliable in climates where distinct seasonal variations occur, because in areas where continuous growing seasons are apparent, more than one growth ring may be produced per year and subsequently the record of the fire may not be maintained. It is not possible to use this indicator for the majority of trees from the Australian environment, with the exception of certain species such as grasstrees (Xanthorrhoeaceae, Liliales), which are distributed widely throughout south, southeast and eastern Australia. Ward *et al.* (2001) demonstrated that the burn history of a site could be evaluated by the analysis of leaf bases of this species as

during a fire, the grassy leaves of the trees are burnt back to their roots at the base (or the trunk), which is durable enough to survive the fire. The charred roots then form a new part of the base, while regrowth of the grassy leaves occurs from the top of the base very soon after the burn. By removing a vertical cross-section from the base, the fire scars within the tree can provide an indication of fire frequency and the degree of damage can be related to fire severity (Lamont and Downes 1979). Difficulties in observing patterns in fire frequency may occur if too much of the outer layer is removed from the base. Although this method is dependent upon favourable growing conditions, the technique can provide location specific records of fire events, despite the fact that the sampling kills the tree.

2.2.3 FIRE MOVEMENT AND BEHAVIOUR

There have been a number of studies regarding fire movement and behaviour because it is of major concern for lives and property. The information obtained from models developed to predict the spread of a fire can be used to recognise the susceptibility of an area to burning, or to aid fire fighters. Fire progresses through an area by transferring radiative energy from the flame front to the fuel ahead of the fire (Wotton *et al.* 1999). Beer and Enting (1990) suggested that fire spread could have three alternative forms of development: uninhibited spread, no spread and geometrically constrained spread. Uninhibited spread is relatively easy to model as the complexities that are introduced by topographic variations do not exist (Speer *et al.* 2001) and the fire will advance in the form of a uniformly expanding circle, however the occurrence of wind will invalidate this model. A fire will not spread unless combustible material or wind to advance the fire forwards is present, as all the fuel will become consumed. Geometrically constrained spread is prevented on one or more sides by natural or man-made barriers such as lakes or concrete structures and can distort theorised results.

The main controlling influences on fire movement and behaviour are determined by the fuel, weather and topographical characteristics, which are discussed in Sections 2.2.3.1-2.2.3.3. These factors determine the way that fire builds up, the duration of the burn, the rate at which the fire front moves forwards and the amount of fuel consumed. These factors also have additional impacts on local conditions such as airflows and currents. They are all interlinked and a change in one characteristic will

have a multiplier effect on other components within the system. These components are of great significance and are important elements that need to be considered in fire behaviour modelling to enable accurate predictions of the possible development of the fire.

2.2.3.1 *The effect of weather on fire movement and behaviour*

The effect of weather patterns on fire movement and behaviour include variations in temperature, humidity, wind speed and atmospheric structure. Weather systems are important in influencing the moisture content of the fuel load through the input of precipitation and the level of drying out of the vegetation through the input of solar radiation (Gill and Moore 1994). The influence of wind is also recognised and is discussed later in this section.

The moisture content of the fuel load determines whether it acts as a 'heat source', by providing material to feed the fire, or a 'heat sink', which absorbs energy by evaporating moisture before the fire is able to proceed (Burgan 1979). The level of moisture content of the vegetation affects a fuel's susceptibility to burning, with the greatest risk of fire in the afternoon (about 15:00h) (Gill and Moore 1994) as morning dew will have evaporated over the course of the day. This is of great significance in terms of the ignition of the fire. However, once a fire is lit, a sudden increase in moisture content provided by a heavy rainstorm can often provide the most effective means of extinguishing an out-of-control wildfire. Apart from the weather contributing to variations in the moisture content through precipitation, atmospheric pressure also controls the speed at which air moves across the Earth's surface. In low pressure conditions, associated high winds help to accelerate fire progress as the flames are tilted with the effect of the wind and so can reach more material, while sparks may also be transported by the wind, initiating so-called 'spotting', where burning material is blown ahead of the fire front and sets alight the ground that it lands on. In connection with atmospheric pressure, movements within the air are also induced by uneven heating of the Earth's surface and are moved in accordance with the local pressure system. Unstable air conditions during a fire encourage a strong convection column to develop over the fire: this upward movement of air may also carry and redistribute burning material and encourage

spotting, while the fire is fuelled by in-draughts replacing the rising air (Luke and McArthur 1978).

In relation to Bryam's (1959) fire intensity equation (equation 2.1), the effects of the wind mentioned above, determine the rate at which fire is able to spread horizontally and vertically. Localised winds also affect the level of fire risk. For example, in coastal areas in southeast Australia warm air blown off the land is frequently hot and dry, which will exacerbate dry fuel situations, increasing the fire risk, especially during summer drought conditions when the vegetation already has a low moisture content (Pook and Gill 1993; Beaty and Taylor 2001).

Micro-climatic conditions underneath the forest canopy affect the moisture content of the vegetation whilst also causing disturbance and slowing of air movement, which can affect fire behaviour. Eddies may also be initiated in the lee of trees, which in turn will influence the behaviour of the fire. Slower and turbulent airflows have a similar effect on a fire's behaviour in prolonging burning of the fuel before it proceeds. There is also an increased occurrence of 'spotting' caused by turbulence randomly redistributing ignited material (Gould *et al.* 1997).

2.2.3.2 *The effect of topography on fire movement and behaviour*

The topography of an area is influential in determining the localised burning conditions. At ridge top locations in South East Australia, the soil and vegetation is usually thinner, drier and more exposed, which means that fires are more likely to occur successfully at ridge tops due to the lower moisture content and greater exposure to winds and turbulent flows (Byron-Scott 1990; Raupach 1990). This may not always be the case if the vegetation at the bottom of the slope has a low moisture content, for example after a prolonged dry season, as the greater fuel load may cause higher severity fires to occur there.

Franklin (1997) suggests that the effect of slope steepness is more influential in determining fire behaviour than components of the fuel structure and loading. This results from the fact that a fire moving up-slope has its progress enhanced by preheated convection currents ahead of the burning line (Dupuy 1995) and an increasing slope angle enhances the radiative transfer of heat due to the increased

flame angle (Baines 1990). The effect of wind on the flames may also strengthen a fire's progress by taking the leading edge forward in spreading arcs (Anderson 1982; Cheney 1990). The aspect of a slope is also influential, as it will determine the physical properties of the vegetation, its moisture content and strength of prevailing wind conditions. Each of these factors influences the characteristics of fire movement, which in turn influence fire intensity, frequency and behaviour.

Non-combustible natural barriers influence the behaviour of a fire (e.g. rock outcrops, creeks or rivers) (Leitner 1991), which cannot burn due either to the lack of combustible material with low heat yield or the high moisture content. In relation to the moisture component within Byram's (1959) fire intensity equation, these barriers inhibit the fire's rate of spread. These areas may provide a safe haven for plant species that are normally unable to survive burning (Ward *et al.* 2001). If high wind conditions occur, ignited wind-borne material may be transported and surpass these fire-tolerant zones allowing the fire to continue. For example in a 7500 kWm^{-1} fire described by Cheney (1990) in a dry eucalypt forest in Australia, firebrands were strewn up to 1km in front of the flame-front causing a severe occurrence of spotting. The extent of spotting potential can be related to species type. For example, the roughbark species of *Eucalyptus* also known as stringy-barks, such as *Eucalyptus marginata*, and peppermints such as *E. robertsonii*, *E. dives* and *E. radiata* (Luke and McArthur 1978) do not fully shed their dead bark. This material is highly flammable and once set alight it can easily be torn off by strong undercurrents and initiate spotting (Hafey 2003).

2.2.3.3 *The effect of fuel load on fire movement and behaviour*

The quantity of the fuel load is a determinant of the peak temperature and the duration of the fire (Iwanami 1973); hence, localised control is used to reduce the potential risk of severe fires (see Section 2.2.1). The size, structural composition, porosity and moisture content of the fuel are also important factors influencing residence times of the fire, with low lying, dense fuels causing greater damage (Anderson 1990; Molina and Llinares 2001). As the fuel bed is heterogeneous and often discontinuous at all scales (Green and Tridgell 1990) the different structural composition and types of fuel (needles, leaves, twigs, bark) will influence the way in which material burns (Pook and Gill 1993). In particular, fine round twigs prove

most flammable (Burrows 2001) due to the increased surface area exposed to the flame in proportion to the volume and the less compact structure.

Differences in structure and composition between the canopy, understorey (vegetation under the canopy) and surface litter induce different burning characteristics. The majority of the canopy is composed of living cells of high moisture content. The green understorey has high foliar moisture, thereby dampening the effect on surface fire behaviour (Agee *et al.* 2002), whilst the litter generally consists of dry organic matter. The different types of fire in these contrasting locations of the forest are an important consideration in developing models of fire spread. Although moisture content is influenced by meteorological conditions (Section 2.2.3.1), variations also occur according to species age. Young plants have a higher water content when compared to maturing plants with additional denser materials in the branches, which contain less moisture and so are more flammable (Baeza *et al.* 2002).

The effect of fuel loading on fire frequency is, as already mentioned, the main reason for the application of prescribed fire. A series of high frequency fires means that there is a reduction in fuel loading and fire intensity in comparison to a site that has not been burnt for a longer period, where vegetation builds up and consequently produces a high intensity burn due to the greater amount of fuel. The distribution of fire intensity is subject to much variation over a very small area, evident in the charred remains on the ground. These variations can be linked to the quantity of fuel loading, topography (Section 2.2.3.2) and weather variations (Section 2.2.3.1), which are the main factors that determine the duration and intensity of the burn. Temperature gradients formed as a result of localised intensity differences and powerful convective currents trigger the formation of conical plumes that entrain air mixed with fine ash and charcoal as mentioned in Section 2.2.3.1 (Figure 2.3). This has the potential to transport burnt material over large distances. The variations in temperature that cause the development of these conical plumes can be attributed to the quantity of fuel load.

Although Gould (1997) dismisses the influence of wind in plume modelling calculations, Raupach (1990) highlights the importance of the links between these entities which are also linked to meteorological stability (Section 2.2.3.1). The

modelling of plumes is very important as it recognises localised and fire-induced wind patterns which are interlinked to other components that are deterministic to the success of a fire.

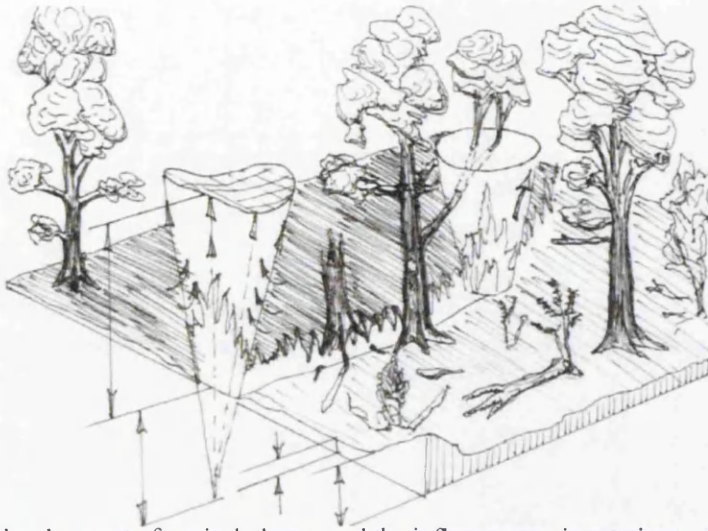


Figure 2.3: The development of conical plumes and the influence on air entrainment (Gould 1951)

Modelling of fire movement behaviour is an important aspect of risk assessment and management. The evolution of technology and software systems has significantly improved the modelling of fires. However, the interlinked complexities that determine fire behaviour and intensity cause problems when trying to create a holistic model. The main components incorporated in such models are shown in Figure 2.4 (Perry 1998).

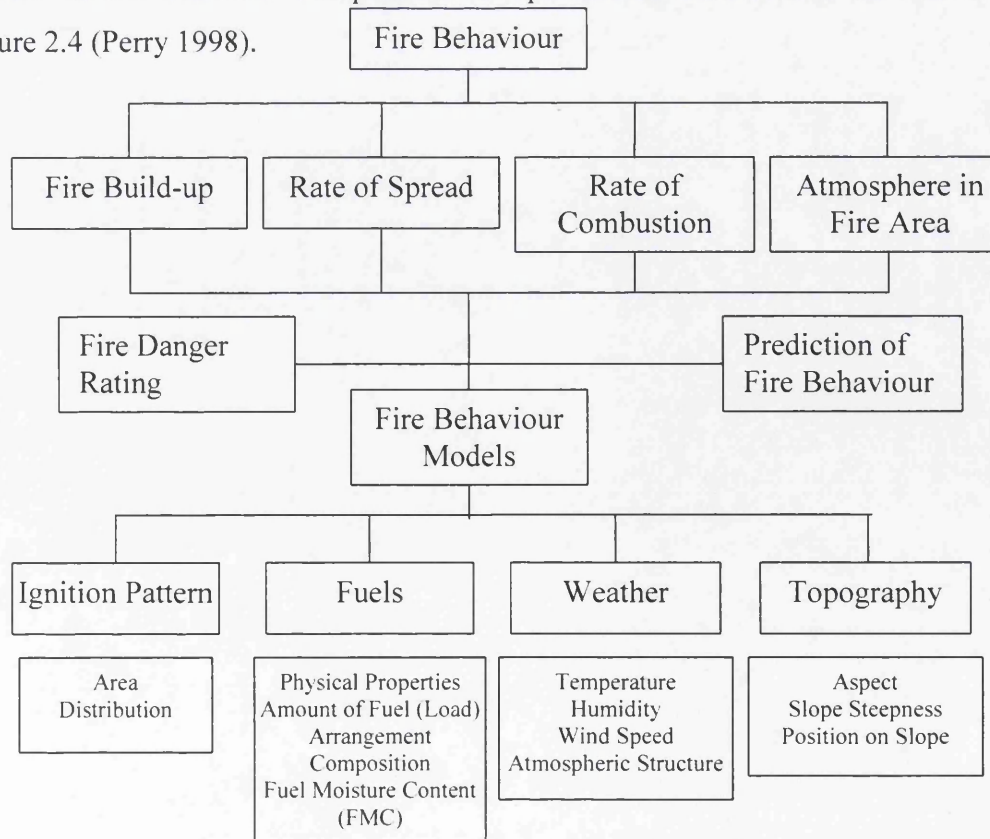


Figure 2.4 – The determinants of wildland fire behaviour and their relation to fire modelling (Perry, 1998).

2.3 FOREST FIRE IMPACTS ON VEGETATION, SOIL AND LITTER

This section firstly details the effects of fire severity on vegetation removal and effects on hydrological processes. It then considers post-fire regeneration, reviews the effects of fire on soils and litter, identifying changes to physical properties of soil. The effect of heating on mineral magnetic properties, thermoluminescence sensitivity (TL χ) and Thermal Activation Characteristics (TAC) are then addressed. It finally reviews the literature relating to the effects of fire on the chemical properties of soil including modifications to soil water repellency.

2.3.1 FOREST FIRE EFFECTS ON VEGETATION

The frequency of fire events has an impact on the biodiversity of an ecosystem. As mentioned in Section 2.2 the natural fire regime of Australia has been modified by human intervention from Aboriginal and European land management practices. The frequent fire regime has led to the establishment of fire tolerant pyrogenic vegetation. The frequency of the fire not only influences the severity of the fire (Table 2.3) but also affects the level of destruction to vegetation (Section 2.3.1.1) and its regeneration (Section 2.3.1.2).

2.3.1.1 *Fire severity and vegetation removal*

The severity of a fire at a burnt site is determined by the type and density of the vegetation, together with the physical aspects of the site, which in turn influences the fire frequency. This causes natural adaptation within species and induces different responses to fire. Eucalypt forests of southeast Australia tend to have higher severity fires than those in the north of the country (Webb 1968; Dickinson and Kirkpatrick 1985; Bowman 1988; Falcon-Lang 2000), because of the higher oil and calorific content of the species in the south caused by localised climatic adaptations and a greater build-up of fuel load due to lower decomposition rates (Walker 1981; Attiwill and Leeper 1987; Ashton and Attiwill 1994).

During a high severity burn, all ground and shrub vegetation will be consumed by fire and the lower tree canopy under 10m will be scorched (Table 2.2). This extent of damage and removal of vegetation on the slope has a large impact on overland flow. Interception of rainfall by vegetation and charred material will be minimal as all the ground litter and understorey vegetation will have been consumed. The

decreased vegetation cover will also cause reduced levels of evaporation, transpiration and interception (Hill and Peart, 1998; Shakesby and Doerr, 2006).

The relationship between increased vegetation cover and reduced levels of runoff and erosion has been well documented (Elwell and Stocking 1976). However, there is evidence that vegetation cover may not be the only controlling factor on erosion. Certainly, Belda and Meliá (2000) argued that the longer the period without plant cover after a fire, the higher would be the soil erosion, but, for example, Cerdà *et al.* (1995) argued that high levels of loss of fine material during early post-fire erosion events are not sustained because of the build-up of a lag of coarser material that remains on the slopes. This identifies a research gap in the literature concerning post-fire soil erosion patterns (Section 2.9).

With a low-severity fire, the extent of damage to the site as identified in Table 2.2 indicates that only ground fuel and shrubs below two metres in height tend to be burnt (Cheney 1981; Jasper 1999). This means that there is a considerable amount of canopy vegetation remaining to protect and stabilise the soil and reduce infiltration rates through rainfall interception by leaves. Visual assessment of the severity of fire (Table 2.2) can identify how burn temperatures vary substantially on a small scale, caused by differential fuel loading (Section 2.2.3.3). This then impacts on the pattern and type of vegetative regrowth and the level of modification to hydrological processes as canopy interception of rainfall at low-severity burn sites regulates the quantity and rate of water reaching the ground. This will also reduce the rate at which saturated overland flow develops, as the slower input of water to the system will minimise the risk of exceeding the infiltration capacity. Overland flow or runoff that occurs on a lightly burnt site will have its progress inhibited as ground vegetation or charred logs may provide an obstacle to the main flow leading to the formation of litter dams (Section 2.5.4.2). The remaining vegetation provides a source for future leaf litter and ground cover, which will aid rapid regeneration and recovery of the environment to pre-fire conditions.

2.3.1.2 *Vegetation regeneration after fire*

Many types of vegetation in fire-prone areas are dependent on burning for regeneration purposes (Gill 1975; Whelan 1995; Whelan and York 1998). Many of

these pyrogenic species have adapted their physical characteristics to increase their flammability levels. The structure of the bark of certain species of eucalypt trees encourages fire to transfer via a 'ladder effect' to the canopy (Cheney 1990). Although high severity fires are associated with the greatest destruction to the vegetation, the temperatures reached during these events are essential to the initiation of regeneration within pyrogenic species.

An aboveground mechanism of fire-induced regeneration is through seed dispersal by the opening of cones. This is dependent upon the severity and residence time of the fire and the height of the cone above the ground. The mechanism is initiated in serotinous cones of *Pinus banksiana* and *Pinus contorta* var. *latifolia* by a two-stage process. Firstly, the heat from the fire weakens and breaks the resin bonds that hold the seedpods closed. This initiates the second process, which is the release of the cone scales from the axis, enabling the dispersion of the seeds. The temperature required for these processes to occur needs to be of a severity sufficient to cause canopy destruction of the tree (Johnson and Gutsell 1993).

The *Banksia* species, which are prominent in various locations around Australia, are renowned for their high tolerance levels to fire and their dependence on heat generated during burning to initiate cone-opening mechanisms in adult species that survived the fire. Regeneration can occur any time between 3 and 30 years after the fire (Witkowski and Lamont 1997). The population growth of this species over time in a fire prone environment is estimated to be zero, as the number of plants unable to survive fire is equal to the number of plants that regenerate. This is because only a few seeds are produced (Drechsler *et al.* 1999). Once a species becomes established in the environment, it may remain there for centuries (Enright and Lamont 1992). Species such as the *Banksia* form an important component of fire-prone areas across Australia, as their roots contribute to stabilising soil in post-fire environments.

As well as the seeds located in the top layers of the soil, there are numerous leguminous plant species that store a seed bank in the upper layers of the soil (Beadle 1940; Bradstock and Auld 1995). The temperatures required to activate these seeds have been recognised by Auld and O'Connell (1991) in a study in the Sydney region of Australia. They observed that temperatures above 60 °C broke

seed dormancy in 50% of the 35 species of Leguminosae (Fabaceae) studied and exposures above 80 °C were required to break dormancy in all the species. The higher temperatures required by fire-dependent varieties need to be experienced throughout at least the top 3 cm of the soil profile where the seeds are located. This is obtained through a longer duration of the fire. In relation to the application of low intensity prescribed fires, the temperatures identified by Auld and O'Connell (1991) are rarely reached, which reduces ecological diversity at these sites as seed dormancy will not be broken (Bradstock and Auld 1995).

It is commonly recognised that once the seeds have been activated or dispersed by the heat from the fire, re-growth is dependent upon a high soil moisture content or rainfall (Bradstock and Bedward 1992; Bond and van Wilgen 1996; Ojeda 1998; Vlok and Yeaton 2000; Cruz and Moreno 2001; Ellis 2001). For example, where rainfall is not strongly seasonal, in areas such as the hinterland of Sydney, post-fire regeneration is dependent upon the timing and magnitude of major rainfall events rather than on seasonal burning (Whelan and York 1998).

As mentioned in Section 2.1, the temperatures reached during burning of prescribed fires are often not high enough to initiate regeneration mechanisms in fire-dependent species. The relationship between fire intensity and effects on re-vegetation were quantified in a study by Dyrness (1976) in which vegetation cover was assessed six years after the burn event with the following results. There was a 30% vegetation cover in a heavily burnt area, a 58% cover in a lightly burnt area, and a 71% cover in an unburnt area. These findings were explained by Dyrness (1976) as the effect of soil hydrophobicity (water repellency) which resists the infinity of soils to water so that they resist wetting for periods ranging from a few seconds to hours, days or weeks (King 1981; Doerr 1997) (Section 2.3.5.2) reducing the rate of succession and recolonization of plants through its influence on moisture availability to the plants (Jungerius and Harkel 1994; Everett *et al.* 1995). An additional consequence of long-lived hydrophobicity is the prolonged susceptibility of a soil to erosion (see Section 2.3.5.1). Other modifications to soil properties should also be taken into account. For example, the presence of nutrient-rich ash immediately after the fire aids regeneration, and can significantly increase ground cover and reduce degradation.

The frequency of the fire regime is a further issue relating to prescribed burning, as the regeneration of vegetation can be seriously hindered if the fire regime is too frequent. Vegetation undergoing re-germination from the previous fire event may not have developed resilience to tolerate the conditions imposed by burning, and fire-sensitive species may become rare and confined to fire shadows in the landscape and effect post-fire erosion. Conversely, if the time interval between fires exceeds 30 years, pyrogenic vegetation, dependent on fire, will decline due to a reduction in the seed bank, causing the genre of vegetation to change drastically (Gill and Bradstock 1995).

The damage to and recovery of vegetation after fire can be assessed by using a Geographical Information System (GIS) approach. This can be carried out by utilising satellite imagery with assessment of the normalized difference vegetation index (NDVI) combined with satellite image analysis (SPOT) (Belda and Meliá 2000). This technique was adopted following the 2001/2002 fires in the Lake Burraborang catchment by Chafer *et al.* (2004) to assess fire severities experienced.

The influence of fire regime on the successful regeneration of vegetation is determined by individual species genetics. Referring once again to the *Banksia* species in Australia, it is estimated that the regeneration of *Banksia goodii* will be most successful with an inter-fire period of 16 years. This estimate is based on a theoretical model of regeneration that is heavily dependent on a number of assumptions, which may have implications on its accuracy. The model enables levels of regeneration to be predicted on a timescale of 100 years, which it would not be possible to achieve through fieldwork. The results indicated the low population growth in this species and highlighted related issues. Research by Auld and O'Connell (1991) and Gill and Bradstock (1995) summarised the influence of fire regime on species diversity and concluded that the greatest species diversity is likely to occur where there is high fire regime variability, where certain species may dominate during the different fire regimes.

2.3.2 FOREST FIRE EFFECTS ON SOILS AND LITTER

As discussed in Section 2.3.1, vegetation build-up strongly influences the potential severity of a fire. The spatial variability of heating in the vegetation influences the properties of the soil and its component particles and may lead to changes to

physical properties including mineral magnetic properties (2.3.4), Thermal Activation Characteristics (TAC) (Section 2.3.5) and chemical properties of aggregates (Section 2.3.6.1) including soil water repellency (Section 2.3.6.2).

2.3.3 FIRE EFFECTS ON SOIL PHYSICAL PROPERTIES

The changes to the physical components of the soil are initiated in the compositional structure of aggregates, as the cohesiveness of the clay particles and organic matter within the soil (which provide binding agents) is reduced or destroyed during combustion (Dyrness and Youngberg 1957; Martinez-Fernandez and Diaz-Pereira 1994; Boix Fayos 1997; Andreu *et al.* 2001). This causes coarse-textured, sand-sized aggregates to be increased after fire (Ulery and Graham 1993; Blake *et al.* 2005b). Greater aggregate stability can occur as a result of fire, because transformations that occur through the oxidation of iron properties cause reorganisation and recrystallization of the compounds (Giovannini 1994).

The extent of physical modifications to the soil is determined by the severity of the fire, with the most pronounced effects being apparent when temperatures are sufficiently high to cause destruction of the organic matter ($\sim >460^{\circ}\text{C}$) (Giovannini 1994). Where severe fires have occurred, the soil loses its plasticity and elasticity and a decline in aggregate stability will be evident for the period after the fire until vegetation cover is established and soil exposure reduced (Imeson *et al.* 1992). However, where low intensity fires have occurred, no significant changes to aggregate stability are likely, as demonstrated in an investigation in New South Wales, Australia (Valzano *et al.* 1997).

Modifications to soil colour may also be noted. Observations have identified a reddening of the soil, especially in areas of high intensity burns, for example, in areas with a high fuel load such as under slash piles or fallen logs (Screenivasan and Aurangabadkar 1940; Ulery and Graham 1993). This is due to the oxidation of the iron minerals within the soil, which contribute to the enhancement of mineral magnetic properties due to the development of a secondary ferrimagnetic form (Maher 1986).

2.3.4 FIRE EFFECTS ON SOIL MINERAL MAGNETIC PROPERTIES

The presence of iron compounds and oxides within soil creates a mineral magnetic signal, determined by the concentration of magnetic grains, their size and mineralogy (Mullins 1977). The ferrimagnetic minerals magnetite and maghaemite, tend to dominate the magnetic signal. Soil-forming processes, fire events, and pollution are some of the factors that can contribute towards changes in the magnetic signal due to mineralogical transformations. Modified signatures that result from these processes can be used in environmental studies for a number of purposes: (i) to discriminate between individual soils or soil horizons; (ii) for soil surveying sediment tagging and tracing; and (iii) to model sediment source linkages (Caitcheon 1993; Blake *et al.* 2006a). Alternatively mineral magnetic techniques have often been applied in archaeological investigations to provide evidence about historical campfire or kiln sites (Canti and Linford 2000; Weston 2004).

This section reviews the literature that has used magnetic measurements for a number of purposes (predominantly focusing on fire enhancement of magnetic properties). It firstly discusses the factors that influence the general mineral magnetic signature of soil, in terms of physical properties and local environmental conditions. It then addresses ways in which magnetic enhancement of grains may occur, before evaluating the use of this technique in environmental studies, and highlights research gaps regarding the effects of heating on mineral magnetic properties.

2.3.4.1 *Magnetic properties of soil*

Soil is primarily composed of mineral fragments and organic matter (Christopherson 2003). The iron minerals within a soil influence physical properties such as its colour, structure and fabric (Maher 1986; Canti and Linford 2000). They also contribute to the magnetic properties of a soil assemblage. The magnetic signal produced by iron minerals is induced by the interaction of magnetic moments within the atomic structure. These are created by the action of negatively-charged spinning electrons circulating the central nucleus within each atom, which initiates an electric current (Mullins 1977).

The interaction of these magnetic moments within the crystal structure determines the type of magnetic behaviour that is initiated. These include: (i) ferromagnetic; (ii) antiferromagnetic; (iii) ferrimagnetic; and (iv) canted antiferromagnetic behaviours (Figure 2.5).

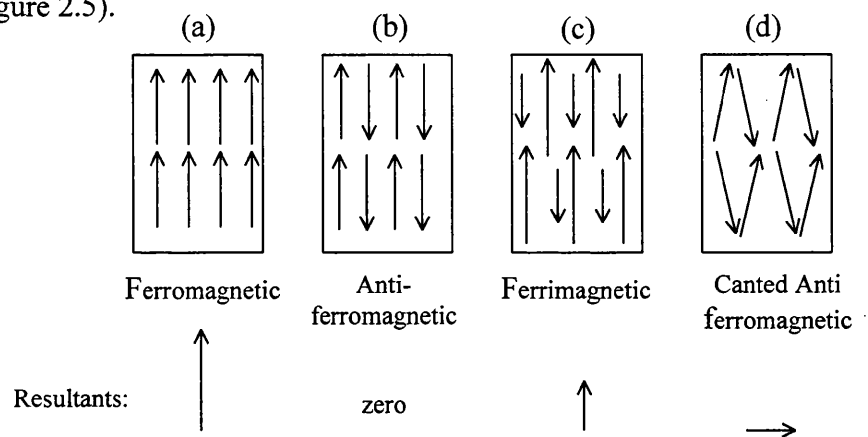


Figure 2.5: Schematic representation of the distribution of magnetisation vectors in crystals showing the resultant spontaneous magnetisation (McElhinny 1973; Smith 1999)

The different types of magnetic behaviour can be used to make inferences about the dominant mineralogy of soil assemblages. Ferromagnetic behaviour (Figure 2.5a) creates the strongest resultant magnetic force, even in the absence of an externally applied field. Minerals including pure iron, nickel and chromium demonstrate ferromagnetic behaviour which means that they are uncommon in environmental studies. Antiferromagnetic behaviour (Figure 2.5b) occurs in samples where there are equal numbers of unpaired electrons. This creates zero resultant magnetic fields as the magnetic vectors within the crystal oppose each other cancelling out the resultant magnetisation. Ferrimagnetic behaviour (Figure 2.5c) occurs where there are unequal magnetic moments which produce a net spontaneous magnetisation. Minerals such as magnetite, maghaemite, pyrrhotite and greigite create ferrimagnetic behaviour (Dearing 1999; Smith 1999). The effect of burning modifies the magnetic behaviour to transform antiferromagnetic alignment to ferrimagnetic alignment by the creation of secondary ferromagnetic iron oxides (Rummery *et al.* 1979). Canted antiferromagnetic behaviour (Figure 2.5d) occurs where the sub-lattices in an otherwise antiferromagnetic alignment are not perfectly parallel and a small residual magnetisation exists. The minerals haematite and goethite demonstrate antiferromagnetic behaviour (Dearing 1999; Smith 1999).

Magnetic measurements are made while a sample is either in a magnetic field or after it has been exposed to an external magnetic field. Low frequency mass specific magnetic susceptibility (χ_{lf}) is a basic measurement conducted while the sample is in an external magnetic field. Values obtained for χ_{lf} are associated with different environmental materials. Comparison of χ_{lf} values with those obtained from other studies by reference to Figure 2.6 (which is composed of data obtained from a range of sources) can be used to make generalisations regarding the dominant type of magnetic behaviour.

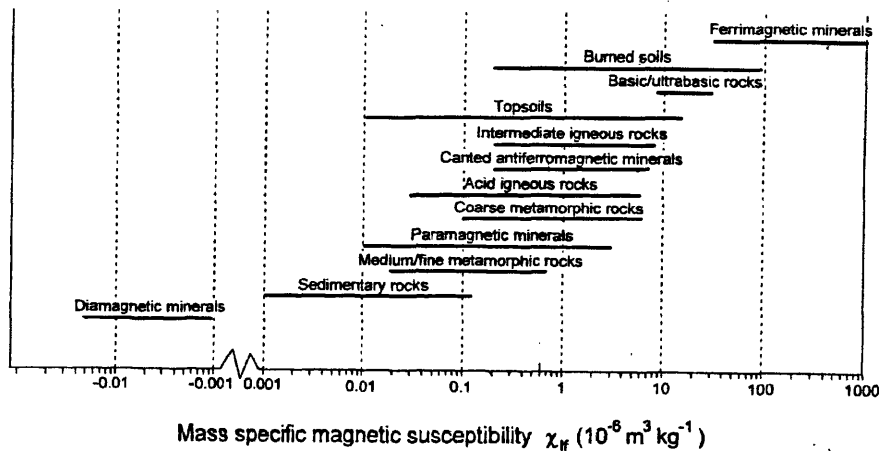


Figure 2.6: The range of magnetic susceptibility values for environmental materials and minerals (data from diverse published and unpublished sources) (Dearing 1999).

Comparison of the results obtained from the measurement of a variety of magnetic parameters enables inferences to be drawn regarding the magnetic domain size, grain size and mineralogy. Figure 2.7 schematically represents the magnetic domain and grain sizes that Blake *et al.* (2006b) found to be enhanced from their study of burnt topsoil. The magnetic parameters used in this study to identify the presence of burnt material and the grain sizes that respond to the various measurements are summarised in Table 2.4

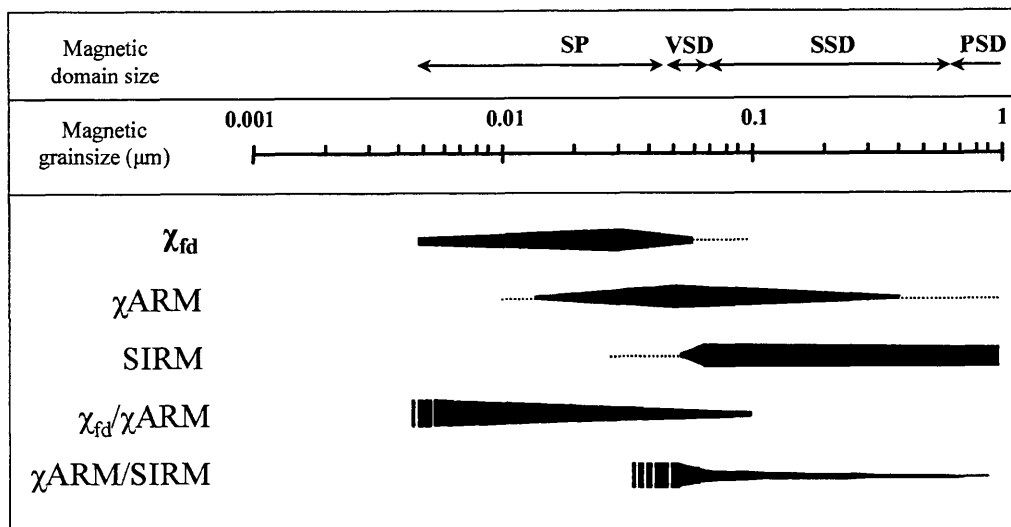


Figure 2.7: The extent and nature of magnetic enhancement in burnt topsoil (Blake *et al.* 2006b)

Table 2.4: Magnetic parameters that respond to heating and their interpretation

| Magnetic parameter | Explanation |
|--------------------------|--|
| χ_{lf} | Low frequency susceptibility (χ_{lf}) measures the ease at which material can be magnetised (Thompson and Oldfield 1986). |
| χ_{fd} | Frequency dependent susceptibility (χ_{fd}) identifies grains lying close to the superparamagnetic (SP) / Stable Single Domain (SSD) grain size boundary (Dearing 1999). |
| χ_{ARM} | Anhyseretic Remanent Magnetisation (χ_{ARM}) identifies predominantly ferrimagnetic SSD) grains in the 0.2-0.4 μm range (Maher 1988). |
| $\chi_{fd\%}$ | Percentage frequency dependent susceptibility ($\chi_{fd\%}$) reflects the presence of the ultra-fine SP ferrimagnetic grains of 0.015-0.025 μm , with lower responses in smaller and larger grain sizes. It is also sensitive to grains between SSD (0.02-0.1 μm) and SP grain sizes (Gedye <i>et al.</i> 2000). |
| Soft _{IRM%} | The 'soft percentage Isothermal Remanent Magnetisation' magnetic parameter detects ferrimagnetic minerals that respond to low magnetic fields after they have been fully magnetised (Oldfield 1991). (0-20mT) (Walden <i>et al.</i> 1997). |
| Mid _{IRM%} | The 'mid percentage Isothermal Remanent Magnetisation' is sensitive to the concentration of canted antiferrimagnetic minerals (20-300mT) (Walden <i>et al.</i> 1997). |
| Hard _{IRM%} | The 'hard percentage Isothermal Remanent Magnetisation' IRM% is sensitive to the concentration of antiferrimagnetic minerals (300-1000mT) (Walden <i>et al.</i> 1997). |
| χ_{ARM}/SIRM | This quotient is particularly sensitive to magnetic grain size changes and can be used to help distinguish between superparamagnetic (SP) (low values) and stable single domain (SSD) (high values) magnetic grain sizes (Gedye <i>et al.</i> 2000). |
| χ_{fd} / χ_{ARM} | This quotient particularly reflects magnetic grains that lie on the SSD/SP grain size transition and is particularly sensitive to magnetic grain size changes (Oldfield 1994). |
| SIRM | Saturation isothermal remanent magnetisation is the highest level of remanence that can be induced in a sample by application of a high field. SIRM is an indicator of the volume concentration of magnetic minerals in a sample but responds to grain size variations (Maher 1986). (Often assumed to be equivalent to 1000mT) |

Parent material, physical composition, dominant minerals and biogeochemical processes have a significant influence on magnetic properties of soil. However, there are also a number of pedological-environmental conditions that modify the magnetic signature by converting antiferromagnetic minerals to a magnetically enhanced ferrimagnetic form (Le Borgne 1955, 1960). These factors include: (i) oxidation and reduction by natural pedogenic processes; (ii) low temperature oxidation of magnetite to maghaemite ($\sim 50^\circ\text{C}$); (iii) dehydration of lepidocrocite and (iv) burning. These factors are influenced by the supply of oxygen (O) to the soil which affects the magnetic properties. The reduced supply of O to the soil causes reduction of other elements to liberate O. Once O levels have dropped, NO_3 will then be reduced, followed by Mn, Fe and SO_4 . (Bohn 1985 in Weston 2002). The reduction of Fe will cause the development of secondary ferrimagnetic minerals.

Oxidation and reduction cycles can result from daily heating and cooling cycles, where decaying organic matter and oscillating wet and dry conditions cause surface soil to often have a higher magnetic susceptibility than lower layers within a soil profile. Differing oxidation and reduction cycles associated with climatic variations

have been demonstrated on UK and Mediterranean soils in the form of contrasting percentages of minerals transformed from an antiferromagnetic to a ferrimagnetic form after heating (Tite and Linnington 1975). Prior to heating, the Mediterranean soils had experienced conversion of minerals, which was explained by the influence of the climate initiating fermentation, with anaerobic (reducing) conditions developed during humid winters and re-oxidation occurring during the summer. Further confirmation was obtained by comparison of tropical soils from sites with and without a significant dry season, with the soils from an area with a distinct dry season having a higher susceptibility caused by the presence of stronger reducing and oxidising conditions during the different seasons (Tite and Linnington 1975).

Catchment particle sorting processes, and local climatic, environmental and pedomicroclimatic conditions can also have a significant effect on the magnetic properties of soil (Maher 1986). Catchment sorting processes can produce a general distinction between material in different landscape units within a catchment in terms of particle size. High parts of the landscape such as summits and ridge tops are generally subject to a high degree of exposure and therefore they experience net removal of fine particulate matter. On the other hand, foot-slope zones tend to provide storage sites due to their low gradient. This redistribution of material through the catchment sorts material in terms of its particle size characteristics but can also cause abrasion and breakage of particles, which influences the resulting magnetic signature (Crockford and Olley 1998).

The different reducing and oxidising conditions associated with different land cover and slope locations are also likely to influence magnetic signatures. This has been exemplified by Magiera *et al.* (2005), who found magnetic signatures of European forest soils to be higher than those obtained for similar soils in open areas such as grassland / arable areas. On a smaller catchment-unit scale, distinctive signatures have been demonstrated following fire in the small sub-catchment of Blue Gum Creek, a tributary to Lake Burragorang (Blake *et al.* in press). The varying microenvironments associated with the different landscape units such as ridge tops, slopes, gullies and rivers are likely to have a strong influence on oxidation and reduction conditions, and additionally produce potentially localised burning conditions. It would be interesting to determine if distinctive signatures can be

linked to different landscape units within the catchment for sediment tracing purposes.

The enhancement of magnetic minerals resulting from burning was first recognised by Le Borgne (1955) who proposed that natural formation of magnetite was related to extreme environmental conditions of high temperature anaerobic conditions. The mechanisms of reduction and biological processes that exist during burning cause the iron compounds within the soil to transform from an antiferromagnetic to a ferrimagnetic alignment (Figure 2.5) thus creating an enhanced magnetic assemblage through the development of secondary ferrimagnetic iron oxides (Rummery *et al.* 1979).

The resulting enhancement of magnetic minerals that occurs from burning of soil has been applied in a number of studies for a range of purposes including: (i) recognition of burnt material within sediment cores to make inferences about historical catchment events (Rummery *et al.* 1979; Rummery 1981, 1983; Gedye *et al.* 2000); (ii) identification of fire-enhanced erosion after heavy post-fire rainfall events (Brown 1972; Brown 1988; Blake *et al.* 2004; Blake *et al.* 2005a); (iii) creation of artificially enhanced tracer material (Oldfield *et al.* 1981; Oldfield 1991; Dearing 2000); and (iv) identification of the location of old campfire or kiln sites during archaeological investigation (Canti and Linford 2000; Weston 2004).

Thermal history experienced by individual grains and soil assemblages may be obtained by comparing magnetic susceptibility during heating and cooling. If the cooling curve differs from the heating curve (following heating to 700 °C), this indicates that further mineralogical changes are occurring during cooling, signifying that temperatures exceeding 700°C have not previously been experienced (Peters *et al.* 2001). This concept has been explored further by Marmet *et al.* (1999) who suggested that this technique could be applied to discover if temperatures higher or lower than 400°C had been experienced by noting the presence of lepidocrocite in the samples (as its transformation temperature range is 250-400 °C). However, this is only possible if lepidocrocite is apparent in the unheated soils. Furthermore, the effect of investigations into the thermal histories of soils will also be dependent on

homogeneous heating and if it relates to a forest fire situation, the effect of mixing and transport processes acting on material on the slope.

2.3.4.2 *The behaviour of fires*

The temperature, duration and rate of heating during a fire have a strong influence on the level of enhanced susceptibility. Taylor and Schwertmann (1974) identified the influence of various parameters on mineralogy resulting from heating. Their laboratory investigations found that oxidising conditions determined by the rate of heating and cooling affected mineralogical modification, in addition to pH and the variability of Fe form. Maghaemite was shown to develop via transformation from magnetite during the following conditions: slow oxidation rates, high Fe concentration, temperatures ranging between 20-60 °C and a pH of 7. Lepidocrocite was formed when faster oxidation conditions prevailed. Soils that originally had a pH of 6 did not produce maghaemite even when the other conditions were favourable.

The importance of oxidising conditions was also highlighted by Oldfield *et al.* (1981), who investigated rates of laboratory-induced heating and cooling, temperature, duration and particle size required to produce an optimum artificial magnetic enhancement of stream bedload material that could be used for sediment tracing purposes. Rapid heating and cooling were found to cause a significant increase in the magnetic enhancement, due to the formation of magnetite. Rapid rates were obtained by inserting samples in a pre-heated furnace (at the optimum heating temperature of 900 °C) and by cooling naturally and through quenching in water, in comparison with slower rates where gradual heating over a 2-hour period and cooling in the furnace occurred. Oldfield *et al.* (1981) also found the duration of the burn to be influential, in that magnetic enhancement increased with heating time, but fell when treatment time exceeded various thresholds. The optimum heating duration for maximum magnetic enhancement for smaller particles was 20-30 minutes, while larger particles required heating for >2 hours.

The findings by Oldfield *et al.* (1981) contradicted the results of experimental hearth fires in America where the temperatures required to produce maximum enhancement were <700 °C and a longer total burn time of 3 hours would produce continued

increasing enhancement (Hathaway 1990b). Similarly, experimental fires in Oxfordshire in the UK tested the influence of heating duration on magnetic enhancement. The fires either lasted 2 hours or were kept alight for 4 days. The results showed that the fires that burned for 4 days produced a greater enhancement of the surface layer of soil and of the ash layer. The ash was enhanced magnetically by a magnitude of 22 times the initial value of the soil. Its initial enhancement was created by a 'roasting' effect of soil in contact with fuel, rather than actual enhancement of the iron minerals within the soil (McClean and Kean 1993; Linford and Canti 2001).

The effect of multiple burn events on magnetic properties has been documented in a number of archaeological studies using campfires and hearths (Hathaway 1990b; Linford and Canti 2001). Results from these studies have shown an increased magnetic enhancement with the number of burn events, with repeated fires ensuring homogeneous mineralogical transformation of the whole soil assemblage. Bellomo (1993) also found that multiple burn events produced a higher level of enhancement associated with archaeological fires when investigating contrasting signatures created during different types of fire. Grass, tree stump and forest fires provided weaker signatures than multiple burn sites such as campfire sites and archaeological hearths. This was due to a more even and thorough heating within man-made fires, while temperatures attained during natural burn events were rarely found to reach adequate levels for producing a significant change in magnetic mineralogy. Contrary to the findings obtained from archaeological and natural fires, laboratory experiments that have investigated the effect of multiple heat treatments on magnetic enhancement have shown little change resulting from multiple heating (Brown 1988; Weston 2004). This is likely to have been caused by the laboratory tests producing uniform and thorough heating conditions, leading to full mineralogical transformations during the first heat treatment.

Studies that have investigated the influence of burning patterns on the enhancement of soil have highlighted the importance of burn duration and oxidising conditions. It is worth noting that these examples are from controlled heating experiments using either laboratory or campfire / kiln situations which are unlikely fully to recreate conditions apparent during natural forest fires.

2.3.4.3 *The type of soil being heated*

Temperature, heating pattern and oxidising conditions have a significant effect on the magnetic enhancement resulting from burning. These factors are also influenced by the soil type in a number of ways: the thermal heat capacity and conductivity of the soil influences the heat transfer rate and the depth at which elevated temperatures are experienced. Thermal heat capacity of soil is a property that determines the energy required to raise the temperature of a unit amount of substance by 1 °C; this is dependent on the individual properties of soil and its water content. The rate of heating and cooling will influence reducing and oxidising conditions, which will have a pronounced effect on the magnetic modifications.

The thermal conductivity of the soil depends on the soil type and arrangement of the particles, moisture and air. Movement of heat through dry soil occurs via the process of conduction, through points of contact between individual grains. Thermal conductivity generally increases if a small amount of water is present, due to the greater contact between particles.

Linford and Canti (2001) assessed the effect of soil type on enhanced temperatures during burning and the resulting magnetic enhancement following either 1- or 4- day experimental campfires in the UK. They highlighted the influence that substrate type had on the depth at which heat penetrated, showing that heat transferred more efficiently through gravelly sand than the clay soil. This was shown to influence directly the level at which magnetic enhancement was noted. The relationship between heating depth and magnetic enhancement has also been confirmed by Morinaga *et al.* (1999). Although soil type affects the transfer of heat through soil, the mineralogies associated with different soils require variable temperatures to cause modification, with clay soil experiencing greater enhancement at lower temperatures than sandy soil (Hathaway 1990b; Linford and Canti 2001; Weston 2004). An additional factor that could have affected the results obtained by Weston (2004) is the influence of the prolonged reducing conditions experienced by the waterlogged clay soil prior to burning (Weston 2004).

The comparatively low temperature required for clay minerals to be transformed mineralogically is likely to be caused by the dominant mineralogy, which is

influenced by grain size. For example, the critical diameter for magnetite is 50 nm (Mullins 1977). Furthermore, the response of magnetite to oxidation is dependent on the grain size, with particles $>600 \mu\text{m}$ converting to haematite, while smaller particles are oxidised to maghaemite (Feitknecht 1965 in Mullins 1977).

As previously mentioned, one of the main findings by Linford and Canti (2001) was the production of a very high magnetic signal in the surface ash. The enhanced ash provides a significant contribution to the magnetic signature of soil following burning. Owing to the fine nature of ash, it easily becomes dispersed throughout the environment via weathering, erosion or its translocation through large pores in the soil during burning, dissipating and diluting the highly enhanced particles. In addition to the bonding of ash to soil particles, other size modifications during fire have been documented. Tite and Mullins (1971) observed a small decrease in the clay-sized fraction and an increase in the susceptibility of medium- to coarse- sand following laboratory based heating. This was attributed to the adhesion of clay particles. Similar findings were documented by Blake *et al.* (2005b) who recognised bonding of particles that had experienced repeated burning on soils located at the foot-slope zone of Blue Gum Creek. Macroscopic evidence of the bonding of particles by heating has been observed by Hathaway (1990a) through the occurrence of botryoidal grains (shaped like a bunch of grapes) .

Soil type influences the content of Fe-bearing minerals. Coarse-textured soils in Europe that are lacking organic matter or clays are more easily leached and iron will be removed, reducing the magnetic minerals (Weston 2002). The importance of the concentration of iron minerals in a sample was highlighted by Morinaga *et al.* (1999) who assessed the response of three different soil types to heating by measurement of χ and remanent magnetisation intensity in detecting heated soils. Owing to the absence of goethite or any magnetic properties in volcanic ash, heating produced no significant increase in χ although an increase was observed for the other soils.

The content of organic matter (OM) within soil has a significant impact on the magnetic properties of an assemblage, as it does not contain any Fe-bearing minerals, so it effectively dilutes the signal emitted by magnetic minerals. The direct

relationship between OM and magnetic properties has been investigated in a number of studies and has been shown to be reliable. Although OM does not carry a magnetic signal, it does provide an important influence on the magnetic minerals as natural decay of OM by microbial action, may produce anoxic conditions that cause the breakdown of carbon compounds. This uses N and consumes O, causing a more rapid onset of the reduction of Fe (Weston 2002).

During a fire, OM also plays an important role influencing: (i) the temperature reached; (ii) the rate of heating and cooling; and (iii) the oxidising conditions. The type and quantity of OM determines the temperatures reached and the duration of a fire event. The type of material influences its structure and the associated oxidation conditions. For example, pine needles burn quickly enabling the fire to consume available fuel and oxygen quickly. This causes elevated temperatures for a short time in contrast to conditions that would prevail under a smouldering log, which would last for a long time and have little O available during re-oxidisation unless the log is fully consumed. A number of laboratory-based heating experiments have simulated anoxic conditions that occur during burning by either using additional OM or heating in reducing environments. Tite and Mullins (1971) found that heating in N₂ then cooling in air (reducing then oxidising conditions) produced a greater enhancement than heating under a constant supply of H₂ (a reducing atmosphere).

An OM content of 10-15% causes elevated temperatures and oxidising conditions that will cause increased enhancement of magnetic properties (Brown 1988). Tite and Mullins (1971) suggested that temperature and iron oxide content had a major influence on the reducing power of the OM. Evidence for full oxidation of the minerals can be demonstrated by reddening of the soil. Canti and Linford (2000) investigated the relationship between temperature and colour change and found that it was complex. Humus provided the essential reducing agent, as soils that had a low OM content generally did not produce reddening. The type of organic matter can also affect the resulting magnetic enhancement by influencing the highly enhanced fuel ash residues. Peters *et al.* (2000) and Peters and Batt (2002) have highlighted the influence that different types of OM have on the enhanced susceptibility resulting from burning. By using room temperature and χ heating and cooling curves, they identified different fuel sources of well-humified peat, fibrous upper

peat, peaty-turf and wood. Comparison of χ_{lf}/χ_{fd} and discriminant analysis of various magnetic parameters measured at room temperature after heat treatment, showed definite groups resulting from fire ash residues created by the different soil types. Hysteresis loops of χ obtained during heating and cooling showed that fibrous upper peat and peat turf had a single magnetic component with a fall in temperature at 600°C, while well humified peat and wood contained one or two distinct magnetic components characterised by reduction in χ at 330 and 550 °C, suggesting the presence of three different magnetic mineralogies within the ash samples (Peters and Batt 2002).

2.3.4.4 *Summary of the effects of heating on mineral magnetic properties of soil*

- The level of magnetic enhancement is determined by the heating rate (more rapid changes produce a greater level of enhancement).
- The level of organic matter within a sample will influence the reducing conditions (increased levels of organic matter produce suppressed enhancement).
- Soil type
 - o Clay minerals tend to obtain magnetic enhancement at lower temperatures than sandy material.
 - o The longevity of the enhanced signature is more likely to be retained in clayey soils than in sandy soils.
 - o Sand transfers heat to lower depths within the profile with a greater efficiency than clay dominated substrates. Therefore, magnetic enhancement for sand is likely to be greater than for clay soil at depth.
 - o Clay retains an enhanced signature for longer than sandy soils due to leaching of ions in sandy soils.
- Laboratory heating produces a more uniform enhancement than experienced in the natural environment, and therefore multiple fires are required to produce significant enhancement to increase the likelihood of thorough heating.

2.3.5 FIRE EFFECTS ON THERMAL ACTIVATION CHARACTERISTICS

Another technique used for the investigation of soil properties is the use of thermoluminescence sensitivity ($TL\chi$) measurements. These have been shown in a number of predominantly archaeological based-studies to become modified following exposure to heating (Göksu *et al.* 1989; Godfrey-Smith *et al.* 2005; Lahaye *et al.* in press). TL measurements have been commonly used for dating purposes by determining the accumulation of charge within the crystal lattice of various materials (including quartz, flint and chert) through exposure to natural environmental radiation. Heating of a sample causes the TL signal to be reset to zero (Figure 2.8), after which point, TL begins to develop again by exposure to ionising radiation and so this is a useful tool for dating fired archaeological artefacts. As the accumulation of radiation occurs at a constant rate (e.g. between points B and C on Figure 2.8) applying a 10 Gy β dose of radiation to the sample prior to measurement enables the equivalent amount of environmental radiation that would have been acquired naturally over a period of *ca.* 10,000 years to be established. By measuring the $TL\chi$ following this procedure it enables simulation of the sample having experienced heating *ca.* 10,000 years ago (Aitken 1985).

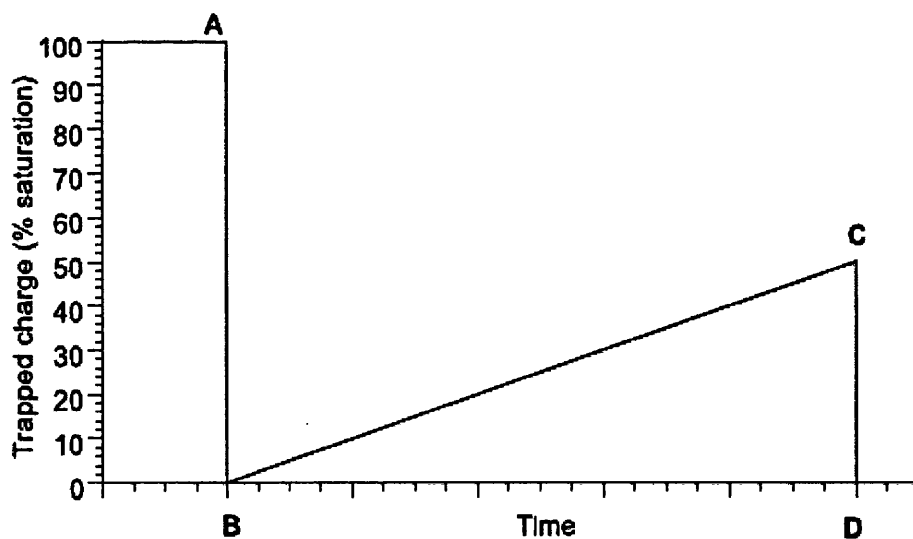


Figure 2.8: Simplified schematic diagram of the physical processes responsible for luminescence dating (Feathers 2003). At point A all traps (e.g. minerals in the raw material of the pottery) have been filled by exposure to natural radiation. Between points A and B, a zeroing event (heating of pottery) empties the traps and the process luminescence is emitted. Through exposure to natural radiation the traps are gradually filled though time, a process shown here as linear although it may not be at all points in time, particularly as saturation is neared. At point C to point D, the traps are again emptied, this time in the laboratory while luminescence is measured. The measured signal is proportional to the amount of trapped charge. If one knows how much radiation is required to arrive at point C, a value called the equivalent dose, then dividing by the average dose rate will yield the time from B to D (Feathers 2003).

In addition to the use of TL measurements to establish the timing of the last heating, the timing of burial can also be ascertained using TL components which have been bleached by sunlight (Rhodes *et al.* 2003b). Optically Stimulated Luminescence (OSL) dating is based on the same principle, but stimulation of the luminescence signal in this instance is initiated by a beam of light (instead of heating used for TL measurements). These techniques have both had wide applications in archaeological (Rhodes *et al.* 2003a) and environmental research (Wilkinson and Humphreys 2005).

Zimmerman (1971) developed a model based on an ionic crystal to explain the thermoluminescence process (Figure 2.9) which contained a valence band where the electrons are contained prior to irradiation, a conduction band where a series of electron traps are located and hole centres which create luminescence when recombination with an electron occurs.

Electrons are released from the valence band (Figure 2.9) in response to natural radiation. The crystal lattice contains positive and negative ions. Defects within the lattice are created where a negative ion is missing. This acts as an electron trap (Figure 2.9) which attracts the electrons that have been released from the valence band because the defects in the lattice (where negative ions are missing) attracts negatively charged ionised electrons (Aitken 1985). Heating the crystal causes increased vibrations within the crystal lattice, which provide sufficient energy that the electrons are 'shaken free' or ejected from the trap. There are various temperatures at which electrons become released. For quartz, the first temperature threshold where this happens occurs between 90-120 °C which produces a peak in electron emission at 110 °C. A luminescence signal (an emission of light) is created when the freed electron recombines with an ion from an electron that has been previously detached (a hole centre) (Figure 2.9) (Halperin and Braner 1960; Zimmerman 1971; Aitken 1985). The luminescence signal is proportional to the number of photons, which is proportional to the number of trapped electrons, which is proportional to the amount of radiation to which the crystal has been exposed. Therefore, the amount of light emitted provides the measurement of TL χ (Aitken 1985).

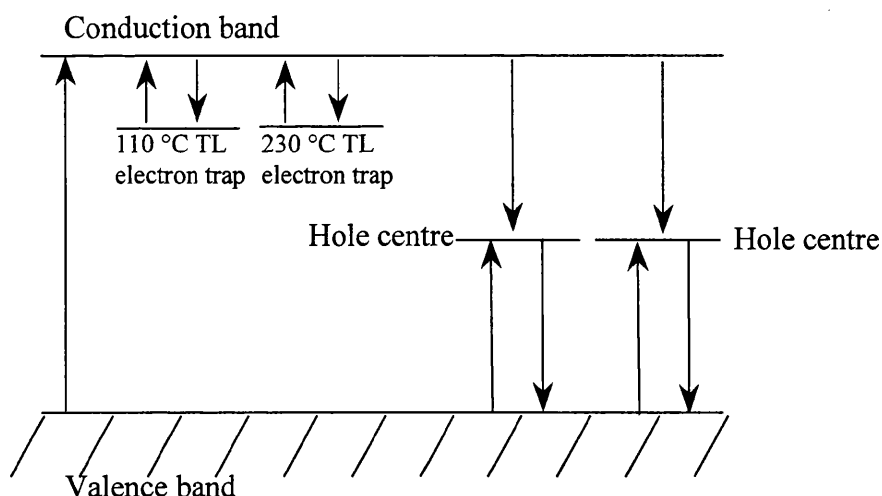


Figure 2.9: Simplified model of electron traps and centres adapted from Zimmerman (1971) and Bailey (2001)

The emission of light is also influenced by impurities within the quartz crystal. This affects the wavelength of the light which results from the recombination of electrons with the luminescence centres. Impurities documented by Anderson *et al.* (1974) include germanium (Ge), aluminium (Al), lithium (Li), sodium (Na) and iron (Fe). They found that the composition of the impurities influenced the response of quartz crystals to heating, by affecting the temperature at which recombination occurs. The $(\text{AlO}_4)^0$ and $(\text{H}_3\text{O}_4)^0$ centres have temperature thresholds that contribute to the 110 °C peak, which is the focus of the present investigation. Other recombination centres are responsible for the TL peaks at higher temperatures (Adamiec 2004). These are located within the conduction band and are activated at 230 and 330 °C, in addition to a deep thermally-disconnected electron centre from which electrons cannot be removed by heating (Bailey 2001).

One major limitation for the use of TL measurements for dating archaeological artefacts has been highlighted by Roque *et al.* (2004), and it concerns the fact that archaeological heat treatments may not have acquired sufficiently high temperatures to fully drain the traps and reset the TL signal to zero. Michab *et al.* (1998) found that to minimise the effects of previous partial heating and bleaching from exposure to sunlight, samples had to have been previously heated to temperatures >500 °C to enable confirmation of accurate dating.

There have been various attempts to ascertain previous temperatures experienced by archaeological artefacts. Melcher and Zimmerman (1977) suggested that TL could be used to determine if a chert artefact was heated to temperatures $>\sim 250\text{ }^{\circ}\text{C}$ by comparing glow curves (obtained during the measurement of the peak in $\text{TL}\chi$) of geological chert and an artefact assumed to have been heated in prehistoric times. David and Sunta (1981) suggested that previous firing temperatures of quartz artefacts could be ascertained by reference to the $110\text{ }^{\circ}\text{C}$ TL peak within a temperature range of $\pm 50\text{ }^{\circ}\text{C}$. Pavlish and Sheppard (1983) were able to distinguish between heated and unheated samples using the TL glow curves of chert. Göksu *et al.* (1989) found that the $110\text{ }^{\circ}\text{C}$ peak could be used to ascertain previous temperatures experienced by flint. However, Watson and Aitken (1985) and Koul *et al.* (1996) were unable to find evidence that the $110\text{ }^{\circ}\text{C}$ TL peak of quartz samples could be used to detect maximum firing temperatures.

The influence of previous heating temperatures had been investigated with reference to TAC by Yang and McKeever (1990), Godfrey-Smith *et al.* (2005) and Lahaye *et al.* (in press). Yang and McKeever (1990) found that the shape of TAC could help to distinguish between samples annealed at 450 and $900\text{ }^{\circ}\text{C}$. Godfrey-Smith *et al.* (2005) were able to distinguish between unheated samples and those heated to 400 and $600\text{ }^{\circ}\text{C}$. Lahaye *et al.* (in press) found that the maximum sensitivity increase in TAC could be used to ascertain previous temperatures experienced ranging between 200 - $800\text{ }^{\circ}\text{C}$.

The use of $\text{TL}\chi$ measurements in archaeological and environmental contexts for dating purposes and for identifying temperatures, to which artefacts had been exposed, highlights how the responses of $\text{TL}\chi$ to heating could potentially be useful in ascertaining the previous temperatures experienced by the soil given the long-lasting nature of the signal. However, the longevity of this modified signal could also pose a problem similar to that found with the mineral magnetic results, i.e. the signals may have been complicated by repeated burn events. Conversely, Wintle and Murray (1999) suggested that some of the $\text{TL}\chi$ changes induced by preheating to different temperatures could be reversed following storage at ambient temperature. This could also have implications for the application of this technique to determining thermal history of soil over recent and geological timescales.

2.3.6 FIRE EFFECTS ON SOIL CHEMICAL PROPERTIES

In this section the effects on soil chemical properties are reviewed. Firstly, the temperature thresholds required to modify chemical properties are presented. Secondly, a review of the effects of fire on water repellency is given in relation to the possible increased erosion that may occur due to modification of catchment hydrology.

2.3.6.1 *Chemical properties*

The chemical properties of the soil are largely determined by the geology and the above-ground biomass characteristics, with the majority of nutrients held in the vegetation tissue. This varies with ecosystem type, species and age, as demonstrated by Kauffmann (1994) through a comparison of nutrient characteristics and pools between grassland and bush ecosystems. During a fire, the chemical components within the biomass can be lost to the soil and atmosphere in a number of ways: with an estimated 50-70% of the above-ground nutrients being vaporised into the atmosphere and only 3% being deposited in the soil surface as ash (Soto *et al.* 1997), however this is likely to vary geographically. These changes are dependent on the severity of the fire. However, different thresholds exist for each element, above which the levels either increase or decline as identified in Table 2.5

Organic matter within the soil generally responds differently to fire compared to the chemical properties of the minerogenic component of the soil. Soils that have experienced low- to medium-severity fires will be dependent upon inputs of organic matter from the remaining vegetation to aid regeneration. However, high-severity burn sites require recolonization of plant communities before the re-accumulation of organic matter can begin (Soto *et al.* 1994; Haslam *et al.* 1998).

The effect of fire in reducing levels of nitrogen and phosphorus is likely to be great due to the high content of these elements within plant tissue (Leitch *et al.* 1983; Soto *et al.* 1994). The first post-fire rainfall events have a significant role in transporting nutrients, as the local topography creates strong fertility gradients between the ridge top, from which the nutrients are removed, and gully sites where they are deposited. This has been identified for dry sclerophyll forests throughout Victoria, Australia (Leitch *et al.* 1983). Gullies provide routes to accelerate the transport of chemical-

rich flows into the water cycle. The increased level of nutrients consequently reduces water quality (Leitch *et al.*, 1983; Davies 1989 quoted in Soto *et al.*, 1997) and may contribute to or cause eutrophication (Section 2.6).

Table 2.5: Effect of fire on soil chemical properties adapted from (Giovannini 1994)

| Soil chemical parameter | Temperature (°C) | General effect |
|-------------------------|------------------|----------------------|
| pH | 220 | Decrease |
| | 460 | Increase |
| | 700 | Increase (4x) |
| Organic matter content | <170 | No detectable effect |
| | 220 | Slight decrease |
| | 460 | Destroyed |
| Nitrogen | <220 | Slight decrease |
| | >220 | Sharp decrease |
| Ammonia | <220 | Increase |
| | >220 | Decrease |
| | >460 | Destroyed |
| Water extractable Ca | >220 | Increase |
| | >460 | Decrease |
| | 900 | Increase |
| Water extractable Mg | 220 | Peak |
| | >700 | Destroyed |
| Potassium | <700 | Increase |
| | >700 | Sharp decrease |
| Water extractable Na | >220 | Increase |
| | <900 | Decrease |

2.3.6.2 *Water repellency*

This section explores the influence of fire on soil water repellency (also referred to as soil hydrophobicity), a condition that causes soils to resist infiltration of water for different periods depending on naturally-induced changes to the surface. Its strength and persistence can be influenced by a number of factors: the initial soil state prior to burning, the severity and the duration of the burn. If extensive water repellency exists this can prevent infiltration of water through surface layers of the soil, this produces enhanced overland flow and accelerated soil erosion (e.g. De Bano *et al.* 1979; Sevink *et al.* 1989; Imeson *et al.* 1992; Shakesby *et al.* 2000)

2.3.6.2.1 *Moisture effect on fire*

In unburnt situations, soil moisture has been demonstrated to be a critical factor controlling water-repellent conditions, which causes it to be temporally variable in certain areas, with effects disappearing during wetter seasons (Walsh *et al.* 1994; Leighton-Boyce 2002). This explains a greater occurrence of water repellent properties in relatively warm dry climates (Shakesby and Walsh 1997), where moisture content of the soil is low due to high levels of evaporation or from the lack

of rain. A more direct association between temperature and water-repellent properties has been observed in soils that have experienced fire. During burning, organic water-repellent substances within the surface matter will either be consumed or volatilised. The vaporized substances may be transferred to lower layers in the soil by a process of 'consequential sequential translocation' (De Bano *et al.* 1976) which is caused by steep temperature gradients between the surface and lower layers of the profile, initiated as a result of the low thermal conductivity of soil (Robichaud *et al.* 2000). In the lower layers, where temperatures are sufficiently low to cause the vapours (to begin) to condense and the water repellent substances to coat the soil particles (De Bano 1981); this produces a subsurface water repellent layer that impedes water infiltration (Zierholz and Hairsine 1995; Ballard 2000). Figure 2.10 shows the water repellent layers in soil before and after the passage of a chaparral fire in California (De Bano *et al.* 1979).

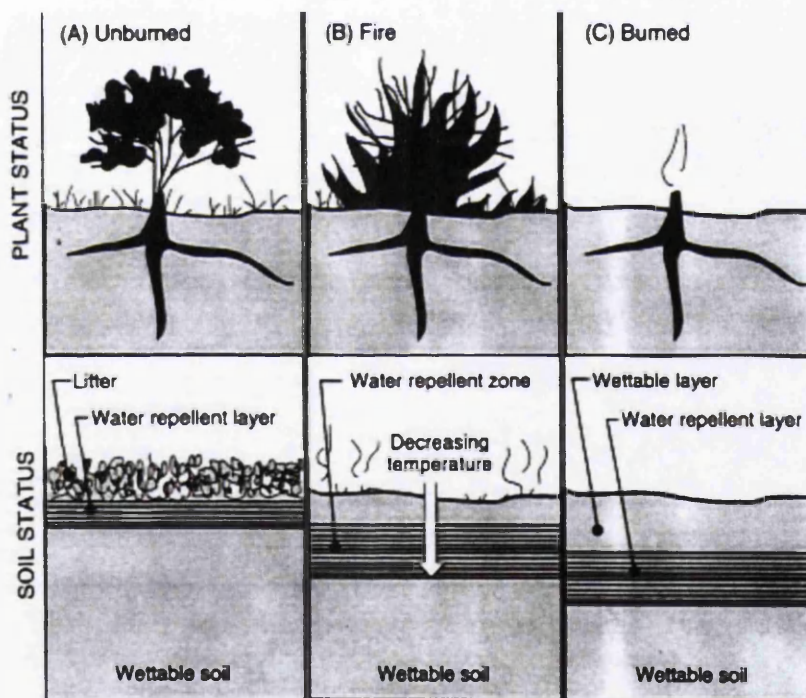


Figure 2.10: (A) Soil water-repellency in unburned brush is found in the litter, fermenting litter and mineral soil layers immediately beneath the shrub plants. (B) When fire burns, hydrophobic substances are vaporized, moving downward along temperature gradients. (C) After the fire has passed, a water repellent layer is present below and parallel to the soil surface on the burned area (De Bano 1981, 2000b).

2.3.6.2.2 *Initial soil state prior to burning*

The initial state of the soil in terms of repellency can influence how the mineral particles will react to the passage of fire. If soils are hydrophobic before the fire, then the effects of fire may appear to be negligible, as discovered in eucalypt forest soil in north-central Portugal (Leighton-Boyce 2002). However, if soils are hydrophilic prior to the fire event, repellency will be more noticeable after the burn, which exemplifies the influence of pre-burn conditions on this property.

2.3.6.2.3 *The severity of the fire*

The severity of the fire influences the degree of enhancement of hydrophobicity and the depth at which it is present (Reeder and Jurgensen 1979; De Bano 2000b). The effects of different temperatures on water-repellent properties are given in Table 2.6.

Table 2.6: Effect of temperature on the enhancement of water repellent properties (after (De Bano 1981).

| Temperature °C | Effect on soil water-repellency |
|----------------|--|
| < 175 | Little effect on water-repellency |
| 175 – 280 | Enhancement of water-repellency |
| 280 – 400 | Destruction of water-repellency due to the consumption of the organic matter |

This link between fire severity and the extent of water-repellency has recently been examined by Shakesby *et al.* (2003) for a eucalypt forest in the Nattai National Park, south-east of Lake Burragorang, southeast Australia, where evidence of the effect of different temperatures on levels of hydrophobicity was confirmed in soils that had been subjected to different levels of fire severity during the 2001/2002 bushfires.

2.3.6.2.4 *The duration of the burn*

In wildfire situations, the time for a fire-front to pass is subject to great variation. The duration of exposure to high temperatures is also of significance to the enhancement of water-repellent properties, as demonstrated in laboratory burning experiments by Robichaud and Hungerford (2000), which highlighted interactions between fire-induced heating, soil water content and soil type.

The effects of fire severity and duration of burning on repellency was explored by Doerr *et al.* (2004) through laboratory investigations. This focused on the duration of heating and fire severity on water-repellent properties of soils through ‘water-

drop penetration tests' for samples obtained from three different sites in the research area. The results obtained identified an increase of soil water repellency during heating up to temperatures of 260-340 °C, which are similar to the temperatures suggested by De Bano (1981) (Table 2.6).

2.3.6.2.5 *Longevity of fire-induced changes to soil hydrophobicity*

The longevity of fire-induced water-repellency is associated with fire severity. Cool temperatures, commonly associated with prescribed fires, give rise only to low levels of hydrophobicity. However, intense, long-term hydrophobicity, caused by high severity fire (usually wildfires) can last for a number of years and restrict vegetation regrowth (De Bano 2000b). The effects of fire on soil water-repellency were reported by Dyrness (1976) for a site in Oregon that had experienced burns of varying severity. When the lightly and heavily burnt sites were compared, the wettability during the first two years after the fire was similar. However, more lightly burnt soils recovered to the pre-burn conditions within 3-4 years after the fire, while the heavily burnt sites took 6 years to recover. The increase of time for water-repellency to become naturally re-established at the surface of the severely burnt sites may also be attributed to the fact that the temperatures reached would have destroyed the organic matter, bacteria and fungi responsible for creation of the water repellent soil coatings. Thus re-establishment of hydrophobicity would be dependent on the recovery of these properties (Widden and Parkinson 1975).

Spatial and temporal variability of water-repellent properties make it difficult to predict where or when they occur. One of the main geomorphological effects of non-wettable soils on the environment is the impact on hydrological processes. Provided the water-repellent layer is consistent and cracks or alternative flow paths provided by degraded root channels do not exist, infiltration is theoretically either impossible where hydrophobicity is apparent at the surface, or its capacity is easily reached where the water-repellent layer has been translocated to lower areas of the soil profile. This causes increased runoff and overland flow, which in turn causes erosion of the soil.

2.4 FIRE EFFECTS ON HYDROLOGY

The severity and type of burn as influenced by the factors identified in Figure 2.4 control the amount of remaining vegetation (section 2.3.1), the state of the soil properties (section 2.3.2), and the depth and consistency of the subsurface hydrophobic layer (section 2.3.5.1), which together contribute to changes within hydrological systems of a post-fire environment. The three processes of infiltration, overland flow and runoff are considered as the most important processes influencing subsequent erosion events and provide the focus for this section.

2.4.1 FIRE EFFECTS ON INFILTRATION

The rate at which infiltration may occur is dependent on the soil properties and the water content of the soil; the speed at which the water permeates through the layers will slow down over time. This is represented in Equation 2.2 (Green and Ampt 1911; Ward and Robinson 2000).

$$f_t = A + B/S_t \quad (\text{equation 2.2})$$

where f_t is the rate of infiltration (mm/s), S_t is the volume of water stored in the depth of soil saturated by infiltration at time t , and A & B are constants for given soil texture and moisture conditions.

In a post-fire environment, a major modification may be observed by reduced vegetation cover and interception of precipitation (Section 2.3.1) causing greater raindrop compaction as a result of the increased rainfall intensity at the surface. The consequence of this is to decrease the infiltration capacity of the soil and encourage enhanced surface water movement, which reduces the cohesion of loose particles. In addition, modifications to the physical and hydrophobic properties of the soil aggregates may also impede infiltration (Sections 2.3.2-2.3.3).

2.4.2 FIRE EFFECTS ON INFILTRATION

An ashy surface layer present immediately after a fire event tends initially to absorb rainfall. However, maximum absorption capacity can be reached over a short period of time during rainfall, due to the hydrophobic nature of the underlying soil. The low cohesion of the ash and the lack of protection from surface raindrop impact (to be discussed in Section 2.5.1) will loosen and disperse the fine soil and ash particles

that could have sealed the surface (De Bano 2000a). As a result, these materials are easily removed by sheet erosion, overland flow or runoff, which thus exposes the buried hydrophobic layer at the surface.

Fire-induced modifications to the microstructure of aggregates (see Section 2.3.2) depend upon the severity of the burn, the slope aspect (Cerdà *et al.* 1995) and the soil type (Scott and Burgy 1956). Heating from fire generally causes reduced aggregate stability. The decline in clay and organic matter content causes a reduction in the water retention capacity (Boix Fayos 1997). This in turn reduces storage of water in the organic horizons (Imeson *et al.* 1992) which determines the location of hydrophobic substances in burnt soils (De Bano *et al.* 1976; Martinez-Fernandez and Diaz-Pereira 1994).

The burnt soil is also susceptible to the formation of crusts and surface seals, which decrease permeability and infiltration, and can also cause increased soil erosion (Farres 1987). This will restrict vegetation re-growth by reducing infiltration and the moisture content of the soil (Andreu *et al.* 2001). The extent to which this occurs has been shown as a three to five times decrease in sorptivity and steady-state infiltration in Israel (Eldridge *et al.* 2000) and between three to six fold in the Sahel (Vandervaere *et al.* 1997). During a rainfall event, the surface area of the crust structure will decline rapidly following contact with water and an initial increase in infiltration may be observed. However, the water initiates reorganisation of soil minerals and the finer materials may clog the soil pores, causing the development of a surface seal, which will consequently reduce the infiltration rate.

The hydrophobic layer has been shown in some studies to impede infiltration seriously (Letey 2001). Where low- to medium- severity burn events have occurred, poor infiltration and rapid initiation of overland flow and runoff are evident soon after the beginning of the rainfall event. These effects result from the comparatively low temperatures being unable to initiate the processes of translocation where hydrophobic substances are moved away from the surface. However, in situations where fires of moderate to high intensity occur, the water repellent layer will have translocated to a deeper subsurface zone. The impact of this subsurface layer on infiltration can be seen in Figure 2.10 where the water is able to permeate the

uppermost hydrophilic layer and travel through the soil profile until it reaches the hydrophobic layer where throughflow or ponding may occur. An analogy can be drawn between this and water travelling through a profile that has coarse permeable sandy soil overlying an impervious clay layer.

2.4.2.1 *The relevance of macro-pores to infiltration processes*

Water movement through the soil (through-flow) initiated at the interface between the hydrophilic and hydrophobic layer will continue until it reaches discontinuities in the water repellent layer, caused by localised differences in fire intensity, cracks or holes from degraded root channels (Dekker and Jungerius 1990; Imeson *et al.* 1992; Shakesby *et al.* 2000). The macro-pores around the plants provide an alternative way of transporting water downwards through the soil profile at burnt and unburnt sites. At burnt locations, where there is minimal leaf litter, macro-pores do not become blocked, thus enabling interception of the overland flow and consequently aiding infiltrating water to pass by the water-repellent layer (Imeson *et al.* 1992).

Roots within soil aid structural stability and might be expected to improve infiltration. However, their effects upon infiltration can also be negative. As the root grows, it requires more space within the soil and compresses soil pores, increasing bulk density and reducing the soil's saturated conductivity (Edwards *et al.* 1996). These effects need to be weighted against the beneficial effects of plants in encouraging infiltration. For example, at unburnt sites leaf interception of rainfall is relatively high. When the plant dies or is burnt by fire, the root decomposes but the modifications to the soil structure remain. Cavities left by the degraded roots improve infiltration by providing channels that transport the water quickly through the soil profile. Vegetation growth and decay cycles within the environment work together to create an equilibrium situation with regard to infiltration; the negative implications of root growth on soil structure, with respect to infiltration, are being compensated by the positive effects of decaying roots (Barley 1954).

Alternative routes for channelling water can be provided by faunal activity, as evident in New South Wales, Australia, where extensive networks built by ants provide routeways for good drainage (Paton *et al.* 1995). The actual pattern of

infiltration remains largely unaffected by fire, although the amounts of water involved change. Where infiltration is not possible, alternative routes are used and flow is concentrated through a few preferred paths such as root channels (Martin and Moody 2001).

The literature discussed has highlighted the main soil modifications that affect infiltration processes in a post-fire environment. There is general agreement that burning tends to reduce infiltration capacity (Cerdà *et al.* 1995). This influences overland flow and runoff processes as discussed in the next section.

2.4.3 OVERLAND FLOW AND RUNOFF

Overland flow is water that travels over the ground surface and into stream channels (Ward and Robinson 2000). Referring to the discussion on infiltration above, this process can take one of two forms: saturation overland flow occurs where shallow water tables rise to the ground surface during rainfall or throughflow events, causing infiltration capacity to be zero (Ward and Robinson 2000). Hortonian overland flow, on the other hand, occurs when rainfall intensity exceeds the infiltration capacity of the ground surface. The latter can be calculated by subtracting infiltration capacity from rainfall intensity. Where the difference is positive, overland flow will be generated (Kirkby 2000). The rainfall patterns and ground conditions are highly influential in determining which of these processes is dominant.

Throughflow and overland flow are runoff processes of water movement through and over soil and may be apparent to the extent that virtually all runoff will be in the form of overland flow, as is typical of semi-arid grasslands and shrub-covered hillslopes (Abrahams *et al.* 1994). Runoff can occur as streamflow, river discharge, or catchment yield and comprises water moving in channels that vary in size from 'trickles' to rivers (Ward and Robinson 2000). As the processes of overland flow and runoff are closely interlinked, the modifications within a post-fire environment will be discussed together in this section.

Overland flow and runoff processes are affected by a number of site-specific factors. The gradient of the slope will affect the infiltration capacity of the soil, as water will run over the surface as overland flow instead of being channelled through cracks and

macropores. In addition, infiltration potential will be influenced by the nature of the surface. A 'rough' surface will slow the flow velocity and increase the likelihood of penetration into the soil, causing the water to have a lower erosive potential. Forest areas that are subjected to slash burning and logging, (especially the logging paths) are likely to experience a high level of overland flow, as these are greatly compacted areas, where infiltration will be minimal (Scott 1997).

The development of a fire-induced subsurface hydrophobic layer can have varying effects on the infiltration patterns within the soil. There is disagreement in the literature concerning the impact of fire on overland flow and runoff. The main points arising are: (i) fire can decrease infiltration and increase runoff and soil loss (Chartres and Mucher 1989; Coelho *et al.* 1990), evidence of this was found for example at a burnt site in Oregon, where the effects of fire-induced water-repellency were long-lived and apparent for up to 5 years after the burn (Dyrness 1976); (ii) the impact on runoff and erosion is short-lived, with water-repellency declining to levels recognised at unburnt sites after the first rainfall event (Mc Nabb *et al.* 1989), alternatively, water-repellency declines within the first year after the fire, as evident in a site in upper Michigan (Reeder and Jurgensen 1979); (iii) macropores provide channels within the soil that allow infiltration to occur, so that localised runoff and overland flow may be evident, but only over a short distance (Kutiel and Inbar 1993). This was a conclusion drawn for example by Leighton-Boyce (2002) who found that on long-unburnt hydrophobic soils, overland flow responses were 16 times greater (with a mean coefficient of 33%) than those experienced on hydrophilic soils. However, the results obtained at a newly burnt site showed that where there were wettable conditions, no overland flow was generated, but where the soil was repellent, the mean overland flow coefficient was up to 70%.

The differences relating to the impact of fire on overland flow and runoff in the literature may have been caused by site-specific factors or variance in fire severity. At the current time, option (iii) seems to be the most likely, as the effect of macropores has been recognised by a number of authors. However, additional factors such as the time interval between the burn and rainfall event may be important, as the most pronounced effects will be apparent immediately following a fire or storms. It is generally agreed that there is an increased likelihood of the development of

overland flow and runoff processes after intense rainfall. The increased volume of flow increases the rate of delivery of water to stream channels, which in turn also increases the erosive capacity of the flow (see Section 2.5) (De Bano *et al.* 1976; Scott 1993).

The variation in the results in literature may be attributed to a number of factors. The severity of the fire is likely to be spatially variable (caused by factors identified in Section 2.2.2). This means that the water-repellent substances may be translocated to varying depths according to temperature differences. These variations with depth will cause discontinuities in the water-repellent layer, complicating the likely overland flow and runoff processes that occur and minimising the effect on infiltration. They will also reduce the likelihood of overland flow generation (Kutiel *et al.* 1995). The severity of the fire will also determine the effect of modifications on the soil properties (see Section 2.3.2) and vegetation (see Section 2.3.1). The reduced vegetation cover will tend to increase the volume and intensity of rain impacting on the surface, which will reduce levels of infiltration and cause the development of Hortonian overland flow at times of intense rainfall.

2.5 FIRE EFFECTS ON SOIL EROSION

This section reports the hydrogeomorphological processes in post-fire environments. The interlinked nature of burn effects on vegetation and soil properties has significant implications on hydrology and erosion at the slope scale which can be identified through various parameters. These effects are highlighted in this section as they are considered an important part of this research. Interactions between the erodibility of soil (the resistance of the soil to both detachment and transport) (Morgan 1979), and the erosivity of rainfall acting upon it will strongly influence the rate of erosion (Thomas 1993).

Fire has been identified in many studies as causing increased levels of erosion. Higher levels of detachment can be attributed to changes to the environment through burning, such as the removal of vegetation, modifications to the hydrophobic, physical and chemical properties of the soil. This has consequent implications for hydrological processes including infiltration and overlandflow (see Sections 2.4). These variables are controlled by the severity of the fire, which in conjunction with

the characteristics of the post-fire rainfall event, is recognised as the main factor influencing levels of erosion (Soler *et al.* 1994; Rubio *et al.* 1997).

The above-mentioned effects of fire on hydrologic processes can be seen to be important in increased post-fire erosion after the 1994 forest fires in the Sydney region, where a high intensity storm occurred soon after a fire event. This rainfall pattern, in addition to modifications to the soil properties induced by fire and large amounts of exposed parent rock caused infiltration to be minimal, leading to the generation of large quantities of overland flow and runoff. Although faster and high-energy flows were created, areas where the remaining vegetation had a dense root format provided resistance to erosion. Areas where the soil was compacted, such as adjacent to walking tracks and fire trails were subjected to major rilling and gullyng (Zierholz and Hairsine 1995). This study provided a comprehensive overview of observed modifications to the post-fire environment, although no quantitative data were included to support the view of major erosion.

Erosion following the 2001/2002 fires in the Lake Burrorang catchment has been reported in a number of publications published by members of the NERC-funded project (Shakesby *et al.* 2003; Blake *et al.* 2004; Chafer *et al.* 2004; Doerr *et al.* 2004; Shakesby *et al.* 2004; Blake *et al.* 2005b; English *et al.* 2005; Blake *et al.* 2006a; Blake *et al.* 2006b; Blake *et al.* 2006c; Doerr *et al.* In press; Shakesby *et al.* in press). Details of these investigations are presented in Section 3.10.

2.5.1 RAINSPASH DETACHMENT

Reduction of vegetation cover by fire (Section 2.3.1) causes rainsplash detachment to have greater significance than in unburnt areas, because of an increased proportion of rainfall impacting directly on the surface. However, the effectiveness of this mechanism must be related to the characteristics of the rainfall event. For example, intense storms are likely to produce raindrops of greater volume, which will affect the terminal velocity and kinetic energy of the drop and determine the level of consolidation and dispersal that will occur on impact with the surface (White *et al.* 1998) (Figure 2.11). Dispersal of soil particles can also occur through the transfer of the kinetic energy to the loose sediment particles lying on the surface, which rebound into the air and transfer their momentum to other particles on

landing, repeating the process. On a slope, the gradient increases the down-slope movement of soil particles when compared to upslope movement due to the gravitational influence (Figure 2.11) (White *et al.* 1998).

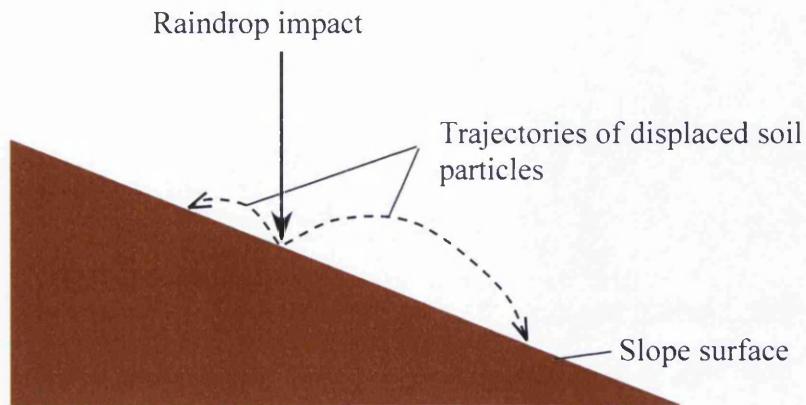


Figure 2.11 Schematic diagram of the displacement of particles by rainsplash (White *et al.* 1998).

The effect of water repellent conditions near the soil surface (associated with low intensity fires) enhances the impact of a raindrop. The contact of a raindrop with the surface of hydrophobic soil disturbs the water-repellent film or protective surface crust (Jungerius and Harkel 1994) which exposes the dry, non-cohesive and easily detachable particles, which can then be displaced and carried by splash ejection droplets. Terry and Shakesby (1993) demonstrated in laboratory experiments for non-aggregated soil samples that the erosive effect of raindrop impact was greater for water-repellent than for non-repellent soils.

Rainsplash detachment has been identified as a major factor in erosive processes. Many studies use a rainfall simulator to try to replicate the effects of a storm event both in field and laboratory situations (Slattery and Bryan 1994; Benavides-Solorio and MacDonald 2001; Johansen *et al.* 2001; Leighton-Boyce 2002). Although this is a very effective method of creating rain when and where it is needed, usually the intensity of the rain remains constant and drops tend to be of the same dimension. This does not occur in reality and hence the results obtained from these studies are unlikely to be representative of natural conditions. Although assessment of erosion under natural conditions is preferable, the rainsplash simulator provides an efficient and reliable means of creating rain under both field and laboratory conditions.

2.5.2 OVERLAND FLOW, RILL AND GULLY DEVELOPMENT

The process of overland flow (as discussed in Section 2.4.2) applies a shear stress to the particles, which is proportional to the velocity of the flow. Rills and gullies may be formed where flow is concentrated into a particular area. The main difference between these features is their size (Morgan 1979), but processes operating in gullies can also differ from processes in rills. Imeson and Kwaad (1980) stated that gullies resemble river valleys, while rills resemble river channels in their behaviour. Kalman (1976) stated that rills are in principle self-stabilising, while gullies are not. Rills are most likely to be formed by overland flow erosion, but gullies can develop in several ways (Hessel 2002).

Resistance to the movement of the particle by the flow depends on the frictional resistance between the particle and the surface on which it rests and the extent to which it is embedded in the surface. Manning's equation (Equation 2.3) quantifies the resistance coefficient (Knighton 1998; Richards 2000).

$$n = k \frac{R^{2/3} s^{1/2}}{v}$$

(equation 2.3)

where n = Manning roughness coefficient (a general measure of channel resistance which ranges from 0.03 for smooth Sections to 0.10 for rocky or heavily vegetated Sections), k = variation of measurement system (1 for SI units), R = Hydraulic radius (mean depth (m) in wide channels), s = slope ($m\ m^{-1}$) and v = velocity ($m^3\ s^{-1}$)

This equation highlights the relevance of the surface roughness and texture. Coarse-textured surfaces reduce the flow velocity of water due to increased energy loss through turbulence, which subsequently reduces the flow's erosive capacity. Caution should be applied when using this equation as surface roughness (n) is not a constant and can be reduced by erosion or weathering.

The combination of heavy rain, hydrophobic soil and reduced vegetation cover at a burnt site can encourage rilling and gullying, especially where surface flows of water are concentrated (Zierholz and Hairsine 1995). The development of post-fire rills up to 60 cm deep was formed on walking tracks in the northeastern part of the Royal National Park, South Sydney region of Australia (Atkinson 1984). Rilling in

a post-fire environment occurs through the following pattern of events: firstly, the top layer of the soil becomes saturated as the water builds up at the subsurface hydrophobic layer, causing the soil to become fluid due to the increased pore pressure. This creates a failure zone between the boundary of the hydrophilic and hydrophobic layers. The fluid zone begins to move as a result of gravity, taking the overlying, saturated material with it. The water repellent layer is left open to erosion from rainsplash and subjected to constant wetting. Once these erosive processes have degraded the hydrophobic layer, the easily damaged underlying dry soil is removed relatively rapidly and rills tend to develop (Figure 2.12; adapted from Wells, 1987; De Bano, 2000).

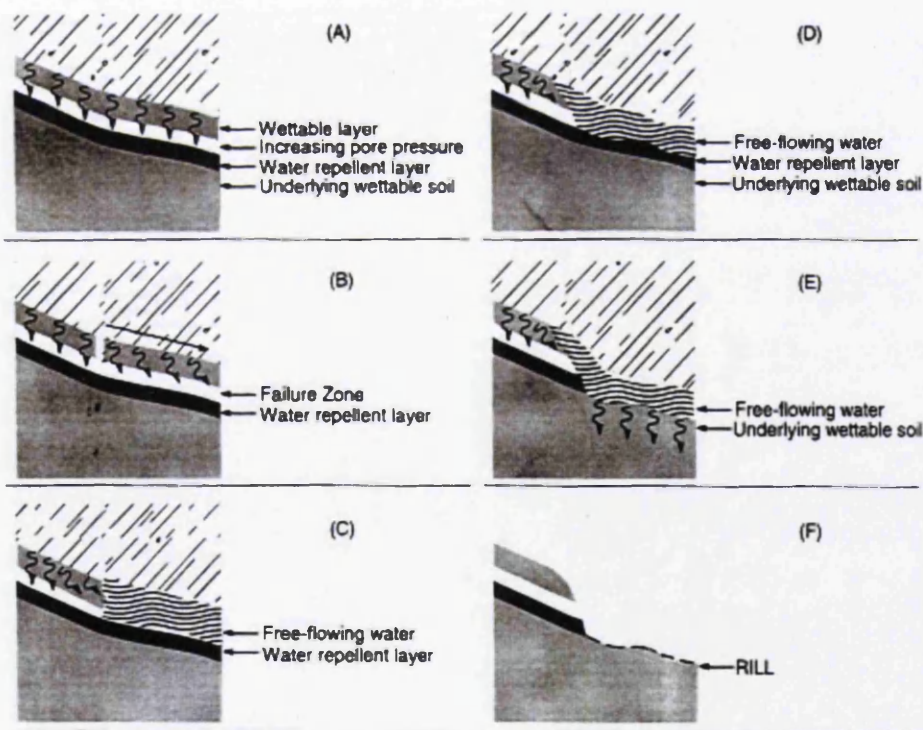


Figure 2.12: Rill formation during rainstorms following fire involves: (A) saturation of the wettable soil surface; (B) a failure at the boundary between wettable and water repellent layers; (C) loss of the wettable surface layer with the flow of water over the water repellent layer; (D) erosion of the water repellent layer; (E) erosion through the water repellent layer and infiltration into the underlying wettable soil; and (F) development of a well-defined rill (adapted from Wells, 1987; De Bano, 2000).

Once rills have been created, they provide efficient channels to move sediment to lower parts of a slope, where the material may either be deposited within alluvial fans or flow into the channels of the stream (Benda *et al.* 2003). (The impacts of increased sediment supply and yields are discussed further in Section 2.6.)

2.5.3 OTHER FIRE-INDUCED EROSIONAL EFFECTS

2.5.3.1 *Wind erosion*

Long dry periods after fire will subject the burnt material to more effective dispersal by the wind (Kutiel and Inbar 1993). As already mentioned, rainfall soon after the fire event will wash some burnt material down-slope. The potential effect of wind on bare soil can have very significant erosive consequences, as was demonstrated in the monitored erosion that followed the 1983 Sydney bushfires. Wind erosion following these fires caused sand from the burnt area to pile up to a height of 8m against obstructions (Atkinson 1984).

2.5.3.2 *Mass wasting*

Mass wasting is a term that refers to the “ processes causing down-slope movement of material under the influence of gravity, and is common in steep mountainous areas” (Wilson 2003 p.391). Creep, flow, slide, fall or subsidence mechanisms can activate the mass movement of material (Summerfield 1991). Severe fires potentially increase the frequency and magnitude of a variety of episodic mass-wasting events by reducing slope stability. Post-fire debris-slides and debris-flows are the most frequently studied forms of mass-wasting, although other processes have also been observed.

2.5.3.3 *Dry ravel*

This is the downhill movement of surface material, rock and debris in a dry-state under the influence of gravity. As with aeolian erosion, this process is not dependent on post-fire storm events (Wondzell and King 2003) and it is the only form of mass wasting that acts independently of rain. Burning removes protective layers of litter and vegetation that stabilize soil, reducing aggregate stability and removing obstacles that prevent movement of material (Section 2.3.2). In addition to the influence of hydrophobicity, fire causes soil to have a lower bulk density and encourages development of dry creep processes, especially on steep slopes

(Krammes and Osborn 1968; Mc Nabb et al. 1989). The extent of the influence of dry ravel on erosion and sedimentation processes was demonstrated after the Wheeler Fire in July 1985 of Matilija Creek, near Ventura, California, where $0.29 \text{ m}^3/\text{km}^2/\text{month}$ of fine gravel was delivered to the channel by the processes of dry ravel. The impact of this was evident in the river, as the first flow after the fire deposited 550 m^3 of fine gravel over 270m, of which 90% was estimated to have been caused by dry ravel on the hillslope (Florsheim et al. 1991).

2.5.3.4 *Debris flows*

These are laminar, sediment gravity flows with a high debris concentration (Matthews 2002). Debris flows can be initiated by either surface runoff or by debris slides. Runoff-initiated flows develop as an extension to the rill or gully formation process, where the water travelling through the channels has sufficient velocity to entrain the quantity of sediment required to form a debris flow. Alternatively the additional sediment may be obtained through channel bank erosion (Wondzell and King 2003). Hydrophobicity is also thought to contribute towards runoff-initiated debris flow in locations where water repellent conditions are integral to the formation of rills and gullies (Section 2.5.2) (De Bano 2000c). However, water repellent conditions are not vital to the formation of debris flows (Cannon and Reneau 2000; Cannon *et al.* 2001).

In addition, debris slides can occur during major storm events when a large quantity of sediment moves en masse on steep hillslopes (Wondzell and King 2003). A combination of the mechanisms and processes mentioned within this section all contribute towards the development of these flows. The extent of material moved by this process was demonstrated following a fire at Storm King Mountain, Colorado in 1994. Rills, gullies and sheetwash-generated debris-flows were formed during a storm event that occurred two months after the fire. The result was 14 ha of highway engulfed by $70,000 \text{ m}^3$ of debris from the surrounding hillslopes (Cannon *et al.* 1998).

2.5.4 FIRE EFFECTS ON EROSION AT THE SLOPE SCALE

Visual evidence of erosion by mass movement processes and material movement can be identified through the development of various features at a slope scale, such as the exposure of soil pedestals and roots, evidence of modified rill and gully systems or disturbance by bioturbation. Evidence of these effects have been identified for the Blue Gum Creek catchment in the Nattai National Park, south-west Sydney by Shakesby *et al.* (2003) after fires of different severities that occurred after the 2001/2002 fires provided an opportunity to investigate water repellency, erosion and sedimentation.

2.5.4.1 *Pedestals and exposed roots*

In post-fire environments, soil pedestals and exposed roots resulting from post-burn erosion are caused by rainsplash removing soil around stones and roots to have columns and ridges of soil capped by these protective features. Slope erosion can be recognised on the slope's large features such as trees, by estimating the volume of material lost from depressions caused by 'the waterfall effect' (Stocking and Murnaghan 2001). This can also be assessed to determine an average volume of soil loss, which can be converted to tonnes/ha equivalent and erosion levels at slope scale. Measurement of a 'waterfall effect' from depressions below large obstacles can provide a crude estimate of the amount of material movement at certain points of the slope. However, this is not fully representative of all erosion mechanisms because it only considers scouring behind obstacles. Despite this, if the erosion has already occurred, a suggestion of the level of the disturbance in the post-fire environment can be ascertained. However, when this information is combined with other slope research techniques the information can provide useful.

2.5.4.2 *Litter dams*

Litter dams are common features that occur globally on both steep and gentle slopes (Eddy *et al.*, 1999). In post-fire environments they are formed where sediment and /or organic matter that is carried by overland flow meets an obstacle and down-slope movement of the material is prohibited. This causes sediment build-up through deposition, initiating the formation of what are called 'litter dams'. These areas of accumulation can continue to develop and create a sheltered area where vegetation becomes re-established which will lead to succession and re-colonisation of both

flora and fauna. Where material has built up against the dam the ground level will be raised in comparison to the slope below the dam, which creates features known as 'microterraces'. These are enhanced by erosion in areas where water is able to pass through the dam. The stages in litter dam and microterrace evolution are shown in Figure 2.13 (Mitchell and Humphreys 1987).

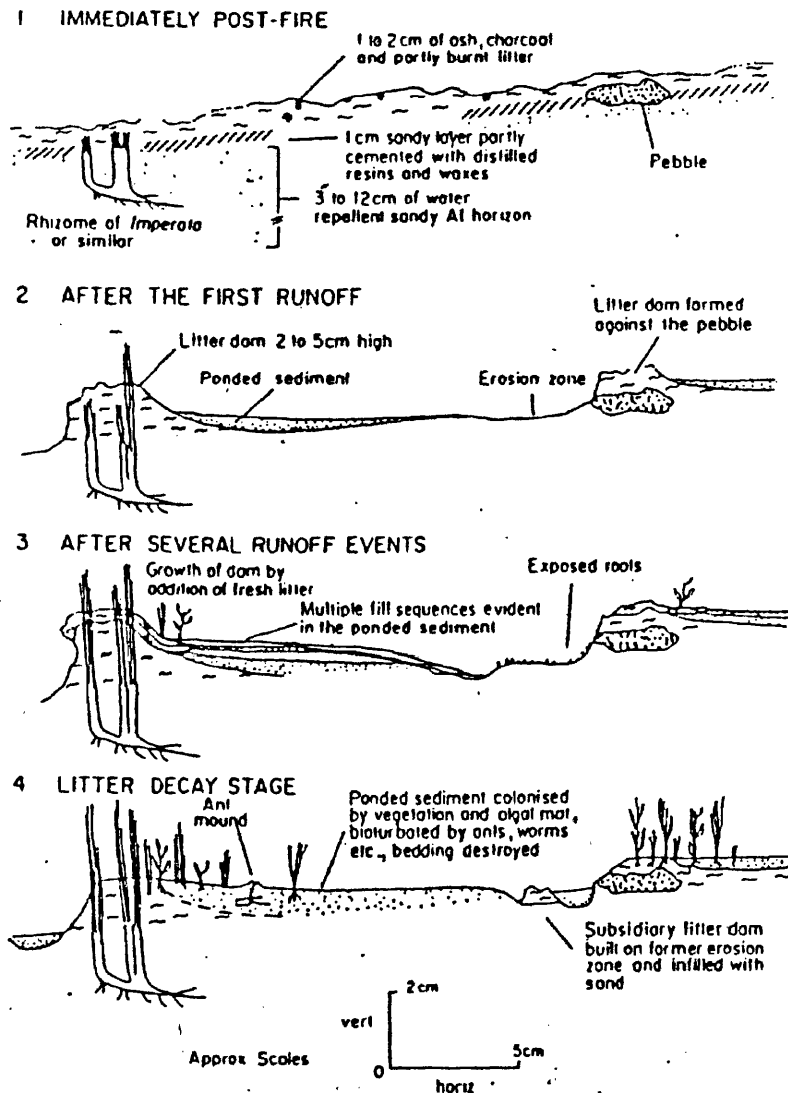


Figure 2.13: Formation of litter dams after fire in the Sydney Basin, Australia (Mitchell and Humphreys 1987).

2.5.4.3 Bioturbation

Other evidence of material movement, by faunal activity, is termed biotransfer of sediment. This produces accentuated downslope surface movement (Dragovich and Morris 2002). In many cases the activities of invertebrates are acknowledged as being essential to the development of the soil through improving its structure by aerating the compacted mineral component of the soil and digesting and mixing organic matter.

The post-fire activity of animals and invertebrates is dependent on the severity of the fire. During the actual burn event the majority of animals are able to move fast enough to escape the fire, whilst the invertebrates are able to survive by moving to lower cooler layers of the soil until the fire passes (Neary *et al.* 1999). High-severity burns have the greatest impact upon the numbers of species able to survive and begin to re-colonise. Recovery of the microbial community is essential to the regeneration of the soil and occurs relatively rapidly following the burn event (Fritze *et al.* 1992 quoted in Haslam *et al.* (1998)), in comparison to the varied response of invertebrates (Whelan 1995; Haslam *et al.* 1998). The rate at which mammals return will be determined by the condition of the habitat. However, animal activity may also hinder regeneration, by consuming new shoots.

Dragovich and Morris (2002) reported biotransfer in a burnt eucalypt forest in south-eastern Australia. They reported relatively little disturbance in areas that had experienced high severity fires. Conversely, high levels of faunal activity were observed in moderately burnt areas, which accounted for 36% of the sediment collected. In their study, the influence of ant mounds and animal scrapings was the prominent factor in loosening the surface soil, making it more susceptible to erosion by overland flow. However, as mentioned in Section 2.4.2.1, the networks created by ants actually improve infiltration and have been observed to cover approximately 20% of the ground surface (Paton *et al.* 1995). Other studies of the effects of faunal activity in Australia have reported that lyrebird scratchings (Dragovich and Morris 2002), goanna activity (Whitford 1998), bandicoot scrapings and the burrowing activity of woylies (*Bettongia penicillata*) (Garkaklis *et al.* 2000) contribute to the process of bio-transfer.

2.6 TRANSPORTATION AND DEPOSITION OF ERODED BURNT MATERIAL AND SEDIMENTS

The focus of the review now extends from the slope to the catchment scale, identifying potential movement of material through rivers and into large bodies of water such as lakes and reservoirs. The quantity of sediment entering a reservoir is dependent upon physical characteristics of the local catchment in terms of geology, topography, size and vegetation cover and climate. Geology will influence the ease with which the underlying bedrock will be eroded. The effect of fire on different soil particles or source material such as sand and clay aggregates is discussed in Section 2.3.2. However, the effects of fire on the generally stable sandstone of the Sydney Basin have been shown to cause an acceleration of weathering (Nanson and Young 1983). In addition to geology, the relief of the land will influence the extent to which gravity aids material in a down-slope direction. Erosion that occurs after a fire (Section 2.5) transports easily dislodged slope material by entrainment within overland flow and stream water flows. The reduced amount of vegetation interception enables rainsplash detachment to be more effective and the surface water to reach higher velocities, which causes a greater erosive and transport effect.

The sediment may be moved to land-based sinks and stores or to stream and river channels and may undergo various stages before finally being deposited in reservoirs or estuaries. These processes can be identified as: (i) entrainment as a result of increased flow velocity; (ii) transportation and deposition through the river system; (iii) deposition at the delta; and (iv) movement within lake and reservoir environments. The effects of increased quantities of sediment entering lakes and reservoirs are discussed with respect to modelling its distribution and the problems these cause, and its implications for water quality.

2.6.1 ENTRAINMENT AS A RESULT OF INCREASED FLOW VELOCITY

The initial entrainment of particles within the flow of a stream occurs as a result of the increased forces acting against the critical shear stress of individual immobile grains. This is caused by the difference in flow velocity between the top and the bottom of the grain, giving lift and the effect of eddies. For the particle to remain in suspension, the vector of the horizontal and uplift forces must exceed the downward forces imposed by gravity. This is dependent on the flow velocity remaining above a

certain threshold, and is determined by grain size and density as identified in Figure 2.14 (Hjulstrom 1935; Knighton 1998).

Following a fire event, the reduced vegetation interception and potential strengthening of the water repellent properties of soil causes the infiltration capacity of the soil to be quickly reached by post-fire rainfall. This means that overland flows are able to reach higher velocities than experienced in unburnt areas due to the lack of obstacles in the flow path and a larger volume of water reducing relative friction, enabling the flow to have a greater capacity to carry material (Figure 2.14).

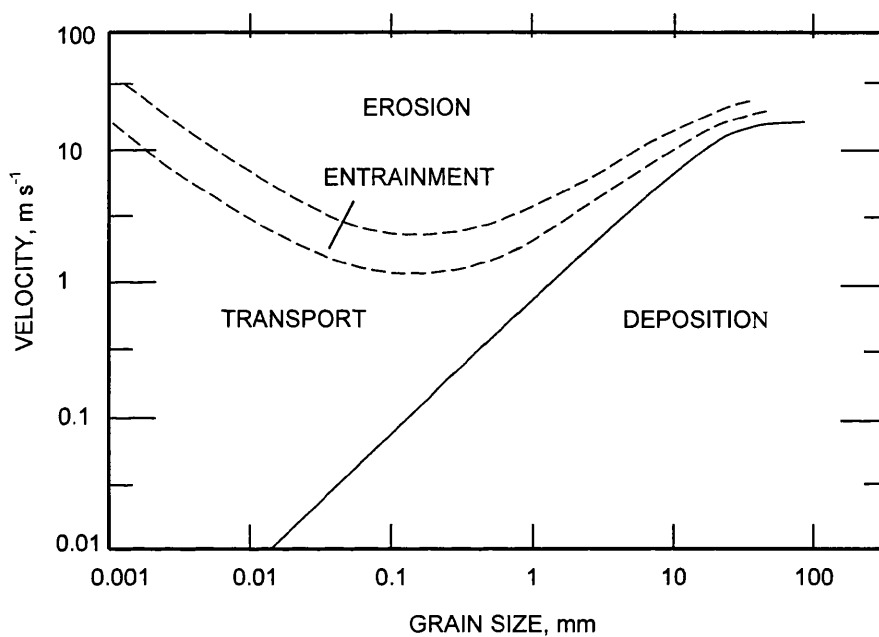


Figure 2.14: Erosion and deposition thresholds in relation to flow velocity (Hjulstrom 1935; Knighton 1998).

2.6.2 RESPONSE OF HYDROLOGIC MECHANISMS IN A POST-FIRE ENVIRONMENT

The first substantial rainfall event after an area has been burnt will initiate an influx of sediment from the easily degraded slope material onto floodplains (Gottschalk 1964) and into channels, which may be subject to terracing due to the greater velocity of the flow (Figure 2.14) (Laird and Harvey 1986; Heede *et al.* 1988; Legleiter *et al.* 2002; Benda *et al.* 2003). The quantity of material moved and the duration of the rainstorm will determine the distance that the sediment is transported. The discharge is ultimately determined by the pattern of the rainfall event, as a moderate to high intensity storm after a fire can cause pulses of water to enter channels and rivers (Miller *et al.* 2003). The increased stream velocity after

rainfall following a fire was demonstrated by an estimated increase of 66% in the median stream power in a river in Yellowstone National Park, USA, in a drainage area that had experienced a 10% burn (Legleiter *et al.* 2002). Brown (1972) compared storm hydrographs of unburnt and burnt sites in the dry and wet sclerophyll eucalypt forests of southeastern New South Wales, Australia. He identified sharp peaks in river storm hydrographs of post-fire areas in comparison to gently curved peaks of unburnt sites. With reference to Figure 2.14, the higher rate of flow had a greater potential to transport more material, thus increasing the amount of particulate material reaching the outlet of the drainage basin (the sediment yield) (Walling 2000). The increased sediment yield in post-fire environments due to increased flow velocity has been well documented, as shown in Table 2.7.

Despite evidence confirming the relationship between increased flow velocity and sediment yield, caution should be applied, as inconsistencies exist in the literature concerning erosion and sediment yield in unburnt situations. Langbein (1958) associated maximum sediment yield with low precipitation and Douglas (1967) demonstrated that annual sediment yield could vary up to a factor of five when comparing a number of rivers. This provides a possible explanation for the inconsistencies in the literature regarding sediment yield, while highlighting the importance of referring to long-term data when considering historical processes. Olive (1985) concluded that there was no single constant relationship between discharge and suspended sediment concentration in a study of five rivers in New South Wales, Australia. This was attributed to storm pattern and subsequent runoff and initial soil moisture conditions (Loughran 1977). Variations in sediment yield in the post-fire period are determined by the rainfall patterns. In Australia, rainfall is influenced by the behaviour of the Southern Oscillation Index, which determines the prevalence of either flood-dominated regimes (FDR) or drought-dominated regimes (DDR), (discussed in Section 3.8) (Warner 1987; Erskine and Warner 1988). Differences in the rates of erosion could also be due to variation of sediment storage in sinks and stores on slope and within river channels amongst other factors (Section 2.5). Major erosion and transport of sediment within the Lake Burragorang catchment has recently been attributed to catastrophic flood events which are not wholly dependent on fire events (Tomkins *et al.* in press).

Table 2.7: Responses of sediment yields to fire events

| Location | Fire details | Rainfall | Rate of flow | | change | | Sediment yield / load | | | Time after fire | Duration of recovery | Reference |
|---|---------------------------------------|----------|---------------|---------------|-----------------|-----------------|-----------------------|--|--------------------|-----------------|----------------------|-----------------------|
| | | | Before | after | change | change | Before | after | change | | | |
| Sydney, NSW Hawkesbury sandstone catchment | Moderately intense | Low | | | | | | 2.5-8.0 t/ha/yr 0.25-0.82 kg/m ² /y | | | 1 year study | (Blong et al. 1982) |
| | | Average | | | | | | Est 20 t/ha/yr | | | | |
| Sydney, NSW Hawkesbury sandstone catchment | | | | | | | | 48,000 kg/ha/yr | | | | (Atkinson 1984) |
| New Mexico | 60% burnt | | | | 100% greater | | | 98,000 mg/l | | 0 yrs | 2-3 yrs | (Bolin and Ward 1987) |
| | | | | | | | | 600 mg/l | | 2 yrs | | |
| Snowey Mountains, NSW, Australia | Severe fire miles ² 280 | | 220 cusecs | 116 cusecs | 104 cusecs | 178 tons/day | 451,000 tons/day | | 44,922 tons/day | Unknown | 4-5 years | (Brown 1972) |

Table 2.7 continued: Responses of sediment yields to fire environments

| Location | Fire details | Rainfall | Rate of flow | | | Sediment yield / load | | | Time after fire | Duration of recovery | Reference |
|---|---|---------------------------------|----------------|------------------------|--------|-----------------------|----------------------------|----------|-----------------|----------------------|--|
| | | | before | after | change | before | after | change | | | |
| NSW, Sydney | Varying severity 3300ha land severely burnt | 80 mm | 0.01 cumecs | 0.096 cumecs | | | 196mg/l | | 3 months | | (Burgess et al. 1980; Burgess et al. 1981) |
| | | | | 0.277 cumecs | | | 283 mg/l | | | | |
| | | | | 0.077 | | | 107mg/l | | 5 months | | |
| | | | | 0.101 cumecs | | | 103mg/l | | | | |
| | | | | 0.118 cumecs | | | 124mg/l | | | | |
| Southern California, Wheeler fire | Severely burnt | 1 st event 110 mm | | 2.1m ³ /s | | | 550 m ³ | | 6 months | 2 years | (Florsheim and Keller 1987; Florsheim et al. 1991) |
| | | 2 nd event 325 mm | | 2.5m ³ /s | | | Above deposits moved | | 7 months | | |
| Colorado Front Range, pine and fir forest | 4690 ha burnt | 90 mm/ha | | 24m ³ /kg | | | | 200 x | 0 years | | (Moody and Martin 2001b; Moody and Martin 2001c) |
| | | 50 mm/ha | | 6.6m ³ /kg | | | | increase | 0 years | | |
| | | 50 mm/ha | | 0.11m ³ /kg | | | | | 3 years | | |

2.6.3 TRANSPORTATION THROUGH THE RIVER SYSTEM

Forest fires initiate a complex set of responses within river channel patterns and forms, which are largely determined by: (i) rainfall events; (ii) slope state; and (iii) fire return interval. Rainstorms of high intensity but comparatively low duration will have a greater ability to transport larger quantities of material than low intensity rain, due to the increased velocity of the resulting stream flow, caused by the larger volume of water at the surface. The slope state refers to the degree of recovery of the vegetation over time. As regeneration becomes more established, less material will be eroded from the surface as it is trapped by vegetation.

At certain points in the channel, for example where it widens or meanders, the velocity of the flow will lessen, causing material to be deposited. In studies that have investigated the response of river channels to fire within a catchment, an initial aggradation of the upper reaches has been observed. After the flow has deposited material, it will still have energy to degrade the lower reaches of a channel. Aggradation of the upper channel will continue for as long as the increased supply persists (Erskine and Melville 1983).

The rapid regeneration of pyrogenic vegetation will provide better ground protection than existed before the fire. This will gradually minimise the amount of material moved. As a result, the inflowing water to the channel will have a reduced sediment yield due to increased obstructions slowing flow velocity and energy with which to erode the upper reaches, causing subsequent aggradation of the middle reaches (Heede *et al.* 1988). This is evidence of the system working to maintain a state of equilibrium. Visual evidence of river response to an influx of sediment may be observed through the development of meandering and reduced pool density (Einstein 1951; Lewin 1983; Florsheim *et al.* 1991) or braiding to dissipate large amounts of energy (Annandale 1987).

2.6.4 DELTA DEPOSITION

A delta begins to develop at the point where the river begins to widen to form a lake, reservoir or estuary; the wetted perimeter of the channel will increase and cause a reduction in flow velocity. This will initiate deposition of progressively finer material away from the source in accordance with Hjulstrom's (1935) thresholds of erosion and deposition (Figure 2.14), which will create a deltaic form, with the

shape determined by the stream power. For example, a low velocity flow will create a steep change in sediment supply, as a lot of material will be deposited at the inflow (Annandale 1985).

The effect of increased sediment transported to a delta in post-fire environments will be seen in the form of greater aggradation and a protrusion of the material into the lake or reservoir. There are only a few studies that have investigated fire deposits within reservoirs, Moody and Martin (2001b) examined the location and thickness of wildfire related sediment deposits on delta formation in Strontia Springs Reservoir, Colorado. Figure 2.15 shows the response of a river delta entering the reservoir before and after a fire that occurred in May 1996, which burnt an area of 4690 ha. The fire initiated a 200-fold increase in erosion rates which subsided three years after the fire. Intense post-fire floods within the first six months following the fire transported burnt bedload in a few hours or days. An estimated 52,000 m³ of material protruded a distance of 10 m into the delta. The burnt material progressed along the delta as a kinematic wave of sedimentation that progressed at varying rates according to the bedload transport rates which ranged between 0.89-310 kg/s. The erratic nature of the sediment movement was attributed to: (i) sediment storage in the channel upstream of the reservoir; (ii) operation of the reservoir water level; and (iii) management of reservoirs upstream of the study site (Moody and Martin 2001a). An estimated 67 % of the initially eroded burnt material was still stored in the deltaic area four years after the fire which suggests that the burnt material in the reservoir has a potential residence time of 300 years. To the author's knowledge, this is the most detailed account of post-fire delta development in a reservoir environment.

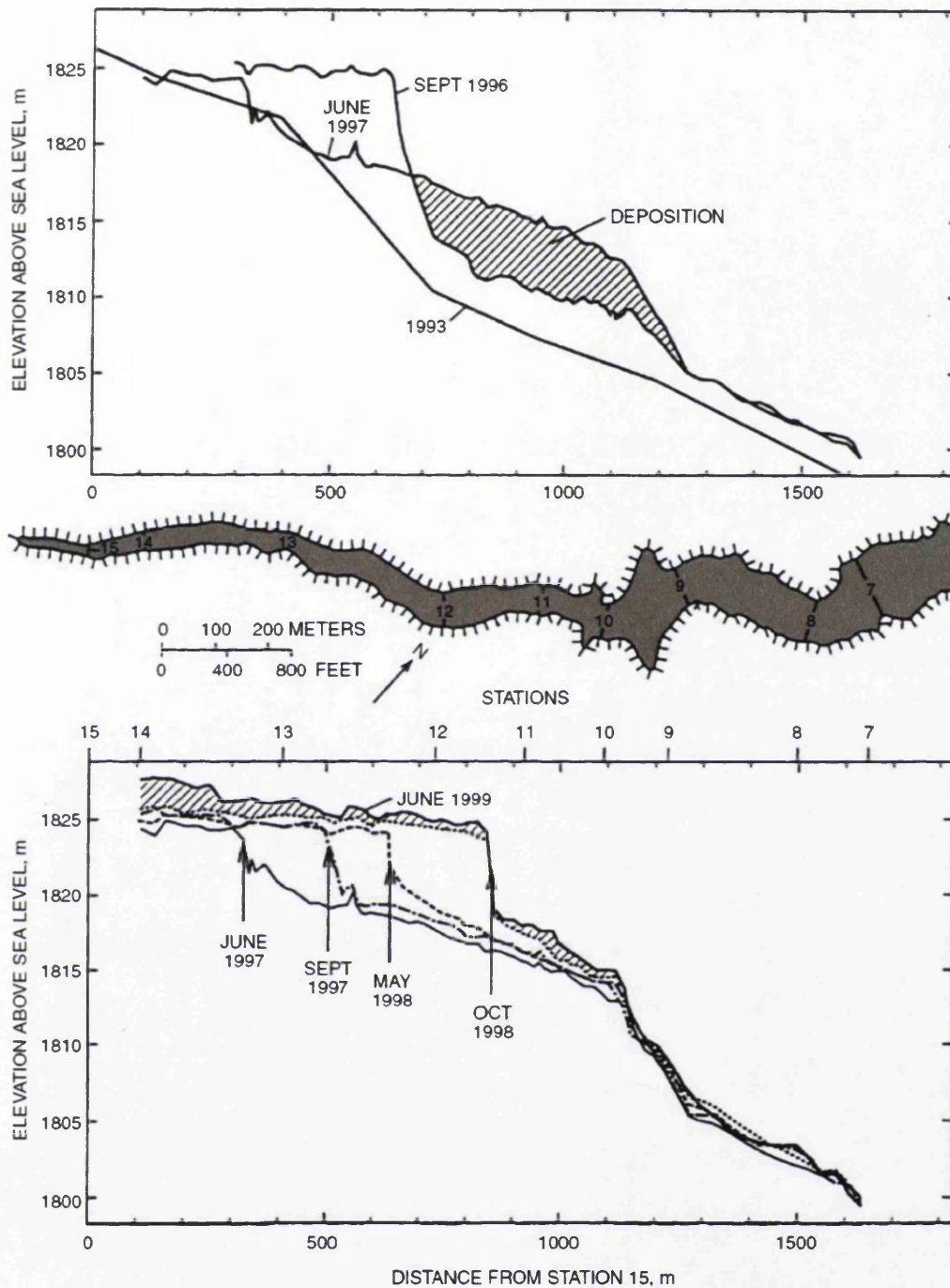


Figure 2.15: Location and thickness of wildfire-related sediment in the upper end of the Strontia Springs Reservoir, Colorado. (A) The pre-fire 1993 surface is shown for comparison with the post-fire September 1996 and June 1997 surfaces. (B) The location of the delta for five surveys in 1997, 1998 and 1999 (Moody and Martin 2001b).

2.6.4.1 *Agradation above the reservoir*

The constantly fluctuating water levels associated with reservoir environments create variable depositional environments at the delta. Increases of water level cause silting, variation in water supply and fluctuations in demand, the delta form will migrate upstream as sediment reaches deeper water earlier, shortening the stream channel. This will reduce the flow gradient, which will cause a decline in stream power, initiating subsequent aggradation (Gould 1951; Gottschalk 1964). The accumulation of material above a reservoir will cause the river to have reduced capacity, which will cause a rise of the local groundwater table, and make adjacent land more susceptible to flooding (Gottschalk 1964). The influx of deposited sediment in channels after fire may encourage growth of water tolerant vegetation such as willows, which provide habitats and improve biodiversity (Armstrong and Mackenzie 2002; Benda *et al.* 2003). However, this may also lead to the formation of pools and backwaters, which may become stagnant and cause deterioration of water quality (Borland 1971).

2.6.5 SEDIMENT MOVEMENT WITHIN LAKE AND RESERVOIR ENVIRONMENTS

Sediment that is transported through the river system can have a dominant effect upon sediment distribution and currents as a result of entrainment into flows within larger bodies of water, such as lakes or reservoirs. The detention-storage time determines the amount of sediment deposition that can occur. If the water is held in the system for a long period, such as in reservoirs where the water balance is altered or controlled by human action (Dussart *et al.* 1973), the currents that keep the particles in suspension will lose energy and deposit material (Gottschalk 1964). This will consequently create high trap efficiency.

The documentation on reservoir processes is limited, but similarities exist between man-made and natural lake environments in terms of dynamics and sediment distribution. For the purpose of this thesis, the comparatively well-documented processes within lake environments will be applied to reservoirs. However, for this to be achieved, consideration of the operation of the reservoir and the size of the inflowing sediment (Borland 1971) needs to be considered.

2.6.5.1 Climate effects on erosion, sedimentation and deposition

Climate affects both the level of weathering that is likely to occur within a catchment and the likelihood of periods of excessive drawdown of water levels in reservoirs. In Australia, the Southern Oscillation Index is a dominant influence upon climatic conditions. It is measured by the pressure difference between Tahiti and Darwin, and gives an indication whether a dry-dominated or flood-dominated regime will occur (Sturman and Tapper 1996; McGregor and Nieuwolt 1998). During wet seasons, increased weathering is likely to occur and sediment yields are likely to be higher than in dry seasons.

The combination of catchment and climatic characteristics provide a dominant influence upon reservoir processes by controlling forcing functions. These are identified by Sly (1994) as wind induced currents, inflowing rivers and density currents formed by water stratification (Figure 2.16).

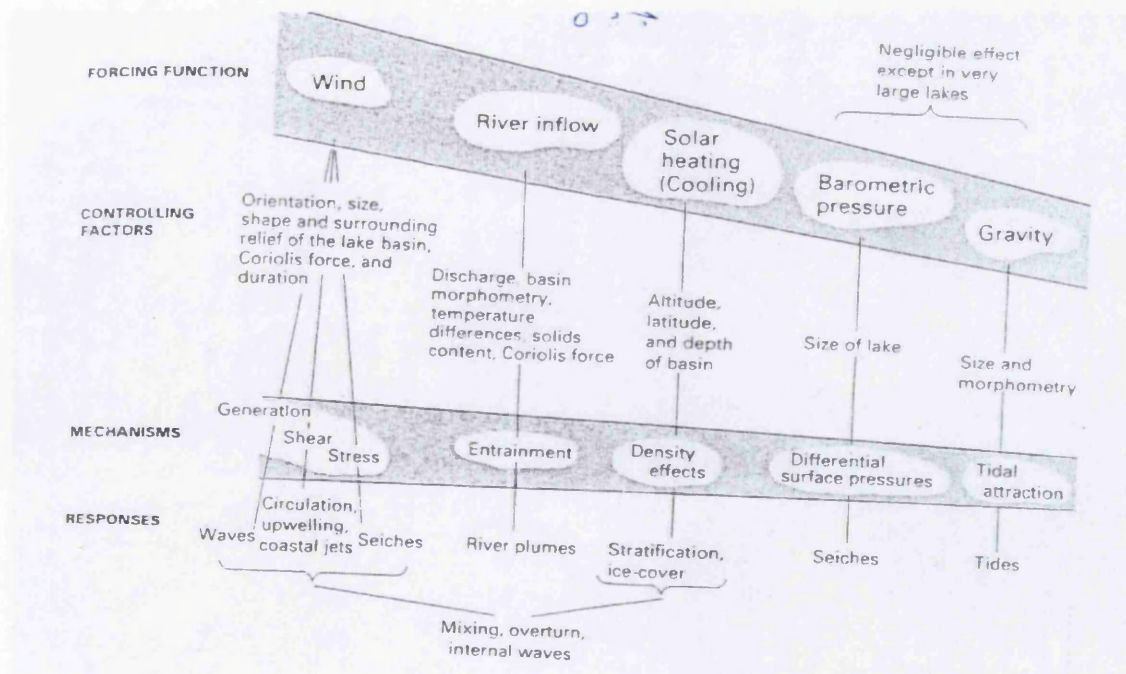


Figure 2.16: Lake responses to various forms of physical forcing functions (Sly 1994)

2.6.5.2 *Processes within lakes and reservoirs affecting sedimentation and deposition*

2.6.5.2.1 *Wind*

Perhaps surprisingly, the dominant forcing function as identified in Figure 2.16 is wind. The local characteristics recognised in Section 2.6.3, such as size, shape and orientation (Sly 1994) and climatic variations, determine the significance of this forcing function. For example, reservoirs or lakes in areas of low relief, which have a large open surface area, will enable a strong fetch to develop. The shear stress imposed on the surface layers of the water will produce rotational movements below the surface and generate waves. This will aid mixing of inflowing currents within the water and increase the movement of the waves to the shore. When the wave enters shallower water, the force may be dissipated by erosion of the banks and potentially cause the development of subaqueous slumps and debris flows (Friedman and Saunders 1978; Sly 1994).

2.6.5.2.2 *River inflow*

The second most dominant forcing function as identified in Figure 2.16, is the influence of river inflow. Sediment laden rivers will deposit larger particles in the headwaters of the river (Hakanson and Jansson 1983), which will contribute to early delta formation. Finer material will remain in suspension and may be carried within turbidity currents or river plumes, which may flow beneath the clear surface water as a result of the greater density (Gould 1951; Leeder 1982).

2.6.5.2.3 *Solar heating*

Solar heating will complicate the forcing function of the river plume effect by the development of thermal stratification of the reservoir water. The inflowing water from the river will become entrained in different ways according to the relative density of the water and the degree of heating (Figure 2.17). For rivers that are warmer than the main body of water, the inflows will occur along the thermocline. These interflows may contain high concentrations of suspended sediment, which will then be dispersed over the lake by wind driven circulation, convection currents and influence of the coriolis force (Leeder 1982). Inflowing waters that are cooler than the lake body will sink and transport oxygenated water to the lower layers, which will help prevent stagnation. Flows that are warmer or less dense than the main body of water will occur as surface flows, which will develop convection currents as they cool. As the flow begins to extend further into the lake, the energy

will become more widely dispersed due to the reduction in velocity of the flow (as identified in Figure 2.17) and the finer material entrained in the flow will also become deposited. The effects of river inflow in a thermally stratified lake are demonstrated in Figure 2.17 (Talbot and Allen 1996).

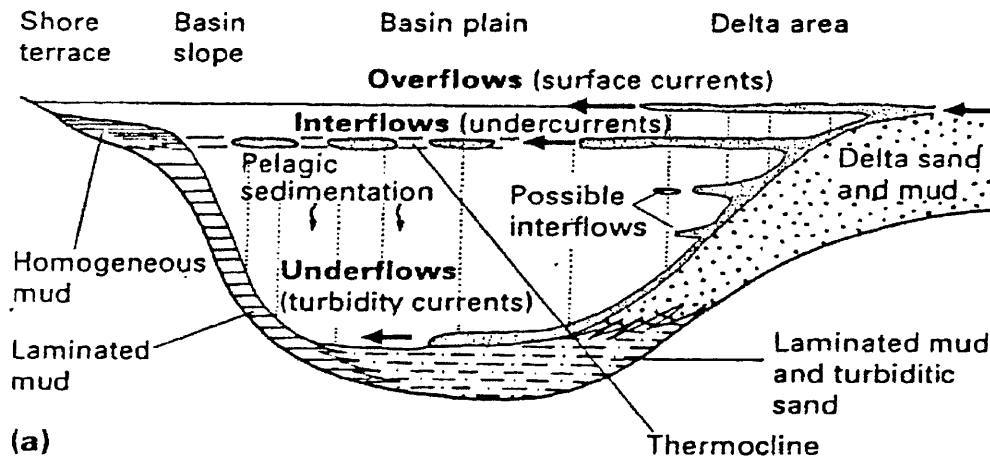


Figure 2.17: Distribution of sediment from a river inflow into a thermally stratified lake (Talbot and Allen 1996).

2.6.5.2.4 Sediment distribution

The forcing functions of wind, river inflow and solar heating will determine the ability of the flow to transport and distribute sediment within the reservoir through the development of currents. The dominant function is subject to variation according to localised factors. However, Annandale (1985) suggested that turbulent suspension is the dominant mechanism of material transport.

The initial stages of reservoir sedimentation after construction will be determined by dominant flows. Although the currents derived by forcing functions will be influential, a dominant flow will continue to run through the thalweg or pre-existing channel and initial deposition will occur adjacent to the original channel, forming levées. This pattern of deposition will continue until the advanced stages of deposition, where the deposits will become smoothed out (Gottschalk 1964), as identified in Figure 2.18. The adjustments in patterns of sediment accumulation with reservoir age are important to recognise for the purposes of identification of primary coring locations. These will affect day to day water levels and depositional environments. Fluctuating water levels may lead to a migratory inflow delta, slumping or reworking of sediments.

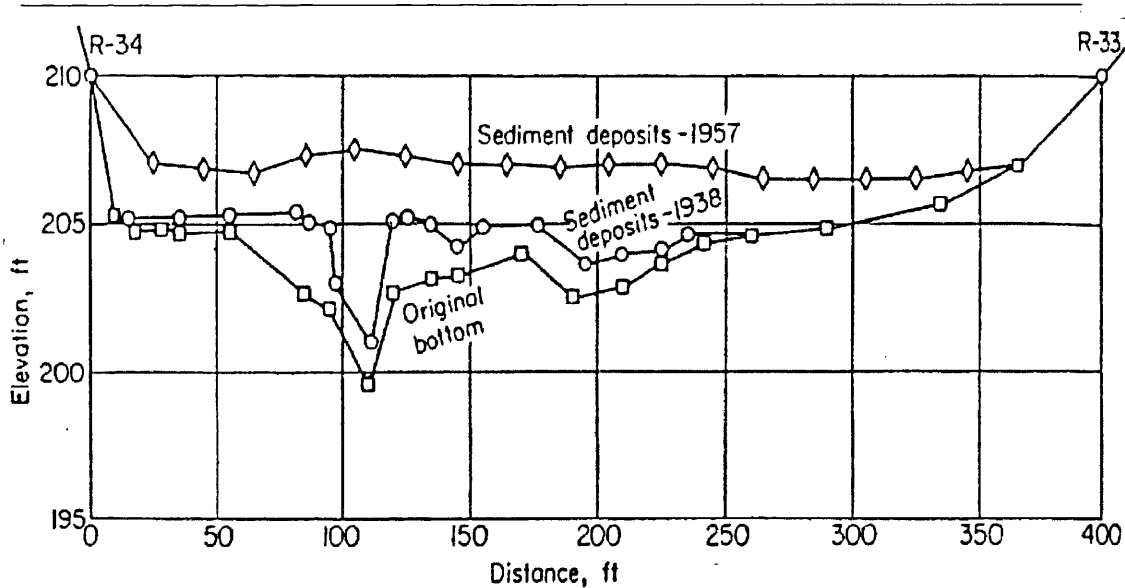


Figure 2.18: Cross section of sediment deposits, Lake Barcroft, Virginia (Gottschalk 1964).

2.6.6 MODELLING SEDIMENT DISTRIBUTION IN RESERVOIRS

Attempts have been made to model sediment distribution in reservoirs. Complexities relating to variations in sediment input and complications imposed by different reservoir operating schedules create difficulties in developing a fully representational model. As a result, assumptions and simplifications have to be made. For example, the computer model of Thomas' (1977) does not take into account meandering or lateral sediment distribution and makes the assumption that the riverbed remains fixed. Improvements have since been made. Young *et al.*'s (1998) model can simulate and predict sediment yield, transport processes in a river system and sediment distribution in a reservoir, based on hydrological, hydraulic, geological and sedimentary characteristics of a catchment.

2.7 RESERVOIR MANAGEMENT

2.7.1 EFFECT OF DRAW-DOWN ON RESERVOIR SEDIMENT MOBILIZATION

Sediment distribution adjusts during periods of drought, increased demand for water will be met by excessive drawdown of the water level. This will cause the deposits at the headwaters to advance into the basin, by streamflow eroding the material deposited at the higher stages. This will also expose shoreland that is usually submerged (Borland 1971). The exposed banks will not initially be vegetated, which will expose fine sediments to mobilisation by aeolian processes, causing an additional input of sediment into the basin (Sly 1994).

2.7.1.1 *Management solutions to sedimentation*

One of the most effective solutions to the management of sediment entering reservoirs in fire-prone environments in the 1960s was to incorporate storage capacity into reservoirs during construction, as it provided a cheaper alternative to controlling erosion (Gottschalk 1964). The increased quantities of sediment entering the reservoir as a result of fire, identified through an increase in river sediment yield (Table 2.7) will shorten the life expectancy of the reservoir through reduced storage capacity. However, more recent management has recognised the value of the sediment trapping capacity of vegetation (Heede *et al.* 1988). Prescribed burning is often chosen to maintain vegetation growth and prevent large quantities of sediment and nitrogen becoming mobilized (Riggan *et al.* 1994; Brose and Wade 2002). However, fire can also impact upon the water quality, in terms of increased evidence of nitrates and ammonium (Riggan *et al.* 1994; Gerla and Galloway 1997). During burning, a large quantity of nitrogen in the tree canopy will be remobilised and transported into the water systems. This is a cause for concern for reservoir environments due to a potential increased contamination of drinking water supplies. Although a large increase in nitrates is observed, mineral loading from P, Fe and Mn was not affected by fires of different severities in a study in the Kakadu National Park, Northern Australia (Townsend and Douglas 2000).

2.7.2 RECORD OF FIRE IN SEDIMENTS

This section examines the reliability of sediments in reconstructing fire events within catchments over time. Sediments can potentially provide a comprehensive record of chronological disturbance events within a catchment. Mohr *et al.* (2000) found a good correlation between records of climate, vegetation and fire history in a lake in California over the last 15,500 years. Similarly Wasson *et al.* (1987) found that the charcoal horizons within sediment cores obtained from a reservoir in NSW Australia held a reliable record of recent fire history when compared with documented evidence of burn events since the construction of the reservoir. However, there have been a number of studies that have found that recent historical fire events were not always reflected in sediment cores (Whitlock and Millspaugh 1996; Mooney *et al.* 2001; Gavin *et al.* 2003). This has led to the identification of a number of limitations regarding the use of sediments to reconstruct fire events within a catchment.

The location of a fire in the catchment influences the amount of material likely to be transported to a lake or a reservoir. In two different studies, Gavin *et al* (2003) and Laird and Campbell (2000) found that charcoal evidence only documented fires that have occurred within close proximity (~500 m) of a lake edge in North America. Higuera *et al.* (2005) suggested that only high severity, large and infrequent fires were reliably recorded within sediments. Laird and Campbell (2000) found that use of a Total Carbon Analyser was a more sensitive way in detecting fire events that had occurred within the catchment as this was able to detect finer ash and atmospherically deposited material. Although this would dependent on the speed and direction of the wind and rain to determine the presence of finer fire ash derived deposits within sediments (Clark 1983).

Clark (1988a; 1988b) and Nichols *et al.* (2000) considered the effect of contrasting buoyancy properties between charred and uncharred plant tissues and sediments and found that this resulted in a separation of material during transport and deposition. This may question the reliability of using charcoal in isolation to detect fire due to the possibility of different depositional patterns in addition to burnt material becoming easily reworked (PlattBradbury 1996). The transport mechanisms required to move material from the catchment to the lake or reservoir are essential in ensuring accurate records are developed. A number of studies have found a lag in charcoal accumulation in sediments with material being deposited as a kinematic wave of sedimentation (Whitlock and Millspaugh 1996; Moody and Martin 2001a). The extent of this lag was documented by PlattBradbury (1996) who recorded charcoal continuing to enter a lake 74 years after the fire had occurred in a catchment in North America.

The limitations identified in this section highlight that caution is required when interpreting chronological evidence stored within sediment deposits. However, consultation of records of ancillary data including rainfall, river flow data and lake level can help to contribute to a comprehensive interpretation of evidence contained within sediments.

2.8 FIRE FREQUENCY AND ITS EFFECTS ON EROSION AND SEDIMENTATION

There is evidence in the previous sections that fire has an effect on hydrogeomorphological characteristics within a catchment. The time interval between fires will influence the severity of a burn, through the effects on vegetation recovery and build up of litter, which in turn will determine the extent of the post-fire erosion. The effect of vegetation regeneration is considered as a primary factor in reducing levels of erosion. Degradation that occurs on the slopes is spatially variable and may transport material relatively short distances to sinks and stores or carry it to stream courses. This causes problems when identifying sediment source locations between systems of different scales (the slope and catchment) because of storage time on slopes and hillsides (PlattBradbury 1996).

2.8.1 TEMPORAL PATTERNS OF FIRE AND EFFECTS ON SOIL EROSION CYCLES

Heinselman's (1978a) fire classification rating given in Table 2.3 highlights the relationship between the return period of fire and the severity of the burn. Together with Table 2.2, the classification of fire events by visual assessment after the burn is a well used and simple means for recognising and predicting fire-return patterns and intervals. It can be noted that although the time since the last burn event and fire severity are linked, with severity generally being greater after longer intervals between fires, they can be subject to variation.

2.8.2 TEMPORAL PATTERNS OF FIRE ON VEGETATION

Vegetation structure and erosion cycles in catchments that are susceptible to burning vary as a result of fire regimes or cycles (intervals between fire events) (Kilgore 1978). This has led to a greater number of fire events occurring on a shorter time-scale. However, temperatures reached on these occasions have tended to be lower due to the reduction in fuel loading, affecting vegetation survival and adaptation, this determines the consistency of the future regenerating ground cover, which in turn affects the level of erosion.

Following medium or long intervals between fire events, (Heinselman's (1978a) classification rating 3 or 4), vegetation builds up, developing a high fuel loading, increasing susceptibility to the occurrence of high severity fires. This also creates good growing conditions for pyrogenic vegetation (Gill and Bradstock 1995). Conversely, if many burn events occur over a short time-scale (less than 25 years

according to Heinselman's (1978a) second classification (Table 2.3) the quick succession of fires will reduce the time for vegetation to regenerate. The reduced fuel load will generally cause low-severity fires. The low temperatures will then not initiate reproduction within pyrogenic vegetation in Australia (Gill and Bradstock 1995).

2.8.3 TEMPORAL PATTERNS OF FIRE AND SOIL EROSION CYCLES

Post-fire vegetation cover and soil erosion are closely linked as interception by the leaf canopy reduces the velocity of surface runoff and its capacity to erode material, by slowing down and deflecting the droplets of water on their way to the ground (Section 3.4). The effects of fire (or other disturbance events that involve vegetation removal) on erosion patterns have been recognised in many studies concerning the recovery of material loss rates back to pre-disturbance levels. The pattern of degradation events generally involves an initial peak in erosion immediately after the disturbance event, which tends to subside in relation to recovery time (Hewlett 1979). However, this pattern is also dependent on rainfall, which will determine the timing, volume and velocity of surface flows. Vegetation regeneration encouraged by good growing conditions will be important to stabilise the soil and to reduce the erosive power of flows.

The pattern of erosion cycles recognised in a hypothetical model proposed by Swanson (1978) is based on sediment yield after fire in two contrasting environments (Figure 2.19). It suggests that recovery of erosion rates to pre-fire values will occur within 10-30 years after fire. The time taken for sediment yield to revert to pre-fire levels is greater than the majority of length of studies in post-fire environments (3-5 years) in Table 2.7. This long recovery time can be attributed to a number of factors, primarily localised conditions such as slope, gradient, or vegetation cover and type (Willgoose *et al.* 2003). However, there are additional complications when using sediment yield as an indicator of erosion, due to inefficient delivery of material from the slope to the catchment (Olive & Rieger 1986; Cammeraat, 2002) as discussed in Section 2.6.

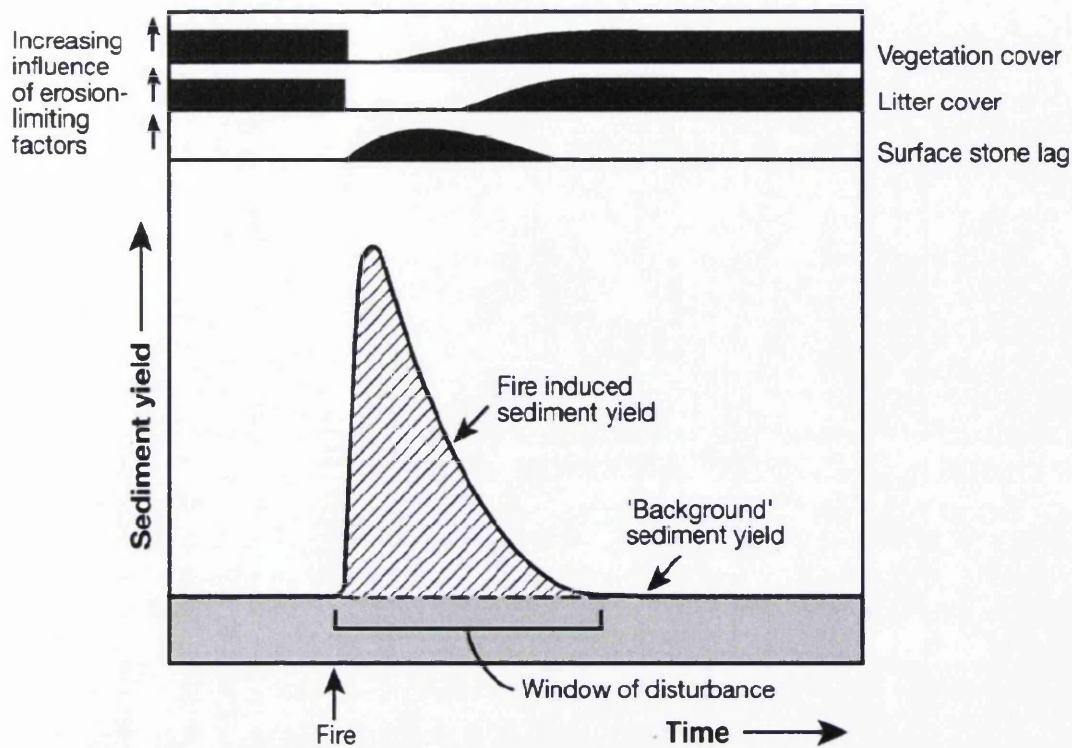


Figure 2.19: A hypothetical decline in sediment yield after wildfire and the role of three factors (vegetation cover, litter cover and stone lag development) in reducing erosion rates (based on Swanson 1981; Prosser and Williams 1998; Shakesby *et al.* 2004; Shakesby and Doerr 2006) in (Shakesby and Doerr 2006).

As post-fire vegetation begins to regenerate, stems trap and hold soil and debris up-slope, root systems start to bind the soil and litter dams begin to change the morphology of the slope. During long intervals between fire events, vegetation tends to recover fully. However, if the period between disturbance events is too long then the lack of under-storey vegetation because of the lack of sunlight will cause greater erosion to occur than would be the case in a newly regenerated area (Brown, 1972). Relatively frequent fire cycles will experience lower severity fires due to the reduced fuel loading (the concept behind prescribed burning). The impact of the increased frequency of fire on soil erosion cycles has not been investigated in any depth. An initial increased level of erosion may occur following a fire caused by the reduced vegetation (Figure 2.19). However, the number of fires in rapid succession will be reduced by the depleted amounts of surviving vegetation. This will cause a lower rate of production of humus and material for soil formation and less easily degraded material. Once degradation has reached bedrock, erosion rates will be reduced to the lowest level before weather erosion begins the cycle again by forming pockets of fine material.

The link between vegetation recovery patterns and soil erosion cycles is a key element that needs to be integrated into the research to help establish a better understanding of erosion patterns at both the slope and catchment scales. Although the recovery of environments to disturbance events has been extensively studied in the literature, to the author's knowledge, no research has directly investigated the impact of changing the frequency of fire events on soil erosion cycles or the effects of different severity fires.

2.8.4 SCALE PROBLEMS (DIFFERENCE BETWEEN SMALL AND LARGE SCALE RESEARCH)

Although erosion cycles induced by disturbance events are recognisable at both slope and catchment scales, the movement of water (Daniell and Kulik 1987; Kuczera *et al.* 1989) and material between these systems is subject to a great deal of variation. This makes it difficult to model, predict and compare quantitatively soil losses on the slopes with the sediment yield reaching the catchment outlet (Slattery *et al.* 2002). Soil loss is caused by inefficient delivery of material through system linkages such as sinks and stores, in addition to the fact that the majority of material is only mobilised during extreme rainfall events (Coppus and Imeson 2002).

Although material movement on hillslopes determines the amount of sediment entering water channels, deposition on slopes within sinks and stores by accumulation behind obstacles or vegetation causes a large proportion of sediment to remain within the slope system. This can account for an estimated 90-95% of material (Slattery *et al.* 2002; Shakesby 2004) as illustrated schematically in Figure 2.20.

The problems associated with scale differences are apparent globally. Research into the inefficiency of sediment delivery through drainage basins in Australia has been attributed to limited sediment supply causing low sediment concentrations, in conjunction with low and variable basin runoff (Olive and Rieger 1986). In a post-fire environment, there is generally increased sediment supply and concentration in streams, although it varies according to rainfall and runoff conditions within the catchment. These large variations of sediment movement question the reliability of studies that use sediment yield as an indicator of erosion (Figure 2.20).

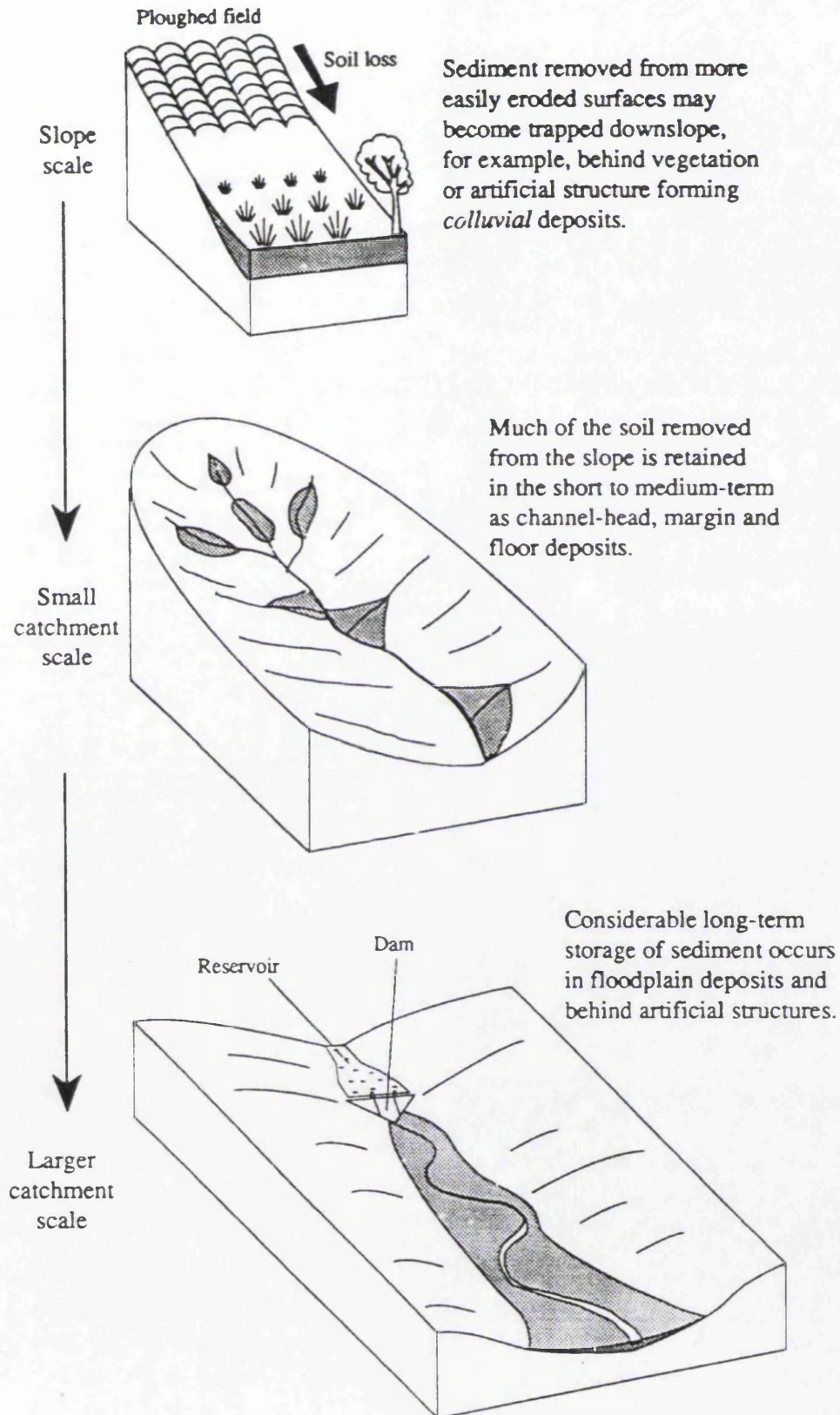


Figure 2.20: The influence of varying catchment scales on sediment losses (Shakesby 2004)

The dependence on rainfall to initiate material movement on a slope, highlights a point where knowledge of hydrogeomorphological processes begins to weaken, as the number of routes that water may take through a system could be extensive and variable (Daniell and Kulik 1987; Kuczera *et al.* 1989). This makes it difficult to predict how much water as runoff or overland flow is available to erode and transport material beyond sinks and stores on the slope (McGlynn *et al.* 2003). This problem has hindered the development of models to predict accurately the movement of sediment through a catchment, which would provide valuable information on predicting the bed load turbidity of water entering river systems and also in determining rates of sedimentation, which are vital when estimating the useful life of reservoir systems.

Bogena (2002) claims to have overcome these problems. He has developed a model applicable at a number of scales, which takes into account the linkages between slope and catchment scales, whilst also considering temporary stores both on slopes and within channels. Cammeraat (2002) disputes whether the development of a model that relates different scales is possible. He proposes an alternative method of improving understanding of catchment systems by recognising the relationships between processes at different scales, although it is not possible to gain quantitative information from this methodology (Figure 2.21).

Figure 2.21 has been developed to show interactions between dominant processes and geocosystem properties at different scale levels and is flexible enough to be applied to a post fire environment, as the connections that are apparent when the land is bare (grey boxes) could also be representative of burnt land and the white boxes are representative of where vegetation has recovered. An additional process would have to be included concerning fire-induced modifications to soil parameters to account for changes in hydrophobicity and aggregate stability (Section 2.3.2). Although this model cannot directly account for quantities of material moved, it gives a better appreciation of the stages within which materials are transported throughout a catchment. Confirmation of the patterns of catchment transport processes may be identified by the use of sediment tracing techniques such as mineral magnetics (Blake *et al.* 2006a) or radionuclide analysis (Fredericks 1994; English *et al.* 2005) to link sediments to original source locations on hill slopes; both techniques have been applied in the Lake Burragorang catchment.

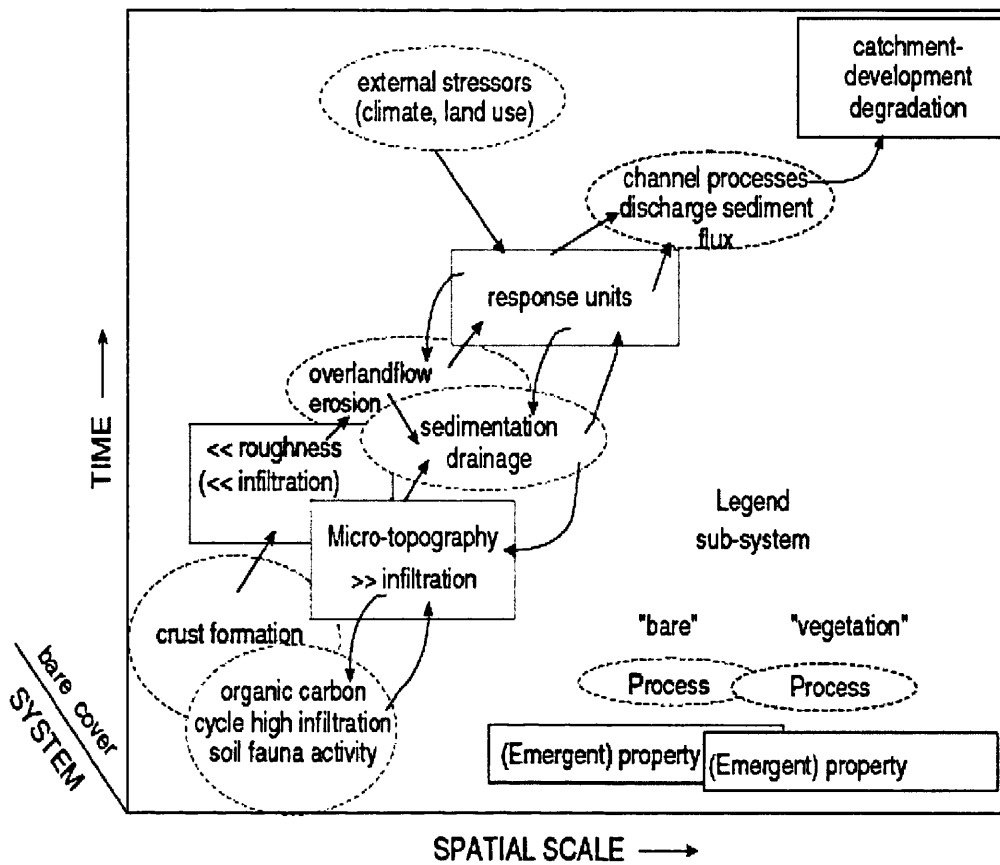


Figure 2.21: Conceptual framework showing process relationships between different scales for a catchment with bare vegetation cover in Spain. The main properties of this model could be applied to a post-fire environment as a result of vegetation destruction and recovery following fire.

2.9 SUMMARY AND RESEARCH GAPS

The review of the literature in this chapter has identified a wide range of factors that need to be taken into account when investigating modifications to hydrogeomorphological processes following the occurrence of fire in an Australian reservoir environment. These include gaps in understanding of: (i) methods of detecting fire events in soil material and sediments in the Australian environment; (ii) methods of reconstructing soil temperatures experienced by fire; (iii) methods for the detection of fire events in reservoir sediment cores; and (iv) the reliability of fire histories reconstructed from reservoir sediments.

There is a good understanding about the behaviour of forest fires owing to its importance in developing effective mitigation measures. Although complex fire models do exist they are unable to account for all catchment-specific factors that will influence the way that a fire progresses. Post-fire techniques available for identifying fire severity include either assessment of vegetation destruction (Cheney 1981; Jasper 1999) or the assessment of the destruction of soil water repellency, which makes it possible to identify whether or not temperatures between 240-360 °C have been reached (Doerr *et al.* 2004). However, Shakesby *et al.* (2003) recently found that there was a poor correlation between these two fire severity indicators. This highlights the first two research gaps for this thesis that require investigation which include: (i) methods of detecting fire events in soil material and sediments in the Australian environment; and (ii) methods of reconstructing soil temperatures experienced by fire to extend the range of fire severities identifiable by the destruction of water repellency in soil.

Temperature thresholds for mineral magnetic properties have been explored in European (Oldfield *et al.* 1981; Linford and Canti 2001; Weston 2002) and North American soils (Brown 1988, 1990); however only investigations by Taylor and Schwertmann (1974) and the more recent work by Blake *et al.* (2004) have investigated fire-derived enhancement of mineral magnetic properties in Australian soils. The preliminary work by Blake *et al.* (2004) highlights a need for a greater understanding of temperature thresholds required to modify Australian soils from different catchment locations.

Investigation of another temperature dependent soil property could extend temperature thresholds identifiable by water repellent and magnetic properties. The use of TL χ measurements and TAC to investigate temperatures experienced by archaeological artefacts has been explored by a number of workers (e.g. Göksu *et al.* 1989; Godfrey-Smith *et al.* 2005; Lahaye *et al.* in press). Examination of the application of this technique to soils could potentially identify the temperatures and timing of heating events in soils.

The third main research gap identified has been the lack of studies that have managed to link erosion at the slope and catchment scales. The work by Blake *et al.* (2004) identified different magnetic signatures derived from soil burnt in different locations within the catchment; however the application of these findings to sediment tracing techniques was not successful due to the non-linearly additive nature of the quotients used to discriminate between the signatures (Blake *et al.* 2006b). Investigation of the parameters required for the production of long-lived enhancement of soil properties could be applied to soils and sediments to provide an indicator of the fire severity that redistributed material had experienced, which would provide a better understanding of areas within the catchment that have the greatest susceptibility to post-fire sediment redistribution and sedimentation.

The final research gap addressed in this thesis investigates the reliability of sediment cores from Australian reservoir environments in preserving a record of catchment fire history. Many studies have used burnt material to reconstruct fire histories over long time-scales in order to make inferences about past climates (MacDonald *et al.* 1991; Millsbaugh and Whitlock 1995; Gedye *et al.* 2000; Gavin *et al.* 2003; Black and Mooney 2006). In contradiction to these studies, there have also been studies that have recognised the need for intense post-fire rainstorms to generate erosion of material from the slopes (Tomkins *et al.* in press). If sufficient post-fire rainfall does not occur, then localized sediment movement and redistribution of material on the slopes as found by Shakesby *et al.* (in press) will occur. In addition to the potential problems of transporting burnt material into sedimentary records it is possible that migratory deltaic systems initiated by fluctuating water levels could lead to complications during deposition of post-fire sediments, or reworking or slumping of material. This highlights the need for detailed work of the complex sedimentary environments contained within reservoirs.

3 STUDY AREA

This chapter introduces the research area, which comprises Lake Burragorang and surrounding sub-catchments. Firstly, it describes the study area and provides justification for the selection of the Nattai sub-catchment of Lake Burragorang as a particular focus of analysis. Secondly, it describes the characteristics of the area in terms of geology, relief, soils, vegetation and land use, together with climate, fire history, hydrology, and bathymetry of Lake Burragorang. It then discusses previous and ongoing work conducted within the catchment of Lake Burragorang relating to soil characteristics, soil water repellency, soil erosion, sediment transport and deposition. Throughout, reference is made to the potential application of mineral magnetism.

3.1 INTRODUCTION

The field research for this study was conducted between February 2002 and April 2005 in the Nattai sub-catchment of Lake Burragorang, New South Wales (NSW), Australia (Figure 3.1). The lake is located approximately 85 km south-west of central Sydney ($34^{\circ}45.2'S$ $150^{\circ}26.52'E$) and is the city's principal water reservoir, providing 80% of its drinking water (SCA 2002). The reservoir was created in 1960 as a result of construction of the Warragamba Dam. The flooded Burragorang valley drowned the lower regions of the Nattai, Wollondilly and Coxs rivers (Figure 3.2). These now form the three major sub-catchments of the lake, comprising respectively 8%, 60% and 30% of the total 9,050 km² area of the hydrological catchment (SCA 2004). Smaller tributaries account for the remaining 2%.

Management of the hydrological catchment is conducted through a series of controlled regions (Figure 3.1). The 'no-entry' zone is currently an area of fenced and prohibited access to the public, managed by the Sydney Catchment Authority (SCA) and contains a 2 km buffer zone around the foreshore of the lake to minimise contamination of its drinking water resource. The SCA owns approximately 470 km² (18%) of the hydrological catchment. Other areas are designated as a restricted access zone (also referred to as a special area), and a nature conservation reserve. Special areas comprise 2584 km², which cover 28% of the hydrological catchment.

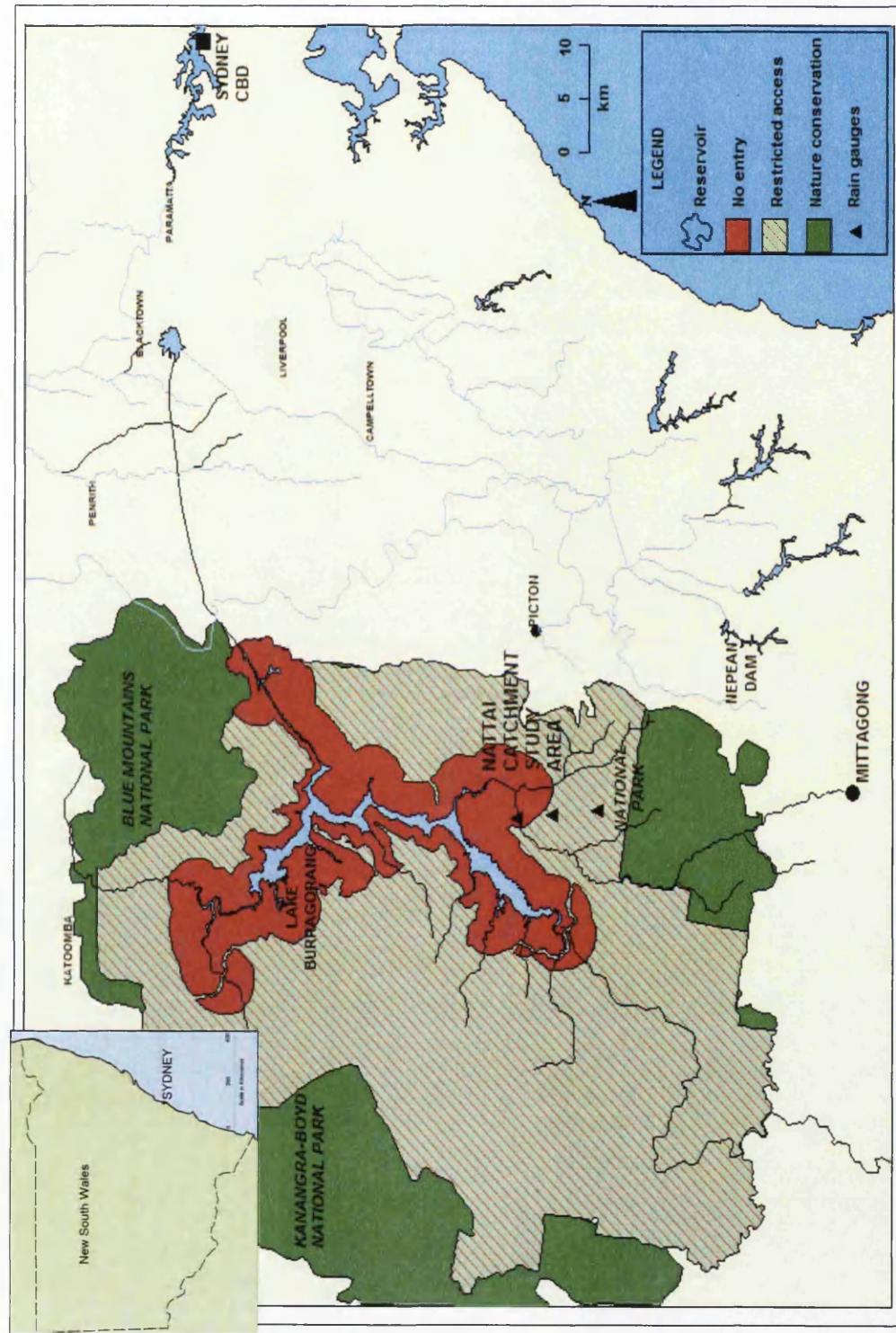


Figure 3.1: Location of Lake Burragorang in New South Wales (NSW), south-east Australia



Figure 3.2: Map of key locations relative to this study and sampling sites.

Within the inner catchment, vegetation is dominated by mature native dry sclerophyll (primarily eucalypt) forests. The outer catchment is of mixed tenure land classified as SCA freehold land, National Parks Wildlife Service (NPWS) managed land, Crown Land and private freehold land (SCA and NPWS 1999). Within the outer catchment, native vegetation has been removed causing higher sediment yields (SCA and NPWS 1999). Table 3.1 gives selected data for the catchment. The area investigated by the research group following the 2001/2002 fire was the Blue Gum Creek catchment (Figure 3.4). This feeds into the Little River, which flows into the Nattai. This area was chosen for their research as it contained slopes of similar topography that had experienced fires of differing severity as suggested by the degree of vegetation destruction.

Table 3.1: Selected data concerning the catchment of Lake Burragorang (SCA and NPWS 1999; SCA 2004)

| Feature | Data |
|--|-------------------------------|
| Capacity | 2.031×10^{12} litres |
| Area of lake | 75 km ² |
| Length of lake | 52 km ² |
| Length of foreshores | 354 km ² |
| Maximum depth | 105 metres |
| Area of catchment | 9,051 km ² |
| Average annual rainfall | 840 km ² |
| Sydney Catchment Authority (SCA) freehold land | 470 km ² |
| NPWS managed land | 18990 km ² |
| Crown Land | 93 km ² |
| Private freehold land | 345 km ² |

At this point it is useful to summarise the advantages of the choice of Lake Burragorang for this research:

- 1 **Homogeneous geology:** The dominance of Hawkesbury Sandstone within the area provides an ideal basis for sediment-tracing purposes, aiding detection of fire enhanced minerals.
- 2 **Largely undisturbed and unpolluted catchment:** This reduces the likelihood of anthropogenic activity creating sediments with enhanced magnetic signatures.

This also provides an area where erosion and sedimentation from the catchment are only influenced by natural factors in an environment that is representative of native flora and fauna. The Nattai catchment was also selected due to its relatively small and therefore more manageable size when compared with the other larger Wollondilly and Coxs catchments.

- 3 **Fire history and severity records:** The Nattai catchment has been subject to four major fire events since the construction of the dam in the 1960s. Additionally, fire severity mapping was available for the most recent 2001/2002 fire event. Access to these records aided interpretation and understanding of processes acting within the catchment. Furthermore, the records allowed useful comparison with the results of this study.
- 4 **Logistical support:** The SCA, which manages a large part of the Nattai catchment, offered a great deal of logistical support to the study, allowing access to all areas of the catchment via fire trails. Additionally, provision of a barge from which sediment coring could be conducted was an invaluable factor in site selection. The SCA have a vested interest in the results from this study, with regard to erosional activity and the implications for water contamination within the catchment.
- 5 **Previous work within the study area by the NERC-funded group:** The results obtained from fieldwork by staff at University of Wales Swansea (and subsequently Plymouth University) in the UK, and Macquarie University and CSIRO in Australia, in 2002 identified research gaps concerning processes operating in Lake Burragorang catchment. The investigations by the NERC-funded group investigated links between fire severity, soil water repellency and soil erosion, which provided an important background to the present study.
- 6 **Reservoir environment:** Although there are many benefits of conducting research within Lake Burragorang catchment, the reservoir environment does pose certain complications with regard to lake floor depositional environments as a result of variable lake level and river discharge. However, a good knowledge of reservoir water levels combined with access to an extensive set of ancillary records of rainfall and river data was available to aid interpretation. Furthermore, the reservoir allows another research gap, that of the viability of using sediment cores to reconstruct fire histories when sourced from complex reservoir environments, to be addressed.

3.2 GEOLOGY

This section describes the main geological characteristics of the study area that have shaped its undulating terrain and dissected gorge systems. The geology is critical not only because of its influence on landforms but also because it affects the nature of the soil, the mineralogy (and therefore its mineral magnetic properties) of its constituent particles, vegetation characteristics, hydrology, and the depth to which elevated temperatures are experienced during fire.

The major land systems within the Nattai catchment are underlain by Wianamatta shales and Hawkesbury Sandstone, deposited in the middle Triassic, which in turn are underlain by Permian coal measures and Shoalhaven Group deposits (Figure 3.3a and 3.3b). Hawkesbury Sandstone comprises primarily quartz and sandstone with minor shale lenses and conglomerates (Haworth 2003) and is the major rock type in the area, dominating 92% of Nattai catchment. The more recently deposited Wianamatta group comprises kaolinite and illite shales and minor interbedded sandstones (Sherwin and Holmes, 1986 cited in Fredericks 1994). Owing to their low resistance to erosion, the Wianamatta shales only cover 8% of the area (Fredericks 1994).

The influence of geology on catchment processes determines the rate of soil production and dominant erosive processes and impacts upon the type of sediments reaching the lake. In catchments where parent material varies, the different magnetic signatures that are produced provide a useful aid for sediment tracing purposes. In contrast, the relative geological homogeneity of the Nattai catchment, dominated by sandstones, with Wianamatta shales apparent only in the higher reaches of the river, provides an ideal situation for examining fire-enhanced sediment properties within this area.

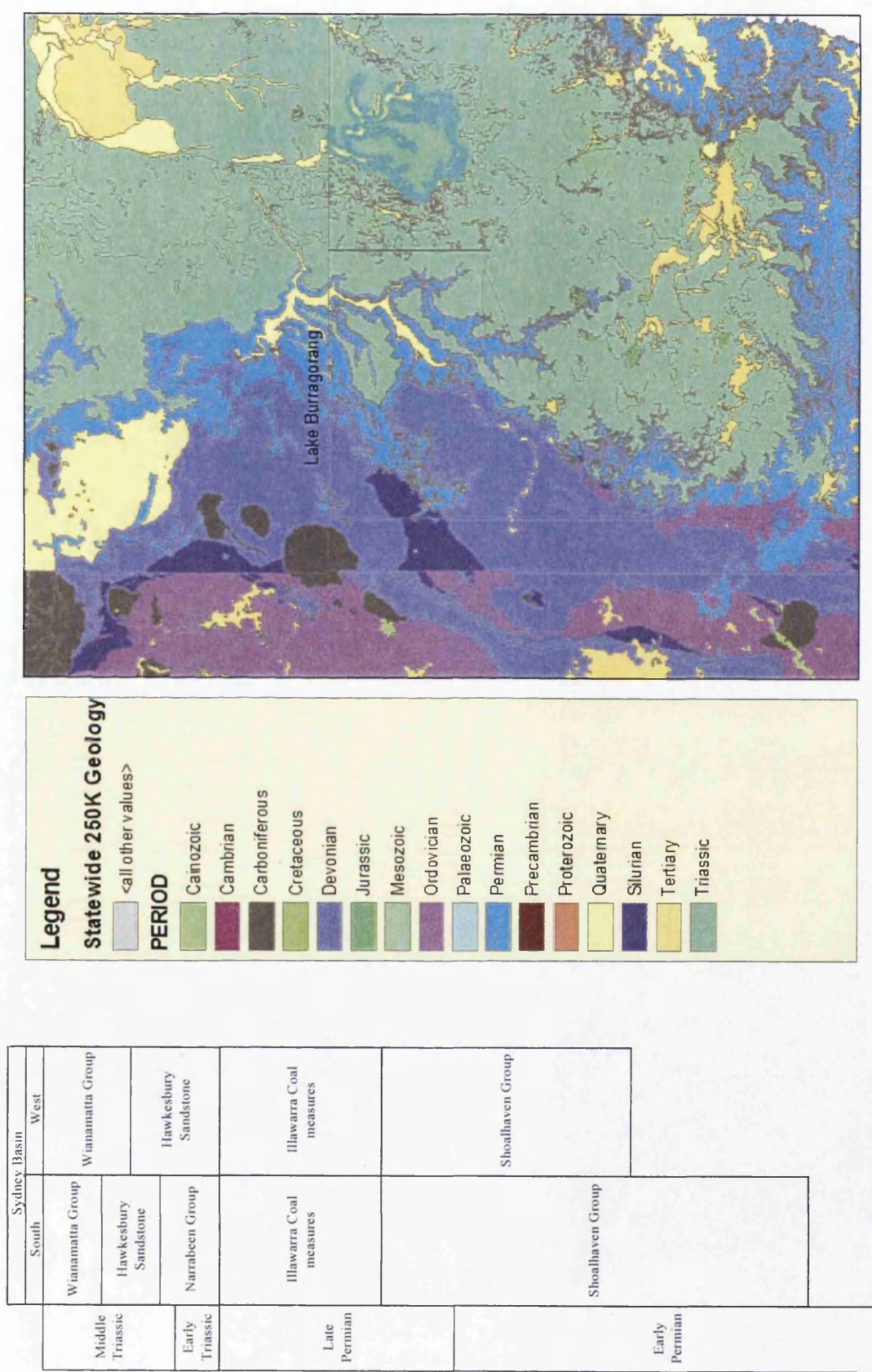


Figure 3.3: (a) Stratigraphic columns for the southern and western sections of the Sydney Basin, NSW (Source: Colliton (2001)); (b) Geology of the catchment of Lake Burragorang

3.3 RELIEF AND SLOPE FORM

The dominance of Hawkesbury sandstone in the Lake Burragorang catchment also plays an important role in determining slope form. This influences slope processes and associated erosion patterns, resulting in the characteristic gorge and plateau topography (Figure 3.4).

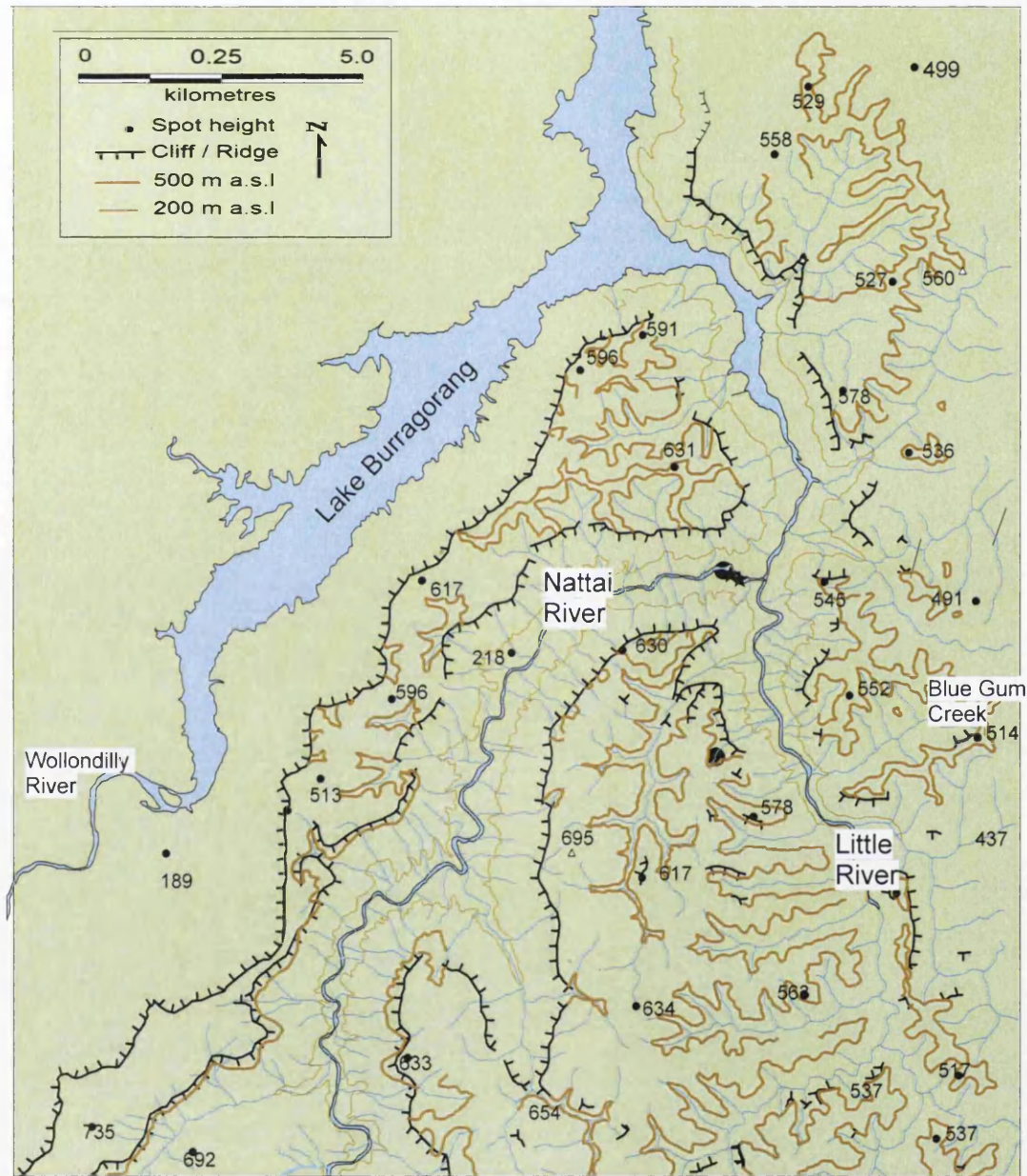


Figure 3.4: Topographical variations within the lower Nattai Catchment

The inner catchment of Lake Burragorang rises from 18m above sea level (a.s.l.) just below the Warragamba Dam to a height of approximately 1300m a.s.l. at Mt Guouogang to the north west of the lake in the Kanangra region of the Blue Mountains National Park. Within the upper reaches of the Nattai, just north of the township of Mittagong, the catchment is dominated by a steeply incised gorge with cliffs reaching 85 m above sea level (a.s.l.). The upper reaches extend to above 700 m a.s.l. Steep-sided valleys characterise the catchment, while the lower reaches of the river (below 200 m a.s.l.) have a well-marked meandering form with gently sloping floodplains and alluvial flats (Figure 3.4). The river is bound by the floodplain, comprised of low-angled slopes (5-10 °) (Figure 3.5). These merge into steeper cliffs upslope that rise to between about 70m and 240m above the river. This topography tends to coincide with areas underlain by rocks of the Shoalhaven group and Illawa Coal Measures that crop out along the Nattai and Little Rivers (Colliton 2001).

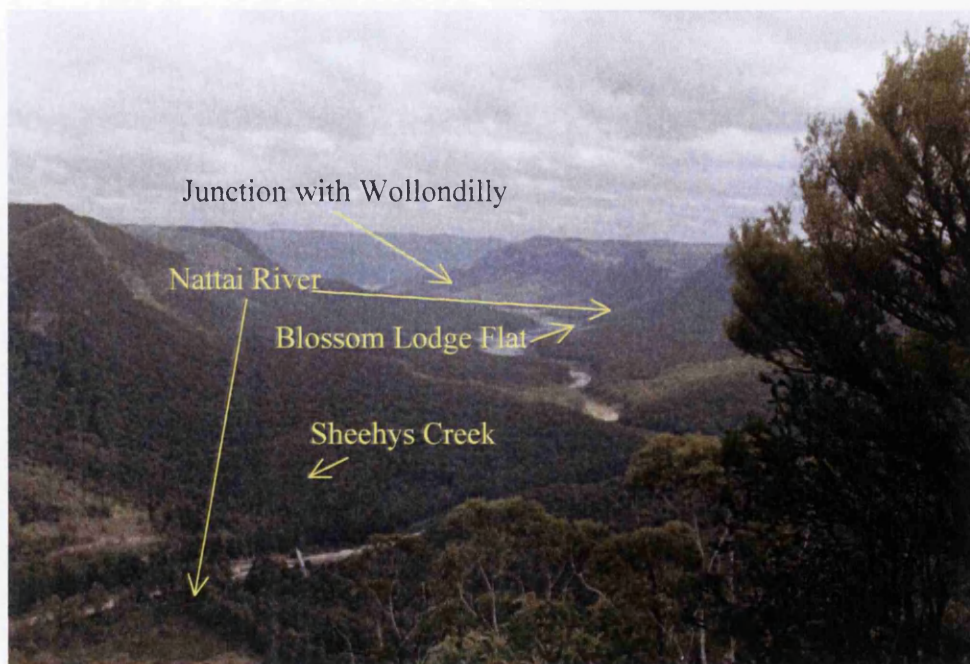


Figure 3.5: The lower reaches of the Nattai River

Slope forms along valley sides within this area of the Sydney Basin have been classified into four main units: (i) gentle ridge-top slopes (2-10°); (ii) steep bedrock exposures and cliffs (70-90°) in the upper mid-slope section; (iii) rockfall and talus-strewn slopes (15-35°) in the mid section; and (iv) foot-slope zones (5-10°), which

continue to the stream or as in the study area, merge with a distinct valley floor (Figure 3.6) (Bishop *et al.* 1980; Shakesby *et al.* 2003). Alternatively, Young and Young (1988) identified the dominant slope features within this landscape as plateaux summits and upland valleys, cliffs and valley floors.

Additional features noted in the plateaux regions within the Blue Mountains, especially where the Narrabeen group dominates, are so-called slot valleys. These features have cross-sections that indicate rates of stream incision that have outstripped those causing valley widening (Holland 1977). The scales of these features vary drastically from minor features of 1-2 cm on plateaux and steep slopes, to large slot valleys, which evolve into entrenched valleys, which dominate the landscape.

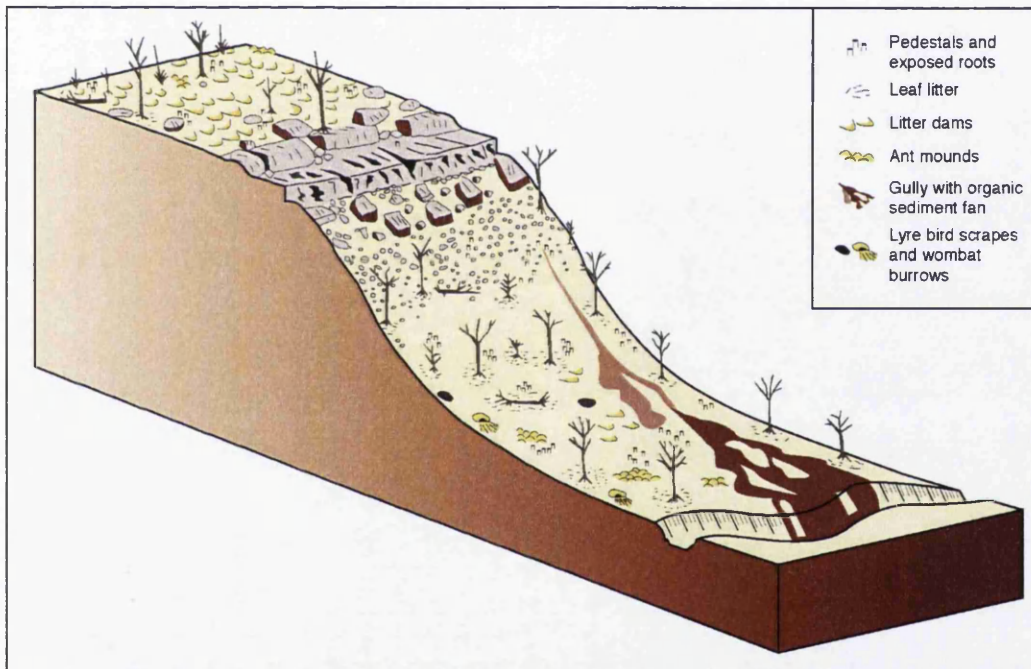


Figure 3.6: General slope formation showing micro- and meso-scale features relevant to post-fire erosion in the catchment of Blue Gum Creek (a tributary to the Nattai) (Shakesby *et al.* 2003).

The first slope form in Bishop's classification of gently sloping ridge tops is related to the sandstone beds. Owing to the low gradient and expansive sandstone plateau units in the area, soil loss is low from this part of the slope (Macris 2001).

The second slope unit within Bishop's classification (Bishop *et al.* 1980), of steep bedrock exposures and cliffs, is a dominant feature of this landscape. Cliff development is triggered by removal of the underlying material caused by

undercutting of the more resistant sandstone material, through the mechanisms of: (i) toppling, which is initiated by sliding, undermining or erosion of the toe slope material; (ii) brittle fracture, induced in sandstones that have experienced undercutting due to the relative weakness of sandstone when in tension of about 5 – 10% of its relative strength when in compression (Young and Young 1988); or (iii) backward rotation, induced by mining-associated subsidence (Cunningham 1988). Where undercutting is not the primary mechanism for cliff instability, the mechanism of gliding may occur. This occurs where very large blocks move outwards from the cliffs along joint planes of gentle slopes. This is a process thought to occur widely within the Sydney Basin, accounting for formation of pinnacles, which are characteristic features of this sandstone environment (Young and Nanson 1983). Only a thin layer of soil can form on these steep bedrock exposures, which is easily mobilised during heavy rainfall events due to the thin layer of relatively infertile soil preventing vegetation from becoming established.

The third slope unit within Bishop *et al.*'s classification, rockfall and talus-strewn slopes in the mid section of the valley side slopes, develops from material derived from the eroded cliffs above. Features within the upper section of the slope, in the rockfall zone, where the sandstone beds are thickest, are caverns, which are weathered, hollowed-out outcrops and boulders. Their formation has been attributed to salt crystallization within the large pores evident in the Hawkesbury sandstone. Growth of the crystals within these confined areas exerts pressure on the rock. When this force exceeds the mechanical strength of the rock, fracturing occurs (Johnson 1974).

The fourth slope unit within Bishop's classification, the footslope zone, often merges with alluvial sediments on the valley floors (Young and Young 1988). In this zone the low gradient enables accumulation and storage of colluvial material for a long period of time. Furthermore, samples collected by Blake *et al.* (2006b) from the Blue Gum Creek catchment demonstrated evidence of multiple burn events suggesting potential evidence of long-term storage on the slopes (Section 3.2). This was supported by radiocarbon dates obtained in the Blue Gum Creek study area, which suggests accumulation of sediments over the mid- to late- Holocene (post-7,000 BP) (Tomkins *et al.* 2004).

3.4 SOILS

Landscapes of the Sydney Catchment Authority have been classified by Henderson (2002) using description of soil profiles according to the Australian soil classification scheme (Isbell 1996). Dominant soil types in the area identified are: Yellow Kandosols (Yellow Earths), Orthic Tenosols (Earthy Sands), Rudosols (Lithosols), Yellow Kerosols and Chromosols (Yellow Podzolic Soils) on shales (Henderson 2002). The underlying geology of the region (Figure 3.3a and 3.3b) has a strong influence on soil type. Soils formed on the Wianamatta group include “*hard acidic duplex soils with Mottle Yellow B horizons and minor gradational red earths with bleached A2 horizons on rises*” (Fredericks 1994 p. 16). Owing to the low resistance of the shales to erosion, these soils are generally located on gentle slopes and therefore produce a deep and fertile material with high clay content. The soils derived from the Hawkesbury Sandstone are influenced by their topographic location. Gently undulating ridges produce shallow stony duplex soils (Dy-Dr) (Northcote 1979). Areas of moderate relief are generally associated with acid leached siliceous earths (Gn2). Areas of high relief are associated with siliceous sands (Ucl-2) (Fredericks 1994).

Textural analysis of soils around Blue Gum Creek indicates that they are sandy loams and loamy sands at the surface with weak pedality. At depth (0.5 - 1.3 m), soils consist of clay loam sands, sandy loams and loamy sands and clays. Soil thickness varies from as little as 1 to 2 cm on ridges to more on mid-slopes and footslopes and on the valley floor (Shakesby *et al.* 2003). Hawkesbury Sandstone produces stable weathered products, which create a relatively homogeneous base signal that can be used to recognise magnetic minerals that have been modified. The high iron accumulation within soils developed on Hawkesbury Sandstone on slopes in swamps in the nearby Avon Catchment, highlights potential problems with using mineral magnetics as iron accumulation and leaching have occurred (Table 3.2).

Table 3.2: Average concentrations of total free iron that is citrate-dithionite extractable; mobile / amorphous iron as oxalate extractable iron in soils of different depths, situated on Hawkesbury Sandstone within the Avon Catchment (Young and Sim (1987) in Young and Young (1988)).

| Soil Type | Total free iron (g /kg) | | Mobile / amorphous iron (g/kg) | |
|--------------|-------------------------|---------------|--------------------------------|----------|
| | at 0.1 m | at 0.5 m | at 0.1 m | At 0.5 m |
| Lithosol | 2.60 | Not available | 0.66 | n.a. |
| Yellow earth | 0.82 | 4.06 | 0.56 | 0.86 |
| Organic sand | 12.02 | 8.91 | 4.83 | 1.83 |

3.5 VEGETATION AND LAND USE

Before European settlement in the Sydney Basin, its vegetation consisted predominantly of *Eucalyptus* woodland, established due to the tolerance of this vegetation to harsh conditions of fire, drought, flooding and insect infestations. After settlement, major deforestation by European settlers occurred leading to clearance of the land for farming and provision of timber for building. Since designation of Lake Burragorang catchment for water supply purposes, the vegetation within the restricted access zone has reverted to mature undisturbed eucalypt forest. The dominant vegetation community within Lake Burragorang's catchment is a dry sclerophyll sandstone woodland type, which covers 65% of the area. The dominant species and structure associated with this group is *Eucalyptus*, which accounts for 50 out of 123 tree species identified in a forest survey of the whole catchment in the 1960s (Wooten 1965). *E. angophora* was found to be the prominent variety, providing canopy cover reaching heights of between 20m and 40m. The understorey consists of taxa such as *Banksia*, *Acacia*, *Hakea* and *Letospermum* (Chafer *et al.* 2004).

Results from a survey of vegetation communities within the Nattai National Park identified predominantly 'Nattai Sandstone Shrub Forest' (NSSF) in this area (Anon 2003). A survey of Blue Gum Creek, (a tributary to Little River) (Figure 3.2) within the Nattai Catchment recognised the presence of a NSSF community, but also identified an influence from adjoining communities of Sheltered Sandstone Intermediate Blue Gum Forest, Exposed Burragorang Sandstone Shrub Woodland and Rocky Sandstone Heath Woodland (Hafey 2004). The main tree species identified by Hafey (2004) within the Blue Gum Creek area are typical of sandstone- and shale-based communities (NPWS 1997) and their associated positions on the slopes are given in Table 3.3.

Table 3.3: Dominant vegetation in the Blue Gum Creek catchment and its respective position in the landscape (Hafey 2004).

| Slope position | Common name | Latin name |
|---|------------------------|-------------------------------------|
| Ridge | Red bloodwood | <i>Corymbia gummifera</i> |
| | Sydney peppermint | <i>Eucalyptus piperita</i> |
| | White stringybark | <i>E. globoidia</i> |
| Valley-side slopes, Sydney Sandstone Gully Forest | Deanes blue gum | <i>E. deanei</i> |
| Moist Escarpment Forest Complex | | |
| The lower foot-slope to mid-slope | Yellow bloodwood | <i>E. deanei</i> & <i>C. eximia</i> |
| | Narrow-leafed ironbark | <i>E. creba</i> |
| | Grey gum | <i>E. punctata</i> |

Understorey vegetation includes *Podcarpus spinulosa* (Plum Pine), *Persoonia linearis* (Fine-leaved Persoonia), *Leptospermum trinervium* (Rough-barked Tea Tree), *L. polygalifolium* (Lemon Scented Tea Tree), *Acacia linifolia* (Flax-leaved Wattle) *A. terminalis* (Sunshine Wattle), *Pimelia linifolia* (Rice Flower), *Lucopogon lanceolatus* (Lance Bearded Heath), *Podolobium ilicifolium* (Native Holly) and *Xylomelum pyriforme* (Woody Pear). These species provide medium-density coverage on the lower slopes, but there is only sparse coverage on the higher slopes. A similar distribution pattern with respect to slope position is evident for the ground cover species of which the dominant species include *Lomandra longifolia* (Mat Rush), *Entolasia stricta* (Wire Grass), *Lomatia salifolia* (Crinkle Bush), *Pomax umbellata* (Pomax), *Ballardiera* (Apple Dumplings) and *Dianell caerulea* (Blue Flax Lily). Potentially, the residue from the burning of these different vegetation types may produce ash with varying mineral magnetic properties (Peters and Batt 2002), although this has not yet been demonstrated for Australian fuel sources.

Many of the species found in the catchment are dependent on fire to activate regeneration and are termed pyrogenic vegetation. Post-fire surveys conducted in the study area found pyrogenic vegetation that survived the 2001/2002 fires experienced rapid regeneration. Research conducted by Bradstock *et al.* (1998) in the Sydney region found that after 3 years of re-growth of sclerophyllous vegetation, enough fuel had accumulated to support another burn event. There are various management options that could be used to minimise the risk of a major fire, including the application of prescribed fires. However, it would not be possible to apply this strategy to the entire Burragorang catchment due to its size.

Prior to the construction of Warragamba Dam, the Burragorang Valley provided ideal conditions for settlement. Artefacts found in the area suggest that the Gundungurra Aboriginal tribe inhabited this area before the arrival of the Europeans, using fertile river flats for farming. Subsequent communities developed in the area around the 1820s after European settlers managed to penetrate the forests. The latter were also drawn to these ideal conditions and raised cattle, sheep, pigs and poultry and grew maize and oats. Coal mining and cedar logging became prominent industries in the late 1800s and early 1900s (Brown, 1976, quoted in Colliton, 2001) as a result of the development of roads providing easier access to the area. Proposals to construct the dam date back to 1867 and the drought between 1934 and 1942 provided the motivation to build it. Construction involved displacing 170 families and flooding 10 schools, 5 post offices, churches and a cheese factory. The silver mining town of Yerranderie became a 'ghost town' due to the loss of access routes through the Burragorang valley (Meredith 1999, 2002). The coal mining industry remained active until 1990.

Land use within the inner catchment following the construction of the dam was restricted in order to limit possible contamination of the reservoir water supply. However, many tributaries extend outside this 2 km buffer zone, passing through private freehold and leasehold land, crown lands, state forest and national parks (Figure 3.2). The restricted access to the Nattai catchment ensures minimal disturbance and reduces potential contamination of water. Within the outer catchment of Lake Burragorang, agriculture comprises 50% of the land use, although crop production is limited, with potato farming on the nutrient-rich, basalt soils and small amounts of barley and oil seed being sown on the alluvial flats (Ferris and Tyler 1985). Some agricultural practices could cause problems in terms of the water quality of Lake Burragorang.

Land use types within the major tributary areas are identified in Table 3.4. The Nattai sub-catchment remains relatively undisturbed, with 83% classed as undisturbed bushland. The 7% of urban development is contained mainly within Mittagong (Figure 3.1), located on private freehold land in the upper reaches, which has led to the removal of vegetation and so has led to increased surface runoff. The land use values for the Nattai River identified in Table 3.4 contrast with those

suggested by Colliton (2001); he considered that 64% of the Nattai catchment was bushland, 32% agricultural and 4% urban. These contrasting figures may be the result of different classifications and changing land use within the outer catchment between 1994 and 2001.

Table 3.4: Percentage distribution of land use in Lake Burragorang catchment in 1992 (Laut *et al.* 1992; Fredericks 1994; Colliton 2001).

| Land use | Wollondilly catchment % | Coxs catchment % | Nattai catchment % | Werriberri catchment % | Total Burragorang Catchment % |
|-------------------|-------------------------------|------------------------|--------------------------|------------------------------|--|
| Bushland | 37 | 75 | 83 | 63 | 53 |
| Grazing | 60 | 22 | 10 | 24 | 43 |
| Urban /peri-urban | 2 | 2 | 7 | 11 | 3 |
| Other | 1 | 1 | - | 2 | 1 |



3.6 CLIMATE

Australia's climatic variability is dominated by the Southern Oscillation (SO), which controls temperature and rainfall across the continent, thus determining the occurrence of either a Dry Dominated Regime (DDR) or Flood Dominated Regime (Sturman and Tapper 1996; McGregor and Nieuwolt 1998) (Section 2.4.4.1.2). El Niño episodes that occur about every 2-7 years (Figure 2.1) are strongly linked to these regimes, but are determined by ocean currents (Perry and Matthews 2003). On average, New South Wales has a humid temperate climate, with moist summers, cool winters and no marked dry season. Major storm events occur between January and February in late summer to early winter months, caused by southward-moving extra-tropical and east coast cyclones (Linacre and Geerts 1997).

The Bureau of Meteorology (BOM) monitors weather data at stations located in built-up areas, near Lake Burragorang. Additionally, individual stations within the catchment belonging to the SCA (Figure 3.1) provide information relating to variations across the catchment. The data available from these sources have been used here to show: (i) temperature and humidity; and (ii) rainfall data derived from stations located within the Nattai catchment of Lake Burragorang.

3.6.1 TEMPERATURE AND HUMIDITY

Records held by the BOM climate station located at Picton Council Depot (34°16'S, 150°61'E) hold data collected since 1880. Mean daily maximum temperatures for the year average 23.5° C and range from 16.8°C in July to 29.3°C in January. Mean daily minimum temperatures average 8.8°C, with the mean daily minimum temperatures ranging between 1.7°C in July and 15.4°C in February. Annual relative humidity averages 73% at 9 am and 52% at 3 pm, deviating by ±7.5% and ±6% respectively (www.bom.gov.au 2004). High temperatures and low humidities tend to dry out litter and vegetation making them susceptible to burning. Therefore, fires tend to start predominantly in summer and in the afternoon due to the reduced moisture levels in the atmosphere (Bradstock *et al.* 1998).

3.6.2 RAINFALL

Daily and annual rainfall data obtained for eight gauging stations located at various sites in the south of the Lake Burragorang catchment (Figure 3.1) is presented in Figure 3.7. The stations located in the Nattai catchment nearest the sampling locations for this study include The Causeway, Starlights and Hilltop. However, the records at these stations only began in 1982, 1982 and 1990 respectively. The longest rainfall record is held at the Joorliands station where records began in 1962, while records at Yerranderie and Byrnes Creek were initiated in 1966. Comparison of the rainfall records within the south of the Lake Burragorang catchment shows that the majority of stations recorded each rainfall event, although there is some variation between the intensity of rainfall at each station which is likely to be due to the spatial variability of rainfall within the catchment.

Reference to the three longest annual records at Joorilands, Yerranderie and Byrnes Creek indicates that exceptionally wet years with annual rainfall > 800 mm were 1963, 1969, 1974, 1978 and the years 1988-1991. The lack of years with rainfall > 800 mm between 1991 and 2004 reflects the drought conditions that Australia experienced during this time. The daily rainfall records show an increased concentration of relatively large rainfall events occurring between 1983 and 1992.

The red horizontal bars on Figure 3.7 reflect the major fires seasons in South Eastern Australia between 1940 and 1992 that were shown to coincide with major El Niño episodes in Figure 2.1. The major fire seasons years when extensive burn events occurred followed years with lower annual rainfall. Comparatively large daily rainfall events often occurred either during years or following major fire seasons.

The mean monthly rainfall for the Causeway and Starlights stations between 1981 and 1991 and for the Causeway, Starlights and Hilltop stations between 1991 and 2003 was 58 mm. During the post-fire study period prior to sediment core collection between 2002-2003 the average rainfall for all three stations was 50 mm. In this period, there was below average rainfall for all months except February, March and November (Figure 3.8). Maximum rainfall occurring in February coincides with regional weather patterns, while the winter months of June and July are relatively dry although they experience cooler temperatures so that moisture levels in the soil

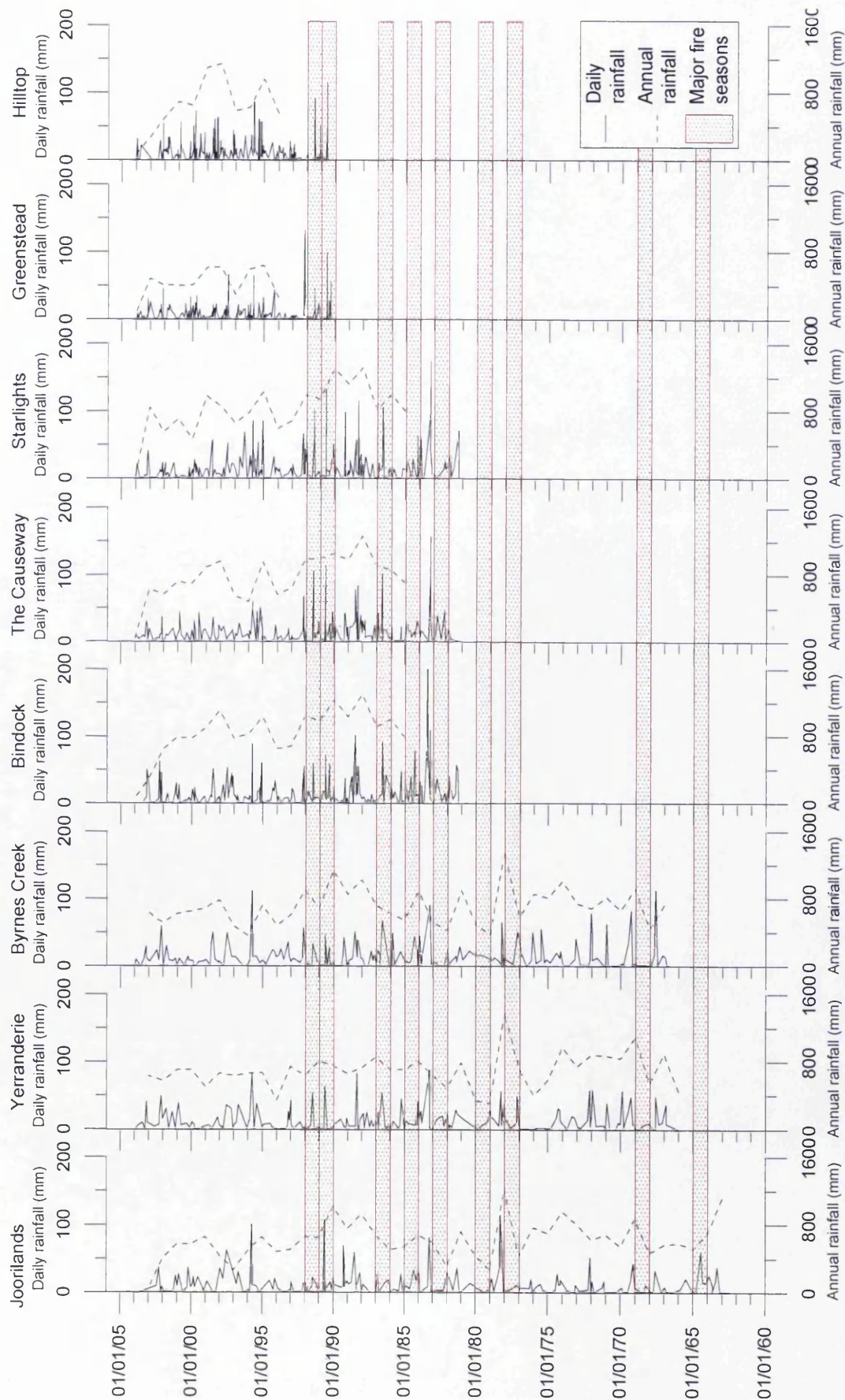


Figure 3.7: Daily rainfall (solid line) and annual rainfall (dashed line) for 8 rainfall stations located in southern Lake Burratorang (See Figure 3.2 for station locations). Major fire seasons (red horizontal dotted bars) in southeast Australia as identified in Figure 2.1.

are maintained, which reduces the likelihood of wildfire. The high levels of rainfall in November and December are associated with precipitation occurring during intense storms. When these events happen after a long period of dry weather, there is a high chance of naturally sparked fire events initiated by lightning strikes. This was the situation that initiated the Christmas 2001-2002 fire, with only 45 mm of rain occurring in December 2001. Extreme rainfall followed this fire with above average rainfall for January, February and March of 75 mm, 154 mm and 87.3 mm, respectively. This contributed greatly to post-fire erosion and enhanced vegetation regeneration.

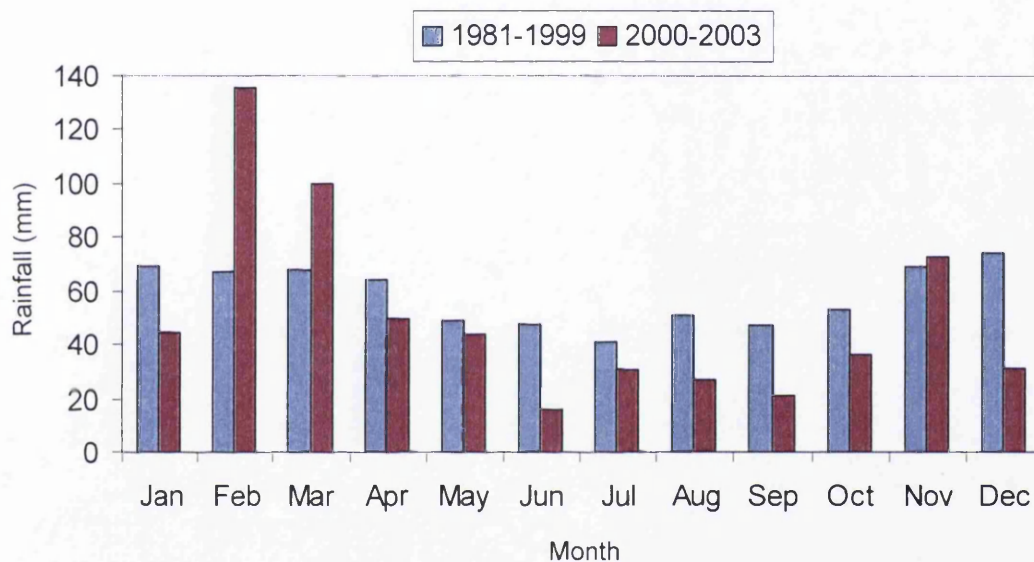


Figure 3.8: Average monthly rainfall for 1981 –1999 and 2000-2003 for the rainfall stations The Causeway, Hilltop and Starlights located in the Nattai Catchment.

3.7 FIRE HISTORY

As already discussed in Section 2.1, bushfires are common in Australia, occurring both naturally and through human action. Around Sydney, the hazard of bushfires has increased as a result of liberal property development encroaching on bushland areas. This section firstly highlights those aspects of the landscape and climate, together with the pyrogenic vegetation that make it prone to burning. Secondly, it identifies the major fire events that have occurred within the catchment since construction of the dam, and thirdly, the major burning events that have occurred within the Nattai catchment.

The Sydney region is susceptible to fire due to the highly combustible sclerophyllous vegetation, in addition to the alignment of the grain of the topography in a north-east to south-west direction causing the prevailing dry inland winds to maximise fire potential (Haworth 2003). Additionally, the rugged and often inaccessible terrain causes difficulties for fire-fighting efforts. The main fire season begins in October and can last until February or March. Fire risk is also enhanced during periods of ENSO- (El Niño Southern Oscillation) driven drought (Section 2.1), caused by the reduced moisture content increasing the easily combustible fuel load. The wet years that often follow long periods of drought, provide ideal growing conditions for regeneration of fire-dependent vegetation (burnt during the drought), which quickly creates high fuel loads (Luke and McArthur 1978).

The fire history of the Lake Burragorang Catchment has been well documented since the creation of the dam. Major burn events occurred in the fire seasons of 1964-1965, 1968-1969, 1997-1998, and 2001-2002. (Figure 3.9). The areas burnt during each fire season are displayed in Figure 3.10. The largest fire experienced in the catchment was in fact a prescribed (i.e. controlled) one that occurred in 1957 and affected more than 50% of the inner catchment. It was conducted in an effort to minimise the possibility of major fire events (Caparero 2004). Since this time, the 2001-2002 fires were the most extensive to have affected the catchment, this was the first burn event to have its fire severity assessed by SPOT and NDVI image analysis (Chafer *et al.* 2004). The 2001/2002 fires occurred after 12 months of officially declared drought. The diurnal temperatures were above average and hot dry north-westerly winds were a regular occurrence (Chafer *et al.* 2004) The fires burnt a

substantial area of the catchment consuming a large proportion of the fuel load. This explains the lack of fires in the catchment during the period between 2001-2002 to 2004-2005 fire seasons despite the continuing drought in 2005.

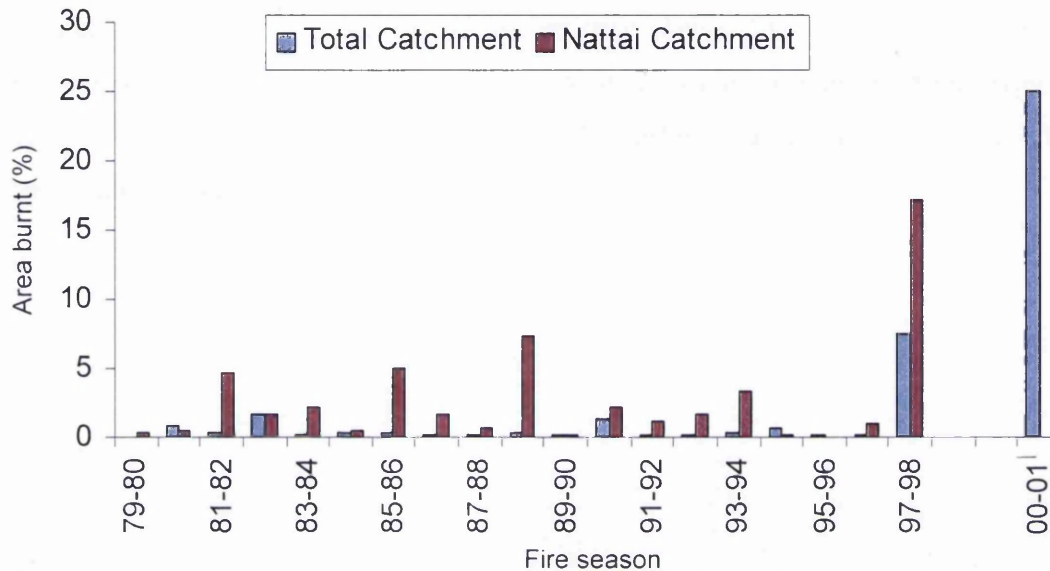


Figure 3.9: Percentage of Lake Burragorang (Total catchment) and Nattai catchments burnt between the 1979/1980 and 2000/2001 fire seasons using data obtained from the SCA.

Figure 3.10 presents fire historical records for the catchment of Lake Burragorang since completion of the dam, and includes data on the areas burnt during each event where available. It demonstrates a ‘jigsaw-burning effect pattern’, for example, the area that was burnt by the fire that occurred in 1964 in the lower reaches of the Nattai catchment did not burn during the 1968 fire event. Although the vegetation is likely to have regenerated to a point where it was able to burn during the latter fire, the vegetation was young and moist enough not to re-ignite. In the intervening 30 years between the fire events of 1967 and 1996-1997, the Nattai catchment experienced very sporadic and patchy burn events. The lack of fire events during this period was also probably influenced by the comparatively ‘wet’ years in the late 1980s (Figure 3.7). It is interesting to note that the fires of 1997-98 covered a similar area to that of 1964. Perhaps the spotting mechanism (Section 2.3) aided the spread of fire across the Wollondilly arm of the lake. The area burnt during the 1997-1998 fire provided a peripheral barrier to the area damaged during the extensive 2001/2002 fires.

Fire severity mapping of the 2001/2002 fires was conducted by Chafer *et al.* (2004) for the SCA with use of pre- and post- fire SPOT satellite imagery to calculate the Normalised Difference Vegetation Index (NDVI). Analysis of these data showed that slope aspect had little impact on fire severity and intensity, while the influence of slope gradient caused gently sloping land to experience the highest severity fires (Chafer *et al.* 2004). Assessment of fire severity (Table 2.1) is important for land management purposes, especially in terms of its expected influence on subsequent erosion. In turn, this has implications for the turbidity and water quality of the tributaries and the patterns of sedimentation in the reservoir.

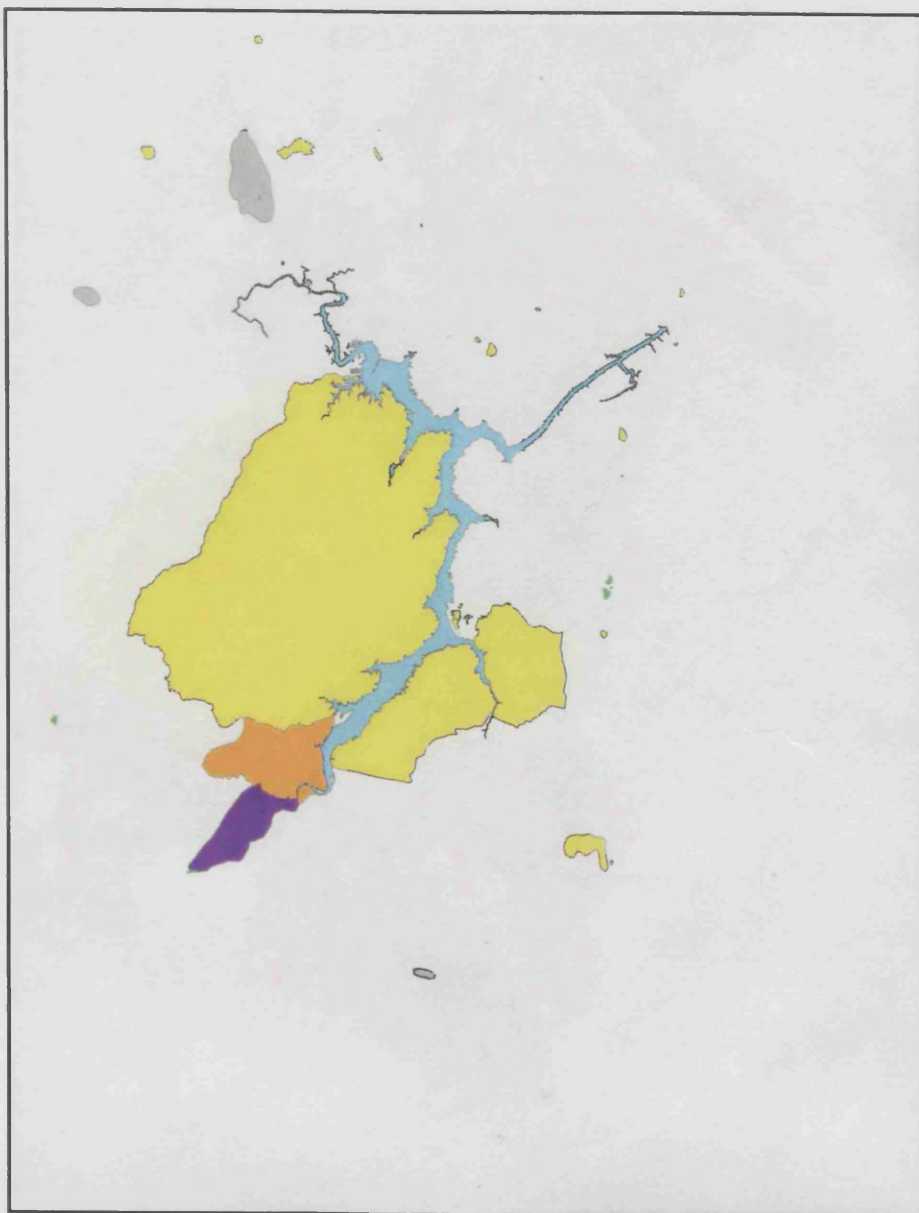


Figure 4.10: Adirondack Park, New York, 1991. Data: Adirondack Park Agency.

Legend

| | |
|---|--------|
| State of New York | Yellow |
| Adirondack Park Agency | Orange |
| Adirondack Park State Thruway Authority | Purple |
| Adirondack Park | Blue |
| Major Roads | Black |
| Water Bodies | Blue |
| Land Development | Grey |

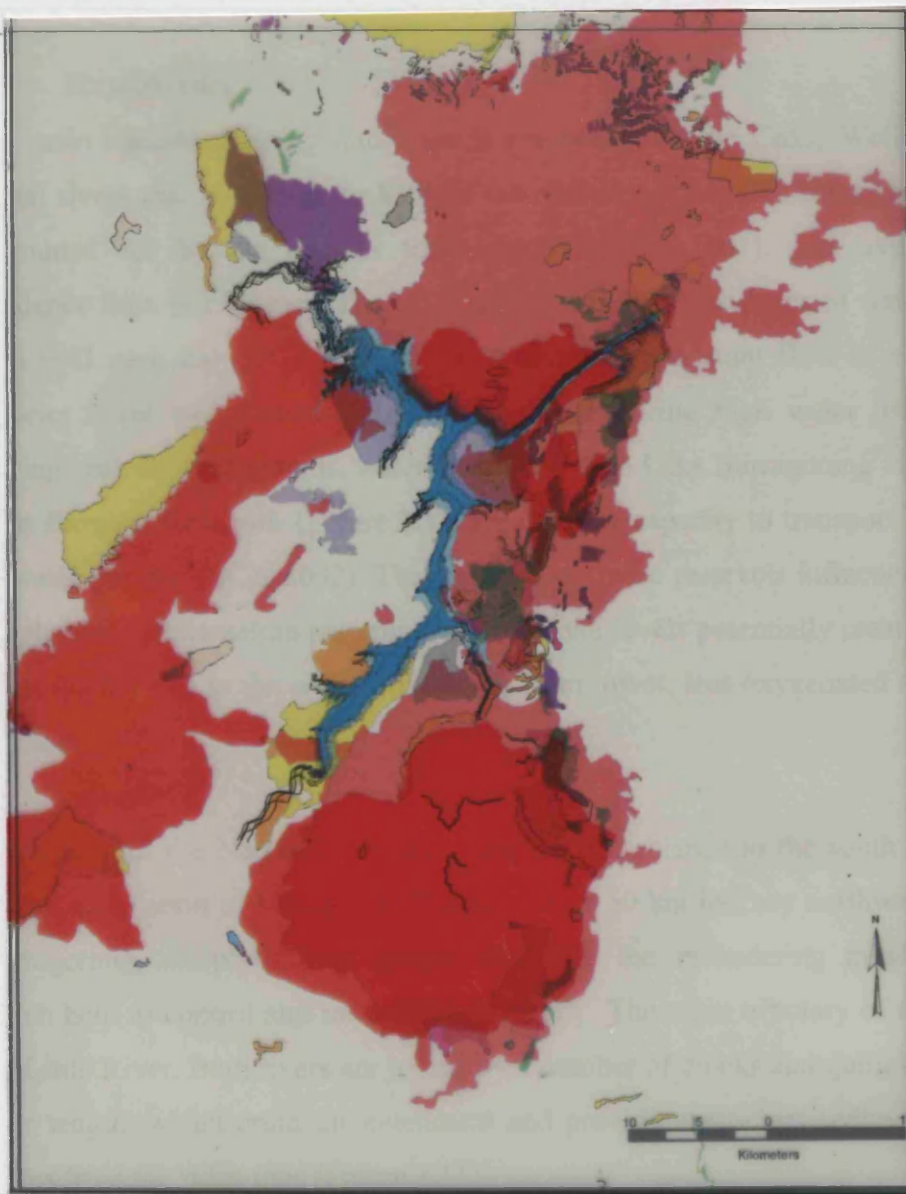


Figure 3.10a: Areas burnt between the 1962/63 and 1967/68 fire seasons

Legend





Figure 3.100: Map of the Lapland region showing land cover.

Lapland

Water

Land

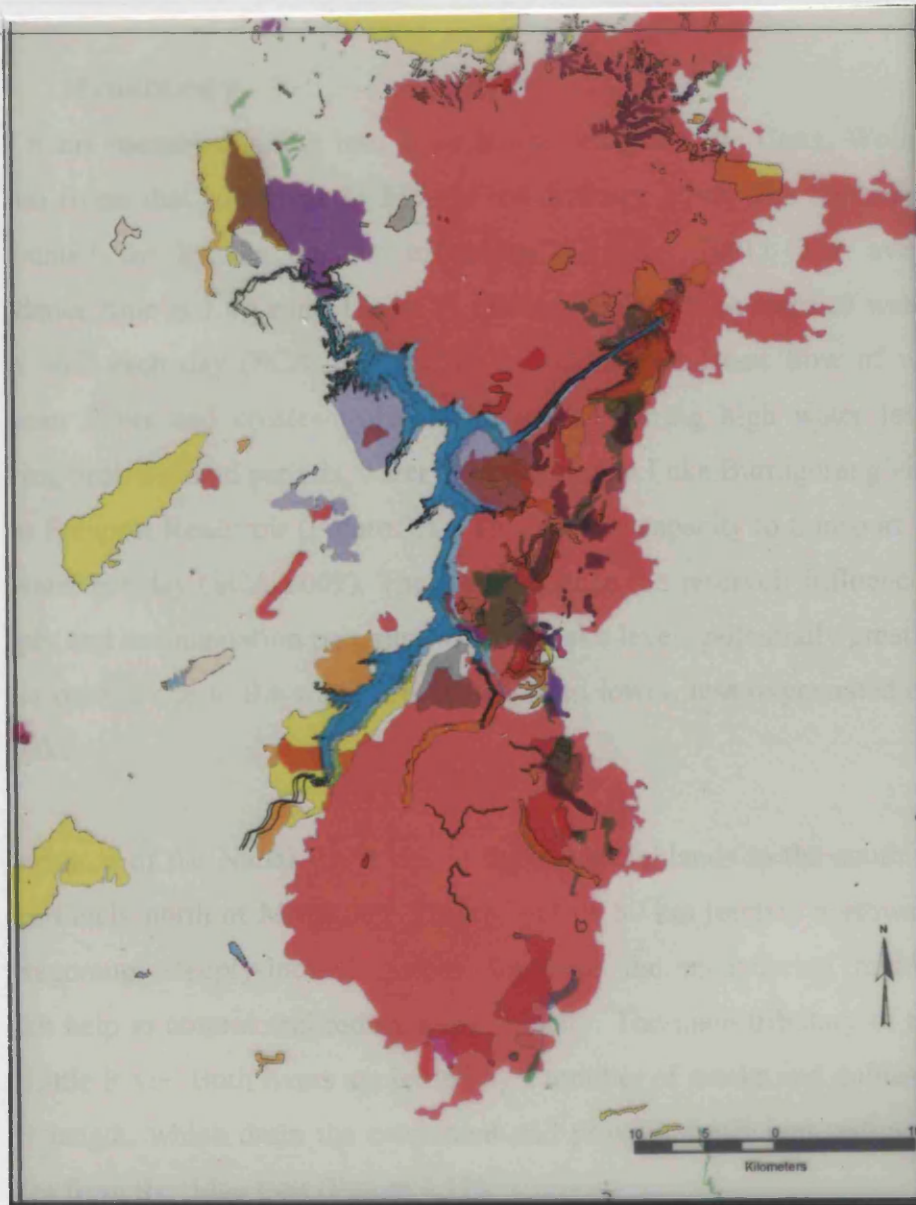


Figure 3.10b: Areas burnt during the 1968-1969 fire season

Legend

- 1968-1969
- Lake Burragorang

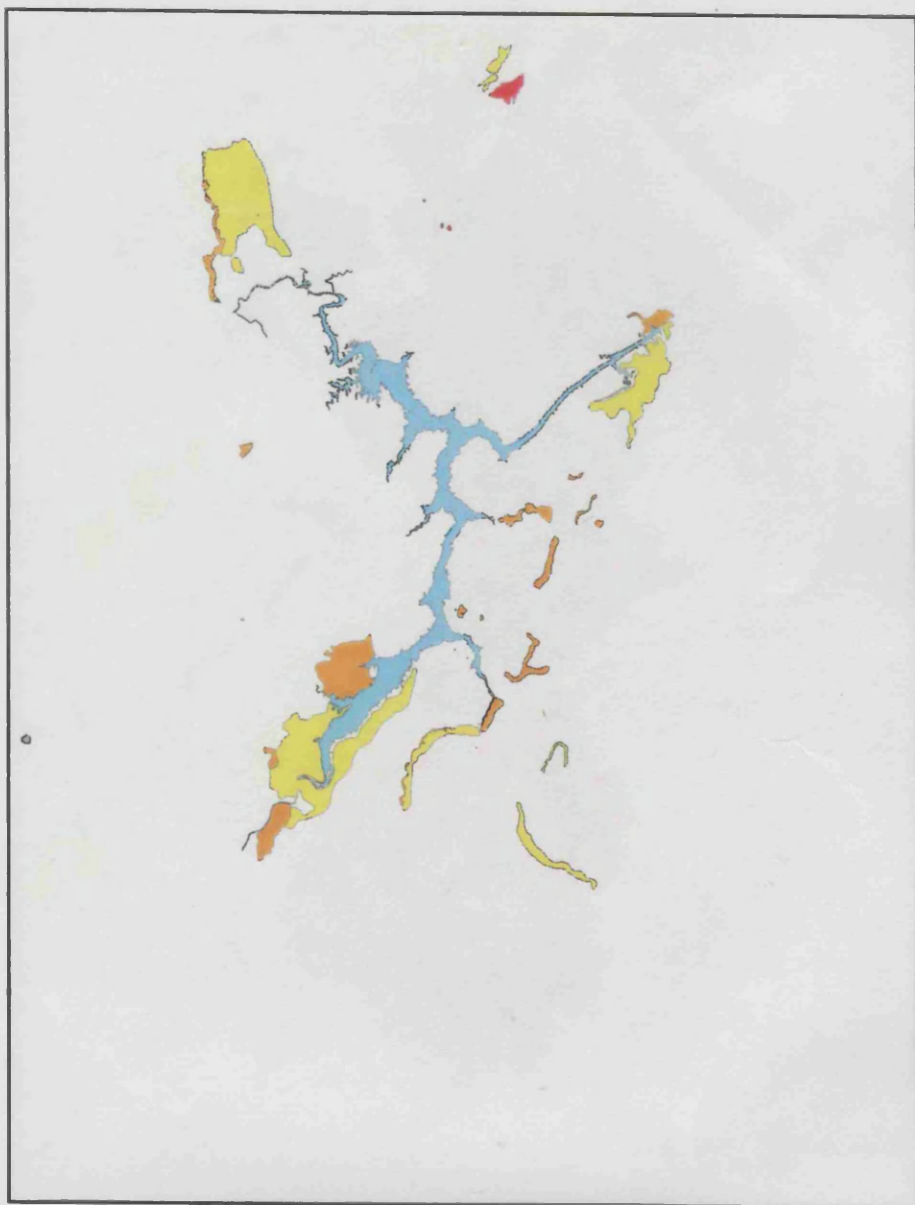


Figure 1. Map of the study area showing the location of the study sites.

Legend

| | |
|--|--------|
| | Water |
| | Land |
| | Marsh |
| | Forest |
| | Urban |

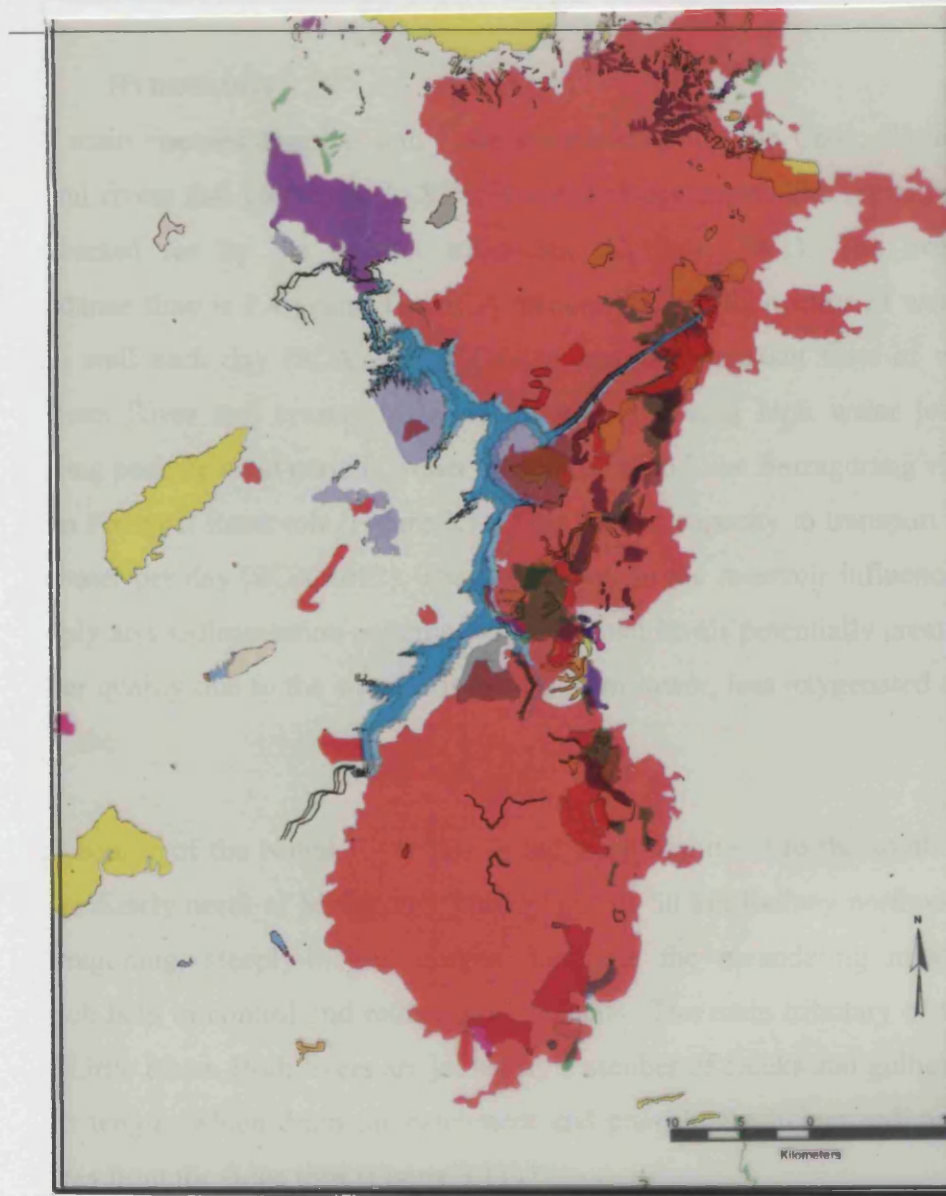


Figure 3.10c: Burnt areas between the 1969/70 and 1974/75 fire seasons

Legend



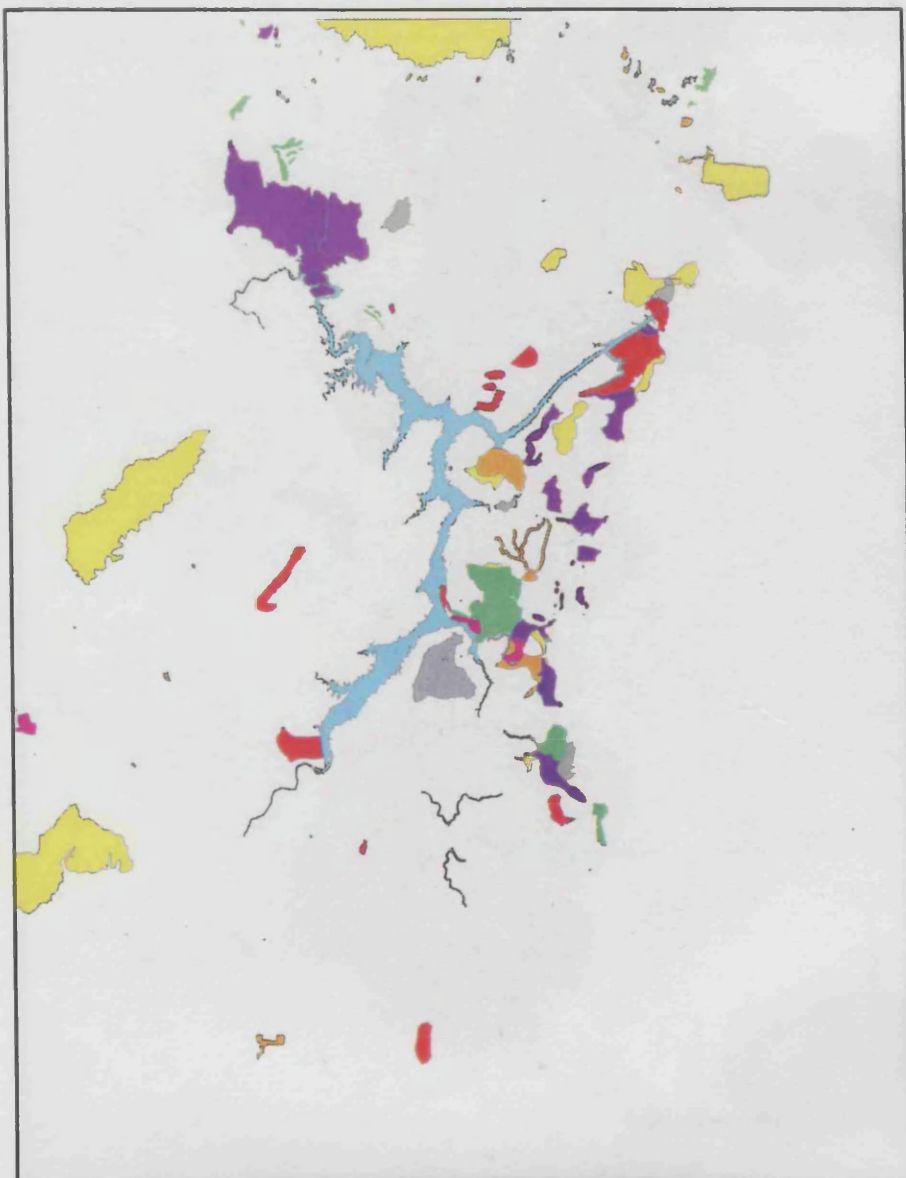


Figure 1. Map of the study area showing the location of the study area.

| Land Use | Area (km ²) | Percentage (%) | Area (km ²) | Percentage (%) |
|-----------|-------------------------|----------------|-------------------------|----------------|
| Water | 1.0 | 1.0 | 1.0 | 1.0 |
| Urban | 1.0 | 1.0 | 1.0 | 1.0 |
| Forest | 1.0 | 1.0 | 1.0 | 1.0 |
| Barren | 1.0 | 1.0 | 1.0 | 1.0 |
| Grassland | 1.0 | 1.0 | 1.0 | 1.0 |
| Shrubland | 1.0 | 1.0 | 1.0 | 1.0 |
| Wetland | 1.0 | 1.0 | 1.0 | 1.0 |
| Other | 1.0 | 1.0 | 1.0 | 1.0 |

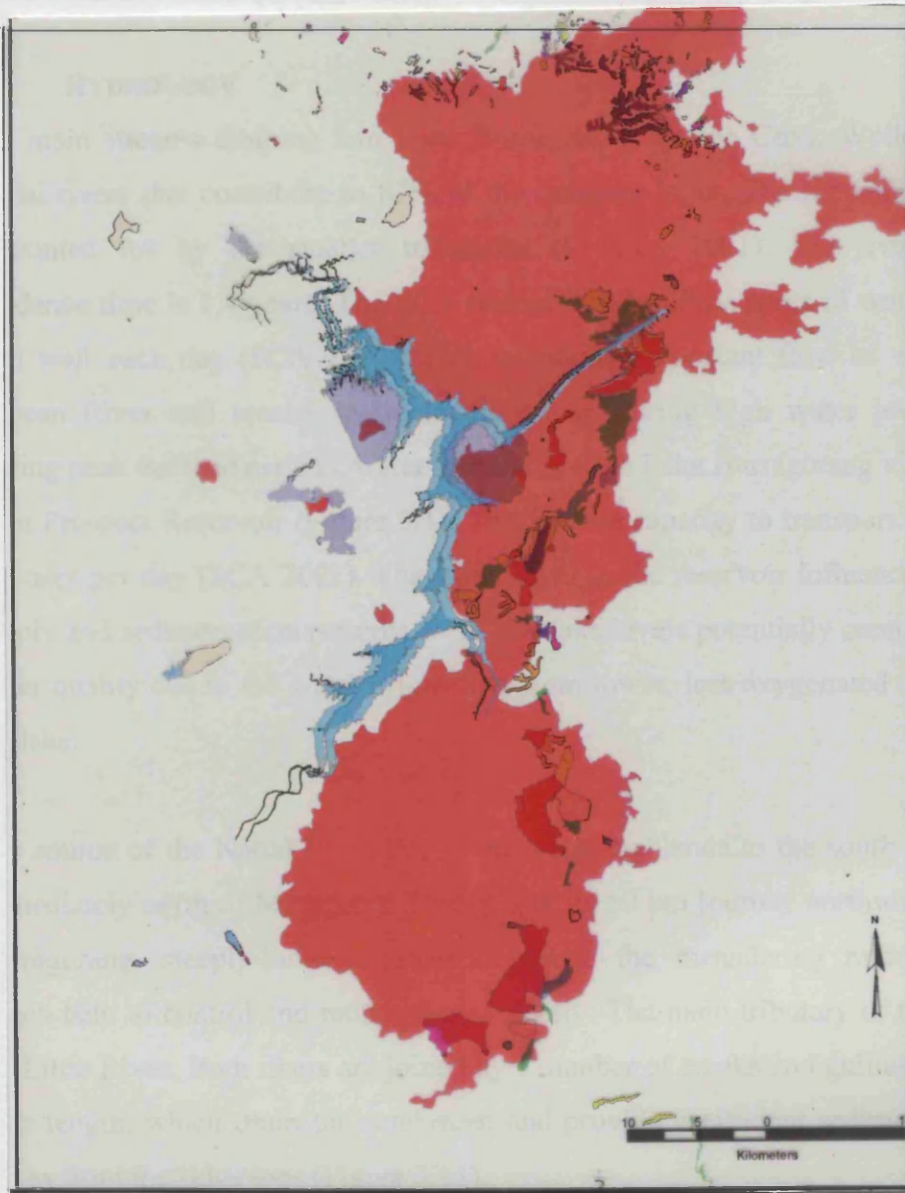


Figure 3.10d: Areas burnt between the 1979/80 and 1985/86 fire seasons

| Legend colour | Legend | Area: total catchment burnt (km ²) | Percentage of total catchment burnt (%) | Area: Nattai catchment burnt (m ²) | Percentage of Nattai catchment burnt (%) |
|---------------|------------------|--|---|--|--|
| | 1979-1980 | 3.15 | 0.035 | 1.30 | 0.35 |
| | 1980-1981 | 75.34 | 0.83 | 1.88 | 0.51 |
| | 1981-1982 | 30.57 | 0.34 | 17.53 | 4.75 |
| | 1982-1983 | 151.43 | 1.67 | 6.08 | 1.65 |
| | 1983-1984 | 22.22 | 0.25 | 8.26 | 2.24 |
| | 1984-1985 | 34.90 | 0.39 | 2.02 | 0.55 |
| | 1985-1986 | 25.96 | 0.29 | 18.39 | 4.99 |
| | Lake Burragorang | | | | |

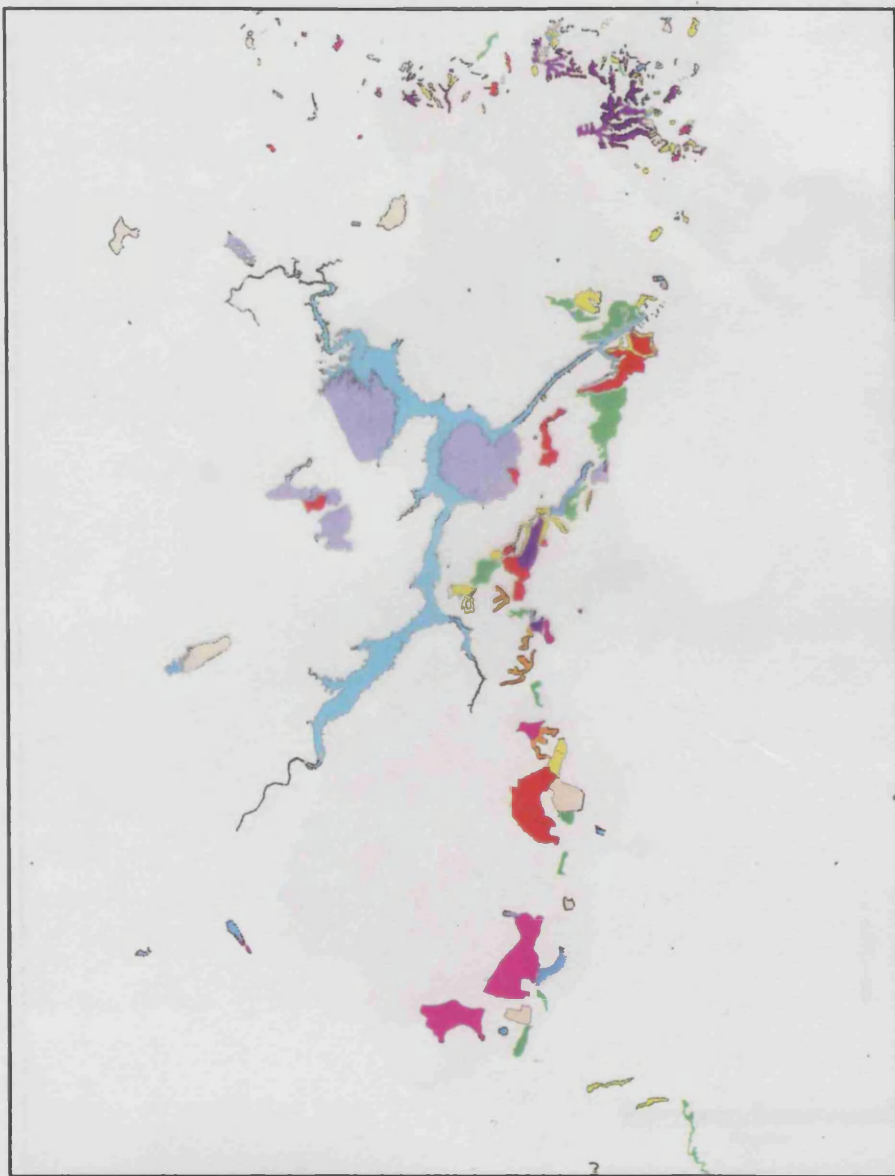


Figure 1. Map of the coastal region of the study area showing the different land use/cover types.

The map was generated using ArcGIS 10.2. The map shows the different land use/cover types in the study area. The map is divided into several zones, each with a different color. The zones are: 1. Urban (red), 2. Agricultural (yellow), 3. Forest (green), 4. Water (blue), 5. Wetland (pink), 6. Barren (purple), 7. Other (grey). The map also shows the location of the study area within the larger context of the region.

| Land Use/Cover Type | Area (km ²) | Percentage (%) |
|---------------------|-------------------------|----------------|
| Urban | 1.2 | 1.2 |
| Agricultural | 2.5 | 2.5 |
| Forest | 3.8 | 3.8 |
| Water | 4.5 | 4.5 |
| Wetland | 5.2 | 5.2 |
| Barren | 6.7 | 6.7 |
| Other | 7.1 | 7.1 |
| Total | 30.0 | 100.0 |

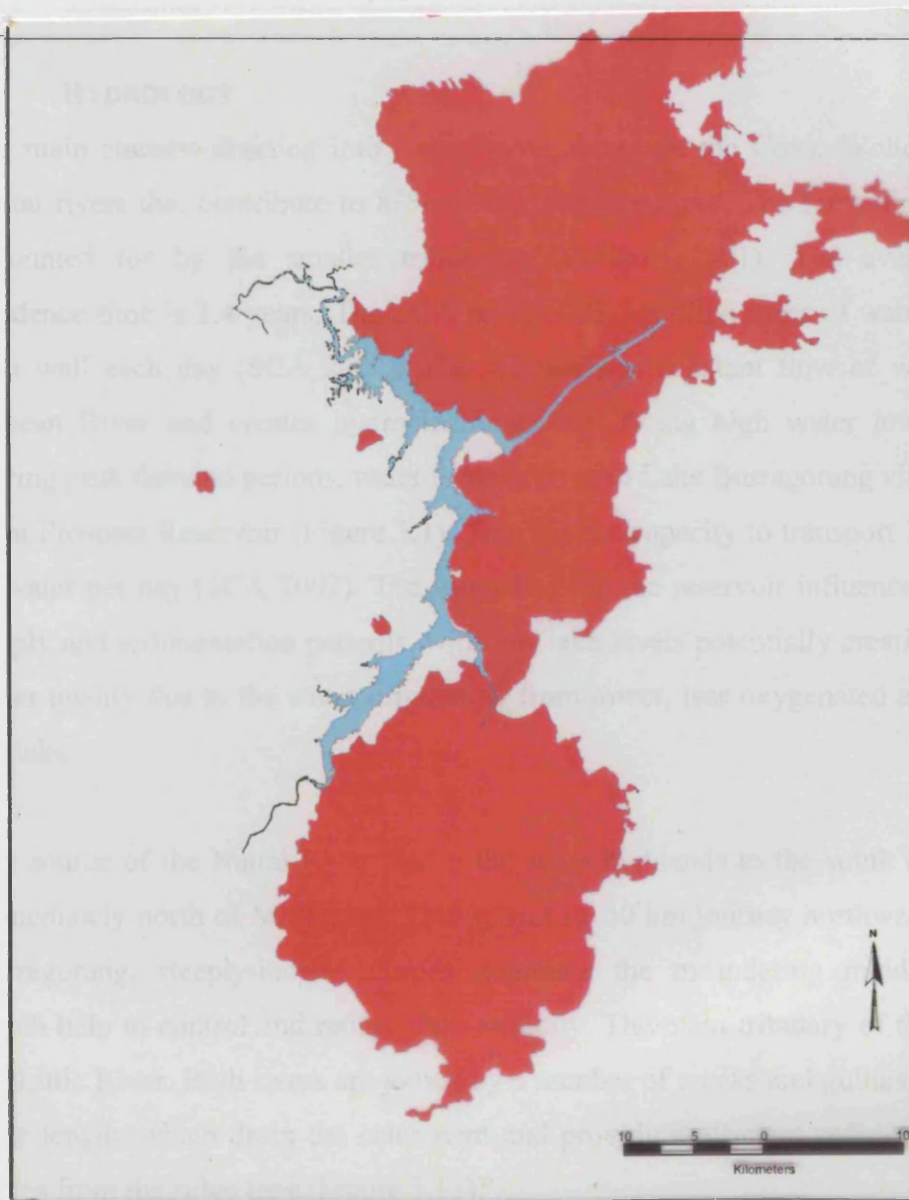
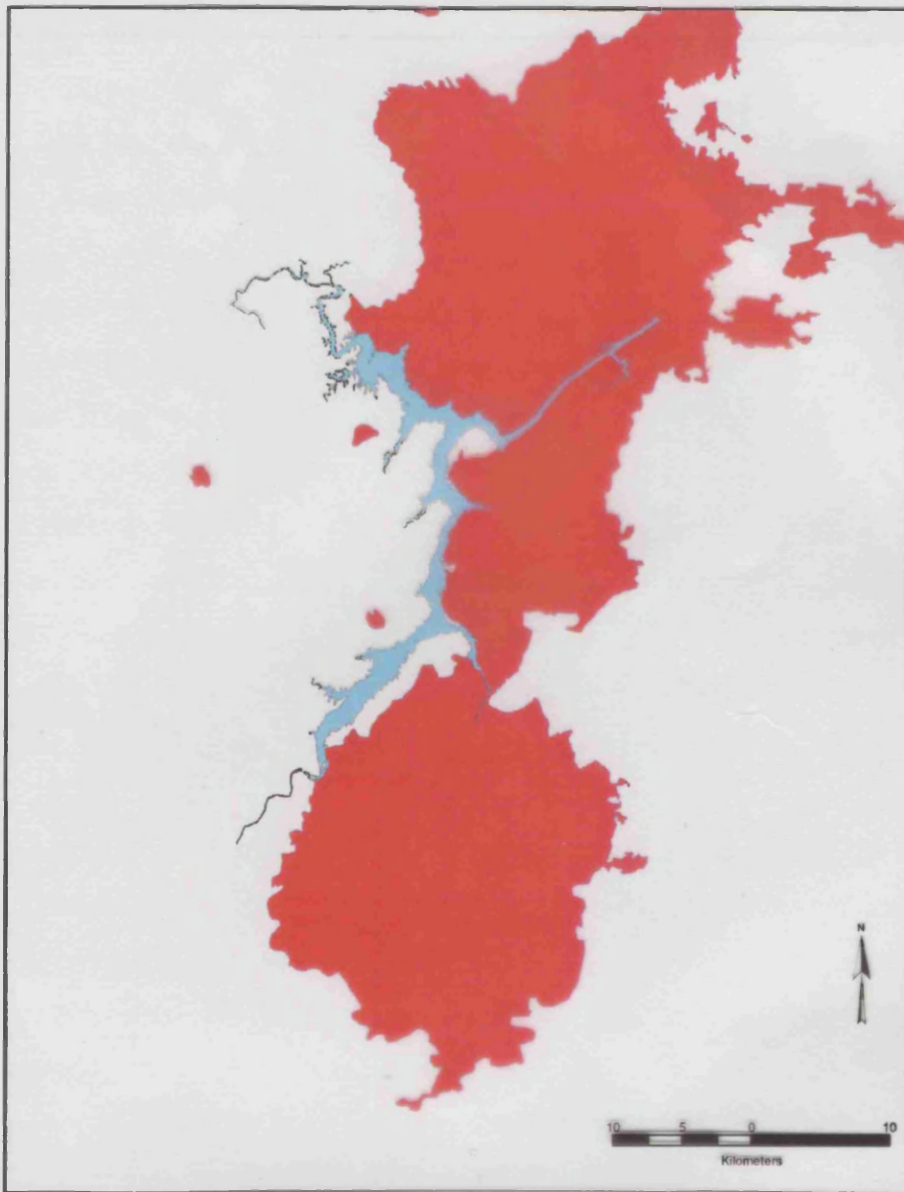


Figure 3.10e: Areas burnt between the 1986/87 and 1996/1997 fire seasons

| Legend colour | Legend | Area: Total catchment burnt (km ²) | Percentage of total catchment burnt (%) | Area: Nattai catchment burnt (km ²) | Area of Nattai catchment burnt (%) |
|---------------|------------------|--|---|---|------------------------------------|
| | 1986-1987 | 21.59 | 0.24 | 6.11 | 1.66 |
| | 1987-1988 | 15.00 | 0.17 | 2.74 | 0.74 |
| | 1988-1989 | 27.18 | 0.30 | 27.18 | 7.36 |
| | 1989-1990 | 19.93 | 0.22 | 0.79 | 0.21 |
| | 1990-1991 | 123.50 | 1.36 | 8.06 | 2.18 |
| | 1991-1992 | 20.31 | 0.22 | 4.50 | 1.21 |
| | 1992-1993 | 13.63 | 0.15 | 6.38 | 1.73 |
| | 1993-1994 | 31.66 | 0.35 | 12.25 | 3.32 |
| | 1994-1995 | 66.43 | 0.73 | 0.42 | 0.12 |
| | 1996-1997 | 10.11 | 0.11 | 3.60 | 0.98 |
| | Lake Burragorang | | | | |



Map of the study area showing the location of the sampling stations.


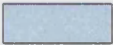
| Station | Date | Avg. Total bacteria count | % Coliform bacteria | % E. coli | % Vibrio |
|---------|----------|---------------------------------|------------------------|-----------|----------|
| 1 | 10/10/00 | 1000 | 25 | 10 | 5 |
| 2 | 10/10/00 | 1000 | 25 | 10 | 5 |
| 3 | 10/10/00 | 1000 | 25 | 10 | 5 |
| 4 | 10/10/00 | 1000 | 25 | 10 | 5 |
| 5 | 10/10/00 | 1000 | 25 | 10 | 5 |
| 6 | 10/10/00 | 1000 | 25 | 10 | 5 |
| 7 | 10/10/00 | 1000 | 25 | 10 | 5 |
| 8 | 10/10/00 | 1000 | 25 | 10 | 5 |
| 9 | 10/10/00 | 1000 | 25 | 10 | 5 |
| 10 | 10/10/00 | 1000 | 25 | 10 | 5 |

3.3 Hydrology

The main rivers discharging into Lake Burragorang are the Castlereagh, Wollondilly and Nattai rivers that contribute to 85% of the catchment input. The remaining 15% are accounted for by the smaller tributaries (Collicott 2001). The average water residence time is 1.4 years. The SCA releases 12.7 million litres of water from the dam wall each day (SCA 2002). This maintains a constant flow of water to the Nepean River and creates hydroelectric power during high water level periods. During peak rainfall periods, water is transferred to Lake Burragorang via a pipeline from Prospect Reservoir (Figure 3.1). This has the capacity to transfer 2.60×10^6 m³ of water per day (SCA 2002). The water level in the reservoir influences sediment supply and sedimentation patterns, with low lake levels potentially causing reduced water quality due to the water originating from lower, less oxygenated areas within the lake.

The source of the Nattai River lies in the steep highlands to the south of the lake, immediately north of Mittagong. Throughout its 50 km journey northwards to Lake Burragorang, deeply incised gorges dominate the meandering riparian reaches, which help to control and reduce flow velocity. The main tributary of the Nattai is the Little River. Both rivers are joined by a number of creeks and gullies throughout their length, which drain the catchment and provide a efficient sediment transport routes from the ridge tops (Figure 3.11).

Figure 3.10f: Areas burnt during the 2001-2002 fire season

| Legend colour | Legend | Area: Total catchment burnt (km ²) | Percentage of total catchment burnt (%) | Area: Nattai catchment burnt (km ²) | Percentage of Nattai catchment burnt (%) |
|---|------------------|--|---|---|--|
|  | 2001-2002 | 2250.00 | 25 | Not Available | Not Available |
|  | Lake Burragorang | | | | |

3.8 HYDROLOGY

The main streams draining into Lake Burragorang are the Coxs, Wollondilly and Nattai rivers that contribute to 83% of the drainage input. The remaining 17% are accounted for by the smaller tributaries (Colliton 2001). The average water residence time is 1.4 years. The SCA releases 33.3 million litres of water from the dam wall each day (SCA 2002). This maintains a constant flow of water to the Nepean River and creates hydroelectric power during high water level periods. During peak demand periods, water is transferred to Lake Burragorang via a pipeline from Prospect Reservoir (Figure 3.1). This has the capacity to transport $2,600 \times 10^6$ l of water per day (SCA 2002). The water level in the reservoir influences sediment supply and sedimentation patterns, with low lake levels potentially creating reduced water quality due to the water originating from lower, less oxygenated areas within the lake.

The source of the Nattai River lies in the steep highlands to the south of the lake, immediately north of Mittagong. Throughout its 50 km journey northwards to Lake Burragorang, steeply-incised gorges dominate the meandering middle reaches, which help to control and reduce flow velocity. The main tributary of the Nattai is the Little River. Both rivers are joined by a number of creeks and gullies throughout their length, which drain the catchment and providing efficient sediment transport routes from the ridge tops (Figure 3.11).



Figure 3.11: Hydrological catchment of the Nattai River (adapted from Colliton (2001))

3.8.1 RESERVOIR LEVEL

The wet periods reflected in the rainfall (Figure 3.7) and river flow data (Figure 3.12b and 3.12c) account to a large degree for the reservoir level variation illustrated in Figure 3.12a. However, the water level is also influenced by management practices, such as transport of water from the Prospect reservoir (Fig 3.2) (SCA 2002).

3.8.2 RIVER FLOW

Daily river flow records for the Nattai and Wollondilly Rivers (Figure 3.2) are shown in Figures 3.12 b and c. Tomkins et al. (in press) suggested that the majority of sediment transport in recent decades is likely to have occurred as a result of low-frequency catastrophic floods rather than high-frequency low-magnitude events. Catastrophic flood events have been defined by Erskine and Saynor (1996) as having a peak discharge of at least 10 times the mean annual flood. Using hourly peak discharge data, Tomkins et al. (in press) identified three major flood events that occurred in the catchment since the completion of the dam in 1960. These occurred during 15-22 April 1969, 21 June – 3 July 1975 and 19-30 March 1978 (Table 3.5), and coincided with the years of highest annual rainfall (Figure 3.7). The smallest of the three events produced a daily flow of 16159 ML. The daily flow data available from the SCA that was available for this PhD (Figure 3.12b and 3.12c) identifies that there were five days when high magnitude events occurred which produced similar volumes of water created during the catastrophic flood events identified by Tomkins et al. (in press). Although the high magnitude events would not have had the same velocity and erosive power as the catastrophic flood events they would have had a greater potential to entrain and transport material than normal daily flow events. Comparison of the flow data of the Nattai and Wollondilly rivers has demonstrated a good correlation between the two rivers in terms of responses to high magnitude events. The flow record for the Wollondilly River is 8 months longer than that of the Nattai and it extends back to 1965. The reservoir level will have also had a significant influence on sediment movement through the river owing to location of the delta during these events.

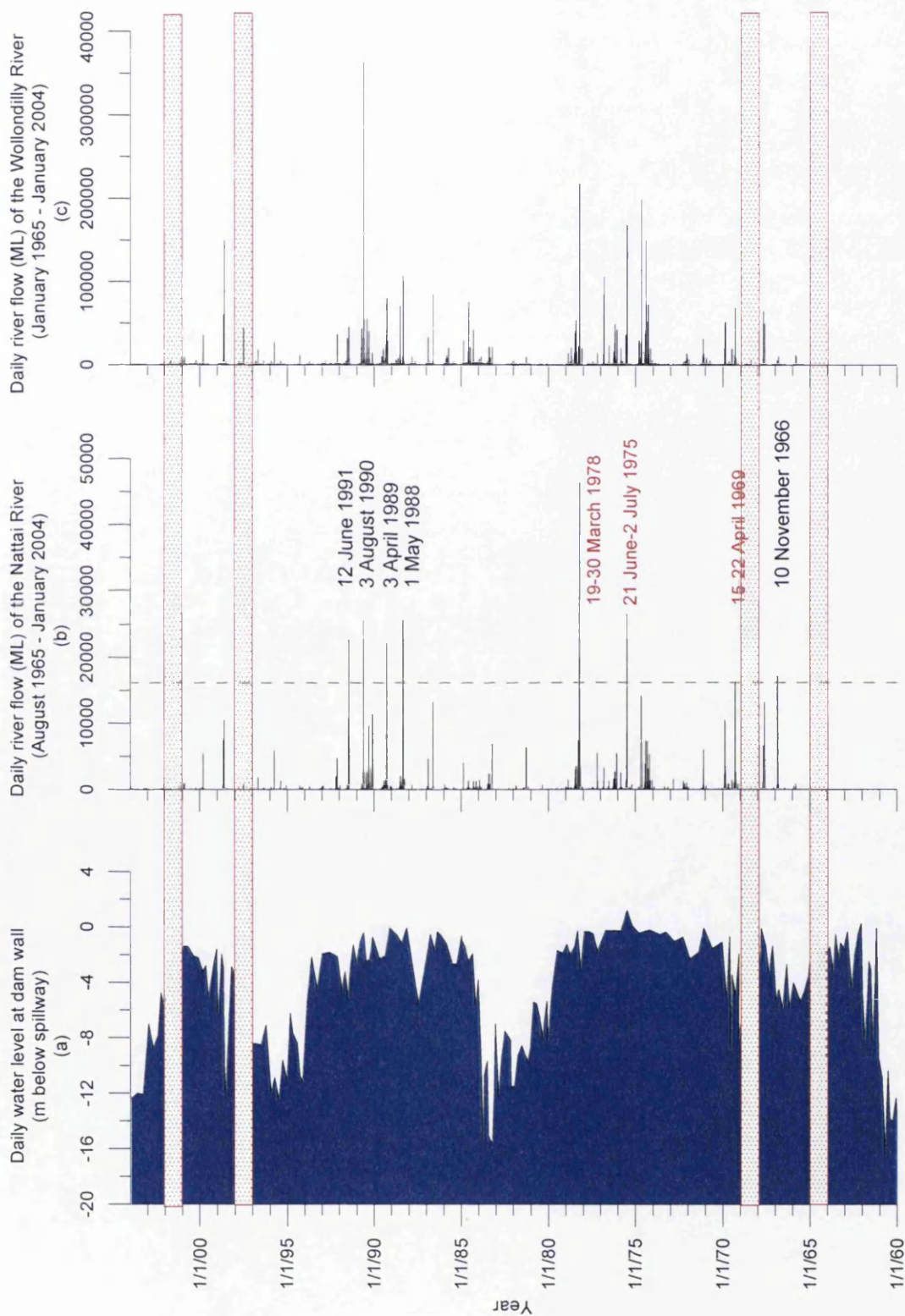


Figure 3.12: (a) Daily reservoir water level since 1960, (b) daily flow data for the Nattai River (catastrophic flood events are labelled in red and high magnitude events are labelled in black), and (c) daily flow data for the Wollondilly River.

Table 3.5: High magnitude (normal font) and catastrophic (bold font) flood events in the Nattai Reservoir and reservoir water level (adapted from (Tomkins *et al.* in press)).

| Date of high magnitude event | Highest daily flow of the Nattai River (10^6l) | Reservoir level (m below and above the spillway) |
|------------------------------|---|--|
| 10 November 1966 | 17134 | -3.66 |
| 17 April 1969 | 16159 | -2.88 |
| 22 June 1975 | 26616 | 1.3 |
| 21 March 1978 | 46470 | 1.01 |
| 1 May 1988 | 25695 | 1.01 |
| 3 April 1989 | 22227 | 0.35 |
| 3 August 1990 | 25709 | -0.92 |
| 12 June 1991 | 22741 | -2.33 |

The volumes of water carried by both rivers are reflective of the catchment size. The response of the river to individual rainfall events can be demonstrated with reference to a series of rainstorms that occurred in February 2002 when the increase in river flow was delayed by two days after the rainfall event. This pattern was also noted during the 2002 fieldwork (Figure 3.13). This highlights the role of vegetation in slowing the movement of surface water through the catchment, thus reducing its erosive potential and the risk of sediment-laden turbid flows.

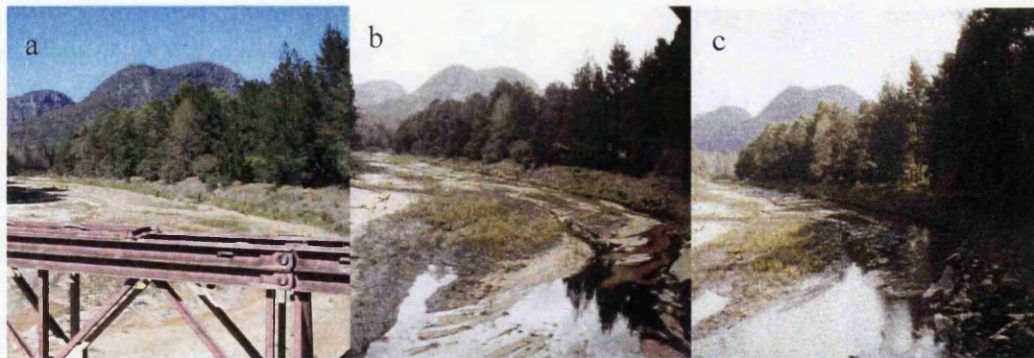


Figure 3.13: Nattai river flow during 2002 fieldwork: (a) before; (b) 3-days after; and (c) 5 days after a storm.

Within the Nattai catchment, turbid flows are generally restricted to the upper reaches of the Nattai River, which minimises the risk of turbidity currents entering the main water body. As a result, turbidity levels are only monitored on a monthly basis. However, additional measurements are made after storm / flooding events, or when very low flows occur (Fredericks 1994). Following severe flooding in 1990, turbidity levels at the dam wall exceeded recommended amounts. Increased flows as a result of flooding have the potential to carry larger amounts of nutrients in the water entering the catchment, with 70% of nutrients in the lake attributed to these events (Bonnet and Wessen 2001). Following fire, increased concentrations of potassium and nitrogen may occur due to modifications by burning that make these elements easier to extract by flowing water (Hollinger and Cornish 2001)

The hydrological characteristics of the Nattai and Little Rivers and their response to storm events highlight the significant role that vegetation plays in reducing sediment supplied to the rivers. However, the location of tributaries in relation to the reservoir is also important, because the distance that the flow travels within channels determines the turbidity of the current in terms of its load and its temperature regulates the type of inflow that it enters the lake (Figure 2.15).

3.9 LAKE BATHYMETRY AND CURRENTS

The topography of the pre-reservoir valleys has provided a complex bathymetric form to the floor of Lake Burragorang, causing the reservoir depth to vary throughout the whole of the lake. The steep mountainous dissected landscape characteristic of the area (Section 3.3) extends beneath the surface of the lake providing a 'Y' shaped cross-profile to the reservoir (Figure 3.14). This has implications for the temperature profiles, which in turn determine the type of inflows that occur. The irregular form also impacts upon currents and water velocity, which affect the patterns of sedimentation. These aspects are discussed in this section.

The bathymetry of the reservoir has a significant role in influencing temperatures that occur within the lake profile. The temperate climate in this area has no distinctive seasonal variation in daily reservoir water temperature (Section 3.6). This means that the inputs are more likely to be constant throughout the year, in contrast to an environment that experiences extreme variations. The 'Y' - shaped form of the lake causes the upper layers of the lake to absorb thermal radiation easily however, this heat does not always penetrate to lower layers of the lake. The differences in density between the two layers cause the upper layers to become more buoyant, whereas the water near the bottom of the lake is cooler and therefore more dense. This creates thermal stratification of the lake (Romero *et al.* 2004).

The thermal stratification of Lake Burragorang has considerable implications for the inflowing water from the tributaries (Figure 2.15) Underflows in the lake do not regularly occur due to the lower water temperatures experienced at depth. This is also evident from the presence of an anoxic hypolimnion recognised by Romero *et al.*, (2004). This is formed as a result the temperature stratification and produces a lack of oxygen in the lower layers of the lake. The effect of a flood on patterns of inflowing water was monitored during an event in 1997: a nutrient-laden underflow was observed that traversed the reservoir for approximately 7 days. During the following weeks, this cool, well-oxygenated underflow displaced the pre-flood hypolimnion upwards which resulted in a mid-depth anoxic region which had negative effects on water quality within the lake and also disrupted recently deposited finer materials (Romero *et al.* 2004).

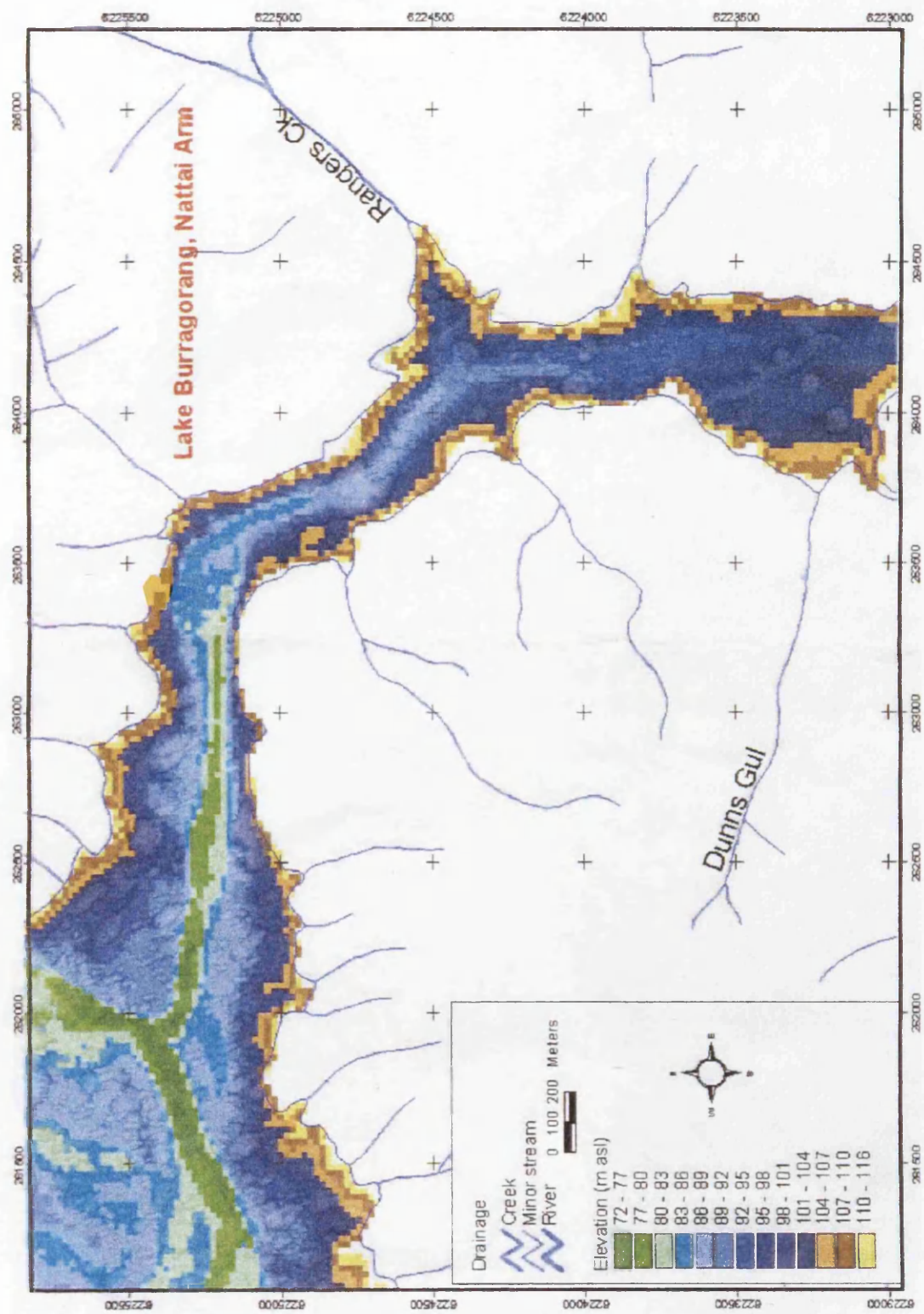


Figure 3.14 - Bathymetry of the Nattai arm of Lake Burragorang (Obtained from SCA records)

Disruption by strong winds to the anoxic region within Lake Burragorang has been observed causing accumulation of biomass on the downwind shore, and upwelling of dissolved phosphorus and other nutrients from deep waters, demonstrating stratification of the water (Bonnet and Wessen 2001). This occurrence of turbidity currents and water flows throughout the lake is important to acknowledge as they have the potential to carry and redistribute sediments over wide areas of the lake and determine the location of sediment deposition, while they also have the potential to affect water quality.

The irregular bathymetric valley form causes variability in the width of inflowing channels, especially in the zone where they meet the reservoir water. At this point, water begins to back-up and it floods lower regions of the river. This forms small, pooled areas or bays. The increased channel width at such locations causes a reduction in flow velocity and the deposition of the heaviest material entrained within the flows. In reservoir environments, migratory deltaic systems are often formed by the fluctuating water levels (Borland 1971).

The information concerning currents within the lake is an important factor in aiding the selection of coring sites feasibly sampled using the available coring equipment. Additionally, recognition of the site of the old river channel before flooding enabled the selection of a site on the old river banks where the highest levels of deposition were most likely to occur (Gottschalk 1964; Borland 1971).

3.10 PREVIOUS WORK ON SOIL EROSION, WATER REPELLENCY, SEDIMENT MOVEMENT AND DEPOSITION IN THE STUDY AREA

This section summarises previous and ongoing research conducted within the catchment of Lake Burragorang. It firstly reviews work carried out on erosion and mass movements within the catchment, highlighting areas of concern to the SCA. It then moves on to discuss the effects of fire on soil properties and hydrogeomorphological systems in the Blue Gum Creek area recognising: (i) small-scale modifications to the soil properties in terms of water repellency and the mineral magnetic signatures; and (ii) research into post-fire ground-level changes and bioturbation. Finally, it summarises the work carried out on historical erosion patterns through examination of the sediments within various sub-catchments of Lake Burragorang, including one study that investigated the potential increased sediment resulting from fire events. These aspects have been studied as part of a 2-year NERC funded project (NER/A/S/2002/00143 by R. Shakesby, S. Doerr and W. Blake in collaboration with G Humphreys and P Wallbrink). This project initiated research into the erosional consequences of different fire severities on soil water repellency in the Lake Burragorang catchment following the Christmas 2001 bushfires. The main aim was to assess how differences in water repellency resulting from the fire severity variations might affect erosion. The research was conducted using a variety of geomorphological and sediment tracing techniques. The main findings are summarised in this section.

3.10.1 SOIL EROSION AND MASS MOVEMENTS WITHIN THE CATCHMENT OF LAKE BURRAGORANG

Slope erosion within the reservoir catchment has long been of concern to land managers due to the potential effect of increased material and nutrients on water quality. An early forest survey by Wooten (1965) identified areas with the highest susceptibility to erosion within the catchment as: (i) roadsides; (ii) open unvegetated areas in which erosion was still active; (iii) burned areas; (iv) gullies; (v) coal washings, drainage from mines etc. (vi) gravel quarries, borrow pits etc; (vii) fire breaks and power line clearings; and (viii) overgrazed areas. The solutions proposed were centred on the importance of ground cover and re-vegetation.

The Department of Conservation and Land Management (CALM) conducted erosion mapping of Lake Burragorang in 1965. A simplified diagram of the erosion mapping is given in Figure 3.15. It shows areas where major gully erosion >1m deep and minor gully and sheet erosion are apparent. The map highlights major gully erosion within the Wollondilly catchment. The dominance of large gully systems within a tributary catchment to the Wollondilly has also been documented (Armstrong and Mackenzie 2002) (Section 3.5). The map shows minimal erosion within the Nattai catchment. Since the production of the map in 1965, the settlement of Mittagong has experienced significant expansion so that increased surface runoff caused by vegetation removal is likely to have made a greater contribution to erosion within the upper reaches of the Nattai.

Landslide events have also been documented in the Nattai catchment. In 1981, a major landslide occurred on a section of the Burragorang Wall escarpment at the mouth of the Nattai (Cunningham 1988). This event was attributed to subsidence, induced by coal-mining activities, combined with the weak nature of sandstone when in tension (Section 3.3). Further mass movement within the Nattai catchment has also been documented in the sub-catchment of Blue Gum Creek (Tomkins *et al.* In preparation). Rockfall evidence is apparent through the chaotic arrangement of Hawkesbury sandstone boulders on the upper slopes. Dating of landslide events was carried out using radiocarbon dating of organic rich sediments in 9 pits and an auger hole (Tomkins *et al.* in prep.). This suggested that a mass movement event occurred during the mid-late Holocene times.

The effects of heavy post-fire rainstorms have been shown to cause frequent accelerated erosion within New South Wales (Atkinson 1984). There had been no studies investigating erosion within the catchment of Lake Burragorang prior to the work carried out in connection with the NERC project, following the Christmas 2001 fires which affected a vast area of the catchment (see Section 3.7). Normalised difference vegetation index (NDVI) and analysis SPOT satellite imagery was conducted by Chafer *et al.* (2004) to obtain information about the severity of the fire by analysis of the level of destruction to the vegetation. The NERC project used one of these site surveys and the fire severity records to identify two sub-catchments that had experienced fires of different severity (moderate-high and low-moderate) on

valley-side slopes located on the eastern slopes of Blue Gum Creek (Figure 3.2) These sites were selected as they had similar landscape characteristics of slope aspect, angle, parent material, altitude and vegetation. An important feature affecting the design of this research project was the occurrence of heavy post-fire rainstorms immediately after the fires, which caused considerable erosion of the burnt topsoil but left some patches of soil intact.

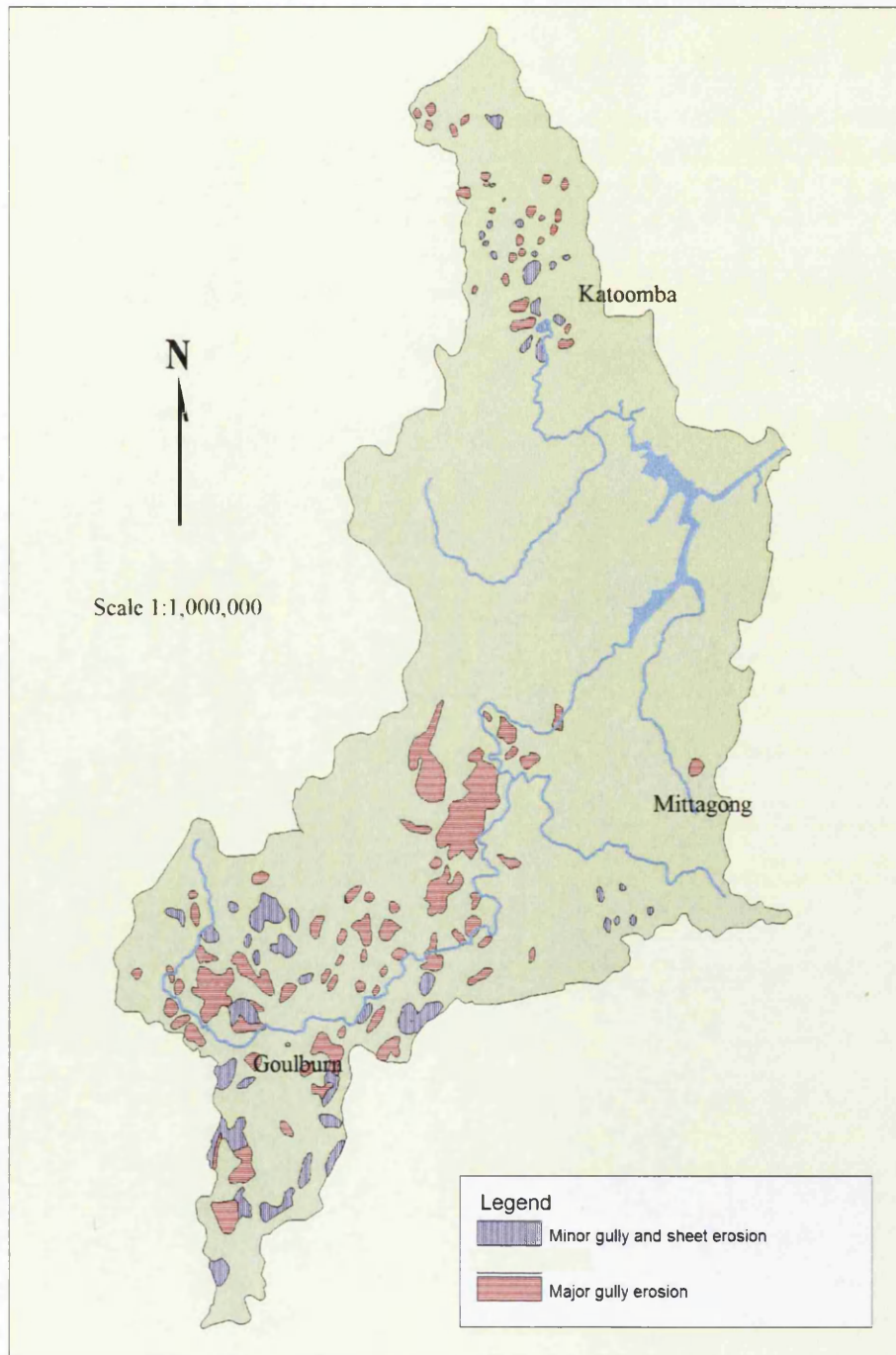


Figure 3.15: Occurrence of erosion in the region of Lake Burragarang identified by CALM survey in 1965 (Fredericks 1994)

3.10.2 EFFECT OF FIRE ON SOIL PROPERTIES WITHIN THE STUDY REGION

At the slope scale, research was carried out into the links between fire severity, soil water repellency and hydrogeomorphological changes following the 2001/2002 event (Shakesby *et al.* 2003; Blake *et al.* 2006a; Doerr *et al.* In press). The results showed that fire severity (Section 3.7) as defined by NDVI analysis (Chafer *et al.* 2004) provided a good indication of the level of destruction of the vegetation. However, investigations showed that NDVI analysis does not provide an accurate indication of the temperature reached within the soil during a fire, as this is dependent on the litter content, not measured by imaging techniques. This was shown to be the case by extensive testing of water repellency (and magnetic susceptibility) at 227 sites located in both the high and low burn severity sites along Blue Gum Creek, and at a long unburnt site since 1961 (Shakesby *et al.* 2003).

The results from Water Drop Penetration tests by Shakesby *et al.* (2003) showed that water repellency existed in 100% of the 29 surface soil sites and in 96% of the 25 sub-surface soil sites tested within the unburnt site. Analysis of the low-severity burn sub-catchment samples showed that 68-74 % of sites were repellent, while 12% of the high burn sites showed surface water repellency. 100% of the subsurface samples at both sites demonstrated subsurface repellency. This confirmed destruction of soil surface water repellency at higher temperatures and translocation to lower layers (Shakesby *et al.* 2003). It is significant that soil water repellency was destroyed at the surface in the severely burnt site because this indicates translocation of the water repellent layer to deeper areas within the soil profile. The destruction of water repellency occurred at temperatures similar to those experienced during severe fires. This was confirmed with laboratory experiments concerning the effect of heating on water repellency (Doerr *et al.* 2004). The samples for this latter study were collected from an unburnt area within the catchment and two other locations within south-eastern Australia, where destruction of water repellency was found to occur at temperatures between 350 and 400 °C (Doerr *et al.* 2004) for heating durations between 2 and 20 minutes.

Modification of the mineral magnetic properties in the samples at higher temperatures used for water repellent testing was investigated by Blake *et al.* (2004). They found that mineral magnetic enhancement of χ_{ARM} and χ_{lf} produced

distinctive signatures for slope units that had experienced different severity fires. These findings were used to suggest the dominant source of downstream sediments to assess the potential tracer application of mineral magnetic signatures derived from different slope locations that had experienced varying fire severities at Blue Gum Creek during the 2001/2002 fires (Figure 3.16). Comparison of the magnetic signatures obtained for surface soils within the catchment showed that the samples from the Little River sediment upstream of the Nattai confluence produced magnetic signatures that suggested the samples were derived from severely burnt sites, whereas the sediment derived from the Nattai upstream of the confluence produced a signature that the sediment originated from unburnt sites. Sediment downstream of the confluence contained a mixture of material from the Little and Nattai Rivers (Blake *et al.* 2006b). One of the limitations that Blake *et al.* (2006b) identified with using magnetic parameters in this study was the inability of the magnetic parameters that were modified by burning to be used to distinguish between the proportion of material from the Nattai and Little Rivers in the samples obtained from downstream of the confluence. This was attributed to the non-linearly additive (Walden *et al.* 1997) nature of additional magnetic parameters that were capable of distinguishing between burnt and unburnt sources (Blake *et al.* 2006b).

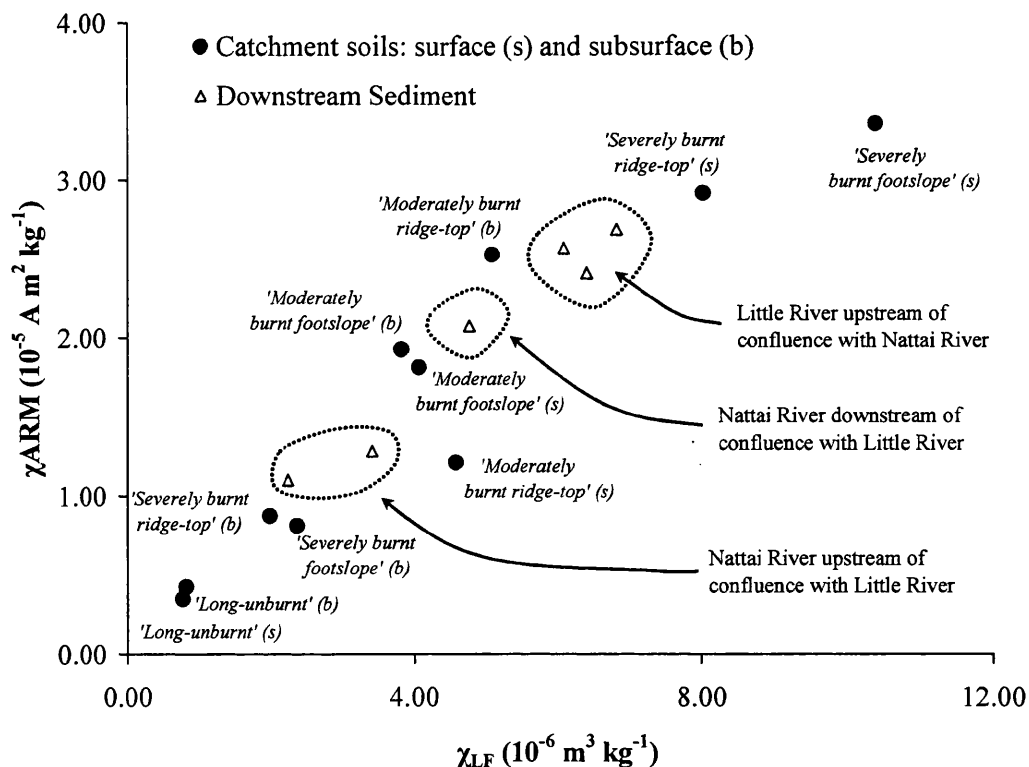


Figure 3.16: Distinctive signatures derived from a bivariate plot of χ_{LF} versus χ_{ARM} for <10 μm source material and downstream sediment from the Blue Gum Creek study site following the 2001 fires.

Comparison of the water repellency and mineral magnetic measurements showed a broad link between these two soil properties. However, different temperature thresholds for the alteration of magnetic properties were found which complicated this relationship. The identification of downstream sediments dominating from areas of moderate to severe fire suggests that post-fire modifications to water repellent properties of soil do not significantly affect the amount of erosion. This was attributed to the intensity of post-fire rainstorms (English *et al.* 2005).

Assessment of sediment redistribution after fire by Shakesby *et al.* (2003) was conducted by means of observations and measurements of: (i) surface ash; (ii) scorch lines on rocks; (iii) the heights of soil pillars and pedestals; (iv) examining and sampling of sediment drapes on ridge tops; (v) ground-level changes on the hillslopes; and (vi) evidence of bioturbation. The results are summarised in Tables 3.6 – 3.8. The presence of surface ash enabled identification of sites where either no post-fire erosion had occurred or where surface ash and burnt material had accumulated following erosion. Scorch lines on surface clasts were able to reveal the depth of material that had been eroded from next to rocks that were embedded into the ground. Soil pedestals were formed beneath stone and root caps predominantly by rainsplash erosion. The height of the pedestals were measured within fifteen 0.16 m² plots for the high- and low- severity burn sites at the Blue Gum Creek study site (Shakesby *et al.* 2006). The indicators of post-fire sediment redistribution in Blue Gum Creek Catchment that were investigated by Shakesby *et al.* (2003), Shakesby *et al.* (2004) and Shakesby *et al.* (2006) are summarised in Tables 3.6-3.8.

Table 3.6: Summary of post-fire sediment redistribution in Blue Gum Creek catchment (Shakesby *et al.* 2003).

| Aspect investigated | Evidence |
|--------------------------------|--|
| Surface ash | Remaining only at sites sheltered from erosion (e.g. downslope from fallen logs) |
| Scorch lines on surface clasts | Up to 2 cm above the soil surface |
| Soil pillars and pedestals | Heights ranging between 6.8 and 14.9 mm (measured in May 2002), |

| | |
|----------------|---|
| Sediment drape | White sand over uneven soil surfaces on ridge tops (Shakesby <i>et al.</i> 2003), indicative of wind erosion and redeposition |
|----------------|---|

Soil pedestals indicated the depth of the surface layer of soil that had been removed primarily by rainsplash erosion (Terry and Shakesby 1993; Stocking and Murnaghan 2001) when compared to material protected by stone caps. The heights of the pedestals were used to estimate topsoil losses of 50-100 t/ha. Evidence of significant topsoil removal was confirmed by the presence of fine organic rich topsoil, noted by Blake *et al.* (2005) in downstream river deposits.

Erosion bridge surveys were conducted at 27 sites in the two research catchments within the Blue Gum Creek following the 2001/2002 fire event and 4 sites within the Cataract River Basin, where sites were installed prior to the first post-fire rainfall event to monitor ground-level changes (Shakesby *et al.* 2006). Results from Blue Gum Creek showed a mean absolute change of ground level (accounting for removal of material by erosion and accumulation of material from eroded sediments upslope) for all measurements taken over the 3-year monitoring period ranging between 3.1 mm and 16.1 mm. Comparison of the 2003-2004 results with the 2002-2003 measurement period highlighted the significant influence that rainfall had on erosion processes, with greater depletion of material recorded in the wetter 2nd year of monitoring, despite the re-vegetation and re-establishment of litter cover (Shakesby *et al.* 2003; Shakesby *et al.* 2006). At the Cataract site (Table 3.7) a mean absolute change of 12.5 mm occurred. The erosion bridge sites were installed before and immediately after the 1st rainfall event. Despite 9 mm of rainfall occurring during the first rainfall event, there was modest mean absolute change of ground level which was attributed to the amount of rainfall not exceeding the storage capacity of the surface 1-2 cm of the soil in which water repellency had been destroyed during burning (Shakesby *et al.* 2006)

Bioturbation plots of 5 x 1 m were set up adjacent to the erosion bridge sites to monitor material translocation by ants and small mammals. Removing the material from the ant mounds allowed determination of the mass and volume of the material moved by ants. Mammal activity was monitored by measurement of the volumes of sediment removed in forming scrapes. Ant activity was shown to move up to 3.8 kg of slope material while small mammals moved up to 11.7 kg between 2002 and

2005 (Table 3.8). This equates to soil translocation of a scale of *c.* 7.8 t/ha over a 14-month period. Fire severity did not affect the extent of faunal bioturbation, but the stone content had a significant impact of the quantity of material moved by ants (Shakesby *et al.* 2006).

Ant activity was found to be more important in limiting erosion than in promoting erosion by providing sediment for removal by rain-splash and overland flow, The ants' nests increased surface roughness and provided sinks for overland flow. However, Dragovich and Morris (2002) argued that ants were important in actually moving material downslope.

Table 3.7: Mean loss/gain and absolute change results for erosion bridge sites: A) on Blue Gum Creek slopes, May 2002-February 2004; and B) on newly burnt terrain in Cataract River basin, January 2003-February 2004 (Shakesby *et al.* 2006).

| Location and fire severity | No. of Sites | Slope of angle(s) | May 11-12 2002-January 30 2003 | | | January 31 2003-February 20 2003 | | | February 21 2003-February 20-24 2004 | | | Whole period ^a | | |
|--------------------------------|----------------|-------------------|--------------------------------|---------------------|-----------------------|----------------------------------|---------------------|-----------------------|--------------------------------------|---------------------|-----------------------|---------------------------|---------------------|-----------------------|
| | | | Rainfall (mm) | Mean loss/gain (mm) | Mean abs. change (mm) | Rainfall (mm) | Mean loss/gain (mm) | Mean abs. change (mm) | Rainfall (mm) | Mean loss/gain (mm) | Mean abs. change (mm) | Rainfall (mm) | Mean loss/gain (mm) | Mean abs. change (mm) |
| A) Blue Gum Creek | | | | | | | | | | | | | | |
| <i>Foot-slope</i> | | | | | | | | | | | | | | |
| High severity | 6 | 6-8 | 166 | -1.8 | 3.1 | 40 | -2.8 | 2.2 | 811 | -1.8 | 4.1 | 1018 | -4.5 | 6.1 |
| Low severity | 3 | 5-8 | 166 | -3.3 | 6.9 | 40 | -0.9 | 3.8 | 811 | -0.6 | 4.9 | 1018 | -4.6 | 7.7 |
| <i>Mid-slope</i> | | | | | | | | | | | | | | |
| V. high severity | 6 | 15-32 | 166 | -3.3 | 6.0 | 40 | 2.0 | 5.4 | 811 | -6.0 | 9.3 | 1018 | -6.9 | 12.1 |
| Low severity | 5 ^b | 19-32 | 161 | -4.2 | 12.5 | 40 | -1.1 | 10.2 | 811 | -7.3 | 13.9 | 1013 | -7.6 | 16.1 |
| <i>Ridge top</i> | | | | | | | | | | | | | | |
| Extreme severity | 3 | 8 | 166 | -2.0 | 4.0 | 40 | -1.7 | 4.3 | 811 | -6.6 | 7.6 | 1018 | -10.2 | 11.3 |
| High severity | 3 | 8 | 153 | -1.8 | 4.3 | 40 | -1.0 | 4.0 | 811 | -1.4 | 7.5 | 1005 | -4.2 | 11.1 |
| B) Cataract River basin | | | | | | | | | | | | | | |
| Severely burnt | 4 | 8 | - | - | - | 29 | -1.8 | 2.3 | 924 | -9.7 | 10.3 | 953 | -11.8 | 12.5 |
| January 2003 | | | | | | | | | | | | | | |

Mean loss/gain values are calculated from negative values at individual measurement points representing ground-level lowering and positive values representing ground-level rise.

Mean absolute changes are calculated from ground-level changes at all individual measurement points recorded as positive values.

The rainfall figures are obtained from Nattai Crossing for Blue Gum Creek and from Cordeaux Office for Cataract River basin (see Fig. 1).

^a The whole period for Blue Gum Creek sites is May 2002-February 2004, that for the Cataract River basin is January 2003-February 2004.

^b One mid-slope site had to be abandoned because of a fallen tree.

Table 3.8. Summary of quantities and rates of different forms of bioturbation for different slope positions in sub-catchments H and L (Shakesby *et al.* 2006).

| Slope position | Surface gravel ^a (%) | Ant mounding ^a (g) | Small mammal scrapes ^a (g) | Total bioturbation ^b (t/ha/yr) | Total bioturbation ^b (mm/yr) |
|--|------------------------------------|----------------------------------|--|---|---|
| Sub-catchment L (mainly low to moderate fire severity) | | | | | |
| Foot-slope | <1 (<1) | 1042 (20-2016) | 2819 (0-8881) | 6.50 | 0.63 |
| Lower mid-slope | 17.3 (9.2-24.3) | 218 (108-397) | 4445 (0-11672) | 7.82 | 0.79 |
| Upper mid-slope | 33.8 (30.8-39.4) | 104 (0-158) | 1698 (0-2934) | 3.02 | 0.31 |
| Ridge top | 8.0 (4.5-14.7) | 777 (0-2146) | 456 (0-1368) | 2.09 | 0.19 |
| Sub-catchment H (mainly high to extreme fire severity) | | | | | |
| Foot-slope | 4.2 (<1-9.7) | 2134 (563-3852) | 950 (0-2313) | 5.24 | 0.47 |
| Lower mid-slope | 24.3 (19.5-29.7) | 26 (13-39) | 288 (0-864) | 0.53 | 0.05 |
| Upper mid-slope | 27.4 (24.3-32.4) | 384 (254-634) | 3560 (0-7748) | 6.62 | 0.66 |
| Ridge top | 6.4 (0-9.8) | 1196 (473-2317) | 329 (0-988) | 2.60 | 0.23 |

Based on measurements conducted on all plots Jan 30 2003 - Feb 28 2003 i.e. up to c. 14 months after fire

^aMean in **bold** and range in brackets based on three 5-m² plots, except for the foot-slope which is based on six plots

^bAnt mounding and surface scraping combined. Corrected for bulk density and expressed as an annual figure by linear interpolation.

Bulk density (g/cm³): ant mounds (n=7) mean=0.85, sd=0.08; surface soil (n=15) mean=0.98, sd=0.13

3.10.3 SEDIMENTOLOGICAL STUDIES WITHIN CATCHMENTS OF LAKE BURRAGORANG

Sedimentation patterns and processes within Lake Burragorang's subcatchments are highly variable. This is due to the strong influence of individual catchment factors. This section details previous research concerned with sediment movement in the Lake Burragorang catchment.

Previous research conducted on sediments in Lake Burragorang has included: (i) an assessment of sediment yields from the Whiteheads Creek subcatchment of the Wollondilly River (Armstrong and Mackenzie 2002); (ii) a comprehensive investigation detailing dominant sediment sources from the major inflowing rivers (Fredericks 1994); (iii) investigations of human induced pollutants in the Nattai River (Colliton 2001), Tonalli River (Harrison 2000), Werri Berri Creek (Rainbow 1999), and the Coxs River (Birch *et al.* 2001); and (iv) more recently, research on post-fire soil erosion and sedimentation has been conducted in the Little River and

the Nattai River catchments (Shakesby *et al.* 2003; Blake *et al.* 2004; Shakesby *et al.* 2006). Details of the findings from these sedimentological studies are summarised in Table 3.9.

Fredericks (1994) attempted discrimination of the different sediments within Lake Burragorang using radionuclide sediment tracing techniques to try to ascertain dominant sources of material entering the lake. His findings identified the Wollondilly and Coxs Rivers as the largest sources of sediment input to Lake Burragorang. He also found some evidence to suggest that contamination of the lower reaches of the Nattai had been caused by material from the Wollondilly, although this may merely have been a result of sorting processes. Total sediment yield was concluded to be comparatively high in comparison to other reservoirs in south-east Australia. This was attributed to the high relief and supported by findings from radionuclide fallout signatures suggesting that between only 20 and 40% of material in the lake was derived from topsoil. The dominance of material from the Wollondilly and Coxs rivers is also likely to be a result of the large catchment size and the high proportion of the area subjected to major gully erosion, transporting material from the ridge-tops to the fluvial system (English *et al.* 2005) (Section 3.8). The dominance of gullies as a means of transporting sediment and material through a catchment has also been recognised by Armstrong and Mackenzie (2002) who found that sediment yields from the Whiteheads Creek Catchment, a small tributary to the Wollondilly River (Figure 3.2), experienced 26% severe gully erosion, 55% moderate and minor gully erosion and 19% streambank erosion. They concluded that areas subject to discontinuously gullied catchments produced sediment yields of an order of magnitude less than for gullied catchments.

Analysis of the sources of eroded sediment by Blake *et al.* (2004) was carried out in an attempt to link the material eroded at the slope scale to the material deposited within the channel and reservoir. Research at the slope scale was conducted in the Blue Gum Creek study area. In summary, the results showed that:

- (i) fires of differing severity produced distinctive signatures attributable to mineral magnetic concentration, grain size and assemblage (Figure 3.16).
- (ii) magnetic material in foot slope zones consisted of fused micro-aggregates, suggesting a coarsening of magnetic grain size at this

location compared to the material sourced on the ridge tops. This change to mineral properties was attributed to diagenesis or to mineral formation processes linked to multiple burning.

- (iii) magnetically enhanced material found within Little River was apparently derived from ridge-top sites and was probably transported into the river mainly via gully systems.
- (iv) foot-slope deposits contributed relatively little to deposits found in the channel.
- (v) fire-enhanced magnetic material derived from the Nattai River had a lower mineral magnetic signal than samples from Blue Gum Creek, suggesting dilution of the bulk signature by deposits sourced from urban and agriculture sources upstream.
- (vi) in a sediment core taken downstream of the confluence of the Little River and Nattai River, magnetic minerals of a coarser grain size were more apparent than those that dominated the samples sourced from upstream regions. This suggests possible loss of the finer mineral magnetic Super Paramagnetic (SP) fraction caused by dissolution processes acting during sub-aqueous storage.
- (vii) mineral magnetic properties of soil and sediment can provide a useful tool for tracing sediment redistributed throughout the catchment.
- (viii) substantial post-fire rainstorm events accounted for 89% of sedimentation in the Nattai arm of Lake Burragorang.

Table 3.9: Summary of investigations on sedimentation in Lake Burragorang

| CATCHMENT | CATCHMENT AREA (KM ²) | SEDIMENTATION RATE | MAIN SOURCES OF SEDIMENTATION OR POLLUTION | REFERENCE |
|-------------------------------|-----------------------------------|---|--|---|
| Lake Burragorang | 9000 | 1.9±0.5 t/ha/y (assuming basal deposits are restricted to channels) | <ul style="list-style-type: none"> Initial rapid infill due to stabilisation of foreshores ~1960 2nd phase demonstrates background deposition rates Subsoil dominance due to steep terrain | (Fredericks 1994) |
| Nattai River | 369.1 | 4.4±1.4 t/ha/y (assuming basal deposits are not restricted to channels) Core 2: 0.6 ± 0.1 cm y ⁻¹ Core 3: 2 ± 2 cm y ⁻¹ Core 5 Zone a: 0.8 ± 0.1 cm y ⁻¹ Zone b: 0.16 ± 0.03 cm y ⁻¹ Core 6: 0.2 ± 0.1 cm y ⁻¹ | <ul style="list-style-type: none"> Increased levels of metal pollutants in the upper catchment due to urbanisation. Pollutants not transported to the lower catchment. Decrease in metal leaching occurred after 1991 coinciding with closure of mine. Charred particles deposited between 1960 and 1970, evidence of fire event in 1968/69. | (Colliton 2001) |
| | 369.1 | No data | <ul style="list-style-type: none"> | |
| Nattai River Tonalli River | 90 | Core 1: Located within the Tonalli River Before 1923: 0.07 ± 0.03 cm y ⁻¹ After 1923: 0.26 ± 0.03 cm y ⁻¹ | <ul style="list-style-type: none"> 89% of reservoir sedimentation in the Nattai arm attributed to substantial post-fire rainstorm events following the 2001-2002 fires Complex depositional patterns in core 2 caused by coring location at the mouth of the river. Increased sedimentation caused by changed land use, or an increase in large rainstorm events. | (Tomkins <i>et al.</i> 2004) (Harrison 2000) |
| | 90 | Core 2: Located at the mouth of the Tonalli River Before 1923: 0.04 ± 0.01 cm y ⁻¹ After 1923: 0.10 ± 0.021 cm y ⁻¹ 1960s: 0.14 ± 0.04 cm y ⁻¹ 1996-2001: 1.2 ± 0.4 cm y ⁻¹ | | |
| Lacy's Creek | 60 | Collected at the mouth of Lacy's Creek Before 1982: 0.14 ± 0.04 cm y ⁻¹ After 1982: 0.5 ± 0.2 cm y ⁻¹ | <ul style="list-style-type: none"> Forested catchment with no mining activity Comparatively small amounts of erosion Low metal concentrations | (Harrison 2000) |
| Werri Berri Creek | 167 | High organic content: 12-13 cm y ⁻¹ Medium organic content: 9 cm y ⁻¹ Low organic content: 4 cm y ⁻¹ | <ul style="list-style-type: none"> 3 major anthropogenic sources of nitrogen in the upper catchment: agricultural sources, storm water runoff and seepage of septic tanks from urban areas High organic content – possibly as a result of heavy post fire storm events. | (Rainbow 1999) |
| Coxs River | 270 | No data | <ul style="list-style-type: none"> Pollutants not transferred from upstream sources into Lake Burragorang as they were trapped in Lake Wallace and Lake Lyell | (Birch <i>et al.</i> 2001) |

The research conducted on sedimentation rates in various sub-catchments of Lake Burragorang identified values ranging between 0.04 cm y^{-1} and 13 cm y^{-1} . The large range highlights the dominance of localised catchment conditions in determining levels and patterns of deposition. The cores obtained from the floor of the Nattai arm of Lake Burragorang by Colliton (2001) demonstrated uniform sedimentation for three of the four cores, whereas all the cores obtained from other rivers identified at least one change in sedimentation rate. The explanations proposed to account for different sedimentation rates in all the studies highlighted the influence of changing land use patterns and the timing of major storm events. Additionally, the considerable sediment storage capacity of the foot-slopes has been a common factor, as indicated by: (i) material located in the foot-slope zones showing evidence of multiple burn events (Blake *et al.* 2004); (ii) ^{137}Cs budget measurements highlighting the dominance of localised redistribution of the material on the slopes to the valley floors, and minimising soil losses reaching the fluvial system, although significant amounts of nutrients and organic matter were found to be removed from the slopes (English *et al.* 2005); and (iii) long-term slope storage identified through continued, but diminishing release of metal pollutants within the sediment core from the Tonalli River, suggesting that ‘tailings erosion’ continued to deposit and remobilise polluted material stored on the slopes (Harrison 2000).

Key findings relating to sedimentation in the Lake Burragorang catchment relevant to the present study can be summarised as follows:

- Erosion of tailings containing heavy metals leached from coalmines may affect mineral magnetic signatures of sediments.
- Sedimentation rates depend on catchment conditions, deposition rates in a pristine catchment of Lacy’s Creek ranged between 0.14 to 0.5 cm y^{-1} (Table 3.9).
- High sedimentation rates in Werri Berri Creek seem to be associated with the movement of large quantities of organic matter.
- Other than being caused by fire, high sedimentation rates seem to occur in catchments: (i) in association with major gully systems; (ii) as a result of major storm events; and (iii) through increased anthropogenic activity.
- Dominance of subsoil contained within sediment from a variety of tributaries to Lake Burragorang reflects the steep terrain, apparent in the southern tributaries.

3.11 SUMMARY OF RESEARCH GAPS ARISING FROM RESEARCH WITHIN THE CATCHMENT OF LAKE BURRAGORANG

In the literature review in Chapter 2 various research gaps were identified. These have been reiterated by investigations conducted within the study area including work by the NERC-funded project group referred to earlier concerned with the effects that forest fires have on the catchment of Lake Burragorang. This research highlighted a broad range of processes that occur at very different scales, from the modification of the properties of individual soil grains to enhanced erosion associated with heavy post-fire rainstorms and the resulting increased sedimentation. This work, combined with previous and ongoing studies, has highlighted a number of potential lines for further investigations, which are summarised below.

Preliminary findings by Shakesby *et al.* (2003) found different magnetic signatures could be derived from areas that had experienced different fire severities. However, this was later found to be of little use for sediment source tracing due to the non-linearly additive nature of the quotients used to discriminate between sources (Blake *et al.* 2006a). These findings confirmed the need for: (i) a better understanding of temperature thresholds required to identify mineral magnetic properties of Australian soils and sediments (research gap 1); (ii) the development of a technique or techniques to identify soil heating levels experienced by soils during fire (research gap 2); and (iii) investigation of the effect of fire location and pedo-environmental conditions on the response of the location-specific mineral magnetic signatures to heating (research gap 3). The fourth research gap, regarding the reliability of fire histories preserved in reservoir sediments, had not previously been explored within the study area and has previously received relatively little attention. It was anticipated that this would prove challenging due to the dynamic nature of this type of sedimentary environment with respect to: (i) variable water levels; (ii) delta migration; (iii) the unreliability of burnt sediment reaching the lake because of highly variable post-fire rainfall; and (iv) turbid flows in the reservoir. Despite these potential problems, an important goal in this thesis was to identify appropriate techniques for reconstructing the fire history from such an environment not only in order to shed light on the hillslope-channel-reservoir transfer of post-fire sediments in the study area, but also to improve techniques for interpreting eroded burnt sediments in a range of sediment sinks including lakes, alluvial fans and reservoirs.

4 RESEARCH DESIGN AND RATIONALE

4.1 INTRODUCTION

In this section, the research design, including aims and methods used for this study, are outlined. The main framework for this investigation is presented in Figure 4.1 and the research questions leading to the specific aims and overall aim are discussed.

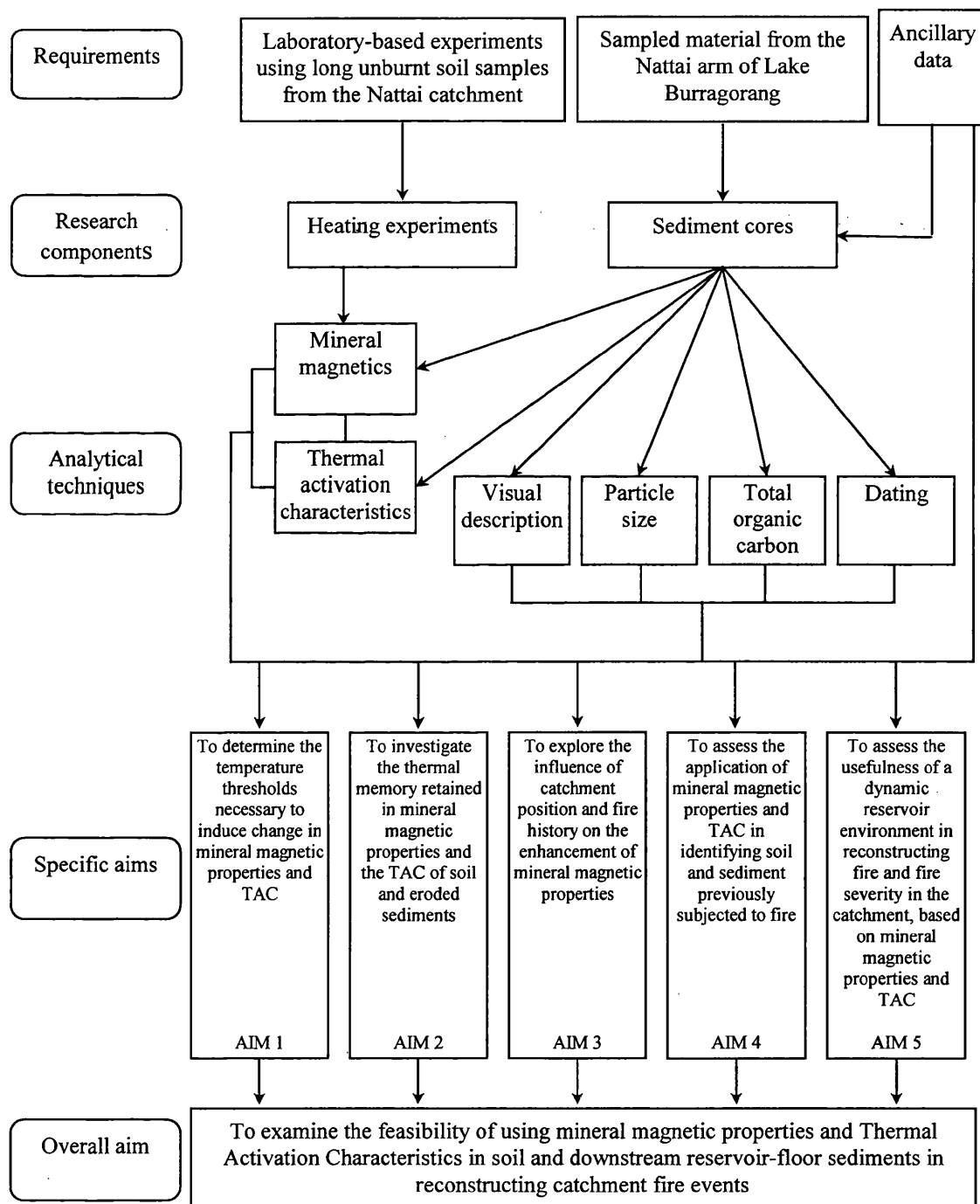


Figure 4.1: Research design

4.2 RESEARCH DESIGN AND RATIONALE

This research design is based on five main aims that have arisen from research gaps identified in the literature review. There have been six stages of experimentation leading to these aims being achieved. The aims (Figure 4.1) have been pursued through a variety of research questions.

The laboratory-based heating experiments were developed in order to investigate the following aims: To determine the temperature thresholds necessary to induce change in mineral magnetic properties and TAC (aim 1); To investigate the thermal memory retained in mineral magnetic properties and the TAC of soil and eroded sediments (aim 2); To explore the influence of catchment position and fire history on the enhancement of mineral magnetic properties (aim 3). These research questions were addressed through four stages of investigation using mineral magnetic measurements (Stages 1 and 2) and Thermal Activation Characteristics (TAC) (Stages 3 and 4). Collection of sediment cores from the Nattai arm of Lake Burragorang were obtained to: assess the application of mineral magnetic properties and TAC in identifying soil and sediment previously subjected to fire (aim 4); and assess the usefulness of a dynamic reservoir environment in reconstructing fire and fire severity in the catchment, based on mineral magnetic properties and TAC (aim 5) (Stages 5 and 6).

Stage 1 of the mineral magnetic investigations was conducted by furnace-heating a long-unburnt, footslope sample using temperature increments between 50 and 800 °C for durations of 5, 10, 20 and 40 minutes. This enabled the following research questions to be addressed: Which magnetic parameters are enhanced by heating? (Research question 1); which temperature thresholds are required to produce enhancement of magnetic parameters? (Research question 2); and what is the effect of heating duration on magnetic parameters? (Research question 3).

Stage 2 of the mineral magnetic investigations involved measurement of changes to magnetic susceptibility (χ) during heating to successively increasing temperatures between 100 and 700 °C and cooling to 40 °C under air and nitrogen atmospheres. This enabled the following research questions to be addressed: what changes occur to χ during heating and cooling? (Research question 4); what is the influence of

reducing conditions on the magnetic enhancement of χ ? (Research question 5); what effect does previous fire severity have on temperature thresholds needed to produce enhancement of magnetic properties? (Research question 6); and how do soils from different slope locations within the catchment respond to the same heat treatments? (Research question 7).

Progressive heating enabled thermal histories experienced by samples to be obtained and also gave information about changes occurring to magnetic properties not apparent in the final enhancement on cooling. This has been investigated by Marmet *et al.* (1999), Peters *et al.* (2001) and Hanesch *et al.* (2006). However, the thermal histories of soils in Australia have not been investigated and neither has the effect that frequent fire events in the Australian environment has had on background mineral magnetic signatures. To improve understanding of the potential use of pyrogenically-enhanced mineral magnetic signatures in sediments, it was important to establish the post-fire locations most susceptible to post-fire erosion. This was carried out by sampling from a range of morphological type sites in the catchment (e.g. footslope, mid-slope and ridge-top locations).

Stage 3 of the investigation was concerned with determining the properties of TAC. This involved investigation of long-unburnt foot-slope soil samples that had been furnace-heated to temperatures ranging between 50 and 800 °C for 40-minute durations, enabling the following research questions to be addressed: which temperature thresholds are required to produce modification of TAC of a long-unburnt foot-slope soil sample by heating? (Research question 8); can thermal histories of grains within a long-unburnt foot-slope soil sample be ascertained from single-grain TAC? (Research question 9); which features in TAC following furnace heating are apparent for the long-unburnt foot-slope sample simulated to represent heating to different temperatures *ca.* 10,000 years ago? (Research question 10).

An investigation of TAC was conducted after the mineral magnetic results had indicated that enhancement occurred at temperatures only exceptionally experienced in soil during wildfire. Previous application of this technique in archaeology suggested that it might prove promising in identifying wildfire-affected soil and eroded sediments, as this work had shown that changes occurred at lower

temperature thresholds than were required to bring about changes to the mineral magnetic properties.

Stage 4 involved investigation of TAC of a previously unexposed bedrock sample furnace-heated to temperatures ranging between 50 and 800 °C for 40-minute periods. This enabled the following research questions to be addressed: which temperature thresholds are required to produce modification of the 110 °C Thermoluminescence (TL) sensitivity (χ) peak (Research question 11); which temperature thresholds are required to produce modification of the shape of TAC plots of unexposed unheated bedrock samples when heated? (Research question 12); and which features of TAC following furnace-heating are apparent for the unexposed, unheated bedrock sample subjected to simulated heating to different temperatures *ca.* 10,000 years ago? (Section 2.3.5) (Research question 13).

Stages 5 and 6 assessed the potential use of mineral magnetism and TAC in identifying burnt material and the degree of soil heating within sediment cores from Lake Burragorang together with their potential for reconstructing fire history. Stage 5 investigated the fire-modified properties within the sediment core profile to detect burnt material and fire severity. This questioned whether the different mineral magnetic signatures identified in the heating experiments were present in burnt material in the cores? (Research question 14); and if it was possible using TAC to identify soil heating levels previously experienced by samples from different depths in a sediment core? (Research question 15). This stage of the research was conducted because previously only enhanced χ has been used in fire detection in sediment cores and this does not provide information on the likely levels of heating experienced by the sediment during wildfire, but this is potentially possible using TAC. Investigation of fire severity and erosion has been extensively carried out in fire-prone terrain, but apart from the work by Blake *et al.* (2006), the levels of heating experienced by sediments subject to fire have not previously been examined.

Stage 6 concerned comparison of the record of closely-spaced sediment cores taken from Lake Burragorang reservoir with documentary records of fires provided by the SCA in order to ascertain the reliability of mineral magnetic parameters and TAC of core sediments obtained from such sediments in reconstructing fire history. This

stage investigated: whether fire indicators were present for each burn event within the recent fire history of the catchment (Research question 16); and which factors influenced deposition of burnt material and the record of fire events within the sediment profile (Research question 17). This stage was carried out in particular to test the reliability of reconstructing fire history from mineral magnetic properties and TAC under difficult conditions. These included a combination of: (i) the dynamic environment of a reservoir (e.g. complex migratory deltaic deposition and fluctuating water levels); with (ii) the unreliability of post-fire transfer of burnt soil from the hillslopes to the channel and reservoir during each wildfire event because of the frequent association of droughts with the critical first few months after fires before vegetation recovery occurs (Prosser and Williams 1998). Overall, these stages in the investigation have been combined to provide an examination of the feasibility of using mineral magnetism and TAC in reconstructing catchment fire events as preserved in soils and reservoir sediments.

5 EFFECTS OF HEATING ON SOIL MINERAL MAGNETIC PROPERTIES

This chapter presents the results and analysis of two heating experiments devised to examine the effects of different laboratory heat treatments on mineral magnetic properties of soil material from the study area. Section 5.1 introduces the thesis aims and sub-aims addressed in this chapter. Section 5.2 describes the methodologies and samples used. Section 5.3 presents the results from stage 1 of the experiments investigating the effect of furnace heating to different temperatures for different durations for various mineral magnetic parameters. Section 5.4 presents the results for stage 2 of the experiments investigating changes to magnetic susceptibility (χ) during progressive heating and cooling. Section 5.5 discusses the implications of the results. Section 5.6 presents key findings relating to the sub-aims of the chapter.

5.1 INTRODUCTION

Enhancement of magnetic parameters has been observed to occur following fire (Le Borgne 1955, 1964; Oldfield *et al.* 1981; Rummery 1981; Gedye *et al.* 2000; Linford and Canti 2001; Blake *et al.* 2006). The heating experiments in this study were conducted in order to address the following thesis aims: to assess the mineral magnetic temperature thresholds apparent for thermally enhanced Australian soils (1a); and to assess the influence of thermal history of samples on mineral magnetic enhancement (1b) (Chapter 4). These thesis aims were addressed via a number of research questions, which were developed to gain a better understanding of: which magnetic parameters are modified by increased temperatures? (Research question 1); which temperature thresholds are required to produce changes to mineral magnetic properties? (Research question 2); what is the effect of heating duration on changes to magnetic properties? (Research question 3); what are the changes to magnetic susceptibility (χ) that occur during heating and cooling? (Research question 4); what is the influence of reducing conditions on the final enhancement of χ ? (Research question 5); what is the effect of the thermal history of the sample on temperature thresholds required to produce enhancement of χ ? (Research question 6); and what is the response of χ of different soils from within the catchment area? (Research question 7).

These research questions were explored in two stages. Figure 5.1 summarises the methods and techniques used in this chapter to address each of the research questions. Research questions 1 – 3 were investigated through a series of furnace heat treatments of 50 °C increments between 50 and 800 °C for durations of 5, 10, 20 and 40 minutes. These were conducted on a sample of long-unburnt surface soil from a footslope site adjacent to Sheehys Creek (34°06'00.1"S, 150°29'23.3"E). Research questions 4 – 7 were addressed by measurement of χ_{lf} changes during progressive heating and cooling in 100 °C intervals up to 700 °C under air and nitrogen environments. The results from this chapter provide a background for the results in Chapters 7 and 8, which focus on the effect of different fire histories on mineral magnetic properties of soil samples from the Nattai catchment and test the reliability of using mineral magnetic enhancement to suggest catchment fire history in sediment records.

Owing to the number of factors that influence fire characteristics (Section 2.2), it was anticipated that magnetic properties would vary according to different heating temperatures and durations. These have never previously been examined for Australian soils. Research questions 1 – 3 attempted to address this research gap.

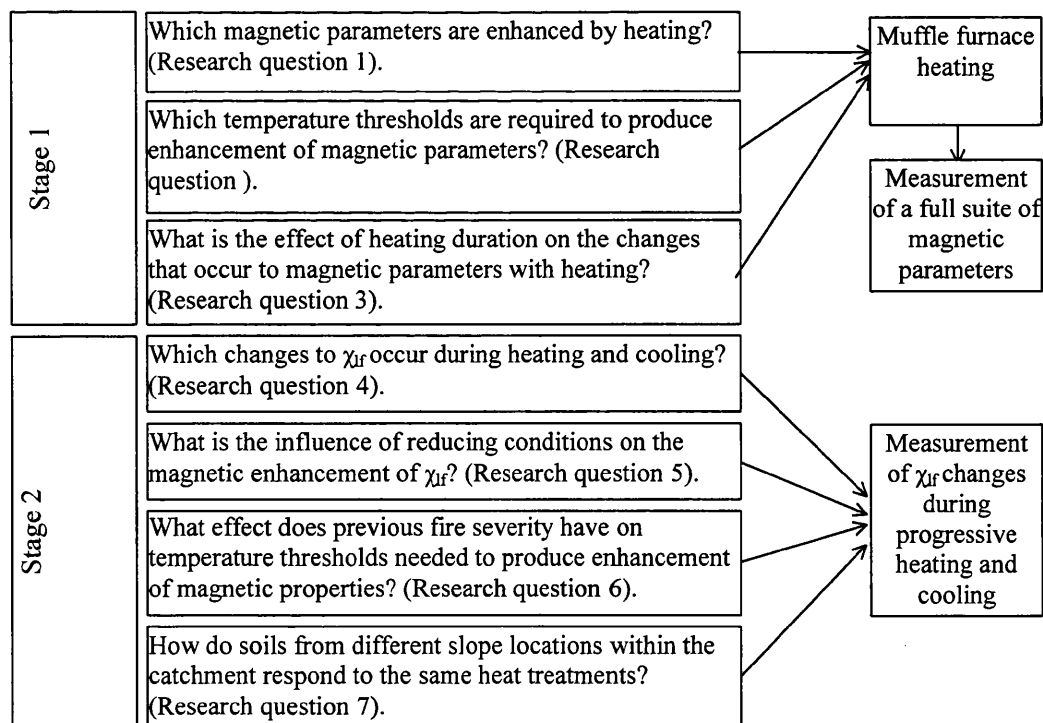


Figure 5.1: Summary of research questions addressed in stages 1 and 2 (Chapter 4) and techniques applied to investigate the effects of heating on mineral magnetic properties of soils from the Lake Burragorang catchment.

Research questions 1-3 were addressed using samples that had been pre-heated in a muffle furnace. Magnetic measurements were conducted using the methodologies outlined in Section 5.2.4. Research questions 4-7 were addressed by measuring χ changes during progressive heating and cooling using methods described in Section 5.2.4. This was done primarily to investigate the different effects of heating in an air atmosphere and a nitrogen atmosphere (to simulate the reducing conditions created by heating in oxygen-reduced situations such as under organic matter). However, it also gave additional information about mineralogical changes that occurred during the heating and cooling process that were not identifiable by furnace heating.

Research question 4 enabled changes to χ that occurred during heating and cooling of the sample to be observed. This procedure enabled inferences to be made regarding the mineralogy of the soil, which influenced the response of the soil to heating (Hanesch *et al.* 2006).

During forest fires, combustion of ground fuel can reduce oxygen levels in the soil, causing heating of the soil to occur in partially anoxic conditions. Research question 5 was conducted by heating the soil in air and nitrogen atmospheres, which enabled simulation of different reducing conditions, to establish if this had an effect on magnetic parameters.

The high frequency of fires occurring in eucalypt forests in Australia made it unlikely that the soil used in this experiment had never previously been heated. Research question 6 was investigated by comparing the χ at 40 °C pre- and post-heating to progressively higher temperatures, which enabled previous temperatures experienced by the soil to be ascertained (Peters *et al.* 2001) and explained the temperature thresholds required for enhancement of the soil to occur.

Gedye *et al.* (2000) suggested that different slope locations could influence magnetic signatures produced by fires. Factors that could have affected the signatures include pedogenesis, previous fire events, the production of bacterial magnetite, waterlogging or wetting (Dearing 1999b). Research question 7 investigated the different slope locations on magnetic enhancement by comparison of responses of soils from different catchment locations.

5.2 METHODOLOGY

This section firstly introduces the samples chosen for use in these experiments (Section 5.2.1). Secondly, it describes the procedure used for furnace heating of the long unburnt soil sample (Section 5.2.2). Thirdly, it describes the methods used to measure the magnetic parameters (Section 5.2.3). Fourthly, it describes the methods used to measure magnetic susceptibility during heating and cooling (Section 5.2.4).

5.2.1 SAMPLE DETAILS

The soil sample used for Stage 1 of this experiment during the furnace heating experiments (Section 5.2.2) was obtained from a foot-slope location adjacent to Sheehys Creek (Figure 5.2). According to SCA records, this site had not been burnt for >30 years. Such a long period without fire suggested that the sample would be composed of a mixture of previously heated and never heated particles of soil, containing relatively un-enhanced magnetic properties. A 2 x 1 m plot was marked out, the litter layer removed and the top 2.5 cm of soil collected.



Figure 5.2: Vegetation at long unburnt footslope sampling site near Sheehys Creek.

Samples used during Stage 2 of this experiment for measuring χ changes during heating and cooling included: (i) the aforementioned long-unburnt foot-slope soil; (ii) a sample from a mid-slope location on Tumbledown Mountain (Figure 3.2) that had last experienced fire in 1984; and (iii) a sample from a ridge-top location above Sheehys Creek (Figure 3.2), that had last been burnt in 1969. The contrasting slope locations were selected to compare their responses after the same laboratory heat treatments. These selected locations provided samples that had not been burnt for a protracted period. Although the samples had experienced different lengths of time since the last fire, in view of the relatively high rates of bioturbation (Shakesby *et al.* in press) thorough removal and mixing of heated and unheated soil particles could be expected. Details of each of the sample sites are provided in Table 5.1 and locations are shown in Figure 3.2.

Table 5.1: Details of soil samples used for measuring χ_f changes during progressive heating and cooling.

| Code | Sample | Latitude and Longitude (E/S) | Site | Number of years since last fire |
|------|---------------|---------------------------------------|-----------------------------|--|
| FS | Foot slope | 34°08' 150°29' | Sheehys Creek | >30 |
| MS | Mid slope | 34°06' 150°28' | Tumble- down Mountain | 20 |
| RT | Ridge top | 34°13.3' 150°29.5' | Sheehys Creek | >30 |

5.2.2 FURNACE HEATING PROCEDURE

This section provides details of stage 1 of the experiment that involved furnace heating of the FS samples in silica trays in a muffle furnace. Samples were heated to temperatures ranging between 50 and 800 °C for durations of 5, 10, 20 and 40 minutes.

Prior to experimentation, the samples were air-dried at room temperature and passed through a 2-mm sieve. Further homogenization and division of the bulk sample was achieved by thorough coning and quartering of the sample into ~20g sub-samples. The sub-samples were spread out on silica trays measuring 155 x 95 mm, which

resulted in a soil layer ~5 mm thick. Silica trays were chosen due to: (i) their non-metallic properties, which would not influence magnetic minerals; (ii) the rapid response of silica to changes in temperatures enabling a fast transfer of thermal energy to the samples; (iii) the ability of silica to withstand temperatures $>1050\text{ }^{\circ}\text{C}$; and (iv) uneven spread of soil thinly and evenly in crucibles, which was required for consistent heating of the soil to the same temperature.

Increments of $50\text{ }^{\circ}\text{C}$, ranging between $50\text{ }^{\circ}\text{C}$ and $800\text{ }^{\circ}\text{C}$ were used in the heating experiments. Samples were heated to between $50\text{ }^{\circ}\text{C}$ and $250\text{ }^{\circ}\text{C}$ in an oven as this provided more accurate heating at lower temperatures than the muffle furnace, which was used to heat samples between $300\text{ }^{\circ}\text{C}$ and $800\text{ }^{\circ}\text{C}$. Before insertion of the trays, the oven or furnace was pre-heated to the desired temperature. Different sub-samples were heated for durations of 5, 10, 20 and 40 minutes to simulate a range of rates at which a natural fire front would progress. It is worth noting that a burning duration >40 minutes is unlikely to occur in natural environments except at particular locations such as under smouldering logs, where very high temperatures can be reached. After heat treatment, the samples were placed on a wire rack and left in their trays to cool to air temperature. After the samples had cooled, they were tightly packed into plastic-film-lined 10 cm^3 sample pots in preparation for mineral magnetic measurements (Section 5.2.3).

5.2.3 MAGNETIC MEASUREMENTS PROCEDURE

This section firstly details the methods used to prepare samples for magnetic measurements (5.2.3.1). Secondly, it describes measurements using the Bartington MS2B dual frequency susceptibility sensor and the Bartington MS2 magnetic susceptibility meter, which were used to measure low and high frequency susceptibility (χ_{lf} and χ_{hf}) and frequency dependent susceptibilities (χ_{fd} and $\chi_{fd\%}$) (Section 5.2.3.2). Thirdly, it describes the procedure used for conducting remanence measurements, including details of how Anhyseretic Remanent Magnetisation (χ_{ARM}) (Section 5.2.3.4) and Isothermal Remanent Magnetisation (IRM) were imparted into a sample (Section 5.2.3.5).

5.2.3.1 Preparation of samples for magnetic measurements

Collection of all sample material for this research was made using plastic tools in order to avoid potential alteration that could occur to the magnetic properties through the use of metal equipment. Once the samples had been collected and air-dried at approximately 22 °C, they were prepared for magnetic analysis by tightly packing soil into plastic film-lined 10 cm³ plastic Azlon sample containers. Once the film-lined pots were nearly full, the corners of the plastic film-liner were gathered and twisted to immobilise the grains so that changes in magnetic field orientation could be recorded accurately.

5.2.3.2 Measurement and calculation of low frequency susceptibility (χ_{lf}) and frequency dependent susceptibilities (χ_{fd} and $\chi_{fd\%}$).

Low frequency mass specific susceptibility (χ_{lf}) was used to identify the volume of ferrimagnetic minerals in a material such as magnetite and maghaemite (Rummery *et al.* 1979). This provided information about the magnetisability of a material (Dearing 1999b). Susceptibility measurements were made at low (0.46 kHz) and high (4.6 kHz) frequencies to calculate frequency dependent susceptibility (χ_{fd} and $\chi_{fd\%}$) this enabled the identification of the presence of ultra fine (<0.03 μ m) superparamagnetic (SP) ferrimagnetic minerals. χ_{lf} and χ_{fd} have both been reported to increase following fire, due to the conversion of antiferromagnetic minerals to ferrimagnetic form (Maher 1986).

χ_{lf} and χ_{fd} were measured using a Bartington MS2B dual frequency susceptibility sensor and a Bartington MS2 magnetic susceptibility meter (Figure 5.3). The MS2B dual frequency sensor contains an electromagnetic coil. When an electric current is passed through this coil, movement of negatively-charged electrons creates a magnetic field. The alignment of the magnetic minerals then change direction to follow the applied magnetic field, such that the more magnetic minerals, the higher the volume susceptibility (κ). This was calculated by the magnetic moment per unit volume of a sample (M), divided by the strength of the applied field (H) and was indicated by the reading obtained on the MS2 meter (Dearing 1999a).

The continuous mode of measurement of the MS2 meter was selected. This produced a new reading every 3 seconds, indicated by a 'bleep'. After a warm-up

period of an hour, the meter was set to zero and readings were conducted with no sample. The level of drift during the ‘air’ readings indicated the background ‘noise’. If the drift was $>0.1 \times 10^{-5}$ SI units) at low frequency, measurement was suspended until interference was reduced. Provided the drift during air readings was minimal, measurement at low frequency was conducted using the following procedure: (i) the equipment was set to zero; (ii) the sample was placed in the centre of the electromagnetic coil; (iii) the first reading was ignored as it did not contain a whole measurement cycle; (iv) the second and third readings of volume susceptibility (κ) were recorded; and (v) the sample was removed from the coil. After all the samples had been measured at low frequency, the meter was switched to measure high frequency values, using the same procedure outlined above.

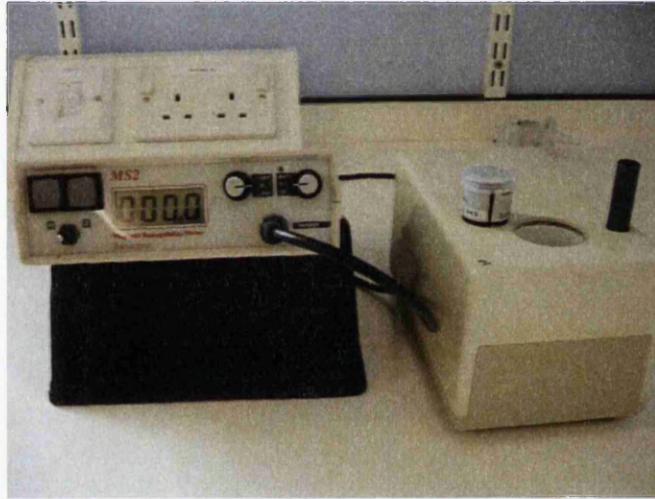


Figure 5.3: The Bartington MS2B dual-frequency susceptibility sensor and Bartington MS2 magnetic susceptibility meter.

Corrected κ was calculated to remove the error from the background readings using an excel spreadsheet. This was calculated by subtracting the average air κ readings from the average sample κ readings (Equation 5.1) (Dearing 1999b)

$$\kappa \text{ (corrected)} = \text{sample } \kappa - \{(1^{\text{st}} \text{ air } \kappa + 2^{\text{nd}} \text{ air } \kappa)/2\} \quad (\text{equation 5.1})$$

where $\kappa \text{ (corrected)}$ is the corrected volume susceptibility reading, **sample κ** is the average volume susceptibility of the sample taken from two readings and $(1^{\text{st}} \text{ air } \kappa + 2^{\text{nd}} \text{ air } \kappa)/2$ is the average volume susceptibility of background air readings taken from two readings.

χ_f was calculated to take into account the quantity of the sample. This was done by dividing κ (corrected) by sample mass (g) and dividing that by 10. χ_f is expressed as:

$$\chi_f = \{(\kappa \text{ (corrected)} / \text{sample mass})/10\} \quad (\text{equation 5.2})$$

where χ_f (expressed as $10^{-6} \text{m}^3 \text{kg}^{-1}$) is the mass specific susceptibility, κ (corrected) is the corrected volume susceptibility reading, and **sample mass** represents the mass of the sample in grams.

The susceptibility of the sample provided an indicator of the total concentration of different types of minerals within a sample. For example, a strong positive susceptibility was indicative of ferrimagnetic materials, whereas weak negative susceptibility indicated diamagnetic minerals. Increased concentration of ferrimagnetic minerals has been commonly associated with high values of χ_f obtained for burnt material (Dearing 1999b). The theory relating to the transformation of minerals to ferrimagnetic form is presented in Section 2.3.3.

Frequency dependent measurements identify superparamagnetic (SP) grains within a sample by comparison of κ values attained at different frequencies. SP grains are very fine magnetic grains that are able to re-align to the orientation of an applied low frequency magnetic field. They are also unable to hold remanence (Smith 1999). Samples that contained SP grains were found by Dearing (1999b) to show slightly lower values for high frequency measurements than those obtained for low frequency measurements. Samples that did not contain SP grains showed identical values when measured at both frequencies. Frequency dependent susceptibility was calculated as either a percentage of the original low frequency κ value ($\chi_{fd}\%$) (Equation 5.3) or as a mass specific frequency dependent susceptibility (χ_{fd}) (Equation 5.4).

$$\chi_{fd}\% = \{(\kappa_{lf} - \kappa_{hf})/\kappa_{lf}\} \times 100 \quad (\text{equation 5.3})$$

$$\chi_{fd} = \{(\kappa_{lf} - \kappa_{hf})/\text{mass}\}/10 \quad (\text{equation 5.4})$$

where $\chi_{fd}\%$ is the percentage frequency dependent susceptibility, χ_{fd} is the mass specific dual frequency dependent susceptibility, κ_{lf} is the corrected volume

susceptibility measured at low frequency, κ_{hf} is the corrected volume susceptibility measured at high frequency and **mass** represents the mass of the sample in grams.

5.2.3.3 *Remanence measurements*

Magnetic remanence was imparted to a sample by the application of a larger magnetic field than used for χ_{lf} and χ_{fd} measurements. This caused the magnetic orientation within the grains to change so that they became aligned in the direction of the applied field. Remanence measurements were conducted immediately after the sample was removed from the applied field. Removing the magnetic field caused some of the magnetic minerals to revert back to their original direction, while other minerals retained the direction induced by the applied field. The type of remanence imparted into a sample stimulates different magnetic behaviour according to the dominant grains within the assemblage. In this study, Anhysteretic Remnant Magnetisation (χ_{ARM}) and Isothermal Remanent Magnetisation (IRM) were used. The information gained from these parameters was then used to make inferences about the ferrimagnetic grains sizes and mineralogy.

Remanence measurements were conducted using a Molspin 1A Magnetometer (Figure 5.4), using the principles of Faraday's Law to measure the remanence retained by a sample. The sample was lowered into the centre of a coil and spun. If the sample had retained any remanence, a magnetic field was generated which produced an electric current proportional to the remanence held by the sample (Walden 1999). The procedure for remanence measurements was as follows: (i) connect the Molspin Magnetometer to the computer and the Spinwin program; (ii) calibrate the Magnetometer using the calibration sample; (iii) place a sample in the holder and lower into the coil; (iv) spin the sample; (v) record the intensity; and (vi) repeat steps (i) to (v) for 10 samples and then re-calibrate the magnetometer.

5.2.3.4 *Anhysteretic Remnant magnetisation: measurement and calculation*

χ_{ARM} was used as an indicator of magnetic grain size and was imparted to a sample using a Molspin a.f. demagnetiser and ARM attachment (Figures 5.4). The sample was placed in a holder and slid into the chamber. The demagnetiser produced an alternating magnetic field, which declined linearly with time. At the same time, the ARM attachment applied a constant biasing field parallel to the alternating magnetic

field (Figure 5.5). This caused diffraction of the alignment of the magnetic grains away from the direction of the alternating field (Walden 1999).

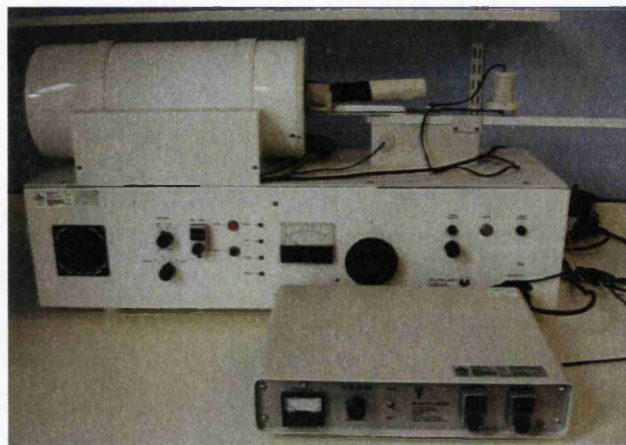


Figure 5.4: The demagnetiser and ARM attachment.

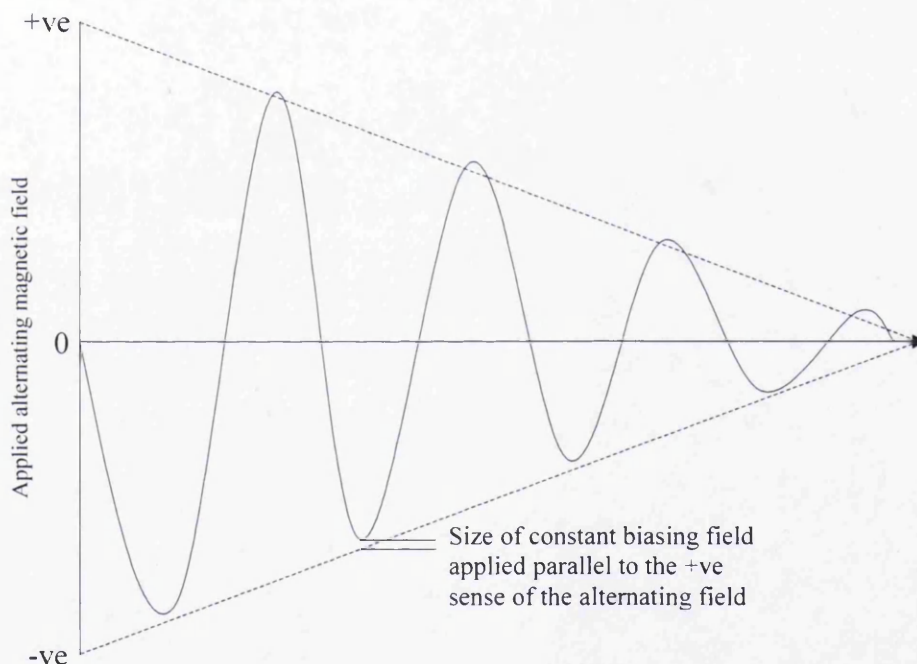


Figure 5.5: Nature of applied magnetic field using the Molspin a.f. demagnetiser and ARM equipment during induction of χ_{ARM} into a sample (Walden 1999).

The procedure used to impart the ARM was as follows: (i) the sample was placed into the holder and slid into the chamber; (ii) the ARM was set at 0.04 mT and the maximum alternating field was set at 100 mT decreasing at a rate of 0.016 mT per cycle; (iii) start was pressed; and (iv) when the cycle was complete (indicated by illumination of the 'finished' light), the sample was removed and the remanence immediately measured, using the Molspin magnetometer as in the procedure outlined in Section 5.2.4.3.

The raw ARM values are added to Equation 5.5a to give a mass specific value:

$$\text{Mass specific ARM} = \frac{\text{Intensity (10}^{-3}\text{ Am}^{-1}) \times 1.29}{\text{Sample weight (g)}} \quad (\text{equation 5.5a})$$

where **Intensity** represents the raw values obtained from magnetometer and the factor **1.29** allows for the volume of the standard 25 mm cylindrical sample pots which have a volume of $12.9 \times 10^{-6} \text{ m}^3$ and for the fact that the sample weight in 10^{-3} g is equivalent to kg (Walden 1999) **Sample weight** represents the mass of sample in grams.

A further calculation was conducted in order to express the mass specific ARM value in the preferred format as χ_{ARM} to account for the size of the biasing field (0.04 mT equivalent to 31.84 Am^{-1}) (equation 5.5b).

$$\chi_{\text{arm}} (10^{-5} \text{ m}^3 \text{ kg}^{-1}) = \frac{\text{ARM (10}^{-5} \text{ Am}^2 \text{ kg}^{-1})}{\text{Steady biasing field (Am}^{-1})} \quad (\text{equation 5.5b})$$

The χ_{ARM} measurements were used to identify stable single-domain ferrimagnetic grains in the $0.02 - 0.4 \text{ }\mu\text{m}$ range. These were slightly coarser than minerals identified by the χ_{fd} parameter (Maher 1988). Increases in the χ_{ARM} parameter have been associated with burnt materials according to Gedye *et al.* (2000).

5.2.3.5 Isothermal Remnant Magnetisation (IRM): measurement and calculation

Isothermal Remanent Magnetisation (IRM) is a measurement of the remanence held by a sample after it has been placed in an externally applied field. Comparison of the IRM values obtained following exposure to increasing sizes of magnetic field was used to provide information about the dominant mineralogy of grains within the sample.

IRM measurements were conducted using the following procedures: (i) the sample was placed in a forward direction in the same alignment of the applied field generated by the electromagnetic coil within the Molspin pulse magnetiser (Figure 5.6); (ii) a magnetic field (H) of specified strength was applied by passing an electric

current (of strength proportional to the desired field) through the electromagnetic coil; (iii) immediately after imparting the IRM, the remanence held by the sample was measured, using the Molspin magnetometer and following the procedure outlined in Section 5.2.3.3. (It was important not to delay this measurement to prevent decay of the remanence); (iv) steps (i-iii) were repeated for increasing field sizes of 20, 40, 60, 80, 100, 200, 300, 500, 600, 800, 1000 mT; (v) steps (i-iii) were repeated, but the sample was placed in an opposite direction to the applied magnetic field created by the Molspin pulse magnetiser. This enabled backfield measurements of -20, -40, -100 and -300 mT to be conducted. The raw IRM measurements were then put into Equation 5.5 to attain mass specific values. The remanence acquisition and decay curves were used to make inferences about the dominant minerals within the samples as magnetically soft minerals have often formed during burning due to the conversion of minerals to ferrimagnetic form (Gedye *et al.* 2000). Soft minerals respond to low backfields during IRM measurement. The values attained for the magnetic parameters described here have been used to form various ratios and quotients to make inferences about magnetic minerals. These are summarised in Table 2.4.

5.2.4 CHANGES IN χ DURING HEATING AND COOLING

Measurement of changes in χ during heating and cooling were conducted to fulfil research questions 4 to 7 (Figure 5.1) using a KLY-3 kappabridge pick-up unit (Figure 5.6).

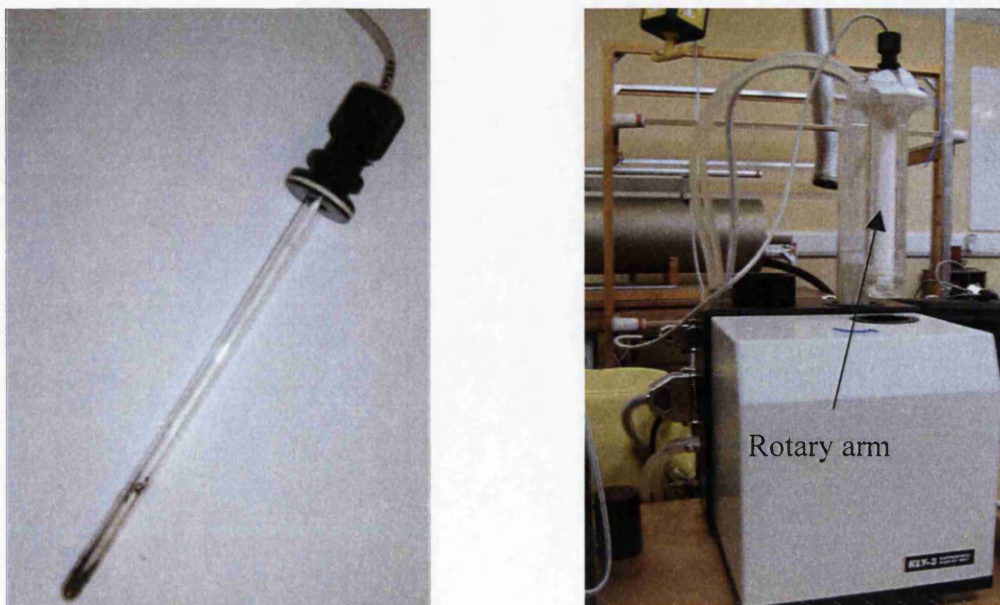


Figure 5.6: (a) Thermocouple inserted in glass vessel with sample. (b) Sample (in glass vessel) inserted in rotary arm.

Preparation of the samples detailed in Table 5.1 involved coning and quartering (described in Section 5.2.2) to create sub-samples of approximately 2-3g. The samples were then inserted into a narrow glass vessel. A glass-encased non-magnetic platinum thermocouple was carefully inserted into the centre of the vessel (Figure 5.6a). Both the vessel and thermocouple were then placed into the holder of a rotary arm (Figure 5.6b), which moves the sample in and out of the furnace to heat the sample and also pauses while the sample is located in the middle of the pick-up coil for measurement of χ to be conducted. Owing to laboratory time constraints, heating was conducted at an 'extra fast' rate of 11 °C / minute. Cold water flowing through the reservoir surrounding the sample vessel regulated the temperature of the sample.

To enable direct comparison of the χ changes caused by heating and cooling with the results from the furnace heating (Section 5.3), different sub-samples that had been coned and quartered from the long-unburnt FS sample were heated from room temperature to 100, 200, 300, 400, 500, 600 and 700 °C. After the specified temperature had been reached, the furnace was shut down. Cooling of the sample began immediately, aided by the movement of water through the reservoir adjacent to the sample. This was maintained until a temperature of 40 °C was reached. In order to establish the replicability of the effects of heating, two runs were conducted on sub-samples from the long-unburnt FS sample. These produced similar results and therefore it was decided that there was no need for further multiple runs.

To simulate natural fire conditions while heating in air, a constant supply of air to the sample was maintained by an open inlet into the sample chamber. To simulate the effect of heating of organic matter under oxygen-deprived conditions, heating of samples in a nitrogen atmosphere was undertaken. To ensure that full reducing conditions were established, the glass tube was filled with nitrogen before the sample and thermocouple were inserted. Constant reducing conditions were maintained throughout the heat treatment by feeding nitrogen through the inlet to the sample chamber. The measurement procedure outlined above was repeated in air for the long-unburnt MS and ridge-top samples (detailed in Section 5.2.1) to compare the responses of the different slope locations to the same heat treatments.

5.3 FURNACE HEATING EFFECTS ON MAGNETIC PROPERTIES OF LONG UNBURNT SOIL

This section presents the results from the furnace heating of the long-unburnt FS sample from near Sheehys Creek. It firstly presents the actual temperatures likely to have been experienced by the samples when compared with the targeted temperatures, taking into account the thermal lag induced by heating of the silica trays (Section 5.3.1). Secondly, it presents the responses of a range of magnetic parameters to the various heat treatments (Section 5.3.2). Thirdly, it explores the relationship of some of the parameters in greater detail by using bi-variate plots (Section 5.3.3).

5.3.1 FURNACE-HEATED SAMPLES: ACTUAL TEMPERATURES

The thermal lag caused by the time and energy required initially to heat the silica trays caused a delay in heating the soil. Figure 5.7 displays the final temperature reached in the centre of the soil layer when heated in the muffle furnace.

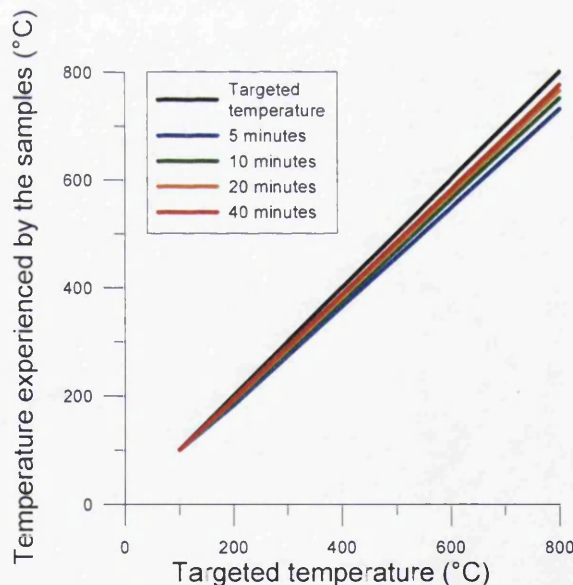


Figure 5.7: Maximum sample temperature during furnace heating, accounting for thermal lag caused by heating the silica trays.

This was calculated following measurement of thermal diffusivity values using a Decagon KD2 thermal meter. Using the thermal diffusivity value (D) of $\sim 0.11 \times 10^{-3} \text{ mm}^2 \text{ s}^{-1}$ of the FS soil and an assumption that an equal heat input from both the top and the bottom of the soil layer occurred, the approximate final temperature T ($^{\circ}\text{C}$) in the centre of the soil layer was derived using Equation 5.6 (Koorevaar *et al.*

1983). This showed that heating duration and targeted temperature both influenced the temperatures obtained by the samples, with larger deviations occurring for samples heated for shorter periods of time that had not experienced such thorough heating. Higher temperatures caused greater deviation from the targeted temperature than for samples heated for short durations. The actual temperatures experienced by the soil during heating have been used throughout this chapter.

$$T = T_b + (T_a - T_b) \operatorname{erfc} \left(\frac{x}{2\sqrt{Dt}} \right)$$

(equation 5.6)

where T_a = initial soil temperature, T_b = oven temperature, t = heating duration (s), erfc = complementary error function (dimensionless), and x = average depth to centre of soil layer (mm).

The values obtained for magnetic measurements from the heating experiments have been presented as normalized values, which were calculated as the fraction of enhancement when compared with the values of the unheated samples (Equation 5.7). This was conducted to mitigate the effect of variability in the initial starting values despite the use of a homogenised soil. This is denoted in the graphs as X_N . Values treated in this way are referred to in the text as ‘non-normalized values’.

$$\frac{X}{X_0} = X_N$$

(equation 5.7)

where X = the actual value obtained, X_0 = the value of magnetic parameter before any form of heat treatment, and X_N = the Normalized value, which is unitless.

5.3.2 RESPONSES OF MAGNETIC PARAMETERS TO FURNACE HEAT TREATMENTS

This section presents the results from the full suite of magnetic measurements (Section 5.2.3) that were conducted on the furnace-heated long-unburnt FS sample. Four main patterns in response to heating occurred: (i) two peaks in enhancement occurred at temperatures of ~450-500 °C and ~650-725 °C; (ii) one peak in enhancement occurred at temperatures between ~600-650 °C; (iii) virtually no

enhancement; and (iv) three peaks in enhancement occurred at temperatures of ~ 150 °C, ~ 450 - 500 °C and ~ 560 - 750 °C.

The first type of response to heating showing two peaks in enhancement at temperatures of ~ 450 - 500 °C and ~ 650 - 725 °C was exhibited by the mineral magnetic concentration parameters of χ_{lf} , χ_{fd} , and χ_{ARM} , presented in Figure 5.8 and Tables 5.3-5.5. These three graphs show two peaks in enhancement occurring between 456 - 484 °C and 621 - 756 °C.

Peak 1 displayed similar patterns in enhancement for χ_{lf} and χ_{fd} , with increases ranging between 2.5 and 7.6 times their initial values. The highest enhancement occurred for χ_{ARM} , with enhancement ranging between 2.0 and 4.8 times the initial values. Heating duration had virtually no effect on the patterns of enhancement produced by χ_{lf} , χ_{fd} , and χ_{ARM} . Peak 2 also produced similar patterns in enhancement of χ_{lf} and χ_{fd} , creating increases ranging between 4.77 and 6.05 times their initial values. The highest enhancement for peak 2 occurred for χ_{ARM} , with enhancement ranging between 4.23 and 10.52 times initial values. A comparison of peaks 1 and 2 showed that the enhancement of peak 2 was greater than for peak 1 for χ_{lf} and χ_{fd} for samples heated for durations of 10 and 40 minutes. For all other samples peak 2 produced higher values than peak 1.

The increase in χ_{lf} , χ_{fd} , and χ_{ARM} at peaks 1 and 2 suggested an increasing concentration of ferrimagnetic material of SSD, and SP grains (Gedye *et al.* 2000). Comparison of the 'non-normalized' values of χ_{lf} of 0.57 ($10^{-6}\text{m}^3\text{kg}^{-1}$) with those obtained from a variety of published and unpublished sources compiled in Dearing (1996b) (Figure 2.5) suggested that the sample contained a mixture of paramagnetic and canted antiferromagnetic minerals. The 'non-normalized' value produced for the maximum enhancement obtained for χ_{lf} was 4.3 ($10^{-6}\text{m}^3\text{kg}^{-1}$). Comparison with values presented by Dearing (1999b) (Figure 2.5) suggested that these values were associated with predominantly canted antiferromagnetic minerals. Although the values obtained for the heated material in this study did not suggest that the sample contained ferrimagnetic minerals, which have been commonly associated with fire

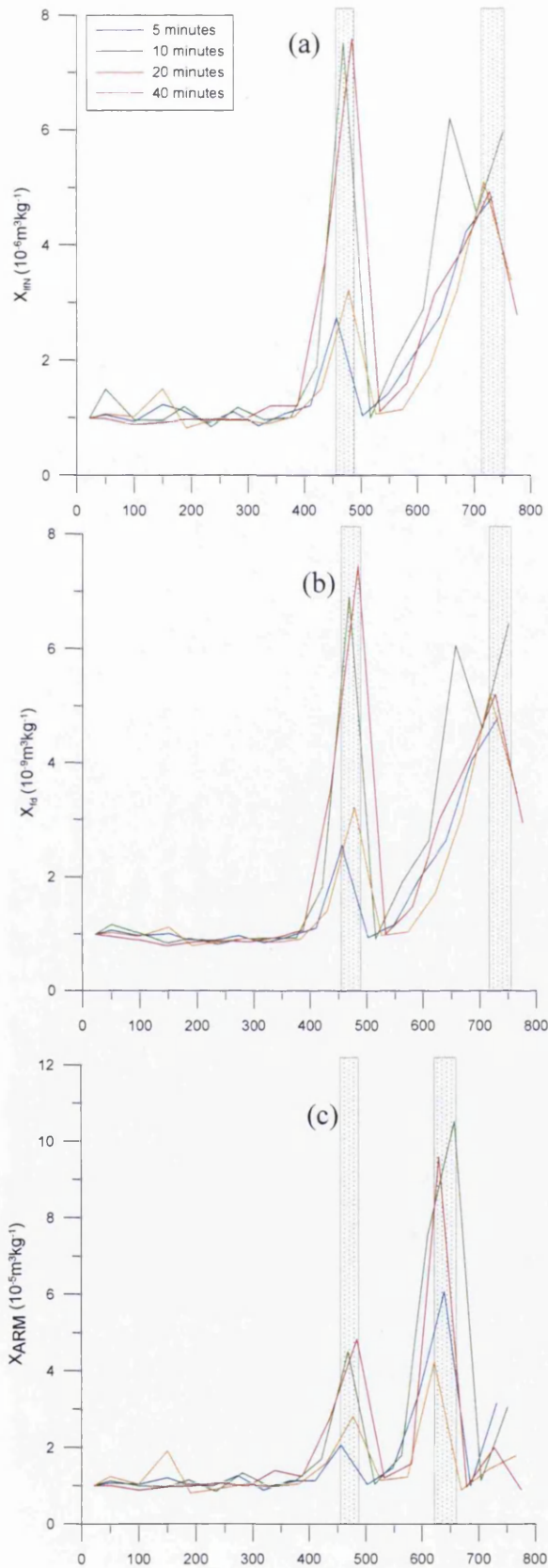


Table 5.3: Peak enhancement and associated temperatures for χ_{if} for heating durations of 5, 10, 20 and 40 minutes.

| Heating duration | T °C | χ_{ifN} Max peak 1 | T °C | χ_{if} Max peak 2 |
|------------------|------|-------------------------|------|------------------------|
| 5 | 456 | 2.75 | 731 | 4.83 |
| 10 | 469 | 7.53 | 657 | 3.51 |
| 20 | 478 | 3.22 | 717 | 5.10 |
| 40 | 484 | 7.6 | 756 | 3.39 |

Table 5.4: Peak enhancement and associated temperatures for χ_{fd} for heating durations of 5, 10, 20 and 40 minutes.

| Heating duration | T °C | X_{fdN} Max peak 1 | T °C | X_{fdN} Max peak 2 |
|------------------|------|----------------------|------|----------------------|
| 5 | 456 | 2.54 | 731 | 4.77 |
| 10 | 469 | 6.90 | 657 | 6.05 |
| 20 | 478 | 3.22 | 717 | 5.20 |
| 40 | 484 | 7.44 | 727 | 5.20 |

Table 5.5: Peak enhancement and associated temperatures for χ_{ARM} for heating durations of 5, 10, 20 and 40 minutes.

| Heating duration | T °C | X_{ARMN} Max peak 1 | T °C | X_{ARMN} Max peak 2 |
|------------------|------|-----------------------|------|-----------------------|
| 5 | 456 | 2.06 | 639 | 6.07 |
| 10 | 469 | 4.50 | 657 | 10.52 |
| 20 | 478 | 2.81 | 621 | 4.23 |
| 40 | 484 | 4.82 | 630 | 9.60 |

Figure 5.8: The influence of furnace heating on (a) χ_{if} (b) χ_{fd} and (c) χ_{ARM} . (Values displayed are normalised to the measurements made at 22 °C.) Grey bars identify the temperature range in which the 1st and 2nd peaks occur.

(Le Borgne 1964), the values fitted within the range commonly associated with burnt topsoils. As these heating experiments were conducted on a bulk sample, it is possible that the magnetic values have been reduced by its sandy nature as magnetic minerals are predominantly found in the clay fraction of a soil (Le Borgne 1955; Mullins 1977).

The increasing values of χ_{fd} at peaks 1 and 2 suggest a greater concentration of ferrimagnetic SP grains (Dearing 1999b). The increasing values for χ_{ARM} occurring at peaks 1 and 2 suggested a greater concentration of SSD grains between either ~ 450 - 500°C or ~ 600 - 650°C (Maher 1988). This suggested that a range of magnetic grain sizes became enhanced with heating.

The second type of response with one peak in enhancement at temperatures between ~ 600 - 650°C , was apparent for $\chi_{fd\%}$ and $\text{soft}_{IRM\%}$ parameters. Enhancement of these magnetic parameters is commonly used to identify burnt material owing to their ability to indicate the presence of ferrimagnetic minerals, which have been created during burning (Gedye *et al.* 2000). Although the $\chi_{fd\%}$ parameter produced one peak in enhancement at temperatures between ~ 600 - 650°C (Figure 5.9b) the magnitude at which this parameter increased (a factor of 0.05) was minimal. A greater uniformity in the responses of the different heating durations was produced following heating to temperatures $>350^\circ\text{C}$. The $\text{soft}_{IRM\%}$ parameter in Figure 5.9a showed a general enhancement in response to increasing furnace temperatures. Below 350°C , there was a fairly high degree of variability for the different heating durations. Similarly to $\chi_{fd\%}$, above 350°C , there was a more uniform response to the furnace heat treatments. Two peaks in enhancement were observed between temperatures of 430 - 530°C and for temperatures of 675 - 750°C . However, the maximum enhancement only produced an increase of 1.48-1.78 times its initial value, similar to the values obtained at $<350^\circ\text{C}$.

The lack of enhancement of $\chi_{fd\%}$ with heating suggested that the material already contained a high proportion of ferrimagnetic minerals. This is confirmed by the high ‘non-normalized’ values of χ_{fd} ranging between 8.64-12.54 % which indicated that the sample comprised virtually entirely SP grains (Dearing 1999b). The low level of enhancement obtained for $\text{soft}_{IRM\%}$ could also be explained by the high ‘non-

normalized' values of $\text{soft}_{\text{IRM}\%}$ suggesting that a maximum of 54% of soft magnetic minerals were contained within the assemblage. As these parameters were enhanced prior to furnace heating, it is possible that the sample had retained an enhanced signal from previous fire events.

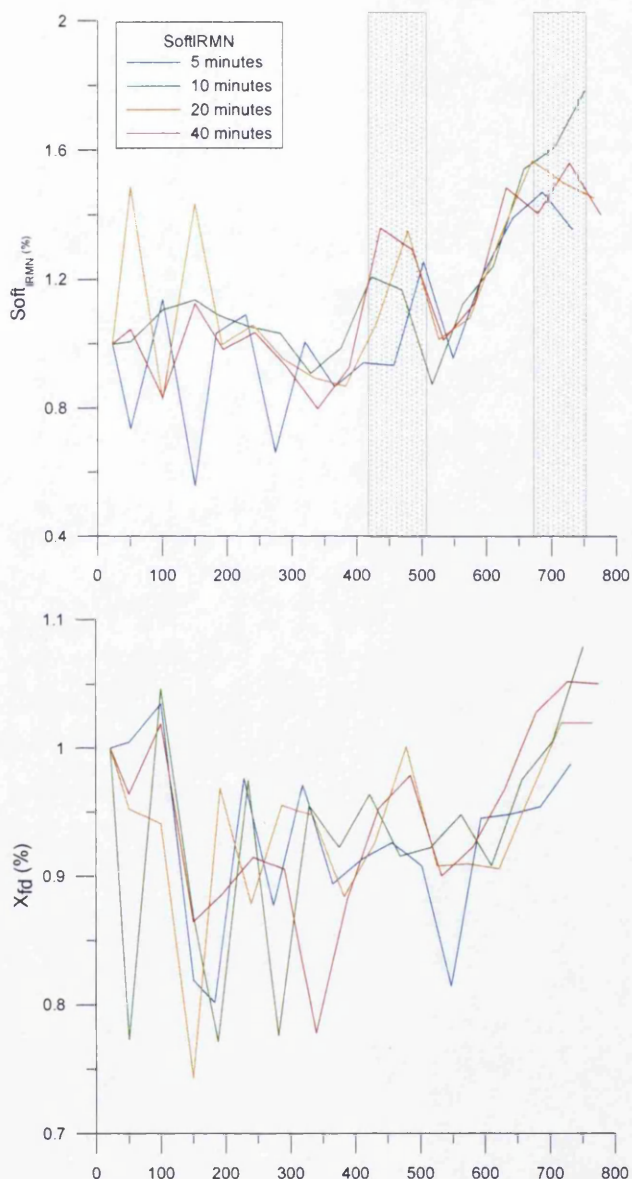


Figure 5.9: The influence of furnace heating on (a) $\text{soft}_{\text{IRM}\%}$ and (b) $\chi_{\text{fd}}\%$. (Values displayed are normalised to the measurements made at room temperature $\sim 22^\circ\text{C}$.) Grey bars indicate the temperature range in which the 1st and 2nd peaks occur.

The third response to furnace heating is evident in the quotients of $\chi_{\text{ARM}}/\text{SIRM}$ and $\chi_{\text{fd}}/\chi_{\text{ARM}}$ (Figure 5.10a and 5.10b and Tables 5.6 and 5.7). Both these parameters only showed one peak in enhancement occurring between 600 and 700 °C. Two

phases of enhancement of these quotients occurred with heating. Initially, $\chi_{\text{ARM}}/\text{SIRM}$ increased to 2.8-4.4 times its initial value between temperatures of $\sim 600\text{--}650\text{ }^{\circ}\text{C}$. It then declined to lower values than experienced at temperatures $<550\text{ }^{\circ}\text{C}$. Secondly, $\chi_{\text{fd}}/\chi_{\text{ARM}}$ increased between temperatures of 650 and 700 $^{\circ}\text{C}$ to between 2.8 and 3.1 times its initial value, then declined slightly. These parameters suggest a coarsening of the grain size assemblage. Initial values of $\chi_{\text{ARM}}/\text{SIRM}$ were low and implied that SP grains dominate the ferrimagnetic assemblage. Higher values created following heating to 600-650 $^{\circ}\text{C}$ suggested an increasing presence of SSD grains (Gedye *et al.* 2000). This transition from SP to SSD form has been confirmed by $\chi_{\text{fd}}/\chi_{\text{ARM}}$, which showed an increasing content of SP grains lying on the SSD / SP boundary at temperatures of 650-700 $^{\circ}\text{C}$ (Oldfield 1994).

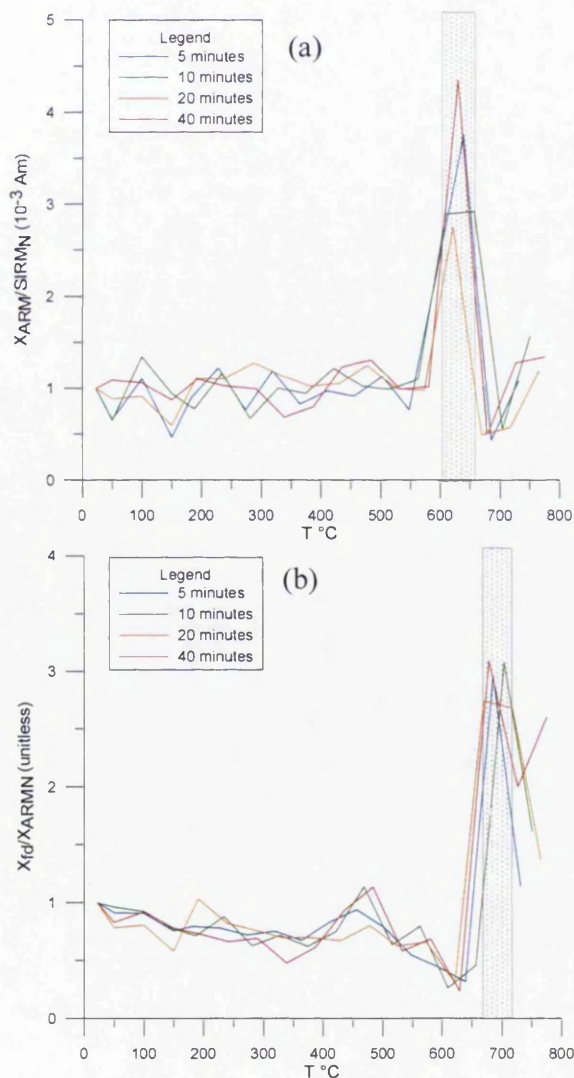


Table 5.6: Enhancement and associated temperatures for $\chi_{\text{ARM}}/\text{SIRM}$ for heating durations of 5, 10, 20 and 40 minutes.

| Heating duration | T $^{\circ}\text{C}$ | $\chi_{\text{fdN}}/\chi_{\text{ARMN}}$ Max peak 1 |
|------------------|----------------------|---|
| 5 | 640 | 3.76 |
| 10 | 657 | 2.92 |
| 20 | 622 | 2.75 |
| 40 | 630 | 4.35 |

Table 5.7: Enhancement and associated temperatures for $\chi_{\text{fd}}/\chi_{\text{ARM}}$ for heating durations of 5, 10, 20 and 40 minutes.

| Heating duration | T $^{\circ}\text{C}$ | $\chi_{\text{fdN}}/\chi_{\text{ARMN}}$ Max peak 1 |
|------------------|----------------------|---|
| 5 | 685 | 2.96 |
| 10 | 704 | 3.08 |
| 20 | 670 | 2.74 |
| 40 | 679 | 3.09 |

Figure 5.10: The influence of furnace heating on (a) $\chi_{\text{ARM}}/\text{SIRM}$ and (b) $\chi_{\text{fd}}/\chi_{\text{ARM}}$ (Values displayed are normalised to the measurements made at room temperature $\sim 22\text{ }^{\circ}\text{C}$.) Grey bars identify the temperature range in which the 1st and 2nd peaks occur.

The fourth type of magnetic response was only demonstrated by SIRM (Figure 5.11). This showed enhancement occurring at three temperature thresholds and highlighted similarities between the samples heated for 5 and 40 minutes and the samples heated for 10 and 20 minutes. The temperature thresholds identified for the samples heated for 5 and 40 minutes produced enhancement at ~ 150 °C, ~ 400 - 500 °C and ~ 700 - 750 °C. The temperature thresholds identified for samples heated for 10 and 20 minutes showed enhancement occurring between ~ 300 - 350 °C, ~ 475 - 500 °C and ~ 625 - 675 °C. SIRM is used to detect the presence of all magnetic material in the sample (Maher 1986). The increased concentration of SIRM at lower temperature thresholds suggested that at temperatures between ~ 150 and 350 °C fine-grained ferrimagnetic material was masking the diluting effects of coarse-grained magnetite and canted antiferromagnetic minerals such as haematite (Walden 1999). Owing to its ability to indicate lower concentrations of enhanced material at a variety of temperatures, SIRM could be a more reliable parameter than using χ_f to identify burnt material. Rummery *et al.* (1979) certainly found SIRM very useful for this purpose.

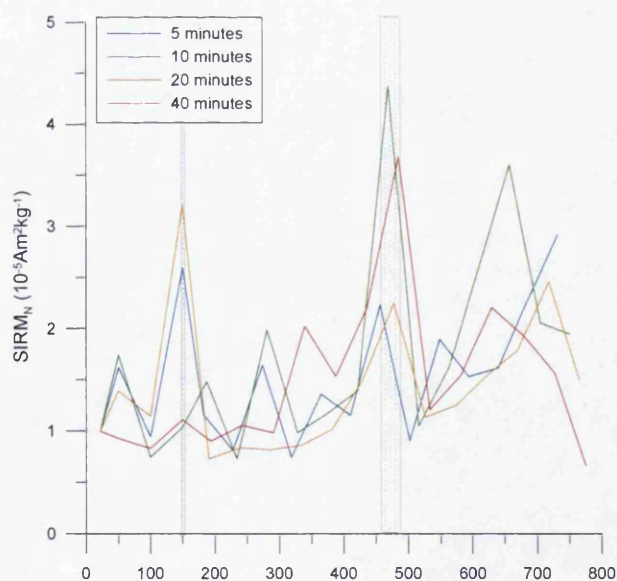


Figure 5.11: The influence of furnace heating on SIRM (Values displayed are normalised to the measurements made at room temperature ~ 22 °C.) Grey bars identify the temperature range in which the 1st and 2nd peaks occur.

The different responses produced by the samples heated for 5 and 40 minutes or 10 and 20 minutes are likely to be a result of the different mineralogies of the sub-samples used, despite attempts to minimise this variability by coning and quartering samples during preparation. As these results show that the variability between different heating durations is greater than the differences of temperature thresholds, this highlights an area in need of further investigation to ascertain the temperature thresholds required to produce enhancement.

The investigation and analysis of the effect of furnace heating long-unburnt foot-slope soil to different temperatures for different durations on various mineral magnetic parameters showed that:

- χ_{fd} , χ_{fd} , and χ_{ARM} are enhanced at ~ 450 °C and ~ 600 °C. This is likely to have been caused by an increase in the concentration of ferrimagnetic minerals of SP and SSD magnetic grain sizes. Owing to the use of a bulk sample, it is likely that non-magnetic minerals may have had a dilution effect on the enhancement.
- $X_{fd\%}$ and $soft_{IRM\%}$ showed virtually no enhancement. Non-normalized values obtained for $\chi_{fd\%}$ indicated that the samples may have already been heated and retained a memory of previous fire events. Alternatively, the high SP content indicated by initially high values of $\chi_{fd\%}$ and $soft_{IRM\%}$ could have been caused by pedogenesis.
- $\chi_{ARM}/SIRM$ and χ_{fd}/χ_{ARM} suggested a coarser mineral magnetic grain assemblage at temperatures between 600-700 °C, demonstrating an increase in a range of mineral magnetic grain sizes.
- SIRM has been shown here to be useful in detecting burnt material as it enabled identification of low concentrations of thermally enhanced fine-grained ferrimagnetic material, allowing enhancement to occur at temperatures as low as 150 °C.

5.3.3 RESPONSES OF MAGNETIC PARAMETERS TO FURNACE HEAT TREATMENTS:

BIVARIATE PLOTS

Bivariate plots are often used in the interpretation of magnetic results as they eliminate concentration problems and can indicate grain size changes (Lees 1999). This section presents bivariate plots that have been used to: (i) discriminate between pollutants (Hunt *et al.* 1984; Oldfield *et al.* 1985); and (ii) identify mineralogy and grain size changes (Maher 1988; Oldfield 1994; van der Post *et al.* 1997; Lees 1999).

Bivariate plots of $\chi_{\text{ARM}} / \text{SIRM}$ and $(\text{IRM}_{300}/\text{SIRM}) / (\text{IRM}_{20} / \text{SIRM})$ have been used to distinguish between dust from fossil fuel combustion, industrial processes and soil erosion processes (Hunt *et al.* 1984; Oldfield *et al.* 1985). Although fossil fuel combustion and natural burning are different, the pyrogenic modifications to secondary magnetic form may be similar. If this is the case, then these plots could potentially be useful in discriminating between material from burnt and unburnt sources.

The bivariate plots of $\chi_{\text{ARM}} / \text{SIRM}$ (Figure 5.12a) and $(\text{IRM}_{300}/\text{SIRM}) / (\text{IRM}_{20} / \text{SIRM})$ (Figure 5.12b) that were produced from results of the furnace heated material were able to distinguish between samples heated to temperatures either above or below 450 °C. Heating to temperatures ≥ 450 °C produced an increasing concentration of ferrimagnetic minerals of both SSD grains (indicated by the increasing χ_{ARM} parameter) and other grain sizes (indicated by increasing SIRM values). This increasing content of ferrimagnetic minerals of a variety of grain sizes was confirmed by an increase in the content of soft minerals (reflected by smaller values of $\text{IRM}_{20}/\text{SIRM}$). Mid-magnetic minerals are likely to have changed to ferrimagnetic form as there was little change to the concentration of magnetically hard minerals identifiable by $\text{IRM}_{300}/\text{SIRM}$.

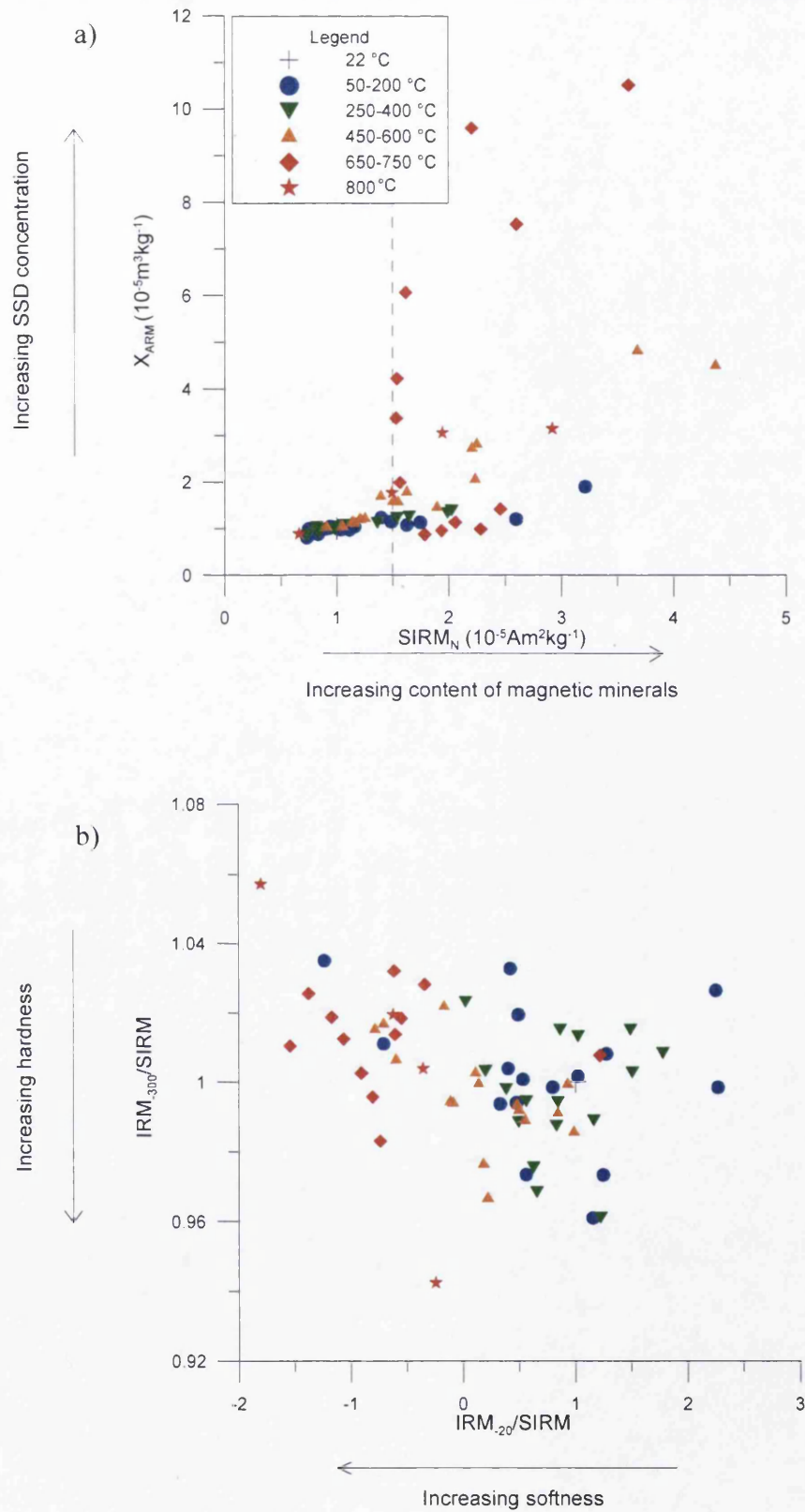


Figure 5.12: Bivariate plot of (a) $\chi_{ARM}/SIRM$ (b) $IRM_{300}/SIRM$ against $IRM_{20}/SIRM$.

The shift in grain-size characteristics suggested by some of the parameters in Section 5.3.2 is seen in the bivariate plot of $\chi_{fd} / (\chi_{ARM}/SIRM)$ (Figure 5.13a). The relationship between these parameters enabled separation of the fine grains from coarser grains within the magnetic assemblage. This suggested a coarsening of the assemblage at temperatures ≥ 450 °C, with finer material contained in the ‘tail’ (Maher 1988). The increasing prevalence of ferrimagnetic material has been supported by Figure 5.13b, where an increase in χ_{fd} in conjunction with an increase in IRM_{100} is represented by higher concentrations of magnetically ‘soft’ minerals at temperatures ≥ 450 °C.

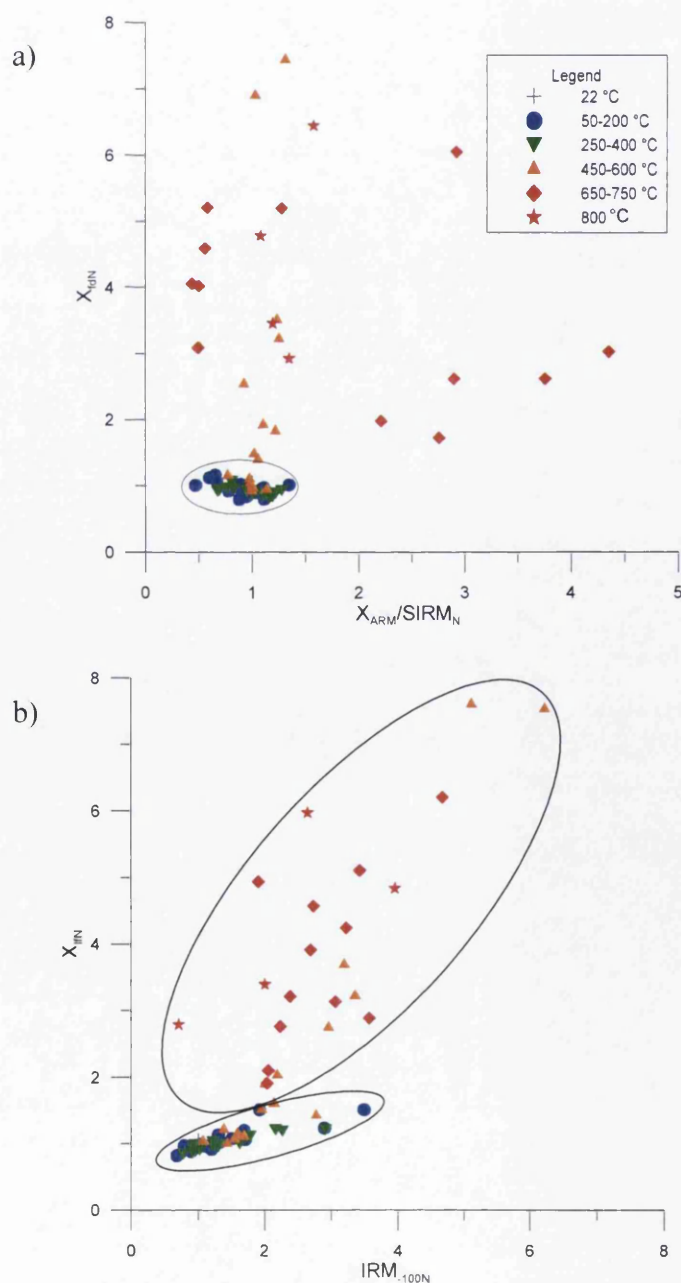


Figure 5.13: Bivariate plot of (a) χ_{fd}/χ_{ARM} against SIRM (b) χ_{fd}/IRM_{100} .

The final transformation of magnetic minerals occurred at temperatures $\sim 700\text{--}800\text{ }^{\circ}\text{C}$. Results have shown an increase in fine-grained secondary ferrimagnetic material, indicated by high $\chi_{fd\%}$ values (Oldfield 1999) and by a fine viscous and SP tail (Figure 5.14) in bivariate plots of $(\chi_{ARM}/\chi_{fd}) / (\chi_{ARM}/\chi_f)$ (Oldfield 1994; van der Post *et al.* 1997).

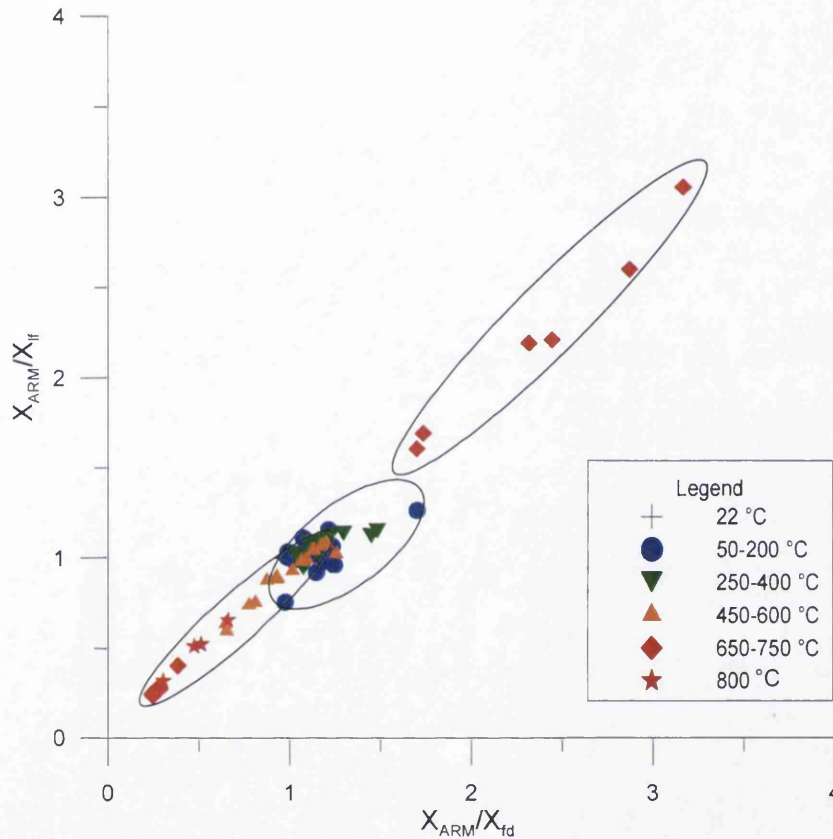


Figure 5.14: Bivariate plot of χ_{ARM}/χ_f against χ_{ARM}/χ_{fd} .

The investigation and analysis of the effect of furnace heating long-unburnt foot-slope soil at different temperatures for different durations on various quotients and bivariate plots of mineral magnetic parameters showed that: (i) all the bivariate plots drawn up identified two distinctive groupings, which differentiated between samples heated either above or below $450\text{ }^{\circ}\text{C}$, with the exception of the sample heated to $550\text{ }^{\circ}\text{C}$; (ii) changes to the levels of magnetic enhancement of various magnetic parameters investigated in this study have been related to an increase in ferrimagnetic minerals, identifiable by an increasing soft ferrimagnetic mineral component of a range of grain sizes; (iii) in this study, Viscous Single Domain (VSD) grains have been shown to have formed by heating to temperatures in excess of $700\text{ }^{\circ}\text{C}$.

In summary, the findings from stage 1 of this experiment in relation to the sub-aims shown in Figure 5.1 indicate that:

- The majority of magnetic parameters investigated here became enhanced at temperatures $>450\text{ }^{\circ}\text{C}$.
- $\chi_{fd}\%$ and $\text{soft}_{IRM}\%$, showed very little enhancement due to high values prior to heating. This suggested that they were retaining a signal from previous fires.
- Sub-sample variation had a greater influence than heating duration on the magnetic properties. This might have been overcome if longer heating durations had been explored, although naturally occurring forest fires rarely burn in the same area for >40 minutes.

5.4 HEATING AND COOLING EFFECT ON χ OF LONG UNBURNT SOIL

This section presents and interprets the results from Stage II of the heating experiments (described in Section 5.2.4). This stage was devised to: (i) investigate the effects of heating and cooling in air and nitrogen atmospheres; (ii) investigate mineralogical changes occurring during heating and cooling; and (iii) compare the responses of three samples from foot-slope (FS), mid-slope (MS) and ridge-top (RT) locations during and following heating and cooling to progressively higher temperatures.

5.4.1 χ CHANGES: FOOT-SLOPE (FS) SAMPLE

Changes in χ during heating at 100 °C intervals between 100 and 700 °C, and cooling to 40 °C in air and nitrogen atmospheres are shown in Figure 5.15. Three main patterns have been identified for samples heated to temperatures of (i) 100-200 °C, (ii) 300-400°C, and (iii) 500-700 °C. Heating to temperatures of between 100 and 400°C and cooling to room temperature produced no change in final χ (Figures 5.15a-d). The peak in χ occurring between 220-270 °C could be an indication of the dehydration lepidocrocite (Tauxe 2002). The general decline in χ with heating was caused by a re-alignment of magnetic moments within the crystal by thermal vibrations destroying the ferrimagnetic alignment, producing paramagnetic behaviour. Schwertmann and Taylor (1989) suggested that some maghaemite in Australian soils may have been formed by the dehydration of lepidocrocite during heating. The conversion of lepidocrocite to maghaemite was shown by the lack of a peak in χ between 220-270 °C in the cooling curve. However, the increased maghaemite in the heated sample did not produce a change in final χ . This may have been as a result of the low concentration of lepidocrocite in the sample owing to its dehydration during previous fire events. Alternatively the peak could have been attributed to the conversion of paramagnetic minerals such as goethite to haematite. Confirmation of the actual minerals contained within the soil assemblage could be attained by XRD analysis (Oldfield 1999). However, the focus of this chapter is on the changes that result from heating, rather than on the actual minerals formed.

Enhancement of χ occurred following heating to temperatures of between 500 and 700 °C (Figures 5.15e-g). Two phases of mineralogical modification were evident. The first peak was associated with the dehydration of lepidocrocite at temperatures of 220-270 °C (Tarling 1983). The second peak was probably associated with the conversion of magnetite at 585°C (Oldfield 1999). Heating to 600°C produced the greatest enhancement of 3.0 times its initial value.

The lack of enhancement of χ following heating to temperatures of 400-500 °C suggested that the sample had previously experienced these temperatures (Peters *et al.* 2001). Alternatively, Marmet *et al.* (1999) suggested that lepidocrocite in the sample indicated temperatures between 220-270 °C had not been experienced. These conflicting interpretations could be explained by a thermal history being retained by the majority of grains within the soil assemblage. The lepidocrocite in the sample is likely to have formed during the period since the last fire by either: (i) input of fresh material; (ii) natural oxidation processes (Schwertmann and Taylor 1989); or (iii) reworking of unenhanced material from greater depth in the soil profile by bioturbation. This last process has been shown to exceed the amount of soil actually removed from a slope by 2-30 times (Mitchell and Humphreys 1987); Dragovich and Morris (2002) calculated that on slopes the bioturbation process led to the net down-slope movement of material following wildfire in similar sandstone terrain to that in the present study amounting to 36% of the total amount of soil loss.

Heating and cooling under a nitrogen atmosphere (Figure 5.15a-h) were conducted to explore the effects of reducing conditions on enhancement since one potential explanation for the lack of a peak of χ in the furnace-heated sample at 200 °C was the lack of reducing conditions created by insufficient organic matter, caused by fire destroying the litter layer. Owing to the complex reduction and oxidation processes that occur in natural fire conditions, the laboratory experiment explored separately heating and cooling in 'full air' and 'full nitrogen' to understand the effect of extreme contrasts in atmospheres.

Heating under nitrogen was conducted to investigate the lack of enhancement at 200 °C as the furnace heating did not show definite enhancement of χ in all samples around 200-300 °C. The lack of enhancement at 200-300 °C was thought to be

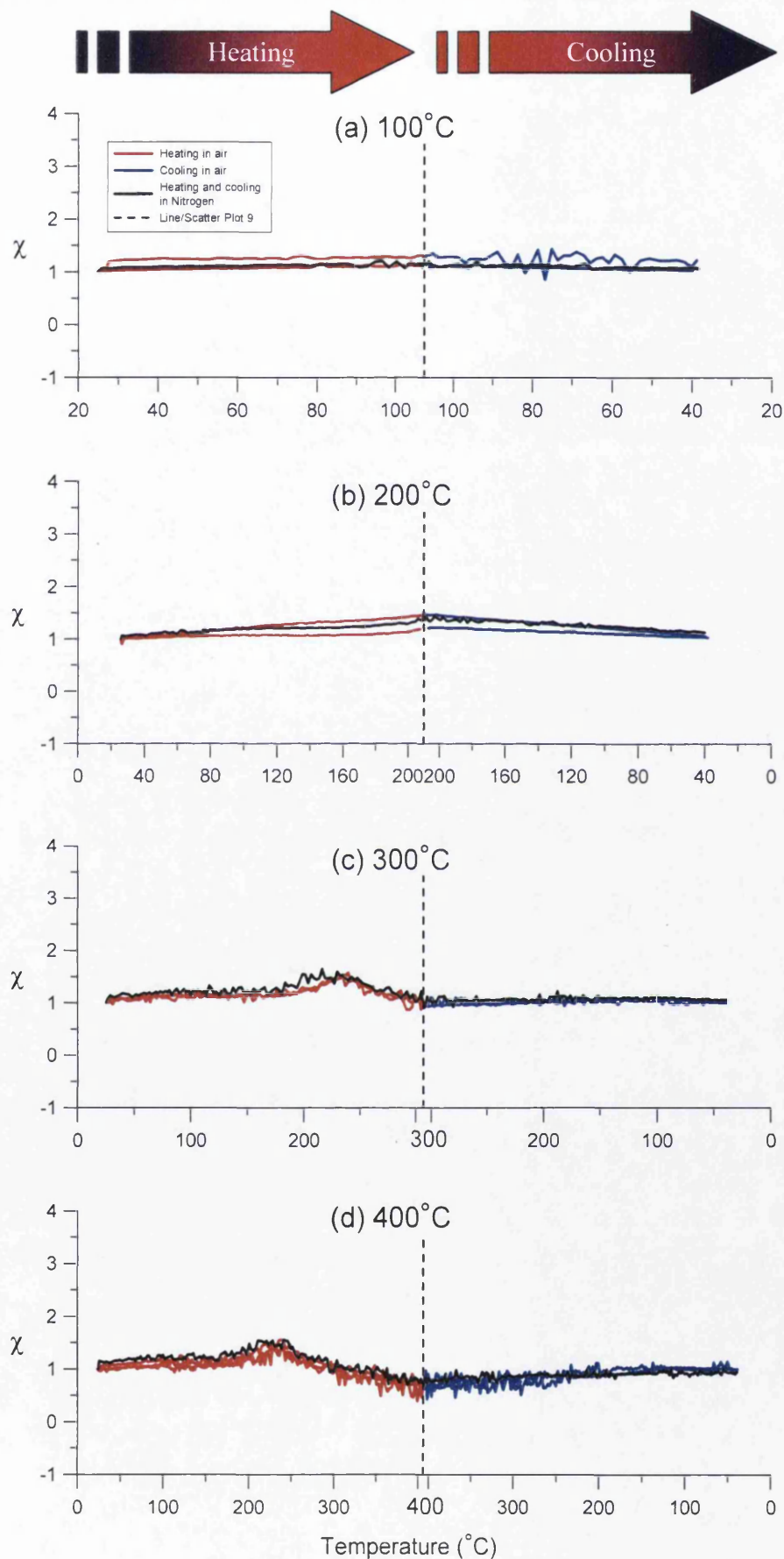


Figure 5.15: χ changes during heating and cooling to temperatures of (a) 100°C , (b) 200°C , (c) 300°C , and (d) 400°C .

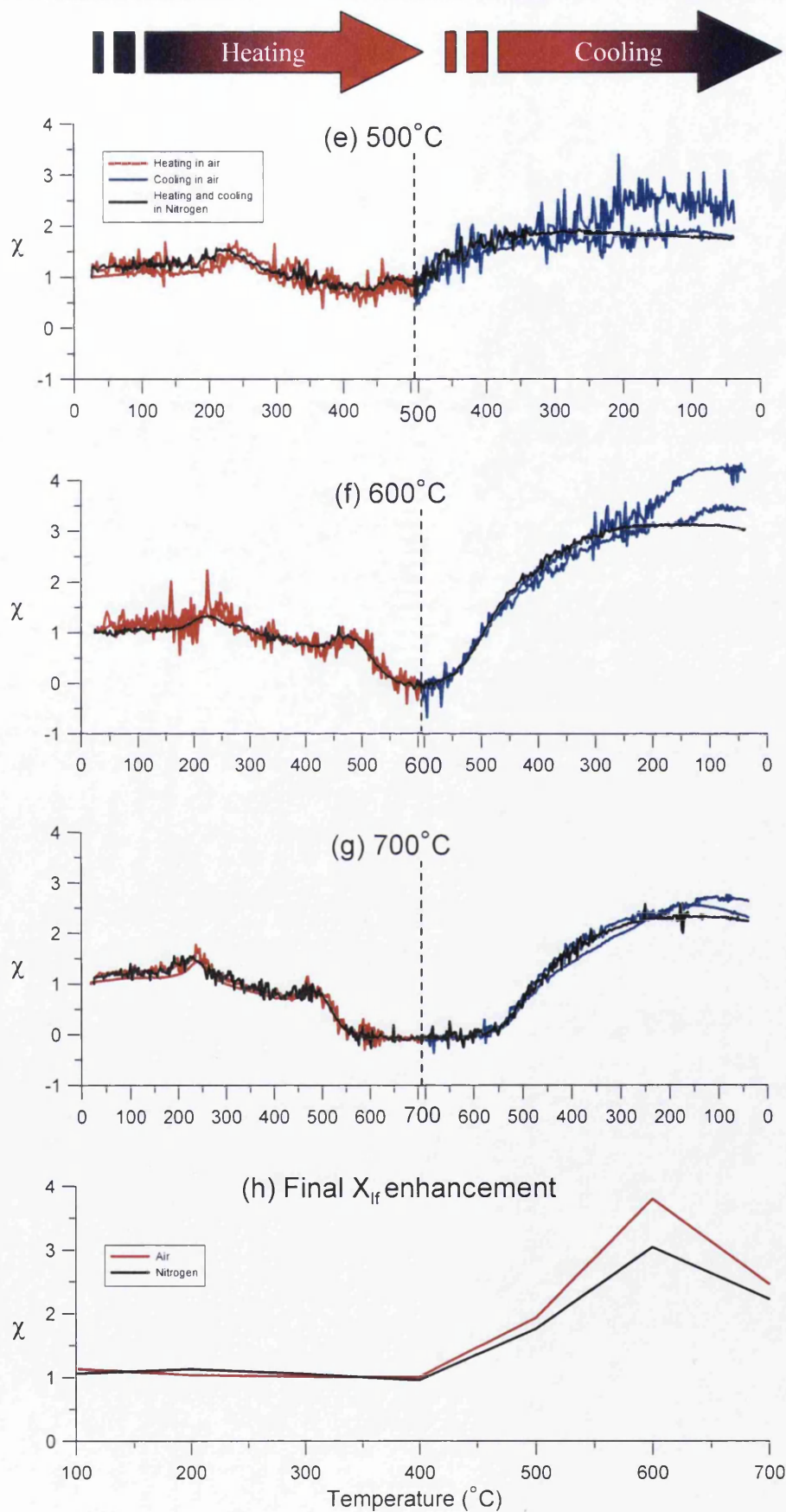


Figure 5.15 continued: χ changes during heating and cooling to temperatures of (e) 500 °C, (f) 600 °C, (g) 700 °C, and (h) final enhancement of χ following heating and cooling.

caused by the generous supply of oxygen, as lepidocrocite can only be formed in specific conditions including oxygen deficiency (Schwertmann and Taylor 1989). If heating at low temperatures ($<200\text{ }^{\circ}\text{C}$) in a reducing atmosphere (i.e. nitrogen) produced lepidocrocite, this would cause enhancement of χ when dehydration of lepidocrocite occurred at temperatures around $220\text{--}270\text{ }^{\circ}\text{C}$ (Tarling 1983; Özdemir and Banerjee 1984; Linford and Canti 2001).

In this experiment, heating the FS sample under a nitrogen atmosphere produced no change of response of χ enhancement for temperatures $<400\text{ }^{\circ}\text{C}$. The same experiment in air (Figure 5.15 a-f) showed that changes to lepidocrocite were apparent in a peak in χ occurring between $220\text{--}270\text{ }^{\circ}\text{C}$ (Figure 5.15a-f). However, this did not produce enhancement of the final χ following heating to $300\text{ }^{\circ}\text{C}$ and cooling to room temperature. The lack of enhancement following temperatures exceeding the thermal alteration temperature of lepidocrocite (at $220\text{--}270\text{ }^{\circ}\text{C}$) (Tauxe 2002) has suggested that: (i) the quantity of organic matter in the sample did not influence the results, which was confirmed by relatively high TOC values (9.58%); (ii) there was only a small proportion of lepidocrocite within the sample producing minimal enhancement; and (iii) changes between 200 and $300\text{ }^{\circ}\text{C}$ could have resulted from the conversion of paramagnetic minerals (Linford and Canti 2001), for example, the transition of goethite to haematite (Tarling 1983).

Comparison of the final enhancement obtained for χ_f changes following furnace heating in stage 1 and the pattern of enhancement following χ changes while heating and cooling in air and nitrogen atmospheres in stage 2 showed differences in the final enhancement. The furnace heating of χ_f produced two peaks in enhancement. However, the χ changes that occurred while heating and cooling only produced a gradual change in enhancement. This may have been caused by the lower resolution of heating increments used for χ changes while heating and cooling, as the 1st peak occurred between $456\text{--}484\text{ }^{\circ}\text{C}$. The differences between temperatures required to produce the peak at $\sim 600\text{--}700\text{ }^{\circ}\text{C}$ could have been caused by the different reducing conditions for the air atmosphere, as the fresh supply of air was greater for the furnace-heated sample. The greater reducing conditions were confirmed by the lower maximum enhancement obtained for χ measurements during heating and cooling in Stage 2, which was ~ 4 times its initial value, compared with enhancement

of ~8 times the initial value for furnace heating in stage 1. Different rates of heating and cooling were found to have a significant effect on final enhancement (Weston 2004). This may explain the differences in final enhancement between Stages 1 and 2 of this experiment. The furnace-heated samples were inserted in a preheated furnace in stage 1, while χ changes during heating and cooling required the sample to be heated from room temperature to the different temperature intervals (at a particularly fast rate of 11 °C per second).

5.4.2 χ CHANGES: MID-SLOPE (MS) SAMPLE

Figure 5.16 presents χ changes to the long-unburnt MS sample while heating and cooling in an air atmosphere. Three main patterns in χ are apparent for samples heated to: (i) 100-200 °C; (ii) 300 °C; and (iii) 400-700 °C. No changes in χ occurred while heating and cooling to temperatures of 100-200 °C. The sample heated to 300 °C produced a peak in χ between 220-270 °C, suggesting dehydration of lepidocrocite or conversion of goethite to haematite. However, in contrast to the FS sample described in the previous section, no final enhancement occurred.

Enhancement of final χ occurred for all mid-slope samples heated to 400-700 °C. The samples heated to 400 °C and 600 °C contained an additional mineral transformation compared to the other sub-samples from MS locations. This was demonstrated by enhancement occurring between heating from room temperature to 60 °C. Taylor and Schwertmann (1974) found enhancement of χ at 60 °C by the formation of maghaemite of samples with an initial pH value of 6. All samples heated to 500-700 °C demonstrated peaks in χ in the heating curve between 220 and 320 °C and between 420 and 520 °C. The main peak at ~585 °C suggested dominance of the mineral magnetite (Oldfield 1999). A different mineral was formed during the cooling curve of the FS sample, as a peak was apparent at 200 °C suggesting the formation of paramagnetic minerals (Linford and Canti 2001).

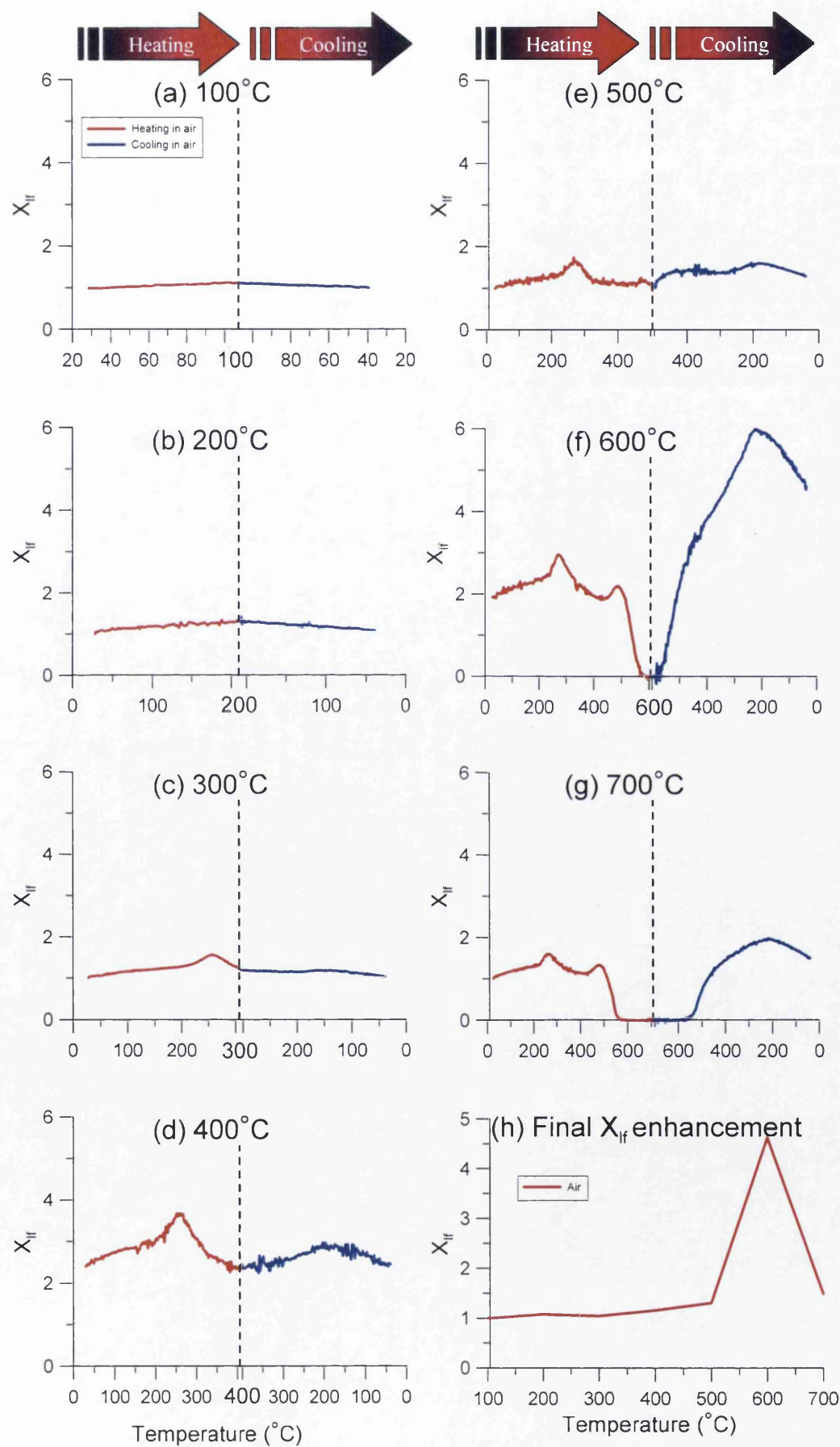


Figure 5.16: χ changes to the long unburnt MS sample during heating and cooling to temperatures of (a) 100 $^{\circ}\text{C}$, (b) 200 $^{\circ}\text{C}$, (c) 300 $^{\circ}\text{C}$, (d) 400 $^{\circ}\text{C}$, (e) 500 $^{\circ}\text{C}$, (f) 600 $^{\circ}\text{C}$, (g) 700 $^{\circ}\text{C}$, and (h) final enhancement of χ following heating and cooling. (Note different scales for graph (h).)

5.4.3 χ CHANGES RIDGE TOP (RT) SAMPLE

Changes in χ of the long-unburnt ridge-top (RT) sample while heating and cooling (Figure 5.17) showed two patterns of change for samples heated to temperatures of: (i) 100-400 °C; and (ii) 500-700 °C. The samples heated to 500-700 °C produced a peak in χ in the heating curve at 400-585 °C, suggesting the dominance of magnetite or maghaemite. The cooling curves showed two phases of change suggesting formation of two different mineral types, with χ peaking at 200 and 500 °C.

Theories developed by Marmet *et al.* (1999) and Peters *et al.* (2001) regarding the possibility of reconstructing thermal history from progressive heating of samples suggested that the ridge-top samples may have previously experienced temperatures of at least 400 °C. Comparison of the large enhancement of χ of ~60 times its initial value obtained for the RT sample heated to 500 °C, with the maximum enhancement of 4-6 times the initial values obtained for FS and MS samples suggested that the RT samples had never experienced thermal enhancement, but that the FS and MS samples had already been enhanced. This accords with the suggestion proposed by Blake *et al.* (2004) that the majority of post-fire erosion occurred from ridge-top locations. Weathering of the exposed ridge-top sites produces fresh, unburnt material, as indicated by the clean white sand deposits on the ridge tops during a reconnaissance visit to the catchment in 2003.

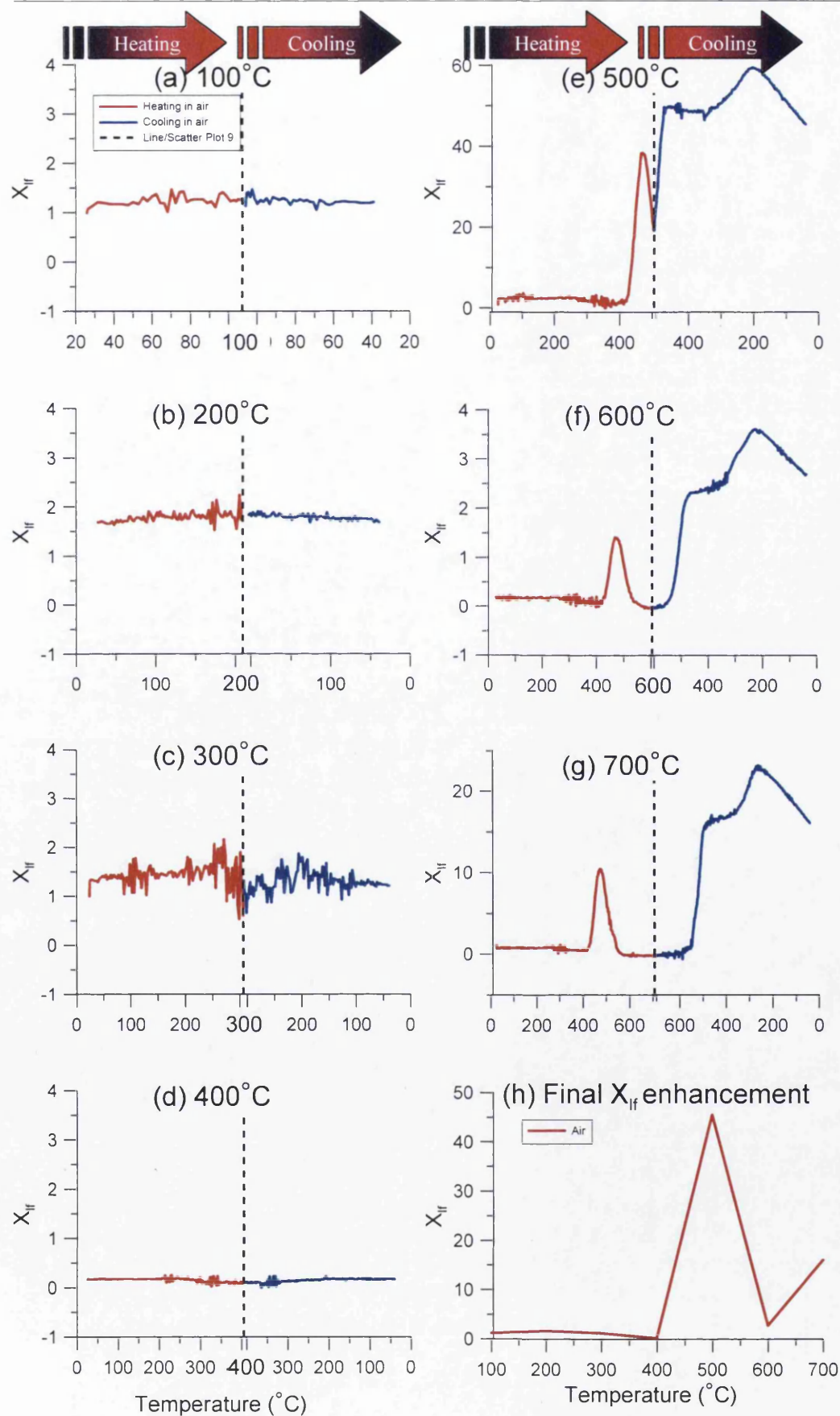


Figure 5.17: χ changes to the long unburnt ridge top sample during heating and cooling to temperatures of (a) 100 $^{\circ}\text{C}$, (b) 200 $^{\circ}\text{C}$, (c) 300 $^{\circ}\text{C}$, (d) 400 $^{\circ}\text{C}$, (e) 500 $^{\circ}\text{C}$, (f) 600 $^{\circ}\text{C}$, (g) 700 $^{\circ}\text{C}$, and (h) final enhancement of χ following heating and cooling. (Note different scales for graphs (e) and (g).)

Examination of χ under air and nitrogen atmospheres for soil samples from long unburnt areas of the catchment from foot-slope, mid-slope and ridge-top locations suggested that:

- Enhancement of material from a range of catchment locations did not produce enhancement of χ until temperatures in excess of 400 °C were reached.
- Reducing conditions imposed by heating the sample under organic matter simulated by heating under a nitrogen atmosphere showed no effect on χ until temperatures > 400 °C were experienced. At this temperature, although the enhancement of χ occurred for the sample, the level of enhancement was lower than that experienced for the sample heated in an air atmosphere.
- A peak in χ occurring between 220 and 270 °C suggests the presence of lepidocrocite in the FS and MS samples.
- The soil assemblage contained a complex mineralogy, which indicates regeneration of the soil and decay of the enhanced magnetic signature following burning.
- Possible retention of a signal from previous fire events was demonstrated by comparing the levels of enhancement created by the FS and MS samples with the RT samples. The material on ridge tops was more likely to have been recently created by weathering of bedrock or lay deep in the soil profile prior to fire and was therefore unlikely to have experienced heating, thus producing a maximum enhancement of ~60 times its initial value.

5.5 DISCUSSION

This section discusses key findings from the results of the heating experiment presented in this chapter. These include: (i) the lack of enhancement of χ until temperatures $>400\text{ }^{\circ}\text{C}$ were reached; (ii) the different temperature thresholds found for enhancement of specific magnetic parameters, suggesting enhancement of a variety of magnetic grain sizes; and (iii) the suppression of enhancement at temperatures $>400\text{ }^{\circ}\text{C}$ when heated in a reducing atmosphere.

5.5.1 ENHANCEMENT OF χ $>400\text{ }^{\circ}\text{C}$

The heat-induced changes to χ identified following the furnace pre-heating in stage 1 and the final enhancement indicated by the FS, MS and RT samples in stage 2 all suggested that enhancement of χ did not occur for some samples until temperatures of $>60\text{ }^{\circ}\text{C}$ had been reached, while others did not become enhanced until temperatures $>400\text{ }^{\circ}\text{C}$ have been reached. This conflicts with findings from some other studies, which have shown enhancement of χ at temperatures between 200 and $300\text{ }^{\circ}\text{C}$ (Brown 1988; Morinaga *et al.* 1999). The differences in temperature thresholds found between studies have been attributed to one or more of the following factors: (i) mineralogy; and soil type; (ii) previous heating history; (iii) rate of heating; and (iv) heating duration.

5.5.1.1 *Mineralogy and soil type*

Mineralogy influenced the enhancement of χ , when temperatures exceeded the alteration temperatures of dominant minerals within the assemblage (Longworth *et al.* 1979; Tarling 1983; Tauxe 2002). The minerals associated with different soil types caused enhancement of χ of clay soils at temperatures $>200\text{ }^{\circ}\text{C}$, whereas sandy soils seem to have become enhanced only at temperatures $>400\text{ }^{\circ}\text{C}$ (Brown 1988; Linford and Canti 2001; Weston 2004). Some of the results from this study conflict with these findings. The foot-slope samples and mid-slope samples (except the MS samples heated to 400 and $600\text{ }^{\circ}\text{C}$ (Figure 5.16d and f) showed no enhancement until temperatures of between 400 and $500\text{ }^{\circ}\text{C}$, while the MS samples heated to 400 and $600\text{ }^{\circ}\text{C}$ and the majority of the ridge-top samples showed change in χ between 40 and $60\text{ }^{\circ}\text{C}$. This suggested that despite the fact that this was a long-unburnt site, either the samples were retaining a memory of previous fire events or the foot-slope samples contained a unique mineralogical signature that was not enhanced by these

temperatures. The concept of the foot-slope sample having experienced previous heating confirms findings by Shakesby *et al.* (2003) who found that foot-slope sites stored much of the burnt soil material eroded from higher up the slope. The mineralogy of the FS sample may well also differ slightly from ridge-top and mid-slope locations as it is likely to have received eroded burnt material from these sites and to have experienced multiple burn events as indicated by fused aggregates (Blake *et al.* 2005). In contrast, following post-fire erosion the MS and RT sites contain previously unexposed unheated material.

These findings imply that the use of mineral magnetic measurements to detect fire events can be an extremely powerful tool to detect the enhancement of soils that have not previously experienced temperatures between 40-60 °C. However, in a fire-prone environment such as the study site, where multiple fire events are common, if temperatures between 40-60 °C have already been experienced, enhancement of χ will not occur until temperatures of between 400-500 °C are reached. The findings from Blake *et al.* (2004) showed that χ_{lf} was a critical parameter for recognising different magnetic signatures associated with fires of different severities. In their study, the samples from the long-unburnt site was thought likely never to have experienced temperatures <40 °C, the samples from the low severity fire likely to have experienced temperatures >60 °C and the samples from the severely burnt site likely to have experienced full conversion of minerals to secondary state by heating to temperatures in excess of 400-500 °C. However, further investigations by Blake *et al.* (2006) highlighted that additional geochemical parameters may provide a more reliable indicator to explore sediment sources as mineral magnetic parameters cannot be used in isolation for sediment tracing purposes to distinguish between fires of low and moderate severity.

The implications of the high temperatures required to produce enhancement of χ where multiple fire events occurs questions the extensive use of χ_{lf} alongside pollen studies to confirm the presence of burnt material in conjunction with an increased occurrence of fire-activated pollen (Long *et al.* 1998). These findings also have implications for archaeological studies, which often use magnetic surveys to detect previous campfire and kiln sites. Kilns are likely to attain temperatures hot enough

to provide enhancement. Single-burn campfires of limited duration may not produce enough heat to modify χ (Bellomo 1993).

5.5.1.2 *Previous heating history*

Mineralogy and soil type have important influences on the temperature thresholds required to produce enhancement of various magnetic parameters. However, these can be affected by previous heating. Experiments by Brown (1988), Weston (2002) and Hanesch *et al.* (2006) investigated the influence of repeated heating and showed that no further modifications to χ occur on heating the second time to the same temperature. This suggested that mineralogical transformation to a secondary state had already occurred. This provided the basis for Peters *et al.*'s (2001) suggestion that by comparing χ at 40 °C pre-and post- progressive heating to temperatures of 700 °C could show the thermal history of an assemblage, by determining the temperature at which enhancement of χ occurred. Furthermore, Marmet *et al.* (1999) and Hanesch *et al.* (2006) also suggested that the presence of lepidocrocite in a sample enabled identification the incidence of temperatures > or <400 °C. According to this suggestion, if lepidocrocite was not present in the sample, then temperatures >400 °C had previously been experienced. However, this was only applicable to locations where lepidocrocite was present before fire. The FS samples showed evidence of lepidocrocite by a peak around its alteration temperature (220-270 °C) (Tarling 1983).

The results for the FS and MS samples in this investigation conflicted with the views expressed by Marmet *et al.* (1999) and Peters *et al.* (2001), as they showed the presence of lepidocrocite, but no final enhancement occurring until >400 °C. The lack of enhancement in χ until temperatures between 400-500 °C could be related to: (i) the dominance of magnetite/maghaemite in the assemblage; or (ii) temperatures <400 °C had already been experienced during fire in the past, but owing to the long time since the last fire event, new lepidocrocite may have been contained within the sample since the last fire event as a result of: (i) eroded sediments from upslope locations; (ii) deposition; (iii) bioturbation mixing unheated subsurface samples with heated samples; or (iv) naturally-occurring reducing conditions (Schwertmann and Taylor 1989).

Comparison of the maximum enhancement following heating soils from the different slope units showed that the FS produced an increase of 3-3.5 times initial values (Figure 5.15h), the MS produced an increase of 5 times initial values (Figure 5.16h), while RT samples produced an increase of 60 times the initial values (Figure 5.17h). The comparatively low level of enhancement obtained for the FS and MS samples could be attributed to the complex fire history of the soil assemblages in the study area containing a mixture of grains with different fire histories.

The high temperatures required to enhance magnetic signatures of the long unburnt FS and MS samples combined with the high $\chi_{fd}\%$ and $\text{soft}_{IRM}\%$ values suggested that some of the grains within the soil assemblage were retaining a thermal memory of previous heating. The implications of these findings are that: (i) soils within the study area retain complex fire histories that are a result of multiple fire events; (ii) the lower proportion of enhancement of χ following heating has resulted from initially elevated signatures derived from previous fire events; and (iii) post-fire erosion processes mix samples of different fire histories.

5.5.1.3 *Rate of heating*

The rate of heating has been shown to be influential in the level of χ enhancement with faster heating creating a greater increase in χ (Oldfield *et al.* 1981; Weston 2004). This was confirmed by differences in the final χ observed for the FS sample in stages 1 and 2 of this experiment. Twice the maximum enhancement was produced for the rapid heating in stage 1 by inserting the sample in a pre-heated furnace when compared with gradual heating conducted while monitoring χ changes with progressive heating and cooling. The implications of the different heating rates in the present study suggest that the enhancement of χ in the catchment is influenced not only by mineralogy and soil type, but also by the rate of progression of the fire front, which is influenced by wind speed, fuel load and moisture content, as shown in Figure 2.2. In general, this agrees with the findings of Oldfield *et al.* (1981) and Weston (2004) who also found that greater enhancement of χ occurs with more rapid heating. It also supports the application of enhanced χ to detect where rapidly igniting fires of greater than moderate severity have occurred such as on shallow and moderate slopes ($<18^\circ$) in the Lake Burragorang Catchment during the 2001 fires (Chafer *et al.* 2004).

5.5.1.4 Heating duration

In this study, variations in mineralogical concentration of the sub-samples produced a greater influence on χ enhancement than heating duration. Similar levels of enhancement were obtained for samples heated for 5 and 20 minutes and 10 and 40 minutes. This contradicts some of the findings by Oldfield *et al.* (1981) who found increasing magnetic concentration with the formation of magnetite, which was followed by its break-up and conversion to haematite after prolonged heating. These differences were likely to have been caused by the different heating durations. Oldfield *et al.* (1981) investigated heating durations ranging between 20 minutes and 2 hours, whereas the experiment here only explored durations between 5 and 40 minutes, as naturally-occurring fires rarely burn for durations > 40 minutes except under smouldering logs. Therefore in most natural forest fires, the rate of progression of the fire front has a minimal effect on final χ .

5.5.2 DIFFERENT TEMPERATURE THRESHOLDS FOR MAGNETIC ENHANCEMENT

Magnetic parameters other than χ_{lf} have been used to identify burnt material. Oldfield *et al.* (1981), Rummery *et al.* (1979) and Rummery (1981) used SIRM and χ_{lf} . Maher (1986) suggested enhancement of χ_{lf} and χ_{ARM} following fire. Linford and Canti (2001) found that χ_{ARM} , $IRM_{2.5T}$ and IRM backfield measurements gave more reliable enhancement than χ_{lf} . None of these studies investigated the temperature thresholds necessary to produce enhancement of these parameters.

High $\chi_{fd}\%$ has been associated with burnt material (Dearing 1999b). As suggested in Figure 5.9b, the lack of enhancement of $\chi_{fd}\%$ and $soft_{IRM}\%$ with heating indicated that the sample had already been enhanced and retained a memory of previous fire events, suggesting that the temperature thresholds required to enhance these parameters had already been reached.

The increase in SIRM at 200 °C reflected increases in magnetic materials for grain sizes not accounted for by other parameters investigated. This could have been produced by the contribution of ultra-fine ferrimagnetic material to the signature, which is usually masked by coarser canted antiferromagnetic minerals (Walden 1999). This highlighted the potential use of SIRM in detecting burnt material resulting from low-moderate severity fires. The implications of the present study are

that magnetic parameters in addition to χ_f should be used to detect burnt material. These findings can also enable tentative suggestions to be made regarding the size of the enhanced magnetic grains and temperatures required to produce enhancement. These findings in general, have highlighted the need for additional parameters to χ in recognising burnt material in environments where magnetite or maghaemite dominate. Enhancement of χ_f only indicates material burnt in fires that reach temperatures in excess of 450 °C.

5.5.3 EFFECT OF REDUCING ATMOSPHERE ON MAGNETIC ENHANCEMENT

The effect of heating and cooling the FS samples in a nitrogen atmosphere in this study produced a suppression of χ enhancement at temperatures > 400 °C compared to the enhancement obtained by the FS samples heated and cooled in air. Brown (1988) and Weston (2004) also found suppression of χ with reducing conditions. However, the suppression observed by Brown (1988) resulted from samples heated at temperatures above 100 °C, while Weston (2004), using a progressive heating technique, did not find suppression of χ enhancement until temperatures were high enough to cause combustion of organic matter, which generally occurs at temperatures >460 °C (Giovannini 1994).

The findings of Weston (2004) are similar to some of the results in this study, probably because of the similarly sandy nature of the samples used. The conflicting findings by Brown (1988) and the present study relate to the different mineralogies of the samples used by Brown (1988), which produced enhancement of χ at temperatures of between 150 and 200 °C.

The present study shows that different reducing conditions in the catchment are likely to affect enhancement. Therefore moist foot-slope or floodplain samples are likely to experience the greatest suppression of enhancement. Drier environments such as ridge-tops are likely to produce comparatively higher levels of enhancement. However, foot-slopes provide an environment that is more likely to suit the development of the mineral lepidocrocite due to the oxygen deprivation experienced in such a location (Schwertmann and Taylor 1989). If large quantity of lepidocrocite is present in the sample, then enhancement of foot-slope samples could occur at lower temperatures than on the ridge-top.

5.6 CHAPTER SUMMARY

This section summarises the key findings from this chapter in relation to the main research questions addressed by these experiments in Section 5.1.

- The magnetic parameters enhanced by heating in this study and their temperature thresholds are shown in Table 5.8 (research questions 1 and 2).

Table 5.8: Temperature thresholds of various magnetic parameters investigated for furnace heating of the long-unburnt samples investigated.

| Magnetic parameter | Temperature thresholds at |
|--------------------------|---------------------------------------|
| | which enhancement occurs (°C) |
| χ_f | 40-60 (in some samples) 450-500, >550 |
| χ_{fd} | 450-500, >550 |
| χ_{ARM} | 450-500, 550-700 |
| $\chi_{fd}\%$ | No thresholds apparent |
| Soft _{IRM} % | 450-500, >600 |
| $\chi_{ARM}/SIRM$ | 550-650 |
| χ_{fd} / χ_{ARM} | >650 |
| SIRM | 450-550 |

- Heating duration did not have an appreciable effect on enhancement of the magnetic parameters investigated. Different concentrations of minerals provided a greater control on the level of enhancement (Research question 3).
- X changes during heating and cooling provided an insight into mineralogical changes that are not indicated by final χ enhancement (Research question 4).
- Reducing conditions suppressed the enhancement of χ . No effects of reducing conditions were identifiable below 400 °C, the point at which enhancement of χ occurred in a 'full-air' atmosphere (research question 5).
- The fire history retained by samples from previous burn events influenced temperature thresholds required to produce magnetic enhancement (research question 6).

-
- Slope location had an effect on the response of χ under the same heat-treatments. This is attributed to the different mineral compositions of the samples obtained from different slope units determined by areas of erosion and deposition (research question 7).

The results presented in this chapter have implications for other aspects of research presented in this thesis. They include:

- the relatively high temperature thresholds (>400 °C) that are required to produce enhancement of mineral magnetic properties of samples that have previously experienced heating to temperatures >60 °C within the Lake Burraborang catchment have implications for: (i) enhanced mineral magnetic signatures that are commonly used to identify burnt material in sediment cores (see Chapter 8); and (ii) the need for investigation of a different soil property such as Thermal Activation Characteristics (TAC) (investigated in Chapter 6) to ascertain the potential use of this soil property in detecting low-severity fires.
- The complex fire histories recorded within soil assemblages are investigated further by assessment of TAC of single grains in Chapter 6.
- The application of mineral magnetic measurements in sediment cores to detect burnt material is investigated in Chapter 7.

6 EFFECTS OF HEATING ON THERMAL ACTIVATION CHARACTERISTICS (TAC) OF QUARTZ GRAINS IN SOIL

This chapter presents the results and analysis of a further development of the heating experiments conducted on mineral magnetic properties of three long unburnt soils investigated in Chapter 5. Two stages of experiments have been devised to examine the effects of different laboratory heat treatments on the Thermal Activation Characteristics (TAC) of quartz within: (i) the long-unburnt foot-slope (FS) soil sample that was investigated in Section 5.3 (Stage 3); and (ii) an unexposed bedrock sample from the Nattai Catchment (Stage 4). Thermoluminescence (TL) properties of soil are commonly used for dating purposes by measuring the luminescence emitted from samples when stimulated by heating. TL differs from Optically Stimulated Luminescence (OSL) in that the latter uses a beam of light to release a luminescence signal (Aitken 1994; Duller 2004).

TAC are established by a series of Thermoluminescence (TL) sensitivity (χ) measurements, made following pre-heating to increasing temperatures ranging between 200 and 680 °C in 40 °C intervals. TAC have been used in some archaeological studies to ascertain temperatures experienced by artefacts (Godfrey-Smith *et al.* 2005; Lahaye *et al.* in press), however this technique has not been widely used to suggest temperatures experienced by soils. Further details of the literature are presented in Section 2.3.5. As measurement of the 110 °C TL peak is carried out by heating to 160 °C, this method may be useful in detecting modification of soil properties that occur if temperatures as low as 200 °C have been experienced. Thus, the method could potentially identify previous heating events at temperatures <400 °C that were not identifiable in samples by mineral magnetic temperature thresholds investigated in Chapter 5.

Section 6.1 outlines the thesis aims and research questions addressed specifically in this chapter. Section 6.2 describes the methodologies and samples used. Section 6.3 presents the results from stage 3 of the experiments investigating the effect of furnace heating of the long-unburnt foot-slope (FS) soil sample on TAC. Section 6.4 presents the results from stage 4 of the experiments investigating the effect of furnace heating of a sample of unexposed bedrock on TAC. Section 6.5 discusses

the implications of the results, and section 6.6 presents a summary of key findings relative to the research questions investigated in this chapter.

6.1 INTRODUCTION

The heating experiments here were conducted in order to address specific thesis aims given in Chapter 4: to assess the temperature thresholds apparent for TL properties of thermally enhanced Australian soils (1a); and to assess the influence of thermal history of samples (1b) (Chapter 4). These thesis aims were addressed via a number of research questions (Figure 6.1), developed to gain a better understanding of: (i) temperature thresholds required to produce modification of TAC of a long-unburnt foot-slope sample by heating (research question 1); (ii) thermal histories of grains contained within a long-unburnt foot-slope soil (research question 2); (iii) features of TAC produced by samples heated to simulate different temperatures *ca.* 10,000 years ago (research question 3); (iv) temperature thresholds required to produce modification of the 110 °C TL χ peak of unexposed unheated bedrock samples by heating (research question 4); (v) temperature thresholds required to produce modification of the shape of the TAC curve produced by unexposed unheated bedrock samples (research question 5); and (vi) features in TAC following furnace-heating that were apparent for the unexposed and previously unheated bedrock sample simulated to have been heated to different temperatures *ca.* 10,000 years ago (research question 6).

These research questions were explored in two stages, which are summarised in Figure 6.1 along with the methods and techniques used in this chapter to address each of the research questions. Research questions 1-3 were investigated using the long-unburnt foot-slope soil sample described in Section 5.2.1 that had been heated in a furnace for 40 minutes. Research questions 4-6 were investigated using a sample of unexposed, unheated bedrock from a road cutting adjacent to the footslope sampling site. All research questions were addressed by measurement of multi-grain aliquots and single-grain samples either directly or following a pre-dose of 10Gy β radiation. Application of the 10 Gy β dose was conducted to simulate the effect of furnace heating *ca.* 10,000 years ago (Section 2.3.5) to assess whether the timing and temperature of fire events could be established. The potential of this parameter in detecting the fire severity experienced by sediments was explored by

investigating TAC in burnt material from different depths in a sediment core obtained from the Nattai arm of Lake Burragorang (Chapter 7). Despite the application of TL χ measurements to gain a better understanding of archaeological prehistoric manufacturing processes and for dating, the use of TAC to investigate the severity or timing of previous fire events in soils and sediments had not previously been explored.

| | | | |
|---------|---|---|--------------------------------|
| Stage 3 | Which temperature thresholds are required to produce modification of TAC of a long unburnt FS sample by heating? (Research question 8) | Multi-grain aliquots | |
| | Can thermal histories of grains within a long unburnt foot-slope soil sample be ascertained by single-grain TAC? (Research question 9) | Single grain samples | |
| | Which features in TAC following furnace heating are apparent for a long-unburnt foot-slope soil sample simulated to have been heated <i>ca.</i> 10,000 years ago? (Research question 10) | Multi-grain aliquots | Measurement following pre-dose |
| Stage 4 | Which temperature thresholds are required to produce modification of the 110 °C TL χ peak of unexposed unheated bedrock samples by heating? (Research question 11) | Multi-grain aliquots | |
| | Which temperature thresholds are required to produce modification of the shape of TAC of unexposed unheated bedrock samples by heating? (Research question 12) | Multi-grain & single grain samples aliquots | |
| | Which features in TAC following furnace heating are apparent for the unexposed unheated bedrock sample subjected to simulated heating <i>ca.</i> 10,000 years ago? (Research question 13) | Multi-grain aliquots | Measurement following pre-dose |

Figure 6.1: Summary of research questions addressed and techniques applied to investigate the effects of heating on TAC of a long-unburnt foot-slope soil sample (Stage 3) and a sample of unexposed unheated bedrock (Stage 4) from the Lake Burragorang catchment.

6.2 METHODOLOGY

This section presents the detailed methodology used for this chapter. It describes sample details (Section 6.3.1); furnace heating procedures (Section 6.3.2); sample preparation for TL measurements (Section 6.3.3); TL measurement procedures (Section 6.3.4) and calculation of $TL\chi$ (Section 6.3.5).

6.2.1 SAMPLE DETAILS

This section describes the two samples used during stages 3 and 4 of this thesis (Figure 6.1), which are detailed in Table 6.1. Preliminary investigations were conducted on the furnace-heated long-unburnt foot-slope (FS) soil sample used in Chapter 5 that had been heated for durations of 40 minutes. These samples were selected as they were most likely to have experienced thorough heating and reached the target temperature. Details about this sample have already been given in Section 5.2.1.

The samples used in Stage 2 of this chapter were derived from a sample of unexposed bedrock (BR), from a road cutting adjacent to Sheehys Creek (Figure 3.2) near to the site of the FS soil sample. This was collected in order to ascertain $TL\chi$ changes in an unequivocally unheated sample. The rock sample was taken from the Hawkesbury sandstone unit, which is dominant in this landscape (Nanson and Young 1983) (Figure 3.2) and contained two distinctive units of white unweathered sandstone and one sample of iron-stained bedrock (Figure 6.2). A sample of the white sandstone was selected for the main part of this experiment, owing to the iron stained sample potentially having a high concentration of uranium.

Table 6.1: Sample details and codes used for investigating the response of TAC to different furnace heat treatments for a (i) long unburnt footslope soil sample and (ii) unexposed unheated sample (since deposition) of bedrock.

| Experiment Stage | Sample code | Location | GPS (S/E) | Description |
|------------------|-------------|---------------|---------------------------|---|
| STAGE 3 | FS | Sheehys Creek | 34°06'00.1 150°29'23.3 | Long-unburnt foot-slope sample >30 years |
| STAGE 4 | BR | Sheehys Creek | 34°13'89.5 150°48'22.1 | Unexposed geological sample Hawkesbury sandstone |

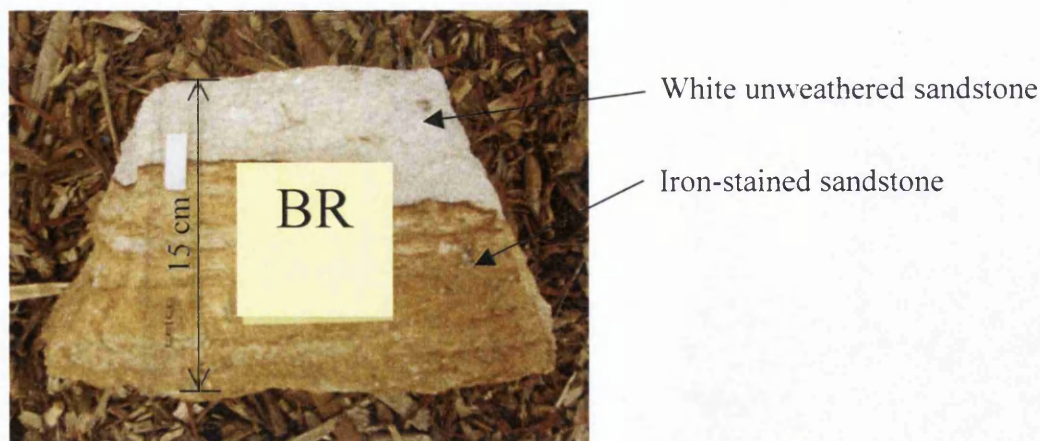


Figure 6.2: Previously unexposed bedrock (BR) sample of Hawkesbury Sandstone – the white un-weathered section was used for this investigation owing to concerns about uranium concentration in the iron-stained sandstone.

6.2.2 FURNACE HEATING PROCEDURE

Details of the furnace heating procedure used for the FS sample can be found in Section 5.2.1.

Preparation of the bedrock (BR) sample was required before furnace heating. Firstly, outer surfaces of the bedrock samples were sprayed with paint in the field and then the sample taken into a light-sensitive laboratory and the outer edges removed to eliminate potential contamination. Secondly, the inner section of bedrock was broken down into individual quartz grains. Thirdly, the previously unexposed bedrock sample was wet-sieved and the 177-210 μm fraction extracted for furnace heat-treatment. Subsets of the crushed white bedrock sample were subjected to furnace heat treatments at 100 $^{\circ}\text{C}$ increments (0-800 $^{\circ}\text{C}$) using the same procedure as outlined in Section 5.2.1. However, 1.5g samples were used here, which were placed on a steel tray and heated in a muffle furnace. The temperature of the sample was constantly monitored during the 40-minute heating using a multimeter attached to a K-type thermocouple in contact with the sample.

6.2.3 SAMPLE PREPARATION FOR $\text{TL}\chi$ MEASUREMENTS

Following furnace heating, extraction of the 125-355 μm fraction from the FS sample was conducted by wet-sieving. Because sieving of the 177-210 μm fraction of the BR sample had been conducted before furnace heating, further sieving was not required. The different grain size ranges used for the FS and BR samples was selected on the basis of the quantity of material available. The furnace-heated foot-

slope and bedrock samples were both subjected to a brief 10-minute treatment in hydrofluoric acid to remove coatings on the quartz grains. Three 3 mm multi-grain aliquots of each of the furnace heated FS and BR samples were mounted onto steel discs using silicone oil. TAC were investigated for 60 discs containing single individually selected quartz grains from the: (i) long-unburnt FS sample heated to 50 °C (used as a proxy for an unheated sample); (ii) unexposed unheated BR sample; and 20 discs from the unexposed BR sample furnace heated to 600 °C were used to ascertain variability in the response of the sub-samples used.

6.2.4 THERMOLUMINESCENCE SENSITIVITY MEASUREMENTS: PROCEDURE

TL χ measurements were conducted at the Research School of Earth Sciences at the Australia National University in Canberra using a Risø TL-DA-10 TL/OSL reader (Bøtter-Jensen 1997) with the following procedure: First, the samples were mounted in the disc holder. Second, approximately 10 ml of phosphorus pentoxide was placed in the instrument to aid in removing H₂O from the atmosphere and improving the vacuum seal. Third, the disc holder was placed in the instrument with the samples positioned so that they were not directly under the irradiator. Fourth, the lid was lowered and the lead blocks positioned between the radioactive source and the photomultiplier to help reduce background count-rate. Fifth, air was extracted from the sample chamber with a vacuum pump and N₂ was allowed to flow into the chamber.

Once the preparation of the instrument had been completed, the following measurement procedure was initiated: (i) application of a 0.2 Gy β dose for 10 seconds; (ii) measurement of the 110 °C TL χ peak by heating to 160 °C; (iii) heating to 200 °C; (iv) application of a 0.2 Gy β dose; and (v) measurement of the 110 °C TL χ peak by heating again to 160 °C. This sequence was repeated for temperatures at 40 °C increments for step (iii) and (iv) until temperatures of 680 °C were reached. Heating of the sample occurred at a rate of 2 °C per second.

In order to simulate the effect of heating *ca.* 10,000 years ago (Aitken 1985) a 10 Gy β dose was applied before beginning the measurement procedure (outlined above).

6.2.5 CALCULATION OF $TL\chi$ AND PRODUCTION OF TAC

$TL\chi$ was calculated from the area under the 110 °C curve, which was proportional to the amount of light emitted by the release of photons from the 110 °C electron trap. The $TL\chi$ measured following progressive heating in 40 °C intervals was used to create the TAC. This showed $TL\chi$ changes following heating to successively increasing temperatures. The shape of TAC for each sample was influenced by the temperatures required to move holes from R- centres to L- centres (Aitken 1985; Bailey 2001) (shown in Figure 2.6). The type of quartz influences the temperature at which $TL\chi$ increases. This is dependent on the position of the trap in relation to the valence band; quartz grains with traps situated closer to the valence band transfer at lower temperatures (Aitken 1985). The influence of this on TAC shape is shown in Figure 6.3.

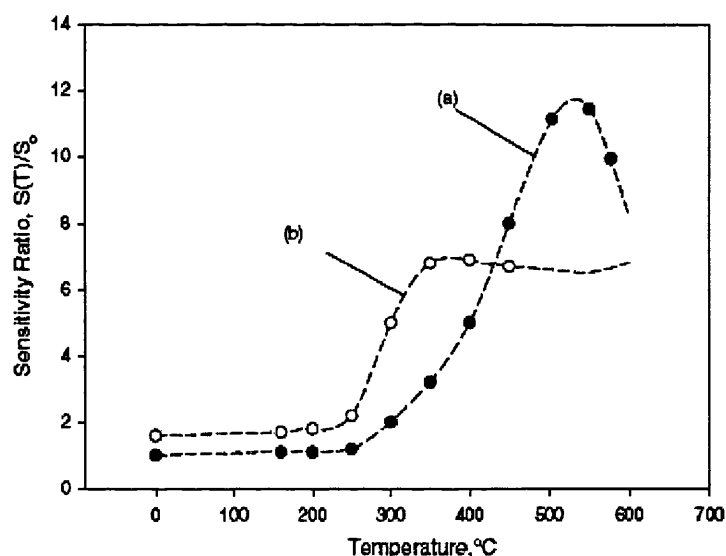


Figure 6.3: TAC showing (a) late activation; and (b) early activation (Fleming and Thompson 1970; Chen and Pagonis 2004)

The TL values were then corrected by removal of the background signal. $TL\chi$ values were then normalized to the $TL\chi$ value of the unheated sample using equation 6.1 to enable comparison of the level of enhancement of $TL\chi$ following furnace heating.

$$\frac{X}{X_0} = X_N \quad (\text{equation 6.1})$$

where: X = Actual values of $TL\chi$; X_0 = Value of $TL\chi$ before any form of heat treatment; X_N = Normalized $TL\chi$ value

6.3 FURNACE HEATING ON TAC OF LONG UNBURNT SOIL

This section presents the results obtained for stage 1 of this heating experiment investigating the TAC of furnace heated long-unburnt foot-slope samples. It firstly shows results for measurement of TAC for samples that have been heated recently. It then moves on to draw comparison with the TAC obtained when measurement was conducted after the application of a 10 Gy β dose to simulate heating *ca.* 10,000 years ago. Finally it presents the TAC obtained for 60 single grains from the FS soil sample furnace-heated to 50 °C and used as a proxy for a previously unheated sample.

6.3.1 TAC OF FURNACE HEATED LONG UNBURNT FOOT-SLOPE SAMPLE

6.3.1.1 *TAC of recently furnace heated sample*

Changes to TAC for the FS furnace heated sample during heating at 40 °C intervals between 160 and 700 °C are shown in Figure 6.4. Three main patterns can be identified for samples heated to temperatures of between (i) 50-400 °C; (ii) 500-600 °C; and (iii) 700-800 °C.

Furnace heating to temperatures of between 50 and 400 °C produced TAC with four phases of change between measurement temperatures of (i) 280-360 °C; (ii) 360-520 °C; (iii) 520-640 °C and (iv) 640-680 °C. Between measurement temperatures of (i) 280-360 °C, an increase in $TL\chi$ of approximately 1.2 times the initial value occurred; (ii) 360-560 °C, a slower increase in $TL\chi$ occurred; (iii) 520-640 °C, a rapid increase in $TL\chi$ occurred producing a peak in $TL\chi$ at 640 °C; and (iv) 640-680 °C produced a decline in $TL\chi$.

Furnace-heating to temperatures of between 500 and 600 °C produced virtually no increase in TAC until measurement temperatures were >560 °C. Between 560 and 640 °C $TL\chi$ increased. The greatest enhancement occurred following measurement temperatures of 640 °C (for the sample furnace heated to 500 °C) and 600 °C (for the sample furnace heated to 600 °C). Measurement temperatures greater than the aforementioned values produced a decline in $TL\chi$.

Furnace-heating to temperatures of between 700 and 800 °C showed a 2-stage pattern of enhancement: (i) a steady increase in $TL\chi$ occurred between measurement

temperatures of 320 and 600 °C producing a peak in enhancement of ~2.6 times initial values; and (ii) a decline in $TL\chi$ occurred following measurement temperatures of 640 °C.

6.3.1.2 TAC of samples with simulated early Holocene heating

The results obtained for the samples exposed to a 10 Gy β dose in order to simulate the effect of heating *ca.* 10,000 years ago and subsequent burial are shown in Figure 6.5. The main shape of the TAC plots for the different heat treatments remained similar for the undosed samples (Figure 6.4). However, a distinctive feature of the dosed samples is a rapid increase in $TL\chi$ following earlier measurement temperatures between 240-360 °C. This suggests that samples heated *ca.* 10,000 years ago are likely to produce an earlier step in TAC enhancement, potentially enabling both the temperature and timing of previous fire events to be established.

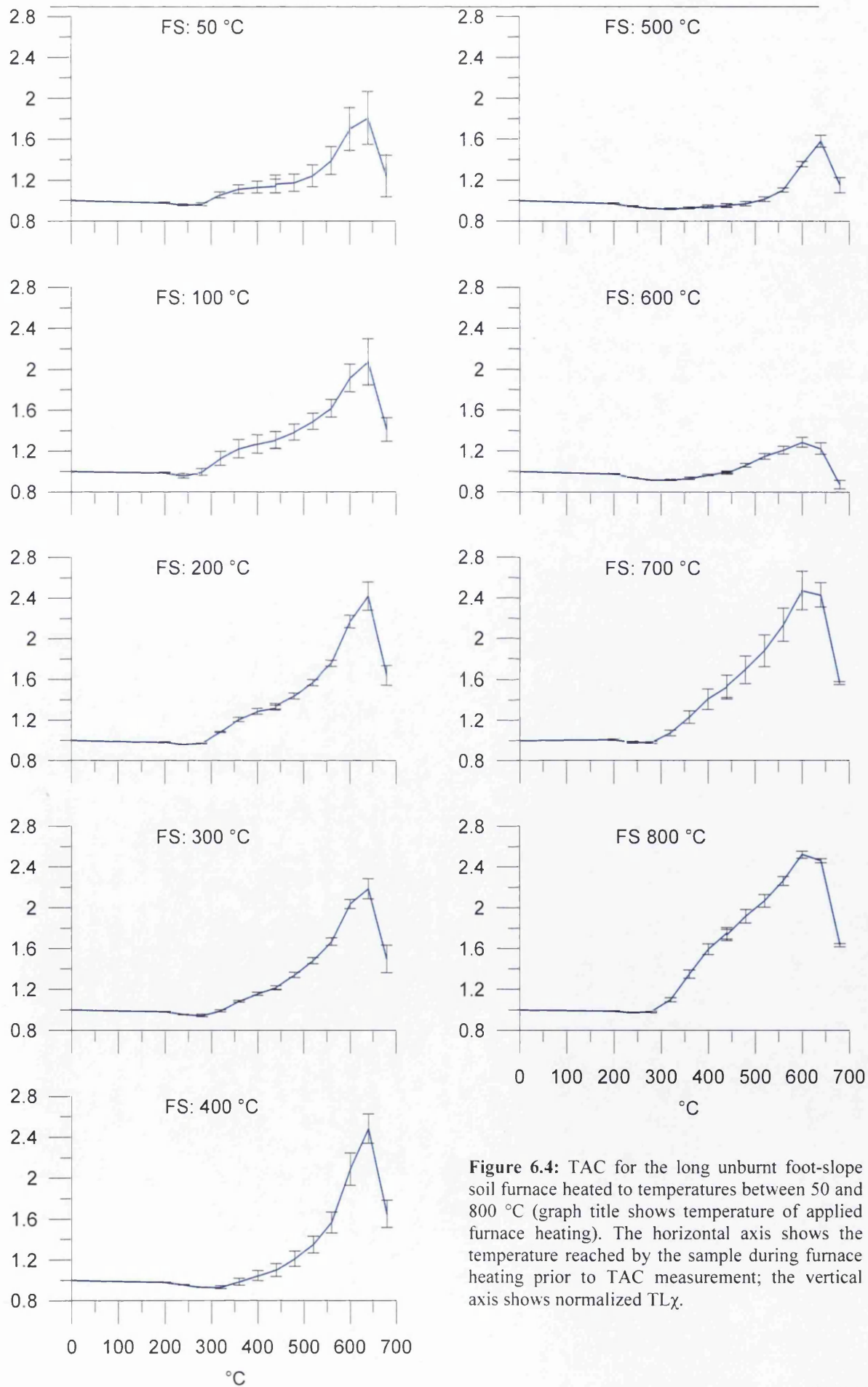


Figure 6.4: TAC for the long unburnt foot-slope soil furnace heated to temperatures between 50 and 800 °C (graph title shows temperature of applied furnace heating). The horizontal axis shows the temperature reached by the sample during furnace heating prior to TAC measurement; the vertical axis shows normalized TL χ .

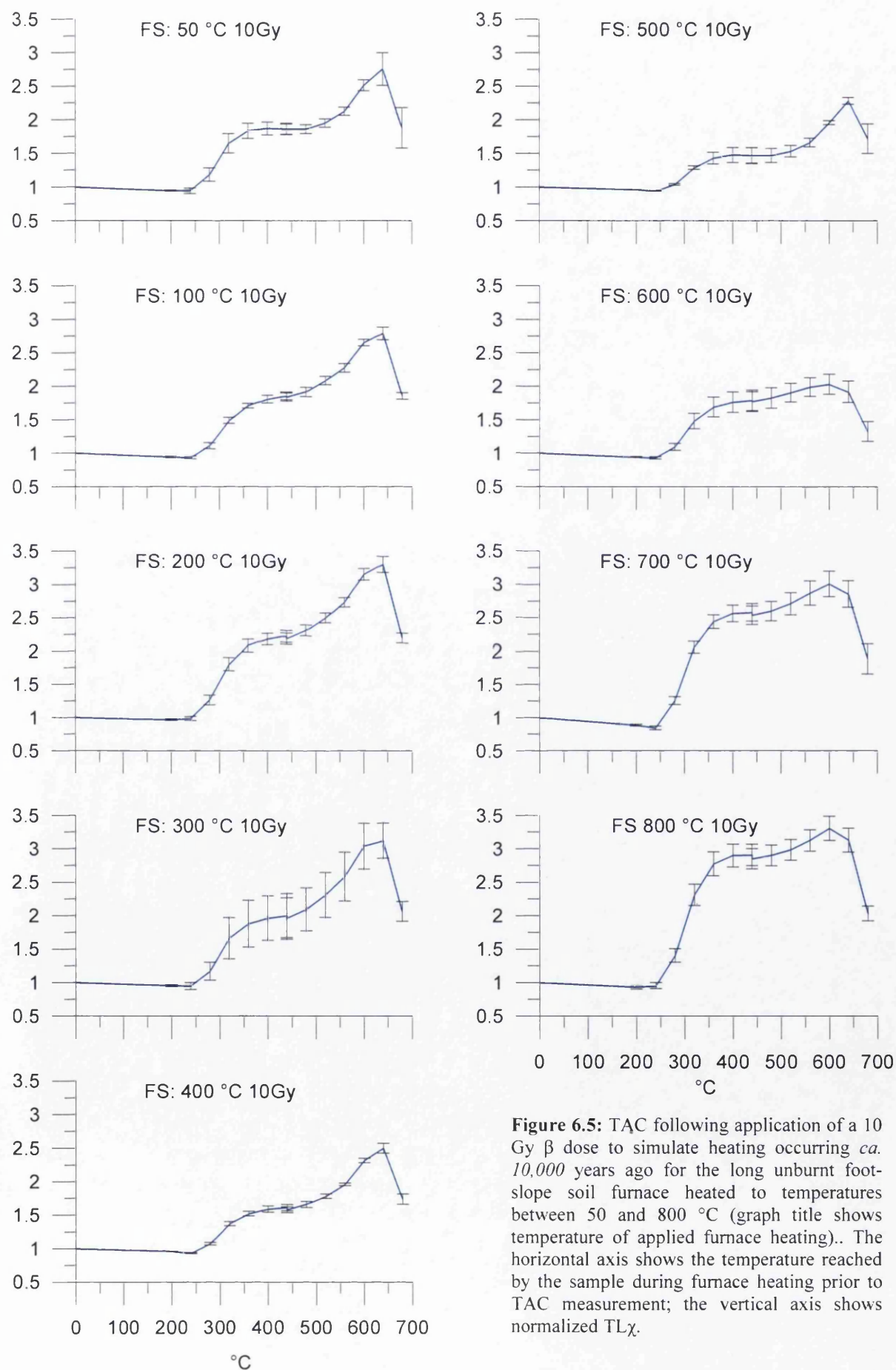


Figure 6.5: TAC following application of a 10 Gy β dose to simulate heating occurring *ca.* 10,000 years ago for the long unburnt foot-slope soil furnace heated to temperatures between 50 and 800 °C (graph title shows temperature of applied furnace heating).. The horizontal axis shows the temperature reached by the sample during furnace heating prior to TAC measurement; the vertical axis shows normalized TL χ .

6.3.2 SINGLE GRAIN ANALYSIS OF 'UNHEATED' SAMPLE

The findings from the investigation of the effects of furnace heating on mineral magnetic properties of the FS sample in Chapter 5 suggested that the samples were already enhanced from previous fires, although temperatures could not be ascertained due to the high thresholds required to produce change in χ_{lf} in these samples. The retention of a thermal memory could explain the low level of enhancement produced by the TAC of furnace-heated samples. This was investigated by assessing the variability of TAC within 60 single grains from the 50 °C sample used as a proxy for an 'unheated' sample.

Comparison of the shape of TAC of 60 single grains from the 'unheated' sample with the multi-grained aliquots of furnace-heated samples enabled inferences to be made about previous temperatures experienced by each individual grain and also about whether the sample had been heated recently or *ca.* 10,000 years ago. The majority of the grains did not show the distinctive sharp increase in $TL\chi$ following measurement temperatures between 240 and 360 °C, indicating that they had experienced recent heating.

The highest temperatures ever experienced by the 60 single grains from the 'unheated (50 °C) sample' were ascertained by simple visual comparison of the shapes of the TAC obtained for the single grains (Figure 6.6) with the shapes of the TAC obtained for the un-dosed and dosed furnace heated samples shown in Figures 6.4 and 6.5. An indication of the temperature allocated to each individual grain is shown by the value in the top left-hand corner of each plot in Figure 6.6. Figure 6.7 shows a histogram of the number of grains allocated to the different temperature thresholds suggested by the shapes of the TAC of the furnace-heated samples (Figures 6.4 and 6.5). This suggests that the majority of the samples had recently been heated to temperatures in excess of 400 °C, as could be expected following wildfire.

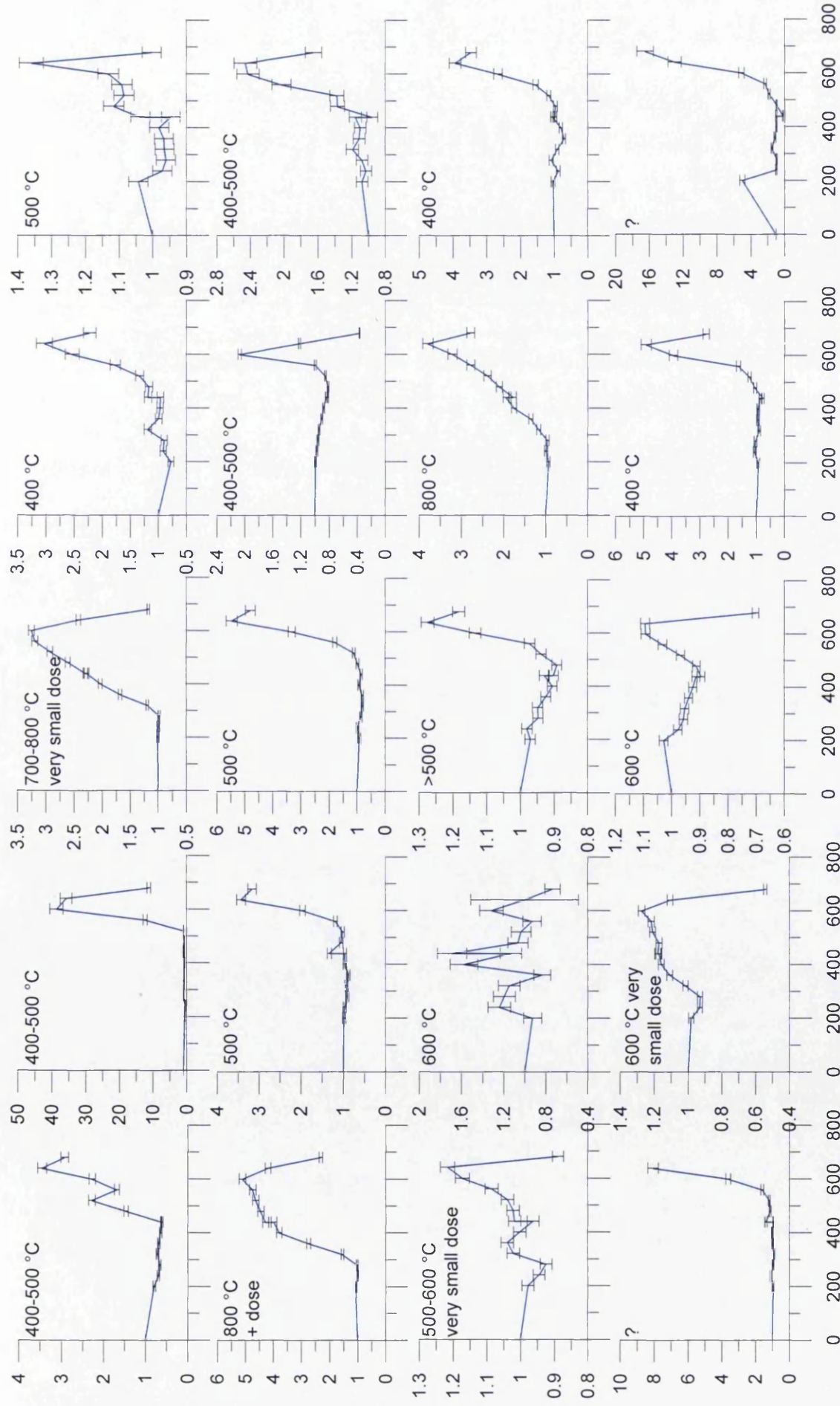


Figure 6.6a: Single grains (1-20) from the sample heated to 50 °C, used as a proxy for an unheated sample. Horizontal axis shows the temperature reached prior to TLX measurement; vertical axis shows normalized TLX. Value in the top left hand corner of each plot reflects maximum temperature previously experienced allocated by comparison of the shapes of TAC obtained for the furnace heated samples (Figures 6.5 and 6.6).

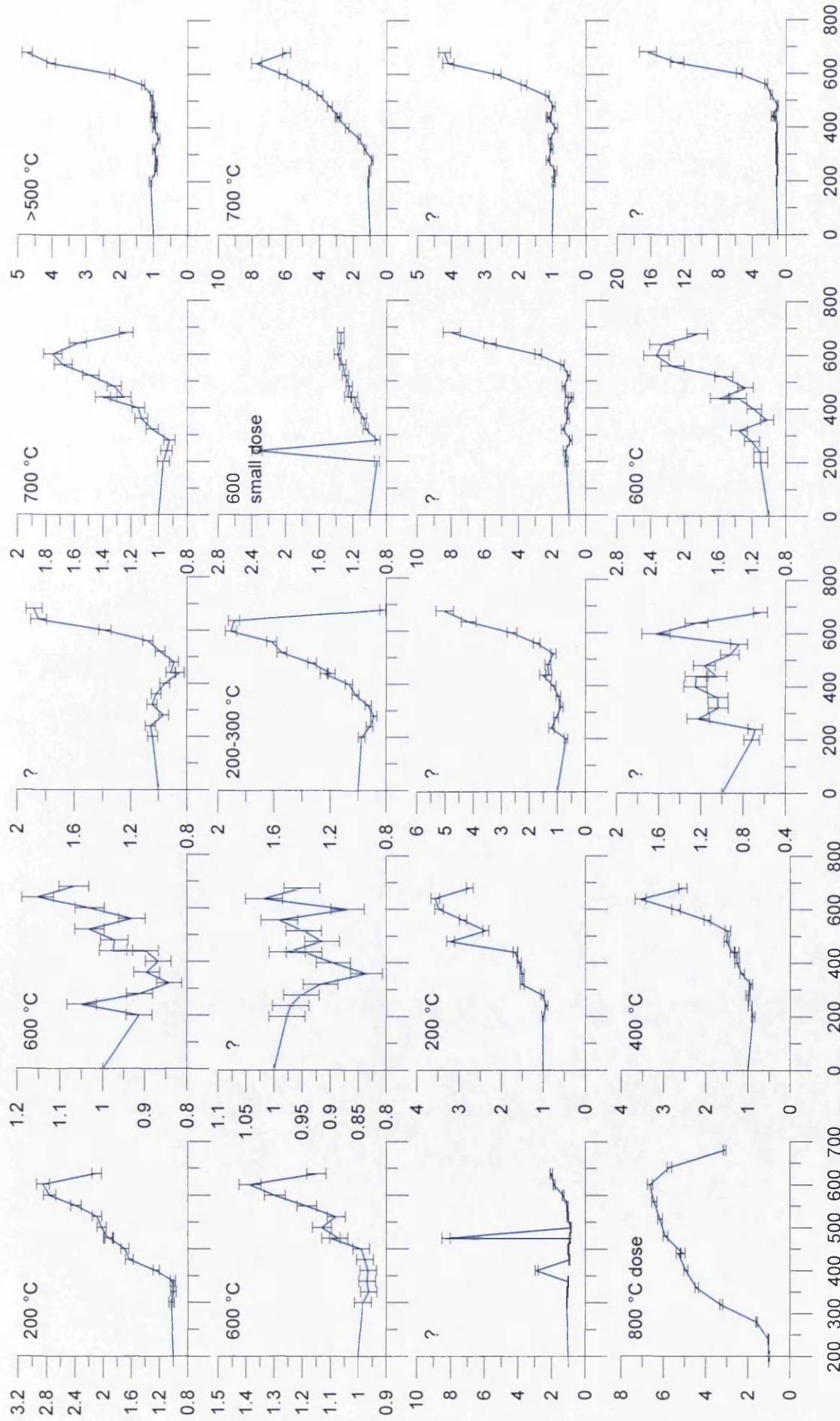


Figure 6.6b: Single grains (21-40) from the sample heated to 50 °C, used as a proxy for an unheated sample. Horizontal axis shows the temperature reached prior to TLx measurement; vertical axis shows normalized TLx. Value in the top left hand corner of each plot reflects maximum temperature previously experienced allocated by comparison of the shapes of TAC obtained for the furnace heated samples (Figures 6.5 and 6.6)

Figure 6.6c: Single grains (41–60) from the sample heated to 50 °C, used as a proxy for an unheated sample. Horizontal axis shows the temperature reached prior to TL χ measurement; vertical axis shows normalized TL χ . Value in the top left hand corner of each plot reflects maximum temperature previously experienced allocated by comparison of the shapes of TAC obtained for the furnace heated samples (Figures 6.5 and 6.6)

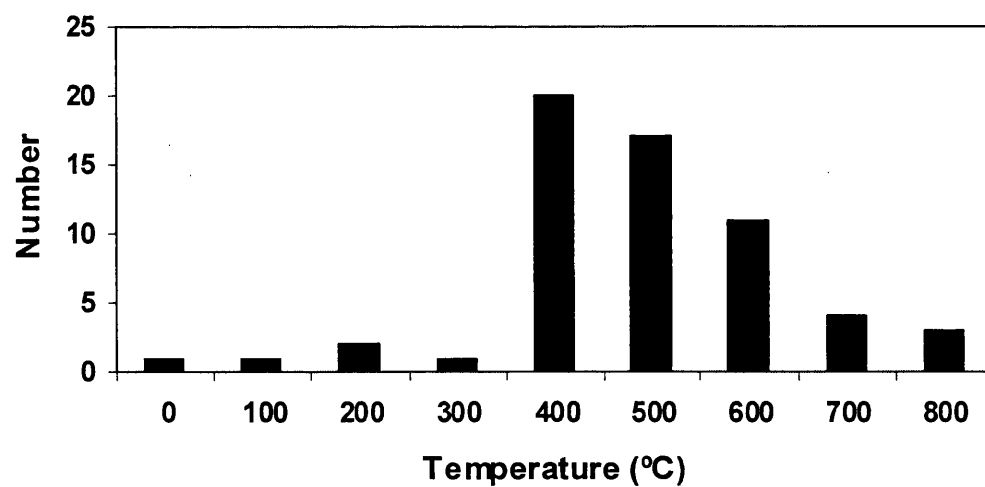


Figure 6.7: Histogram of the temperatures allocated to the 60 single grains from the 'unheated sample' that were suggested by comparison with the TAC plots produced for the various furnace heat treatments in Figure 6.6 and 6.7.

6.4 UN-HEATED AND FURNACE HEATED TAC OF SANDSTONE BEDROCK SAMPLE

This section presents the results obtained for stage 2 of this heating experiment, which deals with the TAC of an unexposed bedrock sample heated in a furnace to temperatures of between 50 and 800 °C. It firstly shows results for measurement of TAC for samples that have been heated recently. It then moves on to draw comparison with the TAC obtained when measurement was conducted after the application of a 10 Gy β dose (to simulate heating *ca.* 10,000 years ago and subsequent burial). Finally it presents the TAC obtained for 60 single grains from the unheated long-unburnt BR sample and 20 single grains that had been furnace-heated to temperatures of 600 °C to assess sub-sample variability.

6.4.1 TL χ OF THE 110°C PEAK

The 110 °C TL χ peak was used to establish the basis of the shape of TAC, as alterations after heating to progressive temperatures were used. The 110 °C TL χ peak obtained during the first measurement of TAC is shown in Figure 6.8. Furnace-heating to progressively increasing temperatures from unheated to 500 °C produced successively increasing values of enhancement for the 110 °C TL χ peak. Temperatures of between 600 and 800 °C produced a reduction in the 110 °C peak.

The increased sensitisation \leq 500 °C was caused by an increasing number of photons recombining with luminescence centres (Zimmerman 1971; Bailey 2001). The decrease in TL χ occurred following the temperature of 573 °C which was the inversion temperature from α to β quartz (Charitidis *et al.* 2000). This suggested that the level of enhancement of TL χ produced during measurement of the 110 °C TL peak could be used to detect whether previous temperatures \leq 400 °C had been experienced.

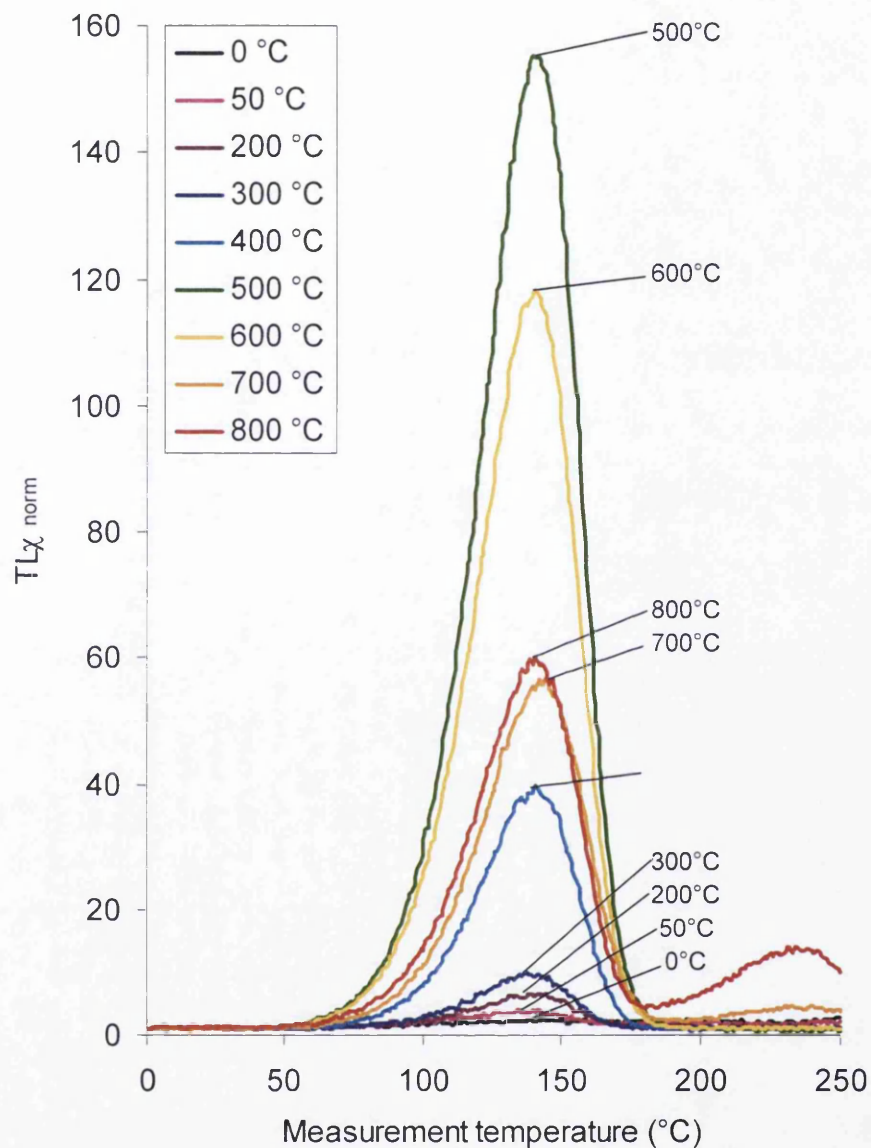


Figure 6.8: Effect of furnace heating of the unexposed BR sample on the 110 °C $TL\chi$ peak. (Values are normalized to the 1st measurement of each sample).

6.4.2 TAC OF FURNACE HEATED UNEXPOSED BEDROCK SAMPLE

6.4.2.1 TAC of a furnace heated unexposed bedrock sample

Figure 6.9 presents the TAC created for the unheated and furnace-heated bedrock samples. The various furnace-heat treatments produced 3 different shapes of TAC for: (i) samples heated to < 400 °C; (ii) the sample heated to 500 °C and (iii) samples heated to between 600 and 800 °C.

For the samples furnace heated between <50 – 400 °C, the TAC showed no increase in TL χ until measurement temperatures of 440 – 560 °C, which produced a peak at either 600 or 640 °C. The sample, furnace-heated to 500 °C produced a unique response showing only one stage of enhancement that occurred after measurement temperatures > 520 °C. Prior to this peak being reached, a slight decline in the TL χ is evident. The samples furnace heated to between 600 and 800 °C produced TAC with a uniform increase in TL χ following measurement temperatures of 280 °C. This enhancement was maintained until measurement temperatures of 600 °C were reached, before TL χ declined at ~ 640 °C.

Simple comparison of the shapes of the TAC would help to differentiate between samples experiencing temperatures ranging between 50 – 400 °C and 600 – 800 °C. However, it was not possible to obtain more detailed information about the heating temperatures previously experienced using this means of analysis owing to similarities between TAC shapes. Therefore, further investigation of the values obtained for the following TAC features was conducted involving: (i) raw number of counts that contributed to the 110 °C TL χ peak; (ii) the temperature at which TL χ began to increase; (iii) the temperature at which the change in rate of TL χ increase occurred; (iii) the temperature at which TL χ peaked; and (iv) the TL χ measured at 680 °C.

6.4.2.2 TAC of unexposed bedrock simulated to have been heated *ca.* 10,000 years ago

The TAC of the furnace heated unexposed BR samples that were created following exposure to a 10 Gy β dose to simulate the effect of heating *ca.* 10,000 years ago are shown in Figure 6.10. The TAC have a distinctive shape with three TL χ peaks. The first peak occurs between 200 and 300 °C; the main increase in TL χ reaches a maximum at a temperature of ~ 480 °C; a third peak is then apparent after measurement following heating to 640 °C.

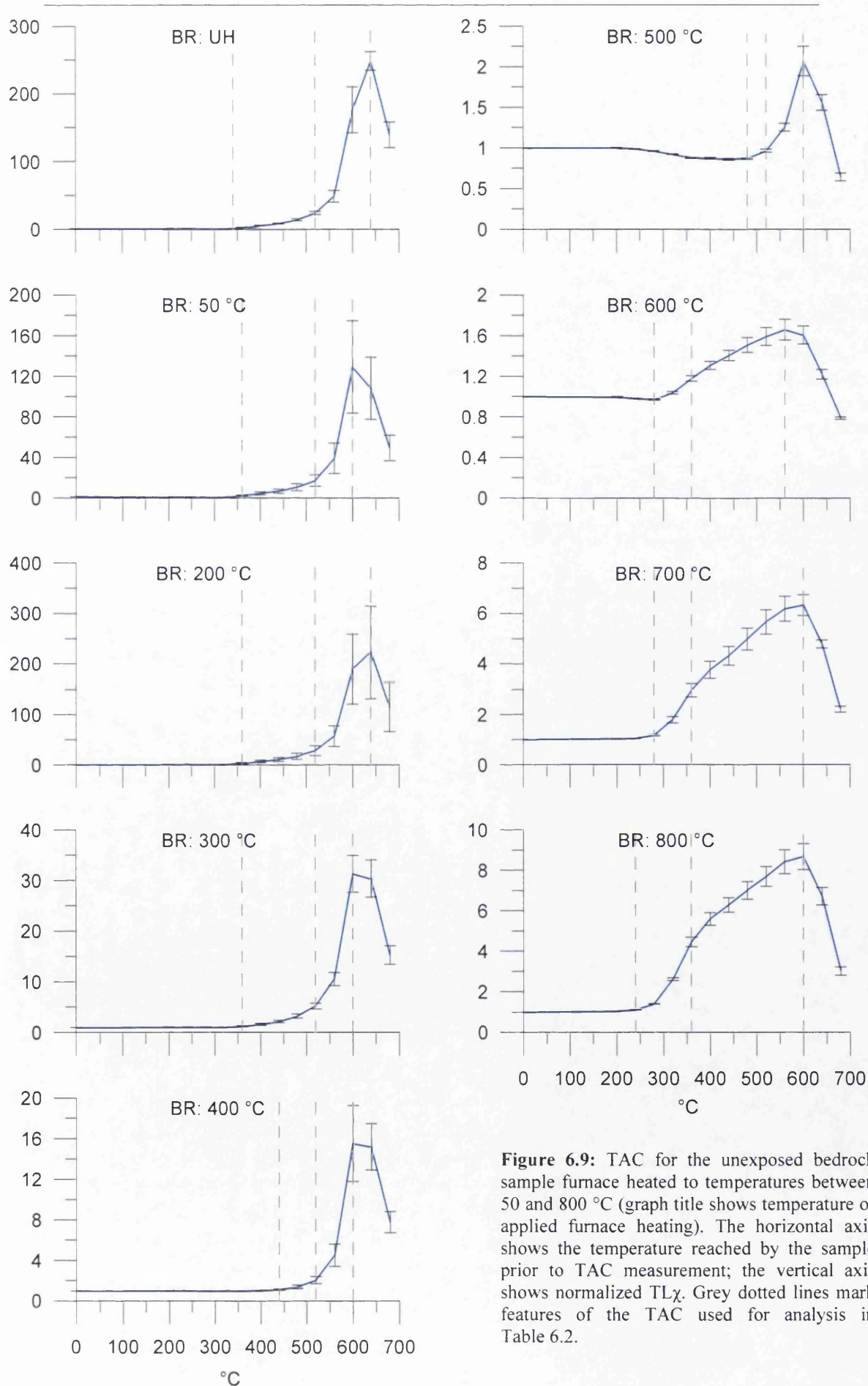


Figure 6.9: TAC for the unexposed bedrock sample furnace heated to temperatures between 50 and 800 °C (graph title shows temperature of applied furnace heating). The horizontal axis shows the temperature reached by the sample prior to TAC measurement; the vertical axis shows normalized TLχ. Grey dotted lines mark features of the TAC used for analysis in Table 6.2.

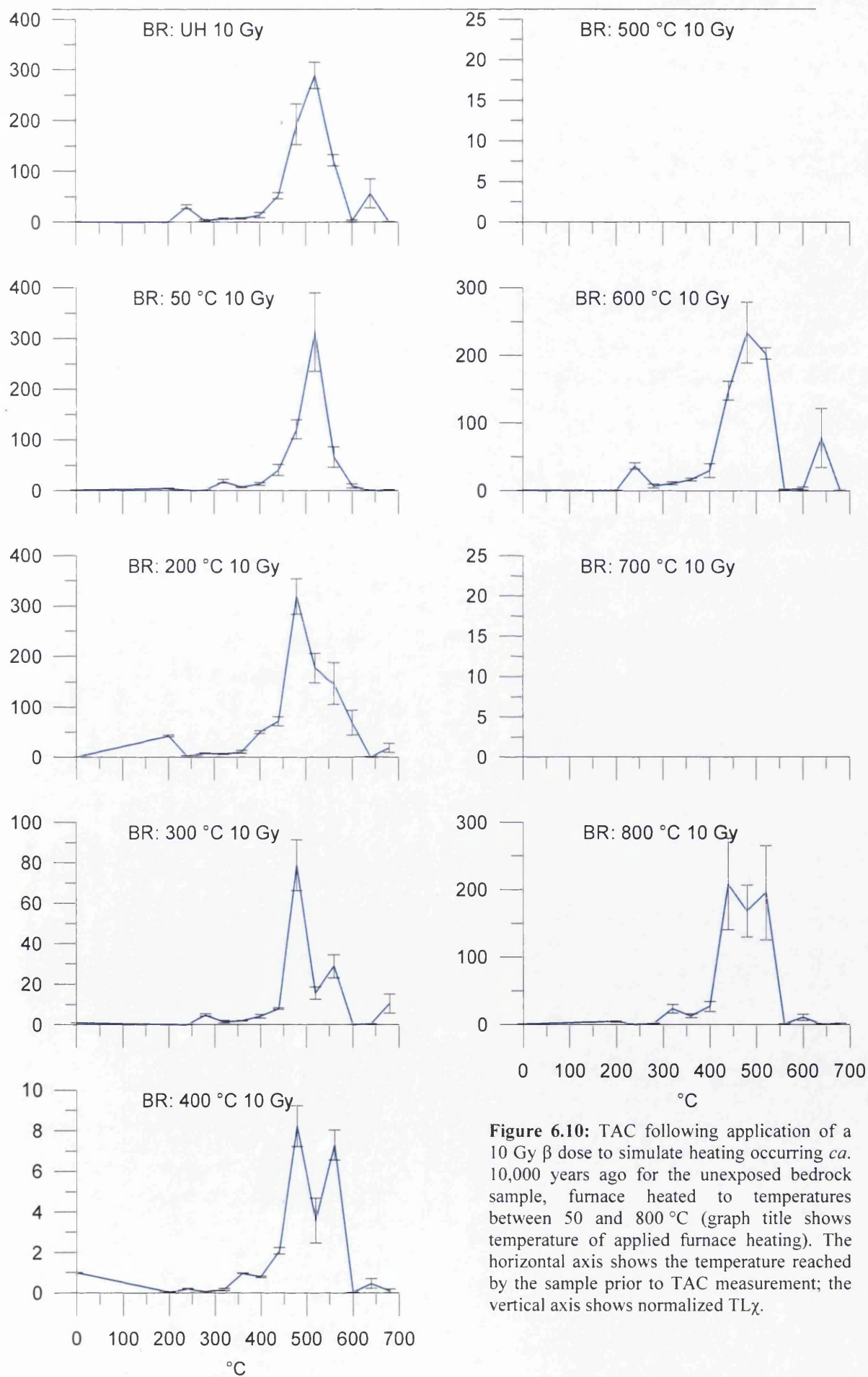


Figure 6.10: TAC following application of a 10 Gy β dose to simulate heating occurring *ca.* 10,000 years ago for the unexposed bedrock sample, furnace heated to temperatures between 50 and 800 °C (graph title shows temperature of applied furnace heating). The horizontal axis shows the temperature reached by the sample prior to TAC measurement; the vertical axis shows normalized TL χ .

6.4.3 SINGLE GRAIN ANALYSIS OF UNEXPOSED BEDROCK

TAC of the 60 single grains from the unexposed BR samples were investigated in order to ascertain whether the grains within the unheated furnace sample showed a high degree of variability or any sign of a retention of a thermal memory (Figure 6.11). Similarly shaped TAC plots were produced for the 60 samples. Generally, a gradual increase in $TL\chi$ to twice its starting value occurred between measurement temperatures of 200-520 °C. Between measurement temperatures of 560 and 640 °C there was a large enhancement of $TL\chi$ ranging between 1.4 and 3000 times the initial value. A decline in $TL\chi$ then occurred after measurement temperatures of either 640 or 680 °C to similar values experienced from heating to measurement temperatures of 520-560 °C. Although the actual value for initial $TL\chi$ varied considerably (2–8204 Counts per 20s integral) this is simply a function of the brightness of the individual grains and content of impurities. Generally, similar shapes of TAC plots were created, regardless of the initial starting sensitivity of the grains.

A comparison of the TAC plots of the 60 single-grain bedrock samples with those obtained for the Sheehys Creek FS soil sample, showed that the single-grain measurements from the former produced similarly shaped TAC, suggesting that the majority of the grains had been previously treated in a similar way thermally, whereas the single grains from the soil sample varied considerably, suggesting that the grains from the long-unburnt soil sample had been subjected to different heating histories.

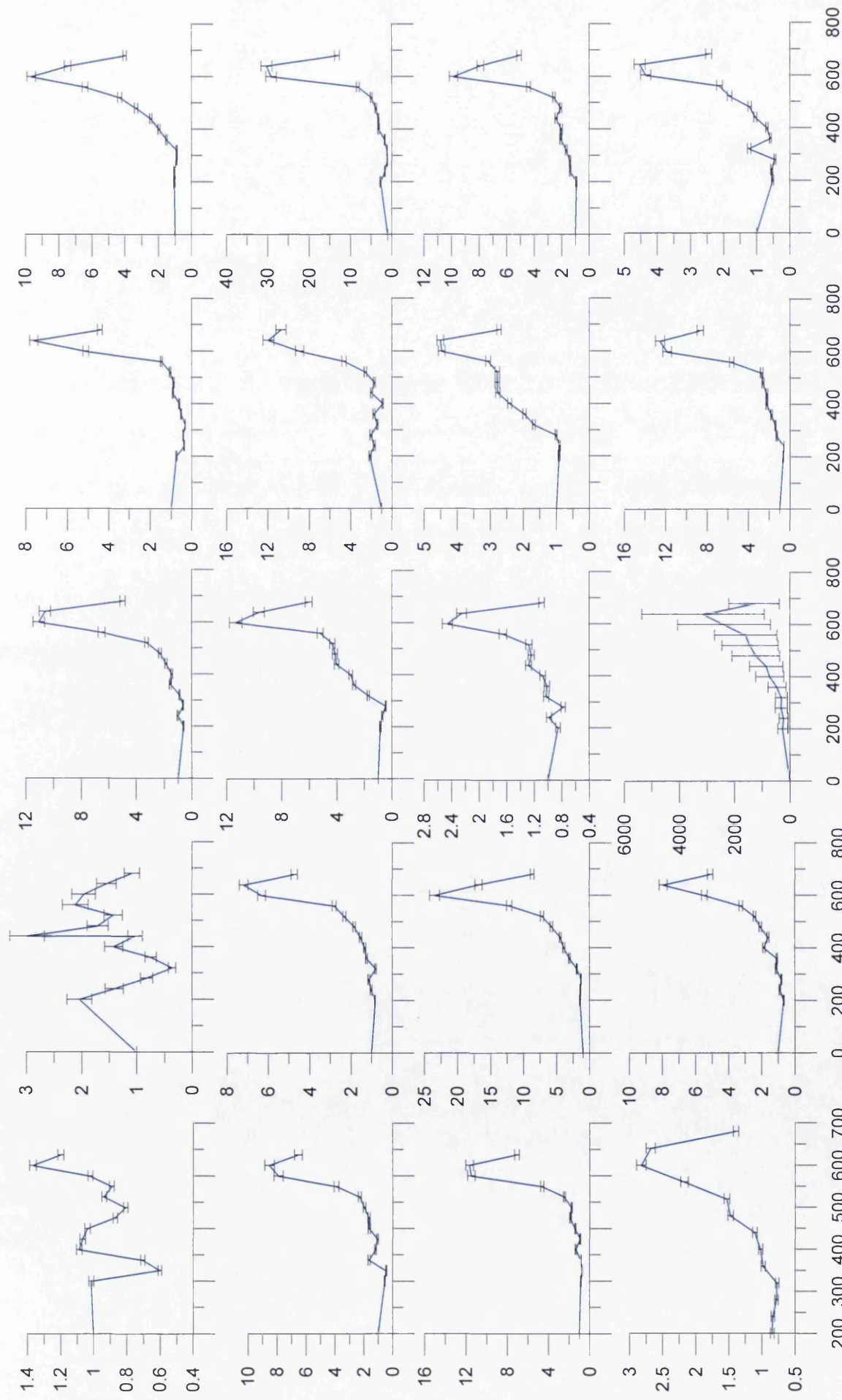


Figure 6.11a: Single grains 1-20 from the unexposed unheated bedrock sample. Horizontal axis shows the temperature reached prior to TL_x measurement; Vertical axis shows the Normalized TL_x. 219

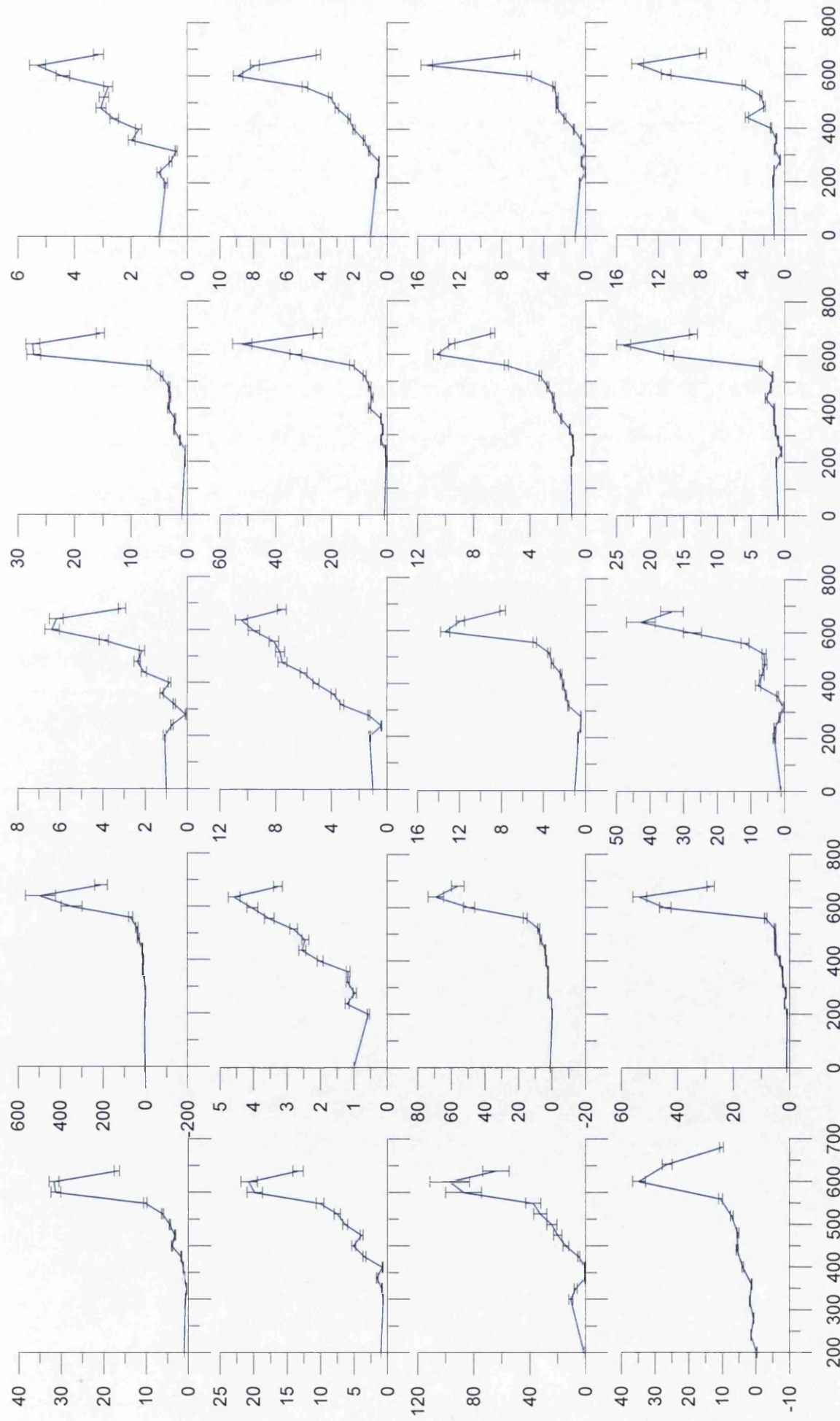
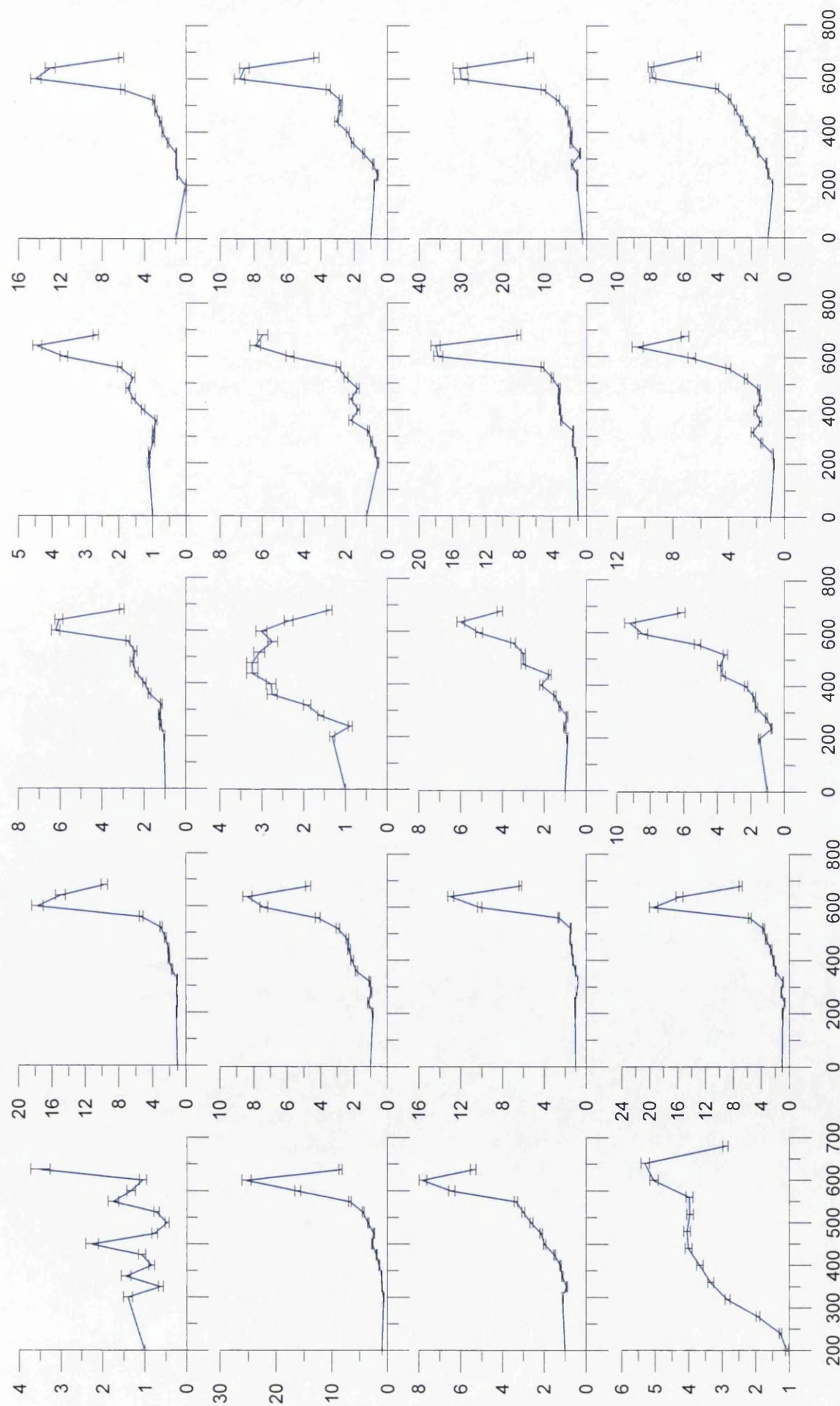


Figure 6.11b Single grains 21-40 from the unexposed unheated bedrock sample. Horizontal axis shows the temperature reached prior to TL_x measurement; Vertical axis 220 shows the Normalized TL_x.



6.4.4 SINGLE GRAIN ANALYSIS OF UNEXPOSED BEDROCK SAMPLE FURNACE HEATED TO 600 °C

To assess the variability in the response of individual grains to heating, TAC were created for 20 grains from the bedrock sample furnace heated to 600 °C for 40 minutes (Figure 6.12). These were then compared with the shape of the TAC obtained for the multi-grained aliquot furnace heated to 600 °C (Figure 6.9). Fifteen out of the twenty plots of single grains investigated showed similar shapes to the multi-grained aliquot. That 5 grains did not follow the pattern produced by the majority of grains heated to 600 °C could be due to the error of ± 10 °C during heating, or to slightly different compositions of these quartz crystals (Rakov *et al.* 1985).

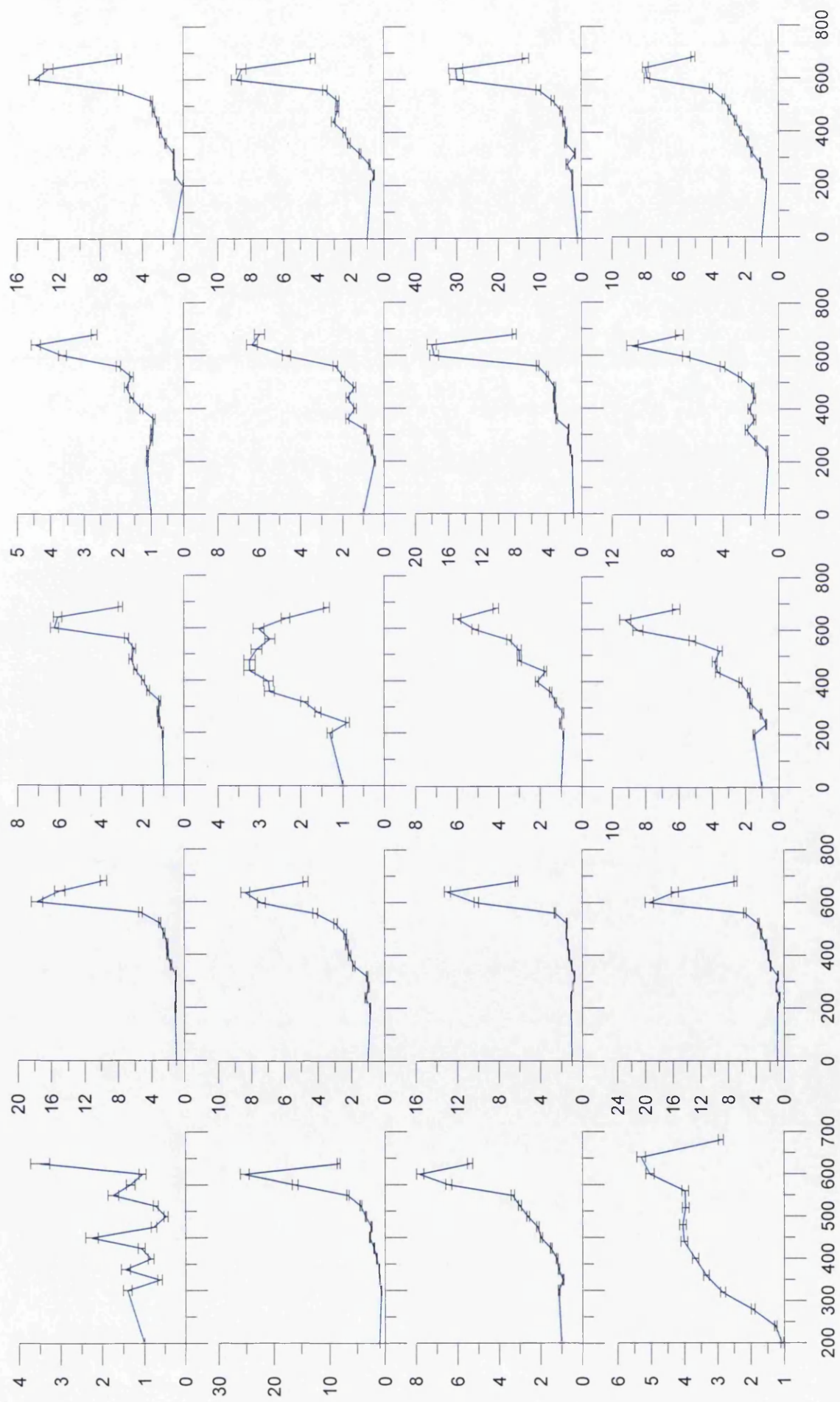


Figure 6.12: TAC for 20 single grains from the BR sample furnace heated to 600 °C Horizontal axis shows the temperature reached prior to TL χ measurement; Vertical axis shows the Normalized TL χ .

6.4.5 FEATURES OF TAC OF THE FURNACE HEATED BEDROCK (BR) SAMPLE

Owing to the subjective nature of visual comparison of the shape of the TAC, further investigations were conducted using features from of the TAC of the furnace heated BR samples. This involved identifying the (i) χ_0 , the raw number of counts contributing to the 110 °C TL χ peak; (ii) T_1 , the temperature at which TL χ begins to increase; (iii) T_2 , the temperature at which a change in the rate of activation occurs; (iv) T_3 , the temperature at which TL χ peaks; (v) χ_{2N} , the normalized TL χ values for (iii); (vi) χ_{3N} , the normalized TL χ values for iv; and (vii) χ_{FN} , the normalized measurement conducted at 680 °C. These features of the TAC are displayed in Table 6.2.

Table 6.2: Table of features identified by the TAC of the furnace heated BR sample.

| Furnace temperature (°C) | χ_0 | T_1 (°C) | T_2 (°C) | T_3 (°C) | χ_{2N} (unitless) | χ_{3N} (unitless) | χ_{FN} (unitless) |
|--------------------------------|----------|---------------|---------------|---------------|---------------------------|---------------------------|---------------------------|
| Unheated | 32036 | 340 | 520 | 640 | 24.2 | 14.0 | 18.9 |
| 50 | 11034 | 360 | 520 | 600 | 17.2 | 129.1 | 49.3 |
| 200 | 22923 | 360 | 520 | 640 | 28.7 | 223.0 | 115.3 |
| 300 | 33978 | 360 | 520 | 600 | 5.2 | 31.3 | 15.3 |
| 400 | 218414 | 440 | 520 | 600 | 2.0 | 15.5 | 7.8 |
| 500 | 1524099 | 480 | 520 | 600 | 1.0 | 2.1 | 0.6 |
| 600 | 1362222 | 280 | 360 | 560 | 1.2 | 1.7 | 0.8 |
| 700 | 377649 | 280 | 360 | 600 | 3.0 | 6.4 | 2.2 |
| 800 | 374605 | 240 | 360 | 600 | 4.5 | 8.7 | 3.0 |

The various features of the TAC identified in Table 6.2 have been plotted against the temperatures of the applied furnace heat treatments in Figure 6.13. None of the TAC features produced a linear response to heating, highlighting the need for comparison of various TAC features to confirm the temperatures previously experienced.

The effect of furnace heating on the raw value of TL χ (χ_0) is presented in Figure 6.13a. This reflects the area under the 110 °C TL χ peak and shows the same pattern demonstrated in Figure 6.8. However, it also emphasises that similar values may be obtained for unheated samples and those heated <300 °C. χ_2 , χ_3 , and χ_F produced

similar responses suggesting difficulty in distinguishing between heating temperatures $<300\text{ }^{\circ}\text{C}$. Attempts to resolve this problem were made by further investigation of features of the TAC by using bivariate plots (Figure 6.14).

A common and unexpected characteristic of the TAC features investigated in Figure 6.13 and all the bivariate plots (Figure 6.14) investigated was that heating to $200\text{ }^{\circ}\text{C}$ produced a change in the behaviour of $\text{TL}\chi$. This suggests that even heating to low temperatures created irreversible change in $\text{TL}\chi$ and showed that the heating required to stimulate measurement of $\text{TL}\chi$ actually produced a change in $\text{TL}\chi$ values. Furthermore, each of the bivariate plots showed evidence of a pattern of hysteresis, suggesting that pre-heating the sample to continuously increasing temperatures $>800\text{ }^{\circ}\text{C}$ could eventually cause the $\text{TL}\chi$ signal to be reset to values similar to those produced by the unheated sample.

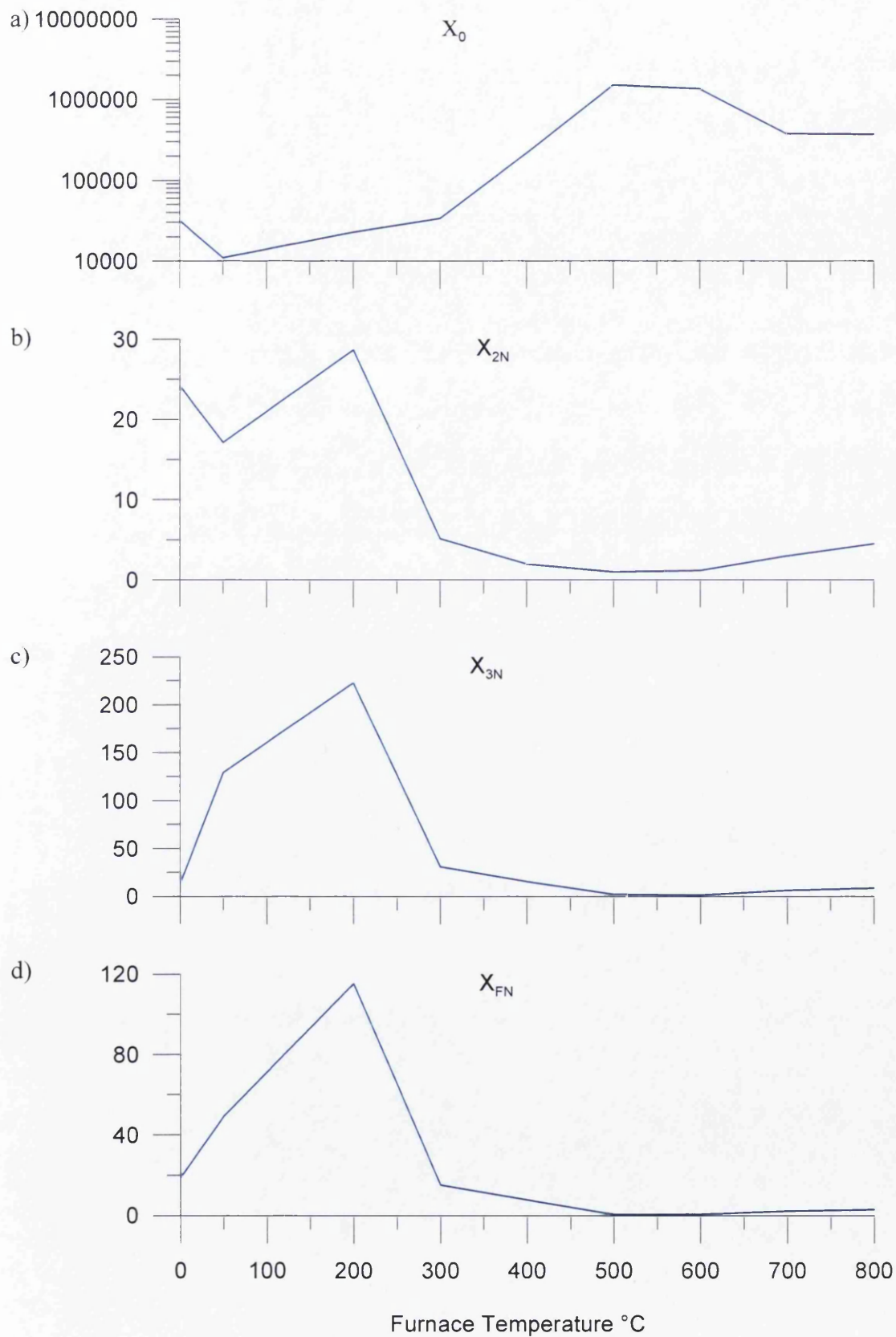


Figure 6.13: Features of the TAC including (a) χ_0 , (b) χ_{2N} , (c) χ_{3N} , and (d) χ_{FN} produced for the bedrock samples furnace heated to temperatures of 0-800 °C.

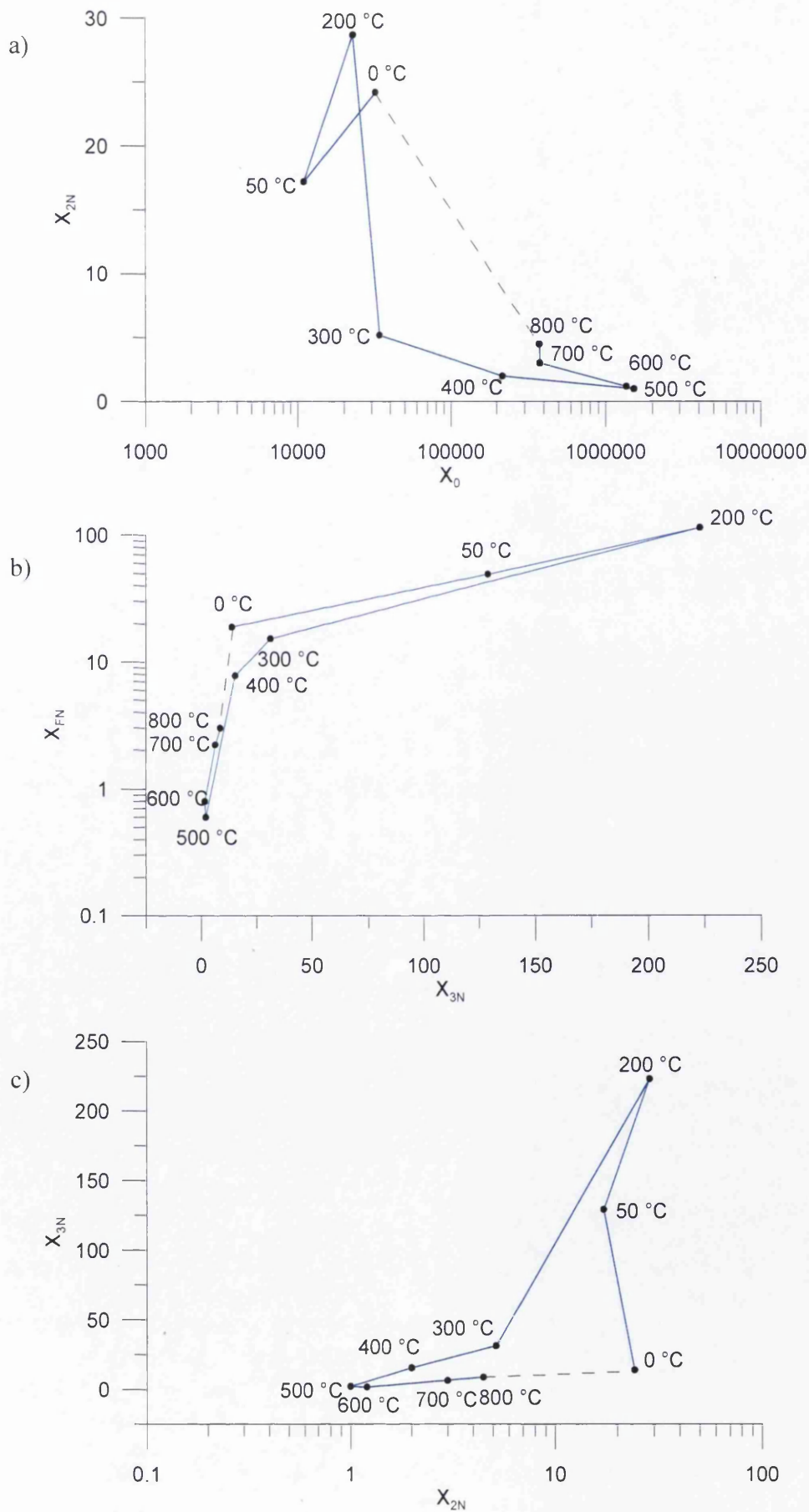


Figure 6.14: Bivariate plots of TAC features: (a) χ_{2N}/χ_0 ; (b) χ_{FN}/χ_{3N} ; and (c) χ_{3N}/χ_{2N} (Dotted lines represent a suggestion of the development of hysteretic behaviour).

In summary, investigation of the effects of furnace heating of samples to temperatures of between 50 and 800 °C on the 110 °C TL χ peak, TAC plot shape and features of the TAC produced by the BR samples have shown that:

- The initial TL χ reflected whether temperatures between 0-400 °C or ≥ 500 °C have previously experienced, with progressively increasing initial values apparent for increasing temperatures ranging between 0 and 400 °C.
- The higher the initial TL χ , the lower the level of peak enhancement.
- TAC plots could be used to distinguish between samples heated to < or > 400 °C.
- Features of TAC could be used for more detailed discrimination of previous temperatures experienced.
- Heating of the sample to <200 °C produced changes to TL χ properties, suggesting that heating during TL χ measurement (which is required to simulate photon emission) modifies results.

6.5 DISCUSSION

This section discusses key findings from the results of the heating experiment on TAC presented in this chapter. These include: (i) the 110 °C TL χ peak increasing with increasing temperature in the furnace to temperatures ≤ 400 °C, (ii) TAC shape and ratios of various TAC features can be used to infer the previous thermal history of individual grains in a soil assemblage, (iii) the shape of TAC can be used to infer the timing and temperature reached during previous heating, and (iv) heating an unexposed unheated bedrock sample to temperatures of < 50 °C produces a change in TL χ properties.

6.5.1 INCREASE IN 110 °C TL χ PEAK WITH FURNACE HEATING TO TEMPERATURES ≤ 400 °C

The heat-induced changes to the 110 °C TL χ peak on the unexposed unheated bedrock sample used in Stage 2 of this experiment (Figure 6.8) suggested that increasing heating temperatures enhanced the sensitivity of the 110 °C TL χ peak at temperatures of between 50 and 500 °C. Temperatures of > 500 °C caused the TL χ to decline. Although this is the first time that the 110 °C TL χ had been used to explore previous temperatures experienced by soil, it had previously been used to estimate firing temperatures of archaeological artefacts by exploration of geological samples, which have been summarised in Table 6.3.

Table 6.3: Summary of the successful use of TL glow curves to detect previous heat treatments.

| Reference | Material | Temperatures identifiable (°C) | Potential to determine previous temperature (°C) |
|------------------------------------|---------------------|-----------------------------------|--|
| (David and Sunta 1981) | Quartz | 500-1200 \pm 50 | Yes |
| (Watson and Aitken 1985) | 5 samples of Quartz | 500-1000 (for 1/5 quartz samples) | No |
| (Chen <i>et al.</i> 1988) | Quartz | 0-950 | Yes |
| (Koul <i>et al.</i> 1996) | Quartz | Past temperature unidentifiable | No |
| (Charitidis <i>et al.</i> 2000) | Quartz | < 500 , 600-900 | Yes |
| (Melcher and Zimmerman 1977) | Chert | $\geq \sim 250$ | Yes |
| (Godfrey-Smith <i>et al.</i> 2005) | Chert | 0, 300, 400, 600 | Yes |
| (Göksu <i>et al.</i> 1989) | Flint | 300-700 | Yes |
| This study | Quartz | 0 – 400, > 400 | Yes |

The results from the present study have found slightly different results regarding the different applications of the 110 °C peak or features of it. Direct comparison with the results shown by Göksu *et al.* (1989) has been possible. The present study showed a uniform increase in TL χ until temperatures of ≤ 400 °C were reached, whereas Göksu *et al.* (1989) found a uniform increase in TL χ increase between 300 and 700 °C. These differences were likely to be caused as a result of the different materials used in the two investigations. Features of the 110 °C TL χ peak have been successfully used in the majority of studies summarised in Table 6.3. The application of these findings to the present study supports the use of TAC to provide further justification about maximum temperatures that have previously been experienced. In general, it has not been possible to make direct comparisons with other studies that have investigated temperature thresholds of quartz by using various ratios because different methods have been used. However, the results presented here do support Watson and Aitken's (1985) suggestion that the 110 °C TL χ peak of quartz could not be used to identify previous heating to temperatures of >500 °C. The variety of findings from the different studies may be related to the different impurities within the quartz structures of the samples used.

6.5.2 USE OF TAC CURVES TO DISTINGUISH BETWEEN SOIL HEATED TO (I) <400 °C; (II) 400-500 °C; AND (III) 600-800 °C.

Investigation of the heat-induced changes to the shape of the TAC showed that simple visual comparison could indicate the thermal history of a sample.

The use of the shape of TAC to establish previous thermal heating has been investigated in a number of archaeological studies. Yang and McKeever (1990) found that differently shaped TAC were produced for samples that had been unheated and heated to 450 and 950 °C. Godfrey-Smith *et al.* (2005) found differently shaped TAC were produced for samples heated to 400 and 600 °C.

Lahaye *et al.* (in press) conducted a similar investigation to that used in the present study by using a bedrock sample of quartz. The general shape of TAC with increasing furnace temperature was different from those obtained in this study. Lahaye *et al.* (in press) found progressively higher activation temperatures with increasing oven annealing until temperatures of 600 °C, with the sample heated to 800 °C producing activation at ~ 550 °C. The present study found that heating to

<400 °C produced activation at ~350 °C, furnace heating to 400 and 500 °C produced activation at ~450-500 °C, and furnace heating to 600-800 °C produced activation <~300 °C. The differences in TAC and response to heating may have been as a result of a different distribution of activation energies of the R-traps within the two different samples (Aitken 1985) before and after heating to 573 °C when inversion from α to β quartz occurred (Charitidis *et al.* 2000).

The implications of the lack of change of shape of TAC at temperatures <400 °C for the present study are similar to those found for the mineral magnetics, to the extent that temperatures <400 °C are associated with severe fires, and therefore the actual shape of the TAC curve could only be used to distinguish between fires heating the soil to: (i) <400 °C; (ii) 400-500 °C; or (iii) 600-800 °C.

In general, the differences between findings from the present study and that of Lahaye *et al.* (in press) suggests that different quartz samples could produce varying responses despite identical heat treatments. This emphasises that site-specific investigations are required for a thermal history to be established. Based on the high temperature thresholds required to modify the TAC shapes found in the present study, it is suggested that the shapes of the TAC observed here could also be usefully applied in determining historical manufacturing techniques of prehistoric tools and the locations of kilns.

6.5.3 USE OF TAC IN DETERMINING TEMPERATURES REACHED IN SOIL.

Various features of the shape of the TAC for the furnace-heated samples (Figure 6.13) proved to be more useful in suggesting heating to relatively low rather than high temperatures. The normalized values of χ_{2N} , χ_{3N} and χ_{FN} of each furnace heat treatment produced a curve that showed a rapid decrease for furnace-heating between 200 and 600 °C, which is similar to the normalized values of furnace-heated TAC reported by Yang and McKeever (1990). Furnace-heating to temperatures > 600 °C began to produce a gradual increase in maximum enhancement of $TL\chi$.

Despite different responses in the shapes of TAC found for the present study and that of Lahaye *et al.* (in press), similarly-shaped curves were produced for the maximum $TL\chi$. However, Lahaye *et al.* (in press) did not investigate the effect of furnace-heating to temperatures of $<300\text{ }^{\circ}\text{C}$. The present study found that the unheated and $50\text{ }^{\circ}\text{C}$ samples did not fit the curve produced by samples heated between temperatures of $200\text{--}800\text{ }^{\circ}\text{C}$, and that a peak in $TL\chi_{\text{MAX}}$ is created between 50 and $200\text{ }^{\circ}\text{C}$. Further investigation of ratios of the features of TAC by bivariate plots (Figure 6.14) suggested that heating the samples to $800\text{ }^{\circ}\text{C}$ (and potentially also higher temperatures) began to produce a hysteresis curve, causing the $TL\chi$ to revert back to similar values produced by the unheated sample.

These findings suggested that for the study area, where Hawkesbury sandstone dominated, the curve of $TL\chi_{\text{MAX}}$ could be used to identify material that has been heated to either $<200\text{ }^{\circ}\text{C}$ or to between $200\text{--}500\text{ }^{\circ}\text{C}$. Confirmation of whether temperatures of $<$ or $> 200\text{ }^{\circ}\text{C}$ have been experienced could be achieved by consulting bivariate plots of features obtained from TAC (as explored in Chapter 8 for burnt material contained within a sediment core). If it is possible to use TAC to detect where fires have heated the ground to $<200\text{ }^{\circ}\text{C}$, this technique could be very useful in detecting low and moderate severity fires that are typical for many fire-prone environments. However, similarly to the magnetism results, one of the limitations of application of this technique in such a fire-prone environment has been that enhanced TAC are likely to be retained by soil samples, and so this technique could only provide an indication of the hottest fires experienced and not the temperature reached in the most recent fire.

Broadening the investigation to ascertain whether or not different temperature thresholds would be required to modify the shape of TAC for Narrabeen sandstone (which is also present in the catchment) would provide a more comprehensive understanding of the maximum temperatures experienced by individual grains of soil samples within the study area catchment.

In the wider context, these findings could be applied in studies where long sedimentary records are available to suggest how fire severity has varied throughout geological timescales. This could also be used to aid in reconstructing climates as

fire severity is a function of a number of climate-related factors shown in Figure 2.3 including fuel load and moisture content. This technique could also have applications in archaeology, and could also be used to help distinguish between campfire and kiln sites due to the different temperatures associated with these two commonly investigated archaeological features.

The findings reported here have also identified a potential problem with the TL χ measurement procedure, as it demonstrated that changes to TL χ occurred with heating to temperatures as low as 50 °C. Heating to 160 °C was required for stimulation of electron emission and recombination within luminescence centres necessary for the emission of light to enable TL χ measurement to be carried out. This suggested that the actual measurement procedure itself changed the properties of the sample, this could be overcome with use of OSL measurements. Further investigation of the effect of heating to temperatures <200 °C could ascertain whether or not TAC could provide a powerful tool in determining previous fire temperatures experienced during low severity fires.

6.5.4 TAC CAN BE USED TO SUGGEST THE TIMING OF PREVIOUS HEATING.

TL dating described by Figure 2.5 (Feathers 2003) has been a well established technique used to date soils and sediments from different environmental situations. For example, in New South Wales, Bryant *et al.* (1994) dated aeolian sand dunes and Nott *et al.* (1994) investigated their reworking; Nanson *et al.* (1995) produced dates for a dune field in the West Simpson desert. The influence of pre-heating on dating has been investigated by Yang and McKeever (1990), Wintle and Murray (1999) and Roque *et al.* (2004), who identified differences between TL χ responses following various heat treatments, and highlighted concerns regarding partial zeroing of TL χ . Chen *et al.* (1988) and Charitidis *et al.* (2000) identified that higher heating temperatures prior to measurement produced a reduction of superlinearity of the increase in TL χ with time (simulated by increasing the pre-dose). This was explained by partial removal of competing traps. These findings have supported the uniquely-shaped TAC obtained for the dosed samples in this study (Figures 6.5 and 6.10).

Differently-shaped TAC were produced for the radiation dosed and undosed unheated and furnace heated BR samples, suggesting that TAC shape could be used to distinguish between samples heated recently and *ca.* 10,000 years ago. The TAC shape for the dosed FS samples showed an earlier step at 200 °C. This is similar to changes to the shape of TAC of samples that had been preheated to 900 °C, as examined by Kitis *et al.* (in press). However, the erratically-shaped curves for TAC that were produced for the BR sample have not been found in other studies.

The dosed samples produced :(i) an earlier peak and desensitisation at $>\sim 500$ °C; and (ii) a reduction of $TL\chi$ at 680 °C to initial values. These features were not demonstrated by any of the undosed samples. This suggested that it was easy to distinguish between recently burnt samples and those burnt once *ca.* 10,000 years ago. The different TAC created for the FS sample that had experienced multiple burns and the BR sample that had never been heated suggested that there is potential to use the shape of the TAC following application of a pre-dose to identify timing of previous heating events for both environmental and archaeological purposes as well as distinguishing between samples that had experienced single burn and multiple burns events. This could prove a powerful indicator of the reliability of dates obtained for thermally-enhanced samples owing to its ability to identify the possibility of partial re-zeroing effects that may occur during secondary heating events at lower temperatures.

6.6 CHAPTER SUMMARY

In this chapter, the temperature thresholds required to modify the shape of TAC in order to establish the timing and maximum temperature experienced by grains within a soil assemblage have been explored. Some aspects, such as features of TAC using bivariate plots and investigation of changes following heating $< 200\text{ }^{\circ}\text{C}$ have been examined here for the first time and the results should be viewed as tentative. The key findings from this can be summarised as follows:

In stage 3 of the experiment using a long unburnt foot-slope sample:

- The temperature thresholds required to produce modification of the long-unburnt FS sample were: (i) $\leq 400\text{ }^{\circ}\text{C}$; (ii) $500\text{--}600\text{ }^{\circ}\text{C}$; or (iii) $700\text{--}800\text{ }^{\circ}\text{C}$. The lack of difference between TAC plots at temperatures of $< 400\text{ }^{\circ}\text{C}$ relate to the previous thermal histories of grains within the soil assemblage.
- The highest temperatures ever experienced by the soil grains could be established by simple comparison of the shape of TAC plots.
- The shape of the TAC plots of soil samples that had undergone simulated heating *ca.* 10,000 years ago produced an earlier rise in activation at $\sim 200\text{ }^{\circ}\text{C}$.

In stage 4 of the experiment using an unexposed sample of bedrock:

- Temperature thresholds required to produce modification of the $110\text{ }^{\circ}\text{C}$ TL_{χ} peak of previously unheated samples showed a uniform increase in TL_{χ} until temperatures $\leq 400\text{ }^{\circ}\text{C}$. The fact that the TL_{χ} increase $> 400\text{ }^{\circ}\text{C}$ was not uniform suggested that successful application of this parameter in identifying fires heating the ground to temperatures $\leq 400\text{ }^{\circ}\text{C}$ would be possible.
- Temperature thresholds required to produce modification of the shape of the TAC plots are: (i) $\leq 400\text{ }^{\circ}\text{C}$; (ii) $500\text{ }^{\circ}\text{C}$; and (iii) $600\text{--}800\text{ }^{\circ}\text{C}$.
- The maximum TL_{χ} values produced by the TAC showed a linear decrease for samples heated to between 200 and $600\text{ }^{\circ}\text{C}$, indicating potential use of this parameter in detecting heating of samples to these temperatures.
- Application of a $10\text{ Gy } \beta$ dose to samples prior to TAC measurement could distinguish between samples heated: (i) recently; (ii) 10,000 years ago; (iii) once; and (iv) on multiple occasions.
- Heating to only $50\text{ }^{\circ}\text{C}$ produces changes to the shape of the TAC plots. This suggests that modification of TL_{χ} properties may occur during measurement of the $110\text{ }^{\circ}\text{C}$ TL_{χ} peak.

The key findings from this chapter highlight the potential use of TAC plots in ascertaining the maximum temperatures previously experienced in sediments. Limitations of using this technique relate to the retention of a thermal memory, and identifying only the hottest temperatures experienced rather than the heating experienced in the most recent fire event. Multiple heating events are likely to occur where localized redistribution of burnt material occurs on the slopes as documented in the Nattai area following the 2001 fires by Shakesby *et al.* (2003). However, if substantial post-fire erosion occurs and the burnt material is transported directly to a lake or reservoir environment, the chronological deposition of this material could provide a very powerful tool in ascertaining how fire severity has varied during different fire events.

Directions for future research include: (i) further investigation of modification of TL χ occurring <200 °C; (ii) investigation of responses of TAC for other types of geological samples; (iii) the application of TAC shape to investigate heating by samples contained in sedimentary sequences to ascertain temperature experienced in the past (explored in Chapter 7) (iv) investigation of OSL to suggest a samples thermal history due to its dependence of light to release luminescence for measurement.

7 EVIDENCE FOR WILDFIRE TIMING AND POST-FIRE EROSION: SEDIMENT CORES FROM LAKE BURRAGORANG

7.1 INTRODUCTION

This chapter presents the methods and results of the analysis of seven closely-spaced sediment cores from the Nattai arm of Lake Burragorang Reservoir. The cores were selected to fulfil two main aims: firstly, to identify the potential of using different techniques to recognise burnt material in sediment cores and secondly, to ascertain the reliability of obtaining sediment cores from a dynamic reservoir environment in order to make inferences about catchment fire history. The research questions used to address these main aims are presented in Figure 7.1.

The sediment cores were obtained in February 2003 when the preliminary results for mineral magnetic and TAC heating experiments had been established. Analysis of the sediment cores (described in this chapter) was conducted following analysis of the results from Chapters 5 and 6. The present chapter attempts to consider the findings from the previous chapters and establish if: (i) mineral magnetic measurements could be used effectively in recognising burnt material within sediment cores despite the rather negative conclusions arising from Chapter 5 (research question 14); (ii) fire severity of samples from different depths of burnt material within a core could be ascertained (research question 15); and (iii) fire history contained within the sediments from closely spaced sediment cores could provide a reliable record of burn events within the catchment (research questions 16 and 17). To implement these research questions, a variety of measurements were taken of the sediments in the cores including: visual description, TC and mineral magnetics (research question 14); TAC (research question 15); dating (research question 16) and ancillary data (research question 17).

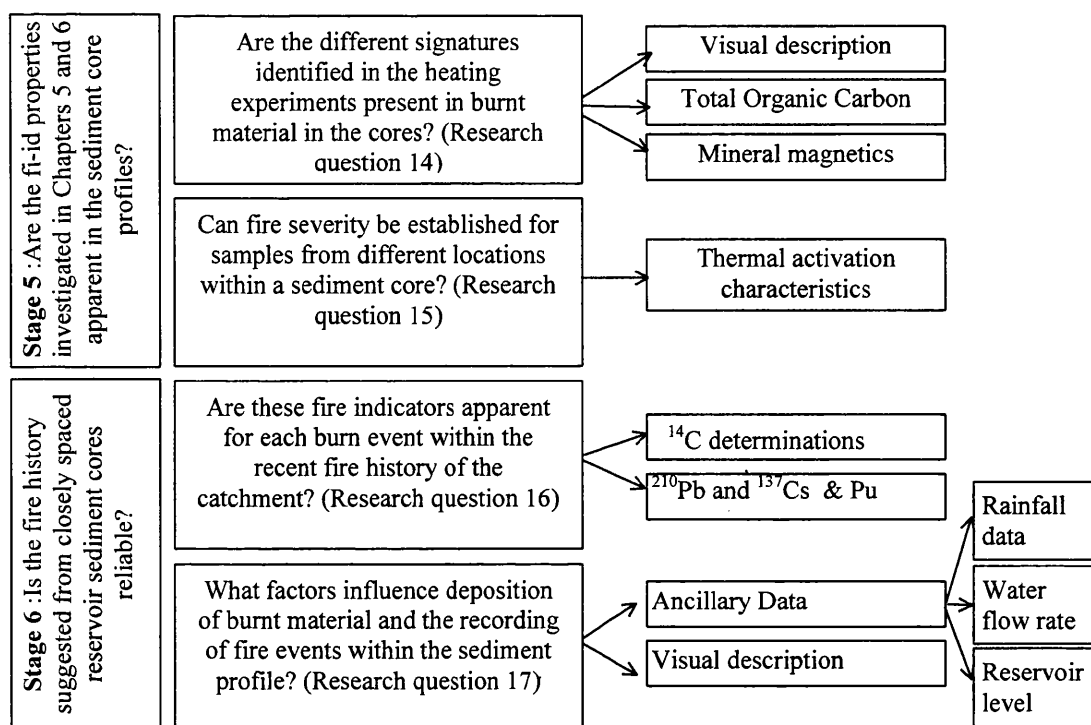


Figure 7.1: Summary of research questions addressed and techniques applied to investigate fire history from the seven closely-spaced sediment cores obtained from two locations in the Nattai arm of Lake Burragorang reservoir.

Although the findings described in Chapter 5 suggested that high temperatures were required to provide enhancement of mineral magnetic properties of soil, mineral magnetic measurements have been commonly used as a tool in detecting burnt material within sediment cores (Rummery 1983; Gedye *et al.* 2000; Blake *et al.* 2004). In Chapter 5, the use of enhanced mineral magnetic parameters to suggest fire events was found to be problematic due to the already enhanced background signature derived from the area experiencing many fire events in the past, causing enhancement of mineral magnetic properties at temperatures > 500 °C. Such temperatures are rarely reached in soils during natural burning of native Australian vegetation (Luke and McArthur 1978). The findings from Chapter 6 have shown that the shape and features of TAC could be used to suggest maximum previous soil temperatures experienced during fire events. TAC have been previously used to suggest temperatures experienced by archaeological artefacts (Göksu *et al.* 1989; Godfrey-Smith *et al.* 2005), but this is the first time that this technique has been applied to the understanding of the thermal history of soil and sediment.

Visual description of the sediment cores was conducted by classifying the sediments according to macroscopic features. Aspects of the method of description by Schnurrenberger *et al.* (2003) were adopted here to: (i) identify locations where burnt material dominated the sediment cores; and (ii) aid in the comparison of the different depositional histories contained within the seven sediment cores. Particle size analysis of the sediment cores was conducted in order to aid correlation and complement the mineral magnetic dataset (Oldfield *et al.* 1985).

Total Carbon (TC) or Total Organic Carbon is often used as an alternative to charcoal counting to indicate burnt material (Clark 1983; Tinner *et al.* 1998; Edwards and Whittington 2000; Figueiral and Mosbrugger 2000). TC measurements were selected in conjunction with the visual description and magnetic parameters to identify burnt material, due to the high sensitivity of TC analysis to detect any form of carbon deposits within the catchment. Charcoal counting on pollen slides was not conducted as it has been shown to be only effective in detecting fires that have occurred in close proximity to the core location, as finer aeolian-derived particles are not accounted for using this technique (Laird and Campbell 2000).

Changes in mineral magnetic properties have been used to make inferences about climatic and anthropogenically-induced variations in sediment patterns (Dearing 1999; Geiss *et al.* 2003). For example, fire frequency has been established by the enhancement of specific temperature-sensitive parameters (Rummery 1983; Gedye *et al.* 2000; Geiss *et al.* 2003; Blake *et al.* 2006a). Additionally, distinctive changes to mineral magnetic parameters have been used as a basis for simple core correlation (Oldfield and Clark 1990; Dearing 1992).

TAC measurements have commonly been used in archaeology to gain a better understanding about previous temperatures used in prehistoric manufacturing techniques (Godfrey-Smith *et al.* 2005). In the present study, TAC were created for samples from different depths in Core 6 where there was burnt material, in order to explore the possibility of identifying the previous maximum fire severity experienced by the sediment. This is the first time that this technique has been used for this purpose. Core 6 was chosen for TAC investigation, as visual description suggested that this core contained the most complete historical record.

Recently, dating of young sediment cores using ^{14}C has been refined to enable leaves and seed pods to be analysed to an accuracy of ± 2 years. This has been possible with the use of elevated ^{14}C values in the atmosphere following nuclear testing in the 1950's (Vogel *et al.* 2002; Hajdas *et al.* 2004; Goslar *et al.* 2005). In addition, ^{210}Pb and ^{137}Cs dating have successfully been applied to sediment cores sourced from the Lake Burraborang catchment (Colliton 2001; Blake *et al.* 2006c). Plutonium (Pu) has been used as a marker in studies where sandy deposits were dominant in order to identify deposition after the nuclear testing in 1963 (Jaakkola *et al.* 1983). This technique is a useful alternative to ^{137}Cs which is unable to attach to sand-dominated material.

Ancillary data including fire history, rainfall, river flow and water level collected by the SCA were used in combination with the findings from the above mentioned techniques to aid assessment of: (i) the reliability of mineral magnetic and TC measurements in identifying burnt material within reservoir floor sediment cores; (ii) the use of TAC in determining fire severity; and (iii) the transport and depositional processes acting within the reservoir environment.

7.2 METHODOLOGY

This section presents a detailed description of the methods used to collect (Section 7.2.1) and analyse (Section 7.2.2) the seven sediment cores from the floor of the Nattai arm of Lake Burragorang.

7.2.1 CORE COLLECTION

Coring was conducted from a barge owned by the SCA, chosen because of its: (i) stable platform; (ii) shallow draught, which enabled access to shallow areas; and (iii) winches that aided smooth extraction of the sediment column. The cores were taken near to Blossom Lodge Flat (Figure 3.4), avoiding locations in front or immediately downstream of inflowing tributaries so as to minimise potential contamination from mineral magnetics emanating from heavy metal deposits associated with mining activities (Harrison 2000). Site selection was aided by the use of an echo-sounding device, which enabled depth transects of the channel to be derived (Figure 7.2). Coring was targeted adjacent to the submerged Nattai River channel, where the longest record of post-dam sedimentation was likely to have occurred (Borland 1971).

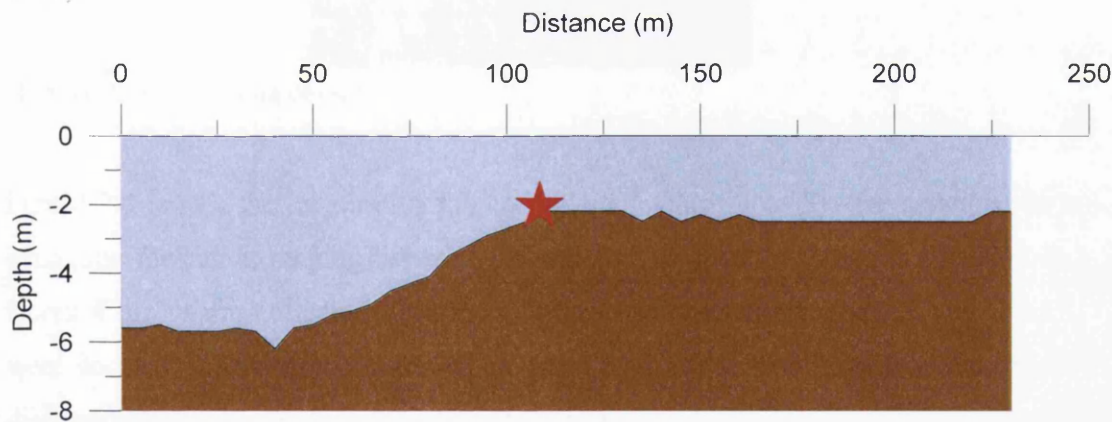


Figure 7.2: Depth transect of the Nattai channel showing targeted coring area on the edge of the submerged Nattai channel for cores 4, 5, 6 and 7.

Coring was conducted using a percussion-coring device (Figure 7.3) from the SCA barge, which was anchored to two fixed points to minimise movement during core extraction. The coring equipment was lowered into the water, supported by a number of ropes holding the equipment in an upright position. Once the percussion corer had reached the lake floor, the weight attached to the top of the plastic coring tube was repeatedly lifted and released, driving the core into the sediment. Hammering continued until the tube had penetrated the sediment to a depth of *ca*

1 m. This depth was indicated by markers on the ropes and through changes in the sound made when the weight hit the top of the core casing. The equipment was then lifted to just below the surface where a bung was inserted at the bottom of the core case to prevent the sediment escaping on exposure to the air. Finally, excess water was drained from the top of the core.



Figure 7.3: The coring device.

Figure 7.4 shows the location of the coring sites. Cores 1 to 3 were arranged in a triangular formation ranging between 5.6 and 25.2 m apart as shown in Figure 7.4a. Cores 4 to 7 were collected ~250.0 m further upstream from where Cores 1 to 3 were located. These cores were taken from a linear transect, with a maximum distance of ~28 m apart (between cores 6 and 7).

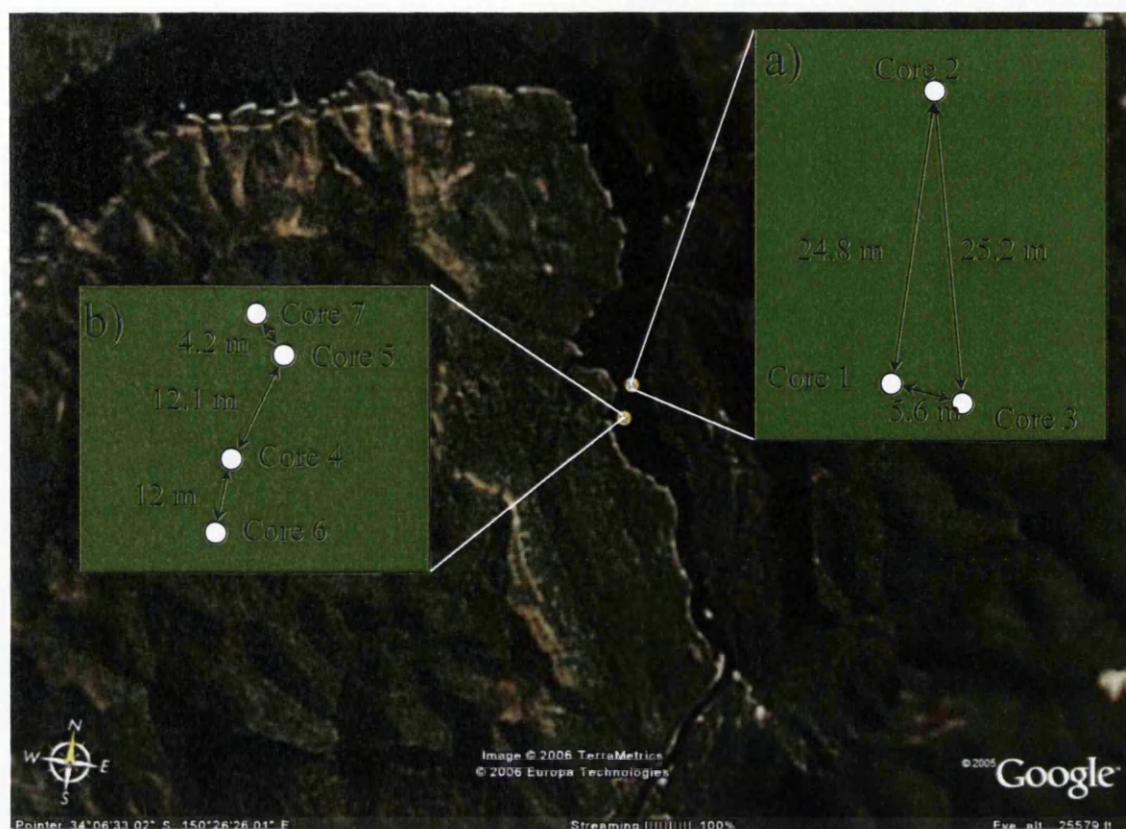


Figure 7.4: Location map of the Nattai cores. Inset a: Spatial relationship between cores 1 to 3; and inset b: spatial relationship between cores 4 to 7 (Imagery from www.earth.google.com).

Following collection, the cores were transported to the CSIRO laboratory in Canberra in an upright position to prevent disturbance of laminations. In the laboratory, the cores were frozen prior to dissection. After freezing, the cores were placed in a cradle and a router was used to split the plastic core casing. Cores were then cut in half using a strip of metal. Dissection of the cores was undertaken, following photography and visual description, in ~1-2 cm segments or where features within the profile changed.

7.2.2 LABORATORY PROCEDURES

7.2.2.1 Core description

Core description was conducted using aspects of the method described by Schnurrenberger *et al.* (2003). Features including: (i) core disturbance; (ii) colour; (iii) strata; (iv) banding; (v) boundaries; (vi) sedimentary structures; (vii) grain size; and (viii) texture were noted. Core disturbance was identified by flexures which are formed where deformation along the edges of the core are produced during

collection. 'Soupy' areas were identified where excess water had caused restructuring of the sediment. Core colour was described using a Munsell colour chart. Strata were identified by changes in distinctive characteristics, with beds identified for strata >1 cm and laminations attributed to strata <1 cm. Bands were characterised by continuous horizontal deposition of a contrasting type of deposit within a core. Features of boundaries were noted in terms of sharpness and abruptness of change. Sedimentary structures were defined by either massive, cross stratification, parallel stratification, graded or reverse-graded bedding. Grain size and texture were estimated using a particle size card, although detailed characterization was later conducted using a laser particle sizer (Section 7.2.2.3). Finally lithostratigraphical units were defined on the basis of similar sediment properties and characteristics.

7.2.2.2 Dating methods applied to the core sediments

Radiocarbon dating (^{14}C) has been commonly used to date Late Quaternary sediments with errors no better than ± 50 years (Worsley 1981), but recent developments using accelerator mass spectrometers have enabled dating to be conducted on seedpods and leaves of post-bomb age with an accuracy of ± 2 radiocarbon years in post-bomb periods (Vogel *et al.* 2002). ^{14}C is a naturally occurring environmental isotope, which is absorbed by plants during photosynthesis. Samples that were deposited before the bomb are also able to be dated using ^{14}C by applying the principle of radioactive decay of C isotopes through time. When an organism dies, it no longer receives new inputs of ^{14}C , so the concentration of ^{14}C declines due to natural radioactive decay. Comparison of the ratio of $^{14}\text{C}/^{12}\text{C}$ of the sample with $^{14}\text{C}/^{12}\text{C}$ ratio for the modern biosphere enables the amount of decay to be established and subsequently a date inferred (Goslar *et al.* 2005).

When this technique was developed, background values of ^{14}C were expressed as a fraction of 100 (%). Following injection of artificial ^{14}C into the atmosphere in 1950, values were elevated above 100%, causing values obtained since 1950 to be expressed as parts per thousand (‰) as percent Modern Carbon (pMC) (Vogel *et al.* 2002). Maximum ^{14}C values in the Southern Hemisphere were reached in 1965 AD (Goslar *et al.* 2005). Following the end of nuclear weapons testing, atmospheric ^{14}C began to decline. This change in ^{14}C values over time is now used to date young

sediments by calibration according to the pMC values measured at the Pretoria Radiocarbon dating laboratory in South Africa (Figure 7.8) (Vogel *et al.* 2002). This technique has been ideal for dating burnt material within sediments, as much of the organic matter will have died during a fire event, provided it is not reworked from older sediments as shown for charcoal in Australian alluvial deposits by (Blong and Gillespie 1978). Preliminary ^{14}C determinations were obtained for four samples from the bases of different units of burnt material in Core 6. Samples from depths of 8.5 cm, 19.5 cm, 29 cm and 43.8 cm were sent to the Poznan ^{14}C dating laboratory in Poland for analysis using an AMS facility. One of the limitations with ^{14}C date is erroneous results that may occur if sediment is reworked through the catchment system as has been demonstrated in various Australian examples by Prosser *et al.* (2001)

Owing to inconclusive results of the ^{14}C dating (Section 7.3.1.5.1), ^{210}Pb and ^{137}Cs dating were also conducted on samples from Core 6 between depths of 0 and 33.5 cm as these techniques had been successfully applied by Colliton (2001) and Blake (2006) to sediment cores from Lake Burragorang. These techniques used the radioactive decay curves from naturally occurring ^{210}Pb and artificially created ^{137}Cs within sediments for dating.

^{210}Pb dating is based on the principle of the radioactive decay of the naturally occurring ^{238}U series (Figure 7.5). ^{226}Ra decays in soil particles to the gaseous isotope ^{222}Rn . This is then emitted into the atmosphere where it decays to form ^{210}Pb . ^{210}Pb atoms become attached to airborne particulate material, which is then returned to the Earth's surface by precipitation or by dry deposition. The radioactive decay of this element can then be used to infer the date of deposition within sediments. There are two models that this data can be applied to: (i) the CRS (Constant Rate of Supply) model which requires a constant rate of ^{210}Pb supply; and (ii) the CIC model (Constant Initial Concentration) which can be applied where there is an abrupt discontinuity in the sediment record (Appleby 2001).

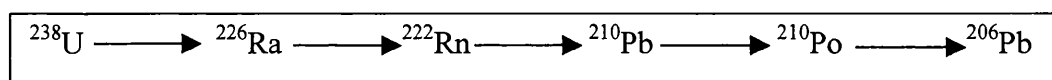


Figure 7.5: Radioactive decay series of ^{238}U leading to the formation of ^{210}Pb (Appleby 2001).

$^{137}\text{Caesium}$ (^{137}Cs) has often been used to support the determinations obtained from ^{210}Pb . ^{137}Cs is an artificial radioisotope, injected into the atmosphere during above-ground nuclear weapons testing between 1953 and 1963 and by the Chernobyl disaster in 1986. (It should be noted, however, that the 1986 ^{137}Cs from Chernobyl did not spread to the Southern Hemisphere.) The ^{137}Cs fallout produced a peak in soils and surface sediments around 1960. The first occurrence of ^{137}Cs activity in a sedimentary sequence could thus be used as a marker for sediments deposited after 1960. ^{137}Cs is only capable of being attached to clay and silt-size particles, and therefore it is not appropriate for the dating of sandy samples. An alternative radioactive isotope arising from the nuclear weapons testing that attaches to sand sized material is Plutonium (Pu) (Jaakkola *et al.* 1983; Ketterer *et al.* 2004). Calculations of the growth of ^{241}Am from ^{241}Pu is able to provide a more reliable confirmation of ^{210}Pb determinations as it is significantly less mobile in lake sediments than ^{137}Cs , and its distribution in cores reflects more closely the fallout record (Appleby *et al.* 1991). Samples from Cores 6 were sent for ^{210}Pb , ^{137}Cs and Pu dating to the CSIRO Dating Laboratory in Canberra. Eleven ^{210}Pb and ^{137}Cs determinations were obtained for Core 6, (Figure 7.7) and two Pu determinations were obtained for the sandy material at depths of 21.5 and 37.6 cm in order to confirm which sediments had been laid down after 1960 (Table 7.3).

7.2.2.3 Particle size analysis

Particle size discrimination was conducted on the mineral content of sediments from all core samples. This was conducted in order to establish the particle size fraction that was contributing to the magnetic signal to give some indication of the relative contribution of particle size to the mineral magnetic results. Removal of organic material from the sample was conducted using a 30% hydrogen peroxide solution (H_2O_2). Between 5 and 10g of sample was placed in a 500 ml beaker. Then, 10 cm^3 of H_2O_2 was added and a watch glass placed on the top of the beaker. The samples were left for >24 hours until reaction of the organic matter had significantly subsided. H_2O_2 treatment was not able to remove the charcoal fragments from the sample, which were therefore also incorporated into the particle size measurements. However, large charcoal fragments were removed by hand. Particle size measurement was conducted in Swansea using a Beckman Coulter® LS™ Series Laser Diffraction Particle Size Analyser. This measured the size of particles by

assessing the level of scatter, in the form of reflection, refraction and diffraction when a particle was placed in a laser beam.

7.2.2.4 Total Carbon (TC) analysis

TC analysis conducted in Swansea on the individual segments of the bulk material using a solid sample Primacs SC Total Organic Carbon analyser. Preparation of the samples before analysis required grinding of samples using a pestle and mortar.

7.2.2.5 Mineral magnetic analysis

Mineral magnetic analysis was conducted on the individual segments of the bulk material using procedures described in Section 5.2.3.

7.2.2.6 Thermal Activation Characteristics (TAC)

Thermal activation characteristics were investigated for quartz grains from 4 sections from Core 6 using both single grain and multigrain measurements, following the procedures described in Section 6.2.

7.2.2.7 Bulk density and porosity

Bulk density was calculated by placing a known mass of each sample in a measuring cylinder and measuring the volume of the sample. The volumes of the voids between each grain of the sample were obtained by measuring the amount of distilled water required to bring the water level in line with the top of the sample. The bulk density was then calculated by dividing the mass of the sample by the sum of the volume of solids and voids (equation 7.1) (Sumner 2000). Porosity was calculated by dividing the volume of the solids by the volume of the voids (equation 7.2) (Sumner 2000).

$$\text{Bulk density (g/cc)} = \frac{\text{mass of the sample}}{\text{Sum of the volume of solids and voids}} \quad (\text{equation 7.1})$$

$$\text{Porosity} = \frac{\text{volume of solids}}{\text{volume of voids}} \quad (\text{equation 7.2})$$

7.3 RESULTS

This section presents the results obtained for four of the sediment cores from the floor of the reservoir. The results from Cores 1-3 are not presented here as they comprised simply of massive sand deposits, with no evidence of fire events. Each core was capped by ~3 cm of fine silty clay. Details of the stratigraphy of Cores 1 and 3 are shown in Appendix 1, which contains: (i) a photograph of the core prior to dissection; (ii) χ_{lf} variation throughout the profile; and (iii) particle size characterisation.

Firstly a comparison of cores 4 to 7 is given by a schematic diagram of the visual descriptions made before dissection of the cores was conducted. This highlights similarities between the core stratigraphies. Secondly, the data for Core 6 is presented as this core appeared to contain the most complete record of sedimentation (Section 7.3.1). This is followed by the results of Cores 5, 4 and 7 (Section 7.3.2). Details of the core stratigraphy include: (i) visual description; (ii) TC measurements; (iii) particle size characteristics; (iv) bulk density and porosity; (v) dating (for Core 6); (vi) mineral magnetics; and (vii) TAC (for Core 6).

Figure 7.6 presents a schematic diagram of cores 4 to 7. Similarities can be drawn by comparing the material within stratigraphic units identified by visual description. All the cores contained a distinctive layer of fine silty material in unit A. Cores 4 and 7 contain an additional unit of burnt organic matter and charred material mixed with clay and silt compared with Cores 5 and 6. This may be caused by different sedimentation patterns resulting from fluctuating reservoir water levels. Cores 4 and 6 both appear to contain a complete record of post dam (i.e. 1960) sedimentation, as the massive coarse sandy deposits in units H and F seem to contain material similar to that present on the floodplain of the original Nattai channel. This complements findings by Blake *et al.* (2006c).

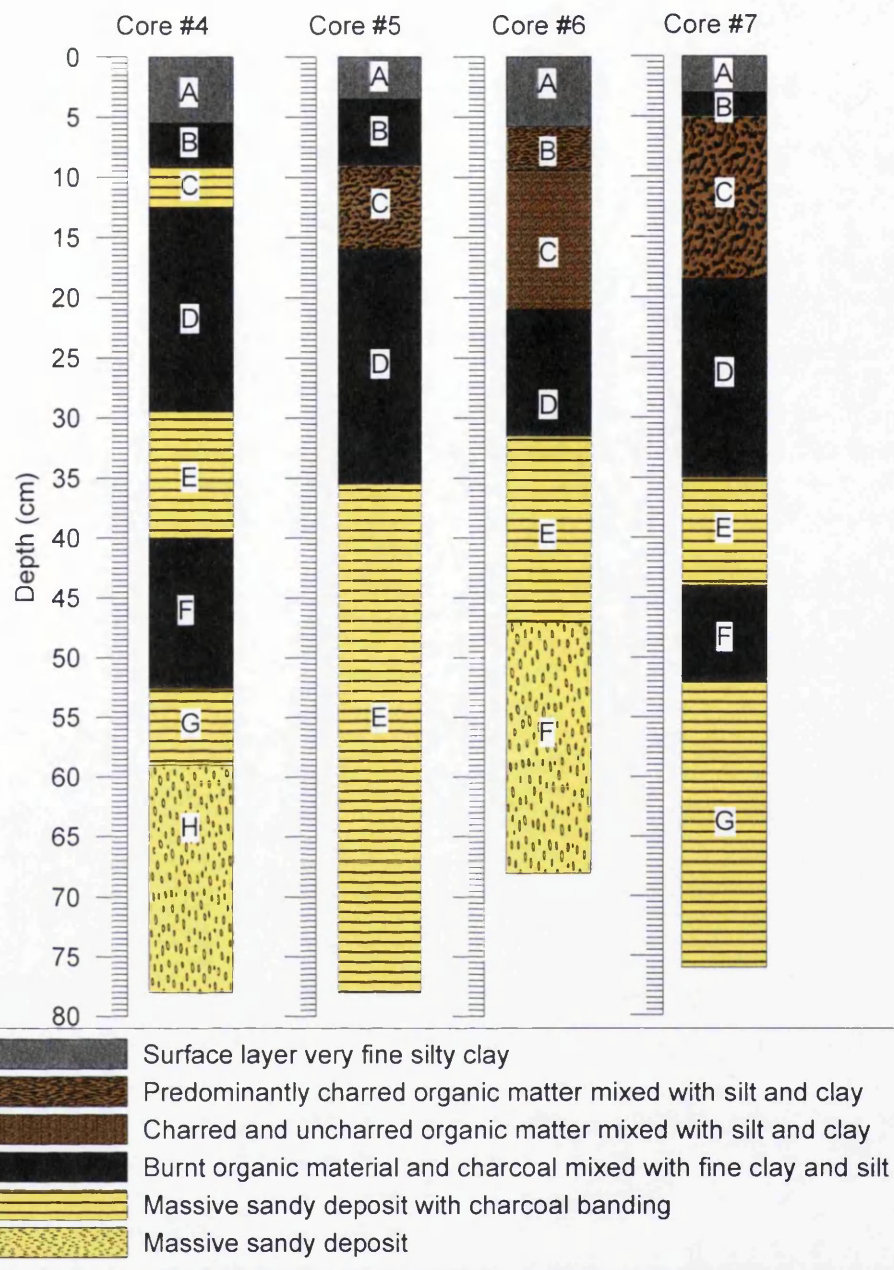


Figure 7.6: Comparison of the visual description of Cores 4-7.

7.3.1 CORE 6

This section presents details of Core 6, which are summarised in Figures 7.6 to 7.11.

7.3.1.1 Visual description

The schematic diagram presented in Figure 7.7a shows that Core 6 contains 6 main sedimentary units. These can be grouped as follows: (i) ~0–5 cm - fine clay / silty material; (ii) ~5–35 cm - fine silty material intermixed with charred and uncharred organic material; and (iii) ~35–68 cm - predominantly sandy deposits with some charcoal bands. The units and their nomenclature are summarised in Table 7.1 and their appearance can be seen in the schematic diagram and photograph (Figure 7.7a and b respectively). The most pronounced changes occur at ~35 cm, where a change in sediment source is apparent from the sandy deposits in the lower part to the charcoal mixed with fine silt and clay above. Horizons thought to represent fire events (Figure 7.7c) have been identified where charcoal dominates units. However, burnt material was evident throughout the top 35 cm of Core 6. The deposition of charcoal and burnt material in unit D below the charred and un-charred material in unit C suggests two phases of material movement through the catchment. The first phase of erosion could have involved the removal of surface ash and charcoal fragments from the slopes. The second phase of erosion is likely to have mobilised the underlying, highly erodible topsoil material.

Table 7.1: Explanation of labels used for units in Core 6

| Unit | Description |
|------|---|
| A | Fine silt / clay material |
| B | Massive burnt organic material intermixed with fine silt /clay material |
| C | Charred and uncharred organic material intermixed with fine silt /clay |
| D | Massive burnt organic material intermixed with fine silt /clay material |
| E | Massive sandy deposit with charcoal banding |
| F | Massive sandy deposit |

7.3.1.2 TC measurements

Figure 7.7d presents the TC measurements for Core 6. TC values ranged between 0.09 and 25.16%. Increased TC corresponds to areas where charcoal and organic matter dominates. Sharp reductions in TC were apparent where 1 cm sections consisted mainly of sandy material, at depths of 14, 26 and 33 cm.

7.3.1.3 Particle size data

Figure 7.7e presents the results from the particle size characterisation for Core 6. The fine surface material in unit A and the boundary between the two main stages of deposition occurring at ~35 cm (suggested by the visual description) is confirmed by the particle size data. The surface layer in unit A contained predominantly clay and silt sized particles. Material between the surface layer and above 35 cm consisted predominantly of silt and clay whereas below 35 cm the sand fraction dominated the assemblage.

7.3.1.4 Bulk density and porosity

Bulk density and porosity (Figure 7.7g) show a strong correlation with particle size characteristics. Higher porosity values which ranged between 0.5 and 0.9 were obtained for material deposited above 35 cm. Below 35 cm, porosity values ranged between 0.5 and 0.7. Conversely, low bulk density values were obtained for material deposited above 35 cm, ranging between 0.2 and 0.8, and high bulk density values ranging between 0.7 and 0.9 occur below 35 cm.

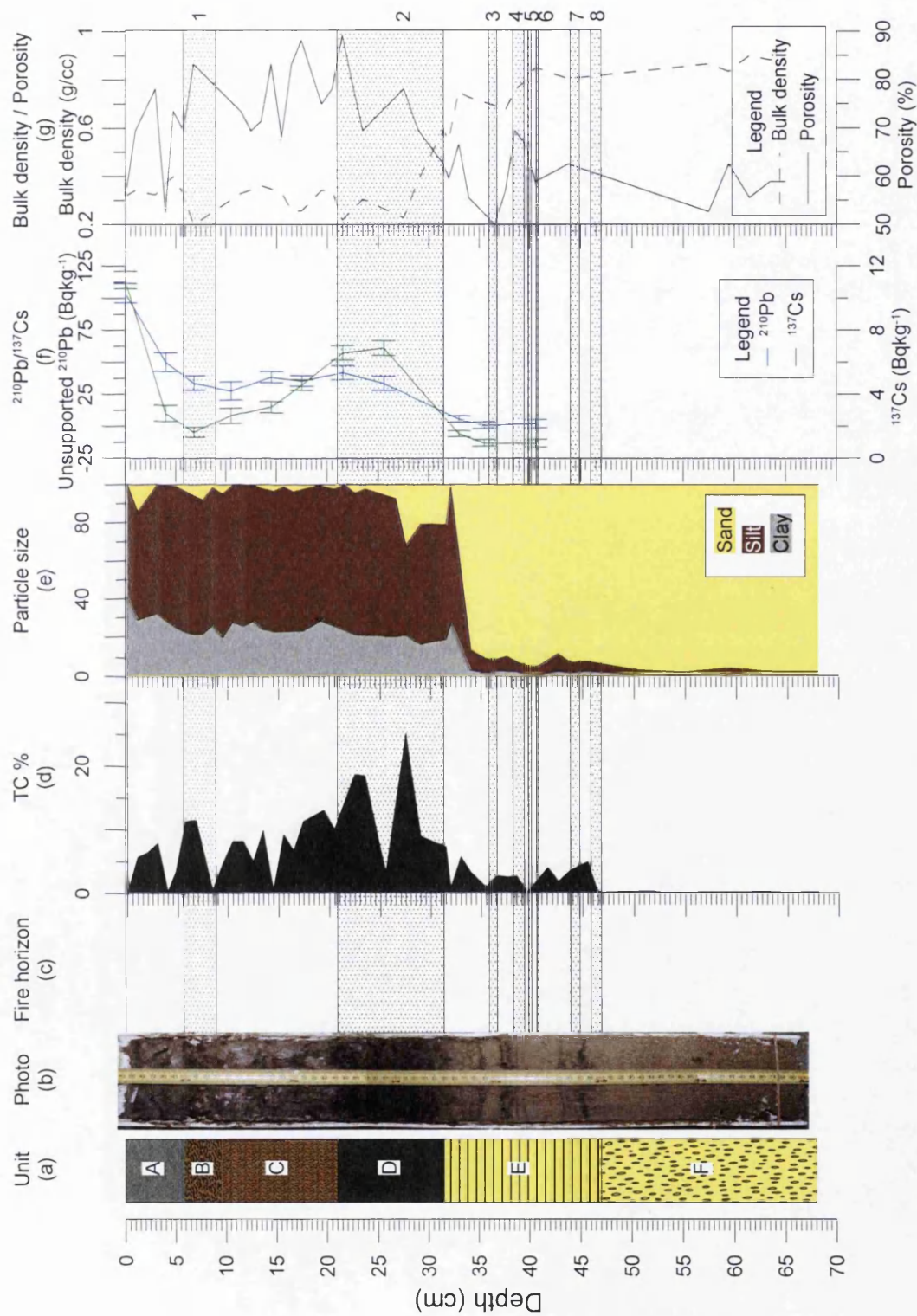


Figure 7.7: Profiles of Core 6 showing: (a) a schematic representation of lithostratigraphical units; (b) photo of core 6 prior to dissection; (c) a schematic representation of fire horizons as defined visually; (d) TC results; (e) particle size composition; (f) ^{210}Pb and ^{137}Cs bulk density and porosity.

7.3.1.5 Dating

In this study, four different dating techniques were explored to attempt to provide accurate dating of cores: ^{14}C (Section 7.3.1.5.1), ^{210}Pb (Section 7.3.1.5.2), ^{137}Cs (Section 7.3.1.5.3) and Pu (Section 7.3.1.5.4).

7.3.1.5.1 ^{14}C

The determinations corresponding to the pMC values obtained from Core 6 at depths of 8.5, 19.5 and 29 cm were ascertained by reference to the ^{14}C calibration curve. This gave two possible dates of deposition, suggesting that the samples were either deposited around 1962-63 or 1984-1986 (Figure 7.8 and Table 7.2). Two determinations were given from the pMC values during the increasing levels before the bomb peak, and during the decline of ^{14}C post-1954, as a result of absorption by oceans and atmosphere. Confirmation of the actual determinations was sought by application of further dating techniques including ^{210}Pb , ^{137}Cs and Pu. Although these dating techniques could also be affected by mixing and reworking of sediments (Nittrover *et al.* 1984; Smith and Hamilton 1985), Blake *et al.* (2006c) and Colliton (2001) have successfully used ^{210}Pb and ^{137}Cs to date sediments from the Nattai catchment.

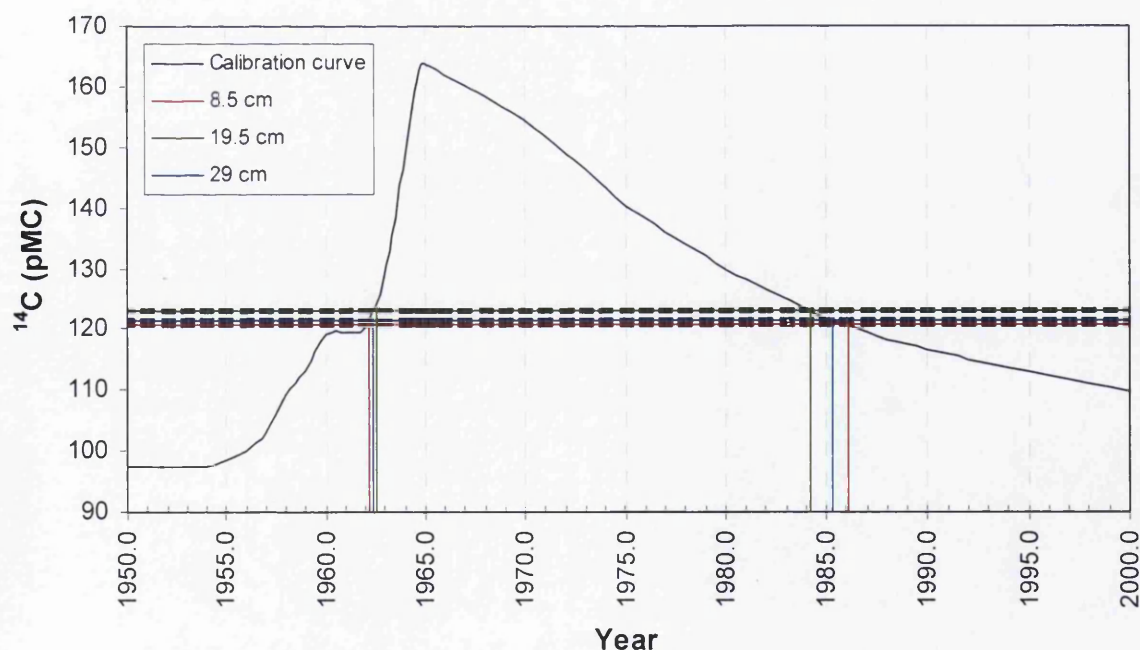


Figure 7.8: Calibration of the ^{14}C values obtained for samples from Core 6 from depths of 8.5, 19.5, and 29 cm. Calibration curve adapted from Robertson *et al.* (2004).

The similar times of deposition and the disordered chronology (shown in Table 7.2) suggests that these samples consist of a mixture of plant tissues formed in different years after the bomb peak in 1955 AD (Goslar *et al.* 2005). The varying ages of plant fragments within each sample produced a mean ^{14}C value of tissues formed in different years. This was also confirmed by the ‘massive’ nature of units C and D. This integration of atmospheric ^{14}C bomb signals (Goslar *et al.* 2005) by reworking of sediments has been shown to be problematic in a number of studies as it seriously limits the accuracy of the determinations (O’Sullivan *et al.* 1973; Björck and Håkansson 1982; Björck and Wohlfarth 2001). This implies long-term storage of sediment on the slopes within the catchment, and the movement of a mass of material in one event, fitting in with the post-fire model of erosion by Shakesby *et al.* (2003), which suggested that following the recent fire in 2001, relatively little material was moved from the footslopes due to their low gradients. Furthermore this reiterates Tomkins *et al.* (in press) suggestion of long term slope storage and that the majority of sedimentation in the region occurred as a result of high magnitude catastrophic rainfall events.

A rather old ^{14}C value of 1288 BP was obtained for the charcoal sample from a charcoal band within the sandy deposits at a depth of 42.8 cm. This was calibrated using the Oxcal calibration program (Bronk Ramsey 2005) which suggested that the charcoal was formed between 680 and 890 AD (with 95% probability) (Figure 7.9 and Table 7.2). This suggests that the sample had either: (i) been subjected to long-term slope storage and reworking (Björck *et al.* 1994); or (ii) been derived from the original floodplain of the Nattai River prior to flooding of the valley by closure of Warragamba Dam (Blake *et al.* 2006c).

Table 7.2: ^{14}C determinations obtained for 4 samples from Core 6.

| Sample depth | Age ^{14}C | Period | Actual date in years |
|--------------|---------------------|--------|----------------------|
| 8.5 | 120.7 ± 0.3 pMC | Modern | 1962-63 or 1984-1986 |
| 19.5 | 123.1 ± 0.4 pMC | Modern | 1962-63 or 1984-1986 |
| 29 | 121.5 ± 0.3 pMC | Modern | 1962-63 or 1984-1986 |
| 43.8 | 1288 ± 30 BP | Old | 680 – 890 AD |

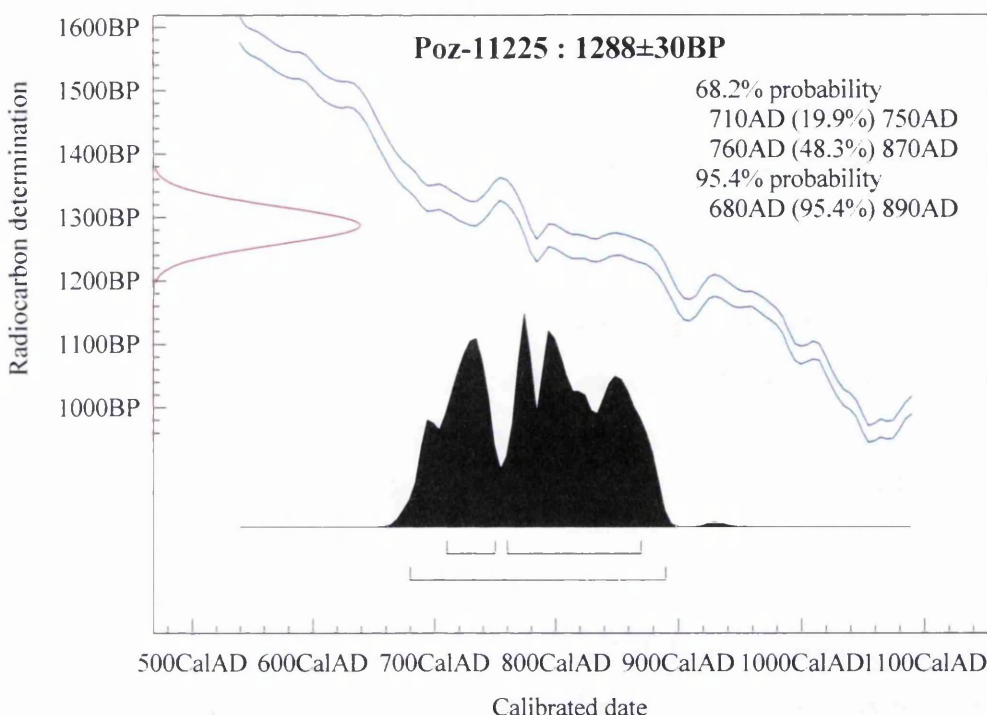


Figure 7.9 ^{14}C date obtained from the charcoal sample from a depth of 42.8 cm in Core 6, using Southern Hemisphere data from OxCal v3.10 (Bronk Ramsey 2005)

7.3.1.5.2 ^{210}Pb

Figure 7.7f presents the ^{210}Pb and $\text{Cs}137$ profiles, which were measured after the ^{14}C determinations had proved inconclusive in dating the reservoir sediments. ^{210}Pb was analysed owing to the potential for the constant rate of decay to provide information on sedimentation rates. However, ^{210}Pb was not detectable for samples below 27.4 cm due to dilution by sand this suggested that sedimentation above this point took place prior to one ^{210}Pb half life (22 years) but later than the age of the first appearance of ^{137}Cs (i.e. 22-48 years ago) (Section 7.3.1.5.3). These results were unable to be applied to either the CIC or CRS model, therefore no further analysis of this data was conducted.

7.3.1.5.3 ^{137}Cs

^{137}Cs values were obtained at the same depths as for ^{210}Pb . The presence of ^{137}Cs in all of the samples measured in Core 6 has suggested that deposition of material above 40.6 cm occurred after 1955-1956 (Figure 7.7f). Owing to the dilution of the signal by increasing sand content below 66 cm, it was not possible to date sediment from deeper in the core or pre-1958 sediments. Between depths of 17 and 25 cm, there is an increase in ^{137}Cs . This could be caused by either: (i) increased

concentration in ^{137}Cs by material being deposited during one event; or (ii) the strong absorption capacity of ^{137}Cs by the decaying organic matter and humus (Ritchie *et al.* 1970; Wise 1980) which dominates this unit. Bishop *et al.* (1991) documented a lack of ^{137}Cs in sediments following high magnitude events removing and depositing material rapidly, which prevented the absorption of the ^{137}Cs isotope. Although there was evidence from the dating and visual description to suggest that units C and D were deposited during a high-magnitude event, ^{137}Cs remains throughout the profile. This suggests that the majority of the material transported from the slopes was of surface soil origin, and any movement of subsurface material was largely restricted to redistribution on the slopes as argued by Shakesby *et al.* (2003).

^{137}Cs was apparent in all samples and was identified down to depths of 40 cm. The lowest sample from the profile showed evidence of ^{137}Cs , signifying that this material was deposited after 1958. It was not possible to obtain determinations at greater depth due to the dilution of the ^{137}Cs by the large sand content, ^{137}Cs not being able to become attached to sand-sized particles (Bishop *et al.* 1991).

7.3.1.5.4 Pu

Plutonium attaches to sand-sized particles and thus it is possible to use this radionuclide to discriminate between samples deposited before and after 1964. The plutonium measurements are presented in Table 7.3. The samples measured between 21.5 and 37.6 cm showed similar $^{238}\text{Pu} / (^{239}\text{Pu} + ^{240}\text{Pu})$ ratios of ~ 0.11 . The first occurrence of Pu in the environment occurred in 1964 from nuclear tests. Assessment of the fallout ratios for $^{238}\text{Pu} / (^{239}\text{Pu} + ^{240}\text{Pu})$, enabled recognition of whether the sediment was deposited pre- or post- 1964. Before 1964, the ratio of Pu produced values of 0.03. Immediately after 1964, this ratio increased to 0.20 for a few years then rapidly declined (Jaakkola *et al.* 1983; Ketterer *et al.* 2004). Pu isotope ratios obtained for Core 6 depths between 21.5 and 37.6 cm were 0.11 ± 0.2 indicating that this particular sediment was deposited around 1964. It also confirmed that the material within units C and D was deposited during one or two large events dating from around this time.

Table 7.3: Plutonium measurements for Core 6

| Core depth (cm) | $^{238}\text{Pu} / (^{239}\text{Pu} + ^{240}\text{Pu})$ | Suggested date |
|-----------------|---|----------------|
| 21.5 | ~ 0.11 | 1964/5 |
| 37.6 | ~ 0.11 | 1964/5 |

Although all of the dating results obtained for the sediment cores contained a degree of uncertainty, the ^{14}C , ^{210}Pb and Pu results obtained for Core 6 all complement each other in suggesting that unit A was deposited after 1964. Material deposited within units B - D are thought to have been deposited during an event around 1964/1965 because of the transition value of the $^{238}\text{Pu} / (^{239}\text{Pu} + ^{240}\text{Pu})$ ratio (Table 7.3). Consultation of the fire history maps in Figure 3.10 suggested that the burnt material is likely to have originated from the fires that burnt the lower Nattai catchment very close to the shoreline during the 1964/1965-fire season. However, this period also coincides with the time when the reservoir first reached its maximum level (Figure 3.12). A large event is likely also to have redistributed loose material on the slopes and from the newly submerged riverbanks. The ^{14}C date for the charcoal sample contained within unit E suggests that this material was deposited well before 1965, indicating that this sediment represented the original Nattai river floodplain before flooding of the valley in 1960. The presence of old river floodplain sediments in the basal unit of a sediment core obtained upstream of the coring sites used in this study was also concluded by Blake *et al.* (2004).

7.3.1.6 Mineral magnetics

The magnetic record from Core 6 (Figure 7.10) has shown two main stages of deposition, with a significant difference between material deposited above and below ~35 cm (i.e. before and after construction of the dam according to the dating evidence). Below this point, there were two main fire horizons at 35.6-37.6 cm and 41-44.5 cm interrupting the massive sandy deposits. The sandy deposits produced low values for all magnetic concentration parameters due to the majority of magnetic minerals being present in material finer than sand. Above 35 cm, the magnetic parameters experienced a general increase associated with the finer composition, identifiable by the particle size graph (Figure 7.7e) and an increase in the contribution of single stable domain (SSD) and superparamagnetic (SP) grains, reflected by the increase in χ_{ARM} , χ_{lf} and χ_{fd} values (Gedye *et al.* 2000). This

change in magnetic composition is likely to have been influenced primarily by the increased sand contained at depths > 35 cm.

In the upper 35 cm of sediment in the core, there are different magnetic signatures, which coincide with the different units identified in the schematic diagram in Figure 7.7a. The fine clay / silt composition of unit A between 0-3 cm produced increased values for all of the measured parameters. This was likely to have been caused by the finer composition of material (confirmed by the particle size analysis shown in Figure 7.7e) as magnetic minerals are predominantly found within clay and silt sizes (Walden 1999). Alternatively, the elevated magnetic parameters in this upper material could have been caused by the relative decay of magnetic signatures in the lower units as a result of the reducing conditions caused by the anoxic hypolimnion on the lake floor (Romero *et al.* 2004). Unit C contained charred and un-charred organic material mixed with predominantly fine silty material. This resulted in elevated values of χ_{lf} and χ_{ARM} between 9-21 cm, while χ_{fd} , $soft_{IRM}$ and χ_{fd} / χ_{ARM} did not show much enhancement, this was caused by the dilution of the magnetic signal by the high organic matter content. Unit D (between 21-35 cm) comprised mainly of burnt organic matter and charcoal, mixed with fine silty material. This produced enhancement of different magnetic parameters to those that were enhanced in Unit C, with elevated values of $\chi_{fd\%}$, $soft_{IRM\%}$ and χ_{fd} / χ_{ARM} . Comparing these values with the results from the heating experiment suggests that both units C and D contained burnt material but in different particle size fractions, with unit C containing coarser magnetic minerals than unit D. Burnt material deposited at depths >35 cm did not correspond directly to an increase in magnetic parameters, although higher values for χ_{lf} , χ_{fd} , $soft_{IRM\%}$, $\chi_{ARM}/SIRM$ and χ_{fd}/χ_{ARM} lay below the tightly banded fire horizons (numbers 3-6 in Figure 7.10). This accords with some of the findings from the furnace heating experiment in Chapter 5 that found enhancement of χ_{lf} , χ_{fd} and χ_{ARM} may have occurred with the sorts of temperatures commonly reached in the soil during wildfire. Although $Soft_{IRM\%}$ and $\chi_{fd\%}$ did not show any clear response to heating, this could have been caused by the high organic content or the retention of a thermal memory from previous fire events. Gedye *et al.* (2000) suggested that χ_{lf} , χ_{fd} , χ_{ARM} , $Soft_{IRM\%}$, $\chi_{ARM}/SIRM$ and χ_{fd}/χ_{ARM} were parameters that demonstrated an increase where burnt material was found.

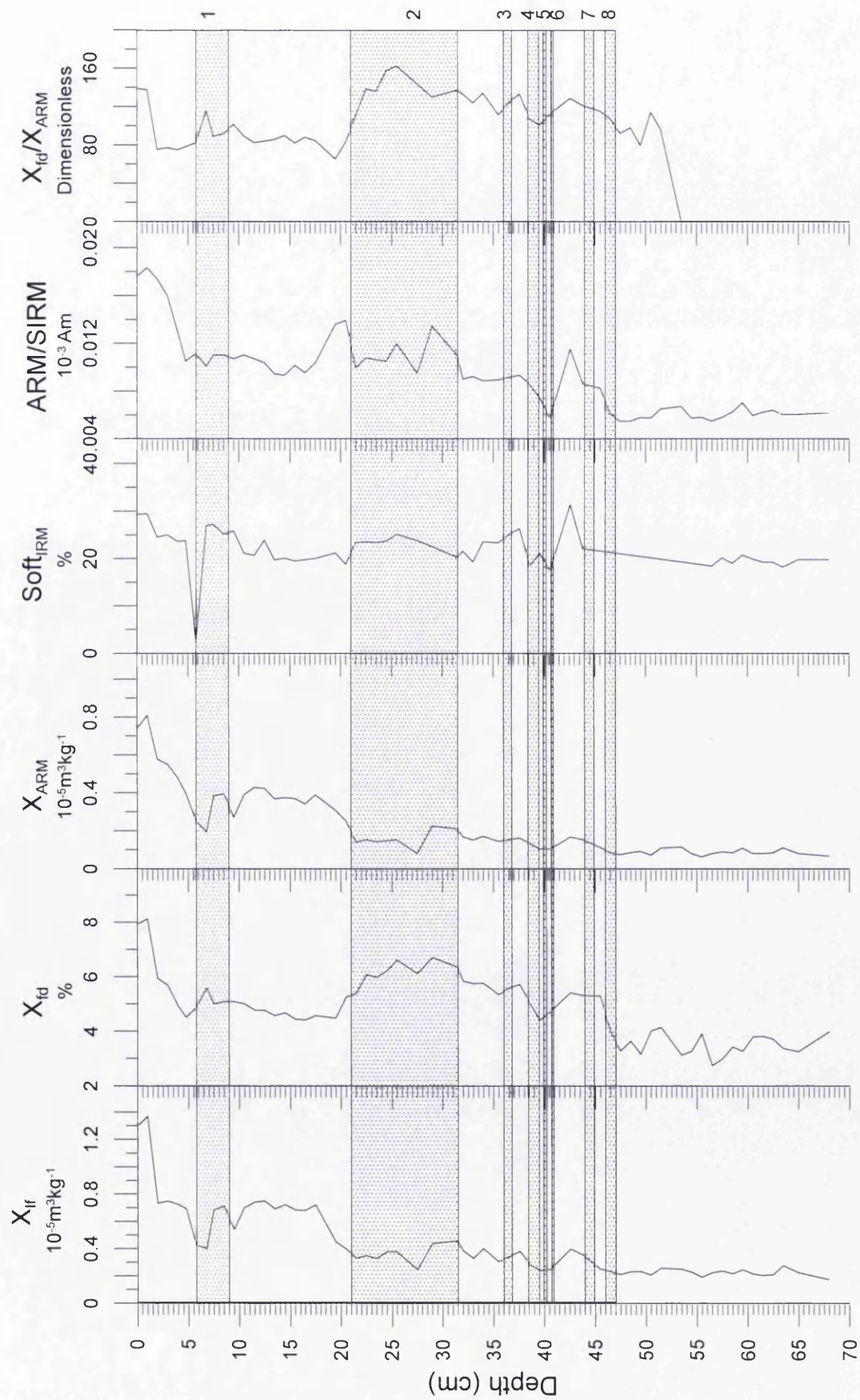


Figure 7.10: Mineral magnetic properties for Core 6.

7.3.1.7 TAC

This section presents the results of the TAC obtained for four samples taken from burnt sections at different depths within Core 6. This was conducted using the methods outlined in Chapter 6. Analysis was conducted with reference to the calibration curves and bivariate plots derived from the furnace heated unexposed bedrock samples in Chapter 6. Firstly, the results for the multi-grain samples are presented. Secondly, the results for single grains from each sample are presented to ascertain the variability of heating histories within the samples. The results and interpretation are provisional given the experimental nature of this work.

Multi-grain TAC were obtained for four samples from core 6, at depths of: (i) 0-5 cm; (ii) 19-29 cm; (iii) 36-37 cm; and (iv) 43-45 cm. Comparison of the shape of TAC of the core samples with the shape of TAC created by the furnace heat-treated bedrock sample (Figures 6.11 and 6.12) suggested that the samples had been heated relatively recently to temperatures between 400-500 °C. Further characterization of the TAC features of the core samples was conducted by comparison of: (i) the normalized maximum $TL\chi$ (χ_{3N}) (Figure 6.13c); (ii) the $TL\chi$ measurement conducted after heating to 680 °C (χ_{FN}) (Figure 6.13d); and (iii) the bivariate plot of χ_{FN} / χ_{3N} (Figure 6.14b) derived for the furnace heated bedrock samples. χ_{3N} (Figure 7.12a) suggested that temperatures of between 480 and 500 °C had been reached; χ_{FN} (Figure 7.12b) suggested that temperatures of between 462 and 480 °C had been reached; the bivariate plot of χ_{FN} / χ_{3N} (Figure 7.12c) suggested that the samples had previously experienced maximum heating temperatures of between 400 and 500 °C.

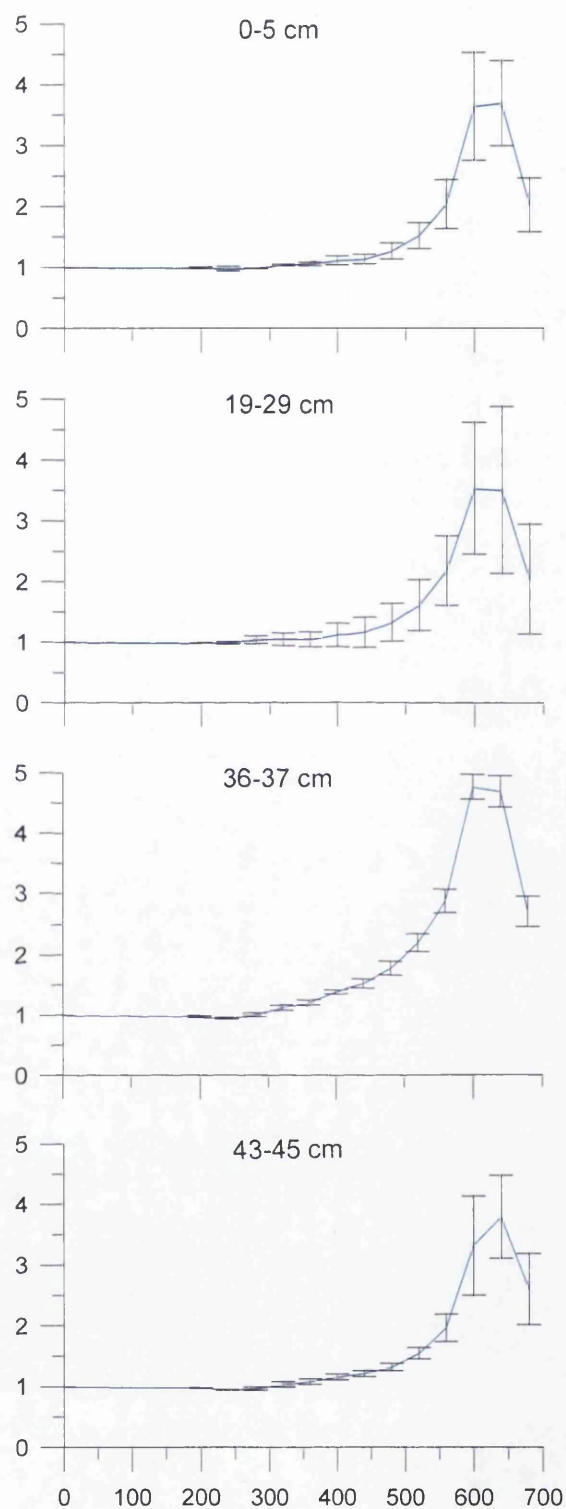


Figure 7.11: TAC for multi-grain samples from Core 6 to elucidate previous heating history.

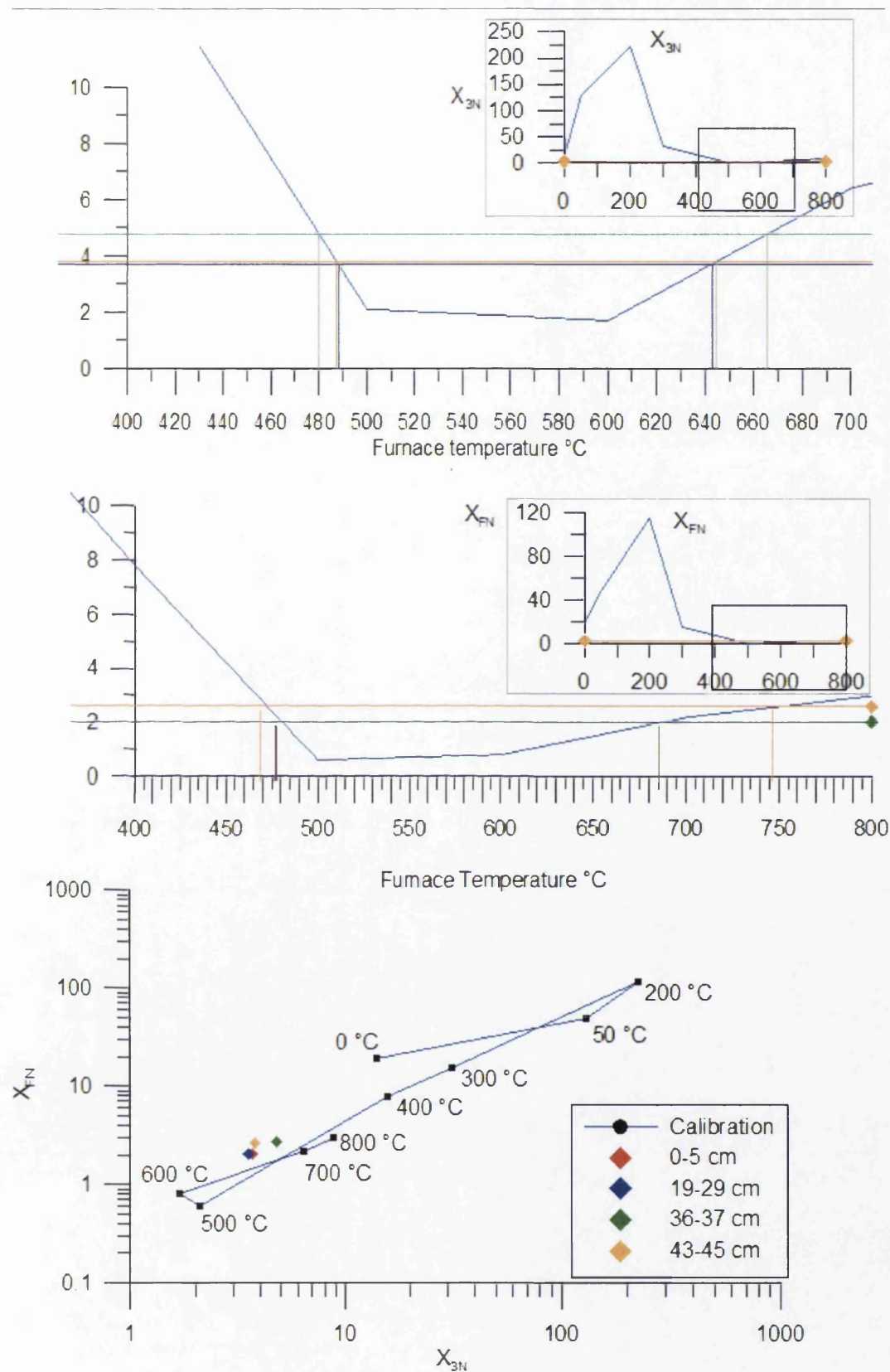


Figure 7.12: Temperatures experienced by samples obtained from Core 6 at depths of 0-5, 19-29 and 43-45 cm suggested by calibration curves derived from features of TAC ((a) χ_{3N} (b) χ_{FN} , and (c) χ_{FN}/χ_{3N}) of furnace heat-treated BR samples (Figures 6.9 and 6.14). The inset graphs in Figures 7.12 a and b show the section of the plots of the TAC features where the values obtained for the core features intersect the calibration curve.

The findings from the preliminary heating experiments in Chapter 6 on the long-unburnt foot-slope sample showed that the soil profile contained grains that had experienced a variety of maximum previous temperatures. Investigation of TAC of 60 single grains from core 6, 20 grains sampled at depths of 0-5 cm, 19-29 cm and 43-45 cm are presented in Figure 7.13a-c. The suggested temperatures allocated to each grain are shown in histograms in Figure 7.14a-c. This identifies that virtually all the grains contained at depths of 0-5 cm and 43-45 cm had experienced maximum temperatures in the range 400-600 °C. The samples from a depth of 19-29 cm contained 3 of the 20 grains that had experienced temperatures <100 °C or were unheated. This could perhaps indicate that the grains were derived from subsurface material.

The similar maximum temperatures experienced by the majority of grains within the sediment core suggested that either: (i) sediment transported from the catchment was predominantly derived from locations that had experienced high severity fires (in excess of 400 °C); or (ii) the complex fire history of the catchment and the longevity of the modified TL χ values of samples meant that at some point in each grain's history it has experienced a severe fire.

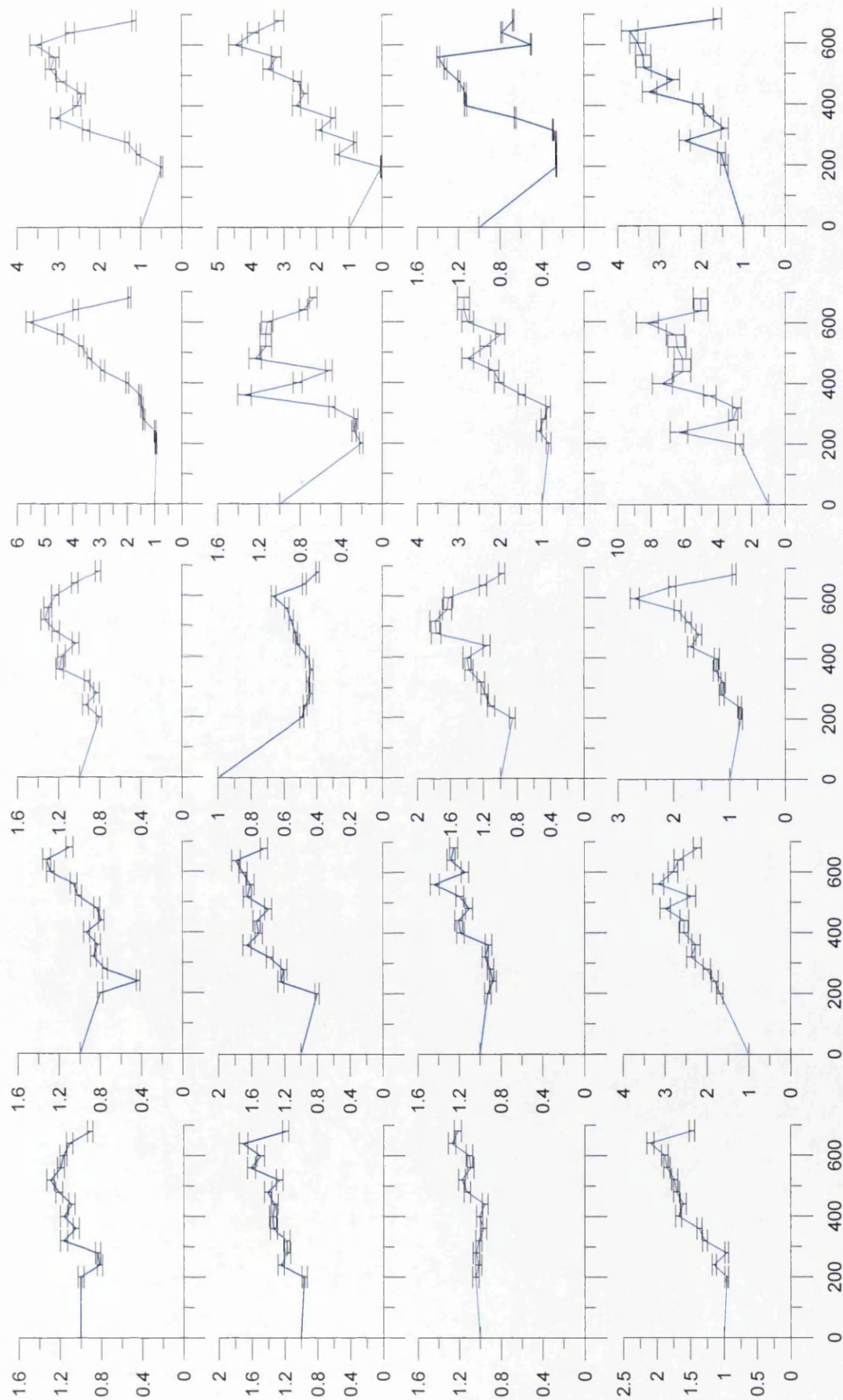
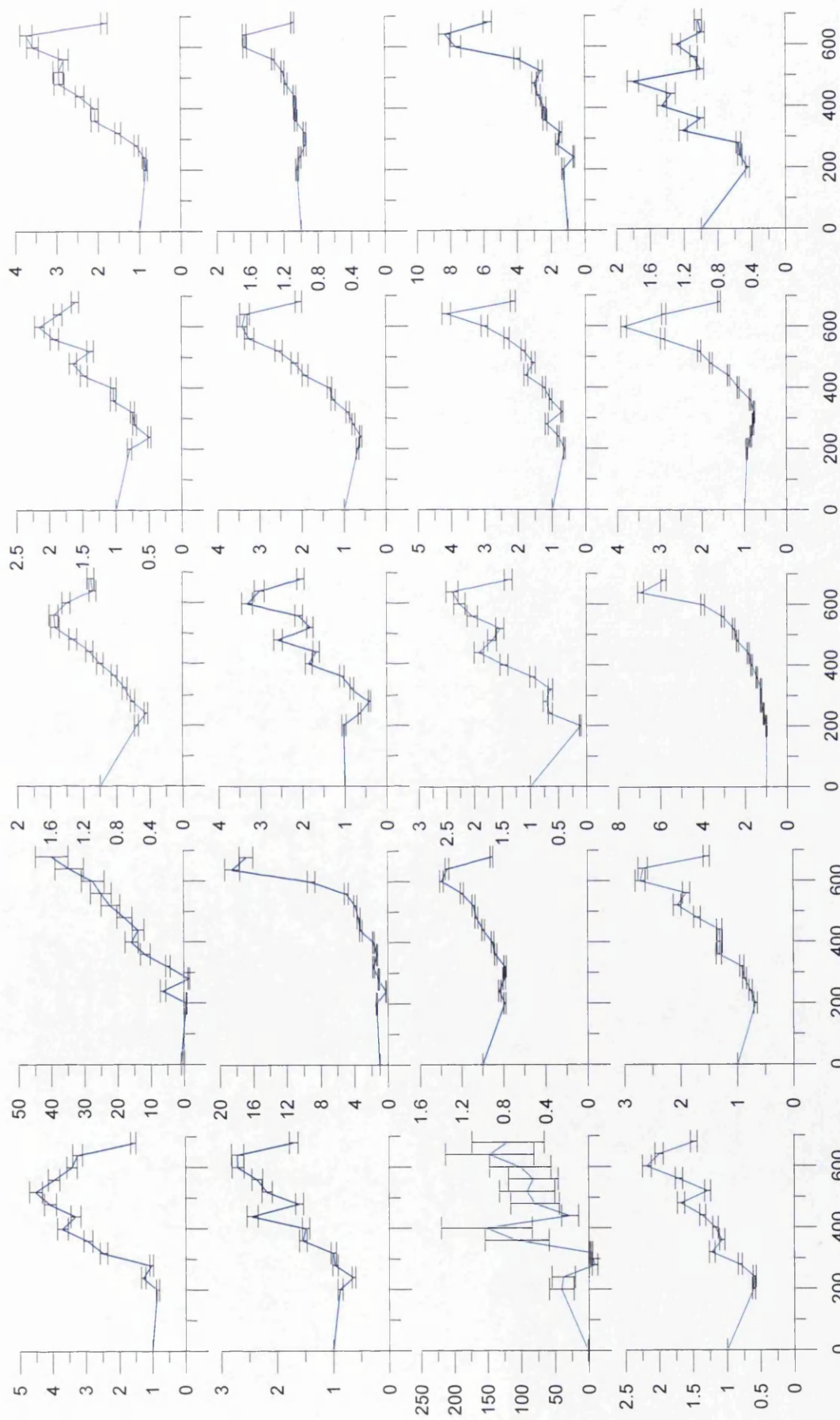


Figure 7.13a: 20 TAC for single grains from the core sampled between 0-5 cm.



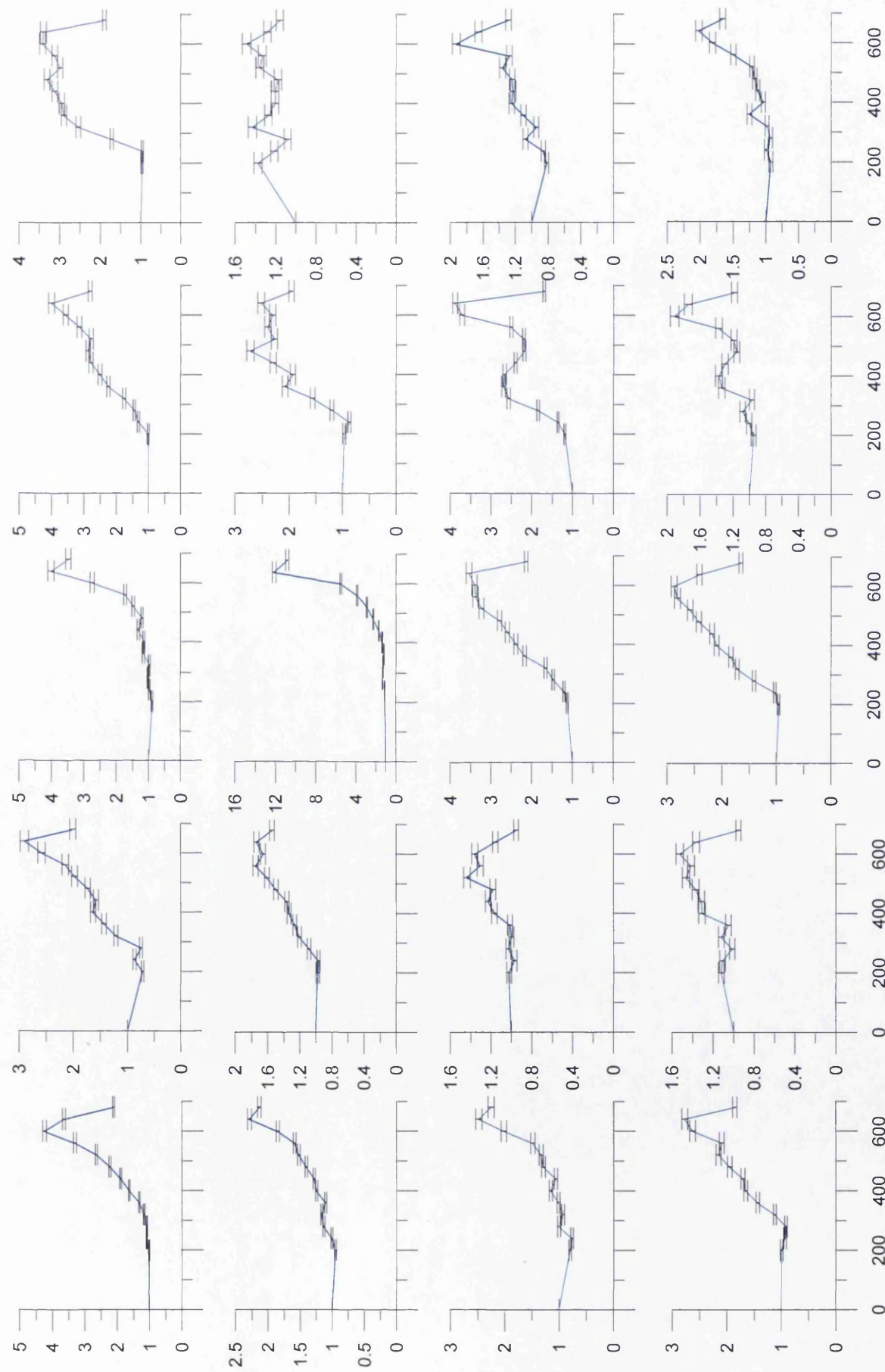


Figure 7.13c: TAC for 20 single grains sampled between depths of 43-45 cm.

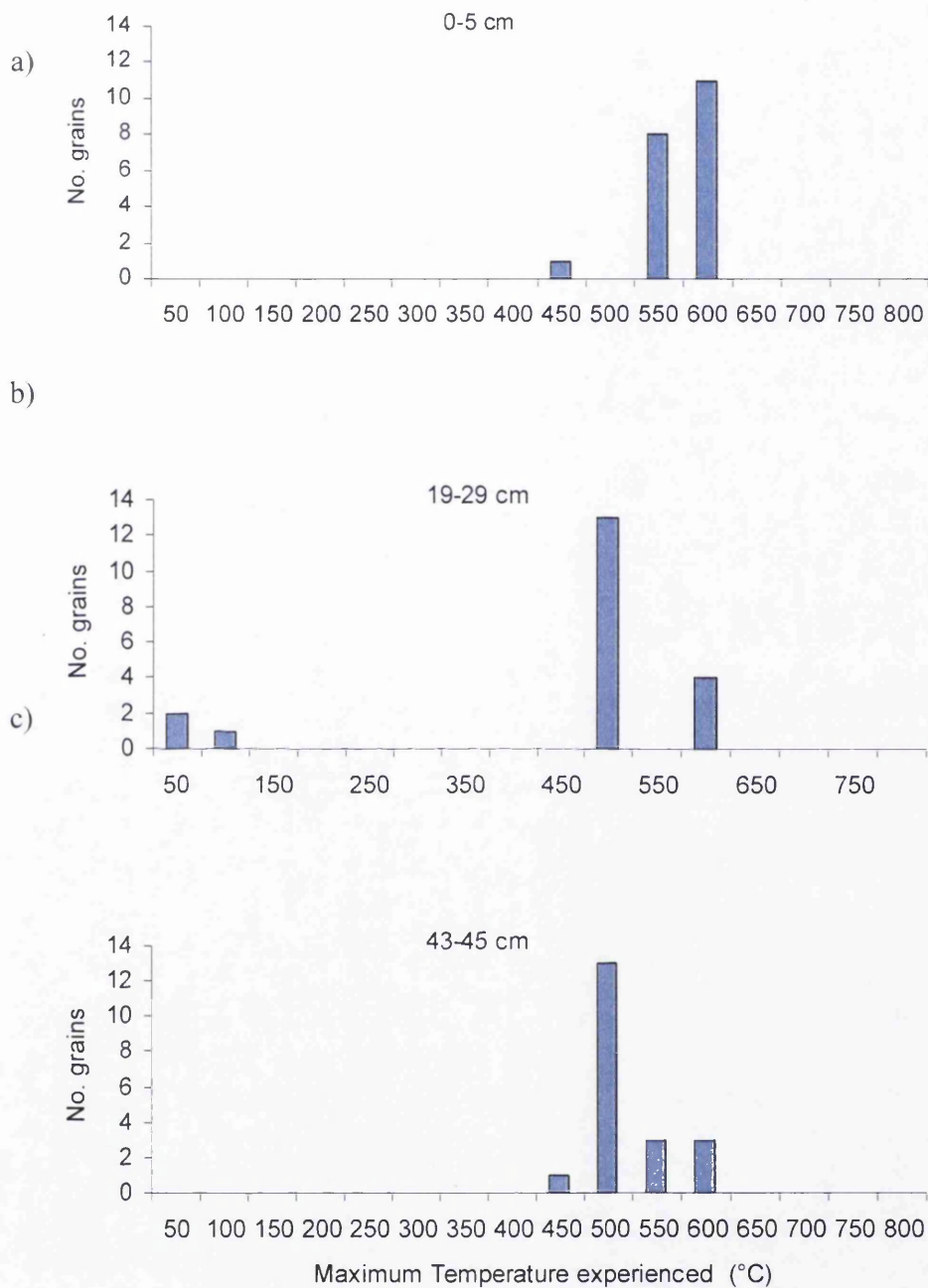


Figure 7.14: Histograms of temperatures allocated to the 20 single grains from the core samples at (a) 0-5 cm, (b) 19-29, and (c) 43-45 cm that were indicated by assessment of the peak value obtained for TAC and comparison with the shape of the TAC curves produced for the various furnace heat treatments in Figures 6.11 and 6.12.

7.3.2 CORES 5, 4 AND 7

This section presents the visual descriptions for Cores 5, 4 and 7. It then compares the responses of TC to particle size variations before presenting the mineral magnetic parameters. For each core, details including: (i) a schematic representation of lithological units contained within the profile, (ii) photo, (iii) schematic representation of fire horizons, (iv) TC and (v) particle size is given (Figures 7.14-7.16).

7.3.2.1 Core 5

Core 5 comprised 78 cm of sediment. Five distinctive sedimentary units could be identified. Unit A comprised ~3.5 cm of fine silty-clay material. Units B and D comprised predominantly of burnt organic material and fine silty material, with some fine banding of sandy material evident. Unit C contained charred and un-charred organic matter, mixed with fine silt and clay. Unit E contained sandy material with bands containing burnt deposits. The schematic diagram presented in Figure 7.6 shows a number of similarities between Cores 5 and 6. As a result, it is not unreasonable to assume that a similar pattern of sedimentation occurred with both cores, with the sediment contained within units C and D deposited following the 1964/1965 fires (i.e. post damming). The magnetic signatures obtained for the different units also showed similar responses for the different sedimentary units. However, the greater variability in $\chi_{fd}\%$, $\text{SOFT}_{IRM}\%$ and χ_{fd}/χ_{ARM} suggested that more distinctive sandy laminations or bands were present.

7.3.2.2 Cores 4 and 7

Similarities could potentially be drawn between cores 4 and 7 by correlating the sandy deposit in between the two units containing charcoal bands. However, the units within Core 4 were more compact than in Core 7 and the sandy basal deposit in unit H showed some similarities with the original floodplain deposit found in Core 6. Core 4 contained 79 cm of sediment and 8 main lithological units. Core 7 contained 74 cm of sediment and 7 main lithological units. In both cores, units 'A' consisted of fine silty ash deposits. Units B, D and F contained burnt material mixed with fine silt and clay. Units E and G were comprised of massive sandy sediment with charcoal banding. The two main differences between Cores 4 and 7 were: (i) Core 4 had an additional unit H, containing a massive sandy deposit; and (ii) unit C

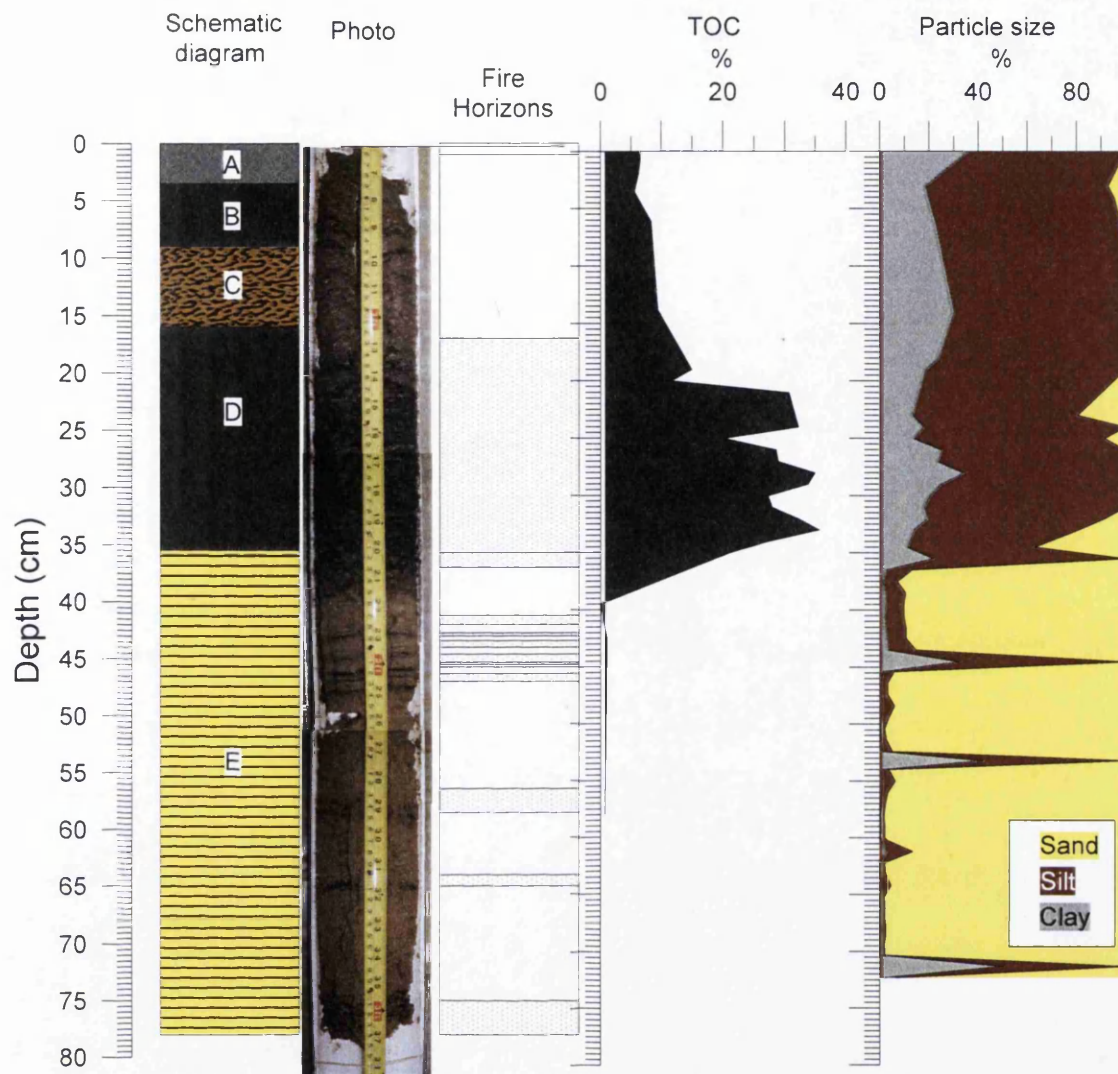


Figure 7.15: Profiles of Core 5 showing (a) a schematic representation of lithostratigraphical units, (b) photo of core 5 prior to dissection, (c) a schematic representation of fire horizons as defined visually, (d) TC, (e) Particle size composition.

in Core 4 contained a similar composition to units E and G, while unit C in Core 7 contained similar material to that found in unit C in Cores 5 and 6.

The particle size composition of each of the cores showed a close correspondence to the lithological units. Unit A in each of the cores showed an increase in the proportion of clay compared with lower units. The units containing burnt organic matter comprised predominantly of clay and silt. Where sandy banding was isolated during dissection, this produced a significant reduction in the percentage of silt and clay. Highest TC values occurred within the units containing burnt organic matter mixed with silt and clay. However, TC values varied according to the mineral content. Charred and un-charred organic

matter mixed with fine silt and clay produced lower TC values. TC values for the banding within sandy deposits were investigated for Core 7, which showed peaks coinciding with the fire horizons.

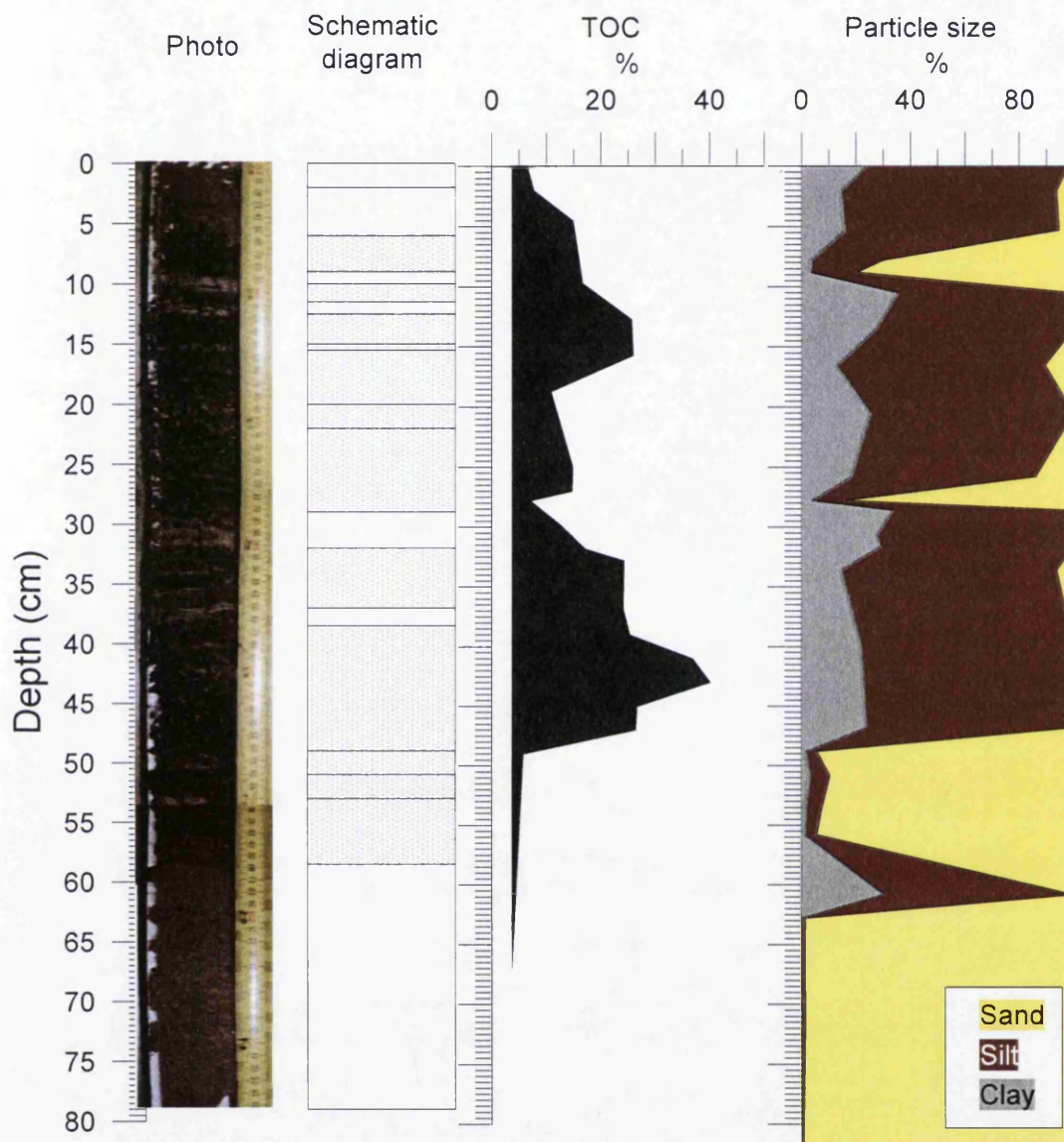


Figure 7.16: Profiles of Core 4 showing (a) a schematic representation of lithostratigraphical units, (b) photo of core 4 prior to dissection, (c) a schematic representation of fire horizons as defined visually, (d) TC, (e) particle size composition, (f) ^{210}Pb / ^{137}Cs , and (g) bulk density and porosity.

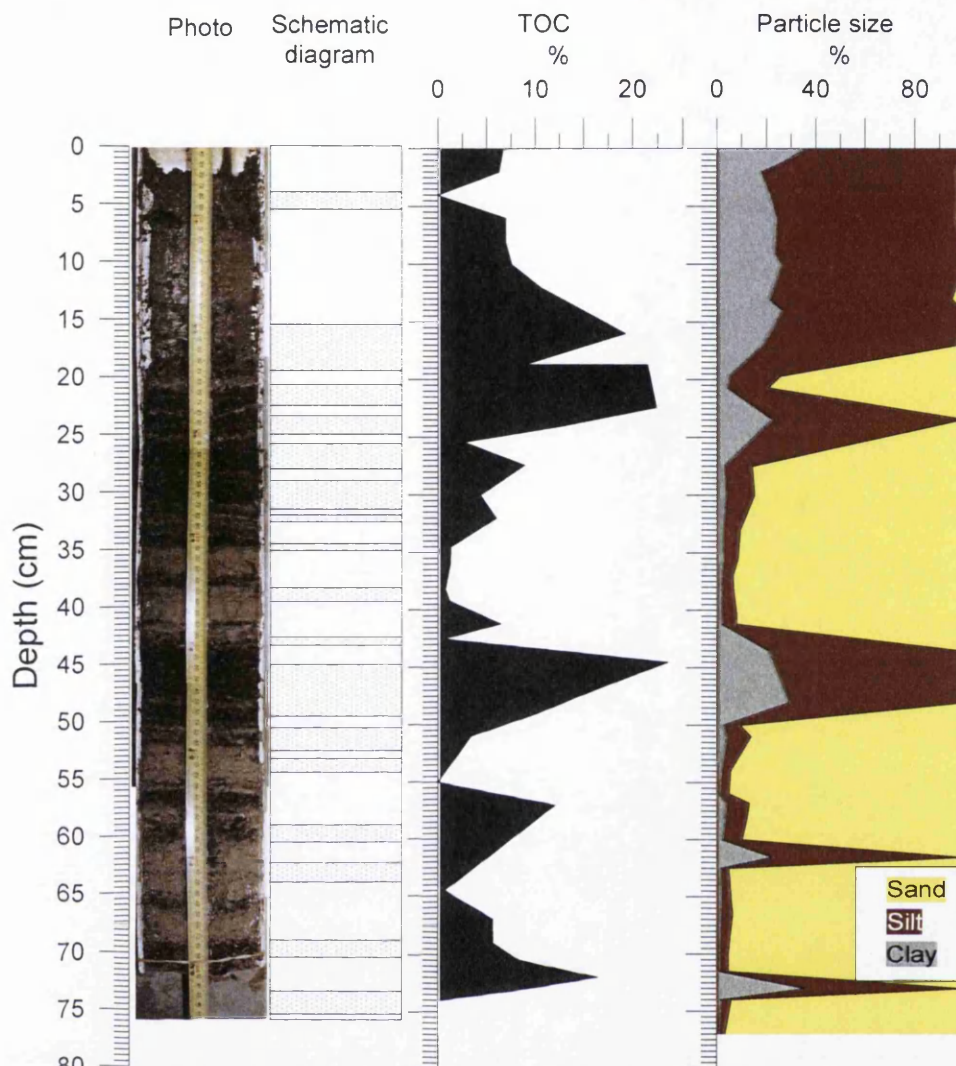


Figure 7.17: Profiles of Core 7 showing (a) a schematic representation of lithostratigraphical units, (b) photo of core 7 prior to dissection, (c) a schematic representation of fire horizons as defined visually, (d) TC, (e) particle size composition, (f) ^{210}Pb / ^{137}Cs , and (g) bulk density and porosity.

7.3.2.3 Mineral magnetic properties of Cores 4, 5 and 7

The mineral magnetic profiles for Cores 4, 5 and 7 (Figure 7.18 to 7.20) all produced increased values for all of the magnetic parameters investigated for the surface layer in unit A (when compared with lower units) apart from the χ_{fd}/χ_{ARM} quotient. The charred and uncharred organic material mixed with fine sediment (i.e. units C in cores 5 and 7) produced increased values of χ_{lf} and χ_{ARM} in both cores. The material at the base of unit C in both of these cases produced an increase in $\chi_{fd\%}$. The units containing burnt organic matter, charcoal and fine sediments produced elevated values of $\chi_{fd\%}$, $\text{Soft}_{IRM\%}$, ARM/SIRM and χ_{fd}/χ_{ARM} . The units containing predominantly sandy material produced lower values in all magnetic parameters investigated, although fluctuations occurred around the depths at which fire horizons were located.

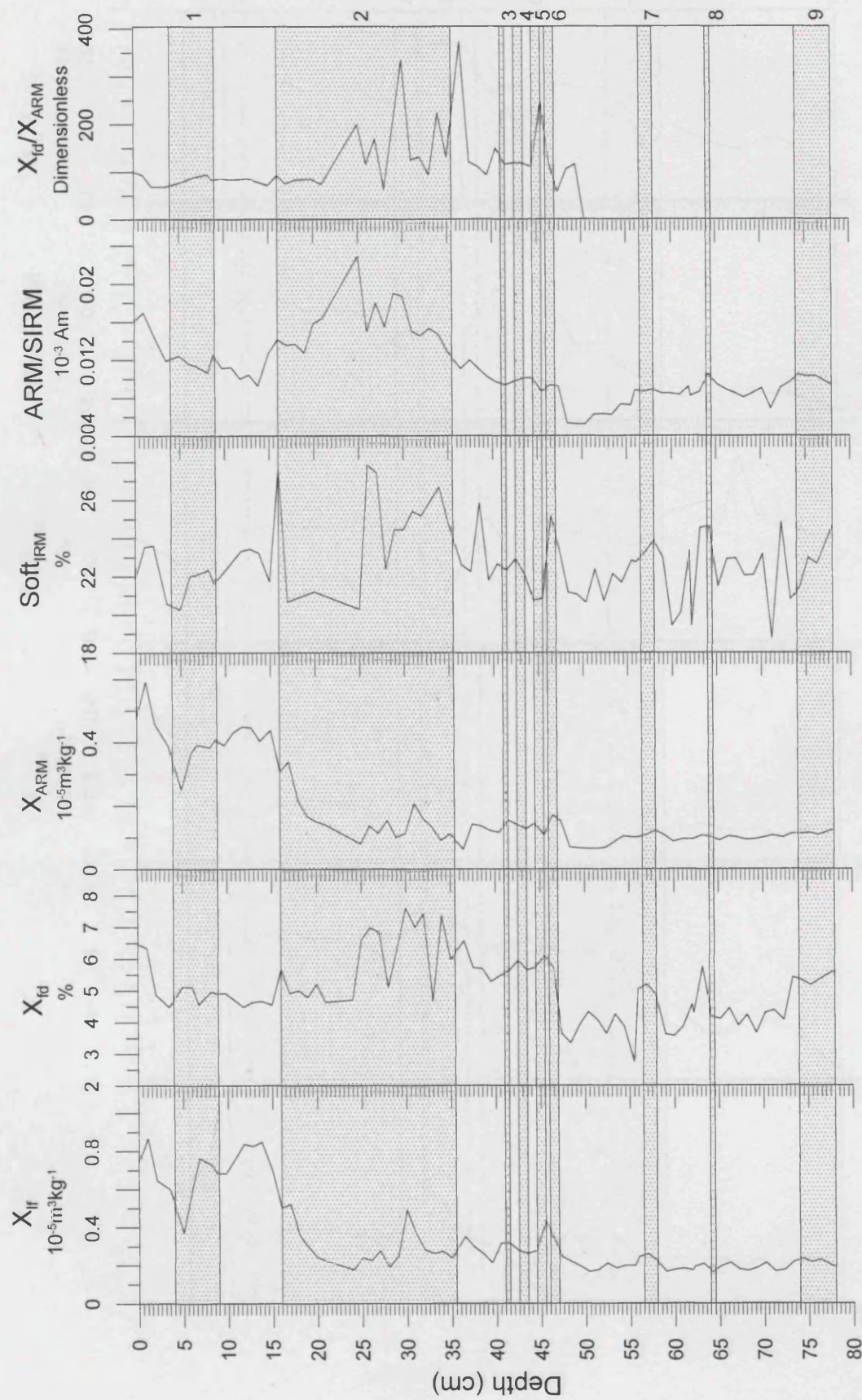


Figure 7.18: Mineral magnetic properties for Core 5.

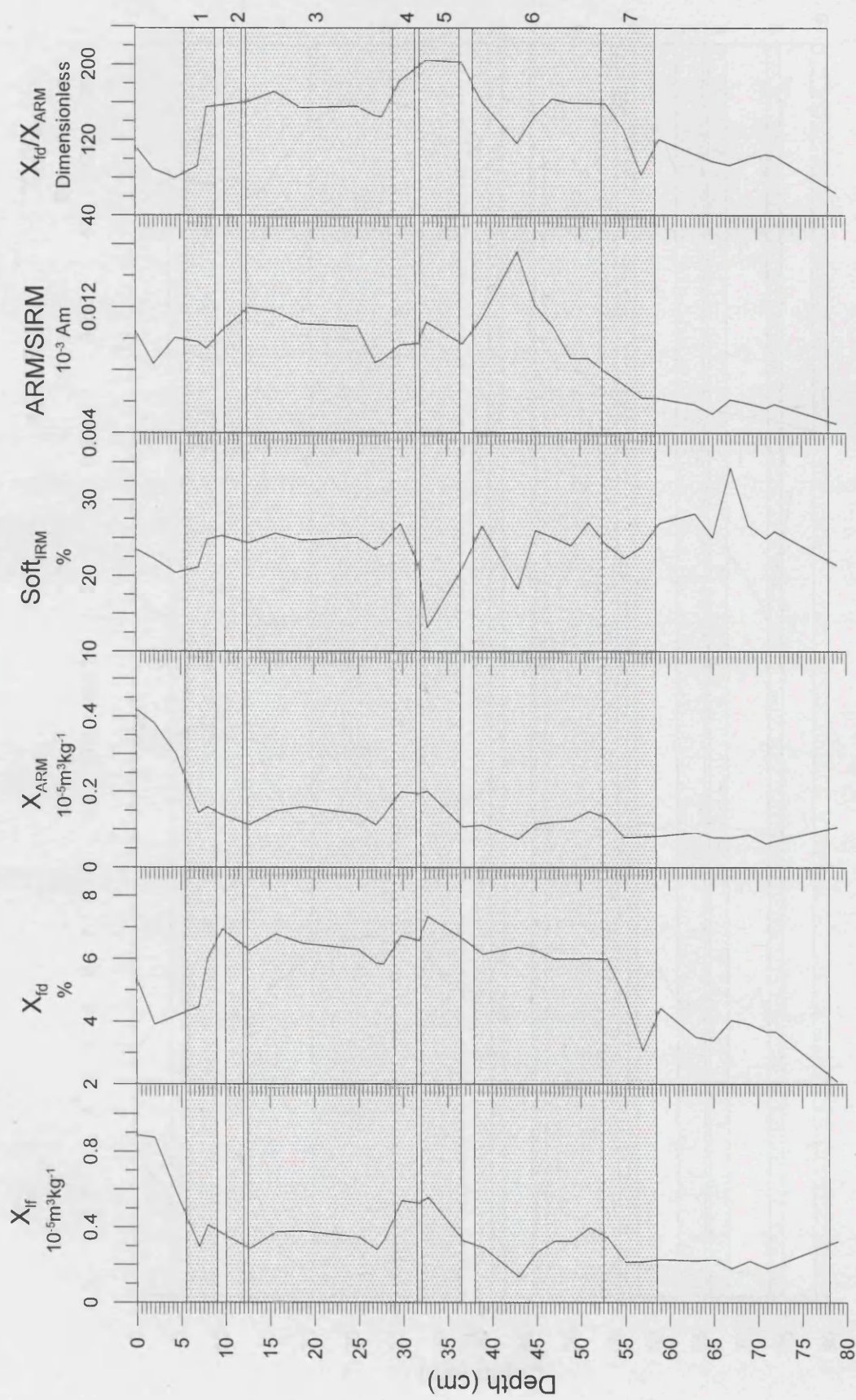


Figure 7.19: Mineral magnetic properties for Core 4.

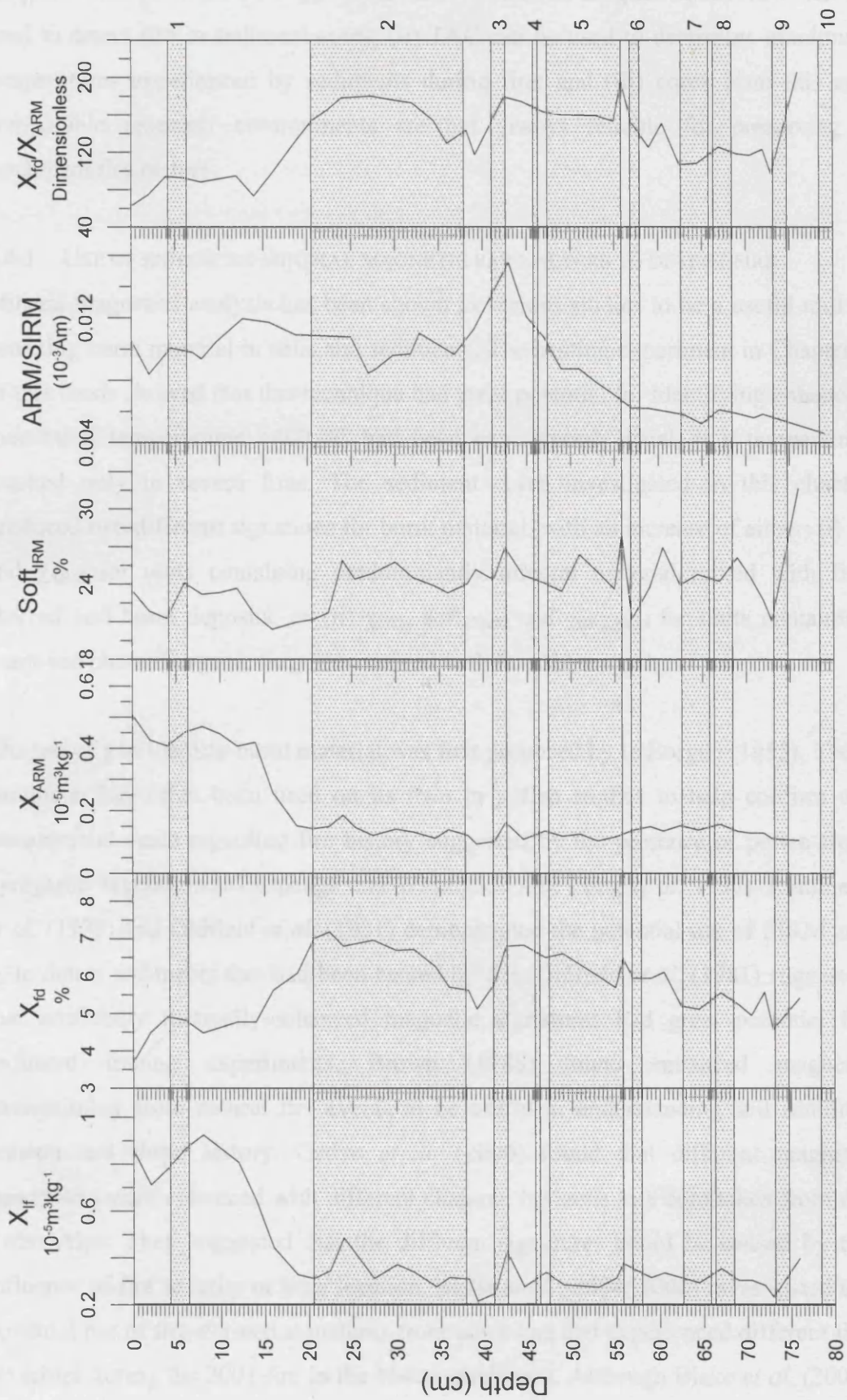


Figure 7.20: Mineral magnetic properties for Core 7.

7.4 DISCUSSION OF FINDINGS

This section discusses key findings from the sediment cores presented earlier in this chapter. These include the suggestions that: (i) mineral magnetic properties can be used to detect fire in sediment cores; (ii) TAC can be used to determine maximum temperatures experienced by sediments during fire; and (iii) cores from this and comparable reservoir environments are not always reliable for preserving a catchment fire history.

7.4.1 USE OF ENHANCED MINERAL MAGNETIC PARAMETERS TO DETECT FIRE

Mineral magnetics analysis has been shown in various studies to be a useful tool in detecting burnt material in soils and sediments. The heating experiment in Chapter 5 of this thesis showed that this technique had great potential for identifying enhanced material if temperatures $>400\text{ }^{\circ}\text{C}$ had been experienced, which is a temperature reached only in severe fires. The sediment cores investigated in this chapter produced two different signatures for burnt material, with an increase of either: (i) χ_{f} and χ_{ARM} for units containing predominantly mineral material mixed with fine charred and burnt deposits, or (ii) $\chi_{\text{fd}}\%$, $\text{soft}_{\text{IRM}}\%$ and $\chi_{\text{fd}}/\chi_{\text{ARM}}$ for units containing burnt and charred organic fragments mixed with fine silt and ash.

The use of χ to identify burnt material was first proposed by le Borgne (1955). The χ parameter has often been used on its own in pollen studies to help confirm the assumptions made regarding fire history suggested by the presence of pollen from pyrogenic vegetation (Millspaugh and Whitlock 1995; Long *et al.* 1998). Rummary *et al.* (1979) and Oldfield *et al.* (1981) demonstrated the potential use of SIRM and χ_{f} to detect sediments that had been heated by fire. Oldfield *et al.* (1981) suggested that artificially thermally-enhanced magnetic signatures had great potential for sediment tracing experiments. Brown (1988) found enhanced magnetic susceptibility from natural fire events to be useful in understanding soil stability, erosion and slope history. Gedye *et al.* (2000) found that different magnetic parameters were enhanced with different charcoal horizons in a core taken from the Swiss Alps. They suggested that the different signatures could be caused by the influence of fire severity or burn location. Blake *et al.* (2004; 2006) investigated the potential use of fire-derived signatures from areas that had experienced different fire severities during the 2001 fire in the Nattai catchment. Although Blake *et al.* (2004)

found different magnetic signatures were apparent for different slope locations and fire severities, Blake *et al.* (2006a) later found that these signatures could not be used for sediment source tracing due to the non-linearly additive nature of the magnetic quotients used to define the burnt material.

The work conducted in this thesis found that χ cannot be reliably used on its own to detect burnt sediment, and comparison with other parameters such as $\text{soft}_{\text{IRM}\%}$ and $\chi_{\text{fd}\%}$ should be used to confirm the presence of burnt material identifiable by eye. The lack of enhancement of χ in each burnt section of the sediment cores investigated in this study could be due to elevated background values from previous fires >50 °C. Therefore, fires >400 °C would have been required to produce enhanced χ . Such temperatures are rarely experienced during natural fires. However, the distinctive signatures derived from ridge-top samples as found by the heating experiment in Chapter 5 and by Blake *et al.* (2004) suggest that the χ values of freshly weathered material would become enhanced following low-severity fires.

The enhanced $\text{soft}_{\text{IRM}\%}$ and $\chi_{\text{fd}\%}$ parameters in this study within the units containing burnt organic matter intermixed with fine silt and ash could have been caused by enhanced ferrimagnetic minerals within the original organic material or by roasting of surface soil with wood fuel (McClean and Kean 1993; Linford and Canti 2001; Peters and Batt 2002). In the light of the dating evidence (Section 7.3.1.5), the suggestions that large charcoal fragments are not transported very far (Patterson *et al.* 1987; Clark 1988b, 1990) and the evidence that the 1964/1965 fires extending to the shores of the lake (Figure 3.10), it is likely that this material was derived from the foot-slope area adjacent to the coring site. The enhancement of χ_{f} and χ_{ARM} may have resulted from surface soil material either: (i) from foot-slope locations heated to temperatures in excess of 400 °C and subsequently exposed by removal of charcoal and burnt organic matter; or (ii) from ridge-top locations that had been subjected to heating to >50 °C, from where sediments had been transported easily down gullies due to their fine nature or lightness (in the case of charred debris).

The importance of these findings for this study and for fire-prone sandy Australian environments elsewhere is that χ cannot be used on its own to detect fire-derived sediments as it does not necessarily become enhanced. A more reliable indicator of

fire-derived deposits can be sought by simply investigating other magnetic parameters such as $\chi_{fd\%}$, or by comparison of mineral magnetic data with visual description or TC values. However, this does not apply in environments where (i) temperature thresholds differ, such as those examined by Brown (1988), where mineral magnetic susceptibility became enhanced at $\sim 200^\circ\text{C}$; or (ii) sufficient post-fire rainfall or annual snow melt occurs, which would remove pyrogenically enhanced material from the slopes, leaving unenhanced background signatures. In these environments, mineral magnetics, particularly χ , can provide a very powerful tool in detecting burnt sediments.

7.4.2 USE OF TAC TO DETERMINE SOIL TEMPERATURES DURING FIRE

There have been many attempts to ascertain the influence of fire severity on erosion and sediment redistribution within catchments. It has commonly been suggested that low severity fires only produce a small increase in sediment yields (Richter and Ralston 1982; Scott *et al.* 1998). However, research in the Nattai catchment area following the 2001 fire events did not support these suggestions. Shakesby *et al.* (2003) found that moderate and severe fires did not result in markedly different responses to erosion. Apart from the investigations by Blake *et al.* (2006a) to identify different magnetic signatures within a sediment core according to previous fire severity, no other studies have attempted to quantify the fire severity experienced by sediments. This chapter has demonstrated that the shape of TAC plot may be a useful tool to identify the maximum temperatures experienced by quartz soil grains within an assemblage.

TL χ properties have previously been used in archaeology to ascertain temperatures experienced by prehistoric heating in kilns and during the manufacturing processes of tools. These applications of TAC have already been discussed in Chapter 6. Only a few other studies have investigated the temperatures experienced by soil and sediment samples, including the work by Blake *et al.* (2006a), Blake *et al.* (2006b) and Blake *et al.* (2006c).

One of the limitations for this application of this technique has been the retention of thermal memory by single grains. This means that TAC is only capable of indicating the maximum temperatures previously experienced, rather than the most recent burn

temperature. However, it seems that it may be possible to distinguish between the samples heated in the distant past (e.g. *ca.* 10,000 years ago) that became buried and those heated recently.

In summary, this investigation of the temperatures experienced by burnt reservoir sediments has shown that it is possible to suggest fire severities experienced burnt soil samples and the timing of the burn event. In this case, as the burnt deposits seem to have been derived from a single fire event, suggested by the interpretation of the visual description, the questionable dating evidence and the similar temperatures experienced by the TAC of grains examined. These findings have revealed the potential for the development of this technique. Directions for further research that could be explored include: (i) investigation of the effect of different fire severities on different geological samples within the catchment; and (ii) investigation of material from a depositional environment spanning different geological timescales in order to ascertain how fire severity has varied in accordance with climatic variations.

7.4.3 RELIABILITY OF FIRE HISTORY RECORDS CONTAINED WITHIN SEDIMENT CORES FROM AUSTRALIAN RESERVOIR ENVIRONMENTS

The presence of burnt material in sediments has often been used to aid reconstruction of fire histories by identification of indicators such as pollen from pyrogenic vegetation and evidence of charcoal (Swain 1973; Long *et al.* 1998; Tinner *et al.* 1999; Gedye *et al.* 2000). For example, studies conducted in annually laminated lakes in Yellowstone National Park have shown a good correlation between dendrochronological and sediment records (Millsaugh and Whitlock 1995) however, the historical accuracy of this information was questioned when variability was found between fire histories in cores taken along a transect, although similar profiles were found for multiple cores from a single sample location (Whitlock and Millsaugh 1996).

Comparison of sediment cores obtained from similar locations has also been conducted for cores from the Burrinjuck Reservoir, southern New South Wales, by Wasson *et al.* (1987) and Tibby (2001). Both studies found a correlation between multiple cores, although Tibby (2001) acknowledged that differences in the thickness of correlated core sections was a result of deposition by density inflows.

This suggestion would explain the variability between the sediment cores obtained in this study, as the fine silty-clay deposits contained within the top 3-5 cm were present for all the cores obtained for this study (overlying the massive fire derived deposits likely to have been deposited by density currents in cores 4-7 and the massive sandy deposits in cores 1-3).

Similarly to this study, Wasson *et al.* (1987) and Mooney *et al.* (2001) compared charcoal bands and documented fire events. Wasson *et al.* (1987) found that each fire event within the Burrinjuck reservoir catchment between 1939 and 1982 was recorded within the sediment profile. This contrasts with findings of this study in the Nattai and those of Mooney *et al.* (2001) (for a lake in NSW) which showed that charcoal evidence does not always corroborate documented fire events within recent history. This may have been influenced by drought-dominated conditions in Australia that have occurred since the study by Wasson *et al.* (1987) was conducted, and highlights the importance of post-fire rainfall events in ensuring that a record of fire is contained within the sediment profile.

Although Wasson *et al.* (1987), Tibby (2001) and the present study have found similarities between cores from reservoir environments, it is likely that fluctuations in water level as shown in Figure 3.12 would affect the location of inflows and create migratory depositional environments (Leeder 1982; Hakanson and Jansson 1983; Clark and Wasson 1986; Annandale 2005).

The variable buoyancy of charcoal (Davis 1967; Renfrew 1973) is likely to determine whether or not burnt material will be transported as suspended sediment or entrained within the bedload of a stream entering a reservoir. The size and integration of the charcoal within the sediments would influence the likelihood of the material becoming re-entrained by turbid flows (Davis 1967) or by rising water levels within the reservoir. These factors together with: (i) the lack of post-fire rainfall following some fire events; and (ii) the proximity of fire to the foreshores of the reservoir; are factors likely to prevent accurate chronologies of fire events being obtained from the sediment cores from the Nattai arm.

7.4.3.1 Post-fire rainfall

One of the main factors influencing the movement of burnt material through a catchment to its final deposition in a sedimentary environment is the occurrence of post-fire rainfall. After a fire has occurred, the slopes are more susceptible to erosion and transfer of material to the river environment following fire events as a result of reduced vegetation and litter cover and often decreased aggregate stability (Andreu *et al.* 2001).

In chaparral environments, low-intensity rainstorms have been shown to trigger debris flows (Wade *et al.* 1987; Weirich 1987) and geomorphic change (Germanoski and Miller 1995). A different situation becomes apparent in sandstone landscapes of Australia, where severe rainstorms appear to be required to produce significant post-fire erosion and movement of sediment to river channels (Blong *et al.* 1982; Atkinson 1984). Similar findings were obtained by Shakesby *et al.* (in press) following the 2001 fires in the Nattai catchment. They found that less material than might have been expected was removed from the slopes due to rainfall that was comparatively moderate in intensity and amount in the first year or so after fire and much of the soil underwent only localized redistribution on the slopes.

In general, erosion of the south-east Australian landscape has been dependent on whether flood- or drought- dominated regimes are prominent (Warner 1987; Erskine and Warner 1988). There has been much evidence to suggest that catastrophic flood events are required to trigger major mass movement of debris (Erskine and Melville 1983). Tomkins *et al.* (in press) have recently concluded that wildfires in recent times have been relatively ineffective in denudation terms compared with longer-term Holocene and pre-Holocene denudation. They have estimated that wildfires only make a modest contribution to the long-term denudation rate of 26 mm kyr^{-1} determined from a range of evidence. The discrepancy between the wildfire-induced denudation and long-term rates, they argue, could be explained by high-magnitude low-frequency catastrophic floods and mass movements that are unrelated to fire. The massive deposit of burnt organic debris and fine sediments seen in units C and D of core 6 (Figure 7.6) and dating evidence both suggest that this material is likely to have been deposited during a high magnitude-low frequency catastrophic flood event. This confirms the inferences of Tomkins *et al.* (in press) and the suggestion

proposed by Blake *et al.* (2004) that 89% of total reservoir sedimentation in Lake Burragorang could be attributed to catastrophic post-fire rainstorm events.

7.4.3.2 Proximity of fire to the coring site

The second possible explanation for the lack of a record of fire events in the sediment cores since the 1964/1965 fire events could be the location of fires within the catchment. The 1964/1965 fire event extended to the shoreline of the Nattai river near to the coring location (Figure 3.10a), whereas more recent fires did not reach this position (apart from the 2001/2002 fires), leaving the vegetation and soils in a stable state.

The delivery of sediment through a catchment has been shown to be strongly influenced by its size (Dearing 2005). Gavin *et al.* (2003) and Laird and Campbell (2000) found evidence to suggest that macroscopic charcoal deposits were only present when fires occurred within close proximity to the edge of the lake. Gavin *et al.* (2003) suggested that this charcoal source area was within about 500 m of the shore. However, this distance is also likely to be influenced by the topography and rainfall events within the catchment. Areas of steep terrain are required to aid this movement of material through the catchment (Clark 1988a), while fine charcoal and burnt material may also enter the lake by wind-blown transport (Clark 1988a). An additional factor in this study that could influence the record of fire events within the sediment column could be related to the proximity of fire to the shoreline, as the 1964/5 fire occurred up to the edge of the lower Nattai River. Although the 2001/2002 fire event also covered a large area around the banks of the lower Nattai River, this event has not been reflected in sediment deposits in the dated cores. This may be as a result of the lack of high-magnitude flow events that occurred up to 2003 (Figure 3.7 and 3.12 and Table 3.5) (when the sediment cores for this thesis were collected). It also suggests that there was no transport of burnt material originating from the 2001/2002 fires into the reservoir, or at least to the area where these cores were obtained. The burnt material mixed with fine ash and silt (e.g. in unit D in Core 6) contained charcoal with diameters $>50\text{ }\mu\text{m}$. Despite its lightness and potentially easy transport, this suggests that the charcoal was not transported very far (Patterson *et al.* 1987; Clark 1988a, 1990; Whitlock and Millspaugh 1996; Long *et al.* 1998), which supports the view that the burnt material did indeed date

from the 1964/1965 fires owing to: (i) its proximity to the coring locations; (ii) the visual description identifying an increased content of burnt material; and (iii) the increased TC values.

These findings imply that: (i) a lack of post-fire rainfall following fire events, and (ii) proximity of fire to the foreshore of the reservoir is a factor likely to influence the accurate chronological reconstruction of fire events from sediment cores. Although this study has shown that cores obtained from reservoir environments appear to contain different chronologies, matching of core stratigraphies is possible by comparing the massively deposited sections of burnt material. However, the variable chronologies obtained for cores 1-3 and 4-7 show that depositional environments can cause substantial variation along a narrow drowned reservoir inlet like that of the Nattai arm. These factors question the reliability of studies that have attempted to reconstruct longer-term fire chronologies in Australian environments, such as that by Black and Mooney (2006).

These findings are likely to be applicable to other Australian environments, but may not be relevant in other climates where post-fire rainfall occurs more reliably or annual snow melt occurs, in which case there is sufficient hydraulic energy to transport material through a burnt catchment. Only in small burnt catchments feeding a reservoir might there be sufficient likelihood of sediment transfer from slopes to catchment outlet such that the reservoir sediments will contain a reliable historical record of catchment fire events. The continued drought conditions in Australia and the resultant lowering of many reservoir and lake water levels are currently providing a unique opportunity to investigate the exposed deltaic sedimentary environment and features of the old Nattai channel and other channels in Lake Burragorang and other reservoirs. Therefore, there is currently an unprecedented opportunity to gain a more complete assessment of the variability of sediments along the courses of rivers as they enter reservoirs than has been possible in the last few decades.

7.5 CHAPTER SUMMARY OF KEY FINDINGS

This section summarises the key findings from this chapter and relates them to the main aims and research questions addressed by the experiments outlined at the beginning of this chapter. These include the investigation of: (i) the appearance of fire-modified mineral magnetic and TAC properties in the sediment core profiles (Stage 5); and (ii) the reliability of fire histories contained within closely spaced reservoir sediment cores (Stage 6).

- The different magnetic signatures that became enhanced with heating in Chapter 5 were found to some extent within sediment cores. Two different signatures were apparent for the sediments investigated, which varied according to the composition of material within the units: these were (i) charcoal and ash dominated material, which showed enhancement of $\chi_{fd\%}$ and $soft_{IRM\%}$, and (ii) mineral material and charred and uncharred organic matter, which produced enhanced values of χ_{lf} and χ_{ARM} . The enhanced magnetic signatures confirmed the visual description of burnt material and elevated TC results.
- TAC of multi-grains from different depths of Core 6 suggest that each part analysed had previously experienced temperatures ranging between 480 and 500 °C. The longevity of the enhanced $TL\chi$ potentially poses a problem as only maximum temperatures and not the most recent ones can be identified. Maximum temperatures experienced by individual grains showed that the majority of grains appeared to have been exposed to high severity fires reaching temperatures of between 400 and 600 °C, suggesting that severely burnt sites were a dominant source of material for sedimentation.
- The dating evidence enables a tentative suggestion to be made that only the 1964-5 fire event is represented in the fire-related sediment in the cores.
- The factors that may have prevented the recording of all fire events in the sediment cores include: (i) the lack of sufficient post-fire rainfall to remove burnt material from the catchment into the reservoir, (ii) the proximity of the fires to the Nattai foreshores and to the coring location (apart from 1964/65 fires); and (iii) fluctuating water levels of the reservoir producing different sedimentary environments. The dependence of chronological records on these aforementioned factors highlights the possibility that reservoir sediments from environments like those investigated here may be less reliable for accurately reconstructing fire histories than has been supposed by some workers.

8 SYNTHESIS AND CONCLUSIONS

8.1 INTRODUCTION

The work presented in this thesis was aimed at addressing four research questions that arose from reviewing the literature summarised in Chapter 2 and also from developments during the work carried out by the NERC-funded URGENCY project following its initial research findings in 2002, immediately after the 2001/2002 fire event had occurred (described in Chapter 3). Four main research gaps in understanding of the detection of burnt material in soils and sediments have been addressed in this thesis. These include the need for developing or assessing: (i) methods of detecting fire events in soil material and sediments in the Australian environment; (ii) methods of reconstructing soil temperatures experienced during fire; (iii) methods for the detection of fire events in reservoir sediment cores; and (iv) the reliability of fire histories reconstructed from reservoir sediments. From these research gaps the following five aims were developed for this thesis. These were to assess:

- 1 temperature thresholds apparent for thermally-enhanced soil parameters;
- 2 thermal memory of soil and sediment samples;
- 3 the influence of catchment location and fire history in producing distinctive magnetic signatures;
- 4 the applicability of mineral magnetic analysis and TAC in identifying burnt material within sediment cores; and
- 5 the reliability of sediment cores obtained from dynamic reservoir environments as indicators of previous catchment fire events.

Chapter 5 investigated the temperature thresholds required to produce enhancement of mineral magnetic properties and found that temperatures $>450^{\circ}\text{C}$ were required to produce an enhancement of foot-slope samples that retained signatures from previous burn events. Chapter 6 investigated the temperature thresholds required to produce enhancement of TAC and found that this technique was capable of indicating both the previous temperatures experienced in the range $0\text{--}800^{\circ}\text{C}$ and the timing of the heating. Chapter 7 explored the potential application of mineral magnetic measurements and TAC for detection of fire-derived material in sediment

cores and found that both of these techniques could successfully be used, provided a full suite of mineral magnetic measurements was acquired. Additionally, the reliability of sediment cores taken from reservoir environments was assessed. This showed that the record of fire events was greatly influenced by the occurrence of post-fire rainfall events, which are not always guaranteed during fire-prone drought conditions.

In this chapter, (Chapter 8) the results from chapters 5-7 are synthesised and the use of mineral magnetism and TAC for the detection of burnt soils and sediments together with the reliability of sediment cores for reconstructing fire history are evaluated. This chapter has six main sections: in Section 8.2 the key findings from each chapter are presented. In Section 8.3, the detection of fire events in soil material and sediments in the Australian environment are evaluated. In Section 8.4, the potential use of mineral magnetic analysis and TAC in reconstructing soil temperatures experienced during fire is explored. In Section 8.5, the potential application of mineral magnetic measurements and TAC for detecting fire events in reservoir cores is investigated. In section 8.6 the reservoir sediment cores are evaluated for their use in reconstructing fire history and severity. Finally, in Section 8.7, conclusions are drawn about the main research gaps that this thesis has addressed.

8.2 KEY FINDINGS

The key findings of this study are summarised in Figure 8.1 in relation to the initial aims identified in Chapter 4. These have provided the basis of the discussion sections at the end of Chapters 5-7. The key findings are that: (1) there is a lack of enhancement of χ for temperatures $<400\text{ }^{\circ}\text{C}$; (2) enhancement of a variety of magnetic grain sizes by heating was suggested by increases apparent in a range of magnetic parameters; (3) suppression of magnetic enhancement occurs at temperatures $>400\text{ }^{\circ}\text{C}$ when heated in a reducing atmosphere; (4) the magnitude of the $110\text{ }^{\circ}\text{C}$ TL χ peak increases linearly for unheated samples when compared with those heated to $\leq 400\text{ }^{\circ}\text{C}$; (5) TAC shape and the peak enhancement of TAC can be used to infer the previous thermal history of individual grains in a soil assemblage; (5) the shape of TAC can be used to infer the timing and temperature reached during previous heating; (6) heating an unexposed unheated bedrock sample to

temperatures $>50^{\circ}\text{C}$ produces a change in TL χ properties; (7) mineral magnetics can be used to detect heating by fire in sediment cores, although additional consultation of a range of parameters is required for reliable assessment; (8) TAC can be used to suggest the maximum temperatures experienced by sediments during fire; and (9) cores from reservoir environments in fire-prone terrain are not necessarily reliable for preserving a catchment's fire history.

| | | | | | |
|--------------|---|---|---|--|---|
| Aim | Assess temperature thresholds apparent for thermally enhanced soil parameters. | Assess thermal memory of soil and sediment samples. | Assess the influence of catchment location and fire history in producing distinctive magnetic signatures. | Assess the application of mineral magnetics and TAC in identifying burnt material within sediment cores. | Assess the reliability of sediment cores obtained from dynamic reservoir environments as indicators of previous catchment events. |
| Sample | Laboratory investigation using soil samples from long unburnt ridge-top, mid-slope and foot-slope sites and an unequivocally unheated bedrock sample. | | | | |
| Technique | Mineral magnetics | TAC | Mineral magnetics | Mineral magnetics | TAC |
| Results | 220-270 °C >400 °C | 0-200 °C 200-600 °C 600-800 °C | Maximum temperature experienced by progressive heating and cooling. | Maximum temperature ascertained by peak value of TAC. Timing of heating ascertained by response to 10 Gy β dose. | Location in catchment influences response to heating due to thermal memory and mineralogy of the sample. |
| Implications | Mineral magnetic measurements and thermal activation characteristics can be used to identify fire events in soils and sediments, and reconstruct temperatures reached. However, the use of Australian reservoir sediments for the purpose of reconstructing catchment fire events is questionable due to the high dependence of post-fire rainfall required to remove material from the slopes to the sediment column and the difficulty in establishing dates to the precision required to distinguish between different fire events within the recent past. | | | | |
| | Reservoir environments produced cores with similar stratigraphy apart from deposits formed by density currents. Unreliable fire records within the sediments are caused by insufficient post-fire rainfall to transport burnt material from the slopes to the reservoir. | | | | |
| | Shape of TAC can be used to detect burnt material and maximum temperature experienced by soil during fire. | | | | |
| | A range of magnetic parameters is required, as X_{ir} does not always show enhancement | | | | |
| | Mineral magnetics, TAC, dating & ancillary data | | | | |

Figure 8.1: Schematic diagram summarising the findings for each research aim identified in Chapter 4 and the overall implications.

8.3 RECONSTRUCTING SOIL AND SEDIMENT TEMPERATURES

Soil temperatures reached during fire have been shown to have an impact on the levels of post-fire erosion, due to a number of factors including vegetation destruction (Bradstock and Auld 1995) and the enhancement or destruction of soil water repellency (Doerr *et al.* 1998). The level of destruction of vegetation cannot be used to assess soil temperatures reached during fire, as demonstrated by Shakesby *et al.* (2003) who found a poor correlation between vegetation destruction and soil temperatures reached. Doerr *et al.* (2004) demonstrated that soil water repellency was eliminated following laboratory-based heating to temperatures between 260-340 °C for three long unburnt soils from eucalypt forests in south-east Australia. Assessment of soil water repellency for samples collected from the Nattai catchment immediately following the 2001 fire by Shakesby *et al.* (2003) suggested that temperatures in excess of 260-340 °C had been reached. In the present study, temperature thresholds of mineral magnetic measurements were investigated to ascertain whether this soil property could also be used to suggest whether or not temperatures >260-340 °C had been reached.

Blake *et al.* (2004) suggested that river and reservoir sediments from the 2001 fires in the Nattai were predominantly derived from ridge-top locations subject to varying fire severities, rather than from mid-slope and foot-slope locations that had experienced high severity fires. These findings led to the examination in the present study of whether or not temperatures experienced during fires could be established for *in situ* and redistributed soil on hillslopes and in downstream reservoir sediments using mineral magnetics. This was done in view of the work by Rummery *et al.* (1979), which showed persistence of enhanced magnetic parameters in sediments. Temperatures reached in the soil and sediment indicated by the destruction or retention of soil water repellency (Doerr *et al.* 2006) could not be applied to the core sediments due to the destruction of this soil property following prolonged wetting (Ritsema *et al.* 1998). The present study has shown that temperature thresholds in the soil, associated only with high severity fires (>450 °C), were required to produce enhancement of mineral magnetic properties of samples from foot-slope locations. This led to the investigation of TAC, to ascertain whether or not this long-lived soil property could be used to suggest if soil temperatures >200 °C had been experienced.

8.3.1 PROBLEMS WITH USING MINERAL MAGNETIC MEASUREMENTS TO RECONSTRUCT SOIL AND SEDIMENT TEMPERATURES

The main problem encountered when investigating mineral magnetic parameters and TAC was the retention of a signal from previous fire events. None of the magnetic parameters investigated for the foot-slope sample became enhanced until temperatures $>450^{\circ}\text{C}$. The high temperature threshold required to produce enhancement of magnetic properties following fire is similar to findings by Oldfield *et al.* (1981), Linford and Canti (2001) and Weston (2002) who investigated sandy soils in the UK. Different temperature thresholds were found in studies investigating clay-dominated soils, which showed enhancement at temperatures $>200^{\circ}\text{C}$ for both the UK (Linford and Canti 2001; Weston 2002) and a chaparral site in California (Brown 1988).

8.3.2 PROSPECTS FOR USING MINERAL MAGNETIC MEASUREMENTS TO RECONSTRUCT TEMPERATURES REACHED IN SOIL AND SEDIMENT

Measurement of χ changes during progressive heating of soil samples showed different responses of the mid-slope and ridge-top samples when compared with the foot-slope samples. The mid-slope and ridge-top samples showed modifications when heated to $50\text{--}60^{\circ}\text{C}$. Taylor and Schwertmann (1974) observed similar temperature thresholds for magnetic enhancement to those samples investigated in this research on soils from the Lake Buragorang catchment. The reason for changes occurring at such low temperatures is likely to have been as a result of the samples never previously experiencing heating. A possible explanation for this is that the samples had been derived from subsurface soil or weathered bedrock with heated material being removed from these mid-slope and ridge-top sites by post-fire erosion. This was confirmed during a reconnaissance visit to the catchment in 2002 in the form of fine white sand on the ridge tops, interpreted as material newly-weathered from exposed bedrock by the passage of the fire. Additionally, Blake *et al.* (2004) suggested that the ridge tops provided a dominant source of material for downstream deposits along the channel of the Nattai River. The minimal enhancement of the FS sample with heating to low temperatures could be explained in terms of the foot-slope zones acting as sediment stores for heated surface soil redistributed from mid-slope and ridge-top positions, as argued by Shakesby *et al.* (2003) and Blake *et al.* (2005). The heated material is thought to have experienced

mixing with previously unheated subsurface soil through bioturbation, which is thought to be particularly effective in the sandstone terrain of south-east Australia (Dragovich and Morris 2002; Shakesby *et al.* 2006). This would have produced a homogenised elevated background mineral magnetic signal retaining a memory of previous heating. However, the unheated samples can still be enhanced, as shown by Blake *et al.* (2006a) who found lower background values of magnetic measurements of long unburnt soils when compared to recently burnt soils. These results suggest that final enhancement of mineral magnetic soils from different slope locations occurs at temperatures of $>400^{\circ}\text{C}$.

8.3.3 FUTURE DIRECTIONS FOR USING MINERAL MAGNETIC MEASUREMENTS TO RECONSTRUCT SOIL AND SEDIMENT TEMPERATURES

Useful approaches in applying mineral magnetic measurements to the reconstruction of heating by fire from *in situ* and redistributed soil could include: (i) assessment of responses of a full suite of mineral magnetic parameters rather than selected ones for sites that may have acted largely as sources rather than sinks of eroded sediment, as is the case for the mid-slope and ridge-top sites in the present study; (ii) investigation of the responses of temperature thresholds from different particle size fractions to heating, thus enabling the potential of different signatures to be used for sediment source tracing; (iii) investigation of the proportion of heated material required to cause enhancement of the assemblage (Crowther 2003); (iv) reconstruction of the temperatures reached by material deposited in lake sediments in order to determine the relative contributions of sediment from areas subject to different fire severities.

8.3.4 PROBLEM WITH USING TAC TO RECONSTRUCT SOIL AND SEDIMENT TEMPERATURES

The main problem encountered in trying to reconstruct the temperature thresholds required to modify TAC in soil and eroded sediment was the possibility of retention of a thermal memory from previous fire events. As a consequence, it was possible only to deduce the maximum rather than the most recent temperature reached. This problem was also encountered by Lahaye *et al.* (in press).

8.3.5 PROSPECTS FOR USING TAC TO RECONSTRUCT SOIL AND SEDIMENT TEMPERATURES

Furnace-heating of a previously unheated bedrock sample showed that the shape of the TAC graph and the maximum value obtained could be used to ascertain the maximum temperature experienced by the samples. Despite the limitation of the retention of the maximum temperature experienced, measurement of TAC following a 10 Gy β dose enabled the timing of heating to be established. This not only enabled temperatures experienced by soil during fire to be reconstructed, but also detection of the temperatures experienced by sediment.

8.3.6 FUTURE DIRECTIONS FOR USING TAC TO RECONSTRUCT SOIL AND SEDIMENT TEMPERATURES

In the future, the exploratory application of TAC in the present study could be extended to: (i) examining temperature thresholds required to modify TAC in other types of sandstone (as, for example sandstone from the Narrabeen complex in the south-east Australian context), or for geological samples that dominate other catchments; (ii) refining the technique in establishing patterns of redistribution of soil on wildfire-affected hillslopes; (iii) applying the technique to lake rather than reservoir sediments and to a small rather than a large catchment, such that the pattern of fire events is easier to unravel; and (iv) exploring heating temperatures reached and the time necessary for zeroing the TAC signal over geological time scales.

8.4 DETECTING FIRE EVENTS IN RESERVOIR CORES

As already mentioned in Section 8.3, both mineral magnetic and TAC soil properties can be used to determine heating experienced by soil samples. This section deals with problems and prospects associated with interpreting the heating experienced by eroded soils deposited in reservoir sediments.

8.4.1 PROBLEMS WITH DETECTING FIRE EVENTS IN RESERVOIR CORES

Within reservoir sediment cores, a comparison of units containing burnt material with mineral magnetic parameters suggested that different signatures were formed in association with different types of burnt material. $\chi_{fd}\%$ and $\text{soft}_{IRM}\%$ showed enhancement in sedimentary units where organic matter and charcoal dominated. On the other hand, in units where mineral material was mixed with charred and un-charred fragments, χ_{lf} and χ_{ARM} increased. This shows that not all magnetic parameters always become enhanced where burnt material is present. Therefore the use of χ on its own is not always reliable in detecting burnt material and a range of parameters needs to be consulted.

The long-term retention of a thermal memory from previous heating events seems to have affected some of the grains since they produced TAC shapes indicative of heating prior to reservoir dam construction. However, the majority of the TAC obtained for single-grain measurements suggest they had been heated recently to similar temperatures, which are associated with high severity fires (between 450 and 500 °C). The similarity in the temperatures suggests that all the sediment was most likely deposited following a single fire, which supports the tentative inferences made by the dating evidence and the relatively limited runoff and erosion associated with most post-dam construction rainstorms is thought to be the 1964 event.

8.4.2 PROSPECTS FOR DETECTING FIRE EVENTS IN RESERVOIR CORES

Mineral magnetic and TAC soil properties have both been shown to be reliable indicators of fire heating in reservoir sediments, although a full suite of mineral magnetic parameters is required to be successful. The sediment cores that were obtained from the Nattai arm of Lake Burragorang did not contain records of all fire events which is mainly attributable to relatively limited runoff and erosion in the critical first few months after many of the fires but also possibly due to the dynamic

nature of the reservoir environment in the Nattai arm (i.e. the influence of considerable reservoir level changes on sedimentation).

8.4.3 FUTURE DIRECTIONS FOR DETECTING FIRE EVENTS IN SEDIMENTARY ENVIRONMENTS

The use of mineral magnetics and TAC to identify fire events and the temperatures reached by soils and sediments could be explored further by: (i) comparing these properties for *in situ* hillslope soils and downstream channel and lake sediments in a small catchment; or (ii) investigating longer fire records in other sedimentary environments such as swamps or lakes. Investigation of additional temperature-sensitive soil properties, such as geochemical indicators (Blake *et al.* 2006b) or levoglucosan (Ellias *et al.* 2001), could also provide further confirmation of temperatures experienced by sediments during fire.

8.5 RECONSTRUCTING FIRE HISTORY USING RESERVOIR SEDIMENTS

Fire histories have been reconstructed by using burnt material contained within sediment cores from lakes in Europe (Gedye *et al.* 2000), North America (Brown 1988) and Australia (Black and Mooney 2006). However, the difficulty in reconstructing fire history in the present study suggests that the combination of reservoir environment and unreliable post-fire rainfall, as is the case for the present study in south-east Australia, may not allow accurate reconstruction of fire events from reservoir sediment cores.

8.5.1 PROBLEMS WITH RECONSTRUCTING FIRE HISTORY FROM RESERVOIR SEDIMENTS

The sediment cores obtained for this study indicate a problem with the use of reservoir sediments in reconstructing fire events within the Nattai catchment, as only burnt material from one fire event was apparent. This was attributed to a combination of the lack of sufficient post-fire rainfall and lower water levels following fire events since 1964/1965.

The burnt material in Cores 4-7 appeared to have been derived from turbid inflows. Correlation of all cores was possible except in the case of sediments apparently deposited by density currents, as was also found by Tibby (2001). As the deposits

derived from the 1964/65 fire, it is possible that more recent fire events could be recorded further upstream of the lake coring sites in similar massive deposits, laid down at a time when the water level was higher. This is likely to have been the case as sediment within the core obtained by Blake *et al.* (2006b) from the Nattai arm 'upstream' of the coring sites in the present study contained material interpreted as dating from the 2001-2 fire. Whitlock and Millspaugh (1996) found that there was a considerable time-lag for burnt material entering a lake, and that material was moved incrementally further downstream in high velocity flows. Owing to the general lack of large flow events in the Nattai catchment after recent fires, material from these events may not yet have been transported very far downstream. Whitlock and Millspaugh's (1996) research was conducted in a lake environment in North America and suggested that the optimum coring location was at the deepest part of the centre of the lake. It was not feasible to follow this principle for Lake Burragorang, as the deepest part of the reservoir exceeds 100m, which was far beyond the working depth of the equipment used in this research. Within the Nattai arm of Lake Burragorang, it is also difficult to assess where deposits from the Wollondilly (Figure 3.2) may encroach.

8.5.2 POTENTIAL FOR RECONSTRUCTING FIRE HISTORY USING RESERVOIR SEDIMENTS

Although the records of fire in the reservoir cores in this study are limited by the heavy dependence on the occurrence of sufficient post-fire rainfall and runoff to lead to deposition of sediment following fire events, reservoir sediments represent one of the few available potential records of fire history as Australian trees do not produce annual growth rings which limits the reliability of dendrochronological records and records of lacustrine charcoal are often location specific (Gavin *et al.* 2003) and affected by reworking (Clark 1988). In the present study, the fire history was known for the reservoir catchment from detailed documentary evidence, but this is not necessarily the case elsewhere where few other records of fire tend to be available. The findings of this study suggests that where there is more reliable deposition of sediment into a reservoir and where reservoir levels are less erratic than for Lake Burragorang, with care, reservoir sediments can be used to reconstruct fire history.

8.5.3 FUTURE DIRECTIONS FOR RECONSTRUCTING FIRE HISTORY USING RESERVOIR SEDIMENTS

Future directions for reconstructing fire history using reservoir sediments are to: (i) investigate suspended flow data in relation to fire events and post-fire rainfall; (ii) obtain cores located along a transect that ensures the inclusion of sediments from fire events reaching the reservoir when the water is at different levels; (iii) obtain sediment cores from deeper areas within the reservoir; and (iv) make comparisons of current river morphology with original floodplain evidence from aerial photographs to gain a better understanding of development of reservoir sedimentation patterns.

8.6 CONCLUSIONS

The findings of the present study in relation to the research gaps outlined in Chapter 2 can be briefly summarised under the following headings:

(i) Methods of detecting fire events in soil material and sediments in the context of the sandstone terrain of south-east Australia

It has been shown that mineral magnetics can provide a useful indicator of burnt material. However, this is dependent upon whether or not there is an enhanced background signature. A full suite of mineral magnetic parameters needs to be consulted in order to enable identification of burnt material. Although it requires considerable development, the exploratory application of TAC in the present study has shown it to be useful in detecting heating as a result of fire in soils and eroded sediment.

(ii) Methods of reconstruction of soil temperatures experienced during fire

Mineral magnetic properties of Australian soils were found to become enhanced at temperatures $>450^{\circ}\text{C}$. This high temperature compared with other studies could be due to previous mineral magnetic enhancement from previous fires. The application of TAC to reconstruct soil temperatures and not just the incidence of fire showed great potential. Although it was only possible to detect the maximum temperature ever experienced, assessment of the timing of the heating could be used to suggest whether or not heating occurred recently or a long time ago.

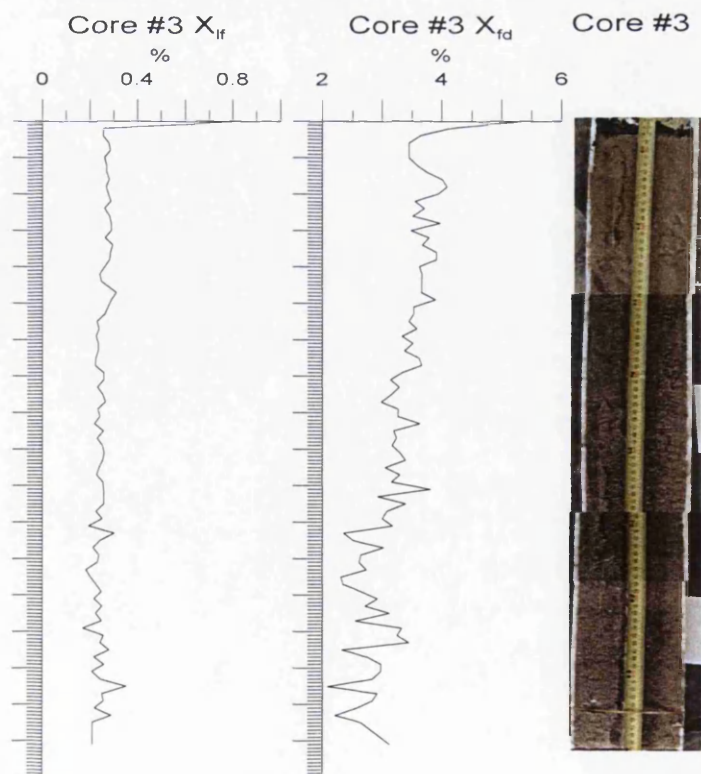
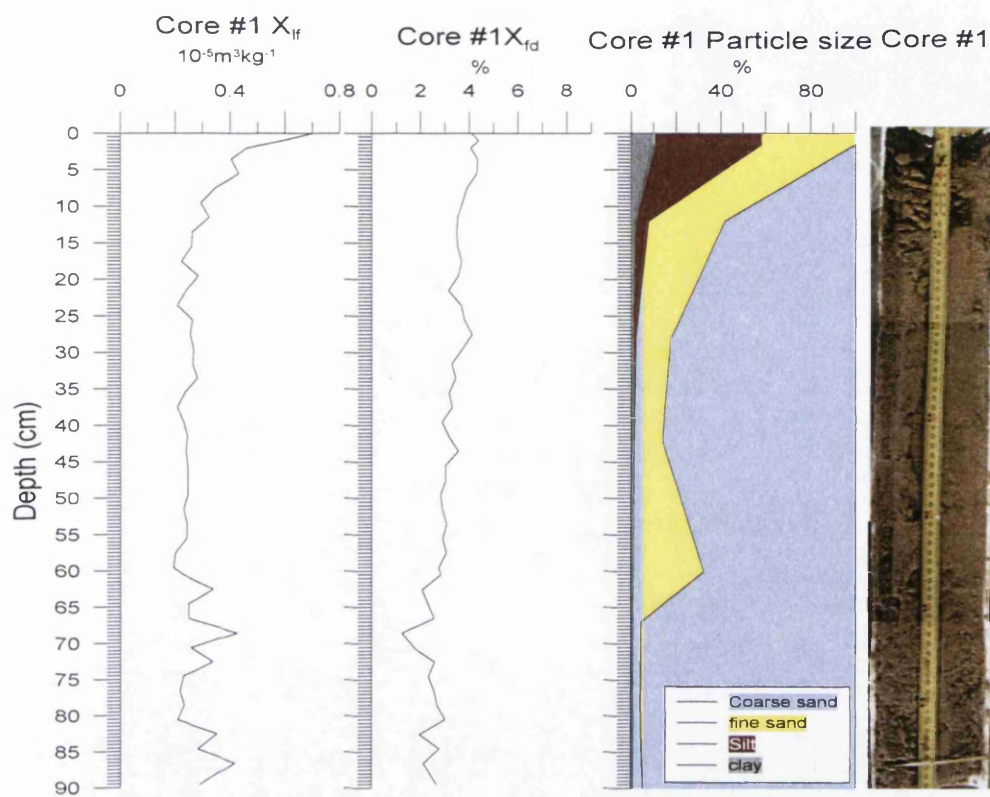
(iii) Methods for the detection of fire events in reservoir cores

The application of mineral magnetics and TAC to sediment cores showed that both techniques could enable detection of burnt material, although a full suite of mineral magnetic parameters would need to be acquired to obtain acceptable levels of accuracy. TAC measured on eroded sediments of known age in sediment sinks such as reservoirs and lakes could provide a great insight into fire severity over geological time and storage retention time of burnt material in sediment stores within a catchment.

(iv) The reliability of fire histories reconstructed from reservoir sediments

Fire histories contained within reservoir sediments, like those in this study from the drought-prone south-east Australian environment, may be difficult to reconstruct because of the unreliability of the transfer of burnt hillslope sediment through the channel system to the reservoir associated with highly variable post-fire runoff following fire events. Given that there may be few other chronological records of fire history in the vicinity, it is nevertheless worth improving this potentially valuable source of evidence both in this type of environment and particularly in environments where post-fire runoff is more reliable such that more fire events are represented.

APPENDIX 1



REFERENCES

- Abrahams, A.D., Parsons, A.J. and Wainwright, J. (1994) Resistance to overland flow on semiarid grassland and shrubland hillslopes, Walnut Gulch, southern Arizona. *Journal of Hydrology*, 156: 431-446.
- Adamiec, G. (2004) Properties of the 360 and 550nm TL emissions of the '110°C peak' in fired quartz. *Radiation Measurements*, 39: 105-110.
- Agee, J.K., Wright, C.S., Williamson, N. and Huff, M.H. (2002) Foliar moisture content of Pacific Northwest vegetation and its relation to wildland fire behaviour. *Forest Ecology and Management*, 167: 57-66.
- Aitken, M.J. (1985) *Thermoluminescence Dating*. Academic Press, London.
- Aitken, M.J. (1994) Optical dating: a non-specialist review. *Quaternary Geochronology*, 13: 503-508.
- Anderson, H.E. (1982) *Aids to determining fuel models for estimating fire behavior.*, USDA Forest Service.
- Anderson, H.E. (1990) *Relationship of fuel size and spacing to combustion characteristics of laboratory crib fires*, USDA Forest Service Research Paper INT-424.
- Anderson, J.H., Feigl, F.J. and Schlesinger, M. (1974) The effects of heating on color centers in Germanium-doped quartz. *Journal of Physics and Chemistry of Solids*, 35: 1425-1428.
- Andreu, V., Imeson, A.C. and Rubio, J.L. (2001) Temporal changes in soil aggregates and water erosion after a wildfire in a Mediterranean pine forest. *Catena*, 44: 69-84.
- Annandale, G.W. (1985) Forecasting sediment distribution in reservoirs during unstable conditions. *Journal of Hydrology*, 80: 361-370.
- Annandale, G.W. (1987) *Reservoir Sedimentation*. Elsevier Science Publishers B.V., Amsterdam.
- Annandale, G.W. (2005) 88: Reservoir Sedimentation. In: M.G. Anderson (Editor), *Encyclopedia of Hydrological Sciences*. John Wiley and Sons, Ltd, pp. 1-13.
- Anon (2003) *The vegetation of the Warragamba Special Area.*, National Parks and Wildlife Service, Hurstville.
- Appleby, P.G. (2001) Chronostratigraphic techniques in recent sediments. In: W.M. Last and J.P. Smol (Editors), *Tracking environmental change using lake sediments. Volume 1: Basin Analysis, coring and chronological techniques*. Kluwer Academic Publishers, Dordrecht, pp. 171-203.
- Appleby, P.G., Richardson, N. and Nolan, P.J. (1991) ^{241}Am dating of lake sediments. *Hydrobiologia*, 214: 35-42.
- Armstrong, J.L. and Mackenzie, D.H. (2002) Sediment yields and turbidity records from small upland subcatchments in the Warragamba Dam Catchment, southern New South Wales. *Australian Journal of Soil Research*, 40: 557-579.
- Ashton, D.H. and Attiwill, P.M. (Editors), (1994) Tall open-forests. *Australian Vegetation*. Cambridge University Press, Cambridge, 157-196 pp.
- Atkinson, G. (1984) Erosion damage following bushfires. *Journal of Soil Conservation*, 40: 4-9.
- Attiwill, P.M. and Leeper, G.W. (1987) *Forest soils and nutrient cycles*. Melbourne University Press, Melbourne.
- Auld, T.D. and O'Connell, M.A. (1991) Predicting patterns of post-fire germination in 35 eastern Australian Fabaceae. *Australian Journal of Ecology*, 16: 53-70.
- Baeza, M.J., De Luis, M., Raventos, J. and Escarre, A. (2002) Factors influencing fire behaviour in shrublands of different stand ages and the implications of using prescribed burning to reduce wildfire risk. *Journal of Environmental Management*, 65: 199-208.
- Bailey, R.M. (2001) Towards a general kinetic model for optically the thermally stimulated luminescence of quartz. *Radiation Measurements*, 33: 17-45.
- Baines, P.G. (1990) Physical mechanisms for the propagation of surface fires. *Mathematical Computer Modelling*, 13: 83-94.
- Ballard, T.M. (2000) Impacts of forest management on northern forest soils. *Forest Ecology and Management*, 133: 37-42.
- Barley, K.P. (1954) Effect of root growth and decay on the permeability of a synthetic sandy loam. *Soil Science*, 78: 205-210.
- Beadle, N.C.W. (1940) Soil temperatures during forest fires and their effect on the survival of vegetation. *Journal of Ecology*, 28: 180-192.
- Beaty, R.M. and Taylor, A.H. (2001) Spatial and temporal variation of fire regimes in a mixed conifer forest landscape, Southern Cascades, California, USA,. *Journal of Biogeography*, 28: 955-966.

- Beaufait, W.R. (1966) An integrating devise for evaluating prescribed fires. *Forest Science*, 12: 27-29.
- Beer, T. and Enting, I.G. (1990) Fire spread and percolation modelling. *Mathematical Computer Modelling*, 13: 77-96.
- Belda, F. and Meliá, J. (2000) Relationships between climatic parameters and forest vegetation: application to burned area in Alicante (Spain). *Forest Ecology and Management*, 135: 195-204.
- Bellomo, R.V. (1993) A methodological approach for identifying archaeological evidence of fire resulting from human activities. *Journal of Archaeological Science*, 20: 525-553.
- Benavides-Solorio, J. and MacDonald, L.H. (2001) Post-fire runoff and erosion from simulated rainfall on small plots, Colorado Front Range. *Hydrological Processes*, 15: 2931-2952.
- Benda, L., Miller, D., Bigelow, P. and Andras, K. (2003) Effects of post-wildfire erosion on channel environments, Boise River, Idaho. *Forest Ecology and Management*, 178: 105-119.
- Bennett, J.L. (1999) Thermal alteration of buried bone. *Journal of Archaeological Science*, 26: 1-8.
- Beringer, J., Kershaw, P., Lynch, A., Marshall, A., Tapper, N., Turney, C. and VanDerKaars, S. (2005) *A report on the scope for the palaeorecord to evaluate historical climate variation and its effect on fire regimes in Australia*. In: Reconstructing past climates for future prediction: integrating high-resolution palaeo data for meaningful prediction in the Australasian region: Canberra. University of Wollongong
- Birch, G., Siaka, M. and Owens, C. (2001) The source of anthropogenic heavy metals in fluvial sediments of a rural catchment: Cocks River, Australia. *Water, Air and Soil Pollution*, 126: 13-35.
- Bishop, P., Campbell, B. and McFadden, C. (1991) Absence of Caesium-137 from recent sediments in eastern Australia - indicators of catchment processes? *Catena*, 18: 61-69.
- Bishop, P.M., Mitchell, P.B. and Paton, T.R. (1980) The formation of Duplex soils on hillslopes in the Sydney Basin, Australia. *Geoderma*, 23: 175-189.
- Björck, S., Bennike, O., Ingolfsson, I., Barnehow, L. and Penney, D.N. (1994) Lake Boksehandsken's earliest postglacial sediments and their palaeoenvironmental implications, Jamson Land, East Greenland. *Boreas*, 23: 459-472.
- Björck, S. and Håkansson, S. (1982) Radiocarbon dates from late Weichselian lake sediments in South Sweden as a basis for chronostratigraphic subdivisions. *Boreas*, 11: 141-150.
- Björck, S. and Wohlfarth, B. (2001) ^{14}C Chronostratigraphic techniques in paleolimnology. In: W.M. Last and J.P. Smol (Editors), *Tracking environmental change using lake sediments. Volume 1: Basin analysis, coring and chronological techniques*. Kluwer Academic Publishers, Dordrecht, The Netherlands., pp. 205-247.
- Black, M.P. and Mooney, S.D. (2006) Holocene fire history from the Greater Blue Mountains World Heritage Area, New South Wales, Australia: the climate, humans and the fire nexus. *Regional Environmental Change*, 6: 41-51.
- Blake, W.H., Doerr, S.H., Shakesby, R.A., Wallbrink, P.J., Humphreys, G.S. and Chafer, C.J. (2005a) *Tracing eroded soil in a burnt water supply catchment, Sydney, Australia: linking magnetic enhancement to soil water repellency*. In: O. p. and C. A.J. Soil Erosion and Sediment Redistribution in River Catchments: Cranfield University. CAB International, Wallingford, UK
- Blake, W.H., Doerr, S.H., Shakesby, R.A., Wallbrink, P.J., Humphreys, G.S. and Chafer, C.J. (2006a) *Tracing eroded soil in a burnt water supply catchment, Sydney, Australia: linking magnetic enhancement to soil water repellency*. In: P. Owens and A.J. Collins Soil Erosion and Sediment Redistribution in River Catchments: Cranfield University. CAB International, Wallingford, UK 62-69.
- Blake, W.H., Droppo, I.G., Wallbrink, P.J., Doerr, S.H., Shakesby, R.A. and Humphreys, G.S. (2005b) *Impacts of wildfire on effective sediment particle size: implications for post-fire sediment budgets*. In: Sediment Budgets: Brazil. 291 IAHS Publication 143-150.
- Blake, W.H., Wallbrink, P.J., Doerr, S.H., Shakesby, R.A. and Humphreys, G.S. (2004a) Magnetic enhancement in fire-affected soil and its potential for sediment-source ascription. *Earth Surface Processes and Landforms*: 1-27.
- Blake, W.H., Wallbrink, P.J., Doerr, S.H., Shakesby, R.A. and Humphreys, G.S. (2004b) *Sediment redistribution following wildfire in the Sydney region, Australia: a mineral magnetic tracing approach*. In: IAHS Publication 288: 288 52-59.
- Blake, W.H., Wallbrink, P.J., Doerr, S.H., Shakesby, R.A. and Humphreys, G.S. (2006b) Magnetic enhancement in wildfire-affected soil and its potential for sediment-source ascription. *Earth Surface Processes and Landforms*, 31: 249-264.

- Blake, W.H., Wallbrink, P.J., Doerr, S.H., Shakesby, R.A. and Humphreys, G.S. (in press) Magnetic enhancement in fire-affected soil and its potential for sediment-source ascription. *Earth Surface Processes and Landforms*.
- Blake, W.H., Wallbrink, P.J., Doerr, S.H., Shakesby, R.A., Humphreys, G.S., English, P. and Wilkinson, S. (2006c) *Using geochemical stratigraphy to indicate post-fire sediment and nutrient fluxes into a water supply reservoir, Sydney, Australia*. In: In Sediment dynamics of the hydromorphology of fluvial systems: IAHS Publication 306 363-370.
- Blong, R.J. and Gillespie, R. (1978) Fluvially transported charcoal gives erroneous ^{14}C ages for recent deposits. *Nature*, 271: 739-741.
- Blong, R.J.M., Riley, S.J. and Cozier (1982) Sediment yield from runoff plots following bushfire near Narrabeen Lagoon, New South Wales. *Search*, 13: 36-39.
- Bogena, H.R. and Diekkruger, B. (2002) Modelling solute and sediment transport at different spatial and temporal scales. *Earth Surface Processes and Landforms*, 27: 1475-1489.
- Boix Fayos, C. (1997) The roles of texture and structure in the water retention capacity of burnt Mediterranean soils with varying rainfall. *Catena*, 31: 219-236.
- Bolin, S.B. and Ward, T.J. (1987) *Recovery of a New Mexico drainage basin from a forest fire*. In: Forest Hydrology and Watershed Management: Vancouver. 167 IAHS Publication
- Bond, W.J. and van Wilgen, B.W. (1996) *Fire and Plants*. Chapman and Hall, London.
- Bonnet, M.P. and Wessen, K. (2001) ELMO, a 3D water quality model for nutrients and chlorophyll: first application on a lacustrine ecosystem. *Ecological Modelling*, 141: 19-33.
- Borland, W.M. (1971) Reservoir Sedimentation. In: H.W. Shen (Editor), *River Mechanics*. Colorado State University, Colorado, pp. 29.1-29.38.
- Bøtter-Jensen, L. (1997) Luminescence techniques: instrumentation and methods. *Radiation Measurements*, 27.
- Bowman, D.M.J.S. (1988) Stability amid turmoil?: towards an ecology of north Australian eucalypt forests. *Proceedings of the Ecological Society of Australia*, 15: 149-158.
- Bowman, D.M.J.S. (1998) The impact of Aboriginal landscape burning on the Australian biota. *New Phytologist*, 140: 385-410.
- Bowman, D.M.J.S. and Wilson, B.A. (1988) Fuel characteristics of coastal monsoon forests, Northern Territory, Australia. *Journal of Biogeography*, 15: 807-817.
- Bradstock, R.A. and Auld, T.D. (1995) Soil temperatures during experimental bushfires in relation to fire intensity: consequences for legume germination and fire management in south-eastern Australia. *Journal of Applied Ecology*, 32: 76-84.
- Bradstock, R.A., Auld, T.D., Ellis, M.E. and Cohn, J.S. (1992) Soil temperatures during bushfires in semi-arid, mallee shrublands. *Australian Journal of Ecology*, 17: 433-440.
- Bradstock, R.A. and Bedward, M. (1992) Simulation of the effect of season of fire on post-fire seedling emergence of two *Banksia* species based on long-term rainfall records. *Australian Journal of Botany*, 40: 75-88.
- Bradstock, R.A., Gill, A.M., Kenny, B.J. and Scott, J. (1998) Bushfire risk at the urban interface estimated from historical weather records: consequences for the use of prescribed fire in the Sydney region of southeast Australia. *Journal of Environmental Management*, 52: 259-271.
- Brian, C.K. and Sillen, A. (1988) Evidence from the Swartkrans Cave for the earliest use of fire. *Nature*, 336: 464-466.
- Bronk Ramsey, C. (2005) Oxcal version 3.10 www.rlaha.ox.ac.uk/orau/index.htm [9 August 2006].
- Brose, P. and Wade, D. (2002) Potential fire behaviour in pine flatwood forests following three different fuel reduction techniques. *Forest Ecology and Management*, 163: 71-84.
- Brown, A.G. (1988) Soil development and geomorphic processes in a chaparral watershed: Rattlesnake Canyon, S. California, USA. *Catena Supplement*, 12: 45-58.
- Brown, A.G. (1990) Soil erosion and fire in areas of Mediterranean type vegetation: Results from Chaparral in Southern California, USA and Matorral in Andalucia, Southern Spain. In: J.B. Thornes (Editor), *Vegetation and Erosion*. John Wiley & Sons Ltd, pp. 269 - 287.
- Brown, J.A.H. (1972) Hydrologic effects of a bushfire in a catchment in south-eastern New South Wales. *Journal of Hydrology*, 15: 77-96.
- Bryant, E.A., Young, R.W., Price, D.M. and Short, S.A. (1994) Lake Pleistocene dune chronology: near coastal New South Wales and eastern Australia. *Quaternary Science Reviews*, 13: 209-223.
- Burgan, R.E. (1979) *Estimating live fuel moisture for the 1978 National Fire Danger Rating System*. INT-226, USDA Forest Service.
- Burgess, J.S., Olive, L.J. and Rieger, W.A. (1980) *Sediment discharge response to fire in selected small catchments - Eden, N.S.W.* In: Hydrology and Water Resources Symposium: Adelaide.

- Burgess, J.S., Rieger, W.A. and Olive, L.J. (1981) *Sediment yield change following logging and fire effects in a dry sclerophyll forest in southern New South Wales*. In: T.R.H. Davies and A.J. Pearce Erosion and sediment transport in Pacific Rim steeplands: Christchurch, New Zealand. IAHS-AISH Publication no. 132 375-385.
- Burrows, N.D. (2001) Flame residence times and rates of weight loss of eucalypt forest fuel particles. *International Journal of Wildland Fire*, 10: 137-143.
- Byron-Scott, R.A.D. (1990) The effects of ridge-top and lee-slope fires upon rotor motions in the lee of a steep ridge. *Mathematical Computer Modelling*, 13: 103-112.
- Caitcheon, G.G. (1993) Sediment source tracing using environmental magnetism: a new approach with examples from Australia. *Hydrological Processes*, 7: 349-358.
- Cammeraat, L.H. (2002) A review of two strongly contrasting geomorphological systems within the context of scale. *Earth Surface Processes and Landforms*, 27: 1201-1222.
- Campbell, G.S., Jungbauer, J.D., Bristow, K.L. and Hungerford, R.D. (1995) Soil temperature and water content beneath a surface fire. *Soil Science*, 159: 363-375.
- Cannon, S.H., Bigio, E.R. and Mine, E. (2001) A process for fire-related debris flow initiation, Cerro Grande fire, New Mexico. *Hydrological Processes*, 15: 3011-3023.
- Cannon, S.H., Powers, P.S. and Savage, W.Z. (1998) Fire-related hyperconcentrated and debris flows on Storm King Mountain, Glenwood Springs, Colorado, USA. *Environmental Geology*, 35: 210.
- Cannon, S.H. and Reneau, S.L. (2000) Conditions for generation of fire-related debris flows, Capulin Canyon, New Mexico. *Earth Surface Processes and Landforms*, 25: 1103-1121.
- Canti, M.G. and Linford, N.T. (2000) The effects of fire on archaeological soils and sediments: temperature and colour relationships. *Proceedings of the Prehistoric Society*, 66: 385-395.
- Caparero, G. (2004) Converstation during fieldwork.
- Cerdà, A., Imeson, A.C. and Calvo, A. (1995) Fire and aspect induced differences on the erodibility and hydrology of soils at La Costera, Valencia, southeast Spain. *Catena*, 24: 289-304.
- Chafer, C.J., Noonan, M. and Macnaught, E. (2004) The post-fire measurement of fire severity and intensity in the Christmas 2001 Sydney wildfires. *International Journal of Wildland Fire*, 13: 227-240.
- Chandler, C., Cheney, P., Thomas, P., Trabaud, L. and Williams, D. (1983) Fire in forestry, *Forest fire behaviour and effects*. Wiley & Sons, New York, pp. 450.
- Charitidis, C., Kitis, G., Furetta, C. and Charalambous, S. (2000) Superlinearity of synthetic quartz: Dependence on the firing tempearture. *Nuclear Instruments and Methods in Physics Research B*, 168: 404-410.
- Chartres, G.T. and Mucher, H.J. (1989) The effects of fire on the surface properties and seed germination in two shallow monoliths from a rangeland soil subject to simulated raindrop impact and water erosion. *Earth Surface Processes and Landforms*, 14: 407-417.
- Chen, R. and Pagonis, V. (2004) Modelling thermal activation characteristics of the sensitization of thermoluminescence in quartz. *Journal of Physics D: Applied Physics*, 37: 159-164.
- Chen, R., Yang, X.H. and Mc Keever, S.W.S. (1988) The strongly superlinear dose dependence of thermoluminescence in synthetic quartz. *Journal of Physics D: Applied Physics*, 21: 1452-1457.
- Cheney, N.P. (1981) Fire Behaviour. In: A.M. Gill, R.H. Groves and I.R. Noble (Editors), *Fire and the Australian Biota*. Australian Academy of science, Canberra, pp. 151-175.
- Cheney, N.P. (1990) Quantifying bushfires. *Mathematical Computer Modelling*, 13: 9-15.
- Christopherson, R.W. (2003) *Geosystems: An introduction to physical geography*, 5th Edition. Pearson Education, Inc., New Jersey.
- Clark, J.S. (1988a) Particle motion and the theory of charcoal analysis: Source area, transport, deposition and sampling. *Quaternary Research*, 30: 67-80.
- Clark, J.S. (1988b) Stratigraphic charcoal analysis on petrographic thin sections: Application to fire history in Northwestern Minnesota. *Quaternary Research*, 30: 81-91.
- Clark, J.S. (1990) Fire and climate change during the last 750 years in northwestern Minnesota. *Ecological Monographs*, 60: 135-159.
- Clark, R.L. (1983). *Fire history from fossil charcoal in lake and swamp sediments*. PhD Thesis, Australian National University, Canberra.
- Clark, R.L. (1986) Pollen as a chronometer and sediment tracer, Burrinjuck reservoir. *Hydrobiologia*: 63-69.
- Clark, R.L. and Wasson, R.J. (1986) Reservoir Sediments. In: D. De Deckker and W.D. Williams (Editors), *Limnology in Australia*. Dr. W. Junk Publishers, Melbourne, pp. 497-506.
- Coelho, A.C., Shakesby, R.A., Walsh, R.P.D., Terry, J.P. and Ferreira, A.J.D. (1990) *Responses of surface and subsurface soil water movement and soil erosion of fire fires in Eucalyptus*

- globulus and Pinus pinaster forest, Agueda Basin, Portugal.* In: V. Xavier Proceedings of the International Conference on Forest Fire Research:Combra. C08-1
- Colliton, J.P. (2001). *The impact of European settlement and coal mining on the Nattai Catchment, NSW.* BSc (Hons) thesis Thesis, University of Technology, Sydney.
- Coppus, R. and Imeson, A.C. (2002) Extreme events controlling erosion and sediment transport in a semi-arid sub-andean valley. *Earth Surface Processes and Landforms*, 27: 1365-1375.
- Crockford, R.H. and Olley, J.M. (1998) The effects of particle breakage and abrasion on the magnetic properties of two soils. *Hydrological Processes*, 12: 1495-1505.
- Cromer, R.N. and Vines, R.G. (1966) Soil temperatures under a burning windrow. *Australian Forestry Research*, 2: 23-34.
- Crowther, J. (2003) Potential magnetic susceptibility and fractional conversion studies of archaeological soils and sediments. *Archaeometry*, 45: 685-701.
- Cruz, A. and Moreno, J.M. (2001) No allocation trade-offs between flowering and sprouting in the lignotuberous, Mediterranean shrub *Erica australis*. *Acta Oecologica*, 22: 121-127.
- Cunningham, D.M. (1988) A rockfall avalanche in a sandstone landscape, Nattai North, NSW. *Australian Geographer*, 19: 221-229.
- Daniell, T.M. and Kulik, V. (1987) Bushfire hydrology - the case of leaking watersheds. *Journal of Hydrology*, 92: 301-313.
- David, M. and Sunta, C.M. (1981) Thermoluminescence of quartz - part VIII: Estimation of firing temperature in ancient pottery samples. *Indian Journal of Pure and Applied Physics*, 19: 1054-1056.
- Davis, R.B. (1967) Pollen studies of near-surface sediments in Maine lakes. In: E.J. Cushing and H.E. Wright (Editors), *Quaternary Paleocology*. Yale University Press, New Haven, pp. 143-173.
- De Bano, L.F. (1981) *Water repellent soils: a state-of-the-art.*, Department of Agriculture, United States.
- De Bano, L.F. (2000a) *Fire-induced water repellency: An erosional factor in Wildland Environments.*, University of Arizona, Tucson.
- De Bano, L.F. (2000b) The role of fire and soil heating on water repellency in wildland environments: a review. *Journal of Hydrology*, 231-232: 195-206.
- De Bano, L.F. (2000c) Water repellency in soils: a historical overview. *Journal of Hydrology*, 231-232: 4-32.
- De Bano, L.F., Rice, R.M. and Conrad, C.E. (1979) *Soil heating in Chaparral fires: effects on soil properties, plant nutrients, erosion and runoff*, United States Department of Agriculture Forest Service.
- De Bano, L.F., Savage, S.M. and Hamilton, D.A. (1976) The transfer of heat and hydrophobic substances during burning. *Journal of the Soil Science Society of America*, 40: 779-82.
- Dearing, J. (1999a) *Environmental magnetic susceptibility: Using the Bartington MS2 System*. Chi Publishing, Kenilworth.
- Dearing, J. (1999b) Magnetic susceptibility. In: J. Walden, F. Oldfield and J. Smith (Editors), *Environmental Magnetism: a practical guide*. London, London, pp. 35-62.
- Dearing, J. (2005) Lake sediments as records of past catchment response. In: M.G. Anderson (Editor), *Encyclopedia of Hydrological Sciences*. John Wiley & Sons Ltd., pp. 1-12.
- Dearing, J.A. (1992) Sediment yields and sources in a Welsh upland Lake-catchment during the past 800 years. *Earth Surface Processes and Landforms*, 17: 1-22.
- Dearing, J.A. (1999c) Holocene environmental change from magnetic proxies in lake sediments. In: B.A. Maher and R. Thompson (Editors), *Quaternary climates, environments and magnetism*. Cambridge University Press, Cambridge, pp. 232-278.
- Dearing, J.A. (2000) Natural magnetic tracers in fluvial geomorphology. In: I.D.L. Foster (Editor), *Tracers in Geomorphology*. John Wiley & Sons Ltd., pp. 57-82.
- Dekker, L.W. and Jungerius, P.D. (1990) Water repellency in the dunes with special reference to the Netherlands. *Catena Supplement*, 18: 173-183.
- Dickinson, K.J.M. and Kirkpatrick, J.B. (1985) The flammability and energy content of some important plant species and fuel components in the forests of southeastern Tasmania. *Journal of Biogeography*, 12: 121-134.
- Doerr, S.H. (1997) *Soil Hydrophobicity: a review*, Aveiro - Swansea : Erosion Research Bulletin.
- Doerr, S.H., Blake, W.H., Shakesby, R.A., Stagnitti, F., Vuurens, S.H., Humphreys, G.S. and Wallbrink, P. (2004) Heating effects on water repellency in Australian eucalypt forest soils and their value in estimating wildfire soil temperatures. *International Journal of Wildland Fire*, 13: 157-163.

- Doerr, S.H., Blake, W.H., Shakesby, R.A., Stagnitti, F., Vuurens, S.H., Humphreys, G.S. and Wallbrink, P. (In press) Post-fire water repellency: an indicator of soil temperature reached during burning?
- Doerr, S.H., Shakesby, R.A. and Walsh, R.P.D. (1998) Spatial variability of soil hydrophobicity in fire-prone eucalyptus and pine forests, Portugal. *Soil Science*, 163: 313-324.
- Douglas, I. (1967) Man, vegetation and the sediment yield of rivers. *Nature*, 215: 925-928.
- Dragovich, D. and Morris, R. (2002) Fire intensity, slopewash and bio-transfer of sediment in eucalypt forest, Australia. *Earth Surface Processes and Landforms*, 27: 1309-1319.
- Drechsler, M., Lamont, B.B., Burgman, M.A., Akcallaya, H.R., Witkowski, E.T.F. and Supriyadi (1999) Modelling the persistence of an apparently immortal *Banksia* species after fire and land clearing. *Biological Conservation*, 88: 249-259.
- Duller, G.A.T. (2004) Luminescence dating of Quaternary sediments: recent advances. *Journal of Quaternary Science*, 19: 183-192.
- Dupuy, J.L. (1995) Slope and fuel load effects on fire behaviour: Laboratory experiments in pine needles fuel beds. *International journal of Wildland Fire*, 5: 153-164.
- Dussart, B.H., Lagler, K.F., Larkin, P.A., Scudder, T., Szesztay, K. and White, G.F. (1973) *Summary of symposium and recommendations*. In: W.C. Ackermann, G.F. White and E.B. Worthington *Manmade lakes: Their problems and environmental effects*: Knoxville, Tennessee, USA. William Byrd Press: Richmod, Virginia
- Dyrness, C.T. (1976) *Effect of wildfire on soil wettability in the High Cascades of Oregon.*, USDA forest Service: Research Paper, Portland, Oregon.
- Dyrness, C.T. and Youngberg, C.T. (1957) The effects of logging and slash burning on soil structure. *Soil Science Society of America Journal*, 52: 444-447.
- Edwards, G.M., Green, A., Quinton, J.N. and Morgan, R.P.C. (1996) The influence of rooting density and root morphology on saturated hydraulic conductivity.: 143-151.
- Edwards, K.J. and Whittington, G. (2000) Multiple charcoal profiles in a Scottish lake: taphonomy, fire ecology, human impact and inference. *Palaeogeography, Palaeoclimatology, Palaeoecology*, 164: 67-86.
- Einstein, H.A. (1951) River Sedimentation. In: V.T. Chow (Editor), *Handbook of applied hydrology*. McGraw-Hill Inc., USA, pp. 17-67.
- Eldridge, D.J., Zaady, E. and Shachak, M. (2000) Infiltration through three contrasting biological soil crusts in patterned landscape in the Negev, Israel. *Catena*, 40: 323-336.
- Ellias, V.O., Simoneit, B.R.T., Cordeiro, R.C. and Turcq, B. (2001) Evaluating levoglucosan as an indicator of biomass burning in Carajas, Amazonia: A comparison to the charcoal record. *Geochimica et Cosmochimica Acta*, 65: 267-272.
- Ellis, L.M. (2001) Short-term response of woody plants to fire in a Rio Grande riparian forest, Central New Mexico, USA. *Biological Conservation*, 97: 159-170.
- Elwell, H.A. and Stocking, M.A. (1976) Vegetal cover to estimate soil erosion hazard in Rhodesia. *Geoderma*, 15: 61-70.
- English, P., Wallbrink, P., Chafer, C., Humphreys, G., Shakesby, R., Blake, W. and Doerr, S. (2005) *Impacts on water quality by sediment and nutrients released during extreme bushfires: Report 2: Tracer assessment of post-fire sediment and nutrient redistribution on hillslopes: Nattai National Park, NSW*, CSIRO Land and Water, Canberra.
- Enright, N.J. and Lamont, B.B. (1992) Recruitment variability in the resprouting shrub *Banksia attenuata* and non sprouting congeners in the northern scrub-heaths of south-western Australia. *Acta Oecologica*, 13: 727-741.
- Erskine, W. and Melville, M.D. (1983) Impact of the 1978 floods on the channel and floodplain of the Lower Macdonald River NSW. *Australian Geographer*, 15: 284-292.
- Erskine, W.D. and Saynor, M.J. (1996) Effects of catastrophic floods on sediment yields in southeastern Australia., *Erosion and sediment yield: Global and regional perspectives*. IAHS Publication, pp. 381-388.
- Erskine, W.D. and Warner, R.F. (1988) Geomorphic effects of alternating flood- and drought-dominated regimes on NSW coastal rivers, *Fluvial geomorphology of Australia*. Academic Press Australia.
- Everett, R.L., Java-Sharpe, B.J., Scherer, G.R., Wilt, F.M. and Ottmar, R.D. (1995) Co-occurrence of hydrophobicity and allelopathy in sand pits under burned slash. *Soil Science Society American Journal*, 59: 1176-1183.
- Falcon-Lang, H.J. (2000) Fire ecology of the Carboniferous tropical zone. *Palaeogeography, Palaeoclimatology, Palaeoecology*, 164: 339-355.
- Farres, P.J. (1987) The dynamics of rainsplash erosion and the role of aggregate stability. *Catena*, 14: 119-130.

- Feathers, J.K. (2003) Use of luminescence dating in archaeology. *Measurement Science and Technology*, 14: 1493-1509.
- Ferris, J.M. and Tyler, P.A. (1985) Chlorophyll - total phosphorus relationships in Lake Burragarang, New South Wales, and some other southern hemisphere lakes. *Australian Journal of Freshwater Research*, 36: 157-168.
- Figueiral, I. and Mosbrugger, V. (2000) A review of charcoal analysis as a tool for assessing Quaternary and Tertiary environments: achievements and limits. *Palaeogeography, Palaeoclimatology, Palaeoecology*, 164: 397-407.
- Flannery, T.F. (1990) Pleistocene faunal loss: implications of the aftershock for Australia's past and future. *Archaeology in Oceania*, 25: 45-67.
- Fleming, S.J. and Thompson, J. (1970) Quartz as a heat-resistant dosimeter. *Health Physics*, 18: 567-568.
- Florsheim, J.L. and Keller, E.A. (1987) *Relationships between channel morphology, unit stream power, and sediment routing and storage in a steep, bedrock controlled channel*. In: Erosion and Sedimentation in the Pacific Rim: Corvallis Symposium, August 1987. 165 IAHS publication 279-280.
- Florsheim, J.L., Keller, E.A. and Best, D.W. (1991) Fluvial sediment transport in response to moderate storm flows following chaparral wildfire, Ventura County, southern California. *Geological Society of America Bulletin*, 103: 504-511.
- Franklin, S.B., Robertson, P.A. and Fralish, J.S. (1997) Small-scale fire temperature patterns in upland *Quercus* communities. *Journal of Applied Ecology*, 34: 613-630.
- Fredericks, D.J. (1994). *Identification of sediment sources for Lake Burragarang*. Unpublished PhD Thesis, Macquarie University, Sydney.
- Friedman, G.M. and Saunders, J.E. (1978) *Principles of Sedimentology*. Wiley, New York.
- Garkaklis, M.J., Bradley, J.S. and Wooller, R.D. (2000) Digging by vertebrates as an activity promoting the development of water-repellent patches in sub-surface soil. *Journal of Arid Environments*, 45: 35-42.
- Gavin, D.G., Brubaker, L.B. and Lertzman, K.P. (2003) An 1800-year record of the spatial and temporal distribution of fire from the west coast of Vancouver Island, Canada. *Canadian Journal of Forest Research*, 33: 573-586.
- Gedye, S.J., Jones, R.T., Tinner, W., Ammann, B. and Oldfield, F. (2000) The use of mineral magnetism in the reconstruction of fire history: a case from Lago di Origlio, Swiss Alps. *Palaeogeography, Palaeoclimatology, Palaeoecology*, 164: 101-110.
- Geiss, C.E., Umbanhowar, C.E., Camill, P. and Banerjee, S.K. (2003) Sediment magnetic properties reveal Holocene climate change along the Minnesota prairie-forest ecotone. *Journal of Paleolimnology*, 30: 151-166.
- Gerla, P.J. and Galloway, J.M. (1997) Water quality of two streams near Yellowstone, Park, Wyoming, following the 1988 Clover-Mist wildfire. *Environmental Geology*, 36: 127-136.
- Germanoski, D. and Miller, J.R. (1995) Geomorphic response to wildfire in an arid watershed, Crown Canyon, Nevada. *Physical Geography*, 16: 243-256.
- Gill, A.M. (1975) Fire and the Australian Flora: a Review. *Australian Forestry*, 38: 4-25.
- Gill, A.M. and Bradstock, R. (1995) Extinction of biota by fires. In: R.A. Bradstock et al. (Editors), *Conserving biodiversity: threats and solutions*. Surrey Beatty and Sons PLY Ltd and NSW National Parks and Wildlife Service, NSW.
- Gill, A.M. and Moore, P.H.R. (1994) *Some ecological research perspectives on the disastrous Sydney fires of January 1994*. In: Proceedings of the 2nd International Conference on Forest Fire Research, November 1994: Coimbra, Portugal. 1 63-72.
- Gill, A.M., Moore, P.H.R. and Williams, R.J. (1996) Fire weather in the wet-dry tropics: Kakadu National Park, Australia. *Australian Journal of Ecology*.
- Giovannini, G. (Editor), (1994) The effect of fire on soil quality. *Soil erosion and degradation as a consequence of forest fires*. Geoforma Ediciones, Logrono, 15-27 pp.
- Godfrey-Smith, D.I., Bouchet-Bert, L., Von Bitter, P.H. and Storck, P.L. (2005) Thermal Activation Characteristics and Thermoluminescence of Chert from the Red Wing, Ontario Region, and its putative heat treatment in prehistory. *Journal of Methods and Applications of Absolute Chronology*, 24: 13-20.
- Göksu, H.Y., Weiser, A. and Regulla, D.F. (1989) 110 °C peak records the ancient heat treatment of flint. *Ancient TL*, 7: 15-17.
- Goldammer, J.G. and Jenkins, M.J. (Editors), (1990) *Fire in Ecosystem Dynamics: Mediterranean and Northern perspectives*, III. SPB Academic Publishing, The Hague.
- Görge, K., Lynch, A., Enticott, C., Beringer, J., Abramson, D. and Tapper, N. (2005) *The impact of abrupt land cover changes by savannah fire on northern Australian climate*. San Diego.

- Goslar, T., van der Knaap, W., Hicks, S., Andric, M., Czernik, J., Goslar, E., Räsänen, S. and Hyötylä, H. (2005) Radiocarbon dating of modern peat profiles: pre- and post -bomb ^{14}C variations in the construction of age-depth models. *Radiocarbon*, 47: 115-134.
- Gottschalk, L.C. (1964) Reservoir Sedimentation. In: V.T. Chow (Editor), *Handbook of applied hydrology*. McGraw-Hill, New York, pp. 17-1-17-67.
- Gould, H.R. (1951) Some quantitative aspects of Lake Mead turbidity currents. *Society of Economic Paleontologists and Mineralogists*, Special Publication no.2: 34-52.
- Gould, J.S., Knight, I. and Sullivan, A.L. (1997) Physical modelling of leaf scorch height from prescribed fires in young *Eucalyptus sieberi* regrowth forests in South-eastern Australia. *International journal of Wildland Fire*, 7: 7-20.
- Green, D.G. and Tridgell, A. (1990) Interactive simulation of bushfires in heterogeneous fuels. *Mathematical Computer Modelling*, 13: 57-66.
- Green, W.H. and Ampt, G.A. (1911) Studies in soil physics, part 1. The flow of air and water through soils. *Journal of Agricultural Science*, 4: 1-24.
- Hafey, J. (2003) Ecological Survey, Blue Mountains, Sydney.
- Hafey, J. (2004) *Flora Assessment; Blue Gum Fire Trail, Nattai National Park*, Unpublished report, Wirrimbirra Environmental Consultants, Sydney.
- Hajdas, I., Bonani, G., Hadorn, P., Thew, N., Coppe, G.R. and Lemdahl, G. (2004) Radiocarbon and absolute chronology of the Late-Glacial records from Hauterive/Rouges-Terres, Lake Neuchâtel (CH). *Nuclear Instruments and Methods in Physics Research B*, 223-224: 308-312.
- Hakanson, L. and Jansson, M. (1983) Sedimentation in Lakes and Water Dynamics, *Principles of Lake Sedimentation*. Springer-Verlag, Berlin, pp. 148-174.
- Halperin, A. and Braner, A.A. (1960) Evaluation of Thermal Activation Energies from Glow Curves. *Physical Review*, 117: 408-415.
- Hanesch, M., Stanjek, H. and Petersen, N. (2006) Thermomagnetic measurements of soil iron minerals: the role of organic carbon. *Geophysical Journal International*, 165: 53-61.
- Harrison, J. (2000). *The spatial and temporal pollution distribution in the Tonalli River, NSW*. B.Sc. (Hons) Thesis, University of Technology, Sydney.
- Haslam, S.F.I., Chudek, J.A., Goldspink, C.R. and Hopkins, D.W. (1998) Organic matter accumulation following fires in a moorland soil chronosequence. *Global Change Biology*, 4: 305-313.
- Hathaway, J.H. (1990a) Determining the source of remanence in archaeological soils: A microscopic study of heated and unheated soils. In: J.L. Eighmy and R.S. Sternberg (Editors), *Archaeomagnetic dating*. The University of Arizona Press, Tucson, pp. 178-194.
- Hathaway, J.H. (1990b) Firing temperature and time as variables affecting the quality of archaeromagnetic results. In: J.L. Eighmy and R.S. Sternberg (Editors), *Archaeomagnetic dating*. The University of Arizona Press, Tucson, pp. 158-167.
- Haworth, R.J. (2003) The shaping of the Sydney by its urban geology. *Quaternary International*, 103: 41-55.
- Head, L. (1989) Prehistoric aboriginal impacts on Australian vegetation: an assessment of the evidence. *Australian Geographer*, 20: 37-46.
- Heede, R.H., Harvey, M.D. and Laird, J.R. (1988) Sediment delivery linkages in a Chaparral watershed following a wildfire. *Environmental Management*, 12: 349-358.
- Heinselman, M.L. (1978a) *Fire intensity and frequency as factors in the distribution and structure of northern ecosystems*. In: H.A. Mooney, T.M. Bonnicksen, N.L. Christensen, J.E. Lotan and W.A. Reiners United States Department of Agriculture - Forest Service - General Technical Report WO-26: Fire regimes and ecosystem properties:Honolulu, Hawaii. 7-57.
- Heinselman, W.L. (1978b) Fire in Wilderness ecosystems. In: J.D. Hendee (Editor), *Wilderness Management*. United States Department of Agriculture Forestry Service, Washington D. C.
- Henderson, L. (2002) *Soil Landscapes in the hydrological catchments of the Sydney Catchment Authority: Burratorang and Wollongong Map Sheets*, Department of Infrastructure, Planning and Natural Resources: Unpublished report and maps, Parramatta.
- Hessel, R. (2002). *Modelling soil erosion in a small catchment on the Chinese Loess Plateau*, Utrecht University, Netherlands.
- Hewlett, J.D. (1979) *Forest water quality: an experiment in harvesting and regenerating Piedmont forest*. In: Research paper for the School of Forest Resources:Athens. 55 University of Georgia. 22.
- Higuera, P.E., Sprugel, D.G. and Brubaker, L.B. (2005) Reconstructing fire regimes with charcoal from small-hollow sediments: a calibration with tree-ring records of fire. *The Holocene*, 15: 238-251.

- Hjulstrom, F. (1935) Studies of the morphological activity of rivers as illustrated by the River Fyris. *Bulletin of the Geological Institute University of Uppsala*, 25: 221-527.
- Hollinger, E. and Cornish, P. (2001) *Establish operational procedures for mobile autosamplers and initiate monitoring of natural bushland*, Water Science Section: NSW Environmental Protection Authority, Sydney.
- Humphreys, F.R. and Lambert, M. (1965) Soil temperature profiles under slash and log fires of various intensities. *Australian Forestry*, 1: 23-29.
- Hunt, A., Jones, J. and Oldfield, F. (1984) Magnetic measurements and heavy metals in atmospheric particulates of anthropogenic origin. *Science of the Total Environment*, 33: 129-139.
- Imeson, A.C., Verstraten, J.M., van Mulligen, E.J. and Sevink, J. (1992) The effects of fire and water repellency on infiltration and runoff under Mediterranean type forest. *Catena*, 19: 345-361.
- Isbell, R.F. (1996) *The Australian Soil Classification*. CSIRO Publishing, Melbourne.
- Iwanami, Y. (1973) *Studies of burning temperatures on grasslands*, Reports of the Institute of Agricultural Research, Tohoku University.
- Jaakkola, T., Tolonen, K., Huttunen, P. and Leskinen, S. (1983) The use of fallout ^{137}Cs and $^{239,240}\text{Pu}$ for dating of lake sediments. *Hydrobiologia*, 103: 15-19.
- Jasper, R. (1999) *The changing direction of land managers in reducing the threat from major bushfires on the urban interface of Sydney*. In: Bushfire 99. Australian Bushfire Conference July 1999: Albury, NSW. 175-185.
- Johansen, M.P., Hakonson, T.E. and Breshears, D.D. (2001) Post-fire runoff and erosion from rainfall simulation: contrasting forests with shrublands and grasslands. *Hydrological Processes*, 15: 2953-2965.
- Johnson, A.R.M. (1974) Cavernous weathering at Berowra, N.S.W. *The Australian Geographer*, 6: 531-535.
- Johnson, E.A. and Gutsell, S.L. (1993) Heat budget and fire behaviour associated with the opening of serotinous cones in two *Pinus* species. *Journal of Vegetation Science*, 4: 745-750.
- Jones, R. (1969) Fire-stick farming. *Australian Natural History*, 16: 224-228.
- Jungerius, P.D. and Harkel, M.J. (1994) The effect of rainfall intensity on surface runoff and sediment yield in the grey dunes along the Dutch coast under conditions of limited rainfall acceptance. *Catena*, 23: 269-279.
- Kauffmann, J.B., Cummings, D.L. and Ward, D.E. (1994) Relationships of fire, biomass and nutrient dynamics along a vegetation gradient in the Brazilian cerrado. *Journal of Ecology*, 82: 519-531.
- Ketterer, M.E., Hafer, K.M., Jones, V.J. and Appleby, P.G. (2004) Rapid dating of recent sediments in Loch Ness: Inductively coupled plasma mass spectrometric measurements of global fallout plutonium. *Science of the Total Environment*, 322: 221-229.
- Kilgore, B.M. (1978) *Fire in ecosystem distribution and structure: Western forests and scrublands*. In: H.A. Mooney, T.M. Bonnicksen, N.L. Christensen, J.E. Lotan and W.A. Reiners Fire regimes and ecosystem properties: Honolulu, Hawaii. General Technical Report WO-26 June 1981 USDA
- King, P.M. (1981) Comparison of methods for measuring severity of water repellence of sandy soils and assessment of some factors that affect its measurement. *Australian Journal of Soil Research*, 19: 275-285.
- Kirkby, M.J. (2000). In: A. Goudie et al. (Editors), *The encyclopedic dictionary of physical geography*. Blackwell Publishers Ltd, Oxford, pp. 256-257.
- Kitis, G., Pagonis, V. and Chen, R. (in press) Comparison of experimental and modelled quartz thermal-activation curves obtained using multiple- and single-aliquot procedures. *Radiation Measurements*.
- Knighton, D. (1998) *Fluvial forms and processes*. Arnold, London.
- Koorevaar, P., Menelik, G. and Dirksen, C. (1983) *Elements of soil physics*. Elsevier, Amsterdam, 228 pp.
- Koul, D.K., Singhvi, A.K., Nambi, K.S.V., Bhat, C.L. and Gupta, P.K. (1996) Feasibility of estimating firing temperature using the 110 °C peak of quartz. *Applied Radiation and Isotopes*, 47: 191-194.
- Krammes, J.S. and Osborn, J. (1968) *Water-repellent soils and wetting agents as factors influencing erosion*. In: Proceedings of the Symposium on Water-Repellent Soils: University of California. pp. 177-187.
- Kuczera, G., Jayasuriya, M.D. and O'Shaughnessy, P.J. (1989) Bushfire hydrology - the case of the leaking watersheds - comment. *Journal of Hydrology*, 106: 377-385.
- Kutiel, P. and Inbar, M. (1993) Fire impacts on soil nutrients and soil erosion in a Mediterranean pine forest plantation. *Catena*, 20: 129-139.

- Kutiel, P., Lavee, H., Segev, M. and Benyamini, Y. (1995) The effect of fire-induced surface heterogeneity on rainfall - runoff - erosion relationships in an eastern Mediterranean ecosystem, Israel. *Catena*, 25: 77-87.
- Lahaye, C., Godfrey-Smith, D.I., Guilbert, P. and Bechtel, F. (in press) Equivalent thermal history (H_E) of ferruginous sandstones based on the thermal activation characteristics of quartz. *Radiation Measurements*.
- Laird, J.R. and Harvey, M.D. (1986) *Complex response of a chaparral drainage basin to fire*. In: R.F. Hadley Drainage basin sediment delivery: Albuquerque, New Mexico. IAHS Publication no.159 165-185.
- Laird, L.D. and Campbell, I.D. (2000) high resolution palaeofire signals from Christina Lake, Alberta: a comparison of the charcoal signals extracted by two different methods. *Palaeogeography, Palaeoclimatology, Palaeoecology*, 164: 111-123.
- Lamont, B.B. and Downes, S. (1979) The longevity, flowering and fire history of the grasstrees *Xanthorrhoea preissii* and *Kingia australis*. *Journal of Applied Ecology*, 16: 893-899.
- Langbein, B.L. and Schumm, S.A. (1958) Yield of sediment in relation to mean annual precipitation. *Transactions of the American Geophysical Union*, 39: 1076-1084.
- Laut, P., Cuddy, S. and Marston, F. (1992) *Land cover, infrastructure and land use in the Hawkesbury-Nepean basin*. 92/46, CSIRO Division of Water Resources Consultancy Report.
- Le Borgne, E. (1955) Susceptibilité magnetique anormale du sol superficiel. *Annals of Geophysics*, 11: 399-419.
- Le Borgne, E. (1960) Influence du feu sur les proprietes magnetiques du sol de du granite. *Ann. Geophys*, 16: 159-195.
- Le Borgne, E. (1964) *The relationship between the magnetic susceptibility and the history of soils*. In: A.E.M. Nairn NATO Palaeoclimates conference: University of Newcastle Upon Tyne. Interscience Publishers: London 666 - 673.
- Leeder, M.R. (1982) *Sedimentology: Processes and Product*. George Allen and Unwin, London.
- Lees, J. (1999) Evaluating magnetic parameters for use in source identification, classification and modelling of natural and environmental materials. In: J. Walden, F. Oldfield and J.P. Smith (Editors), *Environmental Magnetism: a practical guide*. Quaternary Research Association, London, pp. 113-138.
- Legleiter, C.J., Lawrence, R.L., Fonstad, M.A., Marcus, W.A. and Aspinall, R. (2002) Fluvial response a decade after wildfire in the northern Yellowstone ecosystem: a spatially explicit analysis. *Geomorphology*, 1304: 1-18 (article in press).
- Leighton-Boyce, G. (2002). *Spatio-temporal dynamics and hydrogeomorphic implications of soil water repellency within Eucalyptus forests in north-central Portugal*. University of Wales, Swansea, Swansea.
- Leitch, C.J., Flinn, D.W. and van de Graaff, R.H.M. (1983) Erosion and nutrient loss resulting from Ash Wednesday (February 1983) wildfires: a case study. *Australian Forestry*, 46: 173-180.
- Leitner, L.A. (1991) Effects of site, landscape features, and fire regime on vegetation patterns in presettlement southern Wisconsin. *Landscape Ecology*, 5.
- Letey, J. (2001) Causes and consequences of fire-induced soil water repellency. *Hydrological Processes*, 15: 2867-2876.
- Lewin, J. (1983) Changes in channel patterns and floodplains. In: K.J. Gregory (Editor), *Background to palaeohydrology: A perspective*. John Wiley & Sons, Chichester, pp. 303-321.
- Linacre, E. and Geerts, B. (1997) Southern Climates: Australia, *Climates and weather explained*. Routledge, London, pp. 374-380.
- Linford, N.T. and Canti, M.G. (2001) Geophysical evidence for fires in antiquity: Preliminary results from an experimental study. *Archaeological Prospection*, 8: 211-225.
- Long, C.J., Whitlock, C., Bartlein, P.J. and Millsbaugh, S.H. (1998) A 9000-year fire history from the Oregon Coastal Range, based on high-resolution charcoal study. *Canadian Journal of Forest Research*, 28: 774-787.
- Longworth, G., Becker, L.W., Thompson, R., Oldfield, F., Dearing, J.A. and Rummary, T.A. (1979) Mössbauer and magnetic studies of secondary iron oxides in soils. *Journal of Soil Science*, 30: 93-110.
- Loughran, R.J. (1977) Sediment transport from a rural catchment in New South Wales. *Journal of Hydrology*, 34: 357-375.
- Luke, R.H. and McArthur, A.G. (1978) *Bushfires in Australia*. Australian Government Publishing Service, Canberra.

- MacDonald, G.M., Larsen, C.P.S., Szeicz, J.M. and Moser, K.A. (1991) The reconstruction of boreal forest fire history from lake sediments: a comparison of charcoal, pollen and sedimentological and geochemical indices. *Quaternary Science Reviews*, 10: 53-71.
- Macris, J. (2001) Erosion <http://www.wildlife.com/www/biodiversity/management.htm#Erosion:05/02/2005>].
- Magiera, T., Strzyszczyński, Z., Kapicka, A. and Petrovsky, E. (2005) Discrimination of lithogenic and anthropogenic influences on topsoil magnetic susceptibility in Central Europe. *Geoderma*, Article in Press.
- Maher, B.A. (1986) Characterisation of soils by mineral magnetic measurements. *Physics of the Earth and Planetary Interiors*, 42: 76-92.
- Maher, B.A. (1988) Magnetic properties of some synthetic sub-micron magnetites. *Geophysical Journal International*, 94: 83-96.
- Marmet, E., Bina, M., Fedoroff, N. and Tabbagh, A. (1999) Relationships between human activity and the magnetic properties of soils: A case study in the Medieval site of Roissy-en-France. *Archaeological Prospection*, 6: 161 - 170.
- Martin, D.H. and Moody, J.A. (2001) Comparison of soil infiltration rates in burned and unburned mountainous watersheds. *Hydrological Processes*, 15: 2893-2903.
- Martinez-Fernandez, J. and Diaz-Pereira, E. (Editors), (1994) Changes of the physical and chemical properties in a soil affected by forest fire in Sierra Larga (Murcia, Spain). *Soil erosion and degradation as a consequence of forest fires*. Geoforma Ediciones, Logrono.
- Matthews, J.A. (2002) Debris flows. In: J.A. Matthews et al. (Editors), *The encyclopaedic dictionary of environmental change*. Arnold, London, pp. 144.
- Mc Nabb, D.H., Gaweda, F. and Froehlich, H.A. (1989) Infiltration, water repellency, and soil moisture content after broadcast burning a forest site in southwest Oregon. *Journal of soil and water conservation*, 44: 87-90.
- McClean, R.G. and Kean, W.F. (1993) Contributions of wood ash magnetism to archaeomagnetic properties of fire pits and hearths. *Earth and Planetary Science Letters*, 119: 387 - 394.
- McElhinny, M.W. (1973) *Palaeomagnetism and plate tectonics*. Cambridge University Press, Cambridge.
- McGlynn, B., McDonnell, J., Stewart, M. and Seibert, J. (2003) On the relationships between catchment scale and streamwater mean residence time. *Hydrological Processes*, 17: 175-181.
- McGregor, G.R. and Nieuwolt, S. (1998) *Tropical climatology: an introduction to climates of low latitudes*. Wiley, Chichester.
- Melcher, C.L. and Zimmerman, D.W. (1977) Thermoluminescent determination of prehistoric heat treatment of chert artifacts. *Science*, 197: 1359-1362.
- Meredith, P. (1999) *The Australian geographic book of the Blue Mountains*. Australian Geographic Pty Ltd, Terrey Hills.
- Meredith, P. (2002) Burrator: the valley that vanished. *Australian Geographic*, October-December: 26-27.
- Michab, M., Valladas, H., Froget, L. and Mercier, N. (1998) Distinguishing burnt from partly bleached unburnt quartz pebbles of Pedra Furada, Brazil. *Ancient TL*, 16: 5-9.
- Miller, D., Luce, C. and Benda, L. (2003) Time, space and episodicity of physical disturbance in streams. *Forest Ecology and Management*, 178: 121-140.
- Millspaugh, S.H. and Whitlock, C. (1995) A 750-year fire history based on lake sediment records in central Yellowstone National Park, USA. *The Holocene*, 5: 283-292.
- Mitchell, P.B. and Humphreys, G.S. (1987) Litter dams and microterraces formed on hillslopes subject to rainwash in the Sydney Basin, Australia. *Geoderma*, 39: 331-357.
- Mohr, J.A., Whitlock, C. and Skinner, C.N. (2000) Postglacial vegetation and fire history, eastern Klamath Mountains, California, USA. *The Holocene*, 10: 587-601.
- Molina, M.J. and Llinares, J.V. (2001) Temperature-time curves at the soil surface in maquis summer fires. *International journal of Wildland Fire*, 10: 45-52.
- Moody, J.A. and Martin, D.A. (2001a) Initial hydrologic and geomorphic response following a wildfire in the Colorado front range. *Earth Surface Processes and Landforms*, 26: 1049-1070.
- Moody, J.A. and Martin, D.A. (2001b) Post-fire, rainfall intensity - peak discharge relations for three mountainous watersheds in the western USA. *Hydrological Processes*, 15: 2981-2993.
- Moody, J.A. and Martin, D.A. (2001c) *Water Resources Investigative Report 01-4122: Hydrologic and sedimentologic response of two burned watersheds in Colorado*, US Geological Survey, Denver, Colorado.

- Mooney, S.D., Radford, K.L. and Hancock, G. (2001) Clues to the 'burning question': Pre-European fire in the Sydney coastal region from sedimentary charcoal and palynology. *Ecological Management and Restoration*, 2: 203-212.
- Morgan, R.P.C. (1979) *Soil Erosion*. Longman, London.
- Morinaga, H., Inokuchi, H., Yamashita, H., Ono, A. and Inada, T. (1999) Magnetic detection of heated soils at paleolithic sites in Japan. *Geoarchaeology*, 14: 377-399.
- Mullins, C.E. (1977) Magnetic susceptibility of the soil and its significance in soil science - a review. *Journal of Soil Science*, 28: 223-246.
- Nanson, G.C., Chen, X.Y. and Price, D.M. (1995) Aeolian and fluvial evidence of changing climate and wind patterns during the past 100ka in the western Simpson Desert, Australia. *Palaeogeography, Palaeoclimatology, Palaeoecology*, 113: 87-102.
- Nanson, G.C. and Young, R.W. (1983) Environmental concerns in a sandstone landscape with particular reference to the Sydney Basin, N.S.W. In: R.W. Young and G.C. Nanson (Editors), *Aspects of Australian sandstone landscapes*. Australian and New Zealand Geomorphology Group, Wollongong, pp. 4-9.
- Neary, D.G., Klopatek, C.C., De Bano, L.F. and Ffolliott, P.F. (1999) Fire effects on belowground sustainability: a review and synthesis. *Forest Ecology and Management*, 122: 51-71.
- Nichols, G.J., Cripps, J.A., Collinson, M.E. and Scott, A.C. (2000) Experiments in waterlogging and sedimentology of charcoal: results and implications. *Palaeogeography, Palaeoclimatology, Palaeoecology*, 164: 43-56.
- Nittrouer, C.A., DeMaster, D.J., McKee, B.A., Cutshall, N.H. and Larsen, I.L. (1984) The effect of sediment mixing on Pb-210 accumulation rates for the Washington Continental shelf. *Marine Geology*, 54: 201-221.
- Northcote, K.H. (1979) *A factual key for the recognition of Australian soils*. Rellim Technical Publications, Adelaide: Australia.
- Nott, J., Young, R., Bryant, E. and Price, D. (1994) Stratigraphy vs. pedogenesis: problems of their correlation within coastal sedimentary facies. *Catena*, 23: 199-212.
- NPWS (1997) *NSW Urban bushland biodiversity survey*, New South Wales National Parks and Wildlife Service, Sydney.
- O' Hanlon, L. (1995) Fighting fire with fire. *New Scientist*, 1980: 28-33.
- Ojeda, F. (1998) Biogeography of seeder and resprouter Erica species in the Cape Floristic Region - Where are the resprouters? *Journal of the Linnean Society*, 63: 331-347.
- Oldfield, F. (1991) Environmental magnetism - a personal perspective. *Quaternary Science Reviews*, 10: 73-85.
- Oldfield, F. (1994) Toward the discrimination of fine-grained ferrimagnets by magnetic measurements in lake and near-shore marine sediments. *Journal of Geophysical Research*, 99: 9045-9050.
- Oldfield, F. (1999) The rock magnetic identification of magnetic mineral and magnetic grain size assemblages. In: J. Walden, F. Oldfield and J.P. Smith (Editors), *Environmental Magnetism: a practical guide*. Technical Guide, No. 6. Quaternary Research Association, London, pp. 98-112.
- Oldfield, F. and Clark, R.L. (1990) Lake sediment-based studies of soil erosion. In: J. Boardman, I.D.L. Foster and J.A. Dearing (Editors), *Soil Erosion on Agricultural Land*. John Wiley & Sons Ltd, Chichester, pp. 201-228.
- Oldfield, F., Hunt, A., Jones, M.D.H., Chester, R., Dearing, J.A., Olsson, L. and Prospero, J.M. (1985a) Magnetic differentiation of atmospheric dusts. *Nature*, 317: 516-518.
- Oldfield, F., Maher, B.A., Donoghue, J. and Pierce, J. (1985b) Particle-size related, mineral magnetic source sediment linkages in the Rhode River catchment, Maryland, USA. *Journal of Geological Society, London*, 142: 1035-1046.
- Oldfield, F., Thompson, R. and Dickson, D.P.E. (1981) Artificial magnetic enhancement of stream bedload: a hydrological application of superparamagnetism. *Physics of the Earth and Planetary Interiors*, 26: 107-124.
- O'Lear, H.A., Seastedt, T.R., Briggs, J.M., Blair, J.M. and Ramundo, R.A. (1996) Fire and topographic effects on decomposition rates and N dynamics of buried wood in tallgrass prairie. *Soil Biology and Biochemistry*, 28: 323-329.
- Olive, L.J. and Rieger, W.A. (1985) Variation in suspended sediment concentration during storms in five small catchments in southeast New South Wales. *Australian Geographical Studies*, 23: 38-51.
- Olive, L.J. and Rieger, W.A. (1986) *Low Australian sediment yields - a question of inefficient sediment delivery*. In: R.F. Hadley Drainage basin sediment delivery: Albuquerque, New Mexico. IAHS Publication no.159 355-364.

- O'Sullivan, P.E., Oldfield, F. and Battarbee, R.W. (1973) Preliminary studies of Lough Neagh sediments 1. Stratigraphy, chronology and pollen analysis. In: H.J.B. Birks and R.G. West (Editors), *Quaternary plant ecology*. Blackwell Scientific Publications, Oxford, pp. 267-278.
- Özdemir, Ö. and Banerjee, S.K. (1984) High temperature stability of maghemite (α -Fe₂O₃). *Geophysical Research Letters*, 11: 161-164.
- Paton, T.R., Humphreys, G.S. and Mitchell, P.B. (1995) *Soils: a new global view*. UCL Press, London, 70-86 pp.
- Patterson, W.A., Edwards, K.J. and Maguire, D.J. (1987) Microscopic charcoal as a fossil indicator of fire. *Quaternary Science Reviews*, 6: 3-23.
- Pavlish, L.A. and Sheppard, P.J. (1983) Thermoluminescent determination of Paleoindian heat treatment in Ontario, Canada. *American Antiquity*, 48: 793-799.
- Perry, A.H. and Matthews, J.A. (2003) El Niño-Southern Oscillation (ENSO). In: J.A. Matthews et al. (Editors), *The encyclopaedic dictionary of environmental change*. Arnold, London, pp. 187.
- Perry, G.L.W. (1998) Current approaches to modelling the spread of wildland fire: a review. *Progress in Physical Geography*, 22: 222-245.
- Peters, C. and Batt, C.M. (2002) Dating and sourcing fuel ash residues from Cladh Hallan, South Uist, Scotland, using magnetic techniques. *Physics and Chemistry of the Earth*, 27: 1349-1353.
- Peters, C., Church, M.J. and Mitchell, C. (2001) Investigation of fire ash residues using mineral magnetism. *Archaeological Prospection*, 8: 227-237.
- PlattBradbury, J. (1996) Charcoal deposition and redeposition in Elk Lake, Minnesota, USA. *Holocene*, 6: 349-344.
- Pook, E.W. and Gill, A.M. (1993) Variation of live and dead fine fuel moisture in *Pinus radiata* plantations of the Australian Capital Territory. *International journal of Wildland Fire*, 3: 155-168.
- Prosser, I.P., Ruderfurd, I.D., Olley, J.M., Young, W.J., Wallbrink, P.J. and Moran, C.J. (2001) Large-scale patterns of erosion and sediment transport in river networks, with examples from Australia. *Marine & Freshwater Research*, 52: 81-89.
- Prosser, I.P. and Williams, L. (1998) The effect of wildfire on runoff and erosion in native *Eucalyptus* forest. *Hydrological Processes*, 12: 251-265.
- Rainbow, C.M. (1999). *Chronology of sediments and spatial pollutant distribution patterns in the WerriBerri Creek catchment, Wollondillyshire, NSW*, The University of Wollongong, Wollongong.
- Raison, R.J., Woods, P.V., Jakobaen, B.F. and Bary, G.A.V. (1986) Soil temperatures during and following low-intensity prescribed burning in a *Eucalyptus pauciflora* Forest. *Australian Journal of Soil Research*, 24: 33-47.
- Rakov, T.L., Milovidova, N.D., Kuvshinova, K.A. and Moiseyev, B.M. (1985) An ESR Study of Ge Centers in natural Polycrystalline Quartz. *Translated from Geokhimiya, No 9*, 9: 1339-1344.
- Raupach, M.R. (1990) Similarity analysis of the interactions of bushfire plumes with ambient winds. *Mathematical Computer Modelling*, 13: 113-121.
- Reeder, C.J. and Jurgensen, M.F. (1979) Fire - induced water repellency in forest soils of upper Michigan. *Canadian Journal of Forest Research*, 9: 369-373.
- Renfrew, J.M. (1973) *Palaeoethnobotany: The prehistoric food plants of the Near East and Europe*. Methuen, London.
- Rhodes, E.J., Bronk-Ramsey, C., Outram, Z., Batt, C., Willis, L., Dockrill, S. and Bond, J. (2003a) Bayesian methods applied to the interpretation of multiple OSL dates: high precision sediment ages estimates from Old Scatness Broch excavations, Shetland Isles. *Quaternary Science Reviews*, 22: 1231-1244.
- Rhodes, E.J., Chappell, J. and Spooner, N. (2003b) *Age and mobility of arid regolith: assessment by Luminescence dating methods*. In: I.C. Roach CRC LEME:342-344.
- Richards, K.S. (2000) Manning equation. In: A. Goudie et al. (Editors), *The encyclopedic dictionary of physical geography*. Blackwell Reference, Oxford.
- Richter, D.D. and Ralston, C.W. (1982) Prescribed fire: effects of water quality and forest nutrient cycling. *Science*, 215: 661-662.
- Riggan, P.J., Lockwood, R.N., Jacks, P.M., Colver, C.G., Weirich, F.H., De Bano, L.F. and Brass, J.A. (1994) Effects of fire severity on nitrate mobilization in watersheds subject to chronic atmospheric deposition. *Environmental Science and Technology*, 28: 369-375.

- Ritchie, J.C., Clebsch, E.E.C. and Rudolph, W.K. (1970) Distribution of fallout and natural gamma radionuclides in litter, humus and surface mineral soil layers under natural vegetation in the Great Smoky Mountains, North Carolina-Tennessee. *Health Physics*, 18: 479-489.
- Ritsema, C.J., Dekker, L.W., Nieber, J.L. and Steenhuis, T.S. (1998) Modeling and field evidence of finger formation and finger recurrence in a water repellent sandy soil. *Water Resources Research*, 34: 555-567.
- Roberts, W.B. (1965) Soil temperatures under a pile of burning logs. *Australian Forestry Research*, 1: 21-23.
- Robertson, I., Froyd, C.A., Walsh, R.P.D., Newbery, D.M., Woodborne, S. and Ong, R.C. (2004) The dating of dipterocarp tree rings: establishing a record of carbon cycling and climatic change in the tropics. *Journal of Quaternary Science*, 19: 657-644.
- Robichaud, P.R., Beyers, J.L. and Neary, D.G. (2000) *Evaluating the effectiveness of postfire rehabilitation treatments*. RMRS-GTR-63, United States Department of Agriculture Forest Service.
- Robichaud, P.R. and Hungerford, R.D. (2000) Water repellency by laboratory burning of four northern Rocky Mountain forest soils. *Journal of Hydrology*, 231-232: 207-219.
- Romero, J.R., Antenucci, J.P. and Imberger, J. (2004) One- and three-dimensional biogeochemical simulations of two differing reservoirs. *Ecological Modelling*, 174: 143-160.
- Roque, C., Guibert, P., Duttine, M., Vartanian, E., Chapoulie, R. and Bechtel, F. (2004) Dependence of Luminescence Characteristics of Irradiated Quartz with the Thermal Treatment and Consequences for TL Dating. *Journal on Methods and Applications of Absolute Chronology*, 23: 1-8.
- Rubio, J.L., Forteza, J., Andreu, V. and Cerni, R. (1997) Soil profile characteristics influencing runoff and soil erosion after forest fire: A case study (Valencia, Spain). *Soil Technology*, 11: 67-78.
- Rummery, T.A. (1981). *The effects of fire on soil and sediment magnetism*. Unpublished PhD Thesis, University of Liverpool.
- Rummery, T.A. (1983) The use of magnetic measurements in interpreting the fire histories of lake drainage basins. *Hydrobiologia*, 103: 53-58.
- Rummery, T.A., Bloemendal, J., Dearing, J., Oldfield, F. and Thompson, R. (1979) The persistence of fire-induced magnetic oxides in soils and lake sediments. *Annales de Géophysique*, 35: 103-107.
- SCA (2002) *Dams of Greater Sydney and surrounds: Warragamba*, Sydney Catchment Authority, New South Wales.
- SCA (2004) Warragamba dam facts <http://www.sca.nsw.gov.au/dams/facts.html> [21st July 2004].
- SCA and NPWS (1999) *Special areas background document*, Sydney Catchment Authority and NSW National Parks and Wildlife Service.
- Schnurrenberger, D., Russell, J. and Kelts, K. (2003) Classification of lacustrine sediments based on sedimentary components. *Journal of Paleolimnology*, 29: 141-154.
- Schwertmann, U. and Taylor, R.M. (1989) Iron oxides, *Minerals in Soil Environments*. Series, no.1. SSSA, pp. 379-438.
- Scott, D.F. (1993) The hydrological effects of fire in South African mountain catchments. *Journal of Hydrology*, 150: 409-432.
- Scott, D.F. (1997) The contrasting effects of wildfire and clearfelling on the hydrology of a small catchment. *Hydrological Processes*, 11: 543-555.
- Scott, D.F., Versfeld, D.B. and Lesch, W. (1998) Erosion and sediment yield in relation to afforestation and fire in the mountains of the western Cape Province, South Africa. *South African Geographical Journal*, 80: 52-59.
- Scott, V.H. and Burgy, R.H. (1956) Effects of heat and brush burning on the physical properties of certain upland soils that influence infiltration. *Proceedings of the Soil Science Society America*: 63-70.
- Screenivasan, A. and Aurangabadkar, R.K. (1940) Effect of fire heating on the properties of black cotton soil in comparison with those of grey and of humus treated soils. *Soil Science*, 51: 449-462.
- Sevink, J., Imeson, A.C. and Verstraten, J.M. (1989) Humus form development and hillslope runoff, and the effects of fire and management, under Mediterranean forests in NE-Spain. *Catena*, 8: 461-475.
- Shakesby, R.A. (2004) Soil erosion by water, pp. *Pers comm*.
- Shakesby, R.A., Blake, W.H., Doerr, S.H., Humphreys, G.S. and Wallbrink, P. (2004) Post-fire studies - effects on soils of the Little River catchment, *SCA book*.

- Shakesby, R.A., Blake, W.H., Doerr, S.H., Humphreys, G.S., Wallbrink, P. and Chafer, C.J. (2006) *Hillslope erosion and bioturbation following the Christmas 2001 forest fires near Sydney, Australia*. In: O. P. and C. A.J. Soil Erosion and Sediment Redistribution in River Catchments: Measurement, Modelling and Management: Cranfield University. CAB International, Wallingford, UK 51-61.
- Shakesby, R.A., Blake, W.H., Doerr, S.H., Humphreys, G.S., Wallbrink, P. and Chafer, C.J. (in press) *Hillslope erosion and bioturbation following the Christmas 2001 forest fires near Sydney, Australia*. In: O. P. and C. A.J. Soil Erosion and Sediment Redistribution in River Catchments: Measurement, Modelling and Management: Cranfield University. CAB International, Wallingford, UK 51-61.
- Shakesby, R.A., Chafer, C.J., Doerr, S.H., Blake, W.H., Wallbrink, P., Humphreys, G.S. and Harrington, B.A. (2003) Fire severity, water repellency characteristics and hydrogeomorphological changes following the Christmas 2001 Sydney forest fires. *Australian Geographer*, 34: 147-175.
- Shakesby, R.A., Coelho, C.O.A., Ferreira, A.J.D., Terry, J.P. and Walsh, R.P.D. (1993) Wildfire impacts on soil erosion and hydrology in wet mediterranean forest, Portugal. *International Journal of Wildland Fire*, 3: 95-110.
- Shakesby, R.A. and Doerr, S.H. (2006) Wildfire as a hydrological and geomorphological agent. *Earth Science Reviews*, 74: 269-307.
- Shakesby, R.A., Doerr, S.H. and Walsh, R.P.D. (2000) The erosional impact of soil hydrophobicity: current problems and future research directions. *Journal of Hydrology*, 231-232: 178-191.
- Shakesby, R.A. and Walsh, R.P.D. (1997) Forest fires and land degradation in Portugal. *Geographical Review*, 10: 29-33.
- Slattery, M.C. and Bryan, R.B. (1994) Surface seal development under simulated rainfall on an actively eroding surface. *Catena*, 22: 17-34.
- Slattery, M.C., Gares, P.A. and Phillips, J.D. (2002) Slope-channel linkage and sediment delivery on North Carolina coastal plain cropland. *Earth Surface Processes and Landforms*: 1377-1387.
- Sly, P.G. (1994) Sedimentary processes in lakes. In: K. Pye (Editor), *Sediment Transport and Depositional Processes*. Blackwell Scientific Publications, Oxford, pp. 157-186.
- Smith, D. and Hamilton, T.F. (1985) Modelling of ^{210}Pb behaviour in the catchment and sediment of lake Tali Karng, Victoria, and estimation of recent sedimentation rates. *Australian Journal of Marine and Freshwater Research*, 36: 23-32.
- Smith, J. (1999) An introduction to the magnetic properties of natural materials. In: J. Walden, F. Oldfield and J. Smith (Editors), *Environmental Magnetism: a practical guide*. Quaternary Research Association, London, pp. 5-25.
- Smith, M.A., Grant, C.D., Loneragan, W.A. and Koch, J.M. (2004) Fire management implications of fuel loads and vegetation structure in jarrah forest restoration on bauxite mines in Western Australia. *Forest Ecology and Management*, 187: 247-266.
- Snyman, H.A. (2003) Short-term response of rangeland following an unplanned fire in terms of soil characteristics in a semi-arid climate of South Africa. *Journal of Arid Environments*, 55: 160-180.
- Soler, M., Sala, M. and Gallart, F. (1994) *Post fire evolution of runoff and erosion during an eighteen month period*. Soil erosion and degradation as a consequence of forest fires. Geoforma Ediciones, Logrono.
- Soto, B., Basanta, R., Benito, E., Perez, R. and Diaz-Fierros, F. (Editors), (1994) Runoff and erosion from burnt soils in Northwest Spain. *Soil erosion and degradation as a consequence of forest fires*. Geoforma Ediciones, Logrono, 91-98 pp.
- Soto, B., Basanta, R. and Diaz-Fierros, F. (1997) Effects of burning on nutrient balance in an area of gorse (*Ulex europaeus* L.) scrub. *The Science of the Total Environment*, 204: 271-281.
- Speer, M.S., Leslie, L.M., Morison, R., Catchpole, W., Bradstock, R. and Bunker, R. (2001) Modelling fire weather and fire spread rates for two bushfires near Sydney. *Australian Meteorological Magazine*, 50: 241-246.
- Stocking, M.A. and Murnaghan, N. (2001) *Field assessment of land degradation*. Earthscan Publications Ltd, London.
- Sturman, A. and Tapper, N. (1996) *The weather and climate of Australia and New Zealand*. Oxford University Press, Melbourne.
- Summerfield, M.A. (1991) Slope processes and forms, *Global Geomorphology*. Longman Singapore Publishers Ltd, Singapore, pp. 163-188.
- Sumner, M.E. (2000) *Handbook of soil science*. Boca Raton, FL: CRC Press, London.
- Swain, A.M. (1973) A history of fire and vegetation in Northeastern Minnesota as recorded in lake sediments. *Quaternary Research*, 3: 383-396.

- Swanson, F.J. (1978) *Fire and geomorphic processes*. In: H.A. Mooney, T.M. Bonnicksen, N.L. Christensen, J.E. Lotan and W.A. Reiners United States Department of Agriculture - Forest Service - General Technical Report WO-26: Fire regimes and ecosystem properties: Honolulu, Hawaii. 401-420.
- Swanson, F.J. (1981) Fire and geomorphic processes. In: H.A. Mooney, T.M. Bonnicksen, N.L. Christensen, J.E. Lotan and W.A. Reiners (Editors), *Proceedings, fire regimes and ecosystem properties*. USDA Forest services general technical report No. WO-28, pp. 401-420.
- Talbot, M.R. and Allen, P.A. (1996) Lakes. In: H.G. Reading (Editor), *Sedimentary environments: processes, facies and stratigraphy*. Blackwell, Oxford, pp. 83-123.
- Tarling, D.H. (1983) *Palaeomagnetism: principles and applications in geology, geophysics and archaeology*. Chapman and Hall, London.
- Tauxe, L. (2002) *Paleomagnetic principles and practice*. Kluwer Academic, London.
- Taylor, R.M. and Schwertmann, U. (1974) Maghemite in soils and its origin II. Maghemite syntheses at ambient temperature and pH 7. *Clay Minerals*, 10: 299-310.
- Terry, J. and Shakesby, R.A. (1993) Soil hydrophobicity effects on rainsplash: simulated rainfall and photographic evidence. *Earth Surface Processes and Landforms*, 18: 519-525.
- Thomas, A.D. (1993) Fire effects on soil, hydrology and nutrient loss - a review. *Aveiro-Swansea Erosion Research Bulletin*, 3: 1-65.
- Thomas, W.A. (1977) *HEC-6, Scour and deposition in rivers and reservoirs. Users Manual.*, US Army Corps of Engineers, Hydrologic Engineering Centre, California.
- Thompson, R. and Oldfield, F. (1986) *Environmental magnetism*. Allen and Unwin.
- Thonicke, K., Venevsky, S., Sitch, S. and Cramer, W. (2001) The role of fire disturbance for global vegetation dynamics: coupling fire into a dynamic global vegetation model. *Global Ecology and Biogeography*, 10: 661-677.
- Tibby, J. (2001) Diatoms as indicators of sedimentary processes in Burrinjuck reservoir, New South Wales, Australia. *Quaternary International*, 83-85: 245-256.
- Tinner, W., Conedera, M., Ammann, B., Gaggeler, H.W., Gedy, S.J., Jones, R.T. and Sagesser, B. (1998) Pollen and charcoal in lake sediments compared with historically documented forest fires in southern Switzerland since AD 1920. *The Holocene*, 8: 31-42.
- Tinner, W., Hubschmid, P., Wehrli, M., Ammann, B. and Conedera, M. (1999) Long-term forest fire ecology and dynamics in southern Switzerland. *Journal of Ecology*, 87: 273-289.
- Tite, M.S. and Linnington, R.E. (1975) Effect of climate on the magnetic susceptibility of soils. *Nature*, 256: 565-566.
- Tite, M.S. and Mullins, C. (1971) Enhancement of the magnetic susceptibility of soils on archaeological sites. *Archaeometry*, 13: 209 - 219.
- Tomkins, K.M., Humphreys, G.S., Farwig, V.J., Shakesby, R.A., Doerr, S.H., Blake, W.H., Wallbrink, P. and Chafer, C.J. (In preparation) An unusual soil-landscape.
- Tomkins, K.M., Humphreys, G.S., Shakesby, R.A., Doerr, S.H., Blake, W.H. and Wallbrink, P. (2004) *Mass movement events in the south-west Sydney basin during the Holocene*. In: I.C. Roach Regolith: CRC LEME 365-369.
- Tomkins, K.M., Humphreys, G.S., Wilkinson, M.T., Hesse, P.P., Doerr, S.H., Shakesby, R.A., Wallbrink, P.J., Blake, W.H. and Fink, D. (in press) Contemporary versus long-term denudation along a passive plate margin, Australia: the role of extreme events. *Earth Surface Processes and Landforms*.
- Torn, M. and Fried, J.S. (1992) Predicting the aspects of global warming on wildland fire. *Climatic Change*, 21: 257-274.
- Townsend, S.A. and Douglas, M.M. (2000) The effect of three fire regimes on stream water quality, water yield and export coefficients in a tropical savanna (northern Australia). *Journal of Hydrology*, 229: 118-137.
- Turney, C.S.M., Kershaw, A.P., Moss, P., Bird, M.I., Fifield, L.K., Cresswell, R.G., Santos, G.M., DiTada, M.L., Hausladen, P.A. and Zhou, Y. (2001) Redating the onset of burning at Lynch's Crater (North Queensland): implications for human settlement in Australia. *Journal of Quaternary Science*, 16: 767-771.
- Ulery, A.L. and Graham, R.C. (1993) Forest fire effects on soil color and texture. *Soil Science Society of America Journal*, 57: 135-140.
- USDA and NRCS (August 2000) *Fire Burn Intensity Classification Fact Sheet*, United States Department of Agriculture and Natural Resources Conservation Service, Montana.
- Valzano, F.P., Greene, R.S.B. and Murphy, B.W. (1997) Direct effects of stubble burning on soil hydraulic and physical properties in a direct drill tillage system. *Soil and Tillage Research*, 42: 209-219.

- van der Post, K.D., Oldfield, F., Haworth, E.Y., Crooks, P.R.J. and Appleby, P.G. (1997) A record of accelerated erosion in the recent sediments of Blelham Tarn in the English Lake District. *Journal of Paleolimnology*, 18: 103-120.
- Vandervaere, J.P., Peugeot, C., Vauclin, M., Angulo Jaramillo, R. and Lebel, T. (1997) Estimating hydraulic conductivity of crusted soils using disc infiltrometers and minitensionmeters. *Journal of Hydrology*, 188-189: 203-223.
- Verardo, D.J. and Ruddiman, W.F. (1996) Late Pleistocene charcoal in tropical Atlantic deep-sea sediments: climatic and geochemical significance. *Geology*, 24: 855-857.
- Vlok, J.H.J. and Yeaton, R.I. (2000) The effect of short fire cycles on the cover and density of understorey sprouting species in South African mountain fynbos. *Diversity and Distributions*, 6: 233-242.
- Vogel, J.C., Fuls, A. and Visser, E. (2002) Accurate dating with radiocarbon from the atom bomb tests. *South African Journal of Science*, 98: 437-438.
- Wade, D.D. (1993) *Societal influences on prescribed burning*. In: S. Hermann Proceedings of the 18th Tall Timbers Fire Ecology Conference.:Tall Timber Research Statistics 351-355.
- Wade, G., Wells, I.I., Wohlgemuth, P.M. and Campbell, A.G. (1987) *Postfire sediment movement by debris flows in the Santa Ynez Mountains, California*. In: Proceedings of the Corvallis Symposium:IAHS Publication 165 PAGE???
- Walden, J. (1999a) Remanence measurements. In: J. Walden, F. Oldfield and J. Smith (Editors), *Environmental Magnetism: a practical guide*. Quaternary Research Association, London, pp. 63-88.
- Walden, J. (1999b) Sample collection and preparation. In: J. Walden, F. Oldfield and J. Smith (Editors), *Environmental Magnetism: a practical guide*. Quaternary Research Association, London, pp. 26-34.
- Walden, J., Slattery, M.C. and Burt, T.P. (1997) Use of mineral magnetic measurements to fingerprint suspended sediment sources: approaches and techniques for data analysis. *Journal of Hydrology*, 202: 353-372.
- Walker, J. (Editor), (1981) Fuel dynamics in Australian vegetation. *Fire and the Australian biota*. Australian Academy of Science, Canberra, 101-127 pp.
- Walling, D.E. (2000) Sediment yield. In: A. Goudie et al. (Editors), *The encyclopedic dictionary of physical geography*. Blackwell Reference, Oxford.
- Walsh, R.P.D., Boakes, D., Coelho, C.O.A., Goncalves, A.J.B., Shakesby, R.A. and Thomas, A.D. (1994) *Impact of fire induced hydrophobicity and post-fire forest litter on overland flow in northern and central Portugal*. In: 2nd International Conference of Forest Fire Research:Coimbra. II. D.38. 1149-1159.
- Ward, D.J., Lamont, B.B. and Burrows, C.L. (2001) Grass-trees reveal contrasting fire regimes in eucalypt forest before and after European settlement of southwestern Australia. *Forest Ecology and Management*, 150: 323-329.
- Ward, R.C. and Robinson, M. (2000) *Principles of Hydrology*. McGraw-Hill Publishing Company, London.
- Warner, R.F. (1987) *The impacts of alternating flood- and drought-dominated regimes on channel morphology at Penrith, New South Wales, Australia*. In: The influence of climate change and climatic variability on the hydrologic regime and water resources.:Vancouver. IAHS Publication no 168. 327-338.
- Wasson, R.J., Clark, R.L., Nanninga, P.M. and Waters, J. (1987) 210Pb as a chronometer and tracer, Burrinjuck reservoir, Australia. *Earth Surface Processes and Landforms*, 12: 399-414.
- Watson, A.I. and Holle, R.L. (1996) An eight-year lightning climatology of the southeast United States prepared for the 1996 Summer Olympics. *Bulletin of the American Meteorological Society*, 77: 883-890.
- Watson, I.A. and Aitken, M.J. (1985) Firing temperature analysis using the 110 °C TL peak of quartz. *Nuclear Tracks*, 10: 517-520.
- Webb, L.J. (1968) Environmental relationships of the structural types of Australian rainforest vegetation. *Ecology*, 49: 296-311.
- Weirich, F.H. (1987) *Sediment transport and deposition by fire-related debris flows in southern California*. In: Erosion and Sedimentation in the Pacific Rim:Corvallis Symposium, August 1987. 165 IAHS Publication 283-284.
- Wells, C.G., Campbell, R.E., De Bano, L.F., Lewis, C.E. and Fredriksen, R.L. (1979) *Effects of fire on soil - a state - of - knowledge review*. Department of Agriculture Forestry Service General Technical Report WO-7, United States.
- Weston, D.G. (2002) Soil and susceptibility: aspects of thermally induced magnetism within the dynamic pedological system. *Archaeological Prospection*, 9: 207 - 215.

- Weston, D.G. (2004) The influence of waterlogging and variations in pedology and ignition upon resultant susceptibilities: a series of laboratory reconstructions. *Archaeological Prospection*, 11: 107-120.
- Whelan, R.J. (1995) *The Ecology of Fire*. Cambridge University Press, Cambridge.
- Whelan, R.J. and York, J. (1998) Post-fire germination of *Hakea sericea* and *Petrophile sessilis* after spring burning. *Australian Journal of Botany*, 46: 367-376.
- White, I.D., Mottershead, D.N. and Harrison, S.J. (1998) *Environmental systems: an introductory text*. Stanley Thornes (Publishers) Ltd, Cheltenham.
- Whitford, W.G. (1998) Contribution of pits dug by goannas (*Varanus gouldii*) to the dynamics of banded mulga landscapes in eastern Australia. *Journal of Arid Environments*, 40: 453-457.
- Whitlock, C. and Millspaugh, S.H. (1996) Testing the assumptions of fire-history studies: an examination of modern charcoal accumulation in Yellowstone National Park, USA. *The Holocene*, 6: 7-15.
- Widden, P. and Parkinson, D. (1975) The effects of a forest fire on soil microfungi. *Soil Biology and Biochemistry*, 7: 125-138.
- Wilkinson, M.T. and Humphreys, G.S. (2005) Exploring pedogenesis via nuclide-based soil production rates and OSL-based bioturbation rates. *Australian Journal of Soil Research*, 43: 767-779.
- Willgoose, G., Bras, R.L. and Rodriguez-Iturbe, I. (2003) The relationship between catchment and hillslope properties: implications of a catchment evolution model.
- Wilson, P. (2003) Mass Wasting. In: J.A. Matthews et al. (Editors), *The encyclopaedic dictionary of environmental change*. Arnold, London, pp. 391.
- Wintle, A.G. and Murray, A.S. (1999) Luminescence sensitivity changes in quartz. *Radiation Measurements*, 30: 107-118.
- Wise, S.M. (1980) Caesium-137 and Lead-210: A review of the techniques and some applications in geomorphology. In: R.A. Cullingford, D.A. Davidson and J. Lewin (Editors), *Timescales in Geomorphology*. John Wiley and Sons Ltd, London, pp. 109-127.
- Witkowski, E.T.F. and Lamont, B.B. (1997) Does the rare *Banksia goodii* have inferior vegetative, reproductive or ecological attributes compared with its widespread co-occurring relative *B. gardneri*? *Journal of Biogeography*, 24: 469-482.
- Wondzell, S.M. and King, J.G. (2003) Postfire erosional processes in the Pacific Northwest and Rocky Mountain regions. *Forest Ecology and Management*, Article in Press: 1-13.
- Wooten, M.E.T. (1965) *Forest survey of the Warragamba inner catchment area*, Forestry Office, Sydney.
- Worsley, P. (1981) Radiocarbon dating: principles application and sample collection. In: A.S. Goudie and others (Editors), *Geomorphological techniques*. Allen and Unwin, London, pp. 277-283.
- Wotton, B.M., McAlpine, R.S. and Hobbs, M.W. (1999) The effect of fire front width on surface fire behaviour. *International journal of Wildland Fire*, 9: 247-253.
- www.bom.gov.au (2004) Climate Averages for Picton Council Depot http://www.bom.gov.au/climate/averages/tables/cw_068052.shtml [22nd July 2004].
- Yang, X.H. and McKeever, S.W.S. (1990) The pre-dose effect in crystalline quartz. *Journal of Physics D: Applied Physics*, 23: 237-244.
- Young, C.T., Randle, T.J. and Hsu, S. (1998) *Surface erosion, sediment transport and reservoir sedimentation*. In: Modelling soil erosion, sediment transport and closely related hydrological processes: IAHS publication no. 249.
- Young, R.W. and Nanson, G.C. (Editors), (1983) *Aspects of the Australian Sandstone Landscapes*. University of Wollongong, Wollongong.
- Young, R.W. and Young, A.R.M. (1988) 'Altogether barren, peculiarly romantic': The sandstone lands around Sydney. *Australian Geographer*, 19: 9-26.
- Zierholz, C. and Hairsine, P. (1995) Runoff and soil erosion in bushland following the Sydney Bushfires. *Australian Journal of Soil and Water Conservation*, 8: 28-37.
- Zimmerman, J. (1971) The radiation-induced increase of the 100°C thermoluminescence sensitivity of fired quartz. *Journal of Physics C: Solid state Physics*, 4: 3265-3276.